

CCC 2007  
Proceedings



Central European  
Congress on  
Concrete Engineering

Main organizer  
*fib* Hungary



**VISEGRÁD**  
**2007**



FOUNDING MEMBERS

17-18 September 2007  
Thermal Hotel Visegrád  
Visegrád, Hungary

The 3rd Central European Congress on Concrete Engineering



**Innovative Materials and Technologies  
for Concrete Structures**

**Proceedings**

[www.fib.bme.hu](http://www.fib.bme.hu)

**INNOVATIVE MATERIALS  
AND TECHNOLOGIES FOR  
CONCRETE STRUCTURES**





# INNOVATIVE MATERIALS AND TECHNOLOGIES FOR CONCRETE STRUCTURES

Proceedings of the *fib* Congress

**Budapest, Hungary  
16 to 17 September 2007**

**Edited by**

**György L. Balázs**

**Professor**

**Department of Construction Materials and Engineering Geology  
Budapest University of Technology and Economics**

**Budapest, Hungary**

**President of the Hungarian Group of *fib***

**and**

**Salem Georges Nehme**

**Senior Lecturer**

**Department of Construction Materials and Engineering Geology  
Budapest University of Technology and Economics**

**Budapest, Hungary**



This Volume was edited by György L. Balázs and Salem G. Nehme

**© Balázs – Nehme, 2007**

All rights reserved. No part of this publication may be reproduced or transmitted in any form or by any means, electronic or mechanical, including photocopy, recording, or any information storage and retrieval system, without written permission from the publisher.

Both the abstracts and the papers were reviewed by the members of the Scientific Committee.

Although the authors, the editors and the publisher did their best to provide accurate and current information, none of them, nor anyone else associated with this publication, shall be liable for any loss, damage or liability directly or indirectly caused or alleged to be caused by this book.

**Published by the Publishing Company of Budapest University of Technology and Economics**

**ISBN 978-963-420-923-2**



## PREFACE

A new tradition started in 2005 that is called *CENTRAL EUROPEAN CONGRESS ON CONCRETE ENGINEERING*. This is a series of yearly congresses to provide a forum for engineers of our neighbouring countries to meet and exchange experiences regularly. Engineers from all fields are addressed working in design, execution, prefabrication, material production, research or quality control.

In our Congresses new achievements are presented to a specific field of concrete engineering: *Fibre reinforced concrete* was the topic of the 1<sup>st</sup> CCC Congress in Graz, Austria in 2005 and *Concrete structures for traffic network* was the topic of the 2<sup>nd</sup> CCC Congress in Hradec Kralove, Czech Republic.

The 3<sup>rd</sup> Central European Congress on Concrete Engineering will take place in Visegrad, Hungary. The Congress focuses on *Innovative materials and technologies for concrete structures*. Concrete is an ever developing construction material. There is a continuous development on material properties, constructability, economy as well as aesthetics.

The Congress in Visegrad intends to overview properties of new types of concretes (including all constituent materials) and reinforcements as well as their possible applications which already exist or can exist in the future.

Therefore, we selected the following 3 topics:

- Topic 1: Tailored properties of concrete
- Topic 2: Advanced reinforcing and prestressing materials and technologies
- Topic 3: Advanced production and construction technologies.

The Congress in Visegrad will be organized in a beautiful ambient provided by the picturesque Danube Bend.

The host organisation of the Congress is the Hungarian Group of *fib*. Co-organizers of the Congress are the Hungarian Concrete Association and the Association of Hungarian Concrete Elements Manufacturers.

We have a pleasure to invite representatives of clients, designers, contractors, academics and students to take part at this regional event, which will give excellent social and technical conditions for exchange of experience in the field of concrete engineering. We are happy to meet you in Visegrad.

György L. Balázs

Salem G. Nehme

**Scientific Committee**  
**3<sup>rd</sup> European Congress on Concrete Engineering**  
**17-18 September 2007 Visegrád, Hungary**

BALÁZS, György L., Chairman (Hungary)	KOLLEGGER, Johan (Austria)
BELUZSÁR, János (Hungary)	MARIĆ, Zvonimir (Croatia)
BERGMEISTER, Konrad (Austria)	MIHANOVIĆ, Ante (Croatia)
BOROSNYÓI, Adorján (Hungary)	RADIĆ, Jure (Croatia)
CSÍKI, Béla (Hungary)	SITKU, László (Hungary)
DANCS, László (Hungary)	SORIĆ, Zorislav (Croatia)
DOHNALEK, Jiri (Czech Republic)	SPAROWITZ, Lutz (Austria)
DEKANOVIĆ, Đuro (Croatia)	SZARKÁNDI, János (Hungary)
FARKAS, György (Hungary)	UKRAINCZYK, Velimir (Croatia)
HELA, Rudolf (Czech Republic)	VÍTEK, Jan L. (Czech Republic)
JÓZSA, Zsuzsanna (Hungary)	WELZIG, Werner (Austria)
KALNY, Milan (Czech Republic)	ZAMOLO, Michaela (Croatia)
KOHOUTKOVA, Alena (Czech Republic)	ZSIGMONDI, András (Hungary)

**Sponsoring Organizations**

Céh Co.  
CSC Jáklekémia Hungária Ltd.  
DDC Ltd.  
ÉMI-TÜV Süd Ltd.  
Hídépítő Co.  
Holcim Hungary Co.  
Lábatlani Vasbetonipari Co.  
Pont-TERV Co.  
Vegyépszer Co.  
Via Pontis Co.

**Organizing Committee**  
**3<sup>rd</sup> European Congress on Concrete Engineering**  
**17-18 September 2007 Visegrád, Hungary**

POLGÁR, László, Chairman (Hungary)	MOCHANOVA, Alena (Czech Republic)
ARANY, Piroska (Hungary)	NEHME, Salem G. (Hungary)
DUBRÓVSZKY, Gábor (Hungary)	NEMES, Rita (Hungary)
ERDŐDI, László (Hungary)	PAUSER, Michael (Austria)
FEHÉRVÁRI, Sándor (Hungary)	SIMON, Tamás (Hungary)
FENYVESI, Olivér (Hungary)	ŠRŮMA, Vlastimil (Czech Republic)
KOLIĆ, Davorin (Croatia)	SZABÓ, Zsombor (Hungary)
KOLOZSI, Gyula (Hungary)	SZILÁGYI, Katalin (Hungary)
KOPECSKÓ, Katalin (Hungary)	SZILVÁSI, András (Hungary)
KOVÁCS, Tamás (Hungary)	TÁPAI, Antal (Hungary)
LUBLÓY, Éva (Hungary)	ZSIGOVICS, István (Hungary)

**Exhibitors**

NRS AS; OVM China  
Centre for Promotion of Steel Quality  
Novia Ltd.  
Saint-Gobain Specialty Reinforcement  
Holcim Hungary Co.  
BASF Construction Chemicals Hungary Ltd.  
Hungarian Concrete Association  
Association of Hungarian Concrete Elements Manufacturers  
CSC Jäklekémia Hungária Ltd.  
Sika Hungary Ltd.



**Programme overview (Preliminary)**  
**CCC2007 Visegrád**  
**"New materials and technologies for concrete structures"**

Sunday 16 Sept. 2007	Monday, 17 Sept 2007	Tuesday, 18 Sept 2007		
Arrival Registration Welcome	<b>9<sup>00</sup> SESSION 1: Congress Opening</b> Welcome adresses (H, HR, A, CZ) Gy. L. Balázs: "New materials and technologies for concrete structures" 3 Presentations: M7 Kőröshegy viaduct (design and execution)	<b>9<sup>00</sup> - 10<sup>30</sup> SESSION 9</b> <b>SCC + LWC</b> 5 Pres +Disc		<b>SESSION 11</b> <b>UHPC</b> 4 Pres +Disc
	Opening of Poster Session (will be opened all alowy the Congress)			10 <sup>15</sup> - 11 <sup>00</sup> Coffee
	10 <sup>30</sup> - 11 <sup>15</sup> Coffee + Exhibition	10 <sup>30</sup> - 11 <sup>15</sup> Coffee		<b>SESSION 12</b> <b>FRP</b> 6 Pres + Disc
	<b>11<sup>15</sup>-13<sup>00</sup> SESSION 2 Selected Papers</b>  6 Pres + Disc	<b>SESSION 10</b> <b>FRC</b> 5 Pres + Disc		
	13 <sup>00</sup> - 14 <sup>15</sup> Lunch + Exhibition		12 <sup>45</sup> - 14 <sup>00</sup> Lunch + Exhibition	
	<b>14<sup>15</sup> - 15<sup>45</sup> SESSION 3</b> <b>Cements and fresh concrete</b> 5 Pres + Disc	<b>SESSION 5</b> <b>Prefabrication</b>  5 Pres + Disc	<b>SESSION 7</b> <b>Buildings</b>  5 Pres + Disc	<b>14<sup>00</sup> - 15<sup>00</sup></b> <b>SESSION 13: Closing Session</b> 3 Pres M0 North Danube bridges (design and execution) Evaluation of the Congress
	15 <sup>45</sup> - 16 <sup>15</sup> Coffe + Exhibition		<b>15<sup>00</sup> - 18<sup>00</sup></b> <b>Technical Excursion</b> <b>M0 North Danube bridges</b>	
	<b>16<sup>15</sup> - 17<sup>45</sup> SESSION 4</b> <b>Admixtures</b>  5 Pres + Disc	<b>SESSION 6</b> <b>Temperature</b>  5 Pres + Disc	<b>SESSION 8</b> <b>Bridges and tunnels</b>  5 Pres + Disc	
	17 <sup>45</sup> Free time			
	<b>18<sup>45</sup> Congress Banquet</b> <b>Medieval tournament + Dinner</b>			

**3rd Central European Congress on Concrete Engineering  
17-18 Sept. 2007, VISEGRAD, HUNGARY**

**CONTENT**

Preface	I
Content	V

**SELECTED PAPERS**

<i>György L. Balázs</i> Innovative materials and technologies for concrete structures	1
<i>Tamás Mihalek</i> Viaduct of Kőröshegy on motorway M7 in Hungary, movement-limiting the abutments for receiving longitudinal tensile and compressive forces	13
<i>János Magyar</i> Viaduct of Kőröshegy on motorway M7 in Hungary — viaduct with two technologies	21
<i>András Nagy</i> Design of the pier of the Kőröshegy viaduct	29
<i>Jiri Strasky, Ivailo Terzijski, Radim Necas</i> Bridges utilizing high strength concrete	35
<i>Jure Radić, Zlatko Savor, Gordana Hrelja</i> New types of overpasses on Croatian highways	41
<i>Christa Owczakovitz, László Czotter</i> Metro construction in Budapest, Hungary — Construction of the stations Tétényi út and Népszínház utca	47
<i>Zsolt Kassai, Imre Kovács</i> A new construction technology for free shape reinforced concrete sandwich shells	55
<i>Rita Nemes, Zsuzsanna Józsa</i> Differences in mix designs of lightweight and conventional concretes	61
<i>Jan Desmyter, Valérie Pollet</i> On site concreting of architectural concrete: not easy, but possible	67

## **TOPIC 1 TAILORED PROPERTIES OF CONCRETE**

### ***Cement and fresh concrete properties***

- Jürgen Macht, Peter Nischer*  
Testing and improving the stability of concrete with flowable consistency 75
- Thomas Eisenhut, Alexander Pekarek*  
Bleeding of concrete in special foundation engineering 81
- Katalin Kopecskó, György Balázs*  
Effect of ggbs additive on chloride ion binding capacity of slag cements 87
- Vit Černý, Veronika Kalová*  
New production technology of sintered fly ashes aggregate 93
- Veronika Kalová, Vit Černý*  
Optimization of raw material mixtures for new technology of processing of sintered fly ash aggregate 99
- Vladimír Těhnik, Jiri Adámek, Vlasta Juránková, Petr Koukal, Barbara Kucharczyková*  
Concrete durability positively influenced by blast furnace slag in cement 105
- 132. Katalin Szilágyi, István Zsigovics, György L. Balázs*  
Blended cements of the 21<sup>th</sup> century: what makes a concrete 111

### ***Admixtures***

- 314. Peter Kremnitzer, Johannes Horvath*  
Innovative test-methods to determine segregation of concretes with flowable consistency — practical experiences 117
- István Asztalos*  
The evolution of superplasticizer technology new opportunities in concrete industry 123
- Mario Corradi, Rabinder Khurana, Roberta Magarotto, Sandro Moro*  
Innovative superplasticisers for modern concrete structures 129
- Giorgio Ferrari, Francesco Surico, Paolo Clemente, Mariele Gamba, Lino Badesso*  
Chemically reactive superplasticisers with improved workability retention 135
- Jure Francišković, Boris Mikšić, Ivan Rogan, Mijo Tomičić*  
Protection and repair of reinforced concrete structures by means of MCI-inhibitors and corrosion protective materials 143



<i>Vladimíra Vytačilová, Tomáš Dvorský, Alena Kohoutková</i> Problems of permeability of concrete from sight of water diffusion in concrete structure	149
<i>Claudiu Aciu, Zsuzsanna Józsa (advisor)</i> Studies on use of lime milk neutralization sludge in the building material industry	155
<b><i>Self compacting concrete and lighth weight concrete</i></b>	
<i>István Zsigovics</i> Mix design of self compacting concrete	161
<i>Henriette Szilágyi, Adrian Ioani, Ofelia Corbu</i> Self compacting concrete with silica fume – procedure for mix design	167
<i>Katalin Szilágyi, István Zsigovics, Csaba Szautner</i> Experimental studies on concrete with innovative shrinkage compensating admixture system	173
<i>Olga Río, Luis Fernández-Luco, Ángel Castillo</i> Environmental friendly tailor-designed shotcrete	179
<i>Masoud Hosseinpoor, GolnazAlsadat Mirfendereski, Ahmadreza Telebian, Ehsan Fereshte Nezhad, Majid Ebad Sichani,</i>	<i>Behrooz</i>
<i>Esmaelkhanian, Morteza Madhkhan</i> Effect of silica fume on mechanical properties of structural lightweight concrete containing saturated leca fine aggregates	185
<i>Stefan Krispel</i> Increase of safety of concrete pavements – Bright concrete pavements with dark aggregates	193
<i>Aleš Frýbort, Aleš Kratochvíl</i> Microstructure of concrete with micro-fillers	201
<i>Miklós Gálos, László Kárpáti</i> Petrophysical classification of aggregates for concretes	207
<b><i>Fibre reinforced concrete</i></b>	
<i>Fausto Minelli, Giovanni A. Plizzari</i> Fiber reinforced concrete characterization: round panel vs. beam tests toward a harmonization	213
<i>Attila Erdélyi, Adorján Borosnyói</i> Durability studies on steel fibre reinforced concrete	221

<i>María J. Álvarez-Casariego Álvarez, Juan C. Romero Ruiz, Pablo I. Comino Almenara</i>	227
Use of the alkali-resistant glass fibres in reinforced concrete members	
<i>Minh Long Nguyen, Marián Rovňák</i>	233
Shear capacity of steel fiber reinforced concrete beams.	
<i>Alena Kohoutková, Iva Broukalová</i>	239
Simulation as a tool for decision-making process for applications of FRC in precast elements	
<i>Béla Magyari, Géza Tassi</i>	245
Application of glass metal fibres to improve the resistance of concrete	
<i>Florian P. Ackermann, Jürgen Schnell</i>	251
Innovative steel fibre reinforced composite slabs	
<i>Vytlačilová Vladimíra, Věroslav Hrubý, Hana Hanzlová, Jan Vodička, Jaroslav Výborný</i>	257
Fiber reinforced concrete with recycables used in earth structures	
<i>Marijan Skazlic, Dubravka Bjegovic, Mladen Jambresic</i>	263
Study on the properties of high performance fibre reinforced concrete	
<i>Kinga Pankhardt, Salem G. Nehme</i>	269
Experimental studies on carbon fibre reinforced lightweight white cement concrete elements	
<i>Imre Kovács, György L. Balázs, Salem G. Nehme</i>	275
Uniaxial behaviour of steel fibre reinforced concrete	
<b><i>Ultra high performance concrete</i></b>	
<i>Joachim Juhart, Bernhard Freytag, Josef Linder, Lutz Sparowitz</i>	281
Preparation and handling of UHPFRC for the manufacture of thin- walled building elements	
<i>Nguyen Viet Tue, Gunter Schenck, Stefan Henze</i>	289
Product-oriented research on high performance structures	
<i>Marion Rauch, Viktor Sigrist</i>	295
Cracking and deformation behaviour of reinforced UHPC elements	
<i>Bogdan Heghes, Cornelia Măgureanu</i>	301
Rotation capacity of reinforced concrete elements	

*Josef Stryk, Jiri Vyslouzil, Karel Pospisil*  
European knowledge on repair of rigid pavements by using of  
ultra fast concrete 309

### ***Temperature influences***

*Jan L. Vitek*  
Fire resistance of concrete tunnel lining — experimental research 315

*Ivanka Netinger, Dubravka Bjegović, Marija Jelčić*  
Fire resistance of structural concrete 321

*Éva Lubl6y, Gy6rgy L. Balázs*  
Concrete properties in fire depending on types of cement,  
aggregate and fibre 327

*Klaus Meinhard, Martin Hopfgartner, Roman Lackner*  
Insitu temperature measurements to determine properties of jet-  
grouted columns by means of a thermo-chemical analysis 333

*Dita Matesova, Břetislav Teply, Jan Podroužek, Marketa Chroma*  
Probabilistic modeling of steel corrosion in RC structures 337

## **TOPIC 2**

### **ADVANCED REINFORCING AND PRESTRESSING MATERIALS AND SYSTEMS**

*Adorjan Borosny6i, Gy6rgy L. Balazs*  
Comparisons in behaviour of steel or CFRP prestressed beams 345

*L'udovıt Nad', Francesca Nanni, Gualtiero Gusmano,  
Giovanni Ruscito, Daniel Źarnay*  
Reinforcing self-sensing FRP rods as main reinforcement in  
concrete beams 351

*Andrew A. Shilin, Dmitry V. Kartuzov*  
Practical experience of CFRP application for external strengthening  
of reinforced concrete structures 357

*Thanongsak Imjai, Maurizio Guadagnini, Kypros Pilakoutas*  
Analytical study on tensile strength of curved FRP reinforcement 363

*Zsombor K. Szab6, Gy6rgy L. Balazs*  
Behaviour of near surface mounted fibre reinforced strengthenings 369

*D. G. Novidis, S. J Pantazopoulou*  
Beam pull out tests of NSM-FRP and steel bars in concrete 375



*Peter Koteš, Patrik Kotula, Miroslav Brodňan*  
Experimental investigation of strengthened RC girders 381

### **TOPIC 3**

#### **ADVANCED PRODUCTION AND CONSTRUCTION TECHNOLOGIES**

##### ***Prefabrication***

*Jure Radnić, Alen Harapin, Marija Smilović*  
Concrete girder bridges with long prefabricated girders 389

*Andreas E. Kainz, Stefan L. Burtscher, Johann Kollegger*  
Concrete slab with integrated installations 395

*János Beluzsár, Levente Beluzsár, Zoltán Sziklai*  
Application of high strength concrete at the production of railway upper line poles 401

*Kálmán Koris*  
Durability-design of pre-cast concrete members 407

*Markus Schulz*  
Application possibilities of fibres in precast elements 413

*Seng Kiong Ting, Hongsheng Han*  
Cyclic behaviour of precast composite shear walls: experimental results and analysis 419

*Stjepan Lakusic, Vesna Dragcevic, Dalibor Bartos*  
Noise protection barriers by concrete two-layer panels 425

*István Bódi, László Erdődi, Kálmán Koris*  
Parametric analyses of precast reinforced concrete pipes 431

##### ***Buildings***

*Jorge de Novais Bastos*  
The new Amalia Rodrigues Park in Lisbon 437

*S. Kanappan, Sthaladipti Saha*  
Innovative application of high performance self compacting concrete 443

*Marco Preti, Ezio Giuriani*  
Preliminary results on a full scale experiment on seismic rocking of structural walls 449

<i>A. Prota, G. Manfredi, A. Balsamo, A. Nanni, E. Consenza, G. Morandini</i> Innovative technique for seismic upgrade of rc square columns	455
<i>Christian Dehlinger</i> Foundations for offshore wind turbines	463
<i>István Haris, Zsolt Hortobágyi</i> Modelling cast-in-situ reinforced concrete frame stiffened by masonry wall using FEM software	469
<b><i>Bridges and tunnels</i></b>	
<i>Jure Radić, Alex Kindij, Ana Mandić</i> Jarun City Bridge — Preliminary design	475
<i>Ladislav Šašek, Petr Štědroňský</i> The highway bridge at Rzává	481
<i>Andreas Rath</i> New technologies on the project Wienerwaldtunnel, Austria — Optimization of backfill material for segment rings and use of long formworks	487
<i>Jullius Hirscher, Richard Dietze</i> Erection of reinforced concrete segments in Budapest Metro 4 Line	495
<i>Tamás K. Simon</i> Concrete to concrete interaction by constructing the 4 <sup>th</sup> Metro Line in Budapest, Hungary	503
<i>Velimir Ukrainczyk</i> Bridge deck concrete overlays as renewal structures	509
<i>Réka Szécsényi</i> M0 North Danube bridges in Budapest, Hungary — construction technology	515



# **SELECTED PAPERS**



## INNOVATIVE MATERIALS AND TECHNOLOGIES FOR CONCRETE STRUCTURES

*György L. Balázs, Prof.*  
*Budapest University of Technology and Economics*  
*H-1111 Budapest, Műegyetem rkp. 3*  
*balazs@vbt.bme.hu*

### SUMMARY

Concrete must be resistant, serviceable, durable, constructable, economic and aesthetic. Research and technological development should support all of these requirements. Improved properties are reached by new types of cements, aggregates and admixtures. New types of concretes (such as self compacting concrete, fibre reinforced concrete, light weight concrete) also help to improve several properties of fresh or hardened concretes. Non-metallic reinforcements serve to avoid corrosion of steel reinforcements. Externally bonded and near surface mounted applications of non-metallic reinforcements provide new alternatives for strengthening. Prefabrication and new erection techniques serve for faster construction. An overview of last development in materials and constructions are presented herein.

### 1 HISTORICAL BACKGROUND IN HUNGARY

Reinforced concrete structures have been already constructed in Hungary shortly after the invention of reinforced concrete. Fig. 1 presents the pedestrian bridge in the City Park Budapest that was constructed in 1894 with a span of 10.7 m above the surface line of the first underground line in the continental Europe (Balázs, 1994; Mihailich, Haviár, 1966). At the beginning of the 20<sup>th</sup> century many industrial, agricultural or office buildings and residential houses were constructed using reinforced concrete. The girder bridge in Temesvár from 1908 with almost 40 m span and a railway arch bridge with a span of 60 m ment world records at that time (Mihailich, Haviár, 1966; Balázs, Borosnyóí, Tassi, 2004). During the 20<sup>th</sup> century reinforced concrete was widely used for bridges, silos chimneys, large span hangars, shells, storage structures, houses and hydraulic structures.

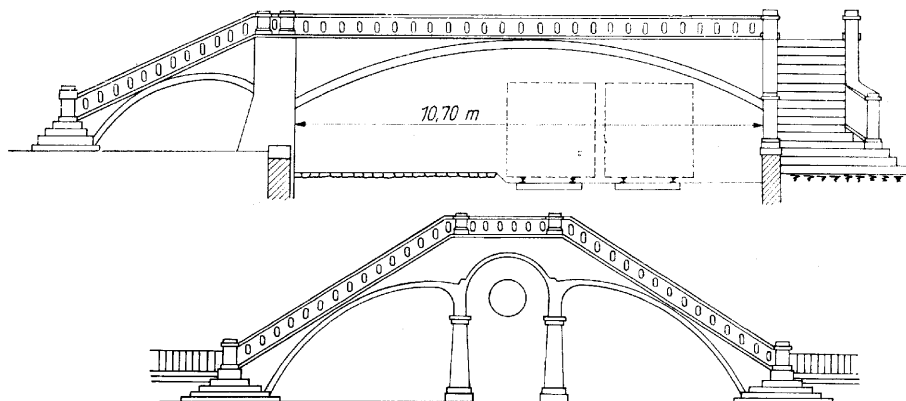


Fig. 1 Still existing concrete pedestrian bridge over the surface line of the first European-continental underground in Budapest (constructed in 1894)

## Cement

*Adam Clark* has burnt Roman cement on the construction site during the erection of the Chain Bridge in 1848 (Balázs, 1994). In 1867 *Ferenc Lichnowszky*, a Polisch Emigrant realized that necessary materials (lime stone and marble) for cement production are available in the vicinity of Lábatlan. The cement factory in Lábatlan was then founded by *Konkoly Thege* in 1868. After Lábatlan several cement factories were founded in Hungary such as: Nyergesújfalu (1870), Újlak (1880), Selyp (1907), Bélápátfalva (1908), Beremend (1909), Tatabánya (1912), Hejőcsaba (1952) und Vác (1964). Today cement is produced in Hungary by two large cement companies in modern fabrics. *Holcim Hungary Co.* has the cement fabrics in Lábatlan and in Hejőcsaba. *Duna-Dráva Cement Ltd.* has the cement fabrics in Vác and Beremend. The cement consumption in Hungary in the last three and a half decades is summarized in Fig. 2. The pro capita cement consumption in Hungary is about 400 kg yearly.

The Hungarian Association for Material Testing started testing of cement already at the beginning of 20<sup>th</sup> century (Zielinski, Zhuk, 1901). *Szilárd Zielinski* has already realized in 1909 the importance of water to cement ratio (Zielinski, 1909). Cements are produced and tested today according to the European Standards (EN 196 and EN 197)

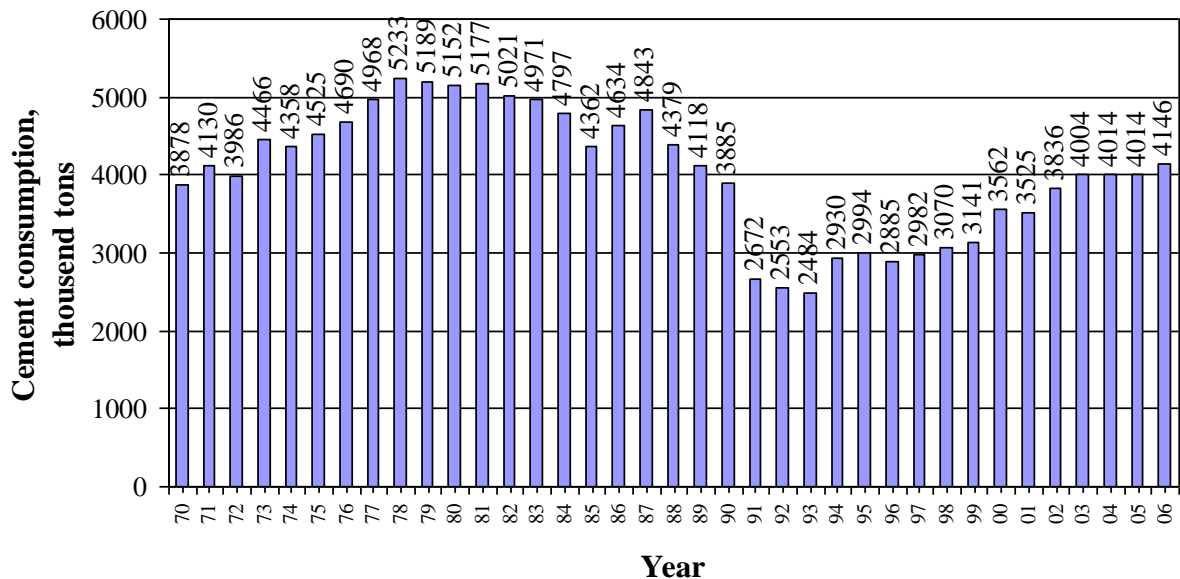


Fig. 2 Cement consumption in Hungary between 1970 and 2006 (based on Hungarian Cement Association, 2005)

## Aggregates

Today mainly natural sand and gravel is used as concrete aggregate. Broken stone is only about 15 percent is used from the whole amount of aggregates. Crushed stone is normally used if relatively high tensile strength is required. Characterizing of available aggregates was carried out by Popovics (1955) and Kausay (1967).

## Concrete

Ready mix concrete is applied in Hungary since 1960. The first ready mix company was BVM. Concrete is produced today mainly by ready mix companies. The overall ready mix concrete production in Hungary is summarized for the last three and a half decades in Fig. 3.

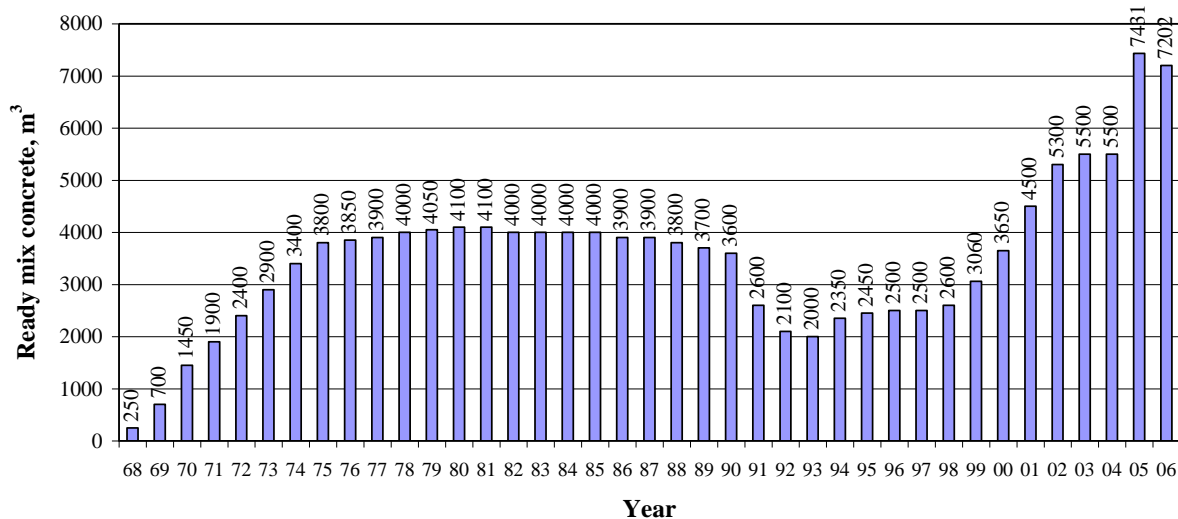


Fig. 3 Ready mix concrete production in Hungary between 1968 and 2006 (based on Szilvási, 2005)

## 2. ACTUAL RESEARCH TOPICS

Most of the research nowadays is related to applications. Research is supported either by companies or by the Hungarian Research Found (OTKA) or by ministries. Research interest is mainly directed towards the following topics: new types of cements, new types of aggregates, new types of admixtures, high strength concrete, high performance concrete, self compacting concrete, durability, service life, fibre reinforced concrete, non-metallic reinforcements, strengthening and upgrading, fire design and seismic design.

### *Chloride ion binding capacity of cements*

Main purpose of research by Kopecskó and Balázs (2005) (Hungarian Research Found Grant T034467) was to study the influence of steam curing on chloride ion binding capacity of  $C_3A$  and  $C_4AF$  clinkers and their mixtures with gypsum. Steam curing is a generally used method in the production of precast concrete elements. Increased temperature accelerates the hydration resulting high early strength (Hooton, Titherington, 2004). Chemically bound chloride content does not induce corrosion of steel reinforcement. Interaction of chloride ions and cements can be modelled by studying directly the interaction of chloride ions and the clinker minerals. Both  $C_3A$  and  $C_4AF$  binds chlorides by the formation of Friedel's salt  $C_3A \cdot CaCl_2 \cdot H_{10}$ , or its iron analogue  $C_3F \cdot CaCl_2 \cdot H_{10}$ , if chlorides are dissolved in the mixing water (Friedel, 1897). This research focused on the influence of de-icing salts. Purpose of research was to answer the following questions:

- What are the influences of the curing temperature (natural hardening at 20°C, steam curing at 60°C or steam curing at 90°C) and gypsum content on the chloride ion binding of hydrated calcium-aluminate clinker minerals ( $C_3A$  and  $C_4AF$ )? (Aluminates to gypsum ratios were from 10/0 to 10/5)
- What is the influence of the curing temperature on the chloride ion binding of cements? (Three different types of cements were studied: OPC, GGBSC and SRPC.)

Semiplastic consistency was used. Samples were subjected to steam curing for 3 hours after casting (60°C or 90°C). Salt-treatment meant to keep the samples in 10% NaCl solution between 28 and 38 days of ages (24 hrs in the salt solution, followed by 24 hrs of drying cyclically). Hydration products were studied by thermal tests (TG/DTG/DTA) and X-ray



diffraction at 1, 7, 28, 90 and 180 days. Splitting tensile tests were carried out to study changes in mechanical properties.

The experimental results on  $C_3A$  and  $C_4AF$  samples prepared without gypsum indicated that Friedel's salt can not be produced from monosulphate; however, it is produced from the stable hydrogarnet. After salt treatment considerable increase of the splitting tensile strength was observed. This can be explained by the volumetric increase of Friedel's salt produced from hydrogarnet. Density of Friedel's salt ( $2,056 \text{ g/cm}^3$ ) is smaller than the density of hydrogarnet ( $2,520 \text{ g/cm}^3$ ); therefore, the decrease of the porosity induces the increase of the splitting tensile strength. Steam curing improves the chloride ion binding capacity of  $C_3A$  és  $C_4AF$  cement clinkers. Steam curing induces higher increase in chloride ion binding capacity for  $C_3A$  clinkers, than for  $C_4AF$  clinkers. In cases of low gypsum content (samples of 10/1 and 10/2 aluminate clinker/gypsum mass ratio) after salt treatment not only Friedel's salt but also Kuzel's salt (sulphate containing chloride-AFm compound) are produced (Kuzel, 1966). Formation of Kuzel's salt increases the amount of chemically bound chloride ions. Production of Kuzel's salt is not followed by the production of secondary ettringite and not induces reduction of tensile splitting strength (Figs. 4 and 5).

It was experimentally shown that steam cured cements (concretes) are able to bind more chloride ions than non-steam cured (naturally hardened) cements (concretes) (Kopecskó – Balázs, 2005). Amount of bound chloride ions is higher in samples steam cured at  $90^\circ\text{C}$  compared to samples steam cured at  $60^\circ\text{C}$ . Various cements have various chloride ion binding capacities. Chloride ion binding capacity of tested cements in decreasing sequence (both for steam cured and non-steam cured samples): CEM III/A 32,5 N (GGBSC), CEM I 42,5 N (OPC), CEM I 32,5 RS (SRPC).

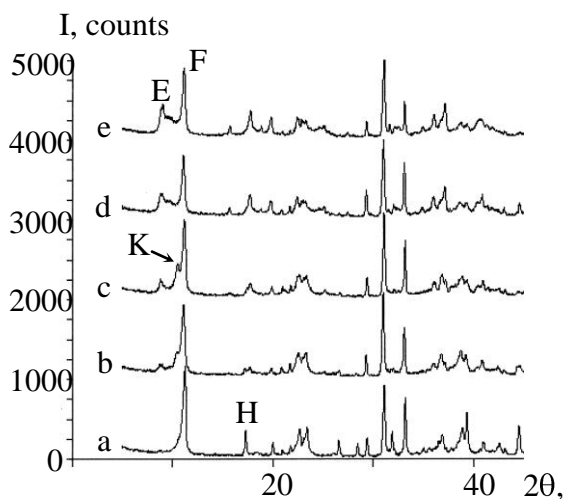


Fig. 4

XRD patterns of 90 days  $C_3A$ /gypsum samples,  
 steam curing at  $60^\circ\text{C}$ ,  
 $C_3A$ /gypsum mass ratios:  
 a) - e) 10/1-től 10/5

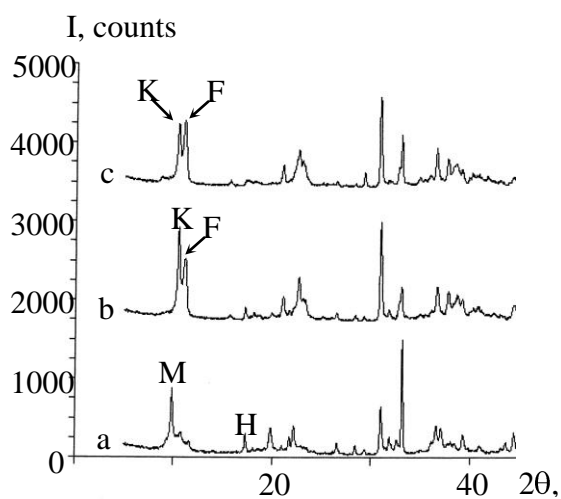


Fig. 5

XRD patterns of hydrated  $C_3A$ /gypsum samples, mass ratio: 10/2, steam cured at  $90^\circ\text{C}$   
 a) before salt treatment, at 28 days  
 b) salt treated, at 90 days  
 c) salt treated, at 180 days

(Notations: F – Friedel's salt, K – Kuzel's salt, E – ettringite, H – hydrogarnet, M – monosulphate)

### ***Light- recycling aggregates***

Recently in Hungary the experimental production of a group of cellular pellet product made of waste glass was started. This new product group was tested for its suitability as lightweight aggregate for lightweight structural concrete or for any other useable purpose. Under the name “Geofil bubbles” a pellet product from industrial and communal (from collected package waste) waste material of high glass content is manufactured by recycling technology (inventor: L. Hoffmann and co., Geofil Ltd. Tatabánya. Registered patent: PCT (HU) 00017). The product is a lightweight artificial gravel with a diameter of 1 to 24 mm having primarily heat and sound insulating properties (Fig. 10). Main properties of foam gravel are:

- particle density: 450 - 1800 kg/m<sup>3</sup>
- loose bulk density: 250 - 1100 kg/m<sup>3</sup>
- crushing strength: 0,3 – 15,1 N/mm<sup>2</sup>
- water absorption capacity: 0,4 - 40 m%.

This new product has three main types called Geofil A, B and C. Type A is used for thermal insulation, type B is used for structural lightweight concrete (LWAC) with thermal insulating property and type C is used for structural LWAC. The water absorption of LWAs Geofil type B and Geofil type C is low. The relationship between water absorption and particle density is well determined. Geofil type A has higher water absorption than the previous ones but it is in all cases lower than in case of other expanded glass or expanded clay product. At the Budapest University of Technology and Economics we have tested several different lightweight aggregate concretes made of different lightweight aggregates. The most important data for mix design is the relationship between particle density and crushing resistance of lightweight aggregate. The density of lightweight concrete with expanded glass aggregate is 15 to 20 % lower than the density of normal weight concrete with the same grade (Nemes, Józsa, 2006).



Fig. 6 Light weight aggregates with different diameters and densities (Józsa, Nemes, 2002)

### ***Fibre reinforced concrete***

The material properties of possible fibres and fibre reinforced concretes are already known more or less. Modelling and new applications still give a lot of possibilities for research. Extensive research was carried out at the Budapest University of Technology and Economics on structural applications of steel fibre reinforced concrete (Balázs, 1999; Kovács, Balázs, 2004). As an example, Fig. 7 indicates the failure loads and failure modes of prestressed pretensioned concrete beams. Fibre contents were 0, 0.5 and 1.0 volumetric percent of Dramix steel fibres. The pretensioned concrete beams did not contain any stirrup reinforcement. The influence of steel fibres was pronounced. Without steel fibres beams failed in shear. However, by increasing the steel fibre content, the failure mode was not only less brittle, but the characteristic crack was formed as a flexural crack for the highest amount

of steel fibres. In this experiments the flexural moment of resistance was reached by 1.0 volumetric percent of steel fibres.

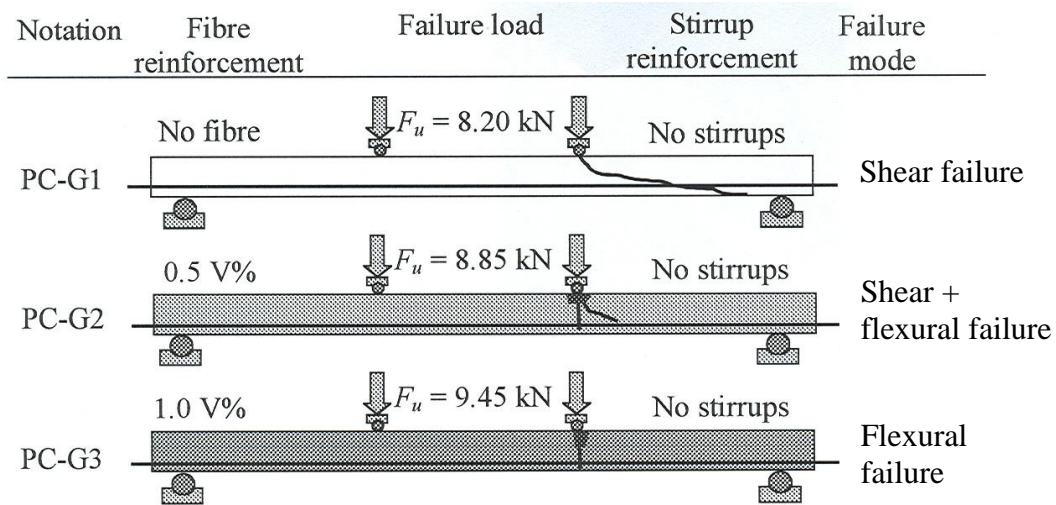


Fig. 7 Failure loads and failure patterns of prestressed pretensioned beams with different steel fibre contents (Balázs, Kovács, 2005)

**Prestressing with non-metallic reinforcements**

Corrosion of steel reinforcement is an important problem also in Hungary especially in bridges owing to the application of deicing salts in winter. Non-metallic reinforcements (prestressed or non-prestressed) can provide an interesting alternative to steel reinforcements at least for specific applications. Among the various high strength fibres (aramid, carbon and glass), carbon fibres seem to have altogether the best mechanical and chemical properties (short term strength, long term strength, fatigue strength, relaxation, durability in alkaline environment, etc). In addition to it, the modulus of elasticity of carbon fibres can be defined during production between 150 000 und 300 000 N/mm<sup>2</sup>.

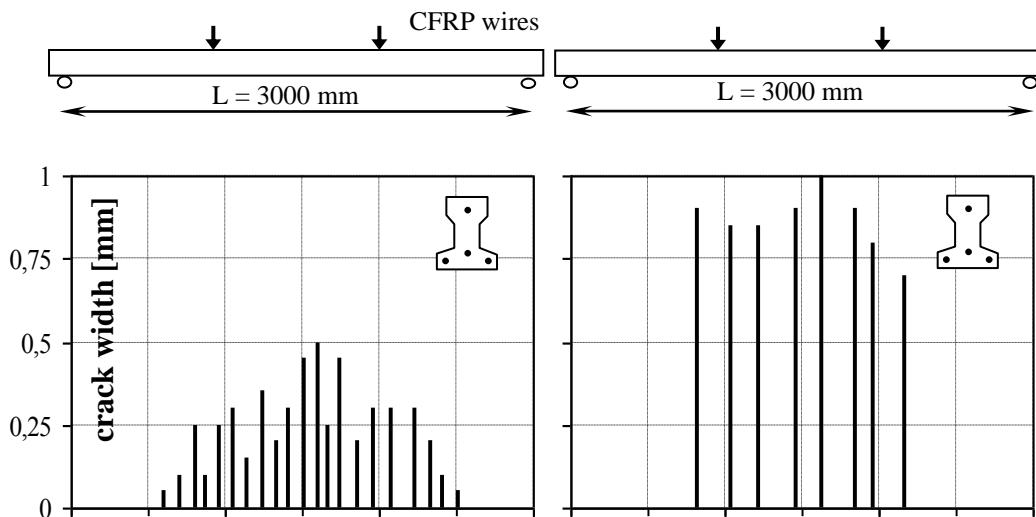


Fig. 8 Crack widths in beams prestressed either with 4 steel wires or CFRP wires (Borosnyói, Balázs, 2002)

A comparative experimental study was carried out at the Budapest University of Technology and Economics on pretensioned concrete beams prestressed either with steel wires or with

carbon fibre wire. The carbon fibre wires had sanded surface. The transfer of prestressing force was reached by bond in both cases. The cross-section of beams had a height of 190 mm and thin web as for typical bridge girders. the span of our laboratory beams was 3 m. The beams did not contain any stirrup reinforcement. (The beams with the carbon fibre wires did not have at all steel reinforcement in them.) Number of prestressing wires in a cross-section was between 1 and 4 in order to reach different failure modes. The observed behaviour indicated the possible use of non-metallic reinforcements (Borosnyói, Balázs, 2002). Fig. 8 gives examples for the crack width distribution in beams prestressed either with 4 steel wires or with 4 carbon fibre wires for a deflection= $\text{span}/75$ . the diagrams indicate favourable comparison for the carbon fibre wires.

### ***Strengthening***

Maintenance and refurbishment of reinforced concrete structures is an important part of the civil engineering activities. The causes are the deterioration of material properties otherwise the increase of loads or other requirements. Typical solution of strengthening nowadays is bonding of high strength fibre strips or wraps to the surface of the member. Various examples from the Hungarian practice are given in Ref. Balázs, Almakt (2000) supported by research results. An interesting example of externally bonded glass fibre fabric in Hungary dates back to 1984 when bauxite concrete columns were strengthened by wrapping of GFRP (Varga, 2000).

## **3. PRECAST CONCRETE**

Development of precast concrete has been already started before the 2nd World War. Precast girders of I, T, TT and U cross-sections were produced up to a span above 30 m. Many of bridges and frames (Fig. 9) were constructed of precast elements. Precast concrete often provides a favourable solution owing to the good quality of concrete. There is a wide range of precast elements produced in Hungary, such as beam and slab elements for dwelling houses, bridge girders, railway sleepers, electric poles, concrete elements for hydraulic and road engineering, etc. Precast bridge girders reach spans above 40 m. The percentage of precast elements of all concrete production is even today very high with new types of elements.



Fig. 9 Precast elements for a hall (Photo: András Leidál)



#### 4. NEW NATIONAL THEATER IN BUDAPEST

The first National Theatre in Budapest was built in 1837. The building became obsolete and demolished during the construction of the 2<sup>nd</sup> underground line. After long debates the New National Theatre was opened on 15 March 2002 (Fig. 10). The New National Theatre is 21 668 m<sup>2</sup> with 610 seats. The building is situated on the bank of the Danube. The stage is equipped with the most modern stage technique (72 pieces of 1×2 m separately movable surface parts). The main load bearing part of the Theatre is made of reinforced concrete extended with steel elements in some places. Interesting solution among the reinforced concrete members are two deep beams with 5 m depth that support the roof system of the audience hall. These were constructed of self compacting concrete with mix proportions of (Zsigovics, Balázs, 2002): cement (CEM II/A-S 42,5 N) 350 kg/m<sup>3</sup>, wasser 150 kg/m<sup>3</sup>, aggregates 8/16 618 kg/m<sup>3</sup>, 4/8 230 kg/m<sup>3</sup>, 0/4 919 kg/m<sup>3</sup>, lime stone powder 150 kg/m<sup>3</sup>, Sika Viscocrete 6 kg/m<sup>3</sup>. The spread with flow table test was between 680 and 750 mm.



Fig. 10 New National Theatre in Budapest

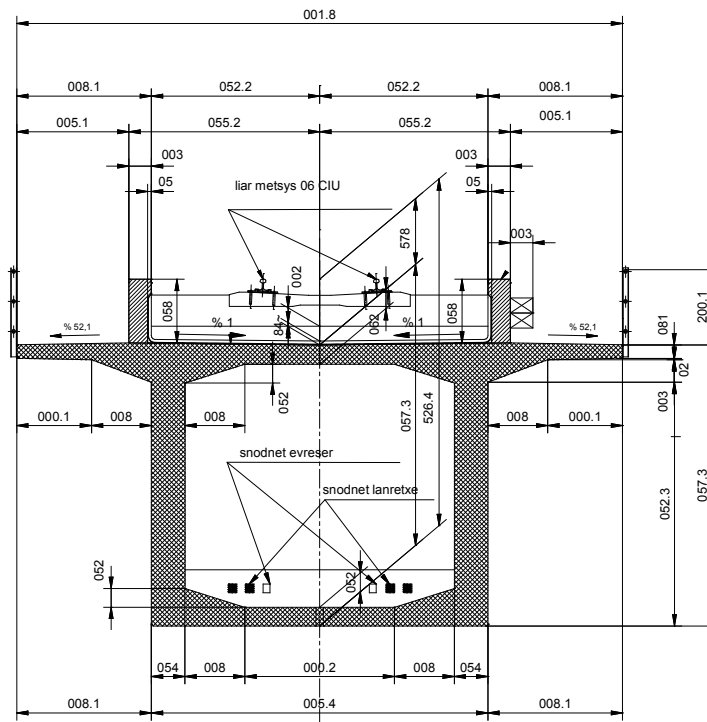
#### 5. SOME RECENT EXAMPLES OF CONCRETE BRIDGES IN HUNGARY

##### **Railway viaduct on the Hungarian-Slovenian railway line**

One of the most modern reinforced concrete viaduct was constructed on the Hungarian-Slovenian railway line in 2001 (Barta, Wellner, Mihalek, Becze, Fodor, 2001; Wellner, Mihalek, 2002). (The railway line was opened in January 2002.) The whole viaduct consists of two pieces of 1400 m and 200 m. The superstructure is a continuous box girder (Fig. 11.a) with an overall width of 8.1 m and overall depth of 3.75 m. Most of the 32 spans are 45 m long on the 1400 m viaduct length. The viaduct has 11‰ inclination. The superstructure was constructed with incremental launching technology. Half of the spans (22.50 m) were cast in construction decks behind both abutments. When the concrete reached its required strength, they were connected to the completed part of the viaduct with prestressing tendons. The superstructure was moved forward parallel to the axis of the viaduct by lifting-pushing jacks placed on the top of the piers (two for each bridge parts) on PTFE sheets. Straight tendons were placed into the bottom and top slabs and curved tendons were placed in vertical alignment (Fig. 11.b).

a)

NOITCES-SSORC



b)

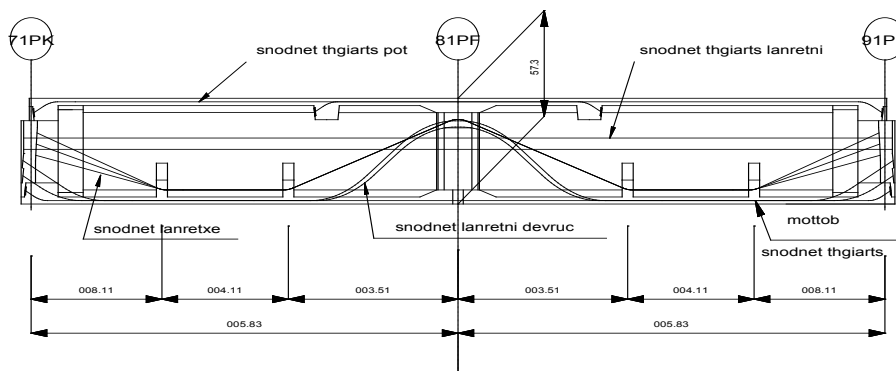


Fig. 11 Prestressed concrete viaduct on the Hungarian-Slowenien railway line (Barta, Wellner, Mihalek, Becze, Fodor, 2001)

a) Cross-section                      b) External cables (Part B)

***The first extradosed bridge in Hungary***

The first extradosed bridge in Hungary was recently opened in South Hungary close to Letenye on the crossing of M7 and M70 freeways (Becze, 2005) (Fig. 12). The reason for the selection of extradosed bridge was to increase the clear span to reach improved traffic conditions. The bridge was constructed with an inclination of  $\alpha=60^\circ$ . The spans are 52,26 + 51,98 m, the overall width is 16.16 m, the depth of the box girder is 2.50–1.60 m. The piers are stiff coupled with the edge beams and are 9.0 m high above the deck. The inclined cables reach the edge beams in a length of 29 to 37 m.



Fig. 12 The first extradosed bridge in Hungary (Becze, 2005)



Fig. 13 Viaduct on the M7 motorway at Kőröshegy (Wellner, Mihalek, Barta, 2005)

### ***Viaduct on M7 motorway at Kőröshegy***

One of the longest viaducts in Europe is the Kőröshegy viaduct on the M7 motorway towards the Croatian border (Wellner, Mihalek, Barta, 2005) (Fig. 13). The overall length of the viaduct is 1872 m with spans of  $(1)+60+95+13\times 120+95+60+(1)$  m. The superstructure is a prestressed concrete box girder of two cells with depth of 3.5 to 7.0 m. The columns reach 80 m heights. The viaduct was opened to traffic on 8 August 2007. Detailed description about the viaduct is given in the next three papers of this Proceedings.

## **6. RECENT HYDRAULIC CONSTRUCTIONS**

Water supply of people and waste water treatment are very important activities of civil engineers (Tóth, 2002). Fig. 14 presents the vertical section of a reinforced concrete sludge digester in Nyíregyháza with a size  $2\times 2000$  m<sup>3</sup>. Top and bottom parts are conical and middle

part is cylindrical. Thickness of wall is 400 mm. Control for for 0.1 mm crack width by 20 m water level is fulfilled.

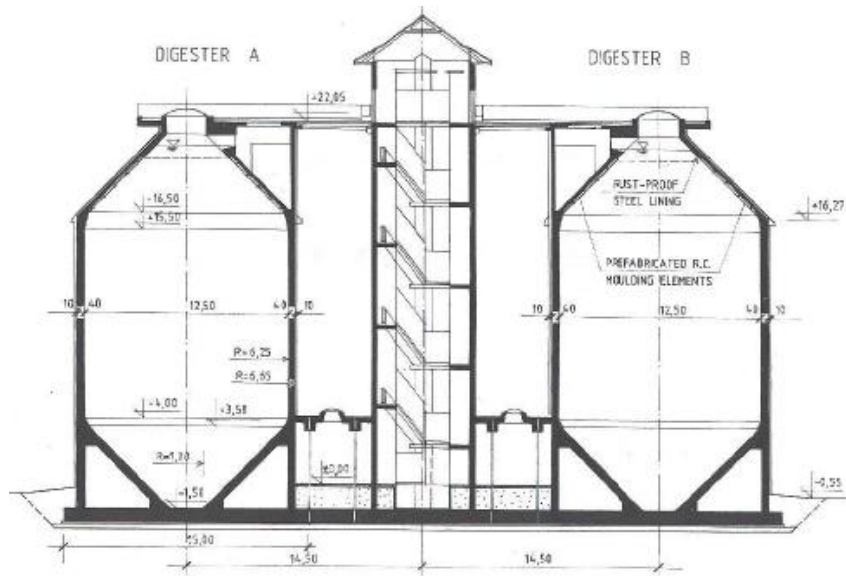


Fig. 14 Vertical section of the sludge digester in Nyíregyháza (Tóth, 2002)

## 7. CONCLUSIONS

Concrete and concrete structures play an important role all over the world in the construction activities. Concrete is a complex material, its properties are defined by the constituent materials and the production process. Research and technological development help to meet the increasing requirements. In the last decade there have been considerable developments in the field of concrete engineering.

In Hungary cement consumption exceeds 4000 tons and ready mix concrete production exceeds 7200 tons in Hungary. As representative examples of high level of concrete technology in Hungary the New National Theatre in Budapest, the first Hungarian extradosed bridge close to Letenye, the railway viaduct on the Hungarian-Slovenian railway line, and the Kőröshegy viaduct on the motorway to Croatia were presented herein.

## 8. REFERENCES

- Balázs, Gy. (1994), „History of concrete and reinforced concrete — Basics“, *Academy Press*, Budapest (in Hungarian)
- Balázs, Gy. L. (1999), „Fibre Reinforced Concrete — from research to practice“, *Proceedings* 4-5 March 1999, ISBN 963 420 589 5
- Balázs, Gy. L., Almarkt, M. M. (2000), “Strengthening with carbon fibres — Hungarian Experiences”, *Concrete Structures Journal*, Vol.1, 2000, pp. 52-60.
- Balázs, Gy. L., Borosnyói, A., Tassi, G. (2004), “Keep concrete attractive – towards the fib Symp. 23-25 May 2005 Budapest”, *Concrete Structures Journal* Vol. 5/2004, pp. 2-4.
- Balázs, Gy. L., Kovács, I. (2005), “Prestressing in Steel Fibre Reinforced Concrete. Proceedings”, *Proceedings of 1<sup>st</sup> Int. Central European Congress on Concrete Engineering*, 8-9 Sept. 2005, Graz, pp. 32-34.



- Barta, J., Wellner, P., Mihalek, T., Becze, J., Fodor, J. (2001), "One of the longest prestressed concrete railway bridges of Europe – executed by incremental launching method in Hungary", *Concrete Structures Journal*, Vol. 2, 2001, pp. 2-13.
- Becze, J. (2005), "The first extradosed bridge in Hungary", *Concrete Structures Journal*, Vol.6, 2005, pp. 52-55.
- Borosnyói, A., Balázs, Gy. L. (2002), "Prestressing provided by CFRP tendons", *Concrete Structures Journal*, Vol. 3, 2002, pp. 75-80.
- EN 196: 1987, : „Cement“, *European Norm*
- EN 197: 2000: „Methods of cement tests“, *European Norm*
- Földvári, G. (2002), "Reinforced concrete structures of the new National Theatre in Budapest", *Concrete Structures Journal*, Vol. 3, 2002, pp. 25-30.
- Friedel, P. M. (1897), „Sur un Chloro-aluminate de Calcium Hydraté se Maclant par Compression“, *Bulletin Soc. Franc. Minéral*, Vol 19, pp. 122-136.
- Hooton, R.D., Titherington, M.P. (2004), „Chloride resistance of high-performance concretes subjected to accelerated curing“, *Cement and Concrete Research*, 34, pp. 1561-1567.
- Hungarian Cement Association (2005), "The Hungarian cement industry in 2004", *Cement International*, Vol. 3, 4/2005, pp. 48-50.
- Kausay, T. (1967), „Characterization of concrete aggregates“, *PhD Thesis*, Bp. (in Hungarian)
- Kopecskó, K., Balázs, Gy. (2005), „Chloride Ion Binding of Cement Clinkers and Cements Influenced by Steam Curing“, *Proc. of the Int. fib Symp. on Structural Concrete and Time* (Eds: Di Mayo and Zega), 28-30 Sept., 2005, La Plata, Argentina, Vol. 1, pp. 147-154.
- Kovács, I., Balázs, Gy. L. (2004), "Structural performance of steel fibre reinforced concrete", *Book, Publishing Comp. of Budapest Univ. of Technology*, 2004, ISBN 963 420 822 3
- Kuzel, H.-J. (1966), „Röntgenuntersuchung im System  $3\text{CaO}\cdot\text{Al}_2\text{O}_3\cdot\text{CaSO}_4\cdot n\text{H}_2\text{O} - 3\text{CaO}\cdot\text{Al}_2\text{O}_3\cdot \text{CaCl}_2\cdot n\text{H}_2\text{O} - \text{H}_2\text{O}$ “, *Neues Jahrbuch Mineralog. Monatsh.*, pp. 193-200.
- Mihailich, Gy., Haviár, Gy. (1966), „Anfang des Betonbaus und die erste Konstruktionen in Ungarn“, *Academy Press*, Budapest (in Hungarian)
- Nemes, R., Józsa, Zs. (2006), „Strength of Lightweight Glass Aggregate Concrete“, *ASCE Journal of Materials in Civil Eng. (USA)* Sept./Oct. 2006, Vol. 18, Nr. 5, pp. 710-714.
- Popovics, S. (1955), „Numerical evaluation of grading of concrete aggregates“, *Acta Technika*, Budapest. Vol. XIII/1955, pp. 93-114. (in Hungarian)
- Szilvási, A. (2005), „Position of the concrete industry based on the increasing requirements“, *World of Construction*, pp. 51-52 (in Hungarian)
- Tóth, L. (2002), "The most up-to-date hydraulic engineering projects in Hungary", *Concrete Structures Journal*, Vol. 3, 2002, pp. 35-40.
- Varga, L. (2000), "Strengthening of bauxit concrete column by GFRP composite", *Research Reports of Dept. of Reinforced Concrete Structures*, Budapest 2000, pp. 299-308.
- Wellner, P., Mihalek, T. (2002), "Viaducts on the Hungarian-Slovenian railway line – Design and construction of the viaducts", *Concrete Structures Journal*, Vol. 3, 2002, pp. 7-10.
- Wellner, P., Mihalek, T., Barta, J. (2005), "Köröshegy viaduct — the biggest in size, prestressed concrete viaduct in Hungary", *Concrete Structures Journal*, V. 6, pp. 56-59.
- Zielinski, Sz., Zhuk, J. (1901), „Vergleichsversuche von Romanzement und der Überprüfung der praktischen Anwendung“, *Kilián Verlag*, Budapest, 1901, p. 33 (in Hungarian)
- Zielinski, Sz. (1909), „Die Erhärtung von Roman- und Portlandzement im Brei, Mörtel und Beton“, *Pátrai Press*, 2.52 (in Hungarian)
- Zsigovics, I., Balázs, Gy. L. (2002), "Self compacting concrete – some Hungarian experiences", *Concrete Structures Journal* Vol. 3, 2002, pp. 52-56.

## VIADUCT OF KŐRÖSHEGY ON MOTORWAY M7 IN HUNGARY, MOVEMENT – LIMITING THE ABUTMENTS FOR RECEIVING LONGITUDINAL TENSILE AND COMPRESSIVE FORCES

*Tamás Mihalek  
Hidépítő Co.  
Karikás F. u. 20  
1138 Budapest, Hungary*

### SUMMARY

The 1872 meter long, 23.8 meters wide continuous, prestressed concrete viaduct has been built on the motorway M7 in Hungary between Zamárdi and Balatonszárszó. The construction of the superstructure was performed starting from the two abutments. During the constructions period the half viaduct has to have a fix point to resist the movement – because all the bearings were movable on the piers. The completed parts of the viaduct was fixed to the abutments ensuring in this way the receipt of pier forces induced by longitudinal movements (changes of length resulting from temperature changes, shortenings resulting from creep and shrinkage).

### 1. SUPERSTRUCTURE

The viaduct rests on 18 supports. Its total length is 1872 meters with the following spans: (1 m)+60 m+95 m+13×120 m+95 m+60 m+(1 m) (Fig. 1). The axis of the viaduct, in plan view, lies in a circular curve with a radius of  $R=4000$  m. The longitudinal slope of the carriageway level is constant, 2.86%, the carriageway has a transverse dedination 2.5%. The superstructure is made of a single box, two-cell cross section with cantilevers of the slab on both sides.

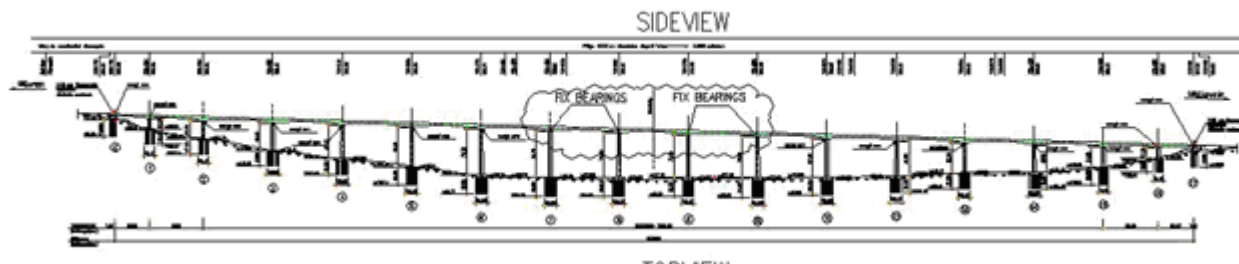


Fig. 1 Side view of the viaduct

The superstructure is constructed in sections. A 115 meters long balanced cantilever was made on each pier, with 5.0 meters long connecting sections at midspans between them (closing segment). The parts of a balanced cantilever: there was a 6.0 m long basic element (starting segment) above each pier to which, on both sides, a 9.5 m long segment-pair was connected. The remaining segment-pairs were 11.25-11.25 m long.

## 2. STRUCTURAL SYSTEMS

### 2.1 Construction stages

The superstructure was built as a balanced cantilever, progressing in two directions from the starting segment over the pier. Two 11.25 meters long segments were made on each end of the balanced cantilever, poured into the hanging formworks, which were held by an auxiliary steel structure (ASS) leaning on the two ends of the balanced cantilever being built (A and B supports). The third (C) support leant on the cantilever-end of the already completed part of the viaduct (Fig. 2).

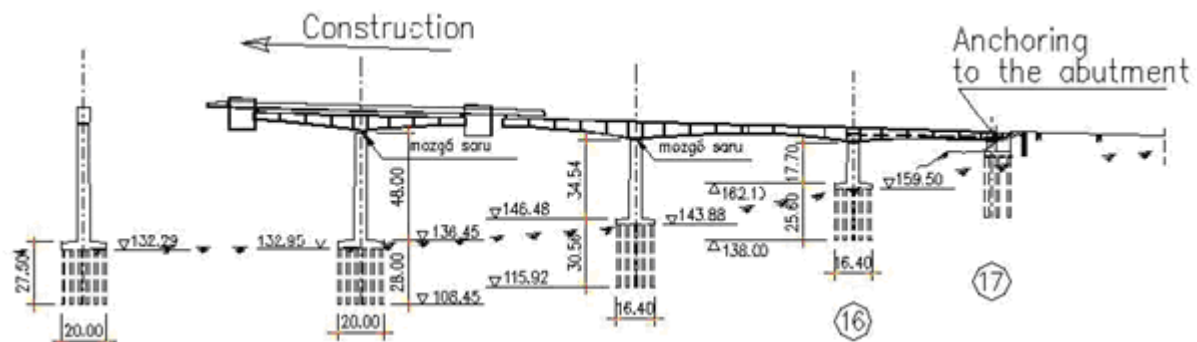


Fig. 2 Side view of the construction

The starting segment was made on two spherical cap bridge bearings. The balanced cantilever can rotate and slip on the bearings. Its stability was ensured by the ASS (Advancing Shoring System). The completed balanced cantilever was connected (closed) backwards, to the completed viaduct part, so longer and longer continuous girder parts with more and more supports were made.

### 2.2 Final state

Finally, the two half-viaducts with 9-9 supports, were closed in the middle to each other, and the continuous superstructure with 18 supports gets configured.

During service, the longitudinal static equilibrium of the bridge was ensured, and horizontal forces are received by the fix bearings built in on the 4 central piers.

## 3. FIXING THE HALF BRIDGE

The construction of the superstructure is performed starting from the two abutments. The completed parts of the viaduct were fixed to the abutments, ensuring in this way the receipt of pier forces induced by longitudinal movements (changes of length resulting from temperature changes, shortenings resulting from creep and shrinkage) (Fig. 3).

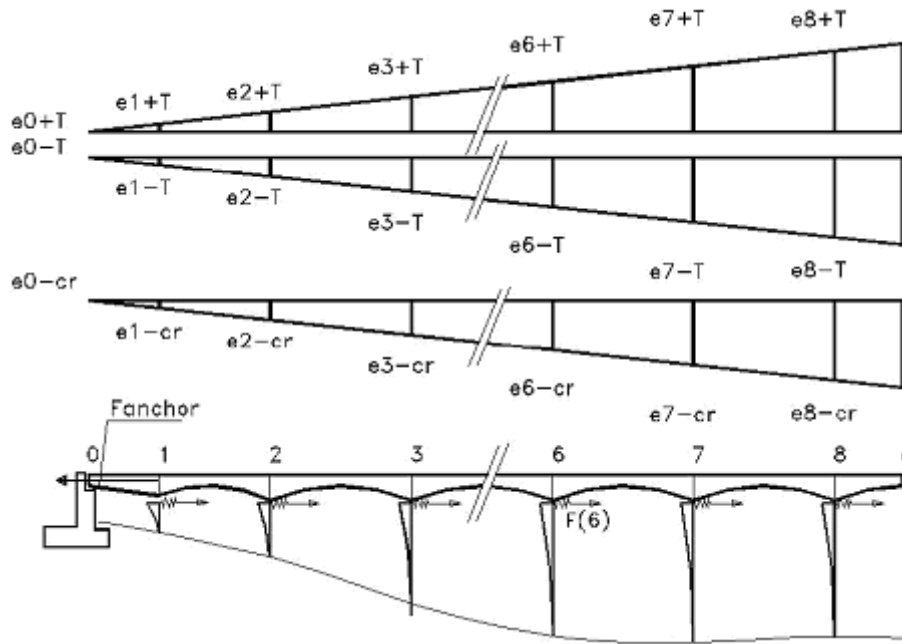


Fig. 3 Effects on the half bridge

### 3.1 Part of the anchoring

For fixing, 2 + 2 pieces of tendons consisting of 19×0,6” strands led inside the box girder were used. One end of the tendon was anchored inside the superstructure, in the crossgirders (diaphragm walls) of the starting segments over piers #16 and #1. The other end of the tendon was anchored in anchoring devices concreted into the thickened (strengthened) section of the retaining walls of the abutments.

Reinforced elastomeric bearings (Neoprene) were built in between the superstructure end and the abutment-wall for ensuring flexible horizontal supporting and occasional rotations. The Neoprene bearings (3 – 3 pieces under the fixing tendons) were placed on auxiliary bearing frames, and were built in vertical plane, with the contingent gap filled in with steel plates. These plates were underlayed in such a way that, when the value of the pier forces exceeds the force in the fixing tendons, during the further elongation of the tendons (accompanied with the increase of the distance of the superstructure from the abutment) the plates, falling out, give a warning that the abutment is receiving a non-admissible force, and it is necessary to decrease the force in the tendons (releasing) (Fig. 4).

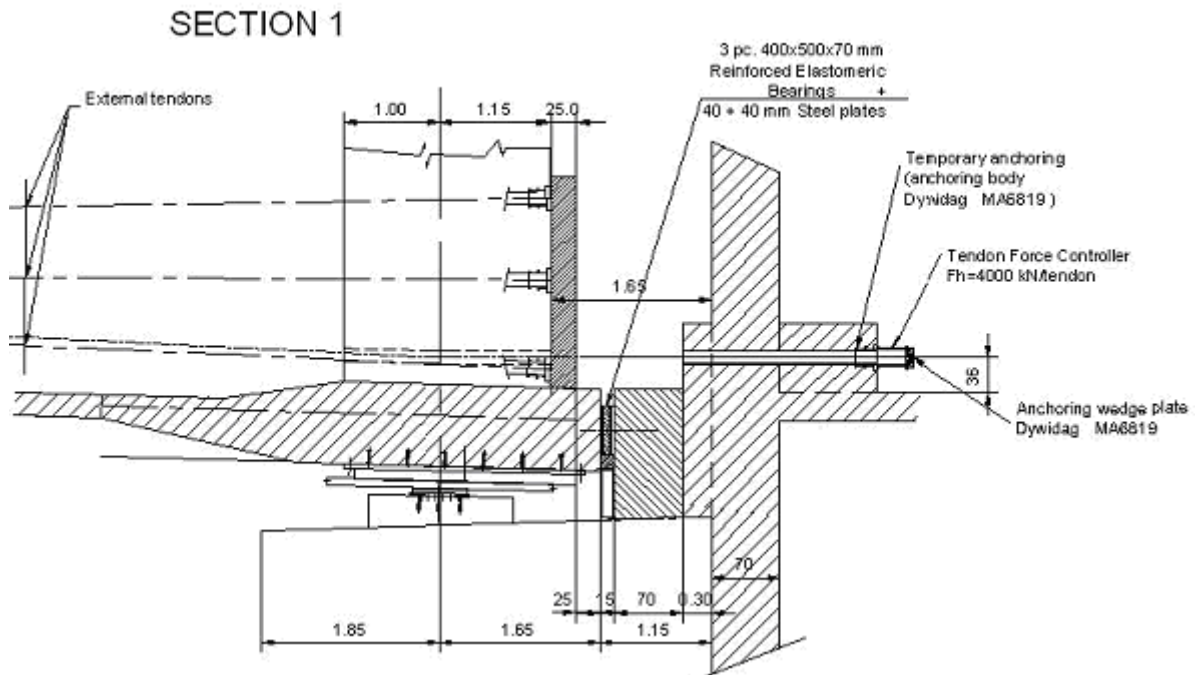


Fig.4 Anchoring – Section 1

### 3.2 Prestressing forces

The prestressing tendons consist of Fp 150/1770 quality strands. Their length is 62 meters. See the characteristics of the anchoring tendons in Tab. 1:

Tab. 1 Characteristics of the anchoring tendons

Applied prestressing force (before anchoring)	$F_{\text{anchor}} = 2800 \text{ kN}$
Calculated elongation of tendon	324 mm
Compression of the neoprene bearing	2 mm
Compression of the superstructure part due to prestressing	2 mm
Tendon elongation, total	328 mm
Tendon force – after wedging	2730 kN/tendon

The tendons were anchored in MA6819 anchoring devices (made by Dywidag SI) concreted into the anchoring block formed in the inner side of the retaining wall of the abutment. For checking the value of the tensioning force in the tendons, force-measuring cylinders were built in between the anchoring head and the anchoring device, at two - two tendons per abutment, whose electrical signals allow us to continuously check the value of the tensioning force in the tendon.

### 3.3 Increasing of the anchoring forces

The anchored half-viaduct will be longer and longer during construction connecting the completed balanced cantilevers to it. Due to these connections, the longitudinal movements of the superstructure (shortening – elongation) will affect more and more piers and, through the bearings, the changes in length will cause the displacement of more and more pier caps. And the displacement of the pier caps can only come about with the resistance of the piers, namely,

the resistance value of the connected piers gets higher and higher. Taking the time schedule of construction into consideration, we plotted the cumulative intensity of the resistance of piers which is shown in (Fig 5.)

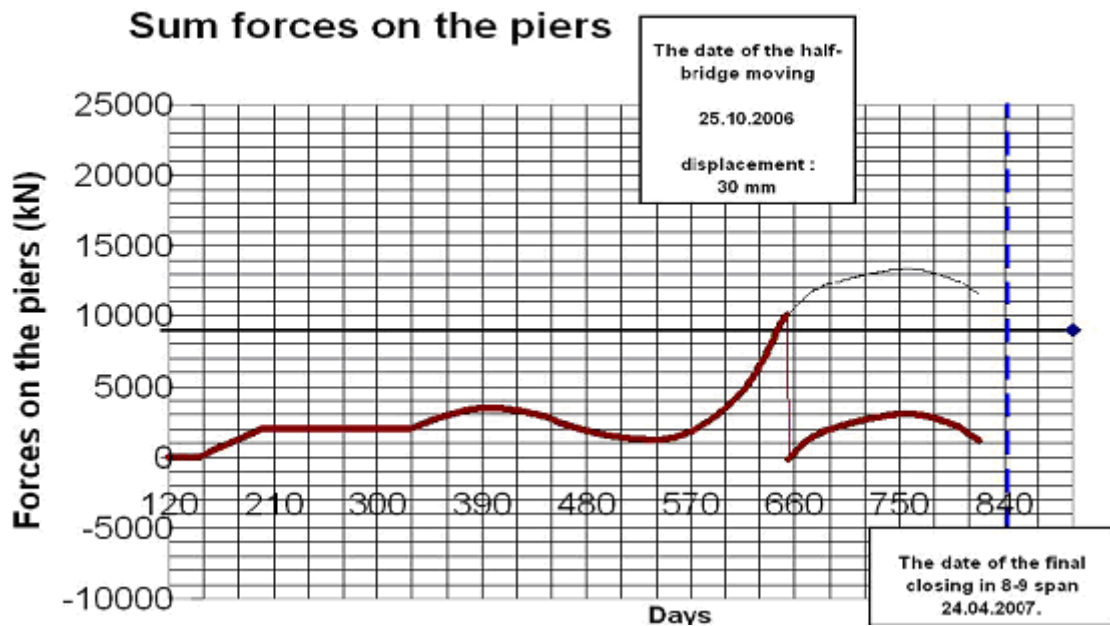


Fig. 5 Cumulated resistance of the piers

The diagram shows the maximum value of force ( $F_{\text{limit-of-abutment}} = 9000 \text{ kN/abutment}$ ) which the foundation (piles) of the abutment can bear (assuming also that the backfill in full width has also been completed). It can be seen from the diagram that at about the  $\frac{3}{4}$  of the construction time (between 600 and 630 days) that is, in September – October 2006, the resistance of piers (the force pulling the abutment) gradually reached, then exceeded the  $F_{\text{limit-of-abutment}} = 9000 \text{ kN}$  value (the piers more and more incline towards the abutment - they were drawn as a bow).

### 3.4 Reduction of the drag-off forces

In order to keep the tensile force on the abutments under the above described limit values, the pier caps were displaced artificially towards the centre of the viaduct (their "updraw" is reduced).

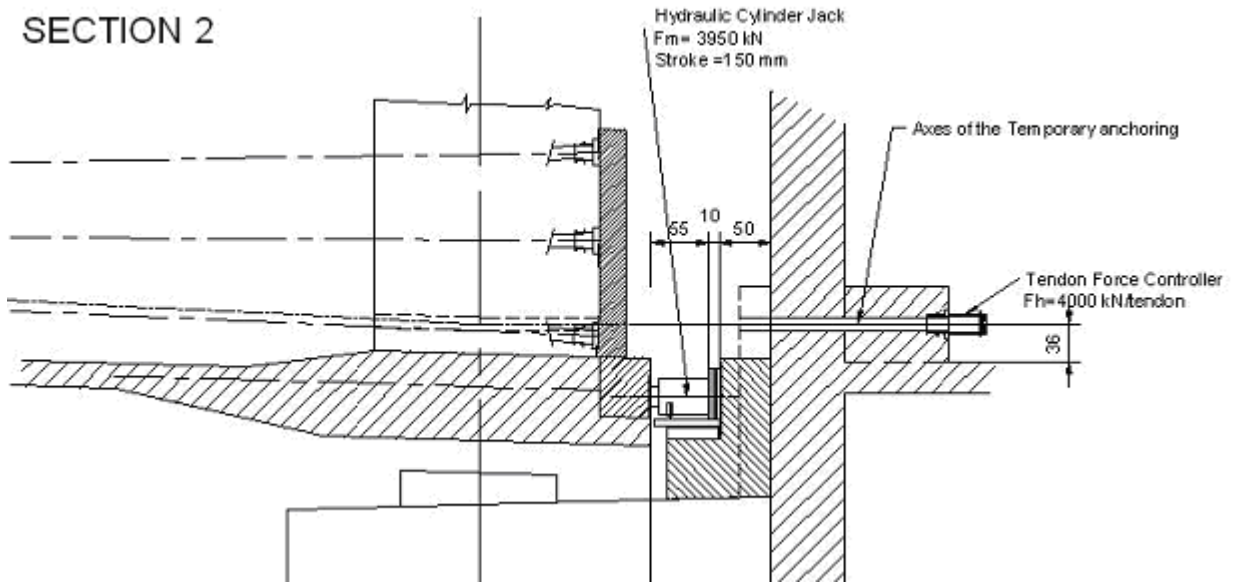


Fig. 6 Shifting the Superstructure by hydraulic jacks

This is reached by shifting the half-viaduct that is, the superstructure is pushed with the help of hydraulic jacks placed between the abutment and the end of the half-viaduct, then, after it has been moved, the increased gap between the abutment and the superstructure is filled up again, and the jacks were removed (Fig. 6). Of course, this shifting elongates the fixing tendons and also increases the tensioning force.

The enclosed diagram shows that, assuming different bearing frictions, to what extent the cumulative forces could increase – the date of exceeding the limit value would not change. On the basis of the evaluation of the figures, it can be seen that the shifting had to be taken place before the date described above (September 2006). The designed value of the shifting is 42 mm. The above operation was performed on both half-viaducts successfully.

The effective value of the shifting was 30 and 28 mm at the abutments, and so we could reach the appropriate value of the dragging forces and the reduction of the pier-forces (Fig. 7).



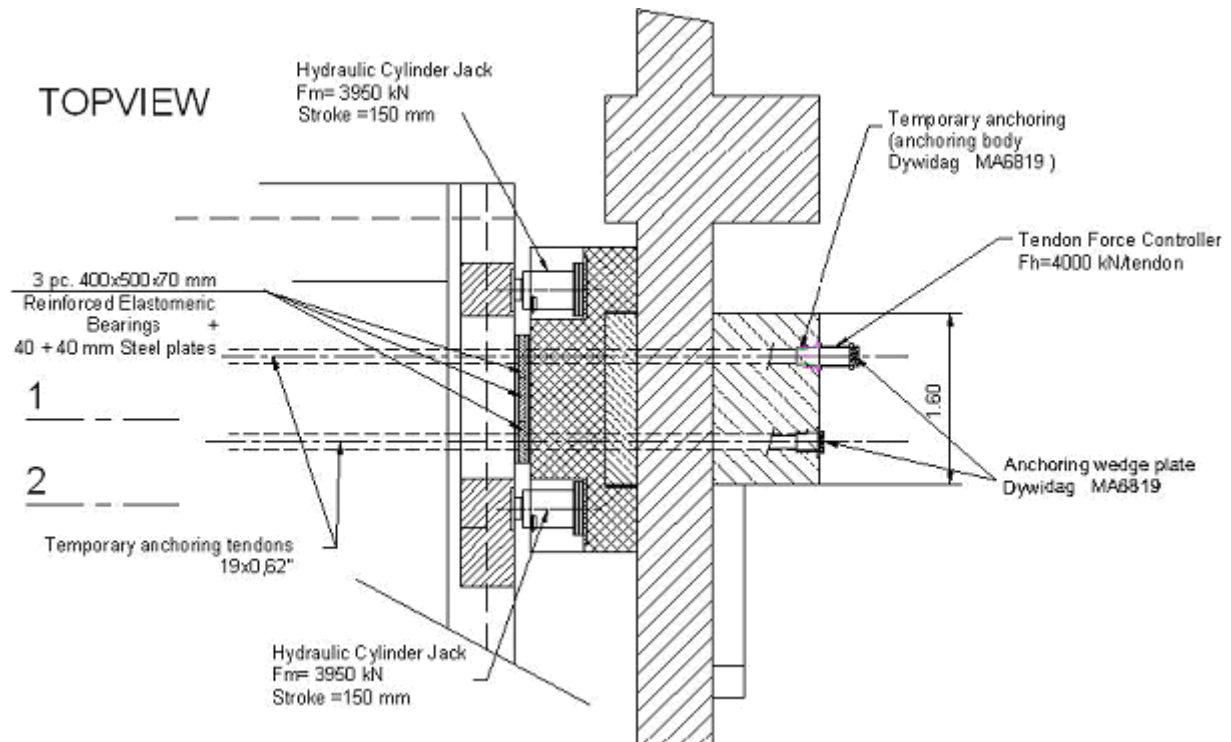


Fig. 7 Shifting of the superstructure by hydraulic jacks

#### 4. DISMANTLING OF THE ANCHORAGE

After the completion of the two half viaduct – the two parts of the superstructure has to be closed to each other. Before the construction of the final closing segment – the anchoring system at the two abutments have to be dismantled – to ensure the possibility of the free movement on both half viaduct. The fix point of the viaduct was in this time at the middle of the bridge – after making temporary press/tensile connection between the ends of the two halvesuperstructure. The dismantling of the anchorage was made by cutting the wires in the strands by the heat of the acetylene/oxygen welding/cutting equipment. The anchoring force was reduced slowly, the tendon was cutting in pieces, step by step.

#### REFERENCES

- Barta, J., Wellner, P., Mihalek, T., Becze, J., Fodor, J. (2001), „Viaducts on the Hungarian-Slovenian Railway Line – Design and Construction of the viaducts“ *Concrete Structures* Vol.2, 2001, pp 2-14.
- DSI – Dywidag System International: Dywidag bonded Post Tension System – Multiplane Anchorage MA (1998)
- Wellner, P., Mihalek, T. (2002), “One of the Longest Prestressed Concrete Railway Bridges of Europe”, *Concrete Structures* Vol.3, 2002, pp 7-10.
- Wellner, P., Mihalek, T., Barta, J. (2005), “Kőröshegy Viaduct – The biggest in size, Prestressed, Concrete Bridge In Hungary”, *Concrete Structures* Vol.6, 2005, pp 56-59.
- Wellner, P., Mátyássy, L., Mihalek, T., Becze, J., Barta, J. (2007), “Viaduct Of Kőröshegy, The largest Prestressed, Concrete Viaduct in Hungary – Design and Construction”, *Concrete Structures* Vol. 8, 2007.





## **VIADUCT OF KŐRÖSHEGY ON MOTORWAY M7 IN HUNGARY, VIADUCT WITH TWO TECHNOLOGIES**

*János Magyar  
Hídépítő Co.  
Karikás Frigyes u. 20  
1138 Budapest, Hungary*

### **SUMMARY**

On the section of motorway M7 between Zamárdi – Balatonszárszó, at Kőröshegy one of the longest road viaducts of Middle-Europe has been constructed. This is an engineer creation of outstanding importance from a number of points of views (top dimensions, completion deadline, constructing-mounting technologies, etc.). The superstructure of 17 spans (in sequence: 60 m, 95 m, 13x120 m, 95 m, 60 m) made of prestressed reinforced concrete has a main girder with two-cells box cross-section, total length of 1872 m, width of 23.8 m leading toward the State Border with a longitudinal gradient of 2.86 %, in a horizontal curve with a radius of 2000 m. At start of the superstructure construction, the blocks were made in formwork wagons suspended on an advancing auxiliary bridge using cast in situ free cantilever technology.

After completion of the first 7 bridge-branch the topographic conditions became yet strongly more favourable and allowed to change for a cantilever erection technology, by transformation of the auxiliary structure, however, kept it further on. By this method the prefabrication of the blocks could be rendered independent of the operations carried out on the bridge, the construction was significantly accelerated and for deadline reserves were created the fulfilment of the expected completion.

### **1. THE AUXILIARY STRUCTURE (Fig. 1)**

The first 7 bridge-branches of the superstructure were made in formwork wagons suspended on an advancing auxiliary structure. The auxiliary structure, having its "maiden name": Peiniger RöRo Advancing Shoring System (ASS), was manufactured according to the demands drawn up by Hídépítő Co. and on the bases of the designs and calculations of Saul Ingenieure GmbH. Further, this complicated structure will be referred simply to as auxiliary structure. The material of the auxiliary structure is steel; its main elements are the two main girders in a distance of 13,500 mm of each other and advancing parallel to the longitudinal axis of the viaduct. The width of the main girders is 2,500 mm, their height is 4,100 mm, their length is 15,732 mm with including the length of the nose is 18,900 m. The cross-section of the main girders is varying along their length. Onto these are suspended the formwork wagons, they are also consisted of two pieces, their outline dimensions are: length of 12,000 mm, width of 28,000 mm and height of 23,595 mm (these parameters are approximately identical with those of an 8-storey block-house) the formwork wagons can be opened since only in this state can they pass over the piers.

On the track mounted onto the inner side of the main girders work 2 cranes with overhead trolleys having bearing capacity of 2x8 t. On the outer side of the main girders was carried out the moving of the persons and the concrete was also forwarded here.



Fig. 1 The auxiliary structure

On the lower chord member of the crane-track move 2 auxiliary scaffolds, the so-called stressing platforms. All technological operations related to the stressing (cable threading, stressing, grouting) can be relatively simply carried out from here. The auxiliary structure is connected to the reinforced concrete superstructure by means of 3 main supports. There are beside the main supports also auxiliary supports which are activated only during the movement of the auxiliary structure. Moving and transporting the structure was a fairly complicated task, more than 150 hydraulic working cylinders must have been operated in harmony within one structure.

The total weight of the structure equals to 1540 t. The structure seems to be complicated, and really it is. Nevertheless, this is necessary since it has to fulfil the following functions in the course of the superstructure construction:

- it holds the weight of the formwork wagons and the weight of fresh concrete,
- it ensures the forward of the materials into the formwork wagons,
- it allows the access to the working area,
- it leads the formwork wagons from the completed balance to the next starting segment without the need of their disassembly,
- due to its own weight it stabilizes the reinforced concrete bridge-balance.

## 2. CONSTRUCTION OF THE SUPERSTRUCTURE (Fig. 2)

### 2.1 Cast in situ free cantilever technology, however, in an other way a little bit

The reinforced concrete structural works of the superstructure were commenced at early May 2005, from the direction of the two abutments and were finished exactly after 2 years on the 9<sup>th</sup> May 2007, when the last closing segment was stressed together. The essence of this technology is that on the two sides of the completed and fixed starting segments were manufactured simultaneously for two elements, each in a length of 11.25 m, fixed by prestressing. Later, this procedure was repeated four times on the right as well as on the left sides, on this way a half of a span was constructed.

This half span of the viaduct weighting 6500 tons was kept in balance by the auxiliary structure, weighting 1540 tons, on the surface of 2 sq. m of the bearings.



Fig. 2 Construction of the superstructure

The half of the span, by manufacturing a closing block in the yet outstanding length of 5 m, was connected to the cantilever sticking forward from the already completed other half of the span, which became by this method one unity, namely a continuous superstructure with more supports. The critical point of the superstructure construction was the exact regulation of the construction shape, in order to give its final form. By the values of adjustment had to be taken into consideration all the changes that might occur in the later phases. The power impulses of the later phases were caused by the movements of the mounting bridge, of the prestressing, of the shrinkage, of the long term deformations and of the temperature changes.

At the end of each phase the pre-calculated values must have been checked up and in many cases corrections had to be applied before next step.

Each of the balance-branches were constructed as independent unities in relation to their own basis-line and they were they tilted to the correct position just at the closure of the arm. In order to evaluate the effects of the temperature, heat-sensors were installed into the structure and their measurements were recorded in each hour by a computer.

## 2.2 The cycle of construction in the case of cast in situ free cantilever method

Fundamentally, the construction of the pairs of blocks was carried out in two phases. In Phase I. the lower slab and the three ribs were prepared, in Phase II. the upper slab in its entire width was prepared. The Phase I. became after hardening and prestressing self-supported. The entire cycle included the following main working processes:

- adjustment of the formwork wagons both vertically and horizontally,
- amplification of the bottom shuttering according to the actual size, preparation of the surface,
- placing the reinforcement of Phase I., placing the tubes of the cables,
- preparing the inner and the face formworks, preparation for concrete cast,
- placing the pairs of Ø36 DSI bars,
- concrete cast of Phase I. and hardening during 36 hours (C45/55 kk, f50, vz4),
- stressing (series DSI MA),
- removing formwork of phase I.,
- lowering by Ø36 DSI bars,

- preparing formwork of phase II.,
- reinforcement for upper slab and placing the tubes of the cables,
- concrete cast of phase II. and hardening,
- prestressing
- moving ASS to the manufacturing position of the next pairs of the elements.

Generally, the cycle period of the segments manufactured in this way came to 14 days and even among the most favourable conditions was at least 10 days.

Concreting in two phases combined with two hardenings consumed too much time within one cycle. The idea of applying cantilever erection technology (stressing in one phase, most of the manufacturing operations on the surface and not in formwork wagons being suspended in a height of 60 to 80 m) raised up. Now this seemed to be applicable because the superstructure construction already leaved the sides of the steep shores and was continued above gently slopes with, almost horizontal surfaces.

### 3. CHANGE OF TECHNOLOGY (Fig. 3)

At the beginning of the year 2006 the leaders already saw that although the speed of a cycle period of 10 or 12 or 14 days, constructing a 45 m long b superstructure with a width of 23.20 m (1044 sq. m), is very quick but in no way enough for keeping the completion deadline.

Nonetheless, the execution was still in a stage where, in case of changing the technology, a shorter cycle period could it the available time. Only that had to be found, how should work the new technology, what cycle period could be awaited from it, how much time takes the acquisition of, and commissioning the new devices, finally, but not insignificantly: what will be the costs of these.

The decision was made: the new technology should be the cantilever erection but with keeping the most part of the auxiliary structure. By this way a cycle period of 7 days could be ensured on long-range. The change of technology will take maximum 175 days, however, this must be limited as short as possible, let's say to 1.5 months! Can this be possible? One must not forget, all these should be carried out in a height of 60 to 70 m! Though to the first moment, or even to the second one, this seemed to be impossible and on the contrary it succeeded. The transformation was finished in 41 days. However, this required special conditions:

- there was no need for new working drawings since basically the segments were manufactured with the same dimensions, with the only difference: not in the formwork wagons rather on the surface,
- nor the prestressing designs had to be changed,
- the "old" auxiliary structure could be applied to the new technology with "minimum" modifications,
- in the course of the transformation, only girders and equipments should have been mounted and dismantled with the dimensions to allow to use of mobilecrane with bearing capacity of 500 t.



Fig. 3 Change of technology

#### 4. THE NEW TECHNOLOGY (Figs. 4 and 5)

##### 4.1 The mode of construction and functions of the "old-new" auxiliary structure

At first sight the mounting bridge did not change but that is not true. The main girders and the running bridge crane, walking paths, transporting cantilevers remained unchanged but:

- The formwork wagon from the direction of the nose has been dismantled and two smaller ones were built from it, for the manufacture of the 1.5 m long monolithic segments,
- The rear formwork wagon has been taken smaller; it was prepared later the closing blocks between the viaduct branches. It has also another important function, to keep thy system in balance by its dead load.
- Two new platforms are installed on top of the main girders and the concrete casting arms were on them placed and also the hauling devices of the new technology:

• lifting presses type HP 200	4 pieces
• hydraulic pump	1 piece
• control panel	1 piece
• cable reversing device	4 pieces
• cable drum	4 pieces.

The "old-new" auxiliary structure, besides keeping the old functions too, received a new mission: lifting to place, exactly adjusting the segments manufactured on the surface and bearing their charge until the monolithic section of the wet joint has been made and the actual segments have been prestressed to the viaduct branch being in progress of construction.



Fig. 4 The new technology



Fig. 5 The new technology

#### **4.2 Cantilever erection technology, however, again in an other way a little bit**

The main change in the new, cantilever erection technology was that the bridge segments were manufactured on the terrain over this prefabricated, shorter by 1.5 m and after their hauling a „wet joint” of 1.5 m will be prepared on site.

The prefabrication of the elements was carried out exactly at the vertically projected trace of their final place and position. The new technology became equal to the expectations, and very soon, after the difficulties of beginning, there was developed the cycle period of seven days that could be later systematically reduced for six days.

The most exciting activity of the new technology was to lift the elements to place and to fix them there. In each cycle the hauling of the pairs of blocks took place according to the following scenario:



- Positioning the auxiliary structure, that means essentially to change the stand over the segment actually to be hauled, with other words that is the same as it was in the former technology, following stressing, to change the stand from one segment over the other one;
- Positioning the lifting platform under continuous geodetic control. It is expedient to exactly position the lifting platform that during the lifting operation should not be necessary to move it together with the load either in transversal or in longitudinal direction, even despite of the fact that the system allows this: in transversal direction 600 mm, in longitudinal direction 1200 mm would have been possible.
- Parallel to the above written adjustments, "underneath" the spreaders were pressed to the upper slab of the segment to be lifted. Each of the spreaders had to be pressed to the upper slab by means of 24 DSI bars, each with a force of 350 kN.
- According to the position of the spreaders underneath, the lifting jacks located on the lifting platform were measured one by one, and slipped on a teflon table to the exact position.
- When everything was on its exact place, the lowering of the lifting cables with the same speed as in the course of lifting started. The duration was expected to be 2.5 to 3 hours, depending on the height.

Some sentences have to be written here about the lifting cables since they differed from the usual ones. One block (its weight reached 670,000 kg) was lifted by 4 cables, each consisted of 14 strands. The characteristics of the strands were:  $A_p = 223 \text{ mm}^2$ ,  $R_m = 1700 \text{ N/mm}^2$ , so-called DYFORM-strands to be purchased from BRIDON, England. The flattened attribute of DYFORM-strand is very important because so it contacted the anchoring wedges on a much larger surface, making possible a great number of reuse. By this way, there was no need to replace the strands till the end of the lifting period, even later they could be used as lifting strands.

- When the cables arrived down, they were connected by transmission of the Banchorages, to the spreaders. After being made the connection, the same initial force had to be obtained in each strand that later, during the lifting operation all the strands should get the same load.
- Following the pre-loading the loads of the two blocks were symmetrically taken, in more steps, by the lifting jacks (that means the lifting was started) until the segments were removed upwards from the formworks.
- After this, the lifting operation was stopped and checked whether the load distribution of the segments was the same as designed or not. In case of deviation (the block was tilted, in one of the jacks the pressure was greater), the block had to be balanced. For this purpose the great cubes of concrete other materials were appropriate.
- After balancing the lifting operation were really begun. Although the equipment was suitable to lift both blocks simultaneously, because of safety reasons, first the rear segment was lifted to place and only then the front one. The position of the segment was continuously checked during the lifting (perhaps being tilted) and the oil pressure was also permanently controlled. In case of deviation in any of the parameters, the segment was again positioned and only then continued the lifting operation.
- When both segments have arrived the final height, newer measurements were carried out for providing a base to the exact adjustments and after that they were fixed to the already completed viaduct branch.
- Following the fixing, the transformed small formwork wagons were placed on the gap of 1.5 m in order to make possible the construction of the wet joint.



- When this connection reached the strength for stressing, the blocks were stressed both to each other and to the already completed bridge-branch. The cable leadings and the stressing forces were maintained in conformity with the former technology.

## **5. CONCLUSION**

Two technologies were applied for the construction of a large engineer structure in a manner, where the technological auxiliary structures were kept and transformed only in a small extent so, that there was no need for re-designing the superstructure and the viaduct could be taken over before the expected completion deadline.

The success is owing to the experienced and in the same time also well qualified technical leaders of Hídépítő Co., nevertheless, also to the physical staff, very well-trained in the construction technologies (cast in situ free cantilever, cantilever erection, incremental launching) of reinforced bridges and committed to bridge construction.

## DESIGN OF THE PIER OF THE KŐRÖSHEGY VIADUCT

*András Nagy  
Pont-TERV Co.  
Budapest, 1119 Thán Károly u. 3-5  
Hungary*

### SUMMARY

The Kőröshegy viaduct is situated on the Balaton section of the M7 motorway. The viaduct is 1872 long and it has 16 piers. The height of the piers varies between 17.70 and 79 m. In close cooperation with the Contractor "Hídépítő", Pont-TERV Ltd has prepared the pier plans, which allowed a quick and simple building technology. For the climbing formwork the reinforcement and diaphragm were prefabricated and lifted with cranes. For the pier cap we used prefabricated bridge girders for formwork.

### 1. PRINCIPLES OF THE DESIGN

The Kőröshegy viaduct is the longest viaduct in Hungary (Fig. 1). Here the motorway crosses a flat valley. During the design, we had to take poor soil conditions and high ground water level into account. The main guideline of the design was to minimize the pier settlements. Due to the short construction time prefabricated reinforcement elements were used.

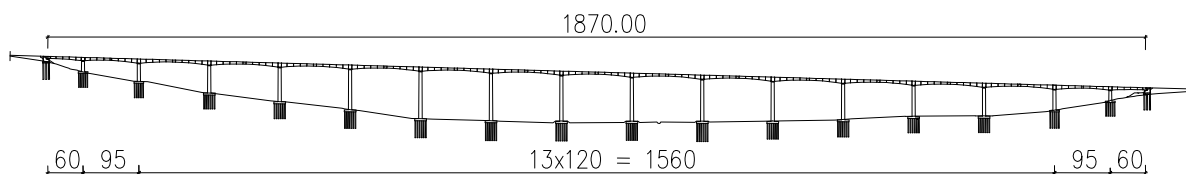


Fig. 1 General layout of the Kőröshegy viaduct

For the structural analysis of the viaduct, several finite element models and programs were used. The interaction of the superstructure, the 16 piers, the aboutment, and the foundations were investigated with a 3D beam program. The loads for the more detailed models were taken from this model.

### 2. PILES AND PILE CAPS

The most important task was to choose the suitable foundation method. The rigid PC box girder superstructure is sensitive to the differences of the piers settlements, so during the construction a settlement monitoring system was installed. Finally  $\phi$  1200 mm diameter bored reinforced concrete piles were applied. In order to take the proper loads and soil conditions into account, the pile caps had 3 different sizes (Figs. 2 and 3).

4 pieces	16.60 * 22.20 * 2.5m with	35 piles
6 pieces	20.00 * 23.60 * 3.5m with	42 piles
6 pieces	20.00 * 27.20 * 3.5m with	48 piles

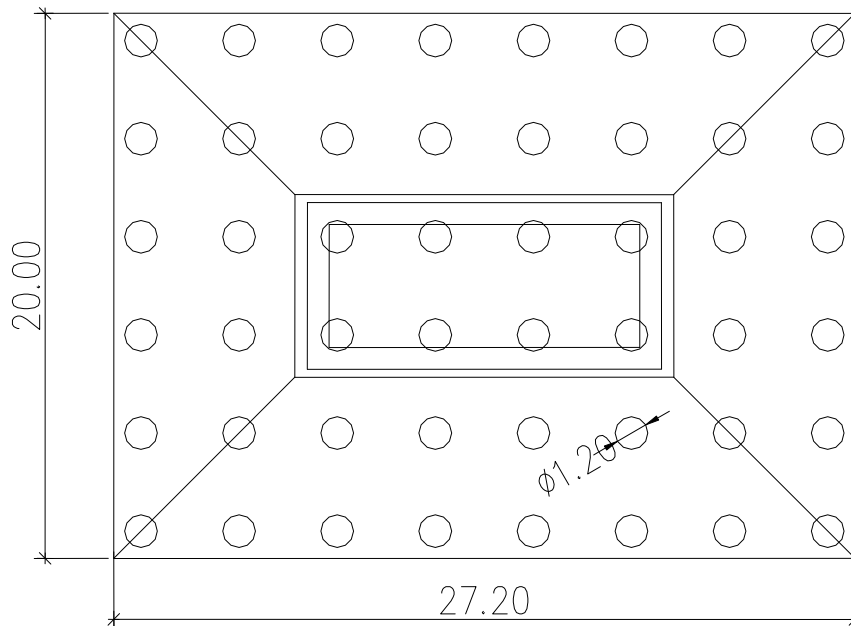


Fig. 2 The plan of the pile cap



Fig. 3 Bored piles and the sheeting for the pile cap

### 3. WALLS AND DIAPHRAGMS

The piers have two cells box cross section, stiffened by horizontal reinforced concrete diaphragms in every 20 meters (Figs. 4 and 5) The contractor has built the piers with climbing formwork. The detailed plans of the piers fit for this technology. Every pier has same geometry from the top to the bottom, so type-plans could be used for the 5m long sections. The thickness of the walls at the starting sections are 80 cm, after it 45 cm and 35 cm.

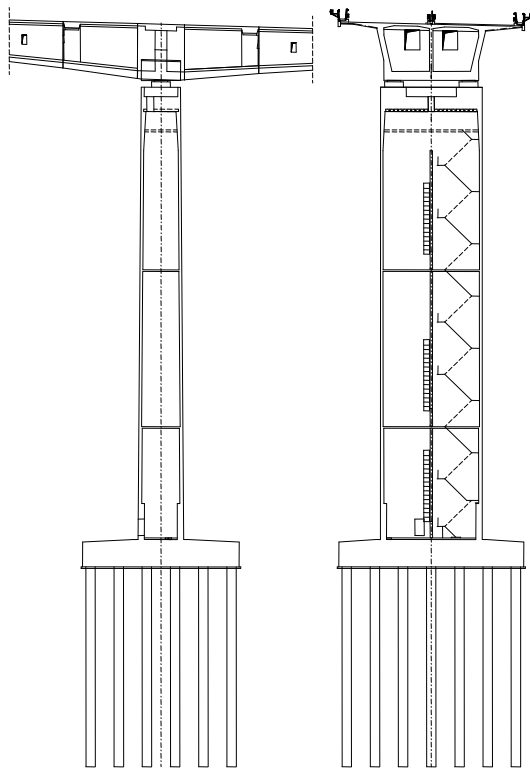


Fig. 4 General plan of the pier



Fig. 5 Piers under construction

The prefabricated wall armatures were assembled on the ground, and lifted by cranes into the formwork. (Figs. 6, 7 and 8) The connections of the armatures were mounted in the formwork.

For the statical analysis of the walls, beam and shell FEM models were made. At the dimensioning of the piers, the biggest effect had the wind load. The bridge is in a 4000 m horizontal curve, so each pier stands in different angle for a certain wind direction. There were many wind directions calculated with  $5^\circ$  steps to find the governing wind load case. The 160 m long auxiliary bridge and the formwork wagons had also big surfaces exposed to wind. Under the superstructure erection, they also have generated big wind loads with 80 m arm of force, and big bending moments in the bottom of the piers due to that.





Fig. 6 Lifting of the prefabricated reinforcement into the formwork

The stiffening diaphragms were made in the ground and lifted in to the right place. The diaphragm was assembled from two lifting unit. On the top of the wall the diaphragms are supported on the inserted HEB girders. After concreting the joint, the good connection between the walls and diaphragms is very important.



Fig. 7 Reinforcement of the diaphragm



Fig. 8 Lifting of the diaphragm

#### 4. PIER CAP BEAM

The most interesting problem was the detailing of the pier cap beam (Figs. 9, 10 and 11). On the top of the piers two big bearings were placed with 65 0000 kN load carrying capacity each. The pier cap has to distribute this big force along the walls. The dimensioning of the pier cap beam was investigated with 3D solid FEM elements. The shuttering of the 3.1 m high pier cap beam in 80 m height is also a difficult engineering problem. Prefabricated FP bridge beams were used as the formwork. With this solution, heavy scaffolding was not needed.



Fig. 9 Prefabricated bridge beams as a formwork for the pier cap beam



Fig. 10 Completed pier cap beam



Fig. 11 Bearing bottom plate in the formwork

The bearing plates have to be placed precisely, because the superstructure was built on it and the position of the bearing determined the end position of the superstructure. The first section of the superstructure was erected on the pier, and it is the support of the auxiliary bridge. And important question was the stability of the starting section. The pier caps and the starting section were stressed together with DYWIDAG bars.



## 5. AUXILIARY ELEMENTS

During the construction many auxiliary structures were needed. Next to every pier were cranes for lifting (Fig. 12). The tallest was 100 m high. Steel anchor structures were put into the pile cap, and the towers were stressed to the walls. (Fig. 12)

For the maintenance works, staircases and mobile lifting devices were installed in each pier (Fig. 13).

In the 6. and 10. piers elevators were mounted.



Fig. 12 Pier 7. with 100 m tall crane



Fig. 13 Staircase in the pier

## 6. CONCLUSIONS

The poor soil conditions, the tall pier and the heavy superstructures were required more precise statical models as usually. From point of view of the piers the wind loads were governing load case both on the erection and the final stages. The pier plans and the building technology allowed a short construction period. The erection of the piers started in October 2004, and finished November 2006. During the two years 16 piers were built with total length of 882 m, consisting of 203 segments. In August 2007, the viaduct was opened to the traffic.

## **BRIDGES UTILIZING HIGH STRENGTH CONCRETE**

*Jiri Strasky, Ivailo Terzijski, Radim Necas*

*Brno University of Technology, Faculty of Civil Engineering, Czech Republic*

*662 37 Brno, Veveri 95, [strasky.j@fce.vutbr.cz](mailto:strasky.j@fce.vutbr.cz), [terzijski.i@fce.vutbr.cz](mailto:terzijski.i@fce.vutbr.cz), [necas.r@fce.vutbr.cz](mailto:necas.r@fce.vutbr.cz)*

### **SUMMARY**

Possibilities of structures utilizing high strength concrete are shown on examples of several highway and pedestrian bridges recently built in the Czech Republic. These structures are discussed from the point of view of their architectural and structural solutions. Also a process of their erection is presented.

### **1. INTRODUCTION**

Recently we have participated in a design and construction of several bridges that utilize high strength concrete (HSC). The main goal in the actual development of HSC was simplicity and economy. Therefore ordinary concrete components without silicafume or similar microfiller were applied. Cement was OPC CEM I 42.5 R in all cases. Maximum of three fractions of aggregate were used. The coarse one was in the most cases basalt, which helps to reach not only the needed strength but also a higher modulus of elasticity. Good common workability and extended pumpability (in time) were guaranteed by careful selection of applied additives/plasticizers. In all cases plasticizers on polycarboxylate or polycarboxylate-ether basis (PCE) were applied. A special demand for limited shrinkage was solved by adding of shrinkage reducer on the basis of multivalent alcohols. High strength concrete was mainly used in structures that are primarily stressed by compression stresses. The possibilities of HSC are presented on the following examples of bridges.

### **2. BURIED BRIDGE ON THE FREEWAY D1 FORMED BY PRECAST GIRDERS**

The freeway D1 Vyskov–Kromeriz close to a village of Brnenske Ivanovice required a construction of a bridge that crosses local creek, rural road and bio-corridor. Since in the place of the crossing the freeway's fill has a depth of 14 m, an over-buried structure represented an optimum solution. Due to very poor geotechnical conditions that were characterized by large long-term deformations of the soil, it was necessary to design a structure that is not sensitive to the differential settlements of the abutments and piers. Therefore, instead of a common continuous three span slab structure, a statically determined structure assembled of precast girders from a high strength concrete of a relatively long span of 34.80 m was designed (Strasky, Terzijski, Konecny, Svadbik, Racansky, 2006) (Fig. 1).

The deck is assembled of precast girders and a composite slab (Fig. 2). At the abutments of the girders are stiffened by diaphragms that also form the end walls. The girders are supported by neoprene pads placed on low abutments. The abutments are founded on a reinforced earth that is founded on the soil which characteristics were improved by gravel piles. The 4.5 m deep fill above the deck is formed by polystyrene. The precast girders are designed from a high strength concrete developed by SKANSKA in collaboration with the Brno University of Technology. Two experimental girders were designed from concrete of the strength class C90/105, all remaining girders from concrete of the strength class C60/75; the composite slab was designed from concrete of the strength class C55/67. Actual average concrete cube



strength after 28 days of the experimental girders was 120 MPa, of the regular girders 101 MPa. Modulus of elasticity for C90/105 concrete was 45.5 GPa and for C60/75 concrete was 46.9 GPa. The girders have simple  $\perp$  shape. They are assembled of three match cast segments. The contact joints that were during post-tensioning filled with epoxy are provided with shear keys. The girders are post-tensioned by 4 tendons of 12-Ls15.5/1800; the ducts are from PE pipes. Similar structures are being designed and built. The construction of the bridges started in autumn 2003; completed is autumn 2005.



Fig.1 Freeway D1 Vyskov-Kromeriz



Fig. 2 Precast girders and composite slab

### 3. THE BRIDGE ACROSS THE RIVER MORAVA IN OLOMOUC

Last month a new bridge across the River Morava and river bypass has been opened. Since the bridge is situated close to a historic fort, it was not possible to build a structure with a load bearing member situated above the deck. Due to the level of the flood, the deck has to be as slender as possible. Therefore a high strength concrete of the strength class C60/75 was used for the deck. Actual average concrete cube strength after 28 days was 103.0 MPa.

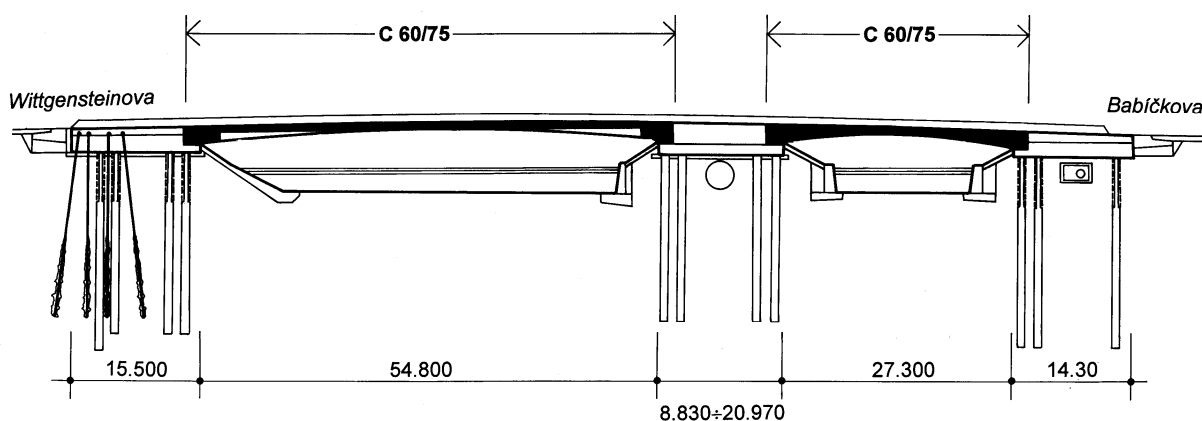


Fig. 3 Bridge across the river Morava in Olomouc

The bridge of two spans (Fig. 3) is formed by a slender slab of variable depth that is fixed into the end abutments. To allow the movement of the structure due to volume changes, the piles are weekend at their top portions. The deck is stiffened by edge girders forming New Jersey barriers. On the outer overhangs the utilities and sidewalks are situated. Since the overhangs are divided by transverse joints, they do not contribute to the resistance of the deck to the load. A solid intermediate support allows an access to the fort. The bridge deck was cast in place in the formwork supported by a steel truss with one support in the river bed.

#### 4. CABLE-STAYED BRIDGE ACROSS THE ODRA RIVER

Near a city of Ostrava the freeway D47 crosses the River Odra and Antosovice Lake on a twin bridge of the total length of 589 m (Strasky, Konecny, Jordan, 2006). Due to a limited clearance, the deck of the structure has to be as slender as possible. Therefore a cable stayed structure suspended on one single pylon was accepted. The main span bridging the Odra River is suspended on a 46.81 m high single pylon. Since the stay cables have a symmetrical arrangement, the back stays are anchored in two adjacent spans situated on the land between the river and lake. The stay cables have a semi-radial arrangement; in the deck they are anchored at a distance of 6.07 m, at the pylon they are anchored at a distance of 1.20 m.

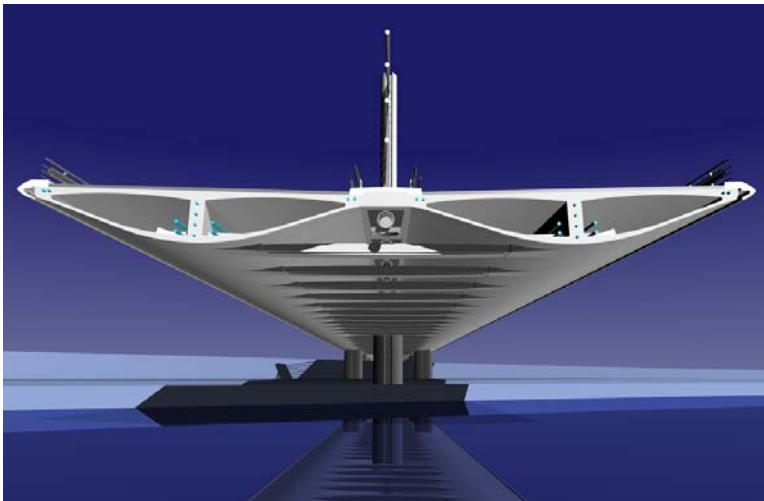


Fig. 4 Cable-stayed bridge over Odra river near to Ostrava



Fig. 5 Pylon

*The decks* of the twin bridge are formed by two cell box girders without traditional overhangs. In the suspended spans the girders are mutually connected by a top slab and by individual struts (Fig. 4). The stay cables of the semi-radial arrangement are situated in the bridge axis. The deck of the bridge is being cast span-by-span in the formwork suspended on the overhead scaffolding system. *The single pylon* is formed by a steel core of the octagonal cross section that is composite with a concrete cover (Fig. 5). Inside of its top part the stay cables are anchored; the bottom part is filled with concrete. The pylon has a constant depth of 3.00 m; the width below the deck is 4.10 m, above the deck is 2.40 m. The precast struts and pylon's fill and cover are designed from high-strength concrete of the strength class C60/75. The construction of the bridge started in 2005; at present, the deck and pylon are completed and the deck is being progressively suspended on the pylon. The completion of the construction is scheduled for autumn 2007.

#### 5. PEDESTRIAN BRIDGE ACROSS THE EXPRESSWAY R35

The bridge crosses expressway R3508 that is being built near the city of Olomouc, Czech Republic. The bridge is formed by a stress-ribbon of two spans that is supported by an arch (Strasky, Rayor, 2007) (Fig. 6). The stress-ribbon of the length of 76.50 m is assembled of precast segments 3.00 m long supported and prestressed by two external tendons (Figs. 7 and 8).

The precast deck segments and precast end struts consist of high-strength concrete of the strength class C60/75. The cast-in-place arch consists of high-strength concrete of the same

strength class. The external cables are formed by two bundles of 31-0.6" diameter monostrands grouted inside stainless steel pipes. They are anchored at the end abutments and are deviated on saddles formed by the arch crown and short spandrel walls. The steel pipes are connected to the deck segments by bolts located in the joints between the segments. At the abutments, the tendons are supported by short saddles formed by cantilevers that protrude from the anchor blocks. The stress-ribbon and arch are mutually connected at the central band of the bridge. The arch footings are founded on drilled shafts and the anchor blocks on micro-piles.

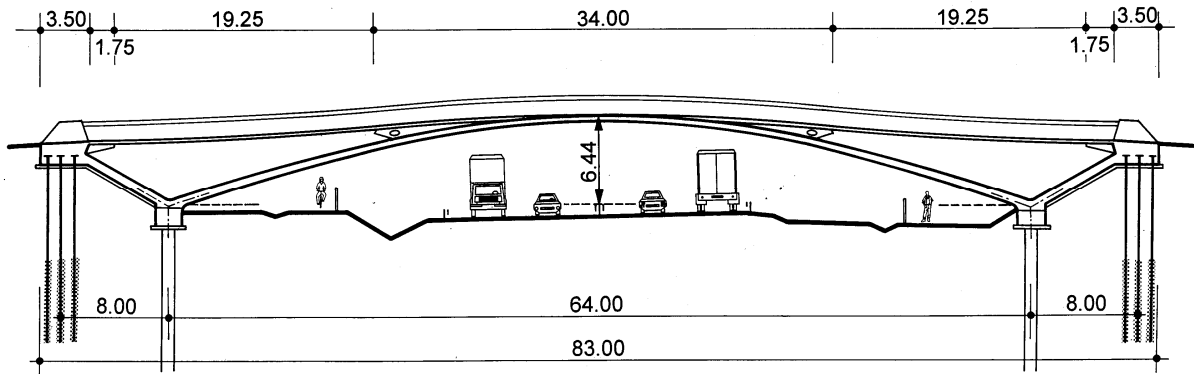


Fig. 6 Pedestrian bridge across the expressway R35

The bridge was erected in several steps. After the piles were placed, the end struts were erected and the arch footings and end anchor blocks were then cast. The arch was cast in formwork supported by light scaffolding. When the concrete of the arch had sufficient strength, the external cables were assembled and tensioned. Then the precast segments were erected (Fig. 7). After the forces in the external cables were adjusted, the joints between the segments were cast and subsequently the external tendons were tensioned up to the design stress (Fig. 9). Since the cables are curved, the radial forces loaded the stress-ribbon and in this way the deck was prestressed.



Fig. 7 Stress-ribbon bridge

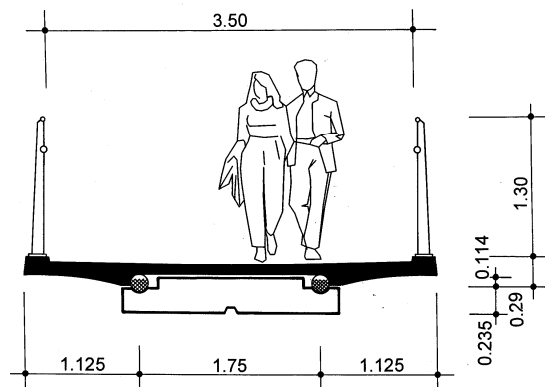


Fig. 8 Cross-section of a stress-ribbon bridge

The structural solution was developed on the basis of the described tests and a very detailed static and dynamic analysis that proved the structure has sufficient margin of safety and a reasonable response to the dynamic loading caused by people and wind.



Fig. 9 After placing the segments

## 6. PEDESTRIAN BRIDGE ACROSS THE SVRATKA RIVER

Another such bridge is being built across the Svratka River in a city of Brno, Czech Republic. The bridge is situated in the vicinity of a new international hotel and prestige office area. Therefore, a great attention was devoted to an architectural solution for the structure. The bridge is formed by a stress-ribbon of length of 43.50 m (Fig. 10) that is assembled of precast segments 1.5 m long, supported and prestressed by internal tendons - see Fig. 12. The end abutments are supported by pairs of drilled shafts.

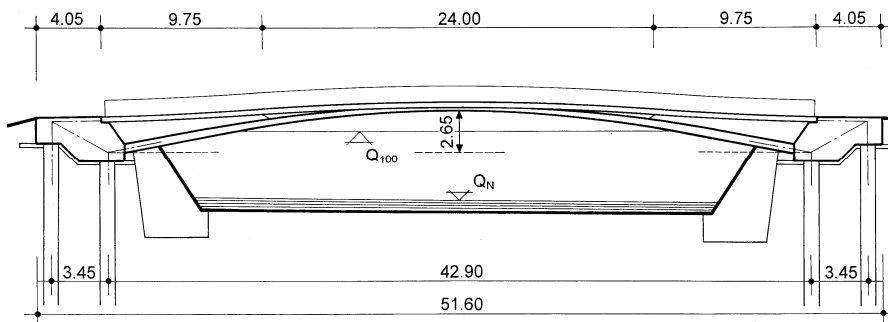


Fig. 10 Stress-ribbon bridge across Svratka river



Fig. 11 Erection

The flat arch is formed by two legs that have a variable mutual distance and merge at the arch springs (Fig. 11). The segments have variable depth with a curved soffit to accommodate prestressing tendons situated close to the bridge axis. The stress-ribbon and the arch are made from high-strength concrete of the strength class C70/85. The arch is assembled from two arch segments temporarily suspended on erection cables anchored at the end abutments. To eliminate the effects of possible deformations of the abutments caused by settlement of the piles, the length of the erection cables allowed adjustment. When the mid-span joints were cast the erection cables were replaced by external cables that tied the abutments.

After that the segments were placed on the arch and external cables and the internal tendons were pulled through the ducts and tensioned. Finally, the external tendons were removed. In this way, the required geometry of the deck was obtained. After casting the joints between the deck segments, the cables were tensioned up to the design stress and, as a result, the deck was prestressed. The structural solution was also developed on the basis of the very detailed static and dynamic analyses. Although the structure is very slender the users do not have an unpleasant feeling when standing or walking on the bridge.



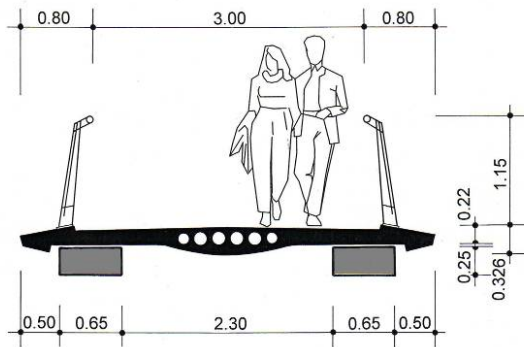


Fig. 12 Cross-section

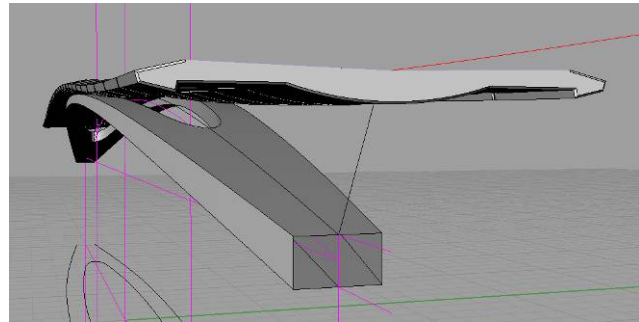


Fig. 13 View

## 7. PEDESTRIAN BRIDGE ACROSS THE VLTAVA RIVER IN CESKE BUDEJOVICE

A composite deck is suspended on one side inclined steel arch of a span of 53.20 m (Fig. 14). The deck is formed by two edge steel pipes mutually connected by diagonal cross beams formed by low plate girders. Composite deck slab together with bottom flanges create a torsionally stiff member that is able to resist an eccentric load. To eliminate a horizontal movement caused by pedestrians, the deck is integral with the abutments.

To increase stiffness of the bridge and eliminate cracks, the deck slab was designed from high strength the strength class C55/67. Actual average concrete cube strength after 28 days was 87.6 MPa. The bridge was opened in June 2006.



Fig. 14 Composite deck suspended pedestrian bridge across Vltava river in Ceske Budejovice

## 8. CREDITS

The development of the described structures has been achieved with the financial support of the Ministry of Education, Youth and Sports of the Czech Republic, project No. 1M0579, within activities of the CIDEAS research centre. The bridges were designed by a consulting firm Strasky, Husty and Partners, Ltd., Brno, Czech Republic. Project Engineers were L.Konecny, R.Broz, L.Hrdina and P.Stefan. The general contractor for all these bridges is SKANSKA DS, Brno, Czech Republic.

## 9. REFERENCES

- Strasky, J., Terzijski, I., Konecny, L., Svadbik, P., Racansky, J. (2006), "Freeway Bridge from Highstrength Concrete", *Structural concrete in the Czech Republic 2002-2005. Proceedings of 2<sup>nd</sup> fib Congress*, Naples
- Strasky, J., Konecny, L., Jordan, J. (2006), "Cable-Stayed Bridge across the Odra River." *Proceedings of 2<sup>nd</sup> CCC Congress Hradec Kralove*
- Strasky, J., Rayor, G. (2007), "Stress-Ribbon Pedestrian Bridges Supported or Suspended on Arches", *International Bridge Conference*. Pittsburgh

## NEW TYPES OF OVERPASSES ON CROATIAN HIGHWAYS

*Jure Radic, Zlatko Savor, Gordana Hrelja*  
*Faculty of Civil Engineering, University of Zagreb*  
*Kaciceva 26, Zagreb, Croatia*  
[jradic@grad.hr](mailto:jradic@grad.hr), [savor@grad.hr](mailto:savor@grad.hr), [hgoga@grad.hr](mailto:hgoga@grad.hr)

### SUMMARY

Due to expansion of highway construction in Croatia, there are a lot of structures to be designed and built in a short period of time. The client Croatian Motorways, designers and contractors are mostly focused on larger structures while the small structures are usually neglected. Highway overpasses are normally relatively short span bridges. Often their alignment is similar and the constructor's wish for maximum unification and standardization to reduce overall building costs usually prevails. The intention of the study made at our department was to develop a few new overpass types for Croatian highways, which will be more functional, safer for highway users and aesthetically more pleasing (Radic, 2007). The result of the study are three new types of overpasses with many alternative designs and details for further application.

### 1. INTRODUCTION

Overpasses are the most visible structures on the highways, so they need to be designed aiming for attractive appearance, with all requirements, regarding traffic safety and clearance, fulfilled. These structures must be functional, safe, durable and economical and harmonizes with their natural surroundings. The civil engineering practice in Croatia often utilizes systems of precast prestressed overpass structures, which puts certain constraints on both the designers and the client.

It is well known that the pier positioned in the median strip of a highway should be avoided, especially in the cut. If the width of a highway is about 30 m, a span of approximately 40 m is needed to avoid the pier in the median strip. The abutments should not be too close to the traffic lanes; if so an overpass will have a barrier effect on the highway users (Leonhardt, 1984).

In many cases, the designers of the overpasses do their best to achieve uniqueness. However, solutions with precast prestressed concrete girders often result in structures of questionable aesthetical value and dubious solutions regarding overall erection, maintenance and durability issues. New overpasses that were considered in the study are of composite type, integral and high strength concrete. After consideration of materials and other aspects of each type of overpasses, a few alternative designs were made for each type and finally the most appropriate one was chosen for the main design. Then the main design was executed for the location specified by the client – Croatian Motorways.

When considerable free space is available between vertical alignment of the overpass and the highway underneath, it is possible to design various structural types (arch, frame, strut frame or beam) and the choice of the superstructure material is wide open (concrete, steel or combination of them). In case of limited height, beam or frame structures with one span are acceptable solutions. In these situations the application of a composite type superstructure or

an overpass made of high strength concrete become economically competitive, and in addition, the visual impact on highway users is improved.

The alternative solutions of each type of differ in the material consumption, the construction method, visual appearance and safety aspects. These are also the parameters used to compare and evaluate the alternative solutions. The static analysis has been performed for each of the solutions to calculate the material consumption of the superstructure and the computer visualizations have been made to assess the visual impact on the highway users.

## 2. COMPOSITE OVERPASS

Composite bridges are usually used for larger spans (50 meters and more), but they can be competitive for small span bridges as well. Composite overpasses open much more possibilities to design economical and durable structures which can also be built in very short time with steel girders completely prefabricated in the workshop and then transported to the site (Schmackpfeffer, 1999). The current market situation in Croatia prefers standard precast concrete overpasses, not because the bids of composite structures are too high, but simply because the standard precast concrete structures are under-priced. Therefore the research and design of composite overpasses should be conducted taking into account special requirements of a specific location. These requirements can derive from many sources, topography uniqueness, visual diversity and local features.

The alternative solutions of the composite overpass were investigated on the Mučići overpass situated on the highway Zagreb – Split – Dubrovnik on the section Šestanovac – Zagvozd. The highway is in the cut, and the overpass is on one side on the embankment and on the other side in the cut. The level difference between the highway and the overpass vertical alignment is 6.80 m. This, together with the minimal traffic clearance of 4.5 m, makes possible the design of different types of composite overpass superstructures. The angle of crossing is  $62.055^\circ$ , and the vertical alignment of the overpass is in a constant slope of 1.626%. The roadway width on the overpass is  $2 \times 3.55 = 7.10$  m with sidewalks of 0.95 m on each side.

Three different solution of composite overpass were analyzed: simply supported beam, integral type bridge and a continuous beam type bridge with a pier positioned in the median strip (Fig. 1).

*The alternative solution "1"* is a simply supported beam with span of 40 m, with abutments not too close to traffic lanes (Fig. 1a). Three different cross sections have been considered for this solution: 1A, 1B and 1C. The cross section 1A comprises two "U" shaped steel girders 1.45 m deep with the concrete deck slab 25 cm thick. The cross sections 1B and 1C comprise two box girders 1.4 m deep, but with different shapes, with concrete deck slab 30 cm thick, comprising 10 cm thick precast plates and 20 cm cast in situ. Precast slabs are used both as the formwork and as part of the composite deck plate.

*The alternative solution "2"* is an integral rigid portal frame with composite superstructure and concrete abutments of 37.5 m span (Fig. 1b). The cross-section comprises two steel box girders of variable depth and concrete deck plate of 30 cm, consisting of 10 cm thick precast plates and 20 cm cast in situ. Precast slabs are used both as the formwork and as part of the composite deck plate.

*The alternative solution "3"* is a composite girder with the pier positioned in the median strip of highway (Fig. 1c). The cross section comprises of two steel plate girders and a concrete deck plate.

Structural steel of S 355 grade, concrete grade of C35/45 and non-prestressed reinforcement grade of S 500B were utilized.

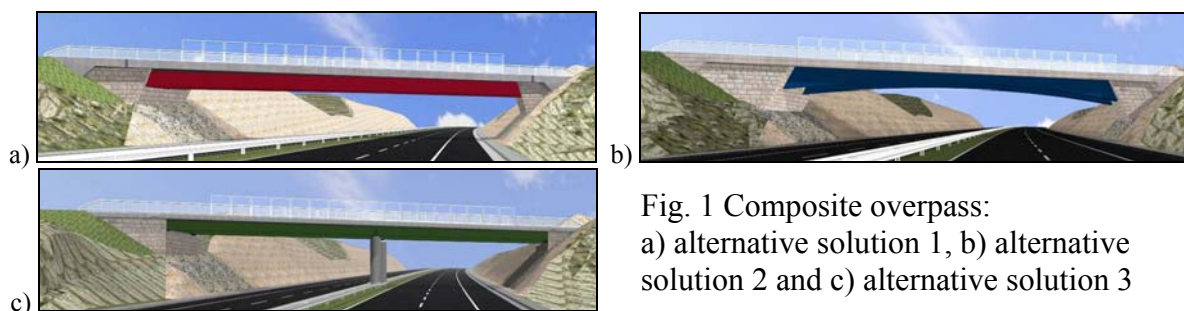


Fig. 1 Composite overpass:  
 a) alternative solution 1, b) alternative solution 2 and c) alternative solution 3

The alternative solution “3” was eliminated at the beginning, because of the a pier in the median strip of the highway. Between the alternative solutions 1 and 2, the alternative solution “1” with cross section “1A” (Fig. 2) was chosen for the next design phase. The main and construction designs are already finished (Savor, 2006) and the construction of the overpass should begin this summer.

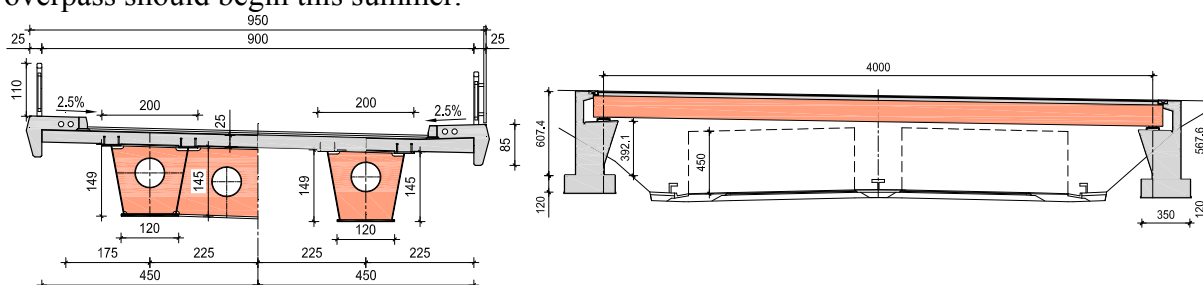


Fig. 2 Composite overpass – cross and longitudinal section of chosen solution

### 3. INTEGRAL OVERPASS

The integral bridges are not new, but there are only a few overpasses of that type recently built in Croatia. Expansion joints and bearings are always causing durability problems, and therefore their number should be minimized. Joints in the bridge deck are very costly to maintain, while detracting from the smoothness of traveling the bridge. To avoid these problems there has been a tendency to eliminate joints as much as possible, particularly in medium and small length bridges such are overpasses. The most frequently used type of integral bridges is a rigid frame in various forms. Integral rigid negative-moment knees greatly reduce the positive span moment and overturning moment at foundation level; single rigid portal frames can be adapted to railways, subways and divided or undivided highways underneath; double-span rigid frames are suitable for divided multilane highways underneath, with sufficient median width; triple- and more span rigid frames can accommodate multilane divided highways with a wider center median. The appearance of this type of bridges is graceful and clean and maintenance costs are low (ACI, 1995).

The alternative solutions of an integral overpass were investigated on the Osijek overpass situated on the highway Beli Manastir–Osijek–Svilaj on the Osijek junction. The highway is in a flat terrain, on low embankment, and the level difference between the highway and the overpass is 6.511 m. The vertical alignment is in a convex curve with 3.500 m radius and the angle of crossing is 82.79°. The roadway width on the overpass is  $2 \times 3.55 = 7.10$  m with sidewalks of 0.5 m and safety barriers on each side. Total width of overpass is 11.70 m.



Three different solution of overpass were analyzed: four and three span rigid frames and a strut frame (Fig. 3).

The solution “1” is a four-span rigid frame with spans of 17.6+22.0+22.0+17.6 m. Total length of the overpass amounts to 87.80 m (Fig. 3a). The cross section is of solid slab type 0.70 m deep and prestressed in longitudinal direction.

The solution “2” is a three-span rigid frame with spans of 22.6+34.0+22.6 m. Total length of the overpass is 79.2 m (Fig. 3b). The cross section comprises two main girders and a roadway slab. The superstructure depth is 1,6 m at mid-span and at abutments and 2.0 m at piers. Cross beams are placed above piers and at mid-span.

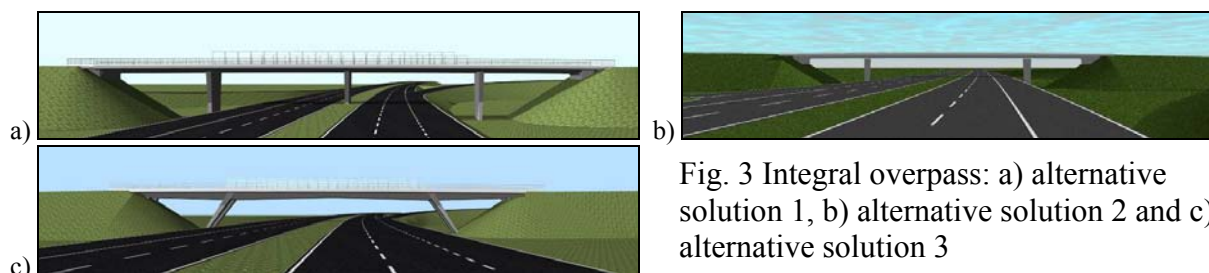


Fig. 3 Integral overpass: a) alternative solution 1, b) alternative solution 2 and c) alternative solution 3

The solution “3” is a semi-integral strut frame with spans of 21.0+42.0+21.0 m. Total length of the overpass is 93.66 m (Fig. 3c). The cross section comprises two main girders and a roadway slab. The superstructure depth is 1.35 at abutments, 1.5 m at mid-span and 2.0 m at piers. Cross beams are placed above the abutments and piers and at mid-span.

Concrete grade of C35/45, non-prestressed reinforcement grade of S 500B and prestressed reinforcement of grade Y1770S7 were utilized for all alternative solutions.

Since the solution “1” has the pier in median strip, it was eliminated at the beginning. Between solutions “2” and “3”, the solution “3” was chosen in accordance with the client’s wishes (Fig. 4). The main design is already finished (Savor, 2006), and the construction of the overpass should begin this year.

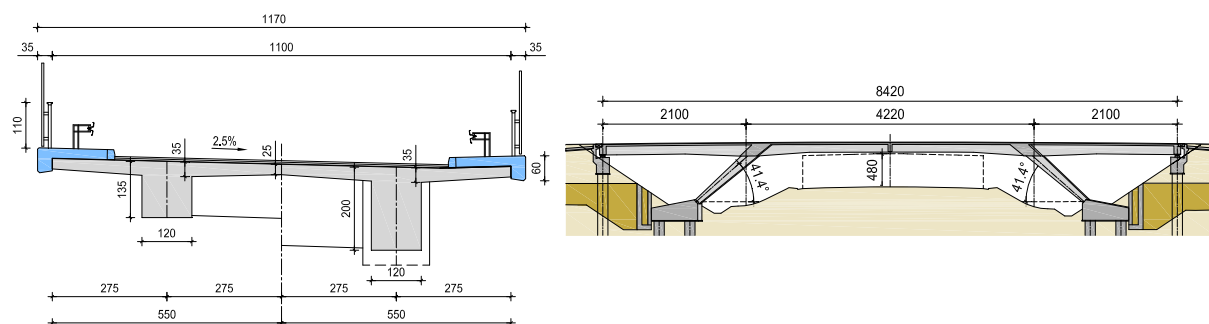


Fig. 4 Cross and longitudinal section of chosen semi-integral overpass

#### 4. HIGH STRENGTH CONCRETE OVERPASS

It was mentioned at the beginning of the paper that the standard precast concrete overpasses are the most often on Croatian highways. One of the main disadvantages of this type of overpasses is their durability and difficult and expensive maintenance. Therefore the overpasses cast in situ and made of high strength concrete are a preferred solution.

Alternative solutions of a high strength concrete overpass were investigated for the Rapain klanac overpass situated on the highway Rupa–Žuta Lokva on the section Senj–Žuta Lokva. The highway is in the cut and the overpass is on a low embankment. The level difference between the highway and the overpass vertical alignment is 8.80 m. This, together with the

minimal required traffic clearance of 4.5 m, makes possible the design of different types of overpass superstructures. The vertical alignment of the overpass is in a constant slope of 1,46% and the angle of crossing is 82.79°. The roadway width on the overpass is  $2 \times 3.55 = 7.10$  m with sidewalks of 1.0 m on each side. Total width of the overpass is 9,60m.

Four different solutions of the overpass were analyzed: a simply supported beam, a rigid integral frame, a strut frame and an arch (Fig. 5).

*The solution "1"* is a simply supported beam with 38 m span, with abutments not too close to traffic lanes (Fig. 5a). The cross section comprises two prestressed main girders and a roadway slab. Total depth of the superstructure is 1.75 m at mid-span and 2.0 m at abutments. Cross beams are placed above the abutments and at mid-span.

*The alternative solution "2"* is an integral rigid frame with 40,0 m span (Fig. 5b). The cross section consists of two prestressed main girders and a roadway slab. Total depth of the superstructure is 1.35 m at mid-span and 2.74 m at abutments. A cross beam is placed at mid-span.

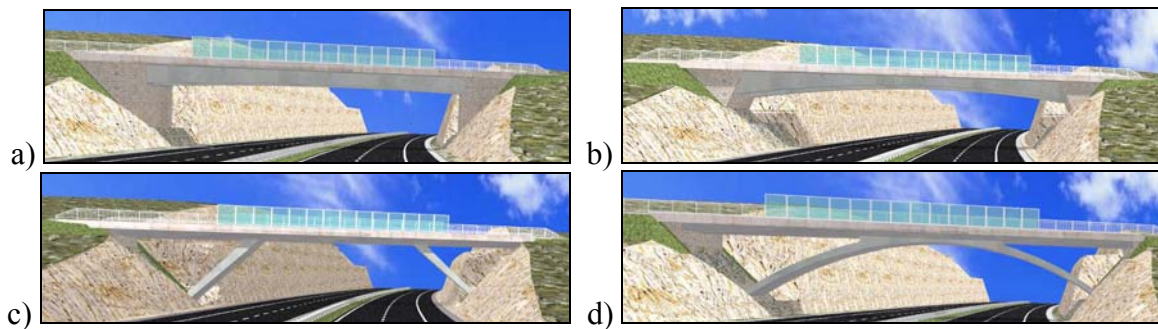


Fig. 5 High strength concrete overpass: a) alternative solution 1, b) alternative solution 2, c) alternative solution 3 and d) alternative solution 4

*The alternative solution "3"* is an integral strut frame with spans of 15.0+21.0+15.0 m. Total length of the overpass amounts to 41.0 m (Fig. 5c). The cross section is of solid slab type 0.90 m deep and prestressed in longitudinal direction.

*The alternative solution "4"* is an arch type structure. As the crossing is not too high above the highway and the arch is thin, the deck slab is joined with the arch at the crown to give an additional appearance of slenderness at this point (Fig. 5d). The arch cross section is of solid box type, with variable depth ranging from 0.5 m at arch abutments to 0.7 m at the crown and of constant 4.5 m width. The slab is solid with constant depth of 0.80 m.

Concrete grade of C70/85, non-prestressed reinforcement grade of S 500B and prestressed reinforcement of grade Y1770S7 were utilized in all alternative solutions.

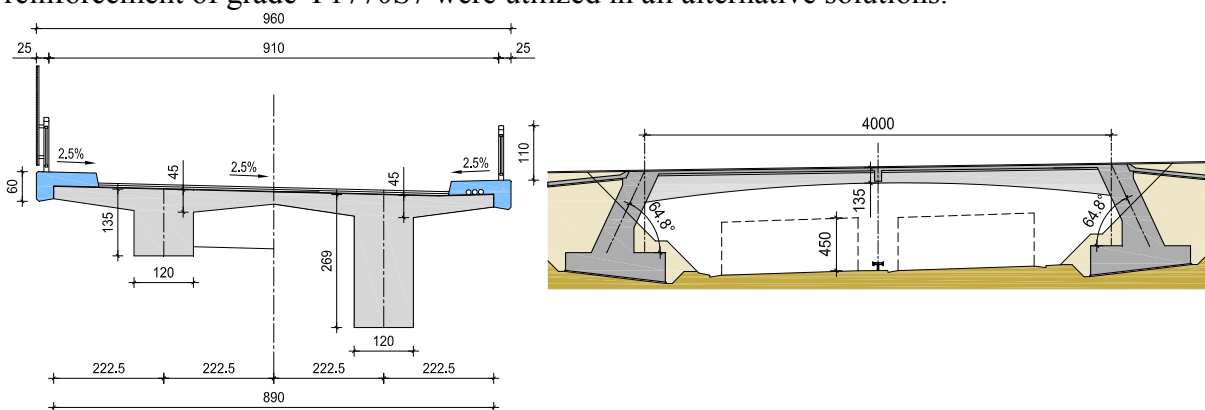


Fig. 6 High strength concrete overpass – cross and longitudinal section of chosen solution

For this overpass the solution “2” – the integral rigid frame was chosen for further design (Fig. 6). It has a pleasing aesthetical appearance, no pier in median strip, abutments are not too close to traffic lanes and it is integral without expansion joints and bearings. The main design is finished (Savor, 2007) and the construction should begin in the year 2008.

## 5. CONCLUSIONS

The results of the study are three new overpasses with many different alternative solutions and details. Aesthetically more attractive appearance can also be achieved by the appropriate choice of the bridge accessories. In this purpose different railings and cornices have been considered for each alternative solution of the overpasses. All alternative solutions are shown with the proper arrangement of the wing wall ending and the connection of the wing wall to the embankment. The abutments of composite and high strength overpass are covered with cut stones and embankments and cut slopes underneath the overpass are paved with dark stones (Fig. 7).

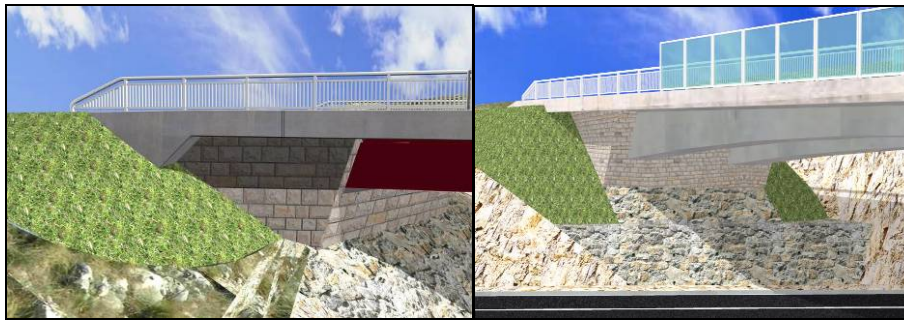


Fig. 7 Details of new overpasses

The proposed alterations have minimal effect on the total cost of an overpass but make a large difference in its appearance.

The attempt to introduce new overpasses to building practice opens many possibilities to achieve richer visual effects without compromising required quality, quantity and durability.

## 6. REFERENCES

- ACI 1995. “Analysis and Design of Reinforced Concrete Structures”, Reported by ACI Committee 343, *American Concrete Institute*, Detroit.
- Leonhardt, F. (1984), “Bridges”, 2nd Edition, Deutsche Verlags-Anstalt.
- Radic, J. (2007), “Study of new types of overpasses on Croatian highways”, Faculty of Civil Engineering, *University of Zagreb*, (in Croatian).
- Schmackpfeffer, H. (1999), “Standardized design for composite bridges – a competitive alternative to prestressed concrete”, *Proceedings of 4th International Symposium on Steel Bridges*, Leipzig, May 1999 (European Convention for Constructional Steelwork), pp. 170-200.
- Savor, Z. (2006), “Main design of Mučići overpass“, Structural Department, *Faculty of Civil Engineering, University of Zagreb*, (in Croatian).
- Savor, Z. (2006), “Main design of Čvor Osijek overpass“, Structural Department, *Faculty of Civil Engineering, University of Zagreb*, (in Croatian).
- Savor, Z. (2007), “Main design of Rapain Klanac overpass“, Structural Department, *Faculty of Civil Engineering, University of Zagreb*, (in Croatian).

## **METRO CONSTRUCTION IN BUDAPEST, HUNGARY – CONSTRUCTION OF THE STATIONS TÉTÉNYI ÚT AND NÉPSZÍNHÁZ UTCA**

*Eng. Christa Owczakowitz (author of the general parts and the part on Station Tétényi út)  
Porr Technobau a. Umwelt AG.  
1103 Wien, Absbergg. 47*

*Eng., MA László Czotter (author of the part on Station Népszínház utca)  
Porr Építési Kft.  
1056 Budapest, Váci u. 81.*

### **SUMMARY**

The following article gives a short overview about the metro line M4 currently under construction in Budapest. The construction of the 1st section of the metro line M4 will be described shortly and particularly the planning and construction of the stations Tétényi út and Népszínház utca will be dealt with in details, in the form of a technical report.

### **1. INTRODUCTION**

Metro construction has an already more than one hundred years old tradition in Budapest. As the development of the Andrassy út as one of the most important urbanistic measures in the last decade of the 19th century, one of the most traffic loaded radial main connections in Budapest was completed, then competent administration pleaded massively for an underground tracing of the public transportation.

The parliament agreed then to the implementation of a metro line under the Andrassy út in 1870 under the precondition that the construction works may only be started if the completion of the metro line can be guaranteed for the millenium festivities in 1896. The metro line started to operate as the first metro on the continent on 2 May 1896 and remained in operation in its original state until 1973.

The metro line received its current state in 1973, when it was fitted to the contemporary standard in the course of a modernization and was also lengthened.

With the construction of metro line M4 a new era has been heralded in the Budapest metro construction, whereby the ambitious purpose of the Hungarian government is to establish such a modern metro again that guarantees an operation for many decades.

### **2. GENERAL DATA OF THE METRO LINE M4**

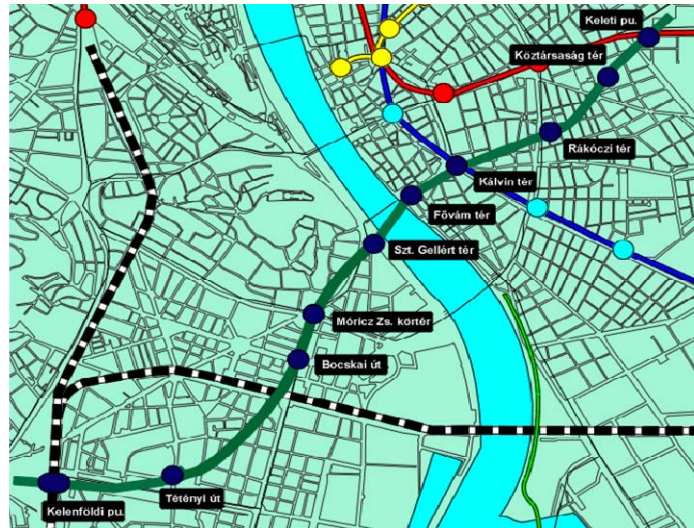
The M4 should be constructed in two sections in which the *first section* leads from the railway station Kelenföld (Kelenföldi pályaudvar), located in South Buda to the Eastern railway station (Keleti pályaudvar), two very frequented railway stations in Budapest. This section has a total length of 7.3 kilometer and includes the construction of ten metro stations.



The *second section*, which is envisaged beyond the Eastern railway station, is still in the planning phase and includes four more stations.

The tunnel section will be built with mining method, with tunnel boring machines, where two separate tunnel tubes will be driven, with a diameter of approx. 6.0 m each.

The stations will be constructed using cut-and-cover method for the most part.



F

ig. 1 overview first section M4

In March 2006 a consortium consisting of Porr, Bilfinger and Vegyépszér was awarded the contract for the construction of the station Tétényi út.

On September 11, 2006 the same consortium was disclosed as the best bidder for the stations Népszínház utca and Keleti pályaudvar. The total contract value is approx. 92.8 million € and is to be spent on the construction till February 2009.

The contract for the construction of the stations includes not only the construction works but the *implementation planning* as well. Thereby an extremely intensive co-operation and coordination is required with the planner during the preparations for the construction. Likewise, the order size includes co-operation with the other contractors of the client as well. It means that the implementation planning has to be co-ordinated also with the constructors of the tunnel, the interior work etc.

During the bidding phase pre-statics had been prepared by the Bureau ISP, a civil engineering bureau in Vienna, based on which the sizes were defined and so it formed the basis for the calculation. According to Hungarian law, for the preparation of the detailed statics and implementation plans it is requisite to assign a planner licensed in Hungary for the metro construction.

Basis for the tender preparation and also for the implementation planning were the tender plans.

### 3. CONSTRUCTION OF THE STATION TÉTÉNYI ÚT

The station Tétényi út will be the first of the 10 stations to be crossed by the tunnel boring machine. In the following the construction of the station Tétényi út will be described:

The construction works for the station Tétényi út have a contract value of approx. 13.5 million euros and cover all the pre-works, public utility replacement, foundation security measures, earthwork and the reinforced concrete works.

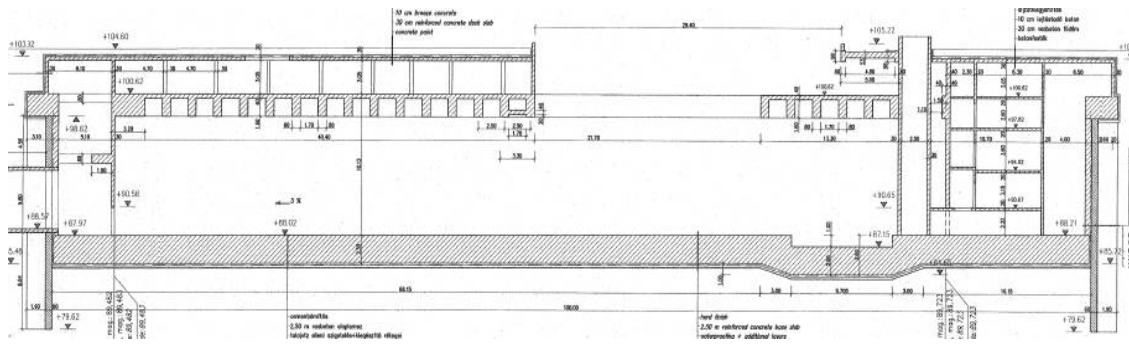


Fig. 2 longitudinal cross section of Tétényi út

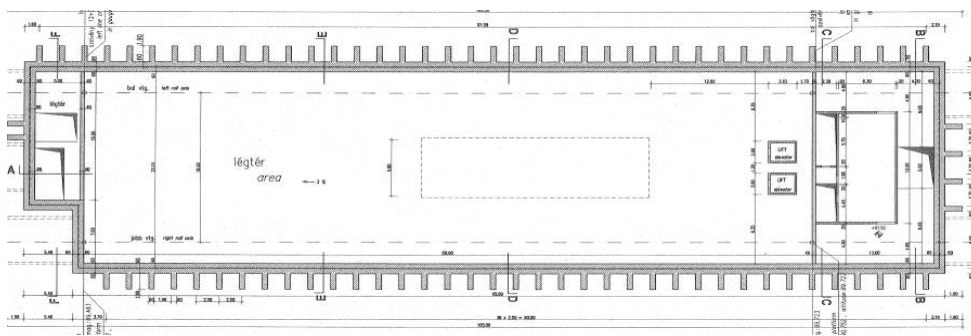


Fig. 3 layout of Tétényi út

The station with the size of approx. 100 m × 25 m and 24 m depth from the top level of the terrain will be constructed by cut-and-cover method. In the following the construction steps of the station Tétényi út are listed, and on the basis of that also the technical aspects of the construction:

- 1.) public utility replacement (ducts, T-Com, Pantel cables, water and gas pipes)
- 2.) Pre-excavation + construction of the sheet-pile wall. The construction of the sheet-pile wall was required to guarantee a dry building pit during all the construction works. The groundwater plane is located approx. 3.00 m under the top edge of the terrain and the bottom edge of the top slab to be constructed is located approx. 6 m under the top edge of the terrain.
- 3.) Construction of the diaphragm wall:  
 Technical data: T-shaped (d=60 cm)  
 Total area approx. 7,600 m<sup>2</sup>  
 approx. 580.000 kg reinforcement

As building pit support a 24 m deep 60 cm wide T-shaped diaphragm wall was constructed. It has the advantage that after the construction of the diaphragm wall and the topmost top slab, the excavation down to the bottom edge of the bottom slab can be carried out without additional temporary struts.

The areas where later the TBM will penetrate the diaphragm wall, reinforcement has been constructed as GRP-reinforcement, so the TBM can penetrate the diaphragm wall and cross the station without damage.



Fig. 4 construction of diaphragm wall

4.) Parallel to the construction of the diaphragm wall the excavation for the top slab construction is already going on and subsequently construction of the top slab took place according to the construction progress

5.) Top slab construction:

Technical data:	Concrete:	approx. 13,150 m <sup>3</sup>
	Reinforcement:	approx. 2,500,000 kg
	Formwork:	approx. 15,000 m <sup>2</sup>

From the constructional point of view the structure has been divided into 3 sections with 2 dilatations.

The top slab was produced as reinforced concrete finned construction. In the second section of the top slab the later opening for the access of the station via escalators was constructed in elliptical shape in fair-faced concrete, in order to meet the architectural requirements.

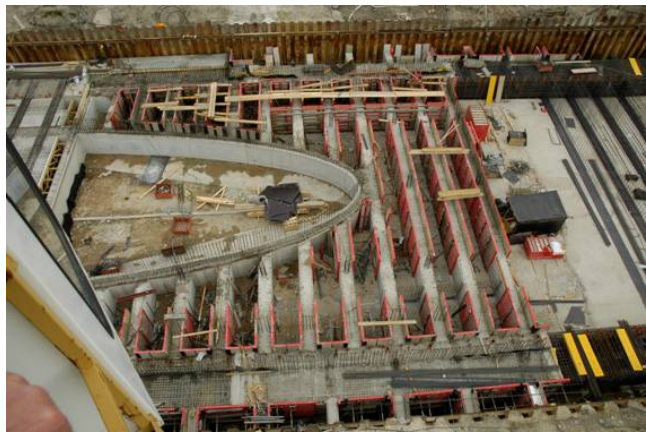


Fig. 5 Construction of top slab part 2

6.) Excavation works, water drainage:

Technical data:	Excavation under the top slab:	approx. 35,000 m <sup>3</sup>
-----------------	--------------------------------	-------------------------------





During the excavation works under the top slab special attention had to be paid so that the building pit support consisting of the T-shaped diaphragm would be dimensioned for earth pressure and the inner shell later to be constructed would take the water pressure. Therefore relief borings were drilled during the excavation, so that behind the diaphragm wall boxes no water pressure can build up.

Fig. 6 Excavation under top slab

Water that leaks from the relief borings shall be discharged till the inner shell has been entirely completed – and so the static system has reached its final state. For this, drainage wells were installed in the bottom slab in order to discharge the water from the relief borings by a drainage system beneath the bottom slab.

7.) Construction of the bottom slab:

Technical data:	Concrete:	approx. 5,600 m <sup>3</sup>
	Reinforcement:	approx. 560,000 kg

The bottom slab and the inner shell will be made of concrete as watertight structures. The construction of the bottom slab and the inner shell takes place on the basis of the specifications of the so-called 'Weiße Wanne' principle. It means that already in the planning phase these specifications have to be considered at the dimensioning of the reinforcement. The construction takes place in 6 concreting sections, approx. 800 m<sup>3</sup>/section each.



Fig. 7 Construction of bottom slab – concreting blinding concrete, reinforcement

8.) Crossing of the TBM + construction of the rails for shuttering traffic by Contract No. 02:



The crossing takes place in September, 2007.

9.) Construction of the inner shell at the time of the track locks:

Technical data:	Concrete:	approx. 1,900 m <sup>3</sup>
	Reinforcement:	approx. 285,000 kg

The inner shell is approx. 10.00 m high, and it should be boarded and concreted in the greatest part without horizontal joints, at once.

10.) This is followed by the construction of the staircase, air shaft and the pedestrian level

## 4. CONSTRUCTION OF THE STATION NÉPSZÍNHÁZ UTCA

### 4.1 Structural description

The station will be situated underneath Köztársaság tér (Budapest, District VII.), with an earth layer of approximately 3.0 – 3.5 m on top. The terrain level as planned, is slightly ascending along the station's longitudinal axis, varying between 105.6 and 106.4 mBf (metres above Baltic Sea level). The highest point of the upper plane of the top slab is at 102.66. The box-shaped station measures 111.50 × 25.60 m, made with a 1.00 m thick diaphragm wall. At both ends of the box-shaped station ventilation shafts are installed enclosed with 60 cm thick diaphragm walls. The connecting planes of the diaphragm walls are set at two different heights. At the sections closer to the park, at 103.8 mBf in a work trench with a slope gradient of 1:1.5, and at the end facing Népszínház utca at 104.80 mBf. The lower plane of the station box's diaphragm wall is at 75.00 mBf.

According to 'Weiße Wanne' specifications, the station contains three dilatation units: their length is 35.50; 36.00 and 40.00 m respectively. Geometrically the station consists of three sections. Engineering areas are situated at the ends of the box-shape object. In the engineering areas monolithic reinforced concrete top slabs will be installed supported with walls and pillars. The middle section, the station itself, is an area of great height featuring reinforced concrete struts on two levels. The diaphragm wall and the internal structure are connected at the joint pockets installed at the level of the struts. This joint is also intended to ensure that the two structures are coupled with negative buoyancy. The bottom slab is not connected to the diaphragm wall. The upward pressure on the bottom slab has to be absorbed by the top slab above.

The highest top slab of the station is a composite of two fundamentally different structures: a monolithic top slab resting on walls and pillars, with diaphragm walls at both ends, and a monolithic beam floor supported by apron-walls. Both structures are employed in the two outermost dilatation units, while the dilatation unit in the middle features beam floors only.

The bottom slab of the station is made of a 3.0 meters thick monolithic reinforced concrete slab. The interior of the station features an exposed concrete finish.

A separate insulation system will not be installed in the station. Water tightness is ensured by the internal reinforced concrete shell, made of watertight mass concrete. In the construction and expansion joints waterproofing is ensured by joint bands, injection grouts and expansion bands.

### 4.2 Technological phases of construction

- Building the diaphragm wall
- Installation of the final and temporary struts at three levels, as per the following:

- Earth excavation up to the bottom of the slabs
- Installation of pockets in the a diaphragm wall to provide temporary support for the slabs
- Installation of formwork and reinforcements for the concrete slabs
- Pouring concrete for an entire dilatation unit, without any interruption
- Installation of temporary steel props
- Earth excavation up to the bottom of the bottom slab
- Bottom slab construction
- Tunnel boring machines passing through the station
- Construction of apron-walls for connecting to the existing platform from below (installation of reinforcements connected to the Lenton coupling units, installation of formwork, pouring concrete through the pipes installed beforehand). The apron-wall is connected to the expansion bands, watertight bands and expansion groutings installed in the breast beams in advance.
- Conventional upward construction of structural works (walls, top slabs), with temporary steel props removed.
- Shuttering panels installed over the upper top slab, conventional formwork installed on the flat slab sections, installation of reinforcements
- Pouring concrete in the top slabs for an entire dilatation unit, without any interruption
- Construction of rising structures on the top slab (e.g. street exit structure)
- Top slab insulation
- Earth filling

## **5. CONSTRUCTION OF THE STATION KELETI PÁLYAUDVAR**

As regards Railway Station East, situated in the vicinity of the hectic traffic junction also called Railway Station East, with a contract value equaling 55.2 million Euros, the construction works has started in the spring of 2007. This unit consists of the station itself and of a separate switch hall. Major dimensions are 130 and 210 m x 35 m respectively, with depths up to 30 m. Construction works here are also carried out using the top down method. The specialty of this project is that it also involves the crossing with an existing Metro line of a greater depth, as well as the relocation of public utilities, roads, road traffic implements.

## **6. CONCLUSIONS**

In summary, it can be stated that the construction of the metro stations are acutely interesting assignment, 'cause in planning and implementation of very different parts of civil-engineering from special civil engineering to top-down method and building a waterproofed structure. Hereby can be mentioned, that building in urban area is an especially challenge also in logistical way for the site. Also the co-ordination at the interfaces with the other contractors, for example contractor for tunnelling, contractor for inner structures etc. and the client poses a great challenge. For all our consortium try for all requests and the short dates to provide the stations in best quality and build in time for the client.



## A NEW CONSTRUCTION TECHNOLOGY FOR FREE SHAPE REINFORCED CONCRETE SANDWICH SHELLS

*Zsolt Kassai*

*Archi Stat Ltd.– Architectural & Structural Design Bureau*

*4400-H Nyíregyháza, Selyem u. 21.*

*Ass. Prof. Dr. Imre Kovács PhD.*

*University of Debrecen Department of Civil Engineering*

*4028-H Debrecen, Ótemető u. 2-4.*

### SUMMARY

Application of shell structures are strongly constrained by their relatively high construction and formwork costs. However, due the suggestive appearance, shells may propose the most environmental-friendly architectural and structural solution for designers. In the light of the motivation a new construction method as well as structural appearance was developed for special reinforced concrete sandwich shell structures. This paper shortly summarises the design philosophy and the construction method of an ongoing investment applying the method.

### 1. INTRODUCTION



Photo 1 Reinforced concrete buildings by Pierre Székely (Bag-Meil)



Photo 2 Free-shape concrete shell structures by Antti Lovag (Pierre Bernard, Cannes)



Photo 3 Shell structures in Provence by René Ligebou



Photo 4 Exterior and interior in Switzerland, by Peter Vetsch (Diatikon, Zürich)

Free shape reinforced concrete shells are one of the most remarkable structural systems has ever been used for buildings. These structural forms offer endless possibilities to form special architectural exteriors and interiors for houses and for other buildings. Only a few remarkable architects follow the way of free shape architecture in Europe. Pierre Székely (Photo 1), Antti Lovag (Photo 2), Christian Chambou, René Ligebou (Photo 3), Daniell Gatolup, Peter Vetsch (Photo 4) are worldwide well known, productive and innovative architects in this field.

However, due to the relatively high construction costs as well as the different and sometimes strange look these buildings are not wide-spread on the world. In the frame of a research group the Archi Stat Architectural & Engineering Design Office and the Department of Civil Engineering at University of Debrecen, Hungary developed a patented, new, economic and environmental friendly construction technology to build reinforced concrete sandwich shells.

## 2. DESIGN ASPECTS AND PHYLOSOPHY

Following Otto Frei's scientific and philosophic achievements on the relationships of the structural and natural forms as well as the Gaia hypothesis, two phases of design procedures are introduced. At the "Global" or architectural phase the free shape of structure is formed following the silhouette of natural bodies. Secondly, at the "Local" or engineering phase the structural behaviour of shell is composed of three different layers which form a sandwich shell with similar structural performance to many natural body such as behaviour of bone, soft stem of plants or structure of molluscs.

### 3. CONSTRUCTION

Construction of free shape sandwich shells composed of different work phases. First step after the foundation is the prefabrication and installation of the steel tube “skeleton” which defines the characteristic points and main curves of the shell surface. Second process is the placing of the two-layer reinforced concrete meshes forming the main reinforcement of the two load bearing reinforced concrete layers as well as the final outstanding shape of the structure. Thirdly, two very fine polypropylene or metal meshes are placed on the two reinforcement meshes which are able to carry the load of concreting during construction. Finally, a calculated thickness of heat insulation layer is injected into the hardened load bearing reinforced concrete layers. After the structural works, soil covering is made on the shell with different thicknesses increasing the heat insulation capacity of the whole structure. Some characteristic joints of the structure are detailed in Fig. 1.

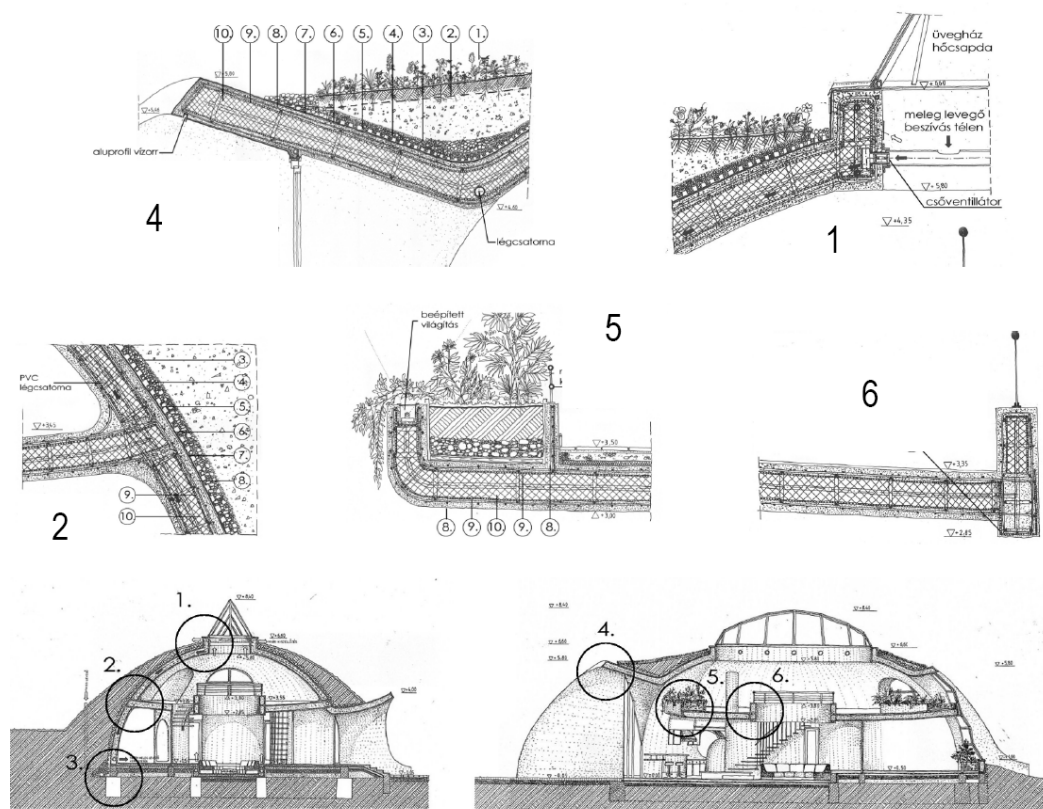


Fig. 1 Structural and architectural detail of some sandwich shell joints

### 4. ACKNOWLEDGEMENTS

The theoretical and the ongoing research work on the behaviour of sandwich structures are financially supported by the INNOCSEKK programme.





Photo 5 Construction of foundation and the steel tube "skeleton"





Photo 6 Release of the double reinforcement meshes  
on the prefabricated steel tube "skeleton"





Photo 7 Inside and outside surfaces of the structure under and after construction together with the views of the building

## **DIFFERENCES IN MIX DESIGNS OF LIGHTWEIGHT AND CONVENTIONAL CONCRETES**

*Rita Nemes, Zsuzsanna Józsa*

*Budapest University of Technology and Economics, Hungary*

*H-1111 Budapest Műegyetem rakpart 3.*

*nemes.rita@gmail.com, zsjozsa@epito.bme.hu*

### **SUMMARY**

Lightweight concrete (LWC) was well-known even by the Romans. Without this innovative composed material the construction of the dome of the Pantheon would have not been possible. For near 2000 years LWC was forgotten, but nowadays – because of its advantages – the construction of high-rise buildings and bridges is possible with this material in many places. Several types of lightweight concrete are nowadays available. Among these there is a type that can compete with conventional concrete. Structural lightweight concretes are typically lightweight aggregate concretes (LWAC) (lightweight pellets in oversaturated cement mortar mixture). Principles of conventional mix design are not available for LWAC, because the load bearing mechanism in case of normal weight concrete is different than that of LWAC. Present paper gives examples for the relationship of compressive strength and density of concrete in case of different LWACs, and presents the main properties of LWAs. Further relevant properties such as deformation and durability are also studied.

### **1. INTRODUCTION**

“Sustainable development meets the needs of present without compromising the ability of future generations to meet their own needs”- defined the UN World Commission on Environment and Development 1987.

Concrete with various shapes is a very good material for load bearing structures however, the relatively low strength-to-weight ratio of concrete can be considered as a disadvantage. The strength-to-weight ratio can be increased, either by increasing the strength (HSC) or by decreasing the self-weight of concrete (LWC).

LWAC was successfully used about 2000 years ago by the Romans and widespread in the past century. Use of this material contributes to sustainable development by improving concrete durability, maximising structural efficiency, lowering transport costs.

The density of structural concrete is between 800 and 2000 kg/m<sup>3</sup> and the compressive strength class is between LC8/9 and LC80/88 according to EN 206-1:2000 European Standard. All of these concretes are lightweight aggregate concretes where the designed air content is assumed being only inside the aggregate and the cement mortar matrix fills the gaps.

### **2. PAST, PRESENT AND FUTURE OF LWAC**

Lightweight aggregates and LWAC were known since the early days of the Roman Empire, the first known use of lightweight aggregate concrete is the Port of Cosa, built in about 273 BC. The four piers (about 4 m cubes) are extending into the sea, and for two millenniums

they have withstood the forces of nature in the harbour with only some surface abrasion. The service life of the structure of the Pantheon is long enough, the dome – with its diameter of 43.3 m – was not exceeded for more than nineteen hundred years. So the Pantheon as the Colosseum were built with different lightweight aggregates, e.g. the foundations of the Colosseum were cast using crushed volcanic lava, the walls were constructed using porous tufa stone, pumice and crushed brick (ACI, 2003).

After the fall of the Roman Empire LWAC was forgotten and reused only at the beginning of twentieth century. At that time the compressive strength of the commercial normal weight concrete was approximately  $17 \text{ N/mm}^2$ , while during the World War I the American Emergency Fleet Corporation built lightweight concrete ships with compressive strength of  $35 \text{ N/mm}^2$  – so we may consider, it was the first modern use of “high-performance” concrete (Ries, Holm, 2004).

In the United States over 100 World War II ships were built in LWAC, ranging in capacity from 3000 to 140000 tons and their successful performance led, at that time, to an extended use of structural LWAC in buildings and bridges (EuroLightCon 2000).

Since LWAC is generally 20-40% lighter than normal weight concrete, the dead load can be reduced, the foundation costs lowered and the concrete and rebar needs lessened. Nowadays multi-storey houses, towers, skyscrapers, office and apartment buildings, hospitals, churches, schools, shell roofs, structures of highway and bridges, prestressed and precast elements, marine structures, platforms are built in many places, the future is the same as from ordinary concrete (high strength and high performance concrete, fibre reinforced concrete etc.) but with the advantages of LWC.

### 3. LIGHTWEIGHT AGGREGATES

LWAs have two main groups. It can be natural material (like the aggregate of historical structures) or the more popular artificial products. Modes of manufacturing can be either the crushing or the heat treatment of the raw material. Most frequently the combination of these two processes are used. The manufactured material can be made of natural materials (e.g. clay or shale) or can be industrial by-product or waste. Wastes have two subgroups, wastes from building industry (used as crushed brick) or communal waste (used as expanded glass). General requirements of LWAs are: low bulk density (max.  $1200 \text{ kg/m}^3$ ) and low particle density (max.  $2000 \text{ kg/m}^3$ ), pressure resistance, thermal insulation capability, mechanical and chemical resistance, fire-resistance, frost-resistance, shape keeping. The most popular and well-known lightweight aggregates are the clay and shale products. The most important LWAs are the expanded clay and glass and the crushed brick.

In case of expanded clay and expanded glass products the relationship between crushing resistance and particle density (except the very low densities ( $<500 \text{ kg/m}^3$ )) is linear (Fig. 1). The crushing resistance of aggregate may reach 70 % of crushing resistance of natural quartz gravel. *The results measured on quartz gravel can be represented on the same line so it is possible to give the strength of lightweight aggregate in percentages of the strength of normal quartz gravel.*

Water absorption capacity of LWAs is usually high as the result of their high porosity. The result is, that the water absorption and the porosity is higher, if the particle density is lower. This is the behaviour of the lightweight aggregates type A (Fig. 2, Tab. 1), where aggregates

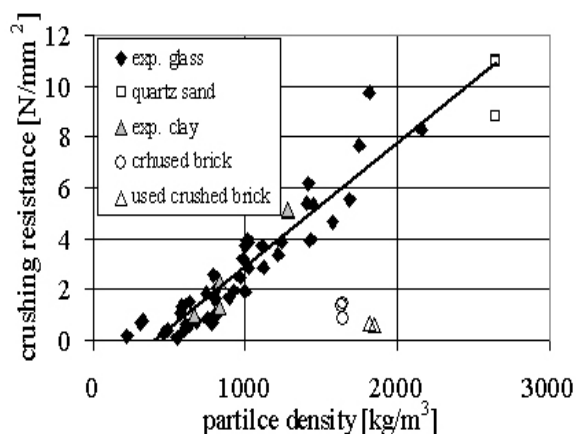


Fig. 1 Relationship between the particle density and the crushing resistance of aggregate

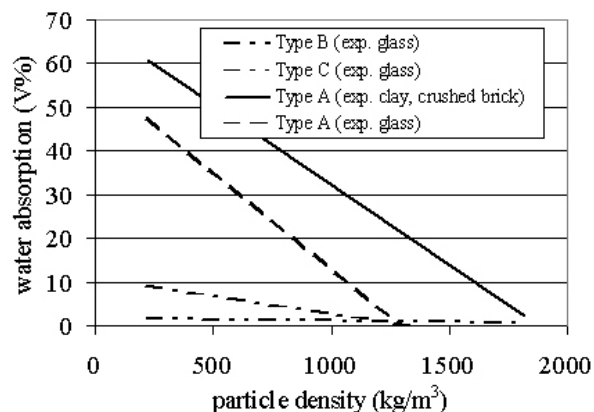


Fig. 2 Relationship between the particle density and the water absorption of aggregate

have open capillary pores. This high water absorption can reach 50 % by mass, usually it results disadvantages in concrete technology (e.g. need extra water to be added (Lin, Chen, Peng, Yang, 2005), the concrete can not be pumped). On the other hand it has an internal water curing effect. The normal process against this phenomenon is to cover the expanded clay aggregates with cement paste on the surface before mixing. It is an extra step in concrete technology (Müller, Haist, 2005), it is time consuming and needs extra costs. In case of expanded glass pellets the surface coating can be produced during the manufacturing process. So type B can be reached, where water-absorbing capacity is inversely depending on the particle density, but the water absorption is not higher than 10 % by mass. The water absorption can be independent from particle density with this coating as well. For type C the water-absorbing capacity of the pellets is very low (under 2 % by mass) and it is available under water pressure, too (Józsa, Nemes, 2002).

Tab. 1 Water absorption and particle density of different types of LWAs and NWA

	Water absorption		Particle density LWA [kg/m <sup>3</sup> ]	Particle density NWA [kg/m <sup>3</sup> ]
	% by mass	% by volume		
Type A	10-60	8-30	200-1800	---
Type B	2-10	2-5	450-1200	2000-2600
Type C	< 2	< 3	500-2000	2600-3000

#### 4. PRINCIPLES OF MIX DESIGN

Basic data for the normal weight concrete are the compressive strength classes. The most important is the water-cement ratio. The first step of mix design is to choose the water-cement ratio. If the water-cement ratio is increasing, the compressive strength is strongly decreasing, but the main load bearing part of concrete is the aggregate skeleton. No significant difference can be realized between the crushing resistances of the normal weight aggregates, so this is not a variable of the concrete mix design. The method of design of LWAC is different due to two reasons. First reason is the load-carrying mode (the load carrying part is the mortar matrix and not the aggregate skeleton). It is very important to find an aggregate that is matching to the matrix stiffness (Bremner, Holm, 1986). Second reason is the different strength of LWAs. The crushing resistance of several LWAs can be considerably different. Usually it is much lower than the crushing resistance of natural stones, but it can achieve that of natural quartz gravel, as well. The water-cement ratio is also important for LWACs, because the load

bearing part is the cement stone, but the concrete strength depends mainly on crushing resistance of LWA.

Density of concrete is the basic information for design similarly to compressive strength of concrete. However, these are opposite requirements. If the strength of aggregate is higher, the particle density of aggregate is higher. It can reach different values in case of LWAs from several materials. The crushing resistance of LWAs limits the compressive strength of LWAC. Normal weight and lightweight aggregate can be applied in combination. The most common combination of aggregates for structural lightweight concrete is, when the sand fraction (lower than 4 mm) is normal weight and gravel fraction is LWA. In case of using different types of aggregates with different particle densities the calculation of grading in volume percent (instead of the usual mass percent) is necessary. LWAC have to be oversaturated.

The strength of LWAC depends on crushing resistance of LWA and strength of cement mortar. If the crushing resistance of LWA is very low (under 1 to 2 N/mm<sup>2</sup> according to EN 13055-1:2002), the influence of aggregate particles can be neglected during mix design of concrete. In this case it is necessary to know the gap ratio of lightweight aggregate bulk. The over saturation should be minimum 10 to 20 % by volume.

## 5. EXPERIMENTAL RESULTS

The most significant property and the input data for design is the crushing resistance of aggregate and the relationship between the crushing resistance and the particle density of LWA. Advantages of artificial products are the better and more constant quality. The three main parameters for mix design are the strength of cement mortar, the strength of LWA and amount of LWA.

Strength of LWAC depends primarily on the strength of the cement mortar, as the main load bearing part is the matrix in LWAC. The importance of the strength of the mortar is more considerable in case of LWAs with low self-weight. During the tests different aggregates (four different expanded glass pellets and natural quartz gravel) and three cement mortar mixtures

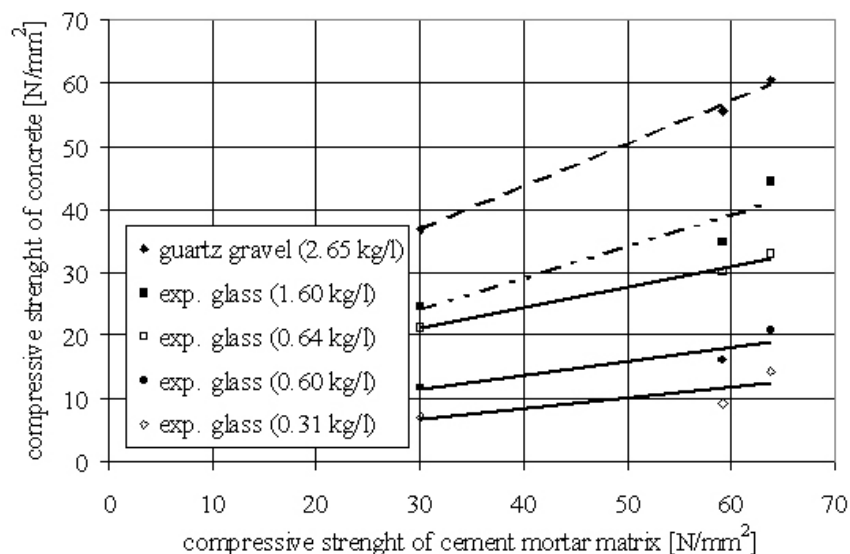


Fig. 3 Relationship between strength of cement mortar and strength of concrete in case of application of different LWAs and natural quartz gravel, amount of LWA is 47 % by volume

(average compressive strength are 63.8, 59.2 and 30.1 N/mm<sup>2</sup>) were used. The cement was the same and the aggregate content was 47 volumetric percent in all cases. Aggregate under diameter of 4 mm was natural sand. Consistency was set to equal by superplasticizer. If the compressive strength of mortar is increasing, the compressive strength of LWAC is increasing. The rate of change in compressive strength of LWAC is independent from the type of LWA, if the volumetric ratio of the aggregate is constant (Fig. 3). Respectively the strength of concrete the higher the density of aggregate is, the more important the strength of cement stone is.

Volumetric ratio of aggregate was applied on the widest possible range. Upper limit can be determined belonging to a paste-oversaturated mixture. Paste-saturated condition can be determined based on the gap ratio of the aggregate (50 to 60 percent by volume). Lower limit is found around 30 to 33 percent by volume. These series of tests were carried out exclusively with the same mortar mixtures (63.8 N/mm<sup>2</sup>). Aggregate content of test specimens was 36 to 56 percent by volume. Fig. 4 indicates results for some types of expanded glass aggregates at different volumetric ratios of aggregate. If the used volume of aggregate decreases from the maximum value (about the applied 56 percent by volume), the strength of concrete increases. But it is not true for the complete density range. If the amount of LWA is very low, the density of concrete increases without the increase of strength (e.g. in case of LWA density 1.0 kg/l under 47 % by volume). Bilinear relationship was experimentally found between compressive strength of concrete vs. density of concrete, it can be concluded that concrete has almost the same compressive strength with further increase in density by reaching the second line. Based on this relationship, the optimum situation can be defined at the point where maximum strength is available at minimum density.

Influence of crushing resistance of the aggregate is essential on the strength of LWAC. If the aggregate has relatively high strength then the behaviour of LWAC is similarly to the normal weight concrete (NWC). The particle density depends strongly on the crushing resistance (Fig. 1). In present test series we defined three classes of expanded glass aggregates according to their particle densities. The relationship between concrete density and cube strength was found to be similar in all cases. If the strength of aggregate is higher, then the strength of concrete to optimum is higher too, but the most advantageous aggregate amount is lower (Fig. 4).

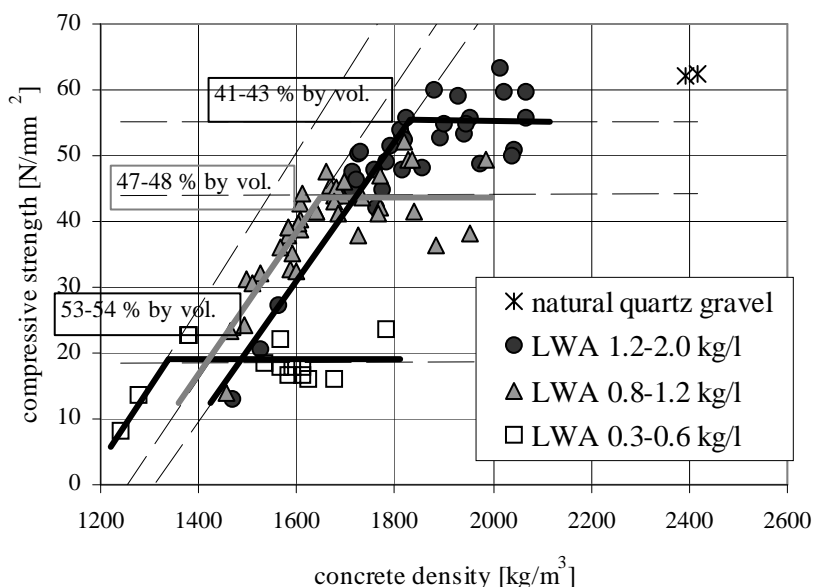


Fig. 4 Relationship between concrete density and compressive strength in case of LWAs of different particle density groups (150 mm cubes, individual values)

## 6. CONCLUSIONS

The long term value of any construction material is predicated on a combination of its properties: durability, total life cycle assessment, cost, and long-term sustainability. Durability and cost depend on the knowledge of use of materials, on finding the optimum among the variable parameters. The past and present of LWAC architecture and engineering are wonderful; our results may serve as improvement to the future of sustainable development of LWAC. Differences in mix design are the following for

	<i>conventional concrete</i>	<i>lightweight aggregate concrete</i>
- <i>requirement:</i>	compressive strength	compressive strength + density
- <i>strength depends on</i>	water-cement ratio	w/c + crushing resistance of LWA
- <i>aggregate grading</i>	percent by mass	percent by volume
- <i>optimal strength:</i>	by paste saturated concrete	by over saturated concrete

Strength of LWAC is influenced by the crushing resistance of the LWA as well as by the strength of the cement mortar. Crushing resistance can be accurately predicted from particle density that is easy to measure. Aim of mix design is to be able to reach the lowest density of LWAC with the possibly highest available strength. For this purpose, an optimum volumetric ratio of aggregate particles should be defined. Strength of LWAC can be predicted from the properties of the constituents and their mixing ratio.

## 7. ACKNOWLEDGEMENTS

Authors wish to express their gratitude to Geofil Ltd. for the collaboration and financial support and to Liapor Ltd. Solvadis Austria and Biotech Hungaria for supplying aggregates.

## 8. REFERENCES

- ACI (2003), „Guide for Structural Lightweight Aggregate Concrete” ACI 213R-03, *American Concrete Institute Farmington Hills, Michigan, Committee 213, chair Ries J.P., pp 1-2.*
- Bremner, T.W., Holm, T.A. (1986), „Elastic Compatibility and the Behaviour of Concrete”, *ACI Journal* March-April/1986, pp. 244-250
- CEB-FIP (1993), CEB-FIP MODEL CODE 1990, *Thomas Telford Services Ltd.*
- EN 13055-1:2002 „Lightweight aggregates – Part 1: Lightweight aggregates for concrete, mortar and grout”
- EN 206-1:2000 „Concrete – Part 1: Specification, performance, production and conformity”
- EuroLightCon (2000) „Durability of LWAC made with natural lightweight aggregates” *EuroLightCon Document BE96-3942/R18*, June 2000
- fib* (2000), „Lightweight Aggregate Concrete, Recommended extensions to Model Code 90; Case studies” *fib bulletin 8 Sprint-Druck Stuttgart*
- Józsa, Zs., Nemes, R. (2002) „Recycled Glass Aggregate for Lightweight Concrete”, *Concrete Structures*, 2002, pp. 41-46
- Lin, C-K, Chen, H-J, Peng, H-S, Yang, T-Y. (2005) „Properties of Self-Compacting Lightweight Aggregate Concrete”, *Proceeding of fib Symposium Keep Concrete Attractive*, 23-25 May 2005, Budapest, Hungary, Eds.: Balázs G.L. and Borosnyói, A., pp. 945-950
- Müller, H.S., Haist, M. (2005), „Pumpable Self-Compacting Lightweight Concrete”, *Proceeding of fib Symposium Keep Concrete Attractive*, 23-25 May 2005, Budapest, Hungary, Eds.: Balázs G.L. and Borosnyói, A., pp. 368-373
- Müller, H. S., Haist, M., Mechtcherine, V. (2002) „Selbstverdichtender Hochleistungs-Leichtbeton”, *Beton- und Stahlbetonbau, Heft 6*, Juni/2002, pp. 326-333
- Ries, J.P., Holm T.A. (2004) „A Holistic Approach To Sustainability - For the Concrete Community – Lightweight Concrete- Two Millenia of Proven Performance” *Information Sheet 7700.1 ESCSI* pp. 1-15



## ON SITE CONCRETING OF ARCHITECTURAL CONCRETE: NOT EASY, BUT POSSIBLE

*Jan Desmyter, Valérie Pollet  
Belgian Building Research Institute (BBRI-CSTC-WTCB)  
Lombardstraat 42, B-1000 Brussels*

### SUMMARY

BBRI is often contacted in cases where architects and clients have high demands and expectations with regard to the quality of the concrete surface. In most of these cases the demands and expectations have not been detailed in the technical specifications and as a result of this, most of the discussions take place during execution of the works, and not before the contract is awarded or the start-up of the jobsite. In this context all parties run a series of risks. Contractors face a series of costs they did not provide at the time of the price offer. Architects and designers, often not well informed about the possibilities and limitations of concrete, fear that their design will be destroyed by bad execution. And clients, well, they will have to live with it... This article gives some general recommendations for on site concreting of architectural concrete. It deals both with specification and execution methods.

### 1 INTRODUCTION

The Belgian Building Research Institute is a private research institute founded in 1960 under impulse of the National Federation of Belgian Building Contractors in application of the so-called "De Groote" decree-law of 1947. Specifically, this decree-law aimed at promoting applied research in industry in order to improve its competitiveness. In application of this law the statutory contributing members of BBRI are the more than 70.000 Belgian construction companies, most of which are SMEs. According to its statutes BBRI has the following three main missions:

- to perform scientific and technical research for the benefit of its members
- to supply technical information, assistance and consultancy to its members
- to contribute in general to innovation and development in the construction sector in particular by performing contract research upon request of the industry and the authorities.

BBRI operates a technical advice service, offering primary advice related to day-to-day (technical) problems on the construction site to all building professionals. As soon as the construction works have started, the advice is however only delivered on the request of and to the (general) contractor. The purpose of this technical advice service is to prevent conflicts and to propose solutions which are acceptable to all stakeholders involved in the construction project. Besides this technical advice service BBRI is also involved in a series of technological advice projects. These projects, which are financially supported by regional authorities such as IWT Flanders (<http://www.iwt.be>), DGTRE (<http://recherche-technologie.wallonie.be/>) and IRSIB-IWOIB (<http://www.irsib.irisnet.be>), have the objective to stimulate the development and use of innovative technologies.

Through these technical and technological advice activities (and especially via the involvement in 2 projects oriented towards the use of special performance concrete technologies) BBRI is often confronted with questions related to the quality of architectural cast-in-place concrete. Sometimes BBRI is asked for advice in the design phase, i.e. before a contractor has been chosen, or right before starting up the concreting operations. However, in too many cases the opinion of BBRI is only requested for *after* the architectural concrete works have been finished partially or wholly. Most of the questions relate to variations in colour and shading, the number and size of bugholes (surface voids) and the presence of local defects in the neighbourhood of form joints and ties holes.

Based upon this practical experience a number of recommendations for the specification and execution of architectural cast-in-place concrete will be given.

## **2 BE REALISTIC ABOUT EXPECTATIONS**

Clients and architects choosing for a design in architectural (or visual) cast-in-place concrete should have a clear understanding of what is possible with the material, and what is impossible or difficult to guarantee. The feasibility of the design should be checked as soon as possible in order to prevent later problems or excessive costs. Demanding uniformity of colour on all concrete surfaces, total absence of pores, a uniform spread of the pore structure in terms of size and distribution, total absence of efflorescence or other defects are perhaps easy to put in specifications, but are impossible to realize and/or guarantee with concrete (Apers, 2000; DBV-BDZ, 2004). It makes therefore no sense to use such terminology in drawings and specifications.

Clients and architects should also realise that some blemishes are avoidable and others are not. Some defects may be present, even if the contractor took all necessary precautions and demonstrated competence, workmanship and a sharp eye for detail (ACI, 2004). Small variations in colour or texture for instance may occur, and their acceptance should be essentially determined based upon the specifications and the sample panels. Occasionally rust stains at the underside of horizontal concrete elements or in vertical surfaces may be present. The same holds for occasional colour changes and aggregate-rich surfaces due to small leakages at form joints. Evaluating the importance of such blemishes and deciding whether or not to accept them, should be done with the overall quality of the concrete structure in mind. Only if rust is present everywhere, nearly all form joints have been leaking or the concrete surface suffers from improper placement or lack of compaction (resulting in pockets of segregated aggregate), judgement may be harsh and one may use terms as execution errors and lack of quality.

The design should furthermore provide for a certain degree of 'flexibility', meaning that it should be adaptable to changes proposed during the concreting operations. This is particularly relevant for the formwork. At the design phase, contractor and/or form manufacturers, who should normally be the most aware of capabilities and limitations of formwork systems, are in general not present. However, the formwork and formwork labour can account for more than half of the overall cost of the concrete structure, and often more in an architectural concrete structure (ACI-ASCC, 1998). The search for a good equilibrium between the owner's budget, the desired appearance of the architectural concrete as defined by the architect and the optimization of the formwork system is, therefore, in most cases a necessity.

### 3 PREPARE PERFORMANCE-BASED SPECIFICATIONS

In most cases where BBRI intervenes, expectations of client and architect with regard to the quality of the concrete surface are high, certainly if they have used the term “visual” or “architectural” concrete in their specifications. However, in most specifications we have been confronted with, the expectations of client and architect haven’t been translated in clear surface quality and appearance requirements. The absence of a standard or guidance document in Belgium for the specification of architectural cast-in-place concrete is probably causing this. Such guidance document does as a matter of fact only exist for precast architectural concrete (PROBETON, 2001).

Belgium has declared the ENV 13670-1 as NBN ENV 13670-1 applicable for the execution of concrete structures in 2000, but only started to use it as a reference in technical specification documents when the standards NBN EN 206-1:2001 and NBN B15-001:2004 for the specification, performance, production and conformity of concrete were put into practice. As can be expected from the provisional nature of the ENV 13670-1, practice has already illustrated the limitations and hiatus of the standard. The practical value of the standard for architectural cast-in-place concrete is also quite doubtful. Only one paragraph of the prestandard deals with the surface finish of concrete structures. This §5.6, entitled “Surface Finish”, states the following: *“If special finishes are required, these shall be stated in the project specification. Trial concrete panels of suitable size may be specified as a basis for approving the surface quality.”* A note was added, probably hoping to give a bit more guidance: *“Surface finish depends on the type of formwork, concrete (aggregates, cement, addition, admixtures), execution and protection during the subsequent construction.”*

Some progress may be expected with the new version of the standard, now already available as a draft prEN13670:2007. In the main body of this draft standard one can find the following in §5.4(6): *“Where the design of the finished permanent structure requires particular surface finish, it shall be stated in the execution specification.”* The same is repeated in §8.8. Apart from these general requirements, the draft standard also includes some guidance on surface finish in the informative annex F on concreting. First of all, it is stated that the specification should include requirements for:

- the formwork face material.
- colour. Interesting to note is that the standard explicitly states that there are no requirements for colour consistency or shade unless it is a special finish using special coloured materials.
- blowholes (size, depth and frequency)
- abrupt irregularities (size and frequency, formwork face irregularities only)
- making good (allowed or not?).

Secondly, it draws the attention to the fact that the type and quality of surface finish for formed and unformed surfaces can vary from basic to special. As a matter of fact it proposes in table F.4 four types, i.e. basic, ordinary, plain and special. With regard to the scope of this article, which is essentially limited to the visual quality of the formed surfaces, only the plain and special finishes are relevant: A *plain finish* is used for surfaces where the visual effect is of some importance. A *special finish* refers to situations where special requirements have to be given, i.e. areas of exposed architectural finish.

Although both versions of the standard stress the importance of specifying surface finish requirements, and the draft standard even proposes a classification, they do not give much

practical guidance on how to specify and execute architectural concrete. In some European countries further guidance is available:

- The German Merkblatt Sichtbeton (DBV-BDZ, 2004) proposes a classification for architectural cast-in-place concrete based upon requirements for the texture, the pore distribution, the colour consistency, flatness, construction joints and formwork seams and associates to this classification the necessity of constructing trial panels before launching the construction work, the quality of the formwork material and the cost implications. Based upon this classification the Merkblatt gives further guidance for specifiers and contractors.
- The Dutch CUR Recommendation on Architectural Concrete (CUR, 2004), which may be considered as a kind of annex to the Dutch Standard NEN 6722:2002, is another interesting document dealing with cast-in-place and precast concrete. NEN 6722:2002 already provides 3 classes of visual concrete A, B and C, but the CUR Recommendation details this further by separating Class B into 2 classes B1 and B2. The Recommendation offers besides this classification criteria for specifying and assessing architectural concrete and guidance for the execution and inspection. Class B1 is considered to be realisable for cast-in-place *and* precast concrete, class B2 is *usually* only to be practiced for precast concrete.
- The Luxemburg Technical Specification Document for Concrete Works CDC-BET (MTP, 2007) and to be considered as a part of the Luxemburg normative framework on concrete, includes a chapter on the specification and assessment of visual concrete. It is clearly inspired on the German approach, but provides in a number of cases more detail. This is amongst others the case for the criteria for assessing the colour homogeneity in which the CIB grey scale (CIB, 1973) is used.
- Finally, also Austria disposes of a standard in which a classification for the surface finish of concrete is defined. ÖNORM B 2211:1998, entitled „*Beton-, Stahlbeton- und Spannbetonarbeiten – Werkvertragsnorm*“, defines „*sichtbetonklassen*“ based upon colour consistency, texture and pore distribution.

For Belgian concrete practice these documents may certainly be helpful and inspiring for writing technical specifications, but they are difficult to be declared as applicable since the Belgian normative framework differs from that of the neighbouring countries. At the moment different stakeholders are envisaging the development of local guidance documents for cast-in-place architectural concrete. In this regard a seminar is organized on the 25<sup>th</sup> of September 2007 by the Belgian Concrete Society and the Royal Flemish Institute of Engineers.

#### 4 INVOLVE ALL ACTORS

Architectural concrete construction necessitates close collaboration between and intense coordination of all building professions present on site. Architect, structural engineer, (general) contractor and ready-mixed concrete supplier, all of them may have an impact on the final result. The architect, together with the client, defines the structure and the desired appearance of the architectural concrete. Architect and structural engineer are the main responsible parties for drawings and specifications on which the price bid, and subsequently the choice of the contractor, will be based. The detail and quality of the specification are therefore key elements for a successful architectural ready-mixed concrete project. If very close tolerances are required, this should be specified. If not, the contractor's bid will not reflect these higher costs and discussions, negotiations and distrust will be the consequence.

One way to involve all actors from the beginning and to avoid misunderstandings is to organize (if legally allowed) a prebid conference or meeting between the architect, engineers, prospective bidding contractors, and if useful the ready-mixed concrete suppliers (ACI, 2004). At such a conference/meeting contractors may even point out that some desires or requirements are impossible to fulfil. In any case such a conference will make it clear to all parties what level of quality is associated to the project.

Using reference samples and providing full-scale sample panels to be constructed on site with typical equipment, materials and procedures (sometimes one may be requested to test multiple execution alternatives) are other ways to draw attention to the surface quality requirements. The aim of such sample panels is to provide for a reference that should be met by all subsequent concreting activities. The sample to be used as reference should therefore be approved by client and architect, and should remain on site until the end of the construction works.

Due to time constraints and the limited size of a lot of architectural concrete construction works the ready-mixed concrete supplier often receives late or insufficient information about the surface quality requirements. As the concrete technology is one of the determinant factors for the final visual quality of the concrete surface, this often poses technical problems or launches financial discussions. The concrete supplier needs to take (costly) precautions to guarantee constant concrete properties and minimal colour differences between subsequent concrete loads. Having a separate or sufficient stockpile for the different constituent materials is in nearly all cases a necessity. Testing the influence of certain admixtures or additives such as fly ash on the surface finish may also be needed. Controlling the stability of the water-cement ratio and the quantity of fine materials has also been proved to be critical.

## **5 ASSURE AND CONTROL QUALITY**

As most of concreting operations in Belgium are taking place on small job sites, experience with the use of quality plans for the execution of concrete works is rather limited. Only contractors working for government agencies or important project developers may have been confronted with the requirement to define quality control and inspection procedures for the execution of concrete structures. It is however a reality that both NBN ENV 13670-1:2000 and prEN13670:2007 deal extensively with quality plan, documentation requirements and inspection activities.

One may expect that the growing use of architectural cast-in-place concrete will result in an increasing demand for specific quality management procedures for concreting activities. The number of people devoted to quality management and control will of course vary with the size of the company, the size of the construction work and its complexity. Aspects which may be covered in quality plans are amongst others:

- the quality control and inspection plan,
- the construction, maintenance and protection of field sample panels,
- the qualifications and responsibilities of contractors, project superintendents, forming and concrete subcontractors, ready-mixed concrete suppliers,
- reports and logs on concrete placements,
- the logistic organisation of the jobsite, and especially the delivery, storage, handling, maintenance and repair of materials and formwork.

## 6 USE QUALIFIED AND EXPERIENCED PERSONAL

One of the drawbacks of (public) procurement systems is that they focus at the bid stage largely on the price of the work, and not enough on the experience and quality image of the contractors. As far as architectural cast-in-place concrete is concerned, qualifications and experience of the contracting company and of its personal at the jobsite are important elements to consider. Experienced crews are not only a key to productivity, efficiency, return and timely delivery, but also to accuracy and quality.

Unfortunately the discontinuous, project-based nature of construction activities leads to evident problems in communication and organisational learning. The experience of a crew with architectural cast-in-place concrete in one project doesn't give any guarantees for other project situations, unless the contractor manages and exploits this experience and know how. The knowledge (and quality) management associated costs should be offset by a greater customer satisfaction, more business, lower uncontrolled costs associated with low-quality work (repair, removal and replacements, unmet schedules, costs of litigation) and (let's hope) higher prices (ACI, 2004).

## 7 CONCLUSIONS

On site concreting of architectural concrete is clearly not easy, but it is possible. It involves organisational and technological measures, it requires an intensive communication between all actors of the concreting process, it necessitates coordination, know how and quality assurance. But most of all on site concreting of architectural concrete needs realistic objectives and adopted technical specifications.

## 8 REFERENCES

- ACI 303R-04, Guide to Cast-in-Place Architectural Concrete Practice, Reported by ACI Committee 303, ACI, 2004.
- ACI-ASCC, "The Contractor's Guide to Quality Concrete Construction", American Concrete Institute and American Society of Concrete Contractors, Second Edition, 1998.
- Apers J. (2000), "Het uiterlijk van beton", Dossier Cement, n°22, Febelcem, Brussels, June 2000.
- CIB n° 24, "Tolerances on Blemishes of Concrete", CIB (Conseil International du Bâtiment), Report n° 24, 1973.
- CUR Bouw en Infra, "Aanbeveling 100 – Schoon beton: Criteria voor de specificatie en beoordeling van betonoppervlakken", CUR Bouw en Infra, Gouda, April 2004.
- DBV-BDZ, "Merkblatt Sichtbeton", Deutscher Beton- und Bautechnik-Verein and Bundesverband der Deutschen Zementindustrie, August 2004.
- MTP, "Cahier des charges concernant les travaux de bétonnage (CDC-BET)", Grand Duché de Luxembourg, Ministère des Travaux Publics, January 2007.
- PROBETON, "PTV 21-601: Geprefabriceerde architectonische en industriële elementen van sierbeton", PROBETON, Brussels, 2001.



# **Topic 1**

Tailored properties of concrete



## TESTING AND IMPROVING THE STABILITY OF CONCRETE WITH FLOWABLE CONSISTENCY

*Jürgen Macht, Peter Nischer*  
*Research Institute of the Austrian Cement Association*  
*A – 1030 Vienna, Reisnerstr. 53*

### SUMMARY

Concrete used for bored piles and diaphragm walls has normally a flowable consistency with a spread of about 60 cm. Problems occur repeatedly in processing this concrete type due to segregation because of settlement of coarse aggregates. This causes the surface-near areas to be enriched with water and powder-fine particles. When these problems do not occur the fresh concrete can be said to be stable. The loss of stability leads to quality problems and additional costs for the repair of the damage. Hence, improving the stability is an important topic for this type of concrete. Powder optimization is the key for improving the stability. Moreover, the testing of the stability is of great importance. Compression tests reflect the behaviour of the concrete during placement and thus allow assessing the concrete before placement.

### 1. INTRODUCTION

When casting concrete components of greater height with concrete with flowable consistency, e.g. bored piles or diaphragm walls, the imposed load acting in the concrete can lead to an enrichment of water and powder particles in the surface-near areas during and following compaction, especially when the concrete has an inappropriate grading curve. This enrichment can be measured by means of a so called pressure test. The apparatus developed for this test by the technical testing and research institute bpv Lanzersdorf comprises a pressure-tight 10 l pot (Eisenhut and Pekarek, 2007). For the test, the desired air pressure (in general 3 bar over a period of 15 minutes) is regulated via a pressure valve and measured with a calibrated manometer. At the end of the test, the cover of the pot is removed and the water content in the surface near layer – i.e. of the upper 2 cm – is tested by drying.

### 2. TEST PROGRAMME AND RESULTS

Several types of concretes - all of them with a maximum particle size  $D_{\max}=16$  mm containing  $208 \text{ l/m}^3$  water were investigated with the pressure test. The cement, addition and superplasticizer contents as well as the spread according to EN 12350-5 of the concretes are compiled in Tab. 1; the grading curves are presented in Tab. 2. The particle size distributions of the powders including the fines of the aggregate were tested by means of the FPIA (flow particle image analyser, for details see (Macht and Nischer, 2006), the particle size distribution of the cements and additions in the concretes investigated are shown in Fig. 1. The reference grading curves in Tab. 2 for the concrete as well as for the powders in Fig. 1 were determined according to (Macht and Nischer, 2006).

Tab. 1 Spread, superplasticizer- and powder-content, water enrichment of the investigated concretes

Concrete	Spread [cm]	Super- plasticizer [kg/ m <sup>3</sup> ]	Cement		Additions		Water- enrichment [%]
			Type <sup>*</sup>	[l/m <sup>3</sup> ]	Type <sup>**</sup>	[l/m <sup>3</sup> ]	
Nr. 1	64	1,96	1	93	-	-	56
Nr. 2	66	1,96	2	93	-	-	12,5
Nr. 3	66	1,96	3	93	-	-	25
Nr. 4	61	4,60	2	87	A	6	5
Nr. 5	66	5,60	2	87	A	6	14
Nr. 6	66	2,30	1	93	B	34	25
Nr. 7	66	2,41	1	127	-	-	12
Nr. 8	66	2,30	2	93	B	34	16
Nr. 9	71	5,40	2	127	-	-	12
Nr. 10	64	3,00	1	117	C	48	10
Nr. 11	75	5,00	1	117	C	48	10

\* 1 = CEM II 42,5N ( $\varphi=3,0$  kg/m<sup>3</sup>); 2 = CEM II 42,5R ( $\varphi=3,0$  kg/m<sup>3</sup>);  
 3 = CEM I 52,5R ( $\varphi=3,0$  kg/m<sup>3</sup>)

\*\* A = microsilica ( $\varphi=3,0$  kg/m<sup>3</sup>); B = rock powder 1 ( $\varphi=2,7$  kg/m<sup>3</sup>);  
 C = Rock Powder 2 ( $\varphi=2,7$  kg/m<sup>3</sup>)

Based on visual assessment, all concretes – except Concrete 4 and Concrete 10 – were approaching the point of segregation and would have been unable to accommodate larger additions of water or superplasticiser. The water enrichment (in percent referring to the amount of mixing water) of these concretes in the surface-near layer determined with the pressure test is shown in Fig. 2 and are summarized in Tab.1.

Tab. 2 Grading curves of the investigated concretes

Concrete	Sieve passing [Vol%] at mm										
	0.01	0.02	0.063	0.09	0.125	0.25	1	2	4	16	22
Reference <sup>*</sup>	5.0	7.0	11	13	15	21	38	48	62	100	
Nr. 1	1.1	2.5	8	11	15	19	38	49	62	95	100
Nr. 2	3.0	6.6	12	14	16	19	38	49	62	95	100
Nr. 3	2.5	6.2	11	13	15	19	38	49	62	95	100
Nr. 4, 5	3.8	7.1	12	14	16	19	38	49	62	95	100
Nr 6.	1.5	3.3	9	14	19	23	41	51	64	95	100
Nr. 7	1.4	3.4	10	15	19	23	41	51	64	95	100
Nr. 8	3.4	7.4	14	16	19	23	41	51	64	95	100
Nr. 9	3.9	9.1	17	18	19	23	41	51	64	95	100
Nr. 10, 11	1.8	4.1	11	18	24	27	45	54	66	95	100

\* see (Macht and Nischer, 2006)

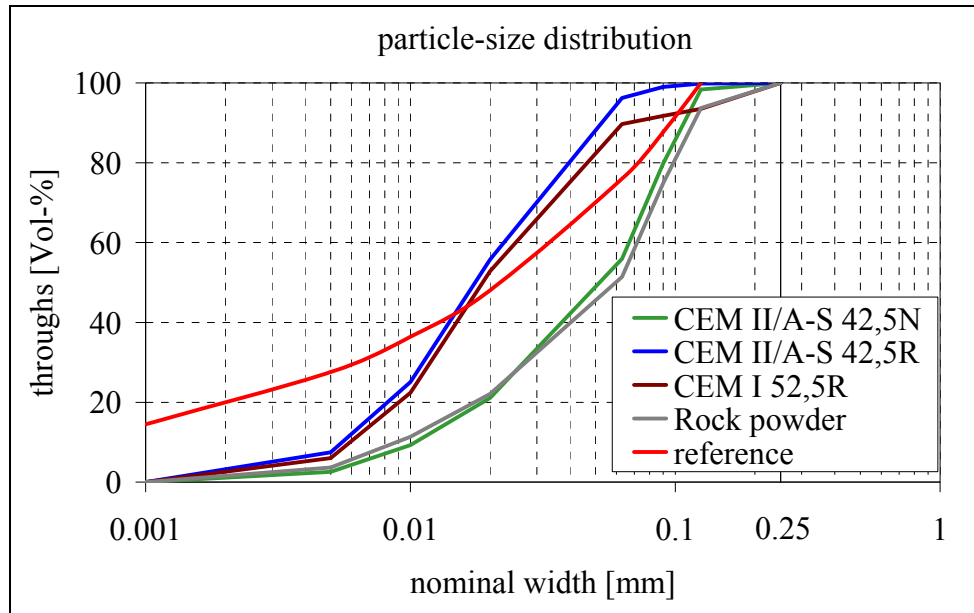


Fig. 1 Grading curves of the powder (Macht and Nischer, 2006)

### 3. DISCUSSION OF RESULTS

#### 3.1 Influence of powder content

A comparison of concretes 1, 2 and 3 with 120 l powder per m<sup>3</sup> concrete (93 l/m<sup>3</sup> cement, 27 l/m<sup>3</sup> aggregate) shows the lowest water enrichment in the surface-near layer for the relatively fine CEM 42.5 R, and the highest for the relatively coarse CEM 42.5 N. All three concretes contained the same amounts of water and superplasticiser and had about the same spread.

When the powder content in the concrete is increased to 153 l/m<sup>3</sup> (127 l/m<sup>3</sup> cement and rock powder, of this 26 l/m<sup>3</sup> from the aggregate), the water enrichment in the surface-near layer in the relatively coarse CEM 42.5 N (Concrete 6 and 7) is significantly lower; in the relatively fine CEM 42.5 R (Concrete 8) slightly higher than in the corresponding concretes with 120 l/m<sup>3</sup> powder. The higher powder content of these concretes required approximately 15% more superplasticiser than the concretes with a lower powder content, the spread being equal. The 127 l/m<sup>3</sup> of powder contained in Concrete 7 and

9 consists exclusively of cement. Concrete 9, made with the relatively fine CEM 42.5 R, achieves a spread larger by 5 cm than Concrete 7, made with the relatively coarse CEM 42.5 N; the water enrichment in the surface-near layer being equal.

When the powder content in the concrete is increased to 190 l/m<sup>3</sup> (165 l/m<sup>3</sup> cement and additions, 25 l/m<sup>3</sup> from the aggregate), the relatively coarse CEM 42.5 N (Concrete 11) can achieve a spread larger by 9 cm than is possible with 127 l cement per m<sup>3</sup> concrete (Concrete 7); the water enrichment in the surface-near layer being equal. The amount of superplasticiser required for a spread of 66 cm is larger by more than 60% than with 120 l powder per m<sup>3</sup> concrete.

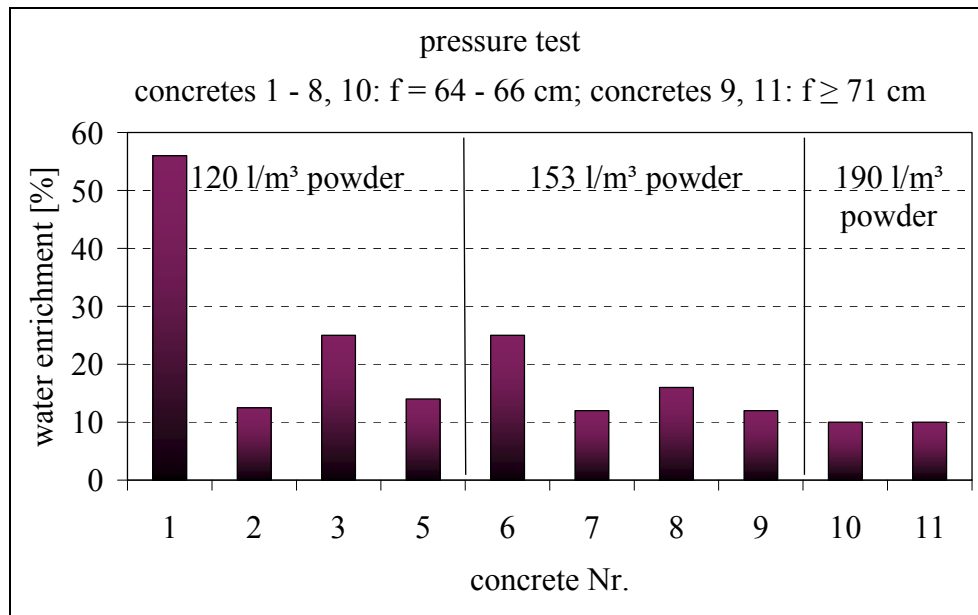


Fig. 2 Water enrichment in the upper 2 cm of the investigated concretes

When exchanging 7% of the relatively fine CEM 42.5 R with microsilica in the concrete containing 120 l powder per m<sup>3</sup> concrete, the superplasticiser required for achieving the same spread of 66 cm (Concrete 5) increases 3.5-fold. The exchange increases the water enrichment in the surface-near layer only slightly, as the superplasticiser requirement is then significantly higher.

### 3.2 Influence of particle size distribution

Based on the particle size distribution (Tab. 2), the results in Fig. 2 can be explained as follows:

1. Concretes with 120 l powder per m<sup>3</sup> concrete (93 l/m<sup>3</sup> cement, including 27 l/m<sup>3</sup> from the aggregate):

The powder content of these concretes is about as large as required for an optimal particle size distribution. The grading curve of the concretes at 0.125 mm and above corresponds to the reference grading curve, see Tab. 2.

- a) Concretes 1, 2 and 3 differ only in respect of the cement type and have the same grading curve in a particle range  $\geq 0.25$  mm. The relative to Concrete 1 significantly lower deviation from the “reference value” in a particle range  $\leq 0.09$  mm in Concrete 2 can explain the good stability of the fresh concrete of Concrete 2. The compared to Concrete 2 significantly poorer performance of Concrete 3 with CEM I 52.5 R can only be partly explained by the less favourable particle distribution.
- b) Larger particle content in the range  $\leq 0.01$  mm: A comparison of Concretes 2 and 5 shows that in the CEM II/A-S 42.5 R investigated, a partial substitution of the cement with microsilica is unfavorable due to the higher demand for superplasticiser and/or water, despite the better adjustment to the “reference grading curve” in the  $\leq 0.01$  mm range (Tab. 1). The larger quantity of fine interstitial particle (microsilica) does here not lead to an improvement.



2. Concretes with 153 l powder per m<sup>3</sup> concrete (127 l/m<sup>3</sup> cement and rock powder, including 26 l/m<sup>3</sup> of the aggregate):

The powder content of these concretes is larger by approx. 30 l per m<sup>3</sup> concrete than required for an optimal particle size distribution. Due to the higher powder content, the grading curve is finer than required also at 0.25 mm and above (Tab. 2).

- a) Concretes 6, 7 and 8 require higher amounts of superplasticiser than Concrete 2 to achieve the same spread and, accordingly, have a higher demand for water, which leads to a worth stability (in comparison with the Concrete 2).
- b) The rock powder added to Concrete 8, compared to Concrete 2, diminishes the ability of the powder to adapt to the “reference grading curve”. This explains the poorer stability of these concretes compared to Concrete 2.
- c) Concretes 6 and 8 contain the same amounts of cement and rock powder; a direct comparison based on the grading curve appears to be possible and explains – due to the better adjustment to the “reference grading curve” (powder content higher  $\leq 0.063$  mm) – the better assessment of Concrete 8.
- d) Concrete 7 has practically the same grading curve as Concrete 6, except that it contains only cement and no rock powder. The particle index of the rock powder is not as good as the particle index of cement (Nischer and Macht, 2006) and, accordingly, has a higher powder requirement. The particles of the rock powder are moreover rougher than the particles of the cement (see (Nischer and Macht, 2006)). This explains why the stability of Concrete 6 in a fresh state is better than that of Concrete 6.
- e) Concrete 9 and Concrete 7 contain the same amount of cement. Concrete 9 contains the relatively fine CEM II/A-S 42.5 R, resulting in a better adjustment to the “reference grading curve.” This enables Concrete 9 to achieve a spread 5 cm larger than Concrete 7.

3. Concretes with with 190 l powder per m<sup>3</sup> concrete (165 l/m<sup>3</sup> cement and additions, including 25 l/m<sup>3</sup> from the aggregate):

The powder content of these concretes is approx. 70 l higher per m<sup>3</sup> than is required for an optimal particle distribution.

Concretes 10 and 11 exceed in the  $\geq 0.063$  mm range the “reference grading curve”, see Tab. 2. The reason for this is the high powder content (cement + rock powder). A larger mortar content in the concrete results in a larger spread than a smaller mortar content – the consistency of the mortar being equal. Concrete 11 has therefore an equally good stability in a fresh state as Concrete 7, although its spread is larger by 9 cm.

When assessing the powder in a concrete with a powder particle index (total sieve passages at 0.01 mm, 0.02 mm, 0.063 mm, 0.09 mm and 0.125 mm; multiplied with the powder content in the concrete), there seems to be a correlation between the spread that can be achieved without segregation and this powder particle index, as shown in Fig. 3. The larger this powder particle index, the larger is the achievable spread without segregation.

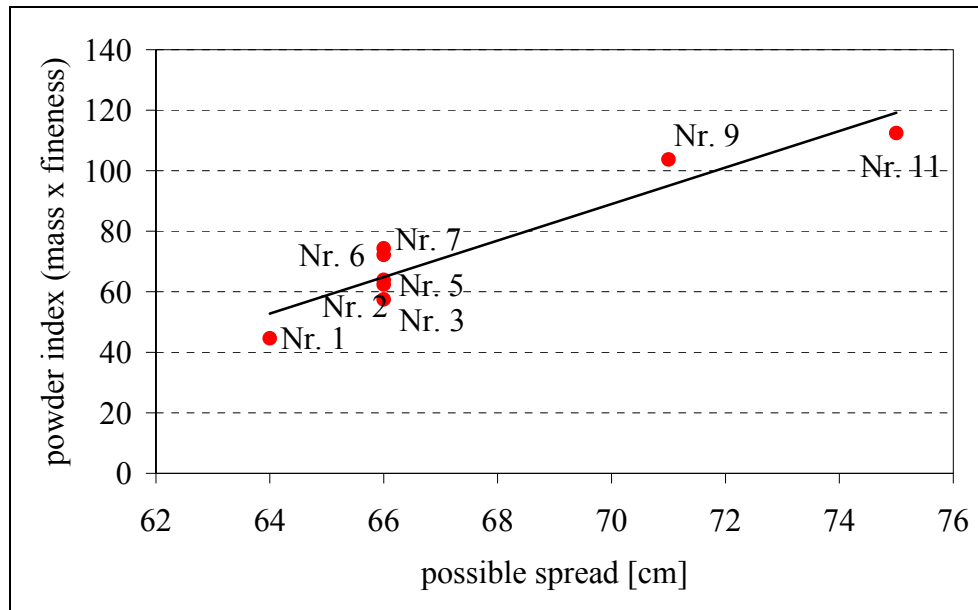


Fig. 3 Correlation between „powder index” and possible spread without segregation

#### 4. CONCLUSIONS

Stable fresh concrete that does not segregate during placement, and in which the coarse aggregate does not settle after compaction, requires more powder: the more flowable the concrete during placement the higher the powder content required. The larger the amount of water and/or superplasticiser is needed to achieve the desired workability, the larger the danger of segregation.

The better the particle distribution corresponds to the “reference grading curve” the less powder is required for a stable fresh concrete. An increase of the powder content will only improve the stability of the concrete if the adjustment of the powder to its “reference grading curve” is not negatively affected. But high contents of particles < 0.01 mm (e.g. microsilica) frequently do not improve the stability due to the higher water and superplasticiser demand.

#### 5. REFERENCES

- Eisenhut, T. and Pekarek, A. (2007), „Bluten von Pfahl- Schlitzwandbeton“, *Pfahl-Symposium*, Braunschweig.
- Macht, J. and Nischer, P. (2006), „Mehlkornoptimierung – Notwendigkeit und Möglichkeiten zur Ermittlung der Korneigenschaften“, *BFT Heft 4*
- Nischer, P. and Macht, J.(2006), „Weiche Betone mit verschiedenem Mehlkorn – Maßnahmen zur Verbesserung der Verarbeitbarkeit“, *FT Heft 8*

## **BLEEDING OF CONCRETE IN SPECIAL FOUNDATION ENGINEERING**

*Dipl.-Ing. Thomas Eisenhut, Dipl.-Ing. Alexander Pekarek  
Bautechn. Prüf- und Versuchsanstalt GmbH (bpv), Grund-, Pfahl- und Sonderbau GmbH  
Industriestr. 27A, 2325 Himberg, Austria  
thomas.eisenhut@bpv.at, alexander.pekarek@gps-bau.com*

### **SUMMARY**

The dead weight of the fresh concrete and the resulting high concrete pressure in special foundation engineering is the major reason for the occurrence of bleeding. Since the fresh concrete pressure can not be proven by the standard method of ÖNORM B 3303:2002, the results are not representative for the construction of piles and diaphragm walls. A comparison of the standard method with the “Betonfilterpresse” (concrete filter press, a new method developed by Bautechnische Prüf- und Versuchsanstalt GmbH) shows, that an evaluation regarding bleeding is not significant due to the low water release of the standard method. However, the concrete filter press method allows a clear evaluation of the individual concrete formula by applying pressure to the fresh concrete.

The grain content  $< 0,125$  mm (M) of the concrete, the particle shape and the grading curve are the determining parameters for bleeding. Therefore, the W/M value represents a excellent way for evaluating the bleeding of concrete under pressure.

Today bleeding of max 40 kg/m<sup>3</sup> after 60 minutes at a pressure of 3 bar with the concrete filter press method seems to represent an acceptable value for the evaluation of concrete for special foundation engineering. This value can be easily achieved by changing the concrete formula.

### **2. INTRODUCTION**

Over the last few years an increased number of defects caused during the manufacturing process of piles and diaphragms walls in special foundation engineering can be noted. These defects mainly occur in cohesive soils. They are not caused by lack of compaction or by too stiff concrete. The defects and the enrichment of fine grain at the horizontal construction surfaces result rather from an insufficient stability of the concrete. Furthermore, at the interface between concrete and soil resp. concrete and reinforcement there is an elutriation of fine grain with simultaneous bleeding due to different densities of the concrete components. The main reason for these effects is the content of fine granularity add-ons as per the European standards ÖNORM EN 206-1:2005 and EN 12620:2005 as well as the national standards ÖNORM B 4710-1:2004 and ÖNORM B 3131:2004, which, together with the low granularity of the cement, cause the high bleeding of such “soft” concrete.

In order to avoid such defects, the Bautechnische Prüf- und Versuchsanstalt GmbH (BPV) was authorized to develop a test method for the determination of the stability of concrete under pressure. Furthermore, the mechanisms, which lead to the bleeding of concrete, should be investigated.

### 3. EVALUATION OF BLEEDING

Bleeding of concrete is measured with the standard method acc. to ÖNORM B 3303:2002, based on ÖNORM EN 480-4. Concrete is inserted into a cylindrical container (height: 250 mm). The segregation of water at the surface is measured until the bleeding stops.

A fast evaluation of bleeding at the construction site is rather impossible because of the duration of the above mentioned test (up to two hours or even longer). Furthermore, concrete pressures in special foundation engineering are typically significantly higher than in structural, e.g. at the bottom of a pile with a length of 12.5 m there will be a pressure of 3 bar. Hence a practical method to simulate the pressure ratios both for piles and diaphragm walls at reduced testing time, was developed by BPV. According to the filter press used for testing bentonite suspensions the BPV developed a concrete filter press, to be used locally at construction sites with minimal additional workload.

The major part of the filter press is a cylindrical container with a volume of about 10 litres and a hole in the bottom (Fig. 1) and a sieve and a filter above this hole. The cylinder is filled with the concrete up to top and slightly compressed by hand. The sealed concrete filter press is now pressurized with compressed air. The segregation of water is collected in a measuring cylinder and recorded over a particular time period. The bleeding of the concrete can be shown as the loss of water over a period in  $l/m^3$ .

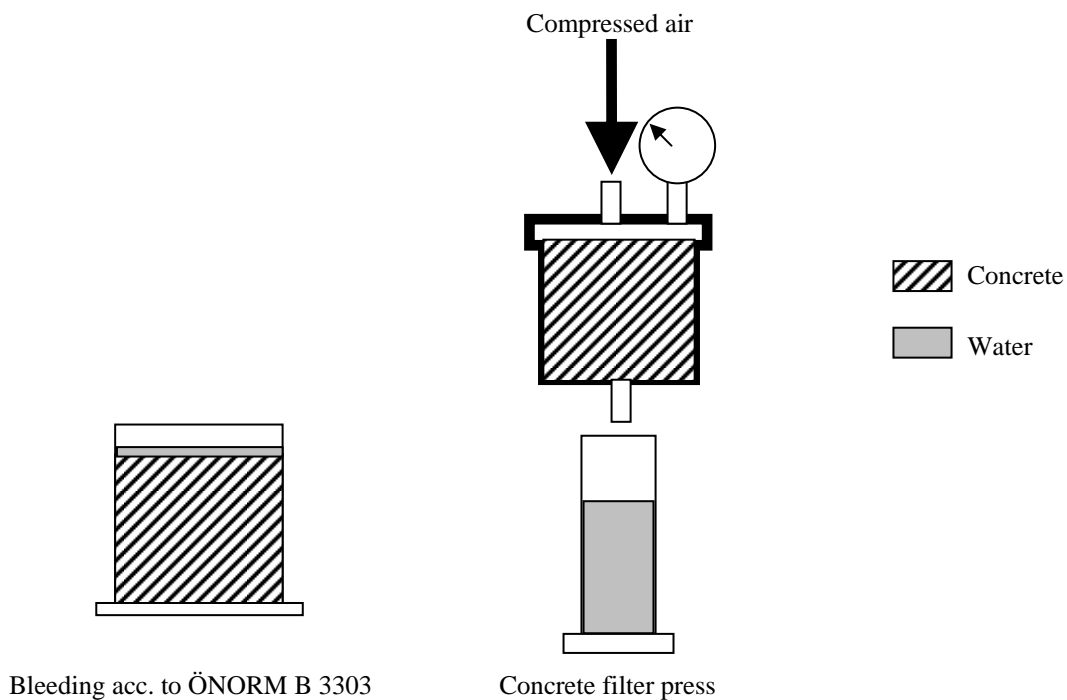


Fig. 1 Measuring equipment for bleeding of concrete

### 4. MECHANISM OF BLEEDING

Bleeding is a partial decomposition of concrete, which is readily mixed, placed and compacted. The segregation of water occurs at the surface during concreting or afterwards and continues until setting and hardening of the concrete (Schießl, 1998).

The major influencing factors of bleeding are the surface and the packing density of the solid parts of the concrete. An optimization of concrete to prevent from segregation of water would be effected by maximizing the surface and packing density of the solid parts (cement, additives and aggregates) of the concrete.

## 5. EXPERIMENTAL STUDIES

Based on a formula for standard concrete the following parameters were varied:

- content of binding ingredients
- content of additives
- content of water.

To ensure comparability of test results the ratio and the grading curve of the aggregates were kept constant.

The following types of cement were used:

- CEM I 42.5 R WT 38 C3A-frei (Portland cement)
- CEM II/A-M (S-L) 42.5 N (Portland composite cement)
- CEM III/B 32.5 N (blast-furnace cement)

The granularity of the cement varied. Fly ash with a latent hydraulic characteristics and granulated lime stone were used as additives.

Tab. 1 Basic composition of the concrete

Cement respectively binder (B)	kg/m <sup>3</sup>	370
Aggregates (0/4, 4/16, 16/32)	kg/m <sup>3</sup>	1880
Grain < 0.125 mm of the concrete (M)	kg/m <sup>3</sup>	400
Water (W)	kg/m <sup>3</sup>	185
W/B-ratio	-	0.46
Flow-table test for fresh concrete	cm	F59 (56 cm to 62 cm)

To allow a comparison of the tested concretes the fresh concrete was limited to 60 cm ± 1 cm at the flow-table test by adding an appropriate plasticizer.

## 6. EXPERIMENTAL RESULTS

### 6.1 Testing Method

To evaluate the differences between the standard method and the concrete filter press method, different concretes were mixed. In comparison to the concrete filter press the standard test acc. to ÖNORM B 3303:2002 shows only small differences between the itemized recipes (Fig. 1). The concrete mixture of the last two recipes (M=450 kg/m<sup>3</sup>, W=185 kg/m<sup>3</sup>) are distinguished by the type of cement and the additive content.

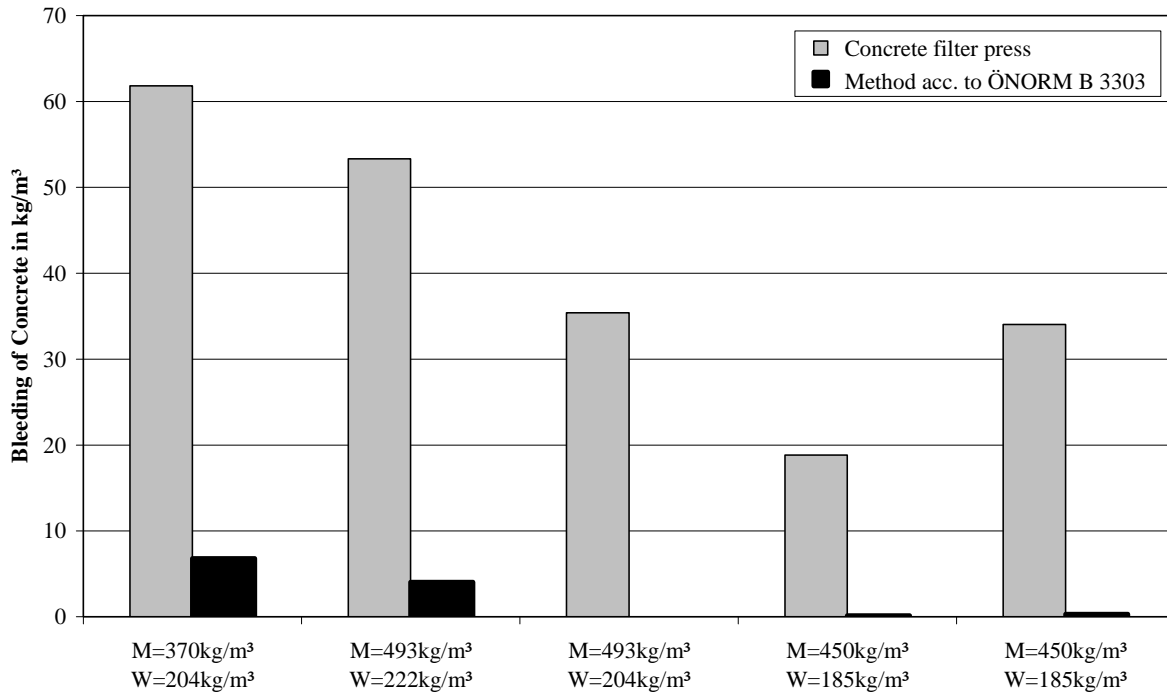


Fig. 2 Comparison of the standard method and the concrete filter press

## 6.2 Water Content and Grain Content < 0,125 mm (M)

The water content, in combination with the grain content < 0.125 mm (M), is one of the most important parameters for the stability of concrete and consequently for bleeding of concrete. The decrease of the water content causes a decrease of bleeding (Fig. 3).

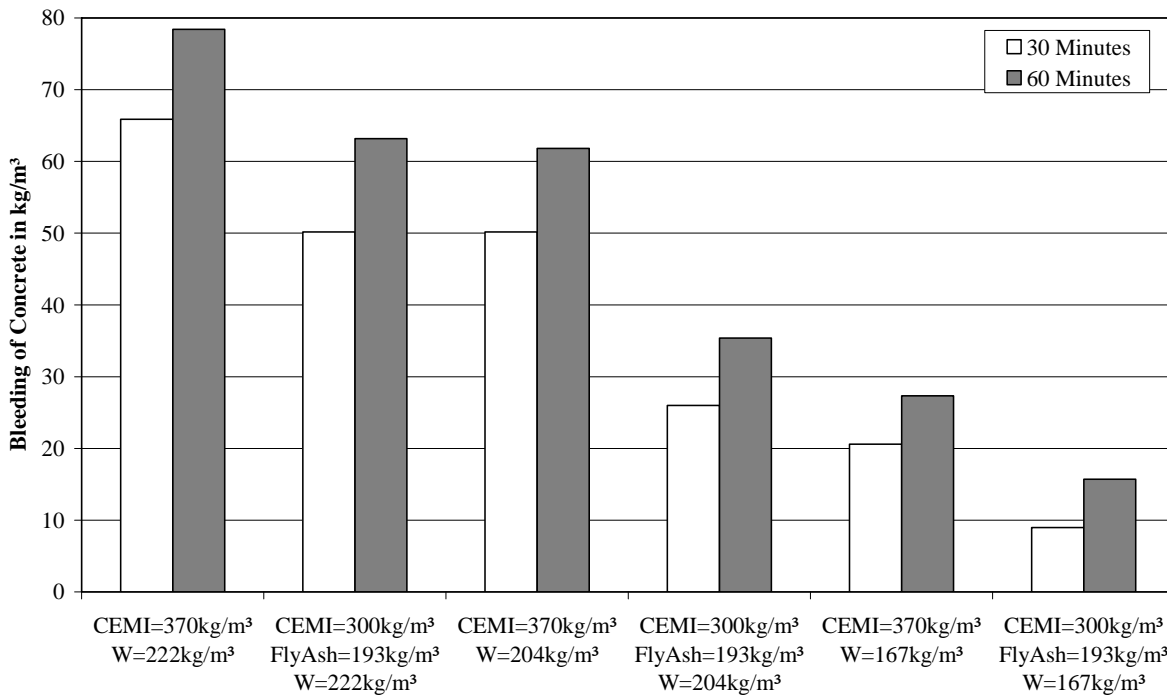


Fig. 3 The influence of water content and grain content < 0.125 mm on bleeding of concrete



As expected, an increasing content of grain < 0.125 mm caused a decreasing bleeding of the concrete. This is irrespective of the type of grain < 0.125 mm (Fig. 4).

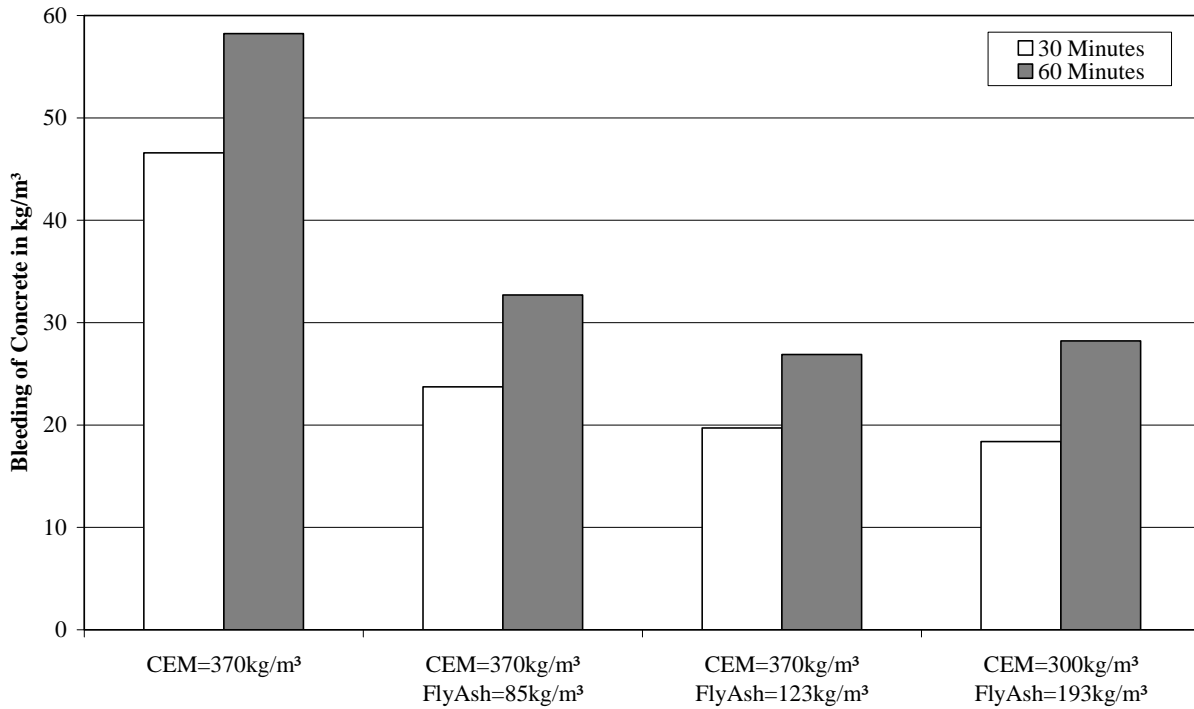


Fig. 4 The influence of water content and grain content < 0.125 mm on bleeding of concrete

## 7. CONCLUSIONS

The experiments show considerable differences between the standard method acc. to ÖNORM B 3303<sup>1</sup> and the concrete filter press method. The standard method shows only tendencies because of the very small quantities of segregated water. However, the results with the concrete filter press show considerable differences between the individual tests. As shown in the performed tests the grain size < 0.125 mm is essential for bleeding of concrete. The amount of grain < 0.125 mm depends on the fineness and the amount of cement and additives as well as the water content. Regarding the bleeding of concrete the water to grain < 0.125 mm ratio (W/M) is significant.

Fig. 5 shows the dependence of bleeding on the W/M-content for several concretes with CEM I. The bleeding is regarded for 60 minutes at a pressure of 3 bar.

The regression line allows to qualify the M-content for concrete. Attentions should be paid to the fact, that the above mentioned regression line is only representative for the used source materials.

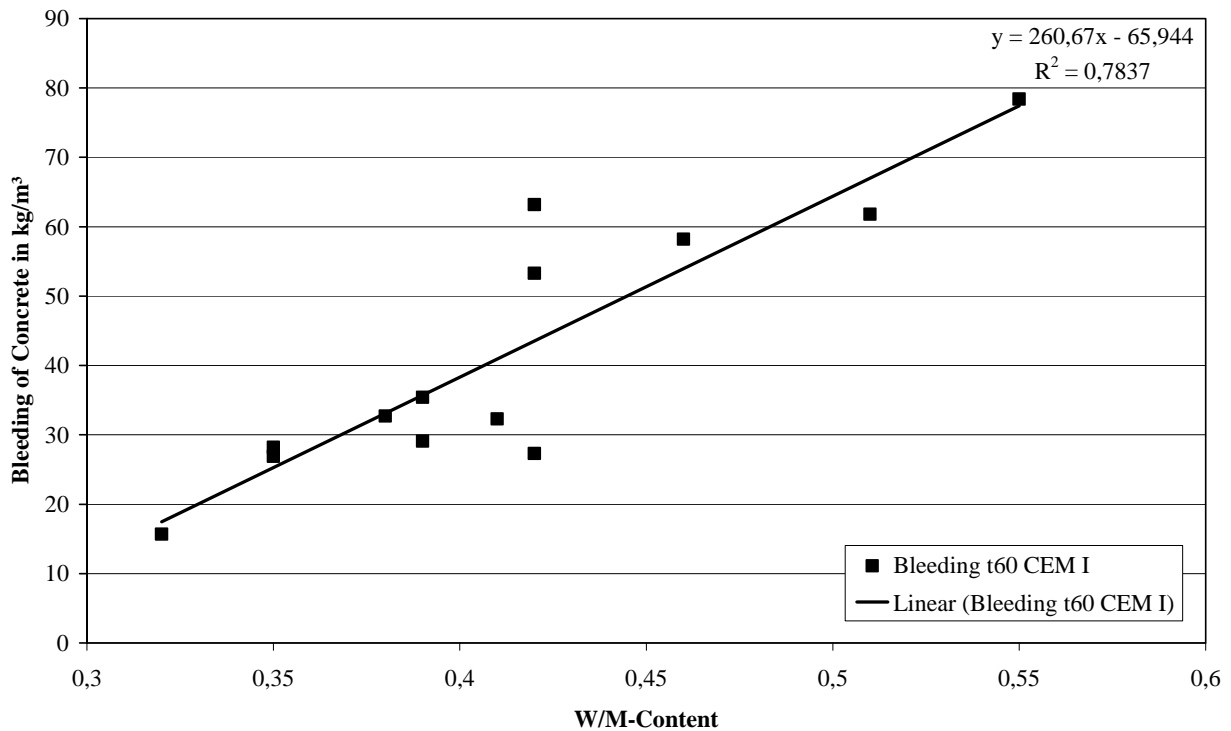


Fig. 5 Bleeding of concrete depending on the W/M-content

## 7. REFERENCES

- ÖNORM B 3303, „Betonprüfung”, Ausgabe 01. 09. 2002.
- ÖNORM EN 206-1, „Beton, Teil 1: Festlegung, Eigenschaften, Herstellung und Konformität”, Ausgabe 01. 11. 2005
- ÖNORM EN 12620, „Gesteinskörnungen für Beton”, Ausgabe 01. 04. 2005
- ÖNORM B 4710-1, „Beton, Teil 1: Festlegung, Herstellung, Verwendung und Konformitätsnachweis, (Regeln zur Umsetzung der ÖNORM EN 206-1)”, Ausgabe 01. 04. 2004
- ÖNORM B 3131, „Gesteinskörnungen für Beton, Regeln zur Umsetzung der ÖNORM EN 12620”, Ausgabe 01. 10. 2004
- ÖNORM EN 480-4, „Zusatzmittel für Beton, Mörtel und Einpressmörtel, Prüfverfahren, Teil 4: Bestimmung der Wasserabsonderung des Betons (Bluten)”
- Pekarek, A. (2007), „Untersuchungen zum Bluten weicher Betone im Spezialtiefbau”, Diplomarbeit, Universität für Bodenkultur, Wien, 02. 2007
- Schießl, P. (1998), „Bluten von Frischbeton, Schlussberichte zu den Forschungsaufträgen 3118 und 3119 der Forschungsgemeinschaft Transportbeton e.V.”, Düsseldorf, Beton-Verlag.

## **EFFECT OF GGBS ADDITIVE ON CHLORIDE ION BINDING CAPACITY OF SLAG CEMENTS**

*Katalin Kopecskó, György Balázs  
Budapest University of Technology and Economics, Hungary  
H-1111 Budapest Műegyetem rakpart 3katalin@eik.bme.hu*

### **SUMMARY**

Main purpose of our research was to study both the hydration and chloride ion binding mechanisms of slag cements. This paper deals with our test results on hardened and afterwards salt-treated cements modelling the influence of de-icing salt. Hydration both of naturally hardened and steam-cured cements were investigated as well as their chloride ion binding mechanisms by thermal tests and X-ray diffraction. The series of samples were cements with different amount of ground granulated slag (CEM I 42.5 N, CEM II/A 32.5 R, CEM III/A 32.5 N and CEM III/B 32.5 N-S). The chloride ion binding mechanism of ground granulated blast-furnace slag without cement clinker content was also studied.

Chlorides were bound in form of Friedel's salt. The formation of Friedel's salt and delayed ettringite increased between the ages 90 to 180 days. Test results indicated that steam cured cements can bind higher amount of chloride ions than naturally hardened ones. Chloride ion binding capacity of tested cements in decreasing sequence was the following: (1) CEM III/B 32.5 N-S; (2) CEM III/A 32.5 N, (3) CEM II/B-S 32.5 R; (4) CEM I 42.5 N. It was also experimentally shown that ground granulated blast furnace slag itself is able to bind chloride ions.

### **1. INTRODUCTION**

One of the most important effects influencing durability of concrete structures is the chloride ion ingress. The chemically bound chloride content does not induce corrosion of steel reinforcement. This paper deals with our test results on hardened and afterwards salt-treated cements modelling the influence of de-icing salt.

Interaction of chloride ions and cements can be modelled by studying directly the interaction of chloride ions and the clinker minerals. Several researchers studied chloride binding of clinkers when the chlorides were added to the mixing water (Balázs, 2001). These studies indicated that calcium-aluminate clinkers bind chloride ions in form of Friedel's salt (Friedel, 1897). Further studies were directed to the interaction of chloride ions and hydrated cements. These studies indicated that also hydrated aluminates and cements are able to bind chloride ions (Neville, 1995; Balázs et al., 1997; Kopecskó et al., 2005).

Steam curing is a generally used method in the production of precast concrete elements. Increased temperature accelerates the hydration resulting high early strength. The accelerated curing affected detrimentally both the long-term strength and the durability. Hooton et al. (2004) concluded that steam-cured concretes containing silica fume or blends of silica fume and ground granulated blast-furnace slag exhibit improved chloride penetration resistance compared to those of Portland cement concretes.

Luo et al. (2003) experimentally studied both the chloride diffusion coefficient and the chloride binding capacity of Portland cement or blended cement made of Portland cement and 70 % GGBS replacement with or without 5 % sulphate. They found that (i) chloride diffusion coefficient decreased; (ii) chloride ion binding capacity improved in samples of blended cement. Moreover the chloride ion binding capacity was lower in case of samples containing 5 % sulphate.

## 2. PURPOSE OF RESEARCH

Purpose of research was to answer the following questions:

- What is the effect of the slag content on the chloride ion binding of cements? Chloride ion binding capacity of cements was investigated in the function of test parameters.
- What is the influence of the curing temperature (natural hardening at 20°C, or steam curing at 80°C) on the hydration processes of cements?

## 3. EXPERIMENTAL STUDIES

Four types of cements were selected with different slag contents. Sulphate contents of cements were not modified (hence the influence of various sulphate contents was not studied separately for the cements). Samples of cements were prepared by the required amount of water to reach the standard consistence (semi-plastic) (MSZ EN 196-3) (Tab. 1).

Tab. 1 Cement types

Cements	Slag content	w/c
CEM I 42.5 N (OPC)	0 m%	0.273
CEM II/B-S 32.5 R	26 m%	0.272
CEM III/A 32.5 N	40 m%	0.285
CEM III/B 32.5 N-S	62 m%	0.302

Tests were carried out to study the influence of salt treatment and steam curing (Tab. 2). Additional tests were carried out to study the chloride ion binding of blast-furnace slag (steam-cured samples for 8 hrs. at 80°C with or without 5 m% sulphate content).

Tab. 2 Experimental programme

Series	Curing and exposure
1	100% r.h. at 22°C
2	100% r.h. at 22°C and salt-treatment
3	steam curing at 80°C and 100% r.h.
4	steam curing at 80°C and salt-treatment

The samples of series of 3–4 were steam cured for 3 hrs at 80°C than samples were kept at room temperature (22±3°C) and 100% r.h. Salt-treatment meant to keep the specimens in 10% NaCl solution, between 28 and 38 days (24 hrs in the salt solution, followed by 24 hrs of drying cyclically). Salt-treated samples were kept then at room temperature (22±3°C) and ~100% r.h. after this time. Tests of hardened samples were carried out in ages of 24 hrs, as well as 7, 28, 90 and 180 days. Hydration process was studied by thermal test (DTA/TG/DTG) using Derivatograph Q-1500 D and X-ray diffraction (XRD) using Philips PW 3710 diffractometer. Simultaneous application of thermoanalytical methods and powder diffraction made possible to carry out detailed analysis of phase modifications.

## 4. RESULTS

### 4.1 Results of XRD

X-ray patterns of salt-treated cements indicated the formation of calcium-aluminate-chlorohydrate, Friedel's salt ( $C_3A \cdot CaCl_2 \cdot H_{10}$ ). We also studied the influence of steam curing on chloride ion binding capacity of cements (Fig. 1).

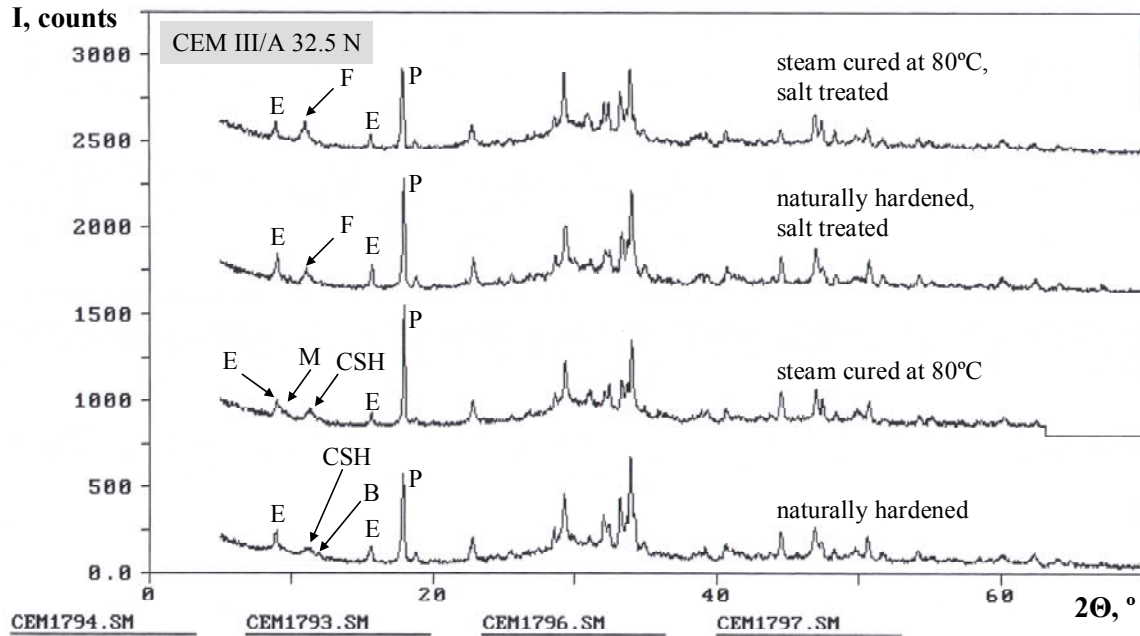


Fig. 1 Influence of steam curing and salt-treatment on cement hydration, X-ray patterns of CEM III/A 32,5 N A at the age of 180 days  
Notation: E-ettringite; F-Friedel's salt; M-monosulphate; P-portlandite, B-Brownmillerite, CSH-calcium-silicate-hydrate

The other  $Cl^-$ -containing hydrate, Kuzel's salt ( $C_3A \cdot 0,5CaSO_4 \cdot 0,5CaCl_2 \cdot H_{12}$ ) did not appear in salt-treated samples (Kuzel, 1966; Kopecskó et al., 2006). The intensity of Friedel's salt was higher in the steam cured samples than those of non-steam cured samples of cements.

X-ray patterns indicated formation of monosulphate ( $C_3A \cdot CaSO_4 \cdot H_{12}$ ) parallel to ettringite ( $C_3A \cdot 3CaSO_4 \cdot H_{32}$ ) formation in the accelerating cured samples (steam curing at 80°C).

The intensity of ettringite was higher in the salt-treated samples compared to the samples kept without salt-treatment. This observation can be explained with the reaction of sulphate ions released by the transformation monosulphate  $\rightarrow$  Friedel's salt. The reaction of sulphate ions and the AFm (aluminate-ferrite mono-) phases lead to the delayed (secondary) ettringite formation.

Additional tests were carried out with GGBS additive. We have experimentally studied if the steam cured granulated slag itself is also able to bind chloride ions. We have shown that the improved chloride ion binding capacity of slag cements is owing to the chloride binding

capacity of slag content even if its hydration was not in the typical environment of cements with high pH value. Chloride ion binding capacity of slag is provided by the hydration of the aluminate containing components of the glass phases. In addition to it we have shown that sulphate content (in our tests gypsum content was 5 m %) produces a decrease in chloride ion binding capacity of slag (Fig. 2).

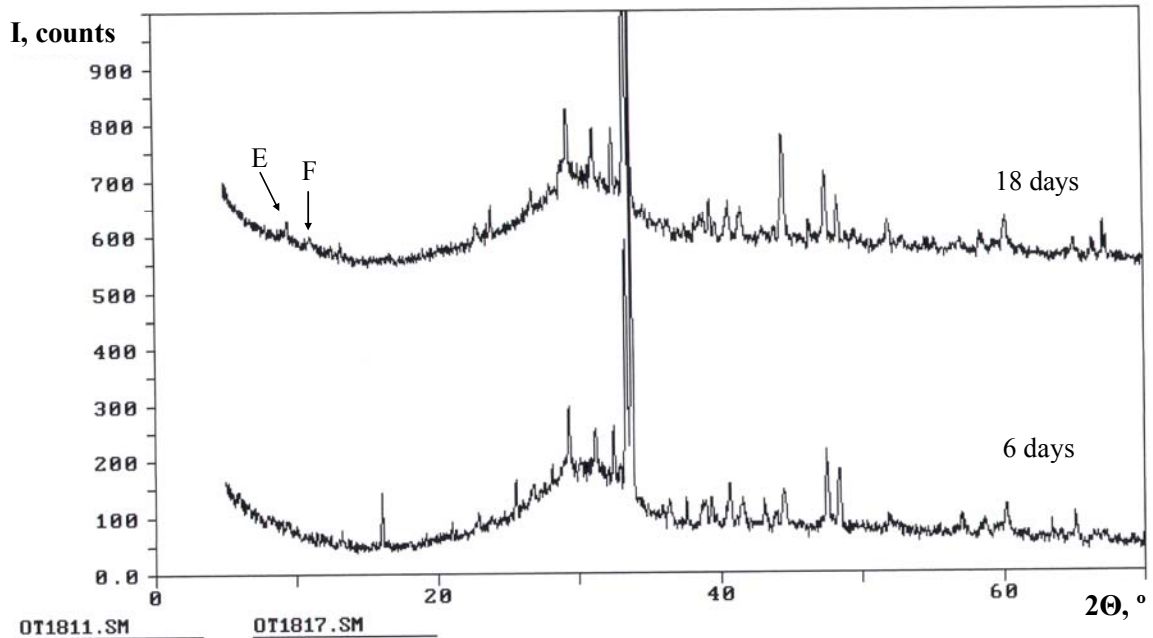


Fig. 2 X-ray patterns of blast-furnace slag (GGBS), steam cured at 80°C for 8 hours,  
a) at the age of 6 days (non salt-treated)  
b) at the age of 18 days (immersed in 10% NaCl solution between the ages of 6-10 days)  
Notation: F-Friedel's salt; E-ettringite

#### 4. 2 Results of TG/DTG/DTA

The most remarkable difference between the results of thermal tests of salt-treated and non salt-treated samples is the presence of a peak at approx. 360°C, which can be attributed to formation of Friedel's salt. About 40% of the water content (4 mole water) of Friedel's salt is lost below 200°C. Previously the chemically bound chloride content was calculated using indirect method where both the total and water soluble chloride content were measured with analytical methods (Dhir et al., 1996). They found that blast-furnace slag cement pastes have higher chloride ion binding capacity compared with the PC control. This conclusion is in accordance with our test results obtained from the thermogravimetric mass loss of the second dehydration step of Friedel's salt using the TG and DTG curves of thermal tests.

Fig. 3 shows the first derivatives of thermogravimetric curves (DTG curves) in case of non salt-treated (non steam cured, age: 90 days) and salt-treated samples steam cured at 80°C at the age of 180 days.

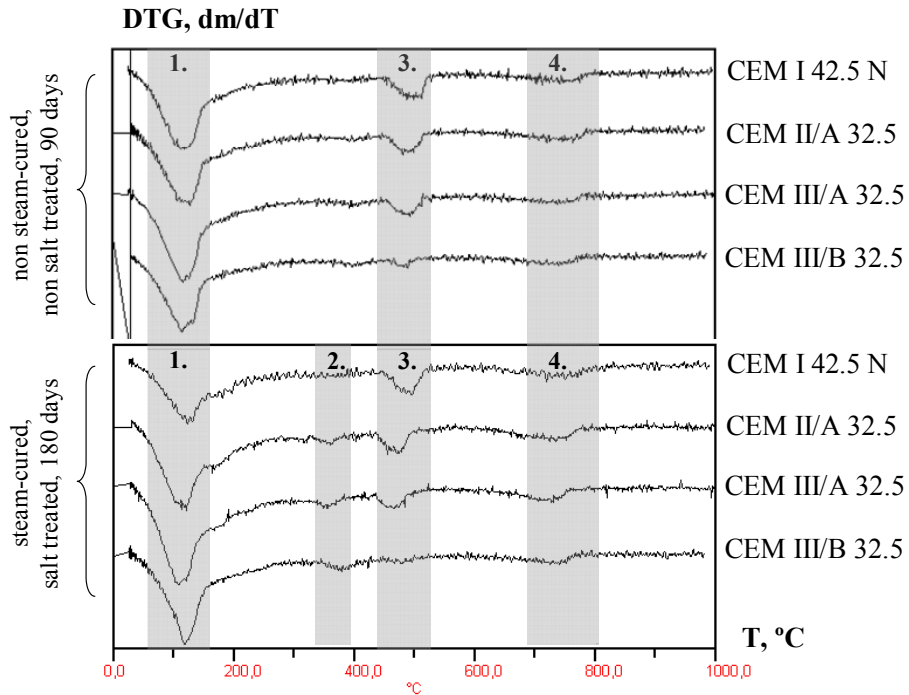


Fig. 3 DTG curves of non salt-treated and salt-treated samples, non steam cured samples (non salt-treated) at the age of 90 days; steam cured then salt-treated samples, at the age of 180 days, salt-treatment between the ages of 28-38 days  
 Notation: 1. ettringite and humidity; 2. Friedel's salt; 3. portlandite; 4. carbonates and CSH

The chemically bound chloride content was calculated from the second step of dehydration of Friedel's salt. 6 moles of water represent 1 mole of Friedel's salt. The stoichiometric factor calculating the amount of Friedel's salt is  $f_{FS} = 5,2$ . The chloride content in Friedel's salt is 12,6%. Fig. 4 shows the diagram of the chemically bound chloride content of salt-treated samples related to the mass of samples without ignition loss.

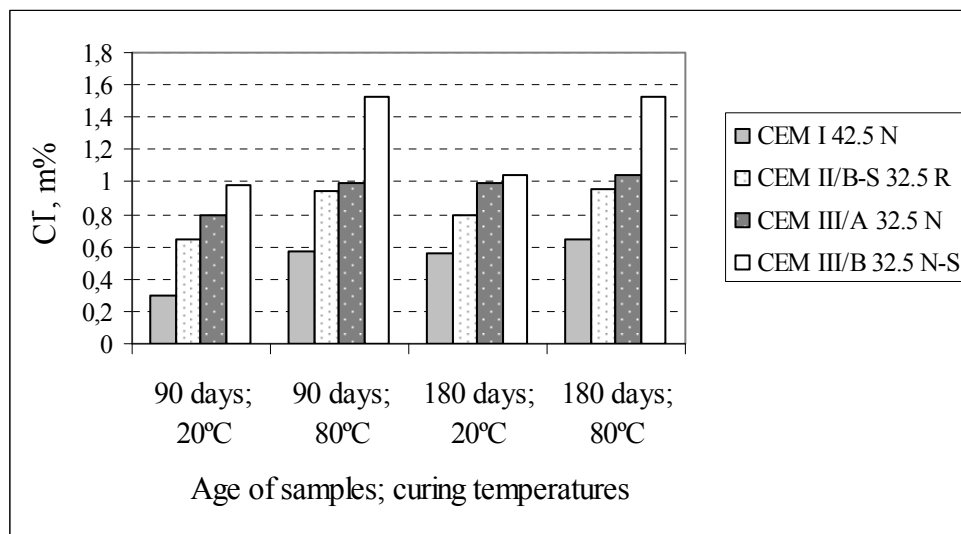


Fig. 4 Amount of chemically bound  $Cl^-$  ions (m%) related to the mass of samples without ignition loss as functions of ages and curing temperatures



## 5. CONCLUSIONS

Purpose of our research was to study the effect of GGBS additive and the influence of steam curing on chloride ion binding capacity of cements. Hydration as well as chloride ion binding mechanisms were investigated by thermal tests (TG/DTG/DTA) and X-ray diffraction (XRD). Four types of cements were selected with different replacement level of GGBS. The hardened samples were cyclically immersed in 10 m% NaCl solution (for 1 day) then kept at 100% relative humidity (for 1 day) between the age of 28 and 38 days, respectively.

We observed in steam cured and salt treated samples higher amount of Friedel's salt compared to those of non-steam cured samples. The chemically bound chloride content increased with the increasing GGBS replacement level. The highest amount of chemically bound chloride content in form of Friedel's salt was found in samples of CEM III/B 32.5 N-S steam cured at 80°C. Low increase in chemically bound chloride content was found as function of age of samples. We have experimentally studied that the steam cured GGBS itself is also able to bind chloride ions. We have shown that the improved chloride ion binding capacity of slag cements is owing to the chloride ion binding capacity of slag content.

## 6. ACKNOWLEDGEMENTS

Authors gratefully acknowledge to Danube-Drava Cement Ltd. for their support of the presented research.

## 7. REFERENCES

- Balázs, Gy. (2001), „My excursions in concrete research”, *Academy Press*, Budapest, pp. 83-102, 120-133. (in Hungarian)
- Balázs, Gy.; Csizmadia, J. and Kovács, K. (1997), „Chloride ion binding ability of calcium-aluminate, -ferrite and -silicate phases”, *Periodica Polytechnica*, Vol. 41 (2), pp. 147-168.
- Dhir, R. K.; El-Mohr, M. A. K. and Dyer; T. D. (1996), „Chloride binding in GGBS concrete”, *Cement and Concrete Research*, Vol. 26 (12), pp. 1767-1773.
- Friedel, P. M. (1897), „Sur un Chloro-aluminate de Calcium Hydraté se Maclant par Compression”, *Bulletin Soc. Franc. Minéral*, Vol 19, pp. 122-136.
- Hooton, R.D. and Titherington, M.P. (2004), „Chloride resistance of high-performance concretes subjected to accelerated curing”, *Cem Concr Res*, 34, 1561-1567.
- Kopecskó, K. and Balázs, Gy. (2005), „Chloride Ion Binding of Cement Clinkers and Cements Influenced by Steam Curing”, Proceedings of the International fib Symposium on Structural Concrete and Time organised by Asociacion Argentina del Hormigon (AAHES), Asociacion Argentina de Tecnología del Hormigon (AATH), Laboratorio de Entrenamiento Multidisciplinario para la Investigación Tecnológica (LEMIT) (Editors: Di Mayo, A.A. and Zega, C.J.), 28-30 September, 2005, La Plata, Argentina, Volume 1, pp. 147-154.
- Kopecskó, K. and Balázs, Gy. (2006), „Chloride binding in concrete, 1. Chloride ion binding capacity of C<sub>3</sub>A and C<sub>4</sub>AF aluminate clinkers”, *Concr Struct*, VIII. 2006/4, pp. 116-124.
- Kuzel, H.-J. (1966), „Röntgenuntersuchung im System 3CaO·Al<sub>2</sub>O<sub>3</sub>·CaSO<sub>4</sub>·nH<sub>2</sub>O – 3CaO·Al<sub>2</sub>O<sub>3</sub>·CaCl<sub>2</sub>·nH<sub>2</sub>O – H<sub>2</sub>O, Neues Jahrbuch Mineralog. Monatsh., 193-200.
- Luo, R.; Cai, Y.; Wang, C. and Huang, X. (2003), „A study of chloride binding and diffusion in GGBS concrete”, *Cement and Concrete Research*, Vol 33 (1), pp. 1-7.
- Neville, A. M. (1995), „Properties of concrete”, *Longman House, Essex, England*, Fourth and Final Edition, pp. 569-571.

## **NEW PRODUCTION TECHNOLOGY OF SINTERED FLY ASHES AGGREGATE**

*Ing. Vít Černý, Ing. Veronika Kalová  
FAST VUT v Brně  
Veveří 95  
602 00 Brno  
Czech Republic*

### **SUMMARY**

The artificial aggregate production from sintered fly ashes is known all over the world for more dozens of years. This aggregate was produced former in the Czech Republic under the trade mark AGLOPORIT in the plant Dětmarovice near Ostrava with utilization of the American (USA) Corson Comp. licensed technology. It was in general proved that the most types of produced fly ashes are usable for this purpose. The best results were obtained in the case of processing black coal fly ashes. The production and the utilization of aggregates from fly ash are stagnating in the world at the present time. The main reason is the uncontrolled technology from the standpoint of achieved economic parameters. The topic of solution is first of all the decrease of high costs for buying the correction fuel (coal) and the decrease of the high natural gas consumption for the batch ignition. Last but not least it is necessary to pay particular attention to the possibility of artificial aggregates production from fly ashes with high content of burnable substances.

### **1. UTILIZATION OF FLY ASHES WITH HIGH CONTENT OF BURNABLE SUBSTANCES FOR THE PRODUCTION OF AGLOPORITE.**

The specific case of the AGLOPORIT solution from fly ash with high content of burnable substances (for instance produced in the heating plant of U.S. Steel Košice) does not concern the problem of securing cheap correction fuel. On the contrary it means the technologically demanding solution of new formulae development and of innovative technological procedures of sintered fly ashes production under conditions, when the produced fly ash contains extra high portion of burnable substances. It is generally true that for the AGLOPORIT production of quality the content of burnable substances has to be mostly adapted to the value 7 – 9 %. This content enables the safe self-burning of the raw material batch on the sintering grate. Deficient sintering of AGLOPORIT grains takes place in the case of lower content of burnable substances. It can lead in extreme case to total stop of the sintering process. On the contrary the abnormal melting of the batch can take place in the case of too high content of burnable substances. This melting in the first moment decreases the porosity of the batch and during further melting air channels are formed, through which flows the excess air. The excessive quantity of burnable substances in the used fly ash can have during the industrial manufacture influence on the value which makes possible the self-sintering process of the batch.

### 1.1. Basic properties of fly ashes

The concrete properties of fly ash samples taken for technological tests of AGLOPORIT production are in the basic extent described in Tab. 1. as the properties survey of all representative samples. The content of burnable substances in fly ash from the USS Košice is in the range 20 – 25 %. This range is in the case of heating plant Přerov 2 – 3 %.

Tab. 1 Basic properties of fly ashes USS Košice and Přerov

Basic properties	Unit	Fly ash USS Košice		Fly ash Přerov
moisture	% of weight	56,7		9,0
Loss by ignition	% of weight	24,5		2,8
Bulk weight	kg.m <sup>-3</sup>	wet	dry	dry
- loose		1076	852	845
- jolted		1162	944	1038
Mesh analysis	% of weight	Rest		
Mesh size 1,000		0,4		0,2
(mm) 0,500		1,0		0,2
0,250		2,2		2,0
0,125		5,4		11,4
0,090		2,6		2,6
0,063		14,4		18,2
< 0,063		74,0		65,4

Tab. 2 Content of burnable substances in fly ash USS Košice and Přerov

Rest on the sieve	Ignition loss ( % by weight)
8,000 mm	0,0
4,000	0,0
2,000	0,0
1,000	0,0
0,500	4,02
0,250	4,86
0,125	19,32
0,063	18,21
< 0,063	9,24

### 1.2 Development of formulae for the agglomeration of aggregates

The technological tests of artificial aggregates production from sintered fly ash were performed in laboratory machinery with the test kiln. This enables the modeling of the batch self burning conditions in the kiln and to determine the basic parameters of the technological process for the design of new equipment for the production.

The possibility was checked of the fly ash (USS Košice) as the basic raw material in combination with clay materials in the first phase of realized tests. The program of tests proceeded from the assumption that the high portion of clay in the mixture up to 33 % will

enable to maintain the character of the ceramic body, even in the case of burnable substances content which exceeds the limit (14.5 %). As the usual portion of the clay admixture can be considered normally the limit 15 %, the higher portion up to the value of 33 % can be still considered as the raw material for AGLOPORIT production. The model formulae of the burned mixture are in the Tab. 3.

Tab. 3 Model formulae

Formula no. 1		Formula no. 2		Formula no. 3	
USS fly ash	74 %	USS fly ash	70 %	USS fly ash	67 %
Clay Tepličany	26 %	Clay Tepličany	30 %	Clay Tepličany	33 %
Water	optimum	Water	optimum	Water	optimum
Burnable substances 14,5 % (Loss by ignition)		Burnable substances 14,5 % (Loss by ignition)		Burnable substances 14,5 % (Loss by ignition)	

The results of burning didn't confirm the preliminary assumption, neither the high content of clay showed good results. The Fig.1 clearly illustrates the over-burnt batch, with melt as the result of the burnable substances high portion.



Fig. 1 The overburnt and insufficiently cooled batch

The second phase of technological tests was concerned with the modeling of burnable substances decrease in the mixture, by the addition of fly ash with lower content of burnable substances. In concrete of the black coal fly ash Přerov in the maximum relation 1: 1 with the fly ash USS Košice and with the addition of 30 % clay. The model formulae you will find in Tab. 4.

Tab. 4 Modeling formulae

Formula no. 1	Formula no. 2	Formula no. 3
Mixture dry substance: % Fly ash Košice 35 Clay 30 Fly ash TPR 35 Water optimum	Mixture dry substance: % Fly ash Košice 48 Clay 20 Fly ash TPR 32 Water optimum	Mixture dry substance: % Fly ash Košice 67 Clay 20 Fly ash TPR 33 Water optimum
Burnable substances <b>8.4 %</b> (Loss by ignition)	Burnable substances <b>9.0 %</b> (Loss by ignition)	Burnable substances <b>10.0 %</b> (Loss by ignition)
Formula no. 4	Formula no. 5	
Mixture dry substance: % Fly ash Košice 58 Fly ash TPR 42 Water optimum	Mixture dry substance: % popilek Košice 68 Clay 15 Flyash TPR 17 Water optimum	
Burnable substances <b>8.8 %</b> (Loss by ignition)	Burnable substances <b>9.0 %</b> (Loss by ignition)	

Better results were achieved in this case. These results enabled to evaluate the suitability of the checked fly ash type for the production of AGLOPORIT. It was further proved that with the adapted content of burnable substances it is possible to produce from the given raw material aggregate of quality even without the addition of clay into the raw mix. The formula which is composed from 68 % of fly ash USS Košice, 17 % of fly ash Přerov and 15 % of clay Vojany can be considered as the optimum. The modulus of compressibility in the cylinder of the material having the optimum formula was in the range 4.5 – 5.5 N/mm<sup>2</sup> in the case of loose bulk weight 720 – 750 g/l. The specimen of agglomerated aggregate of quality is demonstrated in Fig. 2.



Fig. 2 The agglomerate of well burned grains

## 2. CONCLUSION

The fly ash exploited from the uploading place has so high content of burnable substances that it is not possible to process it to AGLOPORIT by classical technological procedures.

The reduction of burnable substances content is theoretically possible by the addition of clay but from the practical point of view the production of aggregates would obtain the character of brick production. This would not fulfill the basic aim of realized tests i.e. first of all the processing of fly ash.

The processing of the checked fly ash type is possible in combination with other fly ash with low content of burnable substances. This would depend on the existence of plants which produce the both types of fly ashes and are situated in economically acceptable distance.

The produced aggregate obtained during technological tests repeatedly achieved the modulus of compressibility in cylinder in the range  $4.5 - 5.4 \text{ N/mm}^2$  with the loose bulk weight  $720 - 750 \text{ g/l}$ . It would be possible under the assumption of acquiring the know-how of the production to warrant the values of these technological parameters in mass production at least with the modulus of compressibility  $5.0 \text{ N/mm}^2$  and with the volume weight maximum  $760 \text{ g/l}$ .

The launching of artificial, lightweight aggregate production of quality from sintered fly ashes based on verified inputs is practically possible only under the condition that the quarried fly ash will be adapted before the final processing technologically in the way which decreases the content of burnable substances in the input raw material.

## 3. ACKNOWLEDGEMENTS

The paper was produced within grant GA 103/05/H044 "Stimulation of scientific development of PhD. students at department of building materials engineering" and within project MPO FI-IM2/183 "New technologies of processing and utilizing of sintered fly ash aggregate".





## **OPTIMIZATION OF RAW MATERIAL MIXTURES FOR NEW TECHNOLOGY OF PROCESSING OF SINTERED FLY ASH AGGREGATE**

*Ing. Veronika Kalová, Ing. Vít Černý  
FAST VUT v Brně  
Veveří 95  
602 00 Brno  
Czech Republic*

### **SUMMARY**

In Czech Republic the fly ash is used for processing concrete, mortar, cement and bricks. The using of fly ash for processing of artificial aggregate was ended a few years ago. Reason of this ending was obsolete and economically ineffective technology of processing. New technology of processing of the sintered fly ash aggregate is going to reduce the power severity of the production thereby its economical effectiveness too.

This paper is focused on optimization of raw material mixtures for this new technology. As a main raw material for processing of artificial aggregate it will be used classical fly ash arises from so-called classical blast furnace combustion at high temperature over 1200 °C, it also can be used fluidized fly ash arises from so-called fluidized combustion at lower temperature about 850 °C. As a binder material clay will be used. Fluidized fly ash may be processed without addition of binder, because it contents free CaO exists in form of so-called soft burnt lime, it means it is reactive.

Fluidized fly ash was not used for this purpose before, but there is a presumption that there can be found a new effective usage by processing of this aggregate.

### **1. FLY ASHES**

All of the high-tech countries make in last decades intensive research of processing capabilities of various kinds of waste as secondary raw materials. The usage of industrial waste is economically and ecologically advantageous; it spares raw materials and energy.

In Czech Republic there is more than 70% of heat energy obtained from coal combustion. It eventuates in relative high production of waste fly ash, which originates from coal combustion as a tough product. Annual production of fly ash was 1.69 million tons in 2004. It was used as a secondary raw material only 178 tons.

Properties of fly ashes are indeterminate and affected by quality of burned coal and by technology of combustion.

Classical fly ash is a reaction product of blast furnace combustion and can be used as a secondary raw material for variety of technologies in production of building materials.

Fluidized fly ashes represent a new category of fly ashes, which are formed by fluidized combustion of powdered coal and lime stone or dolomite at temperature 850 °C. This technology was developed for fuel gas desulphurization; it means removal of sulphur dioxide, which originates by burning of sulphur contained in coal. During the dissociative process the released SO<sub>2</sub> is bound to the CaO by creation of CaSO<sub>4</sub>. Fluidized fly ashes are characterized by increased content of CaO (15 - 35 %). According to the low temperature of combustion, free CaO exists in form of so-called soft burnt lime, it means it is reactive (Rovnanikova, Rovnanik, 2005]). The problem is that the fluidized fly ash is volume and temperature unstable. On this account it almost can't be used for production of building materials.

One of the possibilities where fluidized fly ash can be used is processing of sintered fly ash aggregate. With artificial aggregate we can partially or completely replace natural aggregate in concrete. The goal of sintering of fly ashes into artificial aggregate is to set toxic matter and to reduce undesirable leach.

### 1.1. Properties of used fly ashes

It was used fluidized fly ash from power station Hodonin (designation EHO) and classical fly ash from heating power station Otrokovice (designation TOT).

Tab. 1 Chemistry of fly ashes

Kind of fly ash	Al <sub>2</sub> O <sub>3</sub> [%]	Fe <sub>2</sub> O <sub>3</sub> [%]	CaO [%]	MgO [%]	K <sub>2</sub> O [%]	Na <sub>2</sub> O [%]	MnO [%]	SiO <sub>2</sub> [%]
Fluidized fly ash EHO	39.01	5.27	15.07	1.62	1.00	0.42	0.05	39.66
Classical fly ash TOT	14.07	5.24	1.26	0.2	1.03	0.46	0.02	51.15

Tab. 2 Some properties of fly ashes

Kind of fly ash	Content of free CaO [% of weight]	Decrement after calcine [%]	Weight [kg/m <sup>3</sup> ]
Fluidized fly ash EHO	2.56	2.44	653
Classical fly ash TOT	<0.1	1.86	994

## 2. DESIGNED MIXTURES

It was made several mixtures from above mentioned fly ashes. As an addition it was used clay used in brick kiln Hodonin (designation HO). It was made samples of dimensions 20 × 20 × 60 mm of following mixtures. After hardening the samples were dried in a drying plant at the temperature 90 °C for two hours. Then the samples were burned in a laboratory kiln at several temperatures.

In the first stage they were made mixtures containing only fluidized fly ash and several addition of clay. Samples were burned at temperatures 900, 1000, 1100 and 1200 °C.

Tab. 3 Designed mixtures of first stage

E1H: fluidized fly ash EHO + 10 % of clay HO,
E2H: fluidized fly ash EHO + 20 % of clay HO,
E3H: fluidized fly ash EHO + 30 % of clay HO,
E4H: fluidized fly ash EHO + 40 % of clay HO.

In the second stage they were made mixtures containing both kinds of fly ashes and several addition of clay. These samples were burned at the temperature 1200 °C.

Tab. 4 Designed mixtures of second stage

TOT:EHO=30:70	TOT:EHO=50:50	TOT:EHO=70:30
TOT + EHO	TOT + EHO	TOT + EHO
TOT + EHO + 10 % HO	TOT + EHO + 10 % HO	TOT + EHO + 10 % HO
TOT + EHO + 20 % HO	TOT + EHO + 20 % HO	TOT + EHO + 20 % HO

These properties of samples were then observed: bulk density, compressive strength and absorptivity.

### 3. CHOSEN RESULTS

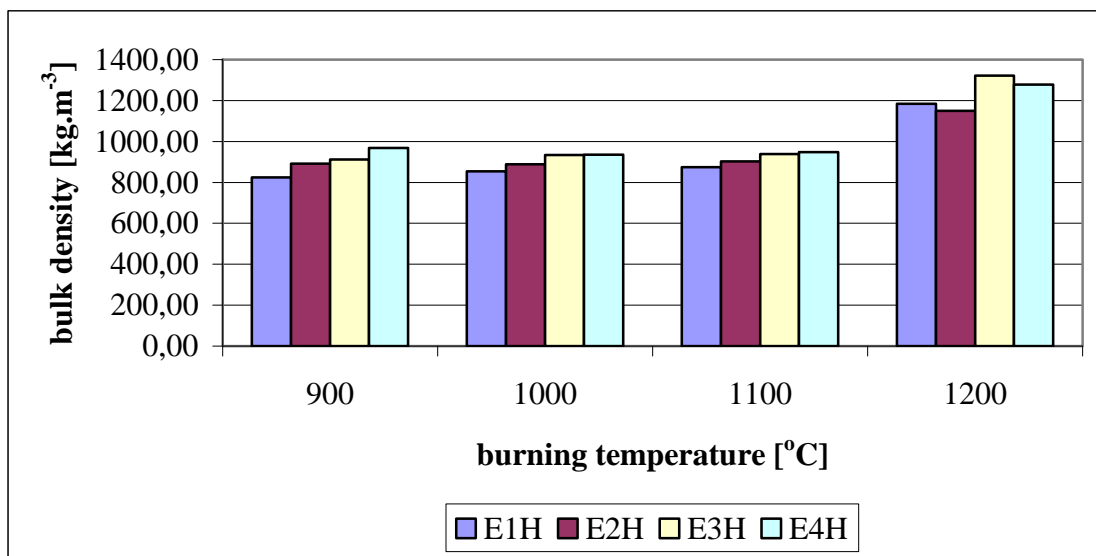


Fig. 1 Dependence of bulk density of samples on burning temperature

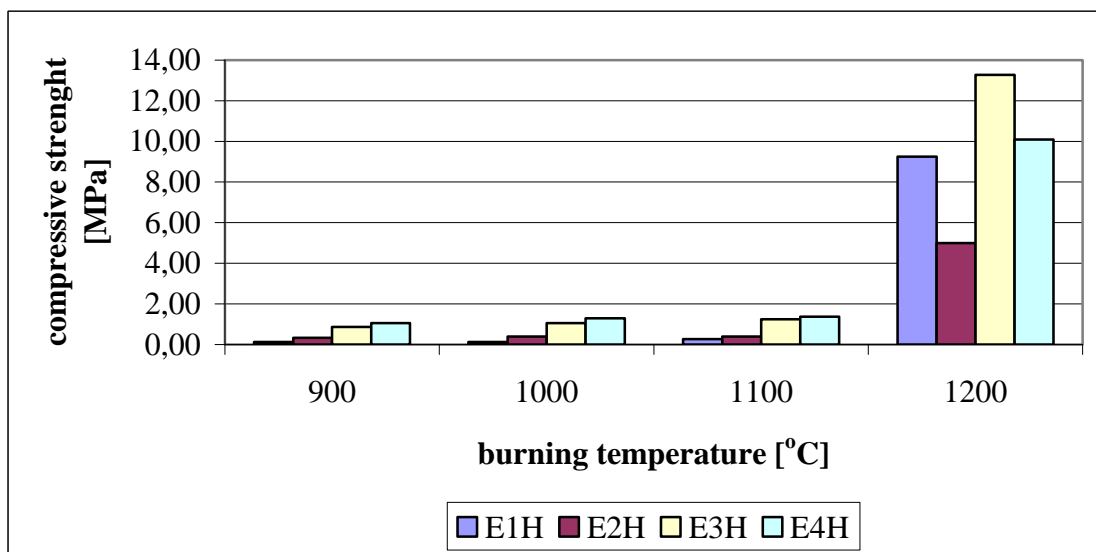


Fig. 2 Dependence of compressive strength of samples on burning temperature

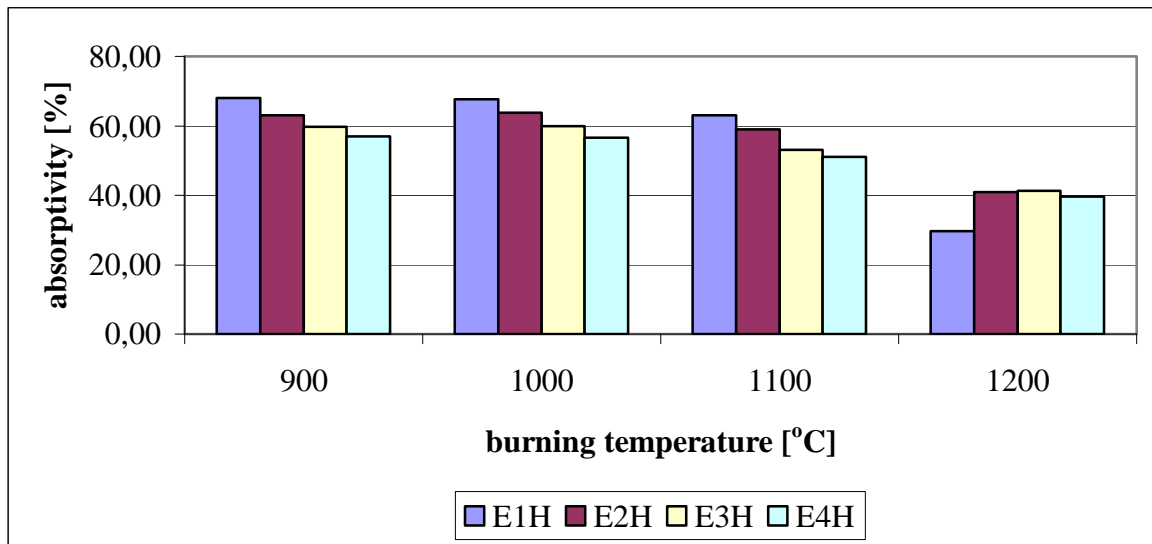


Fig. 3 Dependence of absorptivity of samples on burning temperature

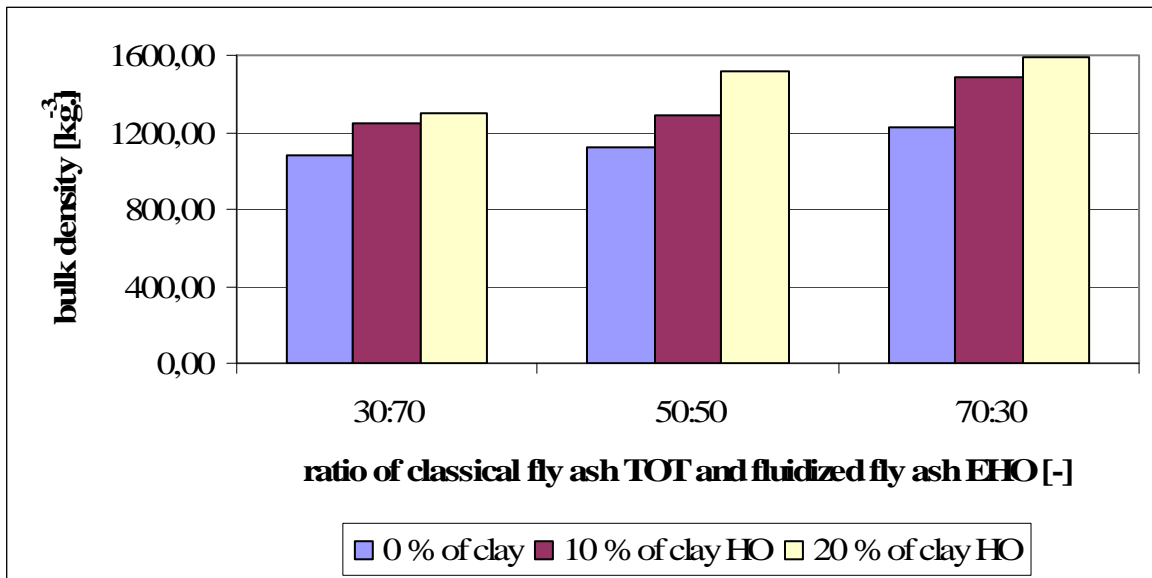


Fig. 4 Dependence of bulk density of samples on ratio of classical and fluidized fly ash

## 5. CONCLUSIONS

The lowest bulk density reaches samples with higher amount of fluidized fly ash. With increasing amount of clay bulk density also increases. Bulk density ranges from 1080 to 1600 kg/m<sup>3</sup>.

The high content of fluidized fly ash in the mixtures reduces compressive strength of samples after burning. It is necessary to use higher content of clay in these mixtures to reach higher compressive strength. Compressive strength of samples ranges from 4 to 33 MPa.

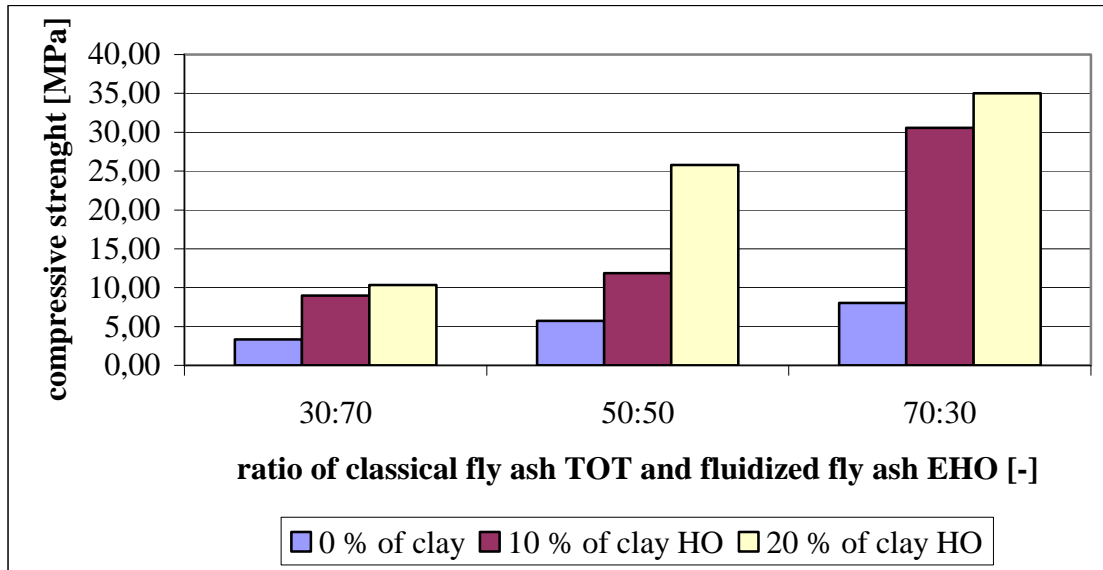


Fig. 5 Dependence of compressive strength of samples on ratio of classical and fluidized fly ash

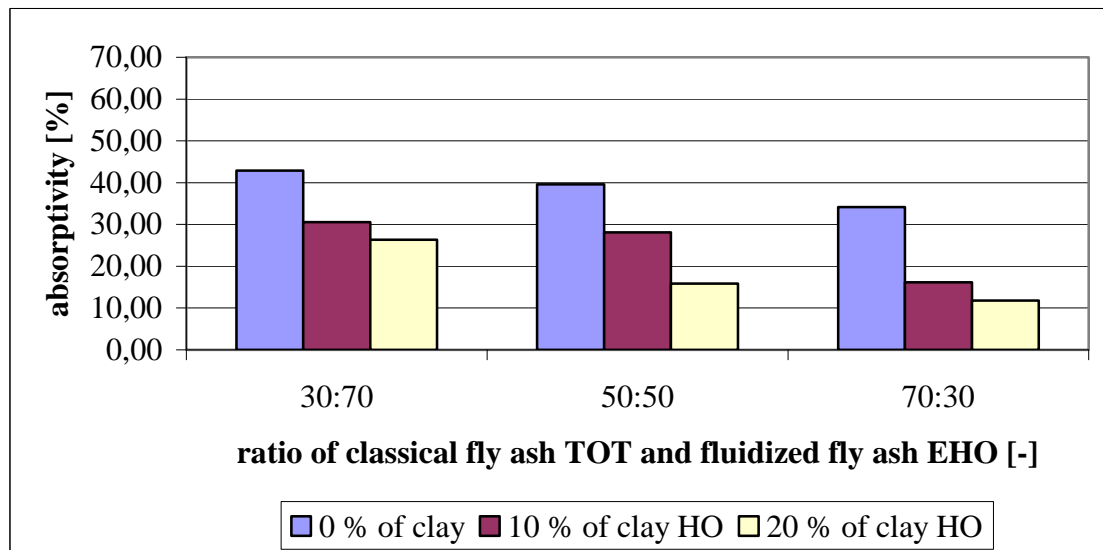


Fig. 6 Dependence of absorptivity of samples on ratio of classical and fluidized fly ash

Increasing amount of classical fly ash in the mixtures implicates a decrease of absorptivity. Mixtures with a higher content of fluidized fly ash reach a higher absorptivity. Clay has positive influence on absorptivity. Mixtures with higher content of fluidized fly ash reach also good absorptivity if they contain higher content of clay. Absorptivity of samples after burning at temperature 1200 °C ranges from 12 to 43 %.

From experimental work results that fluidized fly ash can be used for processing of artificial fly ash aggregate especially when clay is used as an addition. On the other hand mixtures with higher ratio of classical fly ash reach better properties after burning. Therefore processing of mixtures content both kinds of fly ashes – fluidized and classical – is really good technological solution.

## **6. ACKNOWLEDGEMENT**

The paper was produced within grant GA 103/05/H044 „Stimulation of scientific development of PhD. students at Department of building materials engineering” and within project MPO FI-IM2/183 „New technologies of processing and utilizing of sintered fly ash aggregate”.

## **7. REFERENCES**

Rovnaniková, P. and Rovnanik, P. (2005), "Inorganic chemistry and chemistry of inorganic building materials", *CERM*, Brno, Czech Republic, 2005

## **CONCRETE DURABILITY POSITIVELY INFLUENCED BY BLAST FURNACE SLAG IN CEMENT**

*Vladimír Těhnik, VÚSTAH Brno, Hněvkovského 65, Brno*

*Jiří Adámek, BUT Fac. Of Civil Engineering, Veveří 95, Brno*

*Vlasta Juránková, BUT Fac. Of Civil Engineering, Veveří 95, Brno*

*Petr Koukal, Cement Plant Mokrý, a.s., Mokrý*

*Barbara Kucharczyková, BUT Fac. Of Civil Engineering, Veveří 95, Brno*

### **SUMMARY**

In this paper the resulted properties of 5 blended Portland cement sorts with perfectly defined granulated blast furnace slag admixture are presented. By three institutions – USZK FAST BUT Brno, VÚSTAH Brno and Laboratory of Cement Plant Mokra – was developed the methodology of influence testing by variable admixtures of fine – ground granulated BFS to portland clinker. In the laboratory conditions were prepared model equivalents of blended Portland cement types: CEM I without BFS, CEM II/B-S+30%, CEM III/A+50%, CEM III/B+70% BFS laboratory grinded and CEM III/B+70% BFS technology grinded by a factory Kotouč Štramberk. All cements were used for concretes preparation by use of the constant aggregate parameters.

### **1. INTRODUCTION**

A file of experience with monitoring of durability of structures located either nearby or right in the salt water was described by Bijen, (1996). He evaluated a number of reinforced concrete structures had realised in the seas nearby the Netherlands. These structures were mostly constructed from reinforced concretes with slag-portland cement. Even under the severe exposure of the North Sea there was not found increased presence of corrosion of concrete. This fact is predicated just to the slag portland cement, in which strong reduction of chloride ions mobility in comparison to concrete with Portland cement was found. Another important aspect was reduction of water/cement ratio of applied concrete. The effect of sulphate ions on concrete was also significantly lower. The final aspect was the recommendation not to use aggregates which could have been affected by alkali influence.

The slower process of hydration of slag-portland cement in concrete in comparison with concrete with pure Portland cement was favourably demonstrated by the reduction of cracks development in the early stage of setting and hardening (plastic settlement and shrinkage). In combination with sufficient water curing of concrete in the early phase of setting and mainly of hardening of concrete cover, the resistance of concrete against freezing and thawing cycles of salt water increases and at the same time concrete gains very high resistance against crumbling of a surface layer. Substitution of 60 – 70 % of Portland clinker with blast furnace slag of high quality not only reduces the costs of maintenance of salt water structures but it also contributes to emission reducing. This experience inspired us to carry out the evaluation of influence of blast furnace slag volume on durability properties of concrete cover especially of permeability of a porous structure of this layer both on the air and water.



## 2. PROPERTIES OF LABORATORY MANUFACTURED CEMENTS

The first step was the selection of basic components – clinker, blast furnace granular slag and energy-gypsum as a regulator of setting – and their principal properties was determined. The clinker was of saturation by LP = 96.3, silicate modulus MS' = 2.52 and alumina modulus MA = 1.34. A volume of allite C<sub>3</sub>A = 72.6 %, a volume of free CaO = 0.22 %. Blast furnace slag had a volume of Al<sub>2</sub>O<sub>3</sub> 7.50%, index of hydraulic power IH =1.61 and BA = 1.36. Vitreosity of the slag was 77.7 %. In a sample energy-gypsum had a volume of SO<sub>3</sub> = 44.59 % and a content of dihydrate 95.89 %.

For the laboratory manufacturing following types of cements were selected with the slag content and usual content of SO<sub>3</sub> for given type including specific surface:

Tab. 1 Types of cements with content of SO<sub>3</sub>, slag and specific surface

Number of sample	Type	Volume of SO <sub>3</sub> %	Volume of slag %	Blaine m <sup>2</sup> /kg
1	CEM I	2.9 – 3.0	0	360
2	CEM II/B-S	2.5 – 2.6	30	330
3	CEM III/A	2.5 – 2.6	50	410
4	CEM III/B	2.4 – 2.5	70	450
5	CEM III/B-Š	2.4 – 2.5	70	450

For preparation of cement 5 – CEM III/B - Š was used processed milled slag with specific surface 420 m<sup>2</sup>/kg. The slag was laboratory post-milled together with the clinker on the required value. All cements were prepared by separate milling of the slag and clinker with following homogenizing eventually by a short-time post-milling on the required specific surface and volume of SO<sub>3</sub>. The calculation of composition of all cements was based on determination of SO<sub>3</sub> content of individual components with respect to the slag dosing, further properties are presented in Tab. 2 and 3.

Tab. 2 Composition of monitored cements

Type	clinker	slag	gypsum
CEM I	94,77%	0	5,23%
CEM II/B-S	65,87 %	30 %	4,13 %
CEM III/A	46,00%	50 %	4,00 %
CEM III/B	25,35 %	70%	3,65 %
CEM III/B	26,35 %	70 %	3,65 %

Tab. 3 Compressive and bending strengths of cements according ČSN EN 196 - 1

Type	1 Day	2 Days	3 Days	7 Days	28 Days	56 Days
CEM I	15.8 / 3.5	28.2 / 5.1	33.7 / 6.6	49.2 / 7.8	65.4 / 8.4	64.3 / 7.4
CEM II/B-S	8.3 / 2.3	16.8 / 3.9	20.9 / 4.2	32.2 / 5.9	52.2 / 8.3	64.1 / 8.7
CEM III/A	5.9 / 2.8	12.9 / 3.2	15.6 / 4.1	25.8 / 5.4	47.8 / 8.8	59.3 / 9.2
CEM III/B	2.9 / 0.9	6.3 / 2.0	8.5 / 2.6	20.1 / 5.0	40.7 / 9.0	54.5 / 9.7
CEM III/B	1.9 / 0.8	5.5 / 1.5	9.3 / 2.8	19.5 / 5.1	40.2 / 8.0	52.6 / 10.0

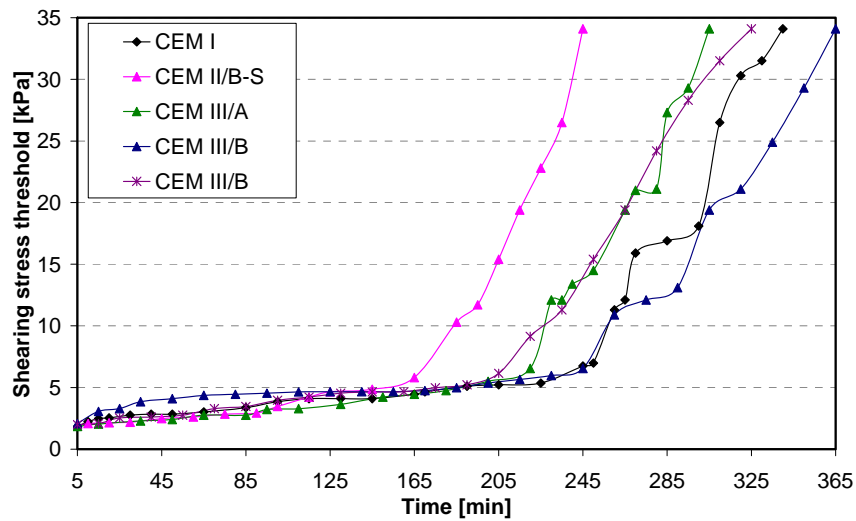


Fig. 1 The course of cements setting by Tussenbrock

Tables 4 and 5 present normal consistency, the start and end of setting and hydration temperature of cements

Tab. 4 Setting according to ČSN EN 199-3

Type	Normal consistency in %	Start of setting	End of setting
CEM I	27.3	3:30	5:00
CEM II/B-S	26.7	3::00	4:00
CEM III/A	26.7	4:20	5:30
CEM III/B	26.7	5:10	6:20
CEM III/B-Š	30.3	4:50	6:00

Tab. 5 Hydration temperature of cements according to ČSN EN 192-8

Type	1 day- J/g	3 days - J/g	7 days - J/g	28 days - J/g
CEM I	261.5	288.2	379.6	600.1
CEM II/B-S	193.5	230.4	266.1	550.6
CEM III/A	172.1	204.9	242.6	525.3
CEM III/B	166.3	198.5	230.7	478.2
CEM III/B	169.5	196.8	261.3	486.5

### **3. PRINCIPAL PROPERTIES OF CONCRETES FROM LABORATORY MANUFACTURED CEMENTS**

Five types of special laboratory manufactured cements with different volume of granular slag were used for concrete mixtures with identical composition of aggregate fractions. These concretes were used for determination of general mechanical characteristics and for the test of durability properties.

All these concretes comprised small quarried aggregates of a fraction 0/4 mm, coarse crushed aggregates 4/8 mm, 8/16 mm and 11/22 mm volume of aggregates in 1 m<sup>3</sup> of fresh concrete was 0,671 m<sup>3</sup>, a volume of cement fills the remaining space. Uniform batch of cements was 380 kg on 1 m<sup>3</sup> of concrete, a volume of the water depends on different measured surface and was dosed so to have possibly the same spillage on a shaking table 480 mm. A super-plasticizer in amount of 0,7% of the cement weight was used for all concretes.

Concretes were marked as follows: concrete G1 from cement CEM I, concrete G2 from cement CEM II/B-S with the slag of 30% of concrete weight, G3 from cement CEM III/A with 50% of the slag, concrete G4 from cement CEM III/B with 70% of the slag. Concrete G5 contained identically with concrete G4 cement CEM III/B 70% of the slag that was technologically prepared in a factory in Štramberk.

The specimens were manufactured using the vibration 2 times 20 seconds on a standard vibrating table. They were de-moulded after two or three days (64, 65). The specimens were after post-forming deposited in the wet environment of relative humidity 90% at the temperature 20-23 °C. To reach the drying of specimen's surface, they were removed from the deposit two days before the test and were subsequently tested after 28 days of maturing. The specimens for long-terms tests are deposited in a laboratory of the relative humidity 50-65% and temperature 20-25%. 12 testing cubes of 150/150/150 mm for determination of compressive strength after 7, 28, 90 and 360 days of curing, 6 cubes of 150/150/150 mm for transverse tension strength after 28 and 90 days of curing, 9 prisms of 100/100/400 mm for determination of dynamic and static modulus of elasticity after 28, 90 and 360 days of curing, 6 tiles of 300/300/80 mm for continuous measurements of air permeability using Torrent Permeability Tester (TPT) method, 6 prisms of 100/100/400 mm for determination of initial surface absorption and absorption capacity of concretes by a method ISAT. On 3 cuts of 75/75/150 mm from the cubes of 150/150/150 mm is determined surface sorption of concretes by B.B. Sabina. After the test ISAT and following drying of the prisms is then determined bending modulus of elasticity. On the tiles were determined the strengths of a surface layer at pull-out tests. Tab. 6 shows physico-mechanical properties of concretes G1 - G5.

### **4. DURABILITY OF CONCRETES**

Durability of concretes is defined by the properties of porous structure of concrete cover. The study of concrete cover of specific specimen, of a part or of the whole structure is considerably complicated. A state of the porous structure of monitored concrete can be described by several kinds of tests, at which its permeability on gases and liquids is monitored. Permeability of air, vapours or water through given structure is best described by determination of coefficient of permeability of these agents through the pores of tested concrete.

By the tests of the samples of concrete with laboratory manufactured cements was determined coefficient of air permeability using TPT method. The contribution describes partial results of these tests, subsequent results will be presented on the conference.

Table 6 Physically-mechanical properties of concretes G1 - G5

property		unit	Concrete indication				
			G1	G2	G3	G4	G5
Volume weight	After 7 days	kg/m <sup>3</sup>	2280	2240	2290	2300	2310
	After 28 days		2260	2230	2290	2300	2340
Compression strength	After 7 days	MPa	33	24	20	17	15
	after 28 days		45	35	38	36	32
Transverse tension strength after 28 days		MPa	3.2	2.6	2.7	2.2	2.6
Modulus of elasticity after 28 days - static - dynamic $E_{bu}$ –ultrasonic method - dynamic $E_{br}$ – resonance method. - dynamic in shear $G_{br}$ – resonance method.		GPa	25.7	26.3	23.9	22.9	
			37.2	38.3	36.1	36.3	35.3
			34.0	35.2	32.9	33.1	33.5
			13.7	14.1	13.3	12.9	13.1
Poisson coefficient		-	0.24	0.25	0.24	0.28	0.28
Cohesion of covercrete		MPa	2.1	2.3	2.0	0.7	1.1

The TPT method consists in determination of coefficient of air permeability  $k_T$  by creating vacuum under stuck measuring cell and by monitoring of the vacuum decrease which happens by the air flow through the pores of concrete after switching off a vacuum pump. The coefficient of permeability is calculated from the change of pressure in the measured time. An author of the apparatus, dr. Torrent, processed a chart based on high-capacity file of tests both in a laboratory and in situ, in which he evaluated examined concrete from the viewpoint of durability into 5 qualitative classes. The least permeable concrete has the lowest coefficient of permeability  $k_T < 0,01 \text{ m}^2 \cdot 10^{-16}$ . On the contrary, concrete in the 5<sup>th</sup> class indicated as very bad has  $k_T > 10 \text{ m}^2 \cdot 10^{-16}$ .

A value of the coefficient  $k_T$  essentially depends on moisture of tested covercrete, a volume of the water or vapours fills up a part of the covercrete porous system and distorts the measured values  $k_T$  - improves durability. For that reason together with the value  $k_T$  is mostly indicated also moisture weight of this layer. Tab. 7 presents  $k_T$  values, values of penetration depth of a fibre into concrete  $L$  and the mean value of the moisture weight  $w$  determined either with a capacity hygrometer Kakaso or with a hygrometer Almero.

## 5. DISSCUSION

- a) Properties of laboratory manufactured cements introduced in Tab. 1 to 5 and Fig. 1 have provided classification of cements as follows:
1. CEM I as CEM I 52.5
  2. CEM II/B-S as CEM II/B-S 42.5
  3. CEM III/A as CEM III/A 42.5
  4. CEM III/B as CEM III/B 32.5
  5. CEM III/B-Š as CEM III/B 32.5

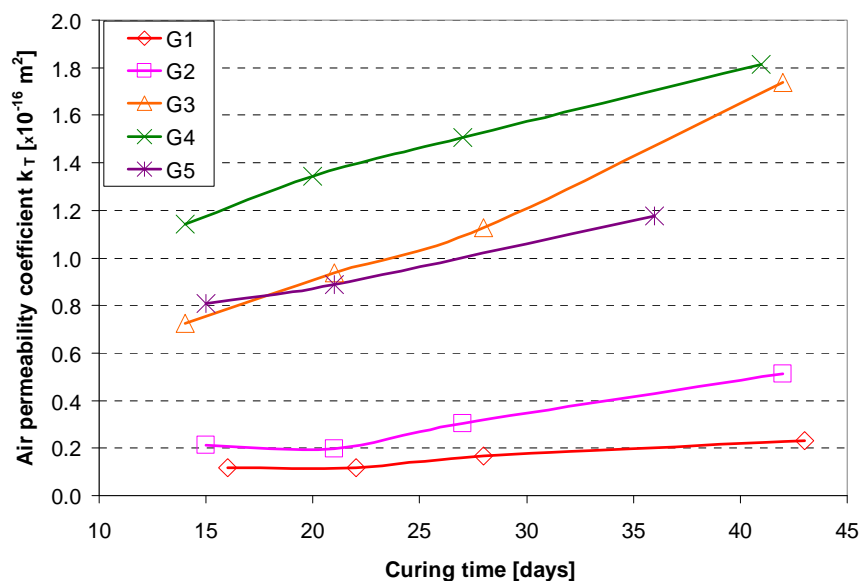


Fig. 2 Dependence of  $k_T$  and curing time

b) Properties of concretes G1 - G5 manufactured from the laboratory prepared cements 1 – 5 may be classified, when considering determined cube strengths to be characteristic according ČSN EN 206-1, as:

G1 – C35/45, G2 – C25/30, G3 – C30/37, G4 – C25/30 a G5 – C25/30

c) Durability properties of concrete are evaluated by determined values of coefficient of air permeability only (Fig. 2). Against expectation, concretes G1 and G2 are of lower permeability than the others. It is presupposed that with increasing ageing the hydration processes, on which the granular slag contributes, will continue. At the hydration new products from the slag will develop and they will fill up the porous structure of concrete with the higher content of the slag.

## 6. CONCLUSION

The influence of different slag in proportion to the clinker in cement was demonstrated itself especially on the mechanical properties of concretes; for the air permeability expected trend wasn't approved. Into the presentation on the Conference in September will be incorporated the results from the long-terms tests and from extension tests relating to the durability of concretes.

## 7. ACKNOWLEDGEMENT

This contribution was prepared under the support of a grant GAČR Nr. 103/05/2683 and a research project MŠMT ČR 1M06005 - CIVAK.

## 8. REFERENCES

Bijen, J. (1996), „Blast Furnace Slag Cement for Durable Marine Structures”, *Association of The Netherlands Cement Industry, Netherlands*

## **BLENDED CEMENTS OF THE 21TH CENTURY: WHAT MAKES A CONCRETE**

*Katalin Szilágyi, István Zsigovics, György L. Balázs  
Budapest University of Technology and Economics, Hungary  
H-1111 Budapest, Műegyetem rakpart 3.*

### **SUMMARY**

In present experimental studies a detailed survey on differences and advantages of blended cements to Portland cement is summarized. Laboratory tests were carried out both on fresh concrete and hardened concrete of 30 different concrete mixtures (with the use of four different blended cements and one Portland cement, with 6 different water-to-cement ratios). Results demonstrated superior behaviour of blended cements of high BFS content (especially CEM III/B) that provides improved durability.

### **1. INTRODUCTION**

Modern cements often include the use of supplementary materials, as hydraulic additives. These materials are often co-products of other processes or natural materials. Some require further processing before they are suitable for cement and concrete. Some of these materials have cementitious properties; others, called pozzolans, do not have cementitious properties when used alone.

Blast furnace slag (BFS) and pulverized fly ash (PFA) are the two most common hydraulic additives used in cements. While chemical similarities exist, these materials have different effects on cements. These differences are based in part on the proportion of oxides in each material. Blast furnace slag is more closely related to Portland cement than pulverized fly ash. Blast furnace slag can replace as much as 50 percent in blended cements (and up to 95 percent in slag cements for mass concrete). Pulverized fly ash content in blended cements is usually limited to 20 or 30 percent.

Blast furnace slag is usually a more uniform product than pulverized fly ash. As a result, concrete made with blended cement of BFS content will generally have more uniform properties than concrete made with PFA content.

Hydraulic additives, although somewhat finer than Portland cement, do not typically have a higher water demand compared to Portland cement in concrete (SCA, 2002). This is believed to be true due to their low absorption and denser packing feature (smaller particles of hydraulic additives can be fitted between the Portland cement grains).

Low permeability in reinforced concrete is important to maintain structural integrity. Permeability is a measure of how easy it is for water, air and other substances such as chloride ions to enter concrete. Low permeability concrete can help to reduce the potential for reinforcing steel to corrode when exposed to chlorides by limiting the diffusion of chlorides into concrete. When Portland cement hydrates, it forms calcium-silicate hydrate gel (CSH) and calcium hydroxide ( $\text{Ca(OH)}_2$ ). Calcium-silicate hydrate (CSH) is the principle binding

material. Permeability is related to the proportion of CSH to  $\text{Ca(OH)}_2$  in the cement paste. The higher the proportion of CSH to  $\text{Ca(OH)}_2$ , the lower the permeability of the concrete. Blended cements (especially blended cements of BFS content) also possess reactive silicon dioxide ( $\text{SiO}_2$ ) in amounts sufficient to provide significant pozzolanic activity. This is largely associated with lowering the calcium hydroxide ( $\text{Ca(OH)}_2$ ) content of concrete by converting it into more CSH binder (*Fig. 1.*). This means that blended cements can exhibit higher strength, reduced permeability, and potentially greater durability in many environments when compared to plain Portland cements (Rendchen, 2002).

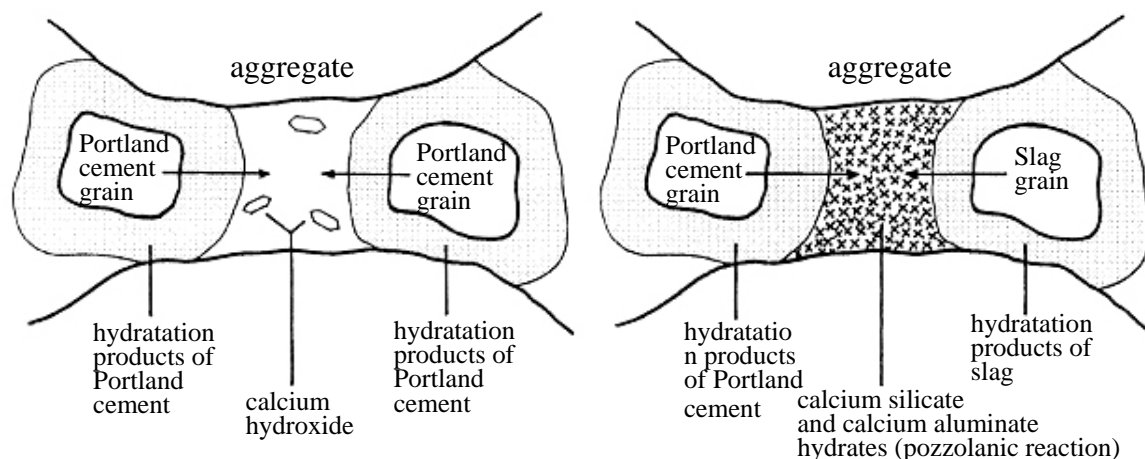


Fig. 1 Hydration products of Portland cement and slag cement (Civil & Marine, 2000)

## 2. AIMS OF STUDY

Due to different hydration processes of Portland cement and that of the hydraulic additives, the behaviour and performance of both fresh and hardened concrete can be improved compared to Portland cement concretes.

Present experimental studies aimed to give a detailed survey on differences and advantages of blended cements to Portland cement (BUTE, 2006). Laboratory tests covered not only standard tests on fresh and hardened concrete, but also detailed analyses of cement properties by means of chemical analyses, differential thermoanalysis, X-ray diffraction analyses and standard cement tests (according to EN 197). Present paper summarizes exclusively the results of the hardened concrete studies focusing mainly on data highlighting influence of permeability.

## 3. EXPERIMENTAL STUDIES

In present experimental studies several tests were carried out at the BUTE Dept. of Structural Materials and Engineering Geology both on fresh concrete and hardened concrete of 30 different concrete mixtures (with the use of four different blended cements and one Portland cement, with 6 different cement amounts). Basic information of cements is indicated in *Tab. 1.* Details of concrete mixes are given in *Tab. 2.* In present comparative analyses we intended to study concrete mixes with different cement amounts, but with the same water amount ( $190 \text{ kg/m}^3$ ). Water amount was chosen to the design consistency class F2, as required by the water demand of the lowest cement amount ( $290 \text{ kg/m}^3$ ) and the grading properties of aggregate used.



Tab. 1 Basic information of cements used (BUTE, 2006)

type of cement	CEM I 42,5 N	CEM II/B-M (V-L) 32,5 R	CEM II/B-S 32,5 R	CEM III/A 32,5 N	CEM III/B 32,5 N-S
hydraulic additive content	0	18% (PFA)	26% (BFS)	40% (BFS)	62% (BFS)
SiO <sub>2</sub> , m%	19,4	24,62	23,02	25,34	29,68
CaO, m%	63,72	53,53	58,91	55,64	48,11
MgO, m%	2,02	1,87	4,12	5,35	7,04
Fe <sub>2</sub> O <sub>3</sub> , m%	3,00	3,54	2,20	2,20	1,59
Al <sub>2</sub> O <sub>3</sub> , m%	4,51	7,60	4,34	5,48	6,95

Tab. 2 Details of concrete mixes tested

type of cement	cement amount, kg/m <sup>3</sup>			water amount, kg/m <sup>3</sup>	water-to-cement ratio			design consistency (flow), mm
CEM I 42,5 N	410	385	350	190	0.46	0.49	0.54	F2 420±20
CEM II/B-M (V-L) 32,5 R								
CEM II/B-S 32,5 R	330	310	290	0.58	0.61	0.65		
CEM III/A 32,5 N								
CEM III/B 32,5 N-S								

Fresh concrete tests covered consistency and consistency endurance studies. Tests on hardened concrete specimens were carried out in terms of standard compressive strength tests, studies of strength development (from the age of 1 day up to 180 days), flexural-tensile strength tests, measurements of Young's moduli up to age of 180 days, standard water penetration (water tightness) tests (according to EN 12390-8:2000) at the age of 42 and 180 days, standard freeze-thaw cycle tests (50 cycles) at the age of 150 days and slab tests (scaling according to prEN 12390-9:2002) at the age of 180 days. Present paper summarizes results of the hardened concrete studies connected to the permeability of concrete (i.e. water tightness tests, freeze-thaw cycle tests and slab tests).

## 4. RESULTS

### 4.1. Water tightness tests

Water tightness was tested according to EN 12390-8:2000 at the age of 42 and 180 days. Due to the same water content and aggregate grading properties, the water penetrations were found to be in the same range for all cement type used (apparently independently of the water-to-cement ratios, *Fig. 2.*). *Fig. 3.* indicates water penetrations of specimens of 330 kg/m<sup>3</sup> cement content at the age of 42 and 180 days. It can be studied that improved water tightness is realized with the use of CEM III/B (having the highest BFS content providing significant pozzolanic activity) and also with the use of CEM II/B-M (having 10% pulverized limestone as additive providing considerably improved packing that is resulted in lower permeability). Different hydraulic additive content of blended cements yields different hydration mechanism that can be studied in the evolution of water tightness of concretes. *Fig. 4.* summarizes the differences in water penetrations (given in percents) between measurements at the age of 42 and 180 days, respectively. Results confirm that high BFS content (CEM III/B) provides a reduced permeability that is developing in time due to the delayed formation of CSH. This behavior was found to be apparently independent from the water-to-cement ratio in present

experiments. Pulverized limestone as additive (CEM II/B-M) yields a behavior that is more sensitive to water-to-cement ratio.

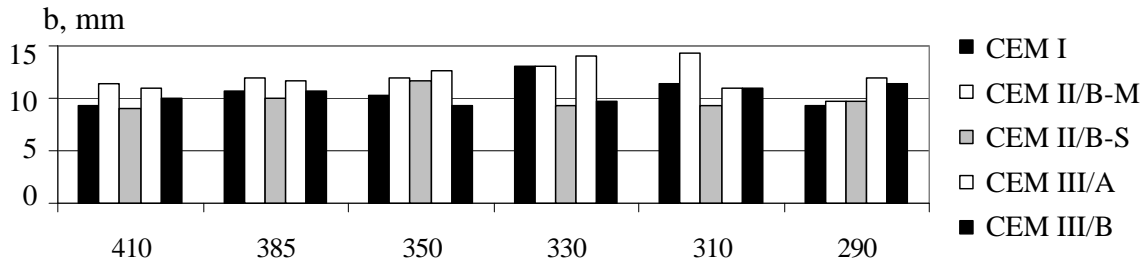


Fig. 2 Water penetrations (b, mm) for specimens of all cement contents at the age of 180 days

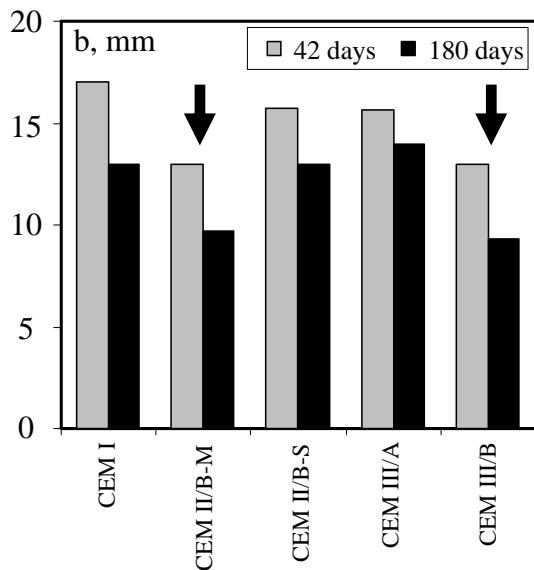


Fig. 3 Water penetration (b, mm) into concrete specimens of 330 kg/m<sup>3</sup> cement content, at the age of 42 and 180 days

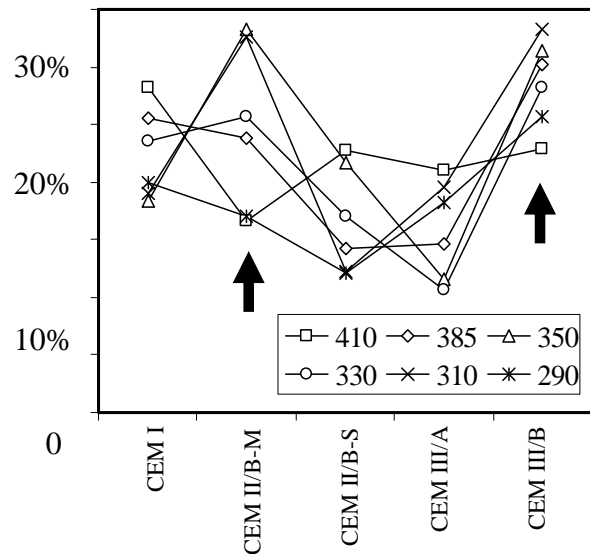


Fig. 4 Differences in water penetrations (percent) for concrete specimens of all cement contents, at the age of 42 and 180 days

#### 4.2. Freeze-thaw tests

Freeze-thaw resistance of concretes was studied in terms of changes in compressive strength, ultrasound pulse velocity (UPV), rebound value and loss of mass after 50 standard freeze-thaw cycles (that were started at the age of 150 days). Results are summarized in Fig. 5. Results indicate that higher amount of hydraulic content yields better freeze-thaw resistance of concretes with a reduced drop in both strength and loss of mass. Results also indicate that non-destructive methods can be suitable for the study of changes in mechanical properties of concretes due to freeze-thaw attack; however, present experimental results did not provide satisfactory sensitivity of ultrasound pulse velocity measurements (Fig. 5a and 5b). Results also highlight a future research need on CEM III/A cement, of which mechanical properties were found to be minor that would be expected based on the BFS content.

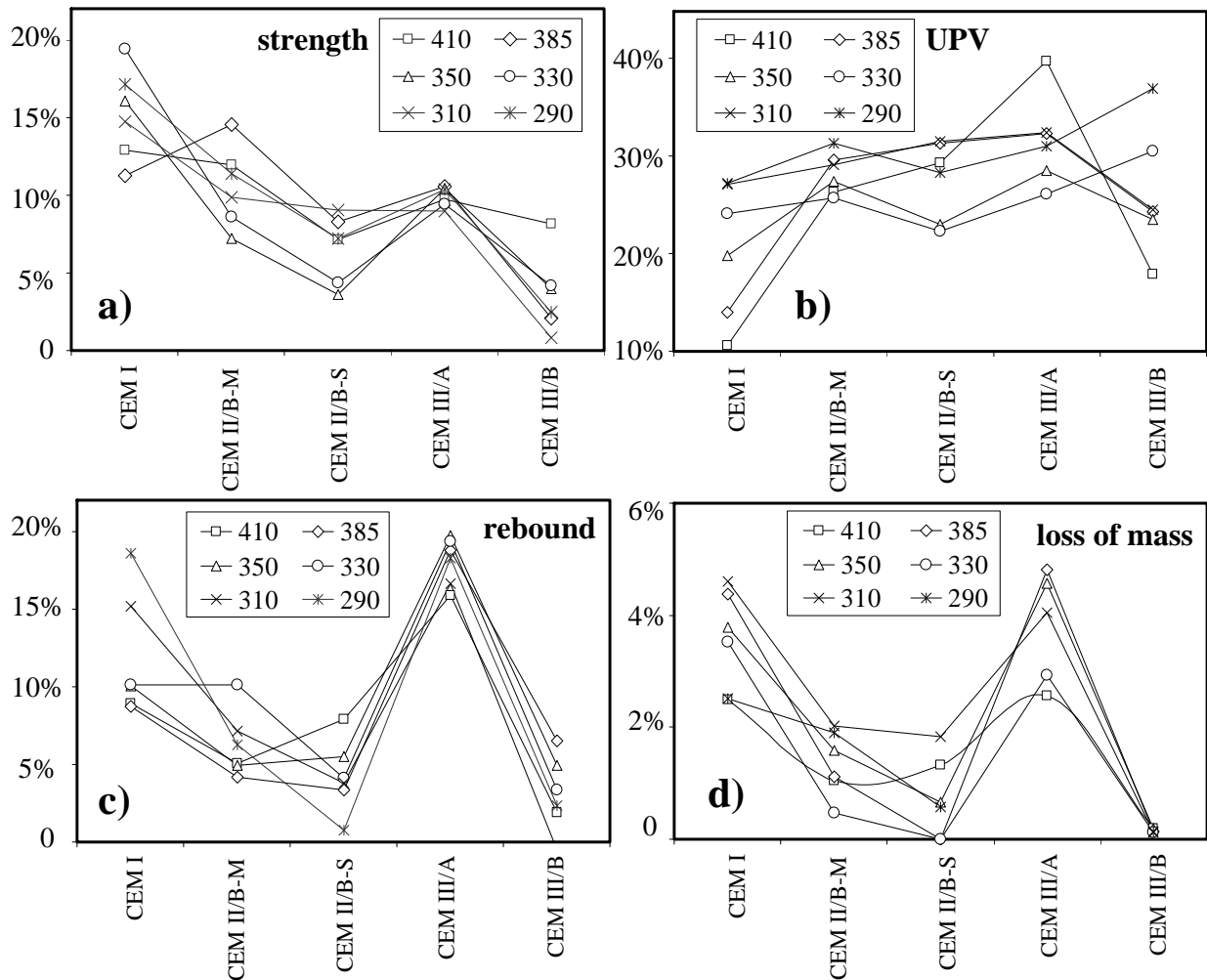


Fig. 5 Mechanical properties of concretes after 50 cycles of standard freeze-thaw tests  
 a) loss in compressive strengths; b) loss in ultrasound pulse velocities (UPV)  
 c) loss in rebound values; d) loss of mass

### 4.3. Scaling tests

Freeze-thaw resistance under the combined influence of 3% NaCl de-icing agent solution was tested at the age of 180 days, according to the prEN 12390-9:2002 recommendations (scaling tests). Results on loss of mass ( $\text{g}/\text{m}^2$ ) are represented in Fig. 6, after 14 cycles applied. Results indicated that increasing water-to-cement ratio yields considerably increasing loss of mass in the case of CEM I and blended cements of moderate hydraulic additive content. CEM III/B shows superior resistance: limited loss of mass almost independently of the applied water-to-cement ratio. Scaling test is modelling the most severe freeze-thaw attack combined with de-icing salt, therefore, it is a suitable measure to indicate concrete or cement sensitivity against freeze-thaw attack. Present experimental results confirmed the experiences with blended cements of high BFS content to provide durable concrete of low permeability. Results also indicate a future research need on blended cements of moderate hydraulic additive content.

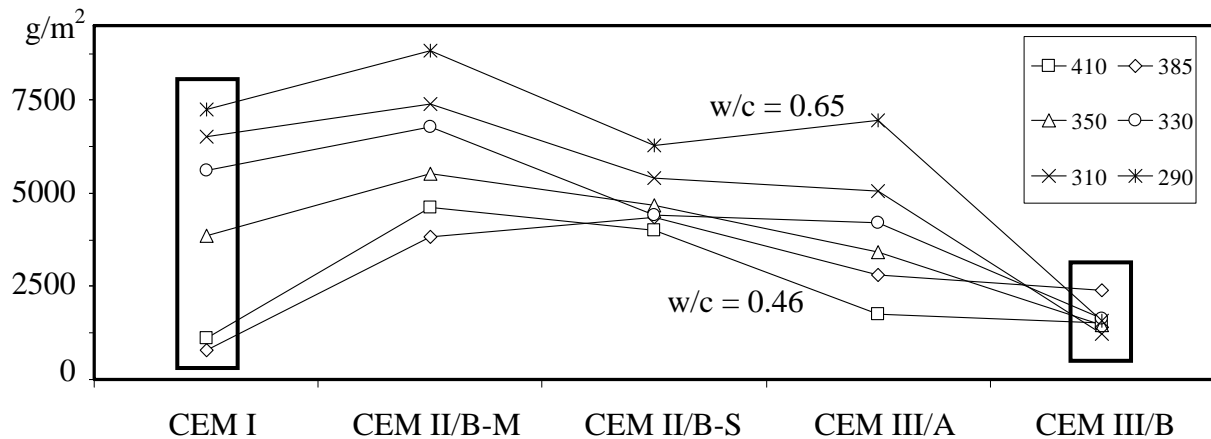


Fig. 6 Loss of mass (scaling) of concretes after slab tests according to prEN 12390-9:2002

## 5. CONCLUSIONS

In present experimental studies a detailed survey on differences and advantages of blended cements to Portland cement was given covering several tests at the BUTE Dept. of Structural Materials and Engineering Geology both on fresh concrete and hardened concrete of 30 different concrete mixtures (with the use of four different blended cements and one Portland cement, with 6 different cement amounts). Results demonstrated superior behaviour of blended cements of high BFS content (especially CEM III/B) that provides reduced permeability yielding advantageous water tightness and freeze-thaw resistance of concretes, thus considerably improved durability. Results also highlight a future research need on blended cements of moderate hydraulic additive content.

## 6. ACKNOWLEDGEMENTS

This research project was supported by the Duna-Dráva Cement Ltd.

Authors wish to present their gratitude to researcher colleagues Csányi, E., Kocsányi, K. and technical staff of the laboratory for their participation in present series of tests.

## 7. REFERENCES

- BUTE (2006) „Cement and concrete studies on blended cements – Final report”, *Research report* for DDC Co. Ltd., BUTE, Dept. of Structural Materials and Engineering Geology, (prepared by Zsigovics, I., Balázs, G.L., Csányi E., Kocsányi, K.K.), 2006 (in Hungarian)
- Civil & Marine Slag Cement Ltd. (2000) „Slag Cement Fact Sheets”, *Technical data*, 2000
- Rendchen, K. (2002) „Hüttensandhaltiger Zement”, *Verlag Bau+Technik*, Düsseldorf, 2002
- SCA Slag Cement Association (2002) „Slag Cement in Concrete”, *Technical data*, 2002

## **INNOVATIVE TEST-METHODS TO DETERMINE SEGREGATION OF CONCRETES WITH FLOWABLE CONSISTENCY – PRACTICAL EXPERIENCES**

*Dipl. Ing. Dr. Peter Kremnitzer*

*Dipl. Ing. Dr. Johannes Horvath*

*ARGE Bautech*

*7. Haidequerstraße 1*

*A-1110 WIEN, AUSTRIA*

### **SUMMARY**

For foundation works concretes with a relatively high flow consistency are used. Construction elements like diaphragm walls and bore piles formed with these concretes sometimes show deficiencies which can be related to the tendency of the used concrete to segregate. To describe this tendency, new methods of testing were proposed, in which at one hand the concrete is filtered under pressure and at the other hand the bleeding under pressure is determined. The goal for the project described here is to correlate these tests with practice and to define limits to distinguish useable concrete lots from insufficient ones. Furthermore a method is under development with which stable concrete mixes shall be obtained by controlling the particle size distribution of fine aggregates and binders. This method shall also be usable for concrete samples with unknown compositions taken from job sites to ex post evaluate the correlation between segregation and particle size distribution.

### **1. SEGREGATION OF CONCRETE IN FOUNDATION ELEMENTS**

At diaphragm walls and bore piles some typical effects can be observed which lead to deficiencies. In soils with a low transmissibility for water the concrete tends to bleeding which leads to pores and cavities and to the formation of areas with a high content of fine aggregates and binder adjacent to areas with rock pockets. In most of these cases an unusual enrichment of fine particles is also found on top of the construction elements. Cast in place bore piles with a length of 20 m and more sometimes show a one to two meters thick layer on top in which only water, binder and sand can be found. Similar effects can be found in diaphragm walls. These deficiencies cause different problems in practice. If the construction elements are meant as foundations the bearing capacity could be affected. In watertight constructions the water tightness could be diminished. That leads to expensive works of repair like injections of cement or polymer resins.

In transmissible soils sometimes a higher than calculated consumption of concrete is observed although the dimensions of the construction elements do not differ significantly from the calculated ones. This is supposed to be caused by a filtration of water through the adjacent ground. This effect is also known from the suspensions of cement, water, stone powder and bentonite used for sealing walls. It does not necessarily lead to deficiencies, sometimes it even increases strength and water-tightness, but it can have economical impacts due to the increased consumption of concrete.



Fig. 1 Rock pockets in a diaphragm wall

It is evident that these effects are depending on the compositions of the used concretes. The recipes of the concretes normally follow the principles for placing under water. That means that the content of binder is at least 350 to 375 kg/m<sup>3</sup>, the water/binder ratio is below 0.60 and the content of powder ( $\leq 0.125$  mm) is at least 430 kg/km<sup>3</sup>. The flow consistency determined according to EN12350-5 generally is between 56 and 62 cm. Nevertheless it turned out at some projects that these requirements are not enough to guarantee that the concrete doesn't segregate under difficult conditions. The assumption was made that the segregation is also highly dependent on the composition of the powder-like constituents of the concrete, on their particle size distribution as well as on their chemical and physical interactions. These effects are currently investigated by some scientific groups. One of these projects was started by a working group of the Austrian Society for Concrete and Construction Technology and this report describes the current state of the attempts to correlate the results obtained in the laboratory with the effects observed in practice.

## 2. TEST METHODS

### 2.1 Segregation

The methods used to determine the stability of concrete against segregation are described by Nischer, Macht (2006) and Eisenhut, Pekarek (2007). A pressure vessel (Fig. 2) is used which can be operated in different ways. The vessel has an outlet at the bottom.

To test the bleeding under pressure the outlet is closed and fresh concrete is put under pressure up to 3 bars for a defined time. The main difference between this test and standard bleeding tests is the pressure which is favourable for the testing of concrete with increased air content. Artificial air voids generally stabilize concrete but they are compacted under pressure. So the stabilizing action of the air voids in a pile or diaphragm wall can be different from that in standard bleeding tests, depending on the area of depth and therefore on the pressure. Tests with concrete without an increased air content showed no clear dependence of

pressure and bleeding in this test. The second difference is that after the test not only volume of water on top of the concrete is measured but also the water content in different layers of the apparently homogeneous concrete underneath. So the test can also be used to distinguish different concrete mixes which show only low bleeding. This test shall simulate the conditions in a construction element in watertight soil like clay, where almost no water is released to the surrounding soil and where the segregation leads to the ascension of the segregated water.

The second mode of operation is with the outlet open and with a fleece (geotextile) and a sieve on bottom of the vessel. These works as a filter and when the vessel is put under pressure excessive water is pressed out of the concrete. This test is similar to the filter press commonly used to characterize the stability of suspensions for sealing walls.



Fig. 2 Test apparatus (bleeding and filtration under pressure)

## 2.2 Particle Size Distribution

To test the dependence of the segregation on the particle size distribution of the fine aggregates and the binder three different methods to determine the particle size distribution were used.

- a) Flow- Particle- Image- Analyses (FPIA)
- b) Laser Granulometric Analysis (LGA)
- c) Hydrometer Analysis with an Areometer (HA).

The goal of these comparative investigations was to determine which method shows a correlation of its results with the results of the pressure tests. The FPIA was considered to be the most effective method to determine the particle size distribution and the shape of particles but this method needs complicated and expensive equipment. The other methods are much more widespread and in the case of the hydrometer analysis the equipment is rather cheap. So they were considered to be the better choice for standard concrete testing, if it could be proved that they show a performance similar to the FPIA.

At the end a procedure should be found with which the particle size distribution of the fine aggregates in a fresh concrete mix can be determined. For this it is necessary to extract the fine aggregates and the binder from the mix. The fresh concrete was taken from transport



vessels on different construction sites. With one part of these samples standard tests on fresh concrete were performed. Another part was dried by evaporating the water with Ethanol. After drying, the concrete was sieved, the fraction  $< 0.125$  mm was separated and the sand and the coarse aggregates were sieved a second time with water. The entire grain size distribution of the concrete was calculated from the result of the second sieving and from the amount of the fraction  $< 0.125$  mm. The fraction  $< 0.125$  mm was used for the three mentioned methods to determine its particle size distribution. It was found, that for LGA and HA the sample preferably should have a grain size  $< 0.063$  mm. So the samples were additionally sieved at 0.063 mm and the fraction smaller than this was tested in LGA and HA.

### 3. SAMPLES OF CONCRETE

Samples were taken from 6 construction sites by two test institutes (Arge Bautech and BPV). From each construction site samples were taken at different occasions to determine the constancy of the production. The pressure tests were performed by each of the institutes on the samples it took. The extraction of the fraction  $< 0.125$  mm was also performed by the institute which took the sample. LGA and HA were performed at Arge Bautech, FPIA at the Research Institute of the Austrian Federation of Cement Producers.

The concrete recipes differed according to the fact that they were produced in different plants for different construction projects. They were all Type C 25/30 according to EN 206-1 with flow consistencies between 56 and 62 cm, powder contents between 400 and 550 kg /m<sup>3</sup> and water/binder ratios  $\leq 0.60$ , binder contents were between 350 and 375 kg/m<sup>3</sup>.

### 4. RESULTS

Arge Bautech compared the two methods of testing in the pressure vessel. The tests of bleeding mostly showed a distribution of the water content as in Fig. 3. The top layer was always enriched with water whereas the next layer showed a significant depletion. In deeper layers the water content approached the average water content of the concrete. This figure was obtained with three different samples from three deliveries of the same recipe. The same samples underwent also the filtration tests. As shown in Fig. 4 there were also significant differences in the amount of filtrate of the three samples.

What should be discussed is, which values should be used to characterize bleeding. There is an indication that the depletion in the layers under the top layer can be measured more exactly than the enrichment in the top layer. There is no parallelism between the results of the tests of bleeding and of filtration. At some construction sites the samples with higher bleeding showed also a higher rate of filtration in the beginning, but with the concrete from other sites this relationship could not be found.

Fig. 5 shows a comparison between the three methods used to determine the particle size distribution of the powder. Obviously the results don't match. Although the contents of fine particles and the flow consistency were rather similar in the three samples of the tested concrete a relation between the graphs of filtration or bleeding and the particle size distributions couldn't be found with any of these methods. Although it is widely accepted that the small particles have an influence on the stability of a concrete mix, the method to regulate the stability by optimizing the particle size distribution has still to be investigated.

The next step will be to correlate the results of the tests of bleeding and filtration with the incidence of deficiencies in practice. For this it will be necessary to perform tests on large series of samples of concretes with high flow consistency and to record the special conditions of placing and casting. Up to now there are too little results to correlate the tests with practice.

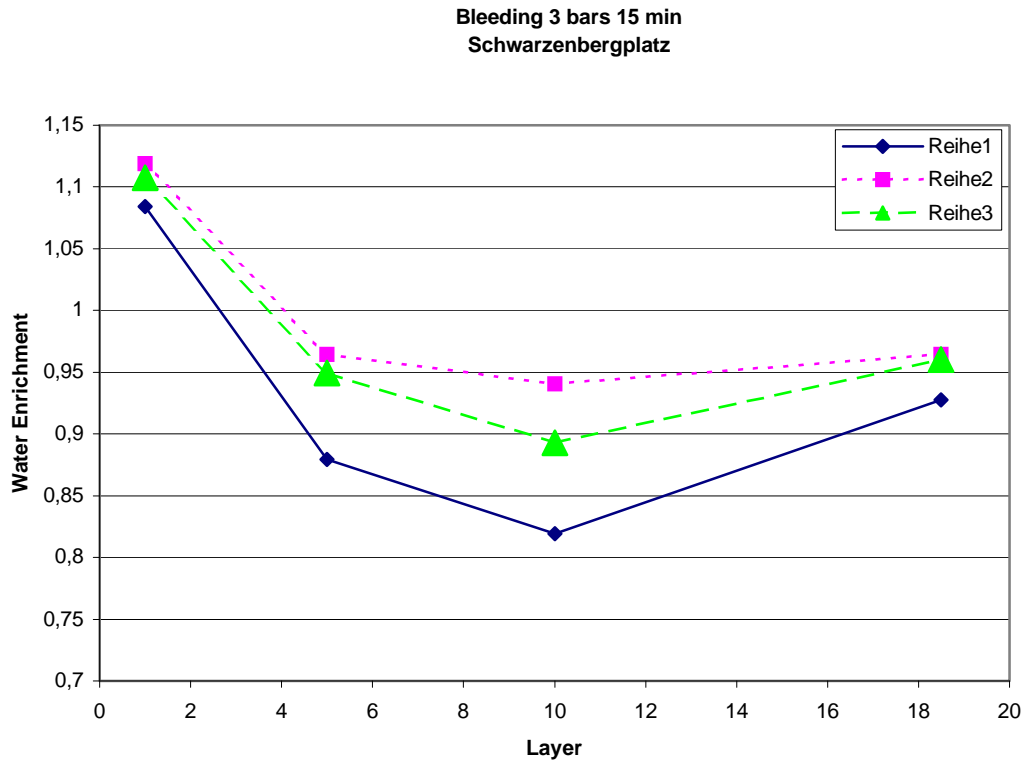


Fig. 3 Bleeding Construction Site: Schwarzenbergplatz

## 5. CONCLUSION

To determine the tendency of segregation of flowable concretes two test methods have been proposed. These tests were applied on various concretes from different construction sites. They show significant differences in the behaviour of different recipes and also of different lots of one recipe. However, the relationships between the results and the appearance of deficiencies in foundation constructions related to bleeding and filtration still have to be found to define specifications according to these tests. Furthermore, the correlation between the results and the particle size distribution of small aggregates and binders were investigated. It is widely accepted that the amount of powdery components has a strong influence on the stability of the fresh concrete, but up to now a definite relationship between the particle size distribution and the tendency to segregate was not detected. For this it will also be necessary to find the right method of determining the particle size distribution. Three methods, Flow-Particle- Image- Analysis, Laser Granulometric Analysis and Hydrometer Analysis have been tested. The differences between their results were rather big. None of them could be correlated with the results of the tests of segregation.

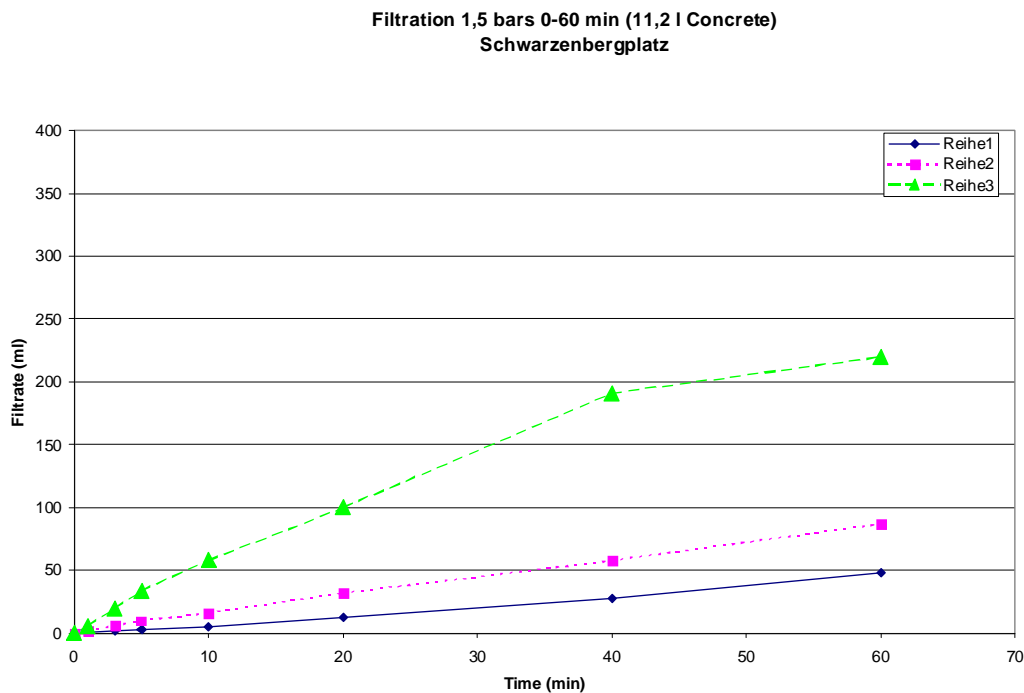


Fig. 4 Filtration Construction Site: Schwarzenbergplatz

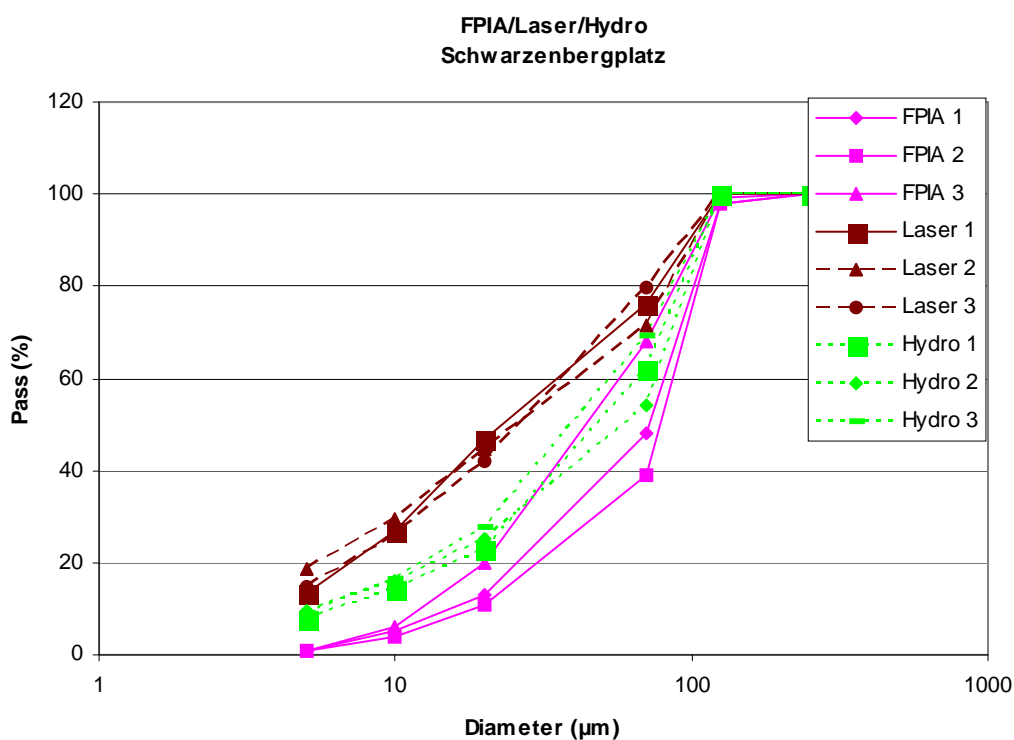


Fig. 5 Particle Size Distribution of different lots of Concrete from Const. Site  
 Schwarzenbergplatz

Eisenhut, Th.; Pekarek, A. (2007), „Bluten von Pfahl- und Schlitzwandbeton“, *unveröffentlichter Bericht der BPV*, Himberg

Nischer, P.; Macht, J. (2006), „Flowable concretes of various powder types, Measures for improving the workability“, *Concrete Technology BFT 08*, page 42-53.

## THE EVOLUTION OF SUPERPLASTICIZER TECHNOLOGY NEW OPPORTUNITIES IN CONCRETE INDUSTRY

*István Asztalos*  
*Sika Hungary Ltd.*  
*H-1117 Budapest, Prielle Kornélia u. 6.*

### SUMMARY

In order to have a better understanding of the current development processes of the concrete industry, it is important to examine polycarboxylate (PCE) based admixtures that are used in the concrete industry, their mechanism and the new opportunities they opened up in concrete technology. These possibilities can only be put into practice effectively if we take the decisive factors of each sector into consideration. The requirements are different in precast concrete, in ready-mixed concrete and site batched concrete industry as well. Today, the admixture production can take these – often largely diverse – requirements into consideration (Fig. 1).

### 1. THE EVOLUTION AND DEVELOPMENT OF ADMIXTURES

Today admixtures constitute an essential part of concrete technology. The most important ones are the superplasticizers, which play the most effective role in this field. Their widespread usage was triggered off by the advancement in both quality and technology related demands. There have been numerous attempts for the mechanization of the exhausting physical work required by the mixing, transportation, placement and compaction of concrete, ever since 1854 in Hungary (Balázs, 1994).

Concurrently, alongside mechanization, there was an increasing need for a more flowable consistency, primarily enable easier handling. Obviously, if this is achieved by additional water, the strength and therefore quality and durability of the concrete will deteriorate.

The first research findings pertaining to the above

efforts were published by the American Duff A. Abrams in 1918 under the title „Design of Concrete Mixtures”. The development of admixtures has always been closely related to the water/cement ratio as well as concrete quality. Tallow and kaolin were applied already in 1885 in order to improve the properties of concrete, while the American Moyer suggested the addition of crude oil in 1909. From 1912 onwards soaps have been applied, which slightly improved workability. In those days even clay was used as an admixture. The first branded admixtures appeared in Germany in 1910 (Pásztor, 1988).

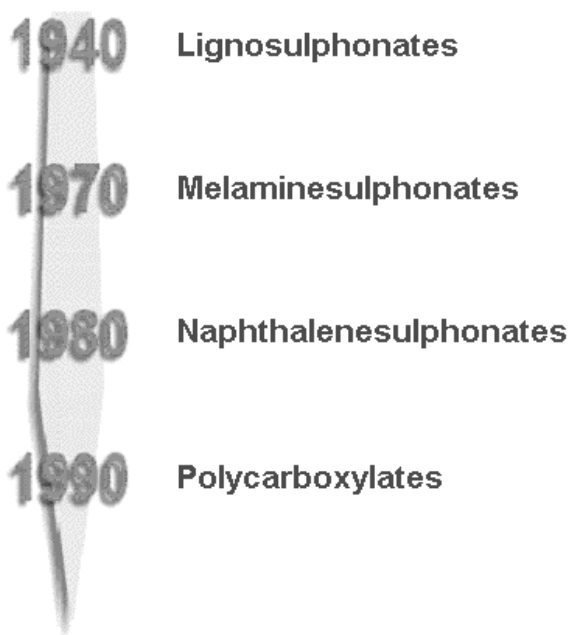


Fig. 1 The development of active ingredients

Interestingly, this date coincided with the foundation of the present-day Sika-Group. Kaspar Winkler – who was born in the Austrian village of Thüring, in Voralberg county next to Bludenz in 1872 – founded his enterprise under the name 'Kaspar Winkler & Co.' in 1910. The first Sika admixtures appeared in 1925 (Heim, 2005).

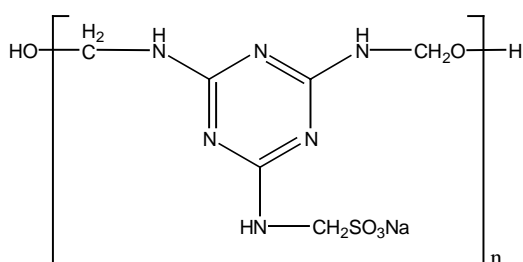


Fig. 2 Melaminesulphonate polycondensate (MFS) (Blask, 2004)

In retrospect it is fair to say that the development of admixtures was a gradual process. The lignosulphonates and their derivatives, the oxycarboxylic acids and their basic salts, the protein decompositions – in concrete technological terms: the plasticizers appeared at the beginning of the 20th century. In 1939, during the pursuit of cement grinding aid in the laboratory of Portland Cement Association Chicago, a certain vinzol-trietanolamin based grinding aid was

found to provide significant frost and freeze/thaw resistance properties for concrete pavements by creating microscopic air voids. With this invention, the term air entraining agent (according

to the terminology of that time: air bubble creating admixture) was introduced. This pool of knowledge only got through to Europe in 1946 because of World War II (Pásztor, 1988).

The application of increasingly effective materials led to the introduction of new terms denoting stronger plasticizing effects. These new materials were named superplasticizers. The plasticizing admixtures, alongside the purified, modified lignosulphonates can be classified into three groups: sulphonated melamine-formaldehyde condensates (Fig. 2), sulphonated naphthalene-formaldehyde condensates (Fig. 3) and sulphonated vinyl polymers (Buday, 1999).

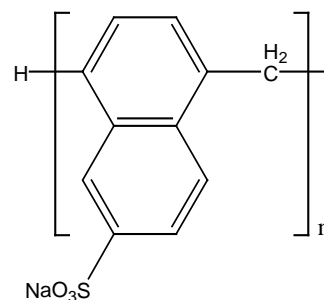


Fig. 3 Naphthalenesulphonate polycondensate (NFS) (Blask, 2004)

To date the latest development in superplasticizer technology are polycarboxylates (PCE, Fig. 4). Generally we can say that Lignos and Gluconates are plasticizers (reduction of the water content between 5 and 12 %) and Melamines, Naphthalenes, Vinylcopolymers and PCEs are superplasticizers (reduction of the water content higher than 12 %).

This advancement was initiated by Japanese research in 1983, which focused on the durability of the concrete. The criteria of durable concrete could only be fulfilled via the vibration of the concrete by well skilled workers. The decreasing number of skilled workers in Japan in construction sites led to a similar decrease in the quality of industrial constructions. This in turn generated a demand for easy and self compacting concrete, which gave a boost for the development. The necessity of the application of this type of concrete was first promoted by Okumara in 1986 (Zsigovics, 2003).

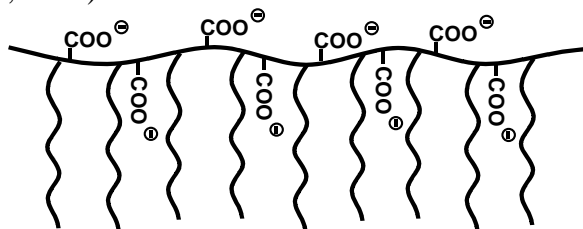


Fig. 4 Polycarboxylate (PCE) (Blask, 2004)

## 2. New opportunities in concrete technology

The latest generation of superplasticizers, the polycarboxylates (PCE) are revolutionizing concrete technology around the world. The PCE based superplasticizers with the help of their giant molecules as barriers between the cement particles causing steric hindrance and resulting in more efficient plasticizing. With the use of these admixtures the production of concrete products with adaptable properties becomes possible. This stands for fresh concrete as well as hardened concrete.

Let us examine and compare the chemicals that are the basis of superplasticisers from a concrete technologist point of view. The sulphonated melamine-formaldehyde condensates, in a word Melamines, constituted the primary materials of superplasticisers, which appeared on the market from the 1960's and 70's onwards (Fig. 5). These products have a strong plasticizing effect, but lose slump relatively quickly. Therefore they are primarily used in precast factories.

### 2.1 The precast concrete industry

In the precast concrete industry strongly plasticized concrete and easy workability are fundamental requirements. However, subsequently we would like to achieve high early strength in order to achieve short stripping times. It is important to note that the various technologies have various demands, which obviously require different mechanisms with machinery.

Before the Melamines appeared in the field of precast concrete industry, steam curing used to be the predominant method for promoting highest early strength. The steam accelerated the hardening process: crystallization processes is accelerated, so does cement hydration, therefore within a relatively short period of time a large proportion of concrete end strength is available. When making warm concrete, in order to accelerate the setting and hardening a significant amount of heat is transmitted into the material during mixing, in a way that its temperature should be between 35-50 °C. Apart from the benefits of steam curing one has to make allowances for maleficent phenomena, such as:

- the final strength of the concrete is decreased
- the structure of the concrete became cracked
- the concrete „burnt” (sudden water loss on the surface) and
- significant amount of energy usage was required (Márkus, 1979).

With Melamines rather high dosages have to be used in order to achieve a good plasticizing effect. The dosage of a 30 % water solution in correlation with the weight of the cement is more than 1%. The softer consistence of the fresh concrete in larger dosages is coupled with a certain „adhesive-effect”, which ensures the coherence of the mixture without it sticking to the mould. In contrast to Lignos, Melamines have no retarding effect; in fact some products even accelerate the hydration of cement (Német, 2006).

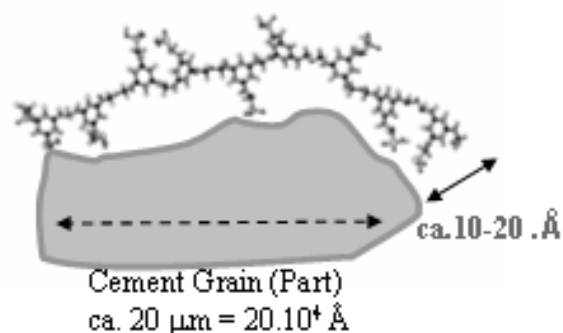


Fig. 5 The size of the Melamine molecule and that of the cement particle (Honert, 2004)

## 2.2 The ready-mixed concrete industry

The ready-mixed concrete is expected to keep its properties, which were configured at the mixing process, for a long time regardless of weather conditions in a controllable way without the separation of the components. We would like to be able to transport ready-mixed concrete to great distances, to pump and mould it easily. Ready-mixed concretes can be produced in building site batched industrial mixers as well as in the carrier vehicle itself: in the mixing truck (Grübl, Weigler, Karl, 2001).

In the Hungarian practice, but also in other parts of the world, the modern construction technology of the 1970's and 80's developed in a way, which led to the termination of building site batched concrete production. On the other hand, the mixing trucks were mostly used for transportation only, and for preventing the separation of the components. Thus, pre-mixed material is placed in them at the concrete factory and they the truck mixing method is rarely executed (Rácz, 1998).

The establishment of the ready-mixed concrete industry was supported by the use of such admixtures, which allowed for longer workability and strong plasticizing. The succeeding basic materials of superplasticizers were the sulphonated naphthalene-formaldehyde superplasticizers, in short: Naphthalenes, which appeared on the market from the 1970's and 80's onward (Fig. 6). These products had a somewhat longer lasting effect due to strong plasticizing.

Thus, they were not only applied in precast factories, but also in ready-mixed factories as well. Naphthalenes had to be dosed to the concrete in much smaller portions. The dosage of a 30 % water solution in correlation with the weight of the cement is effective in 0.2-0.5 % extent. The hydration of the cement is just slightly retarded and no additional air voids are generated. (Német, 2006). However, sometimes there is a need for „after-dosage” at the building site, in case the concrete has to be applied after longer transportation.

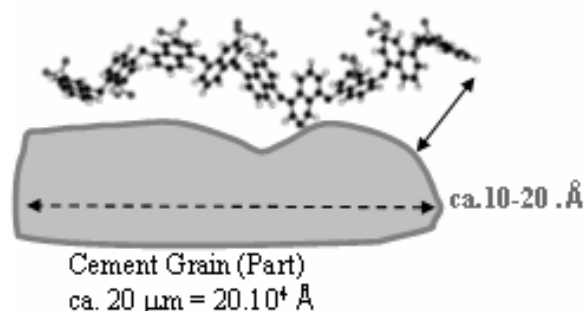


Fig. 6 The size of the Naphthalene molecule and that of the cement particle (Honert, 2004)

## 2.3 PCE based admixtures

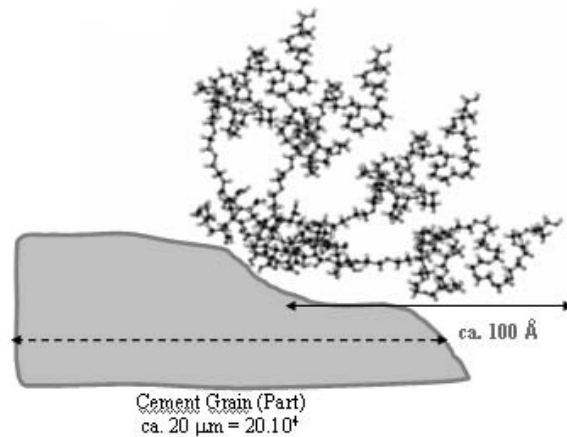
The concrete, which is manufactured in precast, ready-mixed and site batched concrete factories must be able to meet many various requirements. These requirements have generated an advancement in admixture development, which made it possible for superplasticizer production to take the demands of the various industrial sectors into consideration. The manufacturers offer different materials for each segment: the precast, ready-mixed and site batched concrete industries as well. Furthermore, there are other significant special fields, such as: tunnel construction (sprayed concrete), paver production (semi-dry concrete) etc. The active ingredient of the PCE based admixtures is the so called polycarboxylates, the molecule structure of which differs from that of the materials introduced earlier. These old chemicals are such aniono Polymers, which are generated from insaturable carbon acids by polymerization, e.g.:



from acrylic acids, metacrylic acids or malein acids. A bifurcated polymer is created from the fully or partially esterificated/etherificated carboxyl group. The structure of the polymer, which is made of one main chain and many aliphatic side strings, reminds people of a comb, thus this type of the polymer is called comb-polymer (Blask, 2004).

Both the efficiency and economic efficiency of the Polycarboxylates-ether-based admixtures, which represent the latest generation of admixtures, considerably surpass that of the earlier materials. These innovative superplasticisers have been manufactured in Europe since 1997. Owing to their molecular structure, they prevent the cohesion of cement grains (Fig. 7). This way the plasticising effect is stronger than ever before, even if the dosage is very low.

Fig. 7 The size of the PCE molecule and that of the cement particle (Honert, 2004)



## 2.4 Self Compacting Concrete (SCC)

With the application of polycarboxylate based superplasticizers an outstanding fluidity at lowest water/cement ratios could be achieved. The reduction of the water content might be up to 40 %. Special mix design ( $\leq 0.125 \text{ mm}$ ) and adapted grading curve is necessary. Special high performance superplasticizers are necessary to produce SCC in order to ensure a fluid concrete with controlled workability. It's possible to achieve a very high water reduction and a stable and cohesive concrete by using polycarboxylate based superplasticizers.

The Self Compacting Concrete is an innovative concrete that does not require vibration for placing and compaction. It is able to flow under its own weight, completely filling the formwork and achieving full compaction, even in the presence of congested reinforcement. The hardened concrete is dense, homogeneous and has the same engineering properties and durability as traditional vibrated concrete (Honert, 2004).

Nowadays, the admixture factories are able to produce similar basic elements serve to compound polymers for precast industry (quick stiffening and quick strength development) as well as polymers for ready-mixed concrete in high temperature conditions (long workability time combined with good strength development). A further advantageous characteristic of PCEs is that the different structures are compatible among themselves, which means concrete properties cannot only be modified by molecule design but also by combination of two or more polymers with different properties (Wombacher and Hirschi, 2005).

## 3. Conclusions

The fundamental criteria of the concrete durability are the use of concrete, the components, properties, workability, after treatment of which is suited specifically for its purpose. With the help of PCE based admixtures these factors can be influenced specifically. The properties of concrete can be influenced positively and purpose-orientatedly in case of precast concrete-, ready-mixed and site batched concrete production.

#### 4. Acknowledgements

The Author expresses his appreciation of all Sika-Group members (especially for Bastian Bicher and Oliver Blask), whose helpful attitude made it possible that this presentation could provide up-to-date information about the revolutionary rapid changes of concrete technology.

#### References

- Balázs, Gy., (1994), „Beton és vasbeton I. – Alapismeretek története”, *Akadémiai Kiadó, Budapest*
- Blask, O., (2004), „Fließmittel von Sika Addiment – Ein Überblick”, *Sika Addiment GmbH, Leimen*
- Buday, T., (1999), „Betonadalékszerek”, *Építésügyi Tájékoztatási Központ Kft., Budapest*
- Grübl, P., Weigler, H. and Karl, S. (2001), „Beton – Arten, Herstellung und Eigenschaften”, *Ernst & Sohn A Wiley Company, Berlin*
- Heim, W., (2005), „In memoriam Dr. Romuald Burkard”, *Dr. Hans Peter Ming, Chairman of the Board Sika AG, Zürich*
- Honert, D., (2004), „Superplasticizers – Data Pool”, *Sika Addiment GmbH, Leimen*
- Márkus, M., (1979), „Előregyártás I.”, *Tankönyvkiadó, Budapest*
- Német, F., (2006), „Öntömörödő betonok Sika® ViscoCrete® technológiával – Diplomamunka”, *BME Építőanyagok és Mérnökgeológia Tanszék, Szerkezetépítő Szakmérnöki Tanfolyam, Betontechnológiai Ágazat, Budapest*
- Pásztor, R., (1988), „Betonadalékszerek”, *Építésügyi Tájékoztatási Központ Kft., Budapest*
- Wombacher, F. and Hirschi, T., (2005), „Technology and applications of the latest High-Range Water Reducer generation”, *Sika Technology AG and Sika Schweiz AG, Zürich*
- Zsigovics, I., (2003), „Öntömörödő beton, a betontechnológia legújabb forradalma – 1. Fogalmak és vizsgálati módok”, *Vasbetonépítés (Concrete Structures) – Journal of the Hungarian Group of fib, No. 1/2003, pp. 17-24.*

## **INNOVATIVE SUPERPLASTICISERS FOR MODERN CONCRETE STRUCTURES**

*Mario Corradi, Rabinder Khurana, Roberta Magarotto, Sandro Moro*  
*BASF Construction Chemicals Admixtures System Europe*  
*Via Vicinale delle Corti, 21*  
*31100 Treviso, Italy*

### **SUMMARY**

Concrete is a versatile material and offers new opportunities for developing innovative structural forms. The last few years have shown revolutionary developments of new types of concrete, specially self-compacting concrete, whose use is growing rapidly in Europe, and fibre reinforced ultra high performance concrete, whose applications are still in the very preliminary stages. The extraordinary properties of ultra high performance steel fibre reinforced concrete makes it an excellent alternative to steel as a construction material and allows the construction of sustainable and cost effective structures. Recommendations and guidelines on this material are available, but International Standards will have to be developed. This paper presents results of a study made to develop "user friendly" UHPC mixtures. The role of the superplasticiser is examined. Thanks to the innovative superplasticisers, the concrete mixes are self-compacting with high flow and adequate plastic viscosity.

### **1. INTRODUCTION**

Construction began when life appeared on the earth. Birds build nests, bees and ants make complex hives, some animals build shelters or dig tunnels and humans build structures. Human structures started with mud bricks, wood, stones and metal. Bricks and stones are compressive materials and are suitable for arch, dome or barrel structures; which limit the span. Reinforced concrete, as we know it, appeared in 1854 (W.B. Wilkinson). It has a good compressive strength, but a rather low tensile strength. High tensile steel changed the landscape as it allowed building long span girders and trusses. Prestressing provides concrete with a tensile capacity, increasing therefore, the span. Thanks to the advancements of the admixtures science during the past 30 years, significant improvements in the performance of concrete have been made. Compressive strengths of the concrete in the structure have progressively increased from 25 MPa to above 120 MPa. Tensile strengths do not follow the same path, but are provided for by the steel reinforcement (bars, fibres, prestress tendons, etc.)

### **2. DEVELOPMENT OF ULTRA HIGH PERFORMANCE CONCRETE**

The various phases in the development of UHPC may be summarised as below:

- DSP Concept: Ultra fine powder paste fills the voids within the cement particles
- MDF (Macro-Defect Free) cement pastes containing polymers, aluminous cement and hard calcinated bauxite aggregates were developed, but they found very limited applications.
- HPC (High Performance Concrete), a terminology coined in the 80s' which identified concrete mixes with high workability and durability.

- If it was a mix with high strengths (100 MPa) it was called a High Performance High Strength Concrete (HPHSC).
- SIFCON (Slurry Infiltrated Fibre Concrete) is produced by filling the formwork with the bulk of the fibres and injecting a fluid cementitious mortar. This technique also finds some limited applications in repairs and retro-fitting.

Ultra High Performance Concrete is a material with a cementitious matrix that has a characteristic compressive strength in excess of 150 MPa and possibly attaining 250 MPa. It contains steel fibres (1 to 4% volume) in order to achieve appropriate ductile behaviour under tension. It dispenses with the need for passive (non-prestressed) reinforcement. It also may contain polymer fibres (polypropylene fibres) for fire resistance. With respect to normal strength concrete (NSC), which have 4 components (cement, aggregates, water and admixtures) and HSC, that has 5 components (cement, aggregates, other binders, water and admixtures), UHPC has 6 or more components (cement, other binders, fillers, aggregates, fibres of steel or synthetic materials and admixtures). Therefore, the composition of UHPC is more complex. Tab. 1 lists some typical data on the properties of UHPC.

Tab. 1 Typical properties of UHPC

Compressive	180 - 230 MPa
Flexural	40 - 50 MPa
40 - 50 MPa	55 - 60 GPa
Total Fracture Energy	20,000 - 30,000 J/m <sup>2</sup>
Elastic Fracture Energy	20 - 30 J/m <sup>2</sup>
Density	2.45 - 2.55
Entrapped air content	2 - 4%
Capillary porosity	<1%
Total porosity	2 - 6%
Creep coefficient	0.2 - 0.5
Chloride ion diffusion	0.02 x 10 <sup>-12</sup> m <sup>2</sup> /s
Carbonation penetration depth	<0.5 mm
Freeze/thaw (after 300 cycles)	100%
Salt-scaling (loss of residue)	<10 g/m <sup>2</sup>
Abrasion (relative volume loss index)	1.2

Proprietary premixed UHPC mixes are available commercially in small and big bags of up to 1500 kg. However, the handling, logistics and the materials cost limit its use in “niche” and relatively small applications.

To increase the diffusion of UHPC we need to make this material in the most cost effective manner and with materials that are available locally. Other factors that affect its diffusion are the development of new structural concepts that can better utilise its extra ordinary properties. But the situation is evolving and already there are recommendations on UHPC from AFGC/SETRA (2002) Working Group and Concrete Committee of the Japan Society of Civil Engineers JSCE (2006).

### 3. UHPC: COST EFFECTIVENESS AND SUSTAINABILITY

UHPC is basically a new material; even though it is called concrete, it has aggregates of 2 mm maximum size. Its applications will probably not follow the path of normal concrete. With

time new structural concepts will be developed that can better utilise the superb properties of high strength and durability of the UHPC. At present we look for material with 4 distinctive properties:

- strength
- workability
- durability
- affordability (cost).

A structure is not only designed, but it also must be constructed. Workability affects the cost and time required to build the structure. Therefore, time and cost are two factors that decide if the structure will be build. The future of UHPC depends on some breakthrough on these two fronts to push it into popular applications. To fully utilise the capacity of UHPC, new applications must be developed. The very high strength of UHPC will not be necessary if we keep using it on existing types of structures.

New forms of structures will have to be developed for this new material. This will require us to think "outside the box" to find more appropriate applications (Man-Chung Tang, 2004). We have to be innovative.

Besides the ecological advantages, other economical benefits are:

- lower quantities of concrete to be placed
- lower amount of reinforcement
- lesser formwork area
- less dead load, which means smaller foundations.

These result in reduced materials, wage, transport and handling costs.

#### **4. PIONEERING APPLICATIONS OF UHPC**

Ultra High Performance concrete has several particular "niche" applications and there are some pioneering applications in structural concrete. These include Sherbrooke Pedestrian Bridge, Canada, Bourg-lès-Valence Bridge in France, Shawnessy Train Station, Calgary, Canada, Seonyu Pedestrian Bridge, Korea, Toll barrier, Milau Viaduct, France. Other applications are mine construction (shaft lining, chutes), replacement of steel or metallic parts (anchor heads of prestressed concrete, pump impellers, gratings) military applications for missile testing and blast resistant structures. UHPC is used for security applications which require extremely high penetration resistance as well as fire recovery properties and weight reduction. Current security technology uses either metal alloys or concrete-steel composite panel structures that do not satisfy new security and weight requirements. UHPC provides an economical alternative. It also permits monolithic precasting which reduces the numbers of parts to assemble and also reduces the chances for the enclosure to be fractured. The material may allow the elimination of rebar through prestressing or, where geometry requires a very low cover to reinforcement that enables to produce thin, lightweight and long-span structures. Furthermore, the material characteristics enable the achievement of highly sculptural architectural forms. These applications use proprietary premixed material. In Japan a pre-blend binder has been developed for ultra high strength concretes, with the specified design strength of 80-150 MPa. It has been proved experimentally that the structure members using these concretes have a good durability, earthquake and fire resistance. The first example of compact reinforced composite (CRC) was the bridge deck of the Kaag bridges near Sassenheim, Netherlands. A special mix was developed using silica fume and bauxite aggregates. The compressive strength was over 180 MPa.

It is worth mentioning the Gärtnerplatzbrücke across the River Fulda in Kassel, the first example of UHPC in Germany. For the precast concrete segments the UHPC was produced on site with locally available materials.

## 5. TEST PROGRAMME

Objective of the Project is to develop a technology to produce Ultra High Performance Concrete (UHPC) with locally available raw material. UHPC is a concrete having a compressive strength greater than 150 MPa. Due to the presence of steel fibres the tensile strength is above 20 MPa and fracture energy more than 10 kJ/m<sup>2</sup>. It is characterised by its low water binder ratio (usually less than 0.20), low porosity and very high durability against all environmental exposures.

The UHPC technology is based on the following principles:

- Enhancing the homogeneity of the matrix by limiting the maximum size of the aggregates; may be up to 5 mm
- Improving the compacted density by optimising the granular mix (particle packing)
- Increase the ductility of the matrix by incorporating appropriate amount of steel fibres
- Improve the microstructure and durability by post-set heat treatment
- Produce "user friendly" mixtures. That is, the mix constituents are readily available locally and the mixing and the casting procedures as similar to the existing ones.
- Self-compaction of the mix is a must.

For developing a cementitious composite having a compressive strength more than 150 MPa at 28 days and a flexural strength of 35 to 40 MPa also at 28 days, the following test programme was set up:

Cement type	CEM I 42.5 Fintitan	CEM I 52.5 Rossi Fumane
Cement content kg/m <sup>3</sup>	600	600
Undensified silica fume kg/m <sup>3</sup>	100	100
Ground slag kg/m <sup>3</sup>	500	500
Sand 0 - 0.4 mm kg/m <sup>3</sup>	195	195
Sand 0.4 - 1.2 mm kg/m <sup>3</sup>	520	520
Sand 1.2 - 2.4 mm kg/m <sup>3</sup>	195	195
Steel fibres 0.1 dia., l=13mm kg/m <sup>3</sup>	100	100
Admixture	3 PCE superplasticisers	
Dosage	That required for self-compacting. Slump flow retention up to 30'	
Water	Water binder ratio = 0.18 – 0.22	
Test specimens	4x4x16 mm prisms for Rc and Rf @ 1 -7 - 28 days	
Curing	Standard laboratory conditions	

## 5.1 Selection of the superplasticiser

The choice the superplasticiser is very important as it will determine the total water content, the workability and its retention for the time required for transportation and placing of the UHPC. In this respect nanotechnology has brought new light into the Admixture Science. It is now possible that the chemicals or polymers can be engineered to bring together functional groups aimed at targeted performances. Polymers are built for strong or weak adsorption on to the cement particles for dispersion effectiveness and for hydration control (Corradi, Khurana, Magaretto, 2004).

Through investigation of the nano-behaviour, a technology that allows the control of water demand and workability retention of concrete has now been developed. The chemical and physical behaviour of polymers can be controlled through:

- chain length
- side chains length
- electrical charges
- side chain density
- free functional groups.

The superplasticisers selected for test programme are state of the art high range water reducing superplasticiser (HRWR), high range water reducing and early strength enhancing superplasticiser (HWR HE) and long slump retention superplasticiser (LSR).

## 5.2 Test results

For evaluating the flow properties of these mixes, the standard slump flow cone was not suitable as the flow was un-measurable. A small cone was develop having a height of 120 mm, bottom diameter of 140 mm and the top diameter of 100 mm. Tests were carried out to make a correlation with normal SCC. It showed that the slump flow with this “reduced” cone should be > 450 mm and  $T_{35}$  between 2 and 6 seconds. The results of tests made on the fresh and hardened UHPC are shown in Tab. 2.

Tab. 2 Properties of fresh and hardened UHPC

Superplasticiser	HRWR		HRWR HE		HRWR LSR	
Cement type	42.5	52.5	42.5	52.5	42.5	52.5
SP dosage l/m <sup>3</sup>	30	34	32	36	32	35
Water l/m <sup>3</sup>	200	210	195	205	195	210
W/C+SF+Slag	0.17	0.18	0.16	0.17	0.16	0.18
Slump flow @ 5'	490	505	510	530	480	495
Slump flow @ 30'	470	490	480	500	460	470
$T_{35}$ at 5' sec.	7	9	3	4	4	3
$T_{35}$ at 30' sec.	9	11	4	5	5	4
Rc at 1 day MPa	21	27	63	78	Not demouldable	
Rc at 7 days MPa	125	147	138	161	95	137
Rc at 28 days MPa	155	169	158	173	152	164
Rf at 1 day MPa	10.4	13.6	14.2	17.6	Not demouldable	
Rf at 7 days MPa	25.0	31.8	32.1	35.4	21.7	26.5
Rf at 28 days MPa	36.4	40.8	38.6	42.8	38.2	37.7



From the results obtained it is clear that the long slump retention superplasticiser (LSR) is not suitable for the production of UHPC as it delays the setting time and consequently the hardening, beyond the 24 hours. With the high range water reducing superplasticiser (HRWR) the mixes are very cohesive (characterised by the high  $T_{35}$  time) and are therefore, difficult to place as they flow slowly. Also, the strength at 24 hours is not sufficient for utilisation in the precast production.

High range water reducing and early strength enhancing superplasticiser (HWR HE) is the appropriate admixture as it provides a good rheological profile for the UHPC in its fresh state, maintaining the workability for a sufficient time to allow for its placing and finishing. The strength development is excellent even at the early ages (1 day). The 28 day results are also, satisfactory.

## 6. CONCLUSIONS

Ultra High Performance concrete has been on the scene for more than twenty years. Its application has been limited to some “niche” applications stated earlier and to some experimental structures. But the scene is rapidly changing as international recommendations for the design and construction of structures in UHPC have been proposed and more are on the way. This paves the road for the design engineers to think of new structural concepts and innovative architectural forms.

Nanotechnology will help to engineer more efficient polymers to develop more efficient superplasticisers that will meet the challenges posed for the production and use of a “user friendly” and cost effective Ultra High Performance Concrete made with locally available materials.

## 7. REFERENCES

- AFGC/SETRA (2002), “Ultra High Performance Fibre-reinforced Concretes”, Interim Recommendations.
- JSCE (2006) Guidelines for Concrete No. 9, “Recommendations for Design and Construction of Ultra High Strength Fibre Reinforced Concrete Structures” (Draft)
- Man-Chung Tang (2004), “High Performance Concrete – Past, Present and Future”, International Symposium on Ultra High Performance Concrete, Kassel, September 2004.
- Corradi, M., Khurana, R. and Magarotto, R. (2004), “Total Performance Control: An innovative technology for improving the performances of fresh and hardened ready mixed concrete”. Proceedings of ERMCO Congress, Helsinki, June 2004.

## **CHEMICALLY REACTIVE SUPERPLASTICISERS WITH IMPROVED WORKABILITY RETENTION**

*Giorgio Ferrari, Francesco Surico, Paolo Clemente, Mariele Gamba, Lino Badesso*  
*Mapei SpA*  
*Via Cafiero 22, 20158 Milano; [concrete.lab@mapei.it](mailto:concrete.lab@mapei.it)*

### **SUMMARY**

New type polycarboxylate superplasticizers are characterised by higher water reducing ability and better retention of the workability of concrete in comparison to the first generation superplasticizers based on naphthalene sulfonate and melamine sulfonate. Nevertheless, in many cases, mostly when low W/C ratio and long distance transportation are required, even polycarboxylate superplasticizers are inadequate in their capability to retain the workability. Consequently, high dosages of retardants or retempering of concrete cannot be avoided. In the present work, an example of a new type of superplasticizer is presented, specifically developed to overcome the aforementioned drawbacks. These new polymers are chemically reactive in the fresh cement mixture and become active as superplasticizers with time. By using these polymers it is possible to maintain the designed class of consistency of concrete mixtures from the mixing stage at the batching plant to the job site, thus eliminating the need of retempering of concrete and without any delay in the development of mechanical strength. The chemical structure of these polymers is presented, their mechanism of action and performance in cement paste and concrete tests are discussed in comparison with the traditional polycarboxylate superplasticizers.

### **1. INTRODUCTION**

The invention of superplasticizers goes back to more than seventy years ago (Tucker, 1936), but they became increasingly popular in concrete technology just since the last decades of the last century. The earlier class of superplasticizers which was developed, often referred as the first generation superplasticizers, consists of synthetic polymers based on polycondensation products of naphthalene sulfonate with formaldehyde. The dispersion of the cement particles produced by these polymers is mainly due to the electrostatic repulsion induced by these negatively charged macromolecules after their adsorption onto the cement particles. Such polymers require relatively high dosages – normal dosage is 0.4 per cent of active polymer by weight of cement or higher - and have, as a main disadvantage, a pronounced slump-loss with the time of mixing. In fact, the fresh concrete mixtures containing these polymers hardly retain the initial flow for more than 30 minutes. More recently, new types of superplasticizers based on acrylic copolymers have been developed, which are generally referred as polycarboxylate superplasticizers. These polymers, which represent the new type of superplasticizers, are characterised by a “comb-like” structure consisting of a main backbone bearing free carboxylic anionic groups and pendant non ionic side chains. By modifying the type of monomers, their proportions and the reaction conditions, a variety of polycarboxylate superplasticizers with various characteristics and performances have been produced and commercialised with different quality specifications: acrylic superplasticizers (Corinaldesi et al., 2003), polycarboxylic ether superplasticizers (Corradi et al., 2003), nanostructural superplasticizers (Clemente et al., 2005). Thanks to their structure, polycarboxylate

superplasticizers are much more effective in comparison with the first generation ones, both in terms of dosage – normal dosage is about 0.2 per cent of active polymer by weight of cement – and in terms of workability retention. In fact, by using these superplasticizers the initial flow of concrete mixtures can be effectively retained for 60 minutes. These superior effects are ascribed to the better dispersion of cement caused by the polyoxyalkylene side chains, which exert a steric repulsion in addition to the electrostatic repulsion caused by anionic carboxylic groups.

Although polycarboxylate superplasticizers represent a substantial improvement in comparison with the lower effectiveness and the poor retention of the workability offered by the first generation superplasticizers, they are still unsatisfactory in many applications, as in the case of ready-mixed concrete, where the transportation of concrete by truck mixers from the mixing plant to the job site, due to the highly congested traffic of the urban areas, can take more than one hour. In these conditions and particularly in hot climates, even polycarboxylate superplasticizers are ineffective in preventing “slump-loss” and therefore it is necessary to restore the initial workability at the job site by the addition of more water to the mixer. This operation, which is known as “concrete retempering”, increases the water content of the concrete mixtures (water-to-cement ratio) and causes obvious detrimental effects on the mechanical properties and the durability of hardened concrete. The proper remedial action in these cases is an extra addition of superplasticizer at the job site, before placing the concrete, in order to restore the initial workability without affecting W/C. However, this operation requires additional quality control at the job site, and represents a significant disadvantage.

Recently, a new superplasticizer referred as “Slump Loss Controlling Agent” (SLCA) has been developed, based on a reactive polymer framework structure of polycarboxylate polyether type superplasticizer and capable of controlling the slump retention time of concrete for more than 90 minutes without negatively affecting the early mechanical strength development (Hamada et al., 2003). Nevertheless, despite these promising results, due to the afore mentioned reasons, there is the need to develop new superplasticizers capable to further extend the workability of fresh concrete mixtures.

In this paper, a new chemically reactive Superplasticizer (CHRS), capable to maintain and extend the initial workability of concrete mixtures for more than two hours without any adverse effect on mechanical strength development, is presented.

## 2. EXPERIMENTAL STUDIES

*Cement* - The cement used for the tests was a CE II/A-LL 32.5 according to ENV 197/1, typically used for ready-mixed concrete in the Italian market (Tab. 1).

**Test methods** - In all the following tests, CHRS polymer was always compared, at the same dosage, with a conventional polycarboxylate superplasticizer (Dynamon SR3, Mw = 39.000, Mn = 23.000, Mz = 65.000).

Tab. 1 Composition and characteristics of CE II/A-LL 32.5 Portland cement

Component/characteristic	
SiO <sub>2</sub> (%)	18.39
Al <sub>2</sub> O <sub>3</sub> (%)	4.22
Fe <sub>2</sub> O <sub>3</sub> (%)	1.8
CaO (%)	65.9
MgO (%)	2.8
K <sub>2</sub> O (%)	0.6
Na <sub>2</sub> O (%)	3.0
SO <sub>3</sub> (%)	2.7
TiO <sub>2</sub> (%)	0.3
Loss on ignition (%)	11.2
Mean particle size (µm)	19.90

*SEC Analysis* – Analysis of CHRS polymer in terms of molecular weight was performed by SEC (Size Exclusion Chromatography) under the following experimental conditions:

Columns: Water Ultrahydrogel 120, 250, 500, 1000 in series;  
 eluent: 0.1M NaNO<sub>3</sub>/Acetonitrile 80/20 v/v;  
 Flow rate: 1 ml/min;  
 injection: 100 µL of 1.0% aqueous solution of polymer;  
 detector: refractive index;  
 column temperature: 40 °C;  
 molecular weight standards: monodisperse polysaccharide standards with Mw between 750 and 700.000.

*Hydrolysis Test* – The chemical reactivity of CHRS polymer in alkaline conditions was measured by hydrolysis tests in comparison with the reference superplasticizer. In these tests, a known amount of polymer solution was mixed with a predetermined excess of a 24% solution of NaOH at 25° C in order to simulate the alkalinity conditions of the cement mixtures (pH > 12). The residual excess of NaOH was back titrated with 0.1N HCl at different times of mixing, in order to estimate the reactivity of the polymers through the consumption of NaOH caused by the hydrolysis of the ester linkages.

*Mini-slump Test* – The capability of CHRS polymer to maintain the workability of cement mixtures was evaluated in comparison with the reference superplasticizer at the same dosage (0.25% of active polymers by weight of cement) by the mini-slump test (Meyer, Perenchio, 1979). This test consists of the measurement of the spread of a cement paste obtained by mixing water, cement and the superplasticizer (W/C = 0.38) at different times of mixing (from 5 to 240 minutes). The test is performed by filling a small stainless steel cone (upper diameter 20 mm, lower diameter 40 mm, height 60 mm) with the cement paste under test and by measuring the diameter of the circular shape obtained after lifting the cone over a smooth surface.

*Adsorption Tests* – CHRS polymer was added to cement mixture at the dosage of 0.25% as active polymer by mass of cement (W/C = 0.5). At fixed times (from 5 to 240 minutes), a part of the cement suspension was collected and filtered. The liquid phase was analysed by SEC in order to estimate the unadsorbed fractions of the polymer left in the solution after different times. The percent of polymer adsorption was then calculated by comparing the

chromatographic areas of CHRS polymer before and after contacting the cement. The same procedure was adopted for the reference superplasticizer.

*Concrete Tests* – Concrete mixtures containing CHRS polymer and the reference superplasticizer were produced according to the EN 480/1 European standard norm. Natural sand and coarse aggregates (max diameter 20 mm) were used in all the cases. All the raw materials (cement, aggregates and water) were conditioned at 30 °C in order to simulate the operating conditions typical of hot climates. All the concrete mixtures were prepared with the same initial slump values (200 – 210 mm, as measured after 5 minutes from mixing). The slump values were then measured at different intervals (30, 60, 90 and 120 minutes) and the mixtures were “retempered” when the slump values felt below 100 mm. After 120 minutes, if required, the workability of the concrete mixtures was finally restored with the addition of the proper amount of water (“retempering”) within the class S4 of consistency according to EN 206/1 norm (160 – 210 mm) and then placed in 150×150×150 mm plastic moulds. The mechanical strength development was measured after 1, 7 and 28 days of curing at 23 °C. The characteristics of the different concrete mixtures, with the indication of the initial and final (after “retempering”) W/C.

### 3. EXPERIMENTAL RESULTS

#### 3.1 Hydrolysis Tests

The results of hydrolysis tests are shown in Fig. 1. In this figure, the kinetic of hydrolysis for CHRS polymer and for the reference superplasticizer are expressed in terms of mmole of carboxylic groups formed per gram of polymer. In fact, as a consequence of the hydrolysis, the cleavage of each ester bond produces one free carboxylic anionic group along the backbone of the polymer chains. As it appears from Fig. 1, while the reference superplasticizer is stable towards hydrolysis, CHRS polymer is chemically reactive in the alkaline conditions typical of cement mixtures and carboxylic groups are progressively formed in the polymer, thus increasing the initial ratio between carboxylic and ester groups of CHRS polymer with the time.

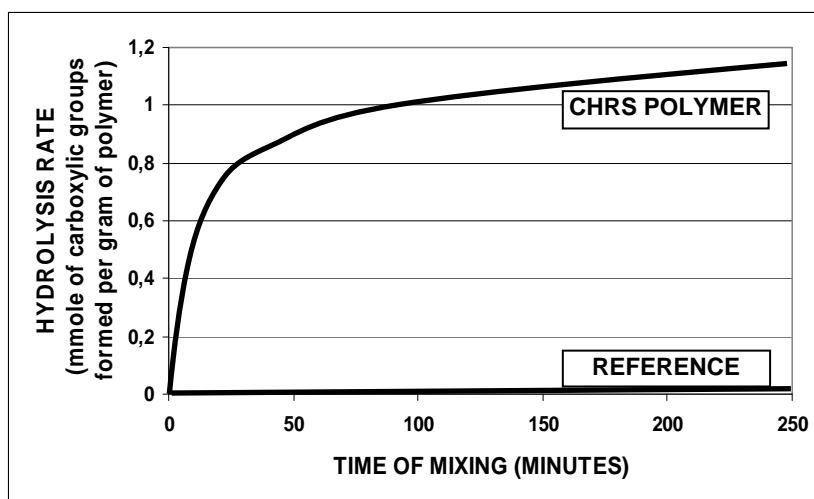


Fig. 1 Kinetics of hydrolysis of ester linkages of CHRS polymer in comparison with reference superplasticizer

### 3.2 Adsorption Tests

The results of adsorption tests are shown in Fig. 2. From this figure, it is possible to observe that the rate of adsorption of the two polymers is quite different. In fact, while the reference superplasticizer adsorbs at a larger extent during the first minutes of mixing (45 % of the superplasticizer is adsorbed within the first 5 minutes of mixing), CHRS polymer initially adsorbs much more slowly (only 12 % is adsorbed in the same period). This situation is completely changed at longer times, because CHRS polymer continues to adsorb with the time of mixing while the reference superplasticizer doesn't. Furthermore, it is important to observe that after 90 minutes of mixing the adsorption of CHRS polymer becomes higher than the reference superplasticizer, indicating a higher plasticizing efficiency at longer mixing times.

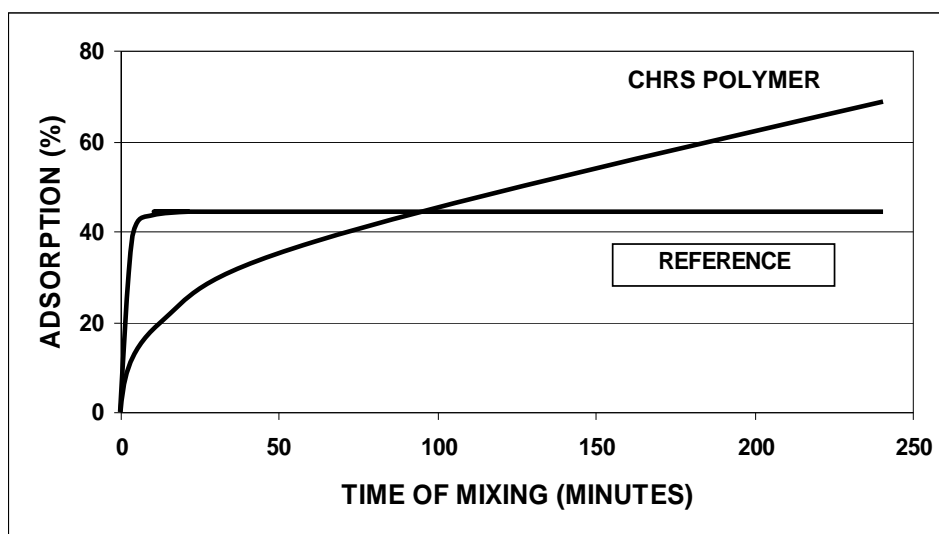


Fig. 2 Adsorption isotherms of CHRS polymer in comparison with reference superplasticizer

### 3.3 Mini-slump test

The results of mini-slump tests (Fig. 3) indicate that the workability of the reference superplasticizer is initially higher than CHRS polymer but, after about 60 minutes of mixing, the latter produces a sharp increase of the workability which exceeds by far that of the reference, reaching the maximum value after 120 minutes (170 mm compared to less than 140 mm). These results are clearly related to the adsorption behaviour of Fig. 2. In fact, when the CHRS polymer is scarcely adsorbed also the workability is low, but when adsorption increases, the workability shows a definite increase, confirming the importance of adsorption in determining the flowability. Furthermore, these results indicate that the flowability is directly related to the presence of carboxylic radicals in the CHRS polymer which, due to their chemical reactivity, progressively increase the density of anionic groups in the backbone, becoming more and more efficient with the time of mixing, confirming that the anionic carboxylic radicals represent the anchor groups for the superplasticizers adsorption (Ferrari et al., 2000).

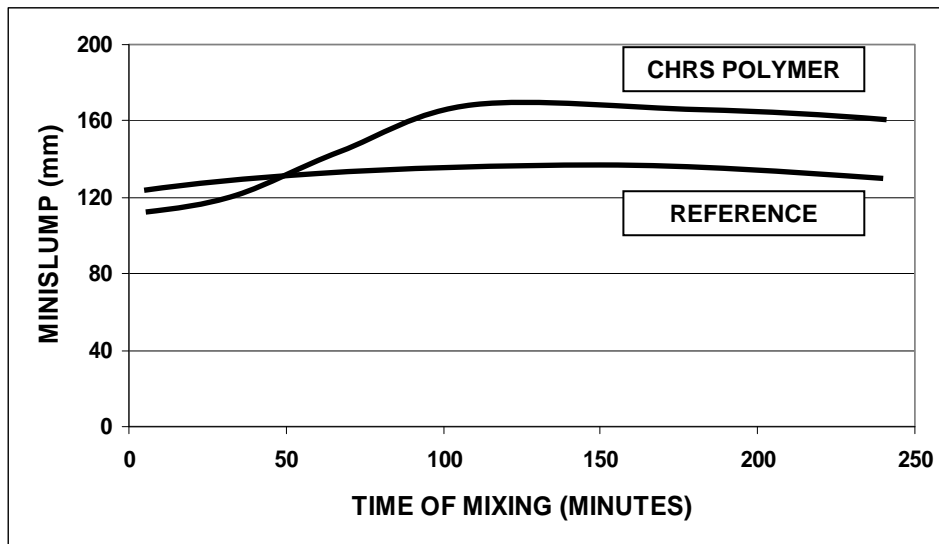


Fig. 3 Flow of mini-slump tests of CHRS polymer in comparison with reference superplasticizer

### 3.4 Concrete tests

The results of the retention of the flow of concrete mixtures with the time of mixing with CHRS polymer and the reference superplasticizer at different dosages of admixture (0.8 and 1.0 % by volume by weight of cement) are shown in Figs. 4 and 5, respectively. Figure 5 indicates that, at both the dosages, CHRS polymer retains the workability of the concrete for two hours without the need of any further water addition (“retempering”) and that, after 2 hours, the concrete mixtures greatly comply with the class of consistency S4, corresponding to a slump interval ranging from 160 mm to 210 mm, according to European norm 206-1. On the other side, the reference superplasticizer (Fig. 5) needs to be “retempered” twice at both the dosages, after 60 and 120 minutes of mixing, confirming that this type of superplasticizer is inadequate to retain the slump for longer times. Moreover, it is important to point out that the “retempering” of the concrete mixtures containing the reference superplasticizers with water increases the final W/C, with detrimental effects on the compressive strength.. On the other side, the concrete mixtures containing CHRS polymer do not require any water addition during the mixing and therefore the initial W/C is not modified and mechanical strength are not affected.

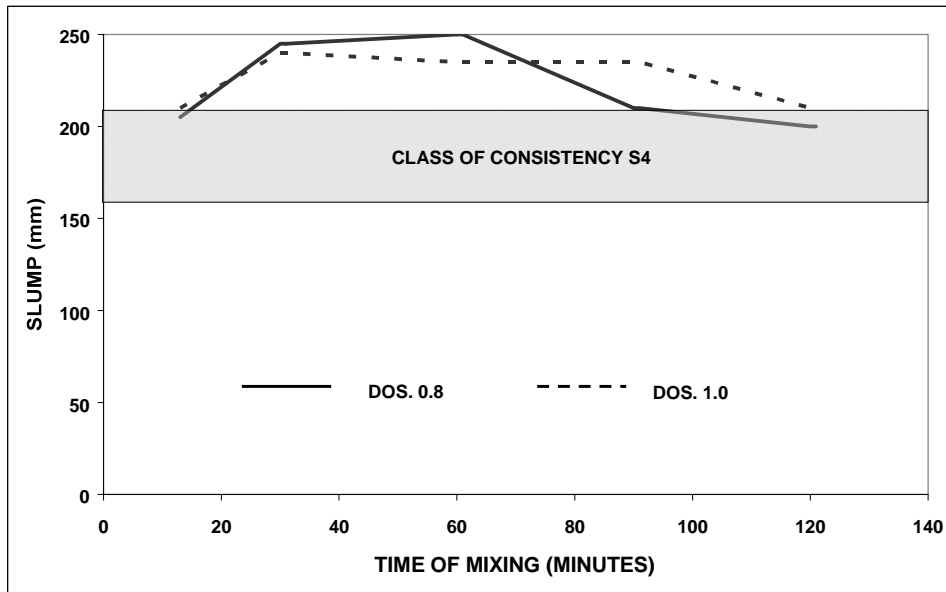


Fig. 4 Slump values of concrete mixtures containing CHRS polymer at different dosages

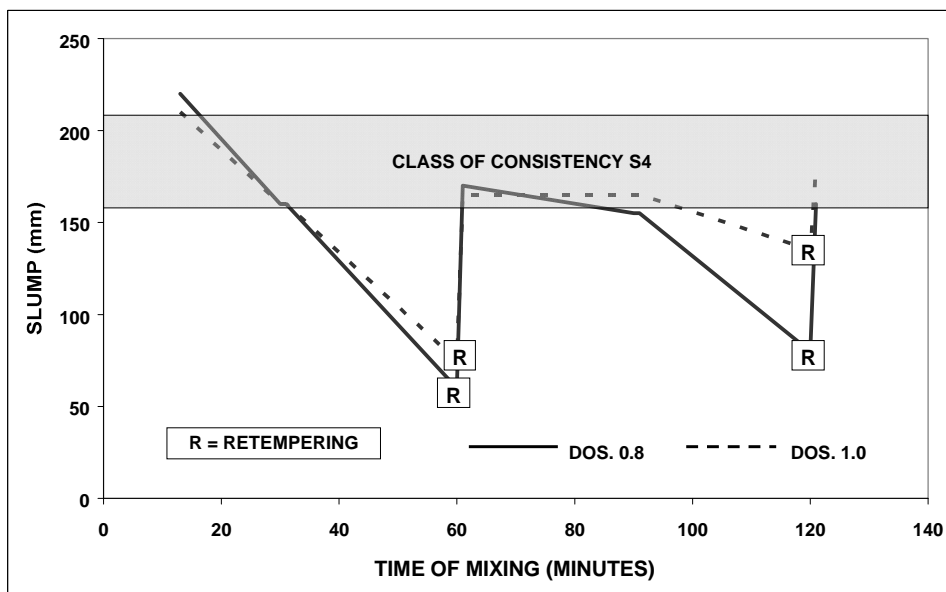


Fig. 5 Slump values of concrete mixtures containing reference polymer at different dosages

#### 4. CONCLUSIONS

The CHRS polymer described in the present paper represents an example of a new type of superplasticizer which, beside the electrosteric mode of dispersion, are characterised by a new mechanism of action based on their reactivity once they are introduced in the cement mixtures. Due to the hydrolysis of selected chemical groups, they become active as superplasticizers with the time of mixing and progressively modify their chemical composition and structure. Due to this new mechanism, they retain the workability of concrete mixtures for longer times in comparison with second generation superplasticizers. It is believed that these superplasticizers actually represent the best assurance to preserve the specifications of concrete mix-design from the mixing plant to the job-site.



## 5. REFERENCES

- Clemente, P., Dal Negro, E., Ferrari, G., Gamba, M., Surico, F. (2005), “Nanostructural Superplasticizers for In-Lining Concrete in Underground Projects”, Eds by: R.K. Dhir, M.D. Newlands, L.J. Csetenyj, Thomas Telford Publ *Applications of Nanotechnology in Concrete Design*, pp. 97-104
- Corinaldesi, V., Moriconi, G. (2003), “The Influence of Mineral Addition on the Rheology of Self-Compacting Concrete”, Eds. by: V.M. Malhotra, *Proceeding for Superplasticizers and Other Chemical Admixtures in Concrete 7<sup>th</sup> CANMET/ACI International Conference, Berlin, Germany*, pp. 227-240,
- Corradi, M., Kurana, R., Magarotto, R. (2003), “New Generation of Polycarboxylate Superplasticizers for Eliminating Steam Curing and Improving Durability of Precast Concrete Elements”, Eds. by: V.M. Malhotra, *Proceeding for Superplasticizers and Other Chemical Admixtures in Concrete 7<sup>th</sup> CANMET/ACI International Conference, Berlin, Germany*, suppl. pp. 347-361
- Ferrari, G., Cerulli, T., Clemente, P., Dragoni, M., Gamba, M., Surico, F. (2000), “Influence of Carboxylic Acid-Carboxylic Ester Ratio of Carboxylic Acid Ester Superplasticizer on Characteristics of Cement Mixtures”, *Superplasticizers and Other Chemical Admixtures in Concrete*, Eds. by: V.M. Malhotra, *Proceeding for Superplasticizers and Other Chemical Admixtures in Concrete 7<sup>th</sup> CANMET/ACI International Conference*, Nice, France, pp. 505-519
- Hamada, D., Sato, H., Yamamuro, H., Izumi, T., Mizunuma, T. (2003), “Development of Slump-Loss Controlling Agent with Minimal Setting Retardation”, Eds. by: V.M. Malhotra, *Proceeding for Superplasticizers and Other Chemical Admixtures in Concrete 7<sup>th</sup> CANMET/ACI International Conference, Berlin, Germany*, pp. 127-141,
- Meyer, L.M., Perenchio, W.F. (1979), *Concrete International*, 36-43, January.
- Tucker, G. (1936), United States Patent 2,052,586.

## PROTECTION AND REPAIR OF REINFORCED CONCRETE STRUCTURES BY MEANS OF MCI-INHIBITORS AND CORROSION PROTECTIVE MATERIALS

*Jure Francišković\**, *Boris Mikšić\*\**, *Ivan Rogan\*\**, *Mijo Tomičić\*\*\**

\**Longus Co. Ltd. Sachsova 4, 10000 Zagreb, Croatia, e-mail [longus@zg.htnet.hr](mailto:longus@zg.htnet.hr)*

\*\* *Cortec Corporation 4119 White Bear Parkway St. Paul MN 55110, USA, e-mail [info@cortecvci.com](mailto:info@cortecvci.com)*

\*\* *CorteCros Co.Ltd. Production & Supply of Corrosion Control Systems, Nova Ves 57, 1000 Zagreb, Croatia, e-mail [info@cortecros.hr](mailto:info@cortecros.hr)*

\*\*\* *Škiljo Gradnja Co.Ltd. 21270 Zagvozd, Croatia*

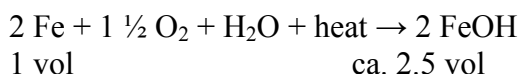
### SUMMARY

In this paper the protection of reinforcing steel in new and existing reinforced concrete structures by using migration corrosion inhibitors (MCI) and corrosion protective materials (CM) which contain MCI is discussed. The composition and criteria of quality for products and systems for protection and repair of new and existing reinforced concrete structures is discussed too. It is also described the procedure of the restoration with the MCI-inhibitors and materials contained this inhibitors of the reinforced concrete structures of the module no. 2 and 3 on the wharf no. 5 in the harbour Ploče.

### 1. INTRODUCTION

Corrosion protection of the reinforcing steel and the protection of the new and the restoration of the old reinforced concrete structures by means of MCI-corrosion inhibitors and anticorrosion materials, as well as with the systems, which contain these inhibitors, represents important contribution and big step forward to the prolongation of the durability and the lifetime of the reinforced concrete structures, and herewith to the major reduction of the maintenance costs, as well as to the effectiveness of the building use. MCI-corrosion inhibitors and anticorrosion materials and the systems, i.e. those, which contain these MCI-inhibitors for the protection of the reinforcing steel and the protection of the new and the restoration of the old reinforced concrete structures, have been used successfully around the world for over 25 years.

*Product of the iron corrosion /Fe is iron oxide /Fe<sub>x</sub>O<sub>y</sub>:*



- “Pure” iron oxide has ca 2.5 times bigger volume than metallic iron.
- Reinforcing steel is not pure iron, but its alloy: steel.
- Products of corrosion are iron oxide mixture, depending on the compound and concentration of the reactants, and on the thermodynamic conditions at which the electrochemical

corrosion reaction unfolds, and the volume of the developed corrosion products is ca 3-12 times bigger than the initial volume of the reinforcing steel/iron.

- Corrosion occurrence on the surface of the reinforcing steel causes not only decrease of adhesion/adherence between the reinforcing steel and the concrete, as well as the reduction of the reinforcing steel section, but also – due to the big increase of the volume of the corrosion products in relation to the initial reinforcing steel volume – huge pressures, which cause appearance of the fissures, setting apart, cracking and scaling of the concrete protection layer above the reinforcing steel.

## 2. MIGRATORY CORROSION INHIBITORS

Migrating corrosion inhibitors are chemical compounds on the amine basis (e.g. aminocarboxylates, amino alcohols, and o.), which through the process of chemical adsorption, so called chemisorptions, »bind»/adsorb on the surface of the reinforcing steel/iron (and other metals), making on the surface an firm and resistant micro layer thick ca 20 µm, resistant to many aggressive substances from the environment, primarily to the impact of the chloride, in the nature omnipresent, and simultaneously very aggressive against the iron oxides, which it chemically destroys.

*MCI-corrosion inhibitors* protect the reinforcing steel against the corrosion in both oxidation ranges: cathode and anode range, in distinction from some other types of corrosion inhibitors, such as e.g. nitrites – therefore are MCI-corrosion inhibitors also designate as mixed corrosion inhibitors. MCI-corrosion inhibitors on the basis of amine compounds belong to the group of so called cathode, respectively cathode-anode inhibitors, which adsorb (through chemisorptions) on the surface of the reinforcing steel, preventing diffusion of the corrosion reactants (O<sub>2</sub>, H<sub>2</sub>O) to the do reinforcing steel, and in this way they protect it against the oxidation processes, in distinction from anode inhibitors on the nitrites and/or chromates basis, which protect the reinforcing steel from the corrosion through the anode passivisation, so that they themselves participate in the anode process, i.e. oxidize instead of main metal.

## 3. QUALITY CRITERIA FOR THE CORROSIVE REPAIR-PROTECTION MATERIALS AND SYSTEMS

### 3.1 Quality criteria of the cleaned concrete

Quality criteria of the cleaned concrete substratum and of the reinforcing steel of the reinforced concrete structures for the application of the Ac-repair-protective systems containing MCI-inhibitors:

1. Tensile strength of concrete substratum and adhesiveness of the concrete and reinforcing steel:  $\geq 1.5 \text{ N/mm}^2$
2. Surface roughness – depending on the repair mortar layer thickness: ca 5 mm for layers with thickness ca 10-50 mm and ca 1mm for layers with thickness 2-10 mm
3. pH: alkaline range  $> 9$
4. Chlorides concentration: without limit (some authors max. 1%)

5. Openness of the concrete surface structure: >50% visible aggregate grains, degree of coverage of the grains with the cement matrix ca 2/3 grain volume 6-Cleaness grade of the cleaned reinforcing steel: min SA 2 resp. St3 (according to international standards ISO 8501-1, SIS 05 59 00 1967, DIN 55 928-Teil 4, ASTM D 2200-67, SSPC VIS) depending on the cleaning method: sandblasting, shot blasting, hydro dynamically, manually.

### 3.2. Quality criteria of corrosion protective

Quality criteria corrosive repair-protective system/layer materials above the reinforcing steel: concrete, resp. repair mortar, protective-decorative coat, resp. hydrophobic impregnations, all containing MCI-inhibitors:

1. Fluids impermeability: Gases permeability coefficient  $\leq 1 \times 10^{-16} \text{ m}^2$  (EN 993-4)
2. Chlorides diffusion:  $< 1 \times 10^{-12} \text{ m}^2/\text{s}$  (GF)
3. Capillary water absorption coefficient  $< 10^{-1} \text{ kg/m}^2\text{h}^{1/2}$  (HRN.U.M8.300)
4. Alkalinity:  $\text{pH} > 9.5$
5. Anticorrosive reinforcing steel protection expressed in corrosion current intensity/density: Accord. to ASTM STP 1065:  $< 0.1 \text{ } \mu\text{A/cm}^2$

## 4. PROCEDURE OF THE RESTORATION OF THE REINFORCED CONCRETE STRUCTURE OF THE MODULE NO. 3 ON THE WHARF NO. 5 IN THE PORT PLOČE CARRIED OUT DURING THE YEAR 2005



Fig. 1 The module No. 3 in port Ploče

#### 4.1 Preparatory works

Cleaning of the concrete surface and reinforcing steel through hydrodynamic removal of the deteriorated material with the high pressure water jet ( $> 2000$  bar) from the reinforcing steel separated and deteriorated protective concrete layer was removed all to the sound, clean and firm substratum (quality criterion: tensile strength of the concrete substratum and adhesiveness between the concrete and reinforcing steel:  $\geq 1.5$  N/mm<sup>2</sup>). Corroded reinforcing steel was cleaned with the hydrodynamic water jet to the cleanness grade min SA2 resp. manually to St3. High pressure pump was placed on the floating platforms from which the applying of the repair mortar and the final superficial treatment with the protective-decorative coat, resp. with the hydrophobic impregnation was performed.

#### 4.2 Impregnation

Impregnation of the entire concrete surface was with the water solution (1:4) of the corrosion inhibitor MCI – in powder. Application was with the brush or roller in 2 layer of the total yield cca 25 m<sup>2</sup>/kg.

#### 4.3 Reprofiling

Reprofiling of the concrete surface and the covering of the exposed reinforcing steel was performed with the repair mortar containing MCI-inhibitor, with the manual application in 1-3 layers depending on the total thickness of the mortar layer (on some areas mortar thickness even to 8 cm). Freshly applied repair mortar was protected from the too fast drying by means of the curing on the basis soya oil containing MCI inhibitor, applied with the brush or roller in one layer, yield ca 5 m<sup>2</sup>/l.

#### 4.4 Protection of the entire surface

Protection of the entire surface, i.e. concrete and reprofiled with the repair mortar, from the impact of the moisture and atmospheric agents was performed with the protective-decorative coat, or hydrophobic impregnation:

- *Wharf face* was treated with the protective-decorative coat (colour light gray) on the basis of 1-k acrylate binder containing MCI-inhibitor, applied with the brush or roller in two layers of the total yield ca 8 m<sup>2</sup>/l and,
- *Concrete surfaces on the soffit and in the interior of the structure* were protected with treatment with the hydrophobic impregnation on the basis of silane-siloxane in the water medium containing MCI-inhibitor, application with the brush or roller in 1-2 layers, treated surface does not change appearance or colour, yield, ca 3.5 m<sup>2</sup>/l.

#### 4.5 Report by the IGH-PC Split

Report by the IGH-PC Split on the quality control of the built in material and on the quality of the realised works is positive, so it is stated in:

1. Preliminary testing of the quality of the chosen material: on the basis of the obtained test results, it was concluded that the restoration corrosive repair mortar conforms to the criteria stated in the Working project of the design company GEOKON.

2. Preliminary testing of the quality of the readiness of the substratum: tensile strength of the concrete substratum „pull off“ comes to  $> 1.5 \text{ N/mm}^2$ , through which fact it conforms to the required criterion, as well as chlorides concentration.
3. Control testing of the quality of the built in material: on the basis of the obtained continuous test results in relation to the repair mortar quality, it was concluded that the repair mortar built in at the wharf no.5, module no. 3 and no. 2, in the port Ploče conforms to the conditions and criteria stated in the Working project.
4. Control testing of the quality of the realised restoration system: on the basis of the daily obtained continuous test results in relation to the repair mortar quality, it was concluded that the repair mortar built in the every porthole of the module no.3 and no.2, in the port Ploče conforms to the conditions and criteria stated in the Working project.
5. Final evaluation of the continuous control quality: it was confirmed that the quality of the materials and works was proved through prescribed and documented testing and that it is in accordance with the conditions and criteria given in the Working design “Restoration of the soffit and the face of the reinforced concrete structure of the wharf no.5” elaborated by the company GEOKON, Zagreb.

## 5. REFERENCES

- Alonso C., Andrade C. (1990), “Effect of Nitrite as a Corrosion Inhibitor in Contaminated and Chloride-free Carbonated Mortars”, *American Concrete Institute Materials Journal*
- Berke N. (1991), “Corrosion Inhibitors in Concrete”, *Concrete International*
- Bjegović D., Mikšić B., Ukrainczyk V., “Corrosion protection of the reinforcing steel through migratory inhibitors”
- Bjegović D., “Designing of the lifetime of the reinforced concrete structures on roads”, *Scientific-research project*
- Broomfield J. (1997), “The pros and cons of corrosion Inhibitors”, *Construction Repair* July/August
- Haynes M., (1997), “Use of migratory corrosion inhibitors”, *Construction Repair* July/August
- Mikšić B., Gelner L., Bjegović D., Sipos L.( 1995), “Migrating Corrosion Inhibitors for Reinforced Concrete”, *Proceedings of the 8th European Symposium on Concrete Inhibitors*, University of Ferrara, Italy
- Report IGH-PC-Split on the testing results of the quality of the built in materials and on the quality of the realised restoration works in 2005., No.3617/340-05/VN, November 2005.
- Technical documentation of the company CORTEC Corporation, Minnesota, USA
- Yongmo, X., Hailong, S, (2004), “Comparison of Amin- and Nitrite-Inhibitorsin Carbonation-Induced Corrosion”, *China Building Materials Academy*, Materials Performance, Jan., pp 42-46



## **PROBLEMS OF PERMEABILITY OF CONCRETE FROM SIGHT OF WATER DIFFUSION IN CONCRETE STRUCTURE**

*Vladimíra Vytlačilová, Tomáš Dvorský, Alena Kohoutková*  
*Faculty of Civil Engineering, CTU in Prague*  
*Department of Concrete and Masonry Structures*  
*Prague 6, Thákurova 7, Czech Republic, [vladimira.vytlacilova@fsv.cvut.cz](mailto:vladimira.vytlacilova@fsv.cvut.cz)*

### **SUMMARY**

Permeability is one of the main factors that affects resulting durability of concrete i.e. immunity against influence of outer forces. Assessment of the durability is nowadays much discussed characteristic above all in relation to permanent sustainable development of concrete construction. The paper deals with problems of incidental permeability of concrete from the point of view of water diffusion in concrete structure - cement stone. It is defined above all by water-tightness, capillarity attraction and absorbability of concrete, whereas all these characteristics depend upon porosity of cement stone.

### **1. INTRODUCTION**

Water-tightness of concrete is an important factor. Reasons are higher requirements on concrete durability. Concrete durability has high importance. For example, water penetration by pressure and capillary rise i.e. suction from wet place or under water submerged and water absorption from air.

The term permeability is often loosely used to describe this general property. Permeability of concrete describes water-tightness, capillarity attraction, absorbability, heat and electric conductivity. While most of the interest in concrete permeability dates back to initial construction of hydroelectric structures in the 30's, there is a renewed awareness of the role that permeability plays for durability of concrete structures.

### **2. WATER MOVEMENT**

Water movement through concrete structures is enabled by continuous paths. These paths arise by pores and cracks. Paths have variable radius from size as cement element to millimetre and bigger.

There are three ways by which water can penetrate into concrete:

- Gross voids arising from incomplete compaction, often resulting from segregation (problem with workability of concrete)
- Micro (or macro) cracks resulting from drying shrinkage, thermal stresses or bleeding settlement.
- Pores or capillaries resulting from mixing water in excess of that which can react with the cement, i.e. water in excess of 0.38 by mass of cement.

In the paths which have bigger radius water flows by pressure. In the capillary paths water does not penetrate, but by capillary forces draws-in. Micro capillaries occurs in cementing



compound every time because volume of hydration products is smaller than volume of cement and hydrated water.

Concrete can be resistant against water pressure only if concrete is without pores and cracks. Important is good workability of concrete. Reduction of permeability can be affected by avoiding bleeding. The most important is to block the channels after formation. Pore blocking takes place as cement continues to hydrate and extends gel formation into the pores. This requires the concrete to be well cured and is greatly affected by w/c ratio. Another possibility is to fill in the pores in the concrete with hydrophobic material. Such materials are marketed as 'waterproofing admixtures' and may be soapy materials such as stearates or materials such as silicones.

### 3. PERMEABILITY OF CEMENT STONE

The permeability of concrete is affected also by the properties of cement. Porosity of structural cement stone enables penetration of the liquid materials and at the same time interference heat transition. Individual characteristics are defined physically (diffusion of water vapours, heat conductivity, electric conductivity) or technologically (hygroscopicity, absorbability, capillarity, water-tightness). Paste permeability is related to water-cement ratio, degree of cement hydration, and length of moist curing. In this article the main mechanisms for water and water vapour transport in concrete are described.

#### 3.1 Hygroscopicity

Hygroscopicity is the capacity to absorb on inner surface water vapour from the atmosphere. Cement stone is hydrophilic material which absorbs water. Water absorption depends on relative humidity and distribution of capillary pores (inside surface area). Thickness of absorbed water layer is:

$$\delta_v = \frac{0,3656}{\sqrt{-\ln \varphi}} \quad (1)$$

Value of thickness layer is from 0.3 to 1.7nm and  $\varphi$  is the relative humidity. Continuation of cement hydration enables increase of humidity absorption so that strength of cement stone grows up.

#### 3.2 Absorption

Absorption is capacity to fill open pores of cement stone with water. It is due to hydrostatic pressure and capillary forces. Absorption units are percents of materials weight. Absorption can be restricted by air pressing in impassable capillaries. (e.g. impassable capillary with radius 1 $\mu$ m have overpressure 230 kPa). Absorption in vacuum per 24 hours is three time higher than absorption in normal compression.

#### 3.3 Capillarity attraction

Capillarity attraction is the difference of the height between water level in capillary and water level in which specimen is placed. After a certain time the balance of capillarity attraction forces and gravity will be stabilize. Contrast to the permeability or diffusion, the rise of the capillary absorption is almost linear with temperature. Height of capillarity action is:

$$h = \frac{2 \cdot \sigma_p \cdot \cos \psi}{r \cdot \rho_v \cdot g} = konst. \left( \frac{1}{r} \right) \quad (2)$$

where:  $\sigma_p$  is surface tension,  $\psi$  is wetting angle,  $r$  is capillary radius,  $\rho_v$  is water density and  $g$  is gravity

### 3.4 Diffusion of water vapour

The most important concrete characteristic, apart from permeability, is diffusion. Water vapour diffusion is characterised by diffusion of water vapour ratio  $\delta$  [s]. For cement stone  $\delta$  has value  $0,010 \cdot 10^{-9}$ s. Quantity of water vapour depends on difference of partial pressure between two surfaces and field of temperature inside material. When temperature drops than pressure of water vapour will be saturated and water vapour will condensate in porous mediums. By this condensation increases material's humidity and at the same time increases heat conductivity of cement stone.

### 3.5 Water-tightness

Water-tightness is reversible value of permeability of porous media. Water-penetration is smaller than ratio of water and air viscosity. On the inside capillaries surface is water absorbed, through profile of capillaries tapers. The laminar flow in capillaries is interrupted. Electrostatic forces of polar liquid act. Speed of the water penetration over capillary system of cement stone is got at the nomogram on the Fig. 1. Water quantity penetrated trough capillary system is determined by Hagen-Poiseuill's principle:

$$V_v = \frac{D_v \cdot S \cdot \Delta p}{\eta \cdot l}; \quad D_v = \frac{r_{ef} \cdot P_K}{8} \quad (3)$$

where:  $D_v$  is specific permeability ratio,  $r_{ef}$  is radius of effective pores,  $P_K$  is capillary porous,  $S$  is surface,  $\Delta p$  is capillary radius,  $\eta$  is water viscosity and  $l$  is pores longitude

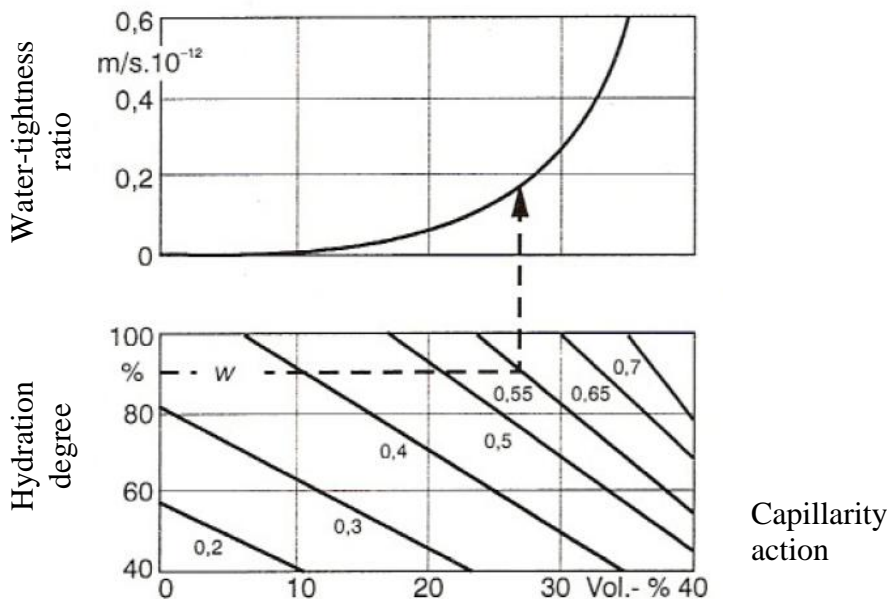


Fig. 1 Nomogram for water-tightness of cement stone

#### 4. CONCRETE PERMEABILITY

Key factors affecting durability are both permeability and other factors (e.g. compressive strength). Low strength and high permeability decrease durability. Concrete permeability is defined by properties which characterize water penetration over porous structure of cement stone (absorption, capillarity attraction and water-tightness), air penetration (diffusion of water vapour), heat conductivity and electric conductivity. All these properties depend on at porosity of cement stone given above. The permeability depends on porosity, time and water-cement ratio (Fig. 2)

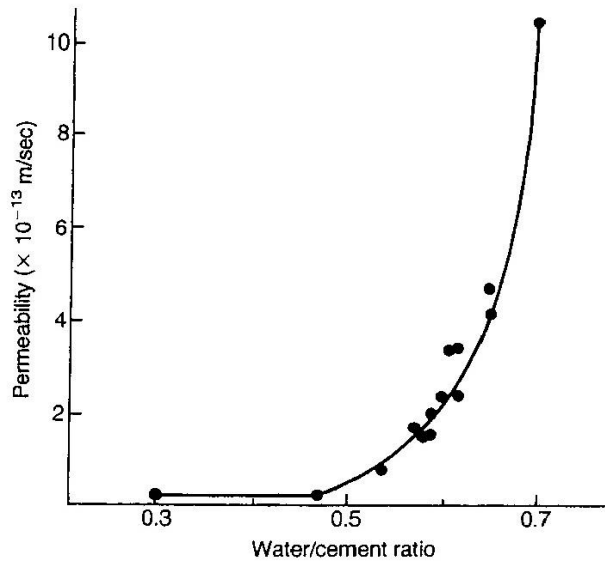


Fig. 2a The relationship between permeability and water-cement ratio

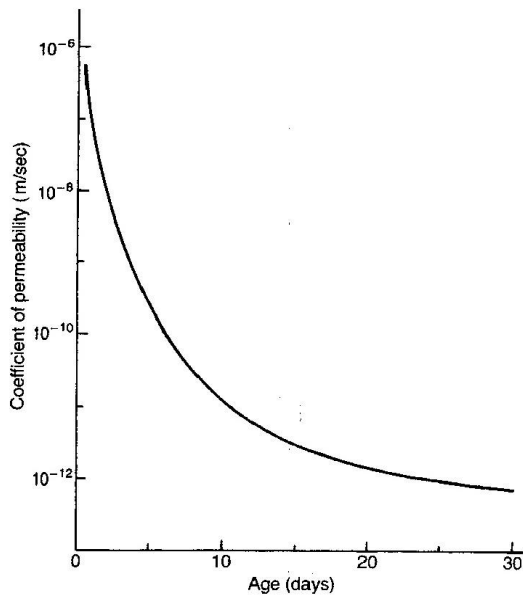


Fig. 2b The effect of hydration on the cement paste permeability

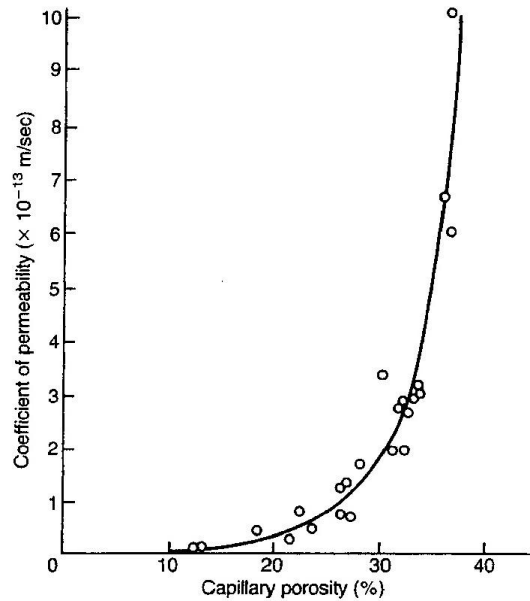


Fig. 2c The relationship between permeability and capillary porosity

Permeability is defined generally as that property of a fluid medium which characterises the easiness with which a fluid will pass through it under the action of a pressure differential. Darcy's law states that the steady-state rate of flow is directly proportional to the hydraulic gradient, i.e.

$$v = \frac{Q}{A} = -K \left( \frac{dh}{dL} \right) \quad (4)$$

where  $v$  is the apparent velocity of flow,  $Q$  is the flow rate,  $A$  is the cross-sectional area of flow,  $I$  is the hydraulic gradient and  $dh$  is the head loss over a flow path of length  $dL$ .  $K$  is called the coefficient of permeability. Darcy's law has been generalised to apply to any fluid flowing in any direction through a porous material, so long as the conditions of flow are viscous.  $dP$  is the pressure loss over the flow path  $dL$ ,  $\mu$  is the viscosity of the fluid and the constant  $k$  is referred to as the intrinsic permeability of the porous medium.

#### 4.1 Concrete water-tightness

Water-tightness is one of the major properties of hardened concrete. Open capillary greater than  $10^{-7}$  m are dominant for concrete water-tightness. Penetration through micro-pores is impossible. Water-tightness depends on distribution of macro-pores and capillaries in a cement stone. Water-tightness is possible defined by permeability ratio:

$$k_p = \frac{V_v}{3600 \cdot S \cdot t \cdot \Delta p} \quad \text{m} \cdot \text{s}^{-1} \quad (5)$$

where:  $V_v$  is water displacement that pass through surface  $S$  during time  $t$  with pressure gradient  $\Delta p = 10^5$  Pa

Quantity of macro-pores in concrete depends on water-to-cement ratio. Over time capillary are filling-up by clinker minerals and water-tightness increases.

In Czech Republic concrete water-tightness test is in agreement with standard ISO 7031. Test is made with three prism specimens with length of edge 150 mm, 200 mm, 300 mm. Ratio of height to length must be greater than or equal to 0.5. Recommended age of concrete is 28 days.

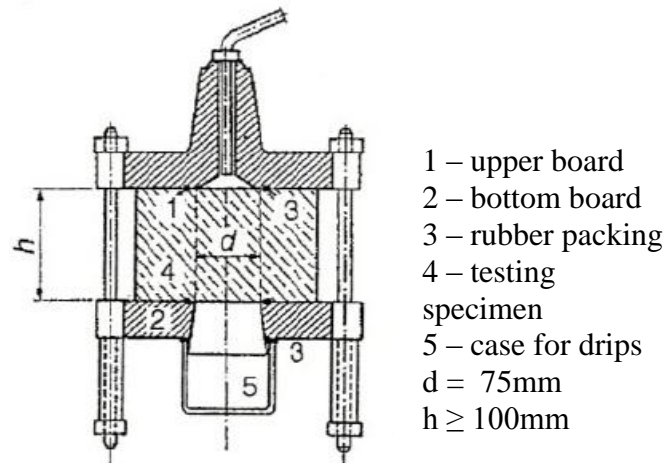


Fig. 3 Measuring installation for assessment water-tightness

#### 4.2 Concrete humidity characteristic

Concrete humidity's characteristic are: balance humidity, absorption, capillarity attraction, absorption characteristic (water content and drying ability). These characteristics depend on porous cement stone. Primarily depend on macro-capillary proportion and cement stone quantity in concrete. Absorption and capillarity attraction drops when water ration drops.

#### 5. CONCLUSIONS

Permeability refers to the amount of water migration through concrete when the water is under pressure or to the ability of concrete to resist penetration by water or other substances. Permeability is an important property that governs many aspects of the durability of concrete structures. Decreased permeability improves concretes resistance to freezing and thawing, resaturation, sulphate, and chloride-ion penetration, and other chemical attack. The permeability of the paste is particularly important because are impasted all constituents in the concrete. Submitted paper is dedicated to the problem of permeability of cement stone and concrete. The contribution deals with basic information about the properties which define the permeability. Assessment of these characteristics is in a many European standards considered one of the basic criteria for appreciation durability concrete therefore it is necessary them pay increased attention.

#### 6. ACKNOWLEDGEMENTS

This research has been supported by the Ministry of Education, Youth and Sports of Czech Republic, under grant No. MSM: 6840770031 and project No. 103/06/2226 of the Grant Agency of Academy of Sciences of the Czech Republic.

#### 7. REFERENCES

- Bílek, V. and Keršner, Z. (2005), "Non-Traditional, Cement & Concrete II", *Brno University of Technology*, ISBN 80-214-2853-8, Brno
- Day, Ken W.(1999), "Concrete mix design, quality control, and specification I", *Published 1999 by E & FN Spon*, ISBN 0-419-24330-5
- Illston, J. M., Domone, P. L. J. (2001), "Construction materials – Thei nature and behaviour", New York, ISBN 0-419-25860-4
- Kosmatka, S. H., Kerkhoff, B., Panarese, W.C. (2002), "Design and Control of Concrete Mixtures", Illinois, ISBN 0-89312-217-3
- Neville, A. M. (2002), "Properties of Concrete", Edinburgh, ISBN 0-582-23070-5
- Pytlík, P. (2000), "Technologie betonu", Vysoké učení technické v Brně, ISBN 80-214-1647-5, Brno

## STUDIES ON USE OF LIME MILK NEUTRALIZATION SLUDGE IN THE BUILDING MATERIAL INDUSTRY

*Claudiu Aciu*

*Technical University of Cluj-Napoca*

*Faculty of Civil Engineering and Building Services*

*25, G. Baritiu Street, Ro-400027 Cluj-Napoca, Romania*

*Claudiu.Aciu@cif.utcluj.ro*

*Zsuzsanna Józsa (advisor)*

*Budapest University of Technology and Economics, Hungary*

*H-1111 Budapest Múgyetem rakpart 3.*

*zsjozsa@epito.bme.hu*

### SUMMARY

Waste materials resulting from technological processes represent a huge problem of mankind nowadays. As a by-product of a new line of wire manufacturing 400 tons of lime milk neutralization sludge is produced every month in Romania. This study shows the results of the experimental program carried out in the laboratory, aiming to find solutions for the reuse of lime milk neutralization sludge for obtaining ecological construction materials. The highest strength values are obtained for a cement dosage of 360 kg/m<sup>3</sup> and 30% sludge using BIBER V 7U plastifying additive. It is found that regardless of the cement dosage, 320, 346, 360 kg/m<sup>3</sup>, for a sludge addition of 50% and using BIBER V 7U plastifying additive, the lowest compressive strength values will be obtained; but all the compressive strength values are higher than 100 daN/cm<sup>2</sup>, which is equivalent to mortar M100.

### 1. INTRODUCTION

One of the strategic objectives of environmental protection in Romania is the use of waste material. The management of waste material aims to use processes and methods that should not:

- a. involve risks for the population, water, air, fauna or vegetation;
- b. produce phonic pollution or unpleasant smell;
- c. affect the landscape or the protected areas.

One of the waste materials in Romanian industry resulting in large quantities and requiring efficient management is sludge. Sludge is known in the literature as a mixture of water and fine mineral matter particles in suspension, resulting from the mechanical wet processing of ore. In Romania, there are commercial companies that produce waste material such as galvanic sludge, which is considered dangerous. Another category of sludge is produced by oil equipment resulting from the extraction of crude oil.

An efficient method of waste management is their neutralization. The team of Craciunescu, Serban, Popescu (1990) and Craciunescu, Serban, Popescu, Matei (1991) proposed the use of bauxite sludge for the obtaining of natural coloured concrete, artificial aggregates, and bauxite sludge bricks. Such studies were also performed by the building materials team of the Faculty of Civil Engineering of Cluj-Napoca (Manea, Aciu, Corbu, 2007). The aims of these studies

were to identify some ecological materials that might use sludge in as high amount as possible.

With the opening of a new line of wire manufacturing about 400 tons of sludge resulting every month, therefore optimal solutions are needed to manage it. The properties of sludge from the lime milk neutralization of acid waters are:

- pH = 7 – 8.5;
- density  $\rho = 1.3 \text{ g/cm}^3$ ,
- chemical composition Fe 24.4; Ca 7.2; Cu 0.05; P 1.0; Zn 0.4; Si 3.1 %

Taking into account the sludge chemical composition, it was proposed to be used as additive for certain mortars, products often used in construction, namely for plasters, masonry or auger bits.

## 2. SLUDGE AS ADDITION

The first stage of the experimental program proposed the elaboration of 9 recipes for a material in which sludge represents an addition, a percentage of the cement dosage used. The chosen variables were the addition percentage: 20%, 30%, and 50% and the cement dosage CEM II A-S 32.5R: 320, 346, 360  $\text{kg/m}^3$ . Tab. 1 shows all these recipes.

Tab. 1 The mortar recipes of the experimental program

	Cement II A-S 32.5R [ $\text{kg/m}^3$ ]	Sludge		A/C	Aggregate [kg]	
		[kg]	%		(0-3)	(3-7)
Recipe 1	320	64	20	0.6	1030.4	809.6
Recipe 2	320	96	30	0.6	1030.4	809.6
Recipe 3	320	160	50	0.6	1030.4	809.6
Recipe 4	346	69	20	0.6	994.0	781.0
Recipe 5	346	104	30	0.6	994.0	781.0
Recipe 6	346	173	50	0.6	994.0	781.0
Recipe 7	360	72	20	0.75	892.1	700.9
Recipe 8	360	108	30	0.75	892.1	700.9
Recipe 9	360	180	50	0.80	865.2	679.8

According to STAS 2634-80, for the determination of tensile bending strength and compressive strength, the test pieces should be prismatic, (4x4x16) cm in size. The bending strength and compressive strength was tested at the age of 7 days and 28 days.(Tab. 2)

Tab. 2 Strength of mortar at 28 days age

	$R_{ti}$ [ $\text{daN/cm}^2$ ]			$R_c$ [ $\text{daN/cm}^2$ ] prism halves								$R_c$ [ $\text{daN/cm}^2$ ] cubes		
	$R_{ti1}$	$R_{ti2}$	$R_{ti}^{med}$	$R_{c1,1}$	$R_{c1,2}$	$R_{c1}^{med}$	$R_{c2,1}$	$R_{c2,2}$	$R_{c2}^{med}$	$R_c^{med}$	$R_{c1}$	$R_{c2}$	$R_c^{med}$	
Recipe 1	37.4	44.8	41.1	114.4	115.0	114.7	102.5	103.1	102.7	108.7	110.2	112.2	111.2	
Recipe 2	49.4	47.9	48.7	123.0	115.0	119.0	115.6	116.8	116.2	117.6	140.0	141.0	140.5	
Recipe 3	28.9	32.9	30.9	70.0	72.5	71.3	71.3	71.8	71.5	71.3	67.3	80.6	73.9	
Recipe 4	55.4	57.5	56.5	160.0	185.0	172.5	218.0	228.0	223.0	198.0	198.0	196.0	197.0	
Recipe 6	40.3	41.6	41.0	145.0	112.5	133.0	145.0	135.0	140.0	136.5	128.0	127.0	127.5	
Recipe 7	52.2	44.9	48.6	118.8	136.3	127.5	109.3	128.2	118.8	123.1	153.0	152.0	152.5	
Recipe 9	38.7	38.3	38.5	158.8	115.6	137.2	122.5	120.0	121.3	129.2	100.0	104.0	102.0	

Fig. 1 represents compressive strengths at 28 days, depending on cement dosage and on the percentage of the added sludge in the recipe: 20%, 30%, 50% of the amount of CEM II A-S 32.5R.

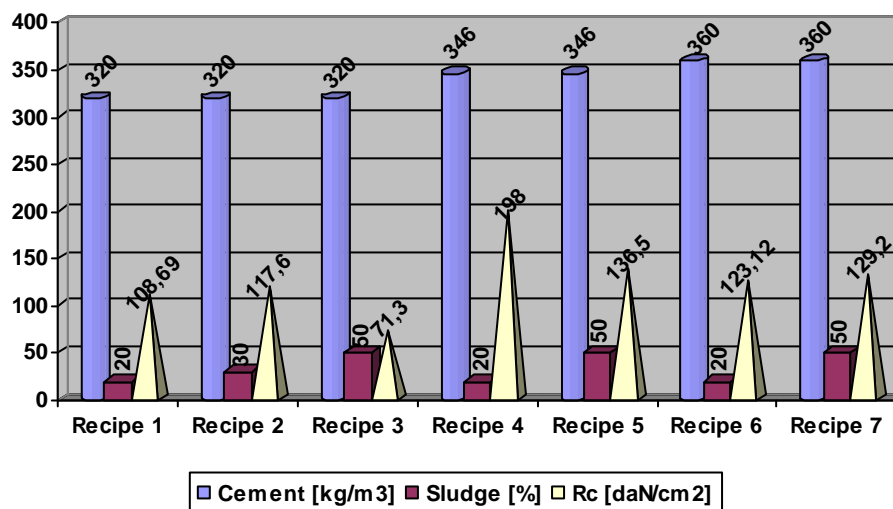


Fig.1 Variation in mortar strength depending on dosage and addition, at 28 days

The following conclusions can be drawn: at the age of 28 days, the material prepared according to the recipes enclosed can be indicated for the casting of some auger bits, having a strength equivalent to mortar M100, using:

- a cement dosage of 320 kg/m<sup>3</sup>, with a sludge addition of 20%, 30%;
- a cement dosage of 346 kg/m<sup>3</sup>, with a sludge addition of 20%, 30%;
- a cement dosage of 360 kg/m<sup>3</sup>, with a sludge addition of 20%, 30%.

It is found that regardless of the cement dosage, 320, 346, 360 kg/m<sup>3</sup>, for a sludge addition of 50%, a reduction in compressive strength occurs. For a cement dosage of 346 kg/m<sup>3</sup> and 360 kg/m<sup>3</sup>, for a sludge addition of 50%, compressive strength values higher than 100 daN/cm<sup>2</sup> are found, which is equivalent to mortar M100.

### 3. SLUDGE AND ADDITIVE AS ADDITION

The additives are chemical substances that are added to concrete in small proportions (less than or equal to 5% of the dried substance in comparison to the cement mass). They influence, directly or indirectly, the properties of concrete both in fresh and hardened states.

The additives have been used since old times even if then they did not have the same name. The Romans added pork grease and blood to the lime concrete with puzzolana in order to increase its durability. After the discovery of the cement concrete (1875–1880) the additives were used to control the setting and hardening, gypsum being used as a setting regulator and calcium chloride for accelerating the hardening (1885). In order to increase the impermeability and the durability of the concrete working in a wet environment there have been used flax oil, soaps and mineral powders. (Manea, Corbu, 2002) The first hydrofuge additives were used in 1910 for building some water tanks. The first air drivers were used in USA in 1939 for building a highway. In Europe the additives were used only after the Second World War.

Additives can have favourable influences on: the processes of hardening, retarding or accelerating the setting of concrete, hydration heat, workability, the possibility of placing of



pumpcrete placement, frost clefiness – repeated freeze-thawing, durability and waterproofness, resistance to chemical agents. The use of additives at international level has particularly developed, and many meetings and conferences have approached this subject (1967 – Brussels, 1973 – Canada, 1981 – Ottawa, 1985 – Mexico, 1989 – Ottawa, etc.).

The additives have a complex effect because they have a major role as well as one or more secondary functions. But the use of these additives must neither influence negatively the physico – chemical – mechanical properties nor produce corrosion of reinforced or pre-stressed concrete.

The main groups of additives are: fluidifiers, plastifiers; superfluidifiers, air entrainers; foaming agents; setting retarders; setting accelerators; antigels; stabilizers, etc (Jebeleanu, 1991).

As part of the experimental program, the use of the BIBER V 7U plastifying additive was proposed. The recommended amount is: 0.25-2.0% of the cement mass; in the case of amounts higher than 0.8% of the cement mass, the secondary effect of setting retardation appears. The usual amount is 0.5% of the cement mass.

The chosen variables were the addition percentage: 20%, 30%, and 50% and the cement dosage II A-S 32.5R: 320, 346, 360 kg/m<sup>3</sup>. The additive represented 0,50% from the cement dosage.

Tab. 3 shows all these recipes.

Tab. 3 The mortar recipes of the experimental programme

	Cement II A-S 32,5R [kg/m <sup>3</sup> ]	Sludge		A/C	Additives BV7U 0,50% [l/m <sup>3</sup> ]	Aggregate [kg/m <sup>3</sup> ]	
		[kg/m <sup>3</sup> ]	%			(0-3)	(3-7)
Recipe 1	320	64	20	0.60	1.60	1030	810
Recipe 2	320	96	30	0.60	1.60	1030	810
Recipe 3	320	160	50	0.60	1.60	1030	810
Recipe 4	346	69	20	0.60	1.73	994	781
Recipe 5	346	104	30	0.60	1.73	994	781
Recipe 6	346	173	50	0.60	1.73	994	781
Recipe 7	360	72	20	0.70	1.80	974	765
Recipe 8	360	108	30	0.75	1.80	974	765
Recipe 9	360	180	50	0.80	1.80	974	765

Tab 4 indicates the values of bending strength and compressive strength at the age of 28 days.

Tab. 4 Strength of mortar at 28 days

	Determination of bending strength (R <sub>ti</sub> ) [daN/cm <sup>2</sup> ]	Determination of compressive strength on prism halves (R <sub>c</sub> ) [daN/cm <sup>2</sup> ]		
	R <sub>ti</sub>	R <sub>c1</sub>	R <sub>c2</sub>	R <sub>c</sub> <sup>med</sup>
Recipe 1	30.52	176.3	168.7	172.5
Recipe 2	32.06	212.7	205.9	209.3
Recipe 3	21.09	108.0	114.1	111.1
Recipe 4	42.89	236.8	216.8	226.8
Recipe 5	30.52	242.8	245.4	244.1
Recipe 6	26.16	138.3	127.6	133.0
Recipe 7	47.53	223.2	249.5	236.4
Recipe 8	34.88	256.6	259.0	257.8
Recipe 9	30.59	161.5	150.0	155.8

Fig. 2 shows the way in which the test pieces were broken following the bending and compressive tests, the sludge granules that remained intact being evidenced.



Fig. 2 Broken test pieces (left – bending; right – compressive tests)

Fig. 3 represent compressive strength at 28 days age, depending on cement dosage and on the percentage of the added sludge in the recipe: 20%, 30%, 50% of the amount of cement II A-S 32.5R, using BIBER V 7U plastifying additive.

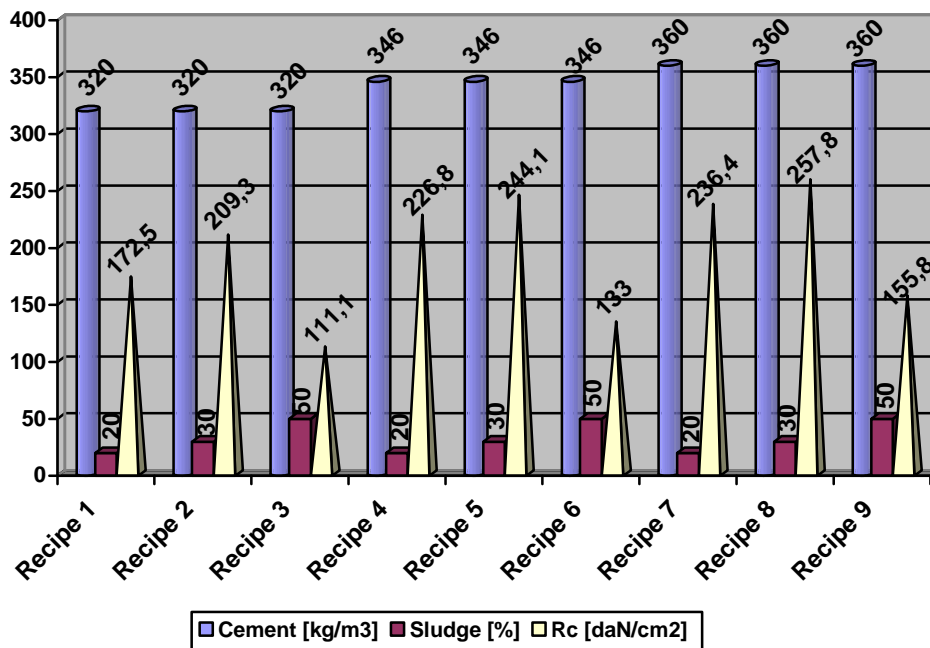


Fig. 3 Variation in mortar strength depending on dosage and addition, at 28 days

#### 4. CONCLUSIONS

From a technical point of view, in the case the plastifier additive is not used, the higher resistances are obtained for a dose of 346 kg/m<sup>3</sup> and 20% sludge.

Tab. 5 presents a comparison regarding the compressive strength of the sludge mortar with and without plastifier.

Tab. 5 Compressive strength of sludge mortar

Cement II A-S 32,5R Kg/m <sup>3</sup>	Sludge %	(R <sub>c</sub> ) [N/mm <sup>2</sup> ]	
		mortar without plastifier	mortar with 0,5% BV 7 U plastifier
320	20	10.87	17.25
346	20	19.80	22.68
360	20	12.31	23.64
320	50	7.13	11.11
346	50	13.65	13.30
360	50	12.92	15.58

In the case the plastifier additive is used (see Table 5), there is a significant increase of the resistance in any of the recipes used. The highest strength values are obtained for a cement dosage of 360 kg/m<sup>3</sup> and 30% sludge using BIBER V 7U plastifying additive.

It is found that regardless of the cement dosage, 320, 346, 360 kg/m<sup>3</sup>, for a sludge addition of 50% and using BIBER V 7U plastifying additive, the lowest compressive strength values will be obtained; but all the compressive strength values are higher than 100 daN/cm<sup>2</sup>(10 N/mm<sup>2</sup>), which is equivalent to mortar M100.

From an economical point of view the material costs of any of the mortar networks using the sludge are markedly lower than in the case of standard mortar. The reductions expressed in percentages range between 20 to 50 %.

An additional advantage is that there is no more need for deposit space that affects the ecological balance. The space, transportation and depositing in ecological conditions require extremely big financial efforts.

## 5. ACKNOWLEDGEMENT

Authors wish to express their gratitude for the help of Prof. Dr. Ing. Mariana Brumaru and Prof. Dr. Ing. Daniela Lucia Manea.

## 6. REFERENCES

- Craciunescu, L., Serban, L., Popescu, M., Matei, V. (1990): Beton aparent cu parament colorat cu șlam de bauxită, *Materiale de construcții*, 20.4.1990. p.203.
- Craciunescu, L., Serban, L., Popescu, M. (1991): Agregate artificiale si cărămizi pe bază de bauxită, *Materiale de construcții*, 21.2-3.1991. p.81.
- Jebeleanu, E. (1991): Contributii la realizarea betoanelor si mortarelor cu aditivi superplastifianti – *Teza de doctorat*, 1991
- Manea, D., Corbu, O. (2002): O noua gama de aditivi pe piata romaneasca ADDIMENT – Ultima inovatie in domeniul constructiilor. Aditivi pentru mortare si betoane, – *Simpozion – 40 de ani de la înființarea catedrei "Beton, Materiale, Tehnologie și Organizare", în cadrul Facultății de Construcții și Arhitectură Iași* – oct 2002; pp.83-96.
- Manea, D., Aciu, C., Corbu (2007): O., Studii privind modalitățile de valorificare a șlamului rezultat în urma neutralizării cu lapte de var a apelor acide provenite din decaparea sârmelor obținute la S.C. Mechel Câmpia Turzii, *Simpozionul International "Inginerie civila 2007" organizat de Facultatea de Constructii Constanta*

## MIX DESIGN OF SELF COMPACTING CONCRETE

*István Zsigovics*

*Budapest University of Technology and Economics, Hungary*

*H-1111 Budapest, Műegyetem rkp. 3. [betonterv@gmail.com](mailto:betonterv@gmail.com)*

### SUMMARY

A new mix design on experimental bases for Self Compacting Concrete was developed based on determining the optimum of powder content. Using our method of mix design, self-compactability can be provided rapidly by laboratory tests. It is not necessary to carry out tests on the paste and mortar. This method was introduced to the practice and applied successfully.

### 1. INTRODUCTION

Self compacting concrete was developed in 1988 in Japan in order to achieve durable concrete structures and to avoid compaction work on site. Investigation for establishing rational mix design and testing methods were carried out to develop standards for self compacting concrete (Skarendahl, Petersson, 2000; Wallevik, 2006).

By Okamura and Ozawa (1995) the main features of the mix design of the self-compacting concrete were:

- Step first designing the mix:  $0.5 \text{ m}^3/\text{m}^3$  bulk volume of coarse aggregate at the most.
- Step second designing the mix: paste tests to determine the water-powder ratio in mass.
- Step third designing the mix: design of the mortar (the fine aggregate content is set at 50 % of the resulting mortar volume, setting the admixture dosage).
- Step fourth designing the mix: checking the self compactability with fresh concrete tests and if necessary the correction has to be carried out for reaching the self compactability.

The steps of the mix design suggest that a correction have to be carried out if the self compactability is not fully activated in the first three steps. The question is what would happen if the paste and mortar tests are not carried out and the self compactability would be set on fresh concrete directly. The results of the research on limestone powder open the door to support this kind of mix design for the self compactability of concrete (Zsigovics, 2004; Zsigovics, 2005).

### 2. DEFINITION OF THE SELF-COMPACTING CONCRETE AND DESIGN

The self compacting concrete is a kind of fresh concrete that can slowly flow without supplementary compacting energy under self-weight without segregation of components, nearly levelling-off, some air goes off during self-compaction, while entirely filling the space of the reinforcement and the formwork and holds its homogeneity.

It follows from the above definition of self-compacting concrete that to produce concrete like honey. In order to reach this there are three technological tools:

- powder content
- super plasticizer admixtures
- admixtures increasing viscosity.

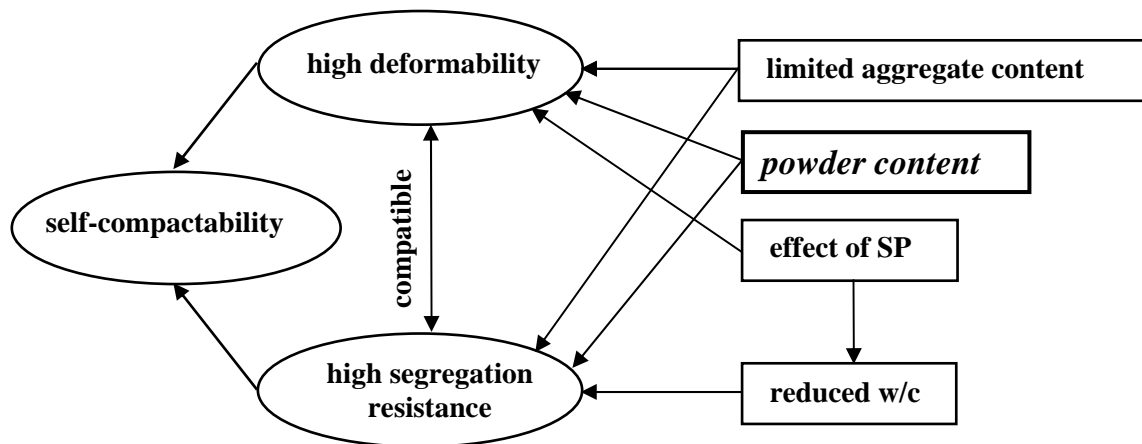


Fig. 1 Methods for achieving self compactability

Okamura and Ozawa (1994) and Ouchi (1998) developed the following method to achieve self compactability (Fig. 1):

- to use limited aggregate content and higher powder ( $\leq 90 \mu\text{m}$ ) content
- to have both of high deformability and high viscosity at the same time.

The coarse aggregate content is determined to be  $\leq 500 \text{ l/m}^3$  in bulk density, the admixture and water content are well determined (these can be optimized also). The maximum self-compactability is reached depending only on the optimized powder content without using viscosity increasing admixture.

If the basic mix is not in the self compactability range then the mix has to be modified to be above the self compactability bottom level by adding water and/or superplasticizer (10-12 seconds V-funnel time and 700-750 mm slump flow) by using the G-ring slump flow and V-funnel tests.

My proposed mix design is to determine the optimum powder content (for instant limestone, silica, slag, fly ash powder) on the fresh concrete mix by trial mixes.

Other design and technology considerations (as strength, water/cement ratio and type of cement) have to be adjusted. In the first step we measure the V-funnel time and slump flow value on mix where the powder content is lower than the expected optimum value.

Afterwards  $20 \text{ kg/m}^3$  limestone is added to the mix and the V-funnel time and slump flow value are measured. The procedure is continued while the slump flow and V-funnel tests results start to decrease (Fig. 2).

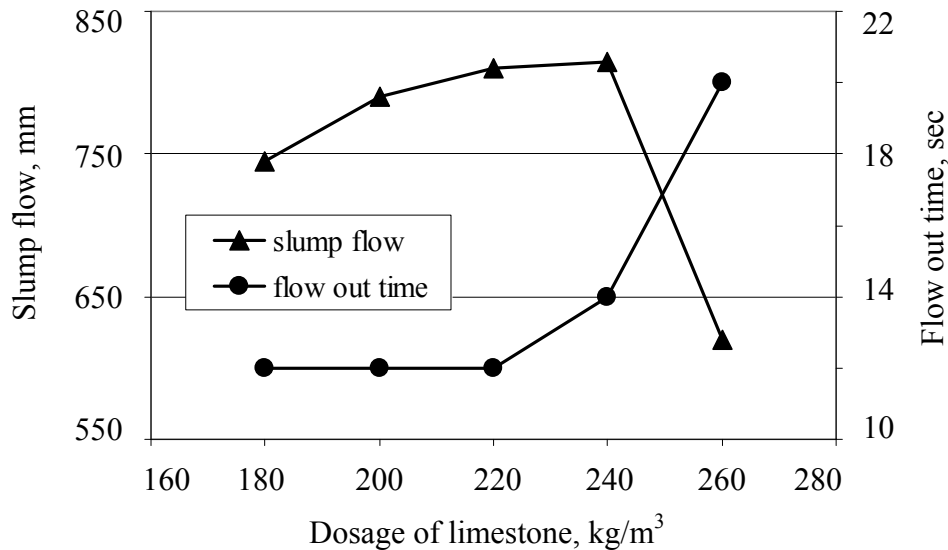


Fig. 2 Effect of the dosage of limestone powder on the consistency and flow out time

Based on the obtained results the optimum dosage of limestone is determined (additional powder content). Thereafter the mix has to be determined for 1 m<sup>3</sup> concrete using the optimum limestone powder content and the finally the consistency is measured (Fig. 3).

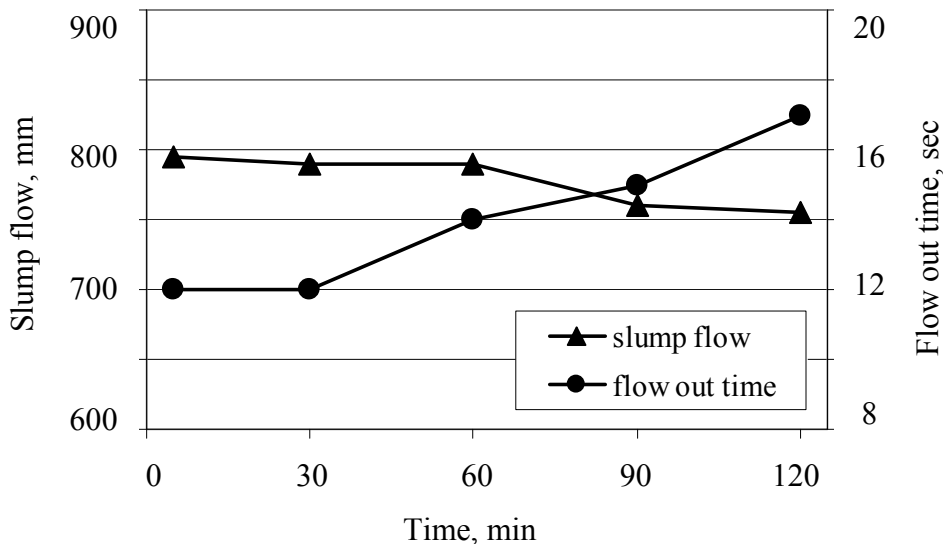


Fig. 3 Slump flow and flow out time against time

The G-ring slump flow and V-funnel time tests are measured for 2 hours. The concrete is considered as high performance self-compacting fresh concrete if the self compactability lasts for two hours. This condition is reached that the slump flow value should be 750±50 mm and the V-funnel time between 10-20 seconds.

These requirements can be adjusted. The aim of the design is to allocate the self-compacting concrete between the given values, and to demonstrate that it remains in that range for one and half or two hours (Fig. 4).

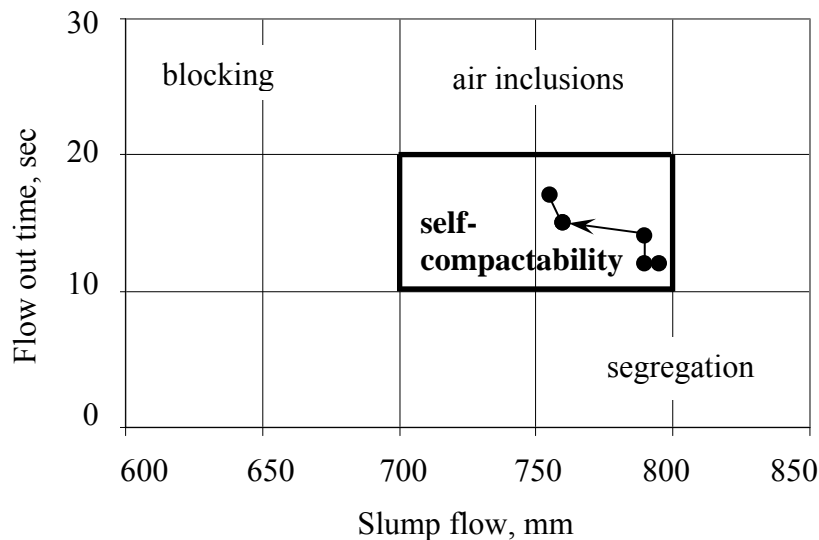


Fig. 4 Range of the workability of the self compacting concrete

The last step of the procedure is to check the homogeneity of the concrete by splitting test. If the concrete homogeneity is not adequate (aggregate settling); the V-funnel time and slump flow test requirements have to be modified.

If the reached concrete maximum performance is not enough for the concrete technology requirements the quality of superplasticizer, sand or cement have to be changed for the mix design until the required target will be reached.

#### 4. CONCLUSIONS

By laboratory tests and successful industrial applications the self compacting concrete can be designed by the following experimental method:

1. The aggregate content is maximalized for 500 kg/m<sup>3</sup> in bulk density.
2. Determination of the type and content of cement and water content (w/c)
3. Choosing the right superplasticizer and determining the dosage of it by the water content.
4. Determination of the optimum powder content (limestone) by the V-funnel test and slump flow test of the fresh concrete.
5. Adjusting the mix for optimum powder content and measuring the V-funnel time and slump flow value of the fresh concrete.
6. Making cylinder specimens. Splitting test on the cylinder specimens for checking the concrete homogeneity.

The above mix design has been used for the high performance reinforced exposed surface concrete structures of the Szécsi Tamás Sport Pool. The design of the self-compacting concrete was done by Budapest University of Technology and Economics Department of Construction Materials and Engineering Geology as a research developing work finalized and supported by Cemex Hungary, Danubiusbeton Betonkészítő Ltd.



Fig. 5 High board of Szécsi Tamás Sport Pool

## 5. REFERENCES

- Okamura, H., Ozawa, K. (1994), „Self-compactable high-performance concrete in Japan”, ACI SP-169, pp. 31-44.
- Okamura, H., Ozawa, K. (1995), „Mix-design for Self-Compacting Concrete”, *Concrete Library of JSCE*, No. 25, June 1995, pp. 107-120.
- Ouchi, M. (1998), „History of Development and Application of Self-Compacting Concrete in Japan” *Proceedings*, International Workshop on Self-Compacting Concrete, 23-26 August 1998, Tosa-Yamada Kochi, Japan pp.1-10.
- Skarendahl, A., Petersson, Ö. (2000), „Self-Compacting Concrete”, State-of-the-Art report of RILEM TC 174-SCC, *RILEM Report 23*, ISBN: 2-912143-23-3
- Wallevik, O.H, (2006), „Why is Self Compacting Concrete so different in different countries?”, *Concrete Plant International* - # 2 – April 2006 pp. 30-36.
- Zsigovics, I. (2004), „Self-compacting concrete”, *PhD Dissertation*, Budapest University of Technology and Economics Department of Construction Materials and Engineering Geology, 2004, p 97.
- Zsigovics, I. (2005), „Effects of Limestone Powder on the Consistency and Compressive Strength of SCC”. *Proceedings of the Second North American Conference on the Design and Use of Self-Consolidating Concrete (SCC) and the Fourth International RILEM Symposium on Self-Compacting Concrete* 30 October-3 November, 2005 Chicago USA, pp. 173-179. ISBN 0-924659-64-5





## **SELF COMPACTING CONCRETE WITH SILICA FUME – PROCEDURE FOR MIX DESIGN**

*Henriette Szilágyi\* , Adrian Ioani\*\* , Ofelia Corbu\*\**

*\* National Institute for Research & Development in Construction and Economy of  
Construction (INCERC) Cluj-Napoca Branch  
117 Calea Floresti, 400524 Cluj-Napoca, Romania.*

*\*\*Technical University of Cluj-Napoca  
15 C. Daicoviciu Street, 400020 Cluj-Napoca, Romania*

### **SUMMARY**

Self Compacting Concrete (SCC), the concrete that is compacted under its own weight with no intervention of vibrating compaction, has many qualities, such as: faster construction with reduction of manpower, increasing productivity during building, high-quality surface finishes, improved durability etc.

The paper presents a research aiming the optimal design and execution of self-compacting concrete in laboratory, following specific mix compositions and establishing the concrete properties in fresh and hardened state.

### **1. GUIDELINES FOR MIX DESIGN**

According to “The European Guidelines for Self-Compacting Concrete”, an efficient design of SCC mixes is based on the rheology of fresh concrete. Therefore:

- limiting the water/powder ratio, adding a high range water reducing admixture (HRWR) and optionally a viscosity modifying admixture (VMA), the viscosity of the paste from SCC is adjusted;
- the volume of the paste must be greater than the void volume in the aggregate, thus increasing fluidity and reduces aggregate friction;
- reducing the coarse to fine aggregate ratio in the mix results an increases of the passing ability of SCC

The relative proportions of the SCC key components are:

- total powder content: 380...600 (kg/m<sup>3</sup>);
- paste content: 300...380 (ℓ/m<sup>3</sup>);
- coarse aggregate content: 750...1000 (kg/m<sup>3</sup>) or 270...360 (ℓ/m<sup>3</sup>);
- water/powder ratio: 0.85...1.10 (by volume);
- fine aggregate content: balances the volume of the other constituents, typically 48-55% of total aggregate weight.

### **2. MIX COMPOSITION**

#### **2.1 Materials**

The selected constituents of the SCC mixes are: Portland cement CEM I 52.5 R, Elkem Microsilica Grade 940 U, fine aggregate (0-4) mm, river coarse aggregate (4-8; 8-16) mm and admixtures. For admixtures were considered: Glenium Ace 30, a high-range water reducing

admixtures (HRWR) and Glenium Stream a viscosity modifying admixture (VMA), in order to optimize the workability and to prevent segregation, both from BASF.

## 2.2 Mix proportions

The aggregate proportions were established respecting the relative proportions of the SCC key components and therewith according to the national regulations, respecting concrete manufacturing. The SCC mixes have the following total grading curve: 56% (0-4) mm; 14% (4-8) mm; 30% (8-16) mm are presented in Fig. 1. An exception is SCC with Index mix 17, which has 40% (0-4) mm; 30% (4-8) mm; 30% (8-16) mm.

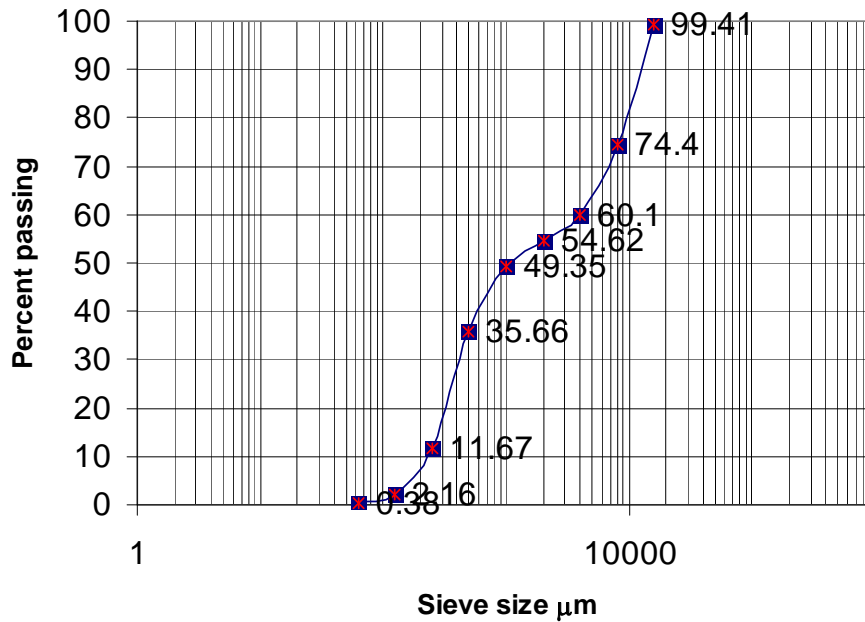


Fig. 1 Total grading curve for aggregates (56% 0-4; 14% 4-8; 30% 8-16)

A few representative SCC mix composition are presented in Tab. 1

Tab. 1 Mix compositions

Mix Index	11	14	15	17	29	30
Cement, kg/m <sup>3</sup>	510	481	450	481	420	420
Microsilica, kg/m <sup>3</sup>	-	25	51	25	54	54
Fine aggregate (0-4) mm, kg/m <sup>3</sup>	920	920	920	657	935	935
Coarse aggregate (4-8) mm, kg/m <sup>3</sup>	230	230	230	493	233	233
Coarse aggregate (8-16) mm, kg/m <sup>3</sup>	493	493	493	493	501	501
HRWR: GLENIUM ACE 30, kg/m <sup>3</sup>	5.61	6.32	7.01	6.32	6.78	7.35
VMA: GLENIUM STREAM, kg/m <sup>3</sup>	-	-	-	3.54	-	2.73
Water, l/m <sup>3</sup>	199	197	195	197	190	190

### 3. EXPERIMENTAL RESULTS

#### 3.1 Test results on fresh SCC

The properties of fresh SCC were assessed using the slump-flow test, the V-funnel test and the L-box test, as shown in Tab. 2, Tab. 3, Tab. 4, Fig. 2, Fig. 3 and Fig. 4.

Tab. 2 Characteristics and test methods for evaluating SCC

Characteristic	Test method	Measured value
Flowability/filling ability	Slump-flow test	total spread
Viscosity (rate of flow)	T <sub>500</sub> Slump-flow test and V-funnel test	flow time
Passing ability	L-box test	passing ratio

Tab. 3 Test results on fresh SCC

Mix Index	Testing time* (min)	Slump-flow (mm)	T <sub>500</sub> time (s)	V-funnel (s)	L-box
11	15	745	3	11.5	-
	30	770	3	-	-
	70	700	5,6	-	-
14	15	650	2,5	7	-
	30	660	2,5	-	-
	60	570	5	-	-
15	15	665	3	6	-
	35	690	2	8	0.83
	60	635	4	12	-
17	15	685	2	5	-
	40	730	2,5	10	-
29	15	600	2,5	7.7	-
	30	560	-	13.5	0.66
30	15	702	-	5.5	-
	30	672	-	9.5	-
	45	-	-	-	0.96

\*After ... min of HRWR addition

Tab. 4 Test reports on fresh SCC

Mix Index	Observations
11	Very good flowability/filling ability and viscosity, stabile mix in time, without segregation.
14	Good flowability/filling ability excellent viscosity, no segregation.
15	Very good flowability/filling ability and passing ability, excellent viscosity, stabile mix in time, without segregation.
17	Very good flowability/filling ability and viscosity, with segregation, corrected with VMA addition.
29	Less flowability/filling ability very good viscosity, unstable mix in time, no passing ability after 30' of HRWR addition
30	Very good flowability/filling ability, excellent viscosity and passing ability, with segregation, corrected with VMA addition.

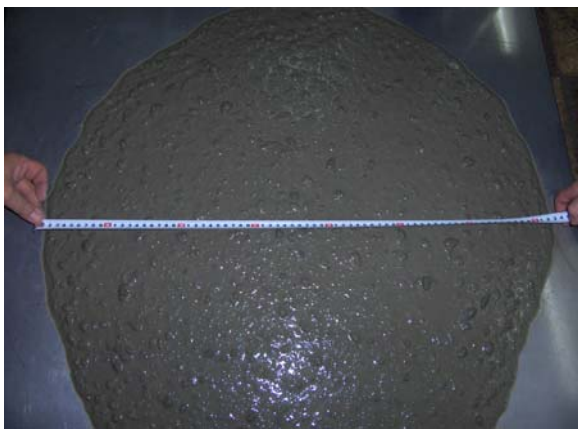


Fig. 2 SCC 11 – Slump-flow



Fig. 3 SCC 17 – Slump-flow before VMA addition



Fig. 4 SCC 17 – Slump-flow after VMA addition

Visual observation was made for all mixes, regarding the edge of the spread concrete at slump-flow, in order to identify the mixes tendency to segregate.

### 3.2 Test results on hardened SCC

The compressive strength for the presented mixes is in Tab. 5.

Tab. 5 Test results on hardened SCC

Mix Index	Compressive strength (N/mm <sup>2</sup> )		
	1 day	7 days	28 days
11	51.1	56.5	70.5
14	45.1	56.9	65.7
15	44.4	60.0	71.0
17	46.7	60.7	69.8
29	41.7	54.2	67.3
30	42.3	57.3	73.4

## 4. CONCLUSIONS

The characteristics of the selected SCC mixes, obtained in laboratory, either in fresh and hardened state, were satisfactory. All mixes had a slump –flow value between 660....750 mm, which classify them in SF2 slump-flow class (exception was SCC 29, with SF1 -550....650 mm). In order to classify the viscosity of mixes after the T<sub>500</sub> time during the slump-flow test or by the V-funnel flow time, results VS1/VF1 class (T<sub>500</sub> ≤ 2 s, V-funnel time: ≤ 8s) for mix 15 and 17 and VS2/VF2 class (T<sub>500</sub> > 2 s, V-funnel time: 9...25 s) for the other mixes.

Our results indicated that self - compacting concrete could be realized even without additions, if the cement content and the fine part of the sand (under 0.125 mm) are high enough to provide the powder need of SCC.

High quality surface finish was achieved, as it shown in Fig. 5, the concrete perfectly filling all the details of the formwork, even in the absence of mould release agent.



Fig. 5 SCC surface finishes

Viscosity modifying admixture (VMA) effects was obvious in the mixes where it was added to the fresh concrete (mixes 17 and 30) increasing cohesion and segregation resistance. The highest compressive strength at 28 days was obtained for mix 30, which has the smallest cement and the largest superplasticiser content.

The next experimental investigation will evaluate the properties of SCC with microsilica at long terms, the shrinkage and the creep coefficients, and also in order to perform the technological transfer between laboratory and prefabricated concrete unit, on the basis of the preliminary mix compositions.

## 5. ACKNOWLEDGEMENTS

The research project was made possible thanks to ASA CONS S.A. Turda, a major prefabricated concrete unit from Romania, who supplying the cement and aggregate. The authors wish also thank to the BASF Construction Chemicals Ltd. and SIKKA<sup>®</sup> Romania Ltd. for providing the necessary admixtures for the self-compacting concrete mixes.

## 6. REFERENCES

- BIBM, CEMBUREAU, ERMCO, EFCA, EFNARC (2005), *The European Guidelines for Self Compacting Concrete. Specification, Production and Use*: 63
- NE 012-1:2007 *Code of Practice for Concrete and Reinforced Concrete. Part 1: Concrete production*: 83
- NE 013-2002. *Code of Practice for Precast Concrete, Reinforced Concrete and Prestressed Concrete*: 166
- Szilagyi, H. Domşa, J. Mircea, A. (2005). "Research upon self –compacting concrete for the precast industry in construction", *fib Symposium "Keep Concrete Attractive"*, Budapest, Hungary, 23-25 May 2005, pp. 235-238.

## **EXPERIMENTAL STUDIES ON CONCRETE WITH INNOVATIVE SHRINKAGE COMPENSATING ADMIXTURE SYSTEM**

*Katalin Szilágyi, István Zsigovics*  
*Budapest University of Technology and Economics, Hungary*  
*H-1111 Budapest Műegyetem rakpart 3.*

*Csaba Szautner*  
*MAPEI Hungary Co. Ltd. H-2040 Budaörs Sport utca 2.*

### **SUMMARY**

In present experimental studies the *Mapecrete* shrinkage compensating and self curing system produced by *Mapei* was studied. Results indicated that the *Mapecrete* system considerably decreases the shrinkage of concretes. The shrinkage compensating action is more effective if the concrete is more sensitive to shrinkage in its origin. Results also demonstrated that due to the combined shrinkage compensating and self curing actions the compressive strength, the consistency, the consistency endurance and the water tightness of concretes can be considerably improved.

### **1. INTRODUCTION**

Crack formation, and particularly shrinkage cracking is one of the major concerns in the durability of concrete structures. Appropriate concrete technology can help to avoid cracking and to provide improved durability in terms of smaller permeability, better water tightness, higher freeze-thaw resistance and higher resistance against aggressive chemical attacks. To avoid shrinkage cracking several possible solutions are available in concrete technology, such as:

- use of expanding cements,
- use of shrinkage compensating admixtures,
- mixing concretes of low cement-paste content,
  - by low water-to-cement ratio,
  - by low cement content,
- mixing concretes of reduced sand content,
- effective curing of concrete.

In present experimental studies the *Mapecrete* system by *Mapei* was studied. The system provides the combined use of the following three components:

- 1) Dynamon SR3 – superplasticizer,
- 2) Expancrete – expansive admixture,
- 3) Mapecure SRA – internal curing admixture.

### **2. DESCRIPTION OF SHRINKAGE AND SHRINKAGE COMPENSATION**

Volume changes (shrinkage) due to loss of water are possible both in the fresh concrete and in the hardened concrete. In the fresh concrete, loss of water by evaporation causes plastic shrinkage and can lead to surface cracking. Withdrawal of water from concrete stored in unsaturated air causes drying shrinkage (Neville, 1995). Autogenous shrinkage (volume



changes due to chemical reactions during hydration) is also discussed in technical literature, however, for practical purposes these relatively small changes need not to be distinguished from drying shrinkage. Factors affecting shrinkage are the followings:

- relative humidity of ambience,
- climatic conditions (temperature, wind speed, etc.),
- volume of cement stone,
- stiffness of aggregate,
- possible water absorbing capacity of aggregate,
- volume-to-surface ratio of the concrete structure.

Prolonged moist curing of concrete delays the advent of shrinkage, but the effect of curing on the magnitude of shrinkage is small (Neville, 1995). Prolonged moist curing helps to avoid cracking due to higher tensile strength of concrete. Shrinkage of concrete stored in unsaturated air can not be avoided as the equilibrium water content in the capillary pores is realized at relatively low water content. No shrinkage of concrete is possible only at ~94RH% of the ambient that is not a usual case in civil engineering. Compensation the shrinkage itself and elimination the shrinkage cracking need the following repertoire of tools in concrete technology:

- 1) concrete mix having low cement paste content,
- 2) shrinkage compensating (expansive) agents,
- 3) prolonged moist curing of concrete.

Above targets can be realized by the following materials (Mapei, 2006; 2007). *Dynamon SR3* superplasticizer consists of a water solution containing 30% of acrylic polymers (with no formaldehyde). The polymers can efficiently disperse the cement grains and they can facilitate a slow development of hydration products within the concrete. *Expacrete* calcium oxide based chloride-free expansive powder is responsible for the volume change compensation during shrinkage of portland cement mortar and concrete. The expansive mechanism is activated when the concrete begin to cure and dissipates after the concrete hardens (Valentine, 2006). *Mapecure SRA* propyleneglycol ether based additive fluid works by reducing the surface stresses of the water present in the capillary pores and as a result, the forces which act upon the walls of the pores are greatly reduced (Maltese et al, 2005).

Tab. 1 Details of tested concrete mixes

type of concrete	cement amount, kg/m <sup>3</sup>	type of cement	water-to-cement ratio	design consistency (flow), mm
steel fibre reinforced concrete (steel fibre content: 30 kg/m <sup>3</sup> )	340	CEM II/B-S 32.5 R	0.45	550-600
concrete of improved water tightness (W)	310	CEM III/B 32.5 N-S	0.55	550-600
high strength concrete (HSC)	410	CEM II/A-S 42.5 N	0.40	550-600
SCC for exposed surfaces (limestone powder content: 220 kg/m <sup>3</sup> ) (SCC)	350	CEM III/A 32.5 N	0.46	700-800 V-funnel time: 15-20 sec

### 3. EXPERIMENTAL STUDIES

In present experimental studies laboratory tests were carried out at the Budapest University of Technology and Economics Department of Constructing Materials and Engineering Geology.

Tests were carried out both on fresh concrete and hardened concrete of four different concrete mixtures (covering self compacting concrete for exposed surfaces, high strength concrete, concrete of improved water tightness and steel fibre reinforced concrete). Details of concrete mixes are given in *Tab. 1*. Fresh concrete tests covered consistency measurements (flow and slump tests for conventional concretes; J-ring tests and V-funnel tests for SCC) as well as consistency endurance studies. Tests on hardened concrete specimens were carried out in terms of standard strength tests, studies of strength development (from the age of 1 day up to 90 days), standard water penetration tests and standard freeze-thaw cycle tests. Present paper summarizes measurements on shrinkage, fresh concrete consistency, compressive strength and water tightness.

#### 4. RESULTS

The applied admixtures had a considerable influence on the decrease of concrete shrinkage for all the four concrete mixes tested (*Tab. 2*). Also, the presence of steel fibres was found to have an effect on shrinkage. Almost the total shrinkage compensating expanding action took place in the first and the second day. Our experiments demonstrated that the shrinkage compensation mechanism for all of our concrete mixes was the same in nature. However, rate and magnitude of shrinkage is strongly depending on the actual mix.

Tab. 2 The 90 days results on shrinkage of tested concrete mixes (average of 2 measurements)

type of concrete	without Mapecrete	with Mapecrete	difference	significance of shrinkage compensation (high+++, low+)
steel fibre reinforced concrete	0.32 ‰	0.08 ‰	0.24 ‰	++
concrete of improved water tightness	0.27 ‰	0.14 ‰	0.13 ‰	+
high strength concrete	0.36 ‰	0.22 ‰	0.14 ‰	+
SCC for exposed surfaces	0.42 ‰	0.11 ‰	0.31 ‰	+++

*In case of the steel fibre reinforced concrete mix*, both Mapecrete and steel fibres are utilized for the shrinkage compensation (*Fig. 1.a*). Therefore, the 90 days shrinkage of this mix is the most favourable (0.08 ‰), however, the shrinkage compensation expanding mechanism itself can not be so significant as in the case of the self compacting concrete mix (0.24 ‰ and 0.31 ‰ decrease, respectively).

*In case of the concrete mix of improved water tightness*, the shrinkage compensating action can not be considerable as the cement paste content of this mix is reduced, according to the design of water tight concretes. The 90 days shrinkage of this concrete mix is rather limited either without the Mapecrete. However, the shrinkage compensation is still remarkable (0.31 ‰ decrease, see *Fig. 1.b*).

*In case of the high strength concrete mix*, the considerably high early age strength was found to reduce the shrinkage compensation expanding mechanism up to the fifth day that can be studied in *Fig. 1.c*. As a result, almost no initial expanding is realized and the 90 days shrinkage of the high strength concrete mix is not so favourable (0.22 ‰) than that of the other mixes studied.

In case of the self compacting concrete mix, the granulated limestone provides a self-curing action, with which the shrinkage compensating expanding mechanism can be maintained for a longer period of time (Fig. 1.d). As a result, the efficiency of the *Mapecrete* is improved (90 days shrinkage is reduced 25% to that of the shrinkage of SCC without *Mapecrete*).

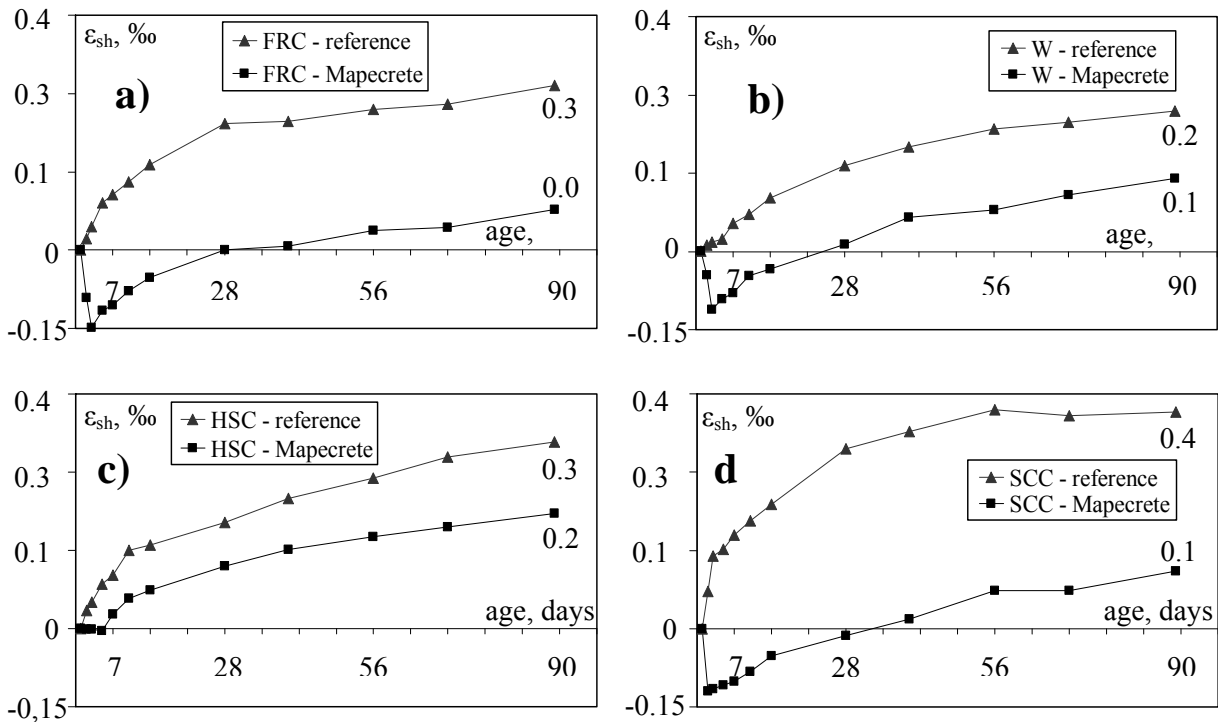


Fig. 1 Shrinkage of concrete specimens without and with Mapecrete (averages of 2 meas.)  
 a) steel fibre reinforced concrete (FRC) c) high strength concrete (HSC)  
 b) concrete of improved water tightness (W) d) SCC for exposed surfaces (SCC)

Present experimental studies demonstrated that the *Mapecrete* system does not have disadvantageous influences on the properties of fresh concrete. Consistency studies were carried out in terms of flow tests and slump tests (with additional V-funnel and J-ring tests for SCC). Results indicated that the *Mapecrete* system is applicable for all the four tested concrete mixes; usually with a beneficial influence on consistency that was not expected originally (e.g. the same consistency is reached at 0.1% lower superplasticizer content in the mix). Consistency endurance was also slightly improved even in spite of the reduced superplasticizer content. In Fig. 2 the 5 min and the 1.5 h results of consistency endurance tests (using flow table) can be studied. The considerable improvement of fresh concrete properties is due to the addition of fine particles of the expansive powder admixture into the matrix.

Early age-, 28 days age- and 90 days age compressive strength are considerably increased by the application of *Mapecrete*. For concrete mixes with CEM II (the high strength concrete mix and the steel fibre reinforced concrete mix in present experiments) the increase in early age strength reaches 100% (Fig. 3). Note, that results indicated in Fig. 3 are corresponding to concrete specimens without any moist curing and stored at laboratory conditions up to 90 days age. The difference in the compressive strength realized is decreasing in time, but it is still considerable at the age of 90 days. Results demonstrated that strength level of standard moist cured concretes can not be reached by the simple use of *Mapecrete* as a substitute for

curing. For concrete mixes with CEM III the increase in early age strength is not remarkable, however, considerable increase in the 90 days strength is realized. These favourable influences are attributed to the combined action of shrinkage compensation and self curing. Experiments also demonstrated that *Mapecrete* is not effective in gaining strength to the concretes tested at a standard moist curing condition: i.e. no difference in the compressive strengths of reference and *Mapecrete* concretes could be realized at the age of 90 days.

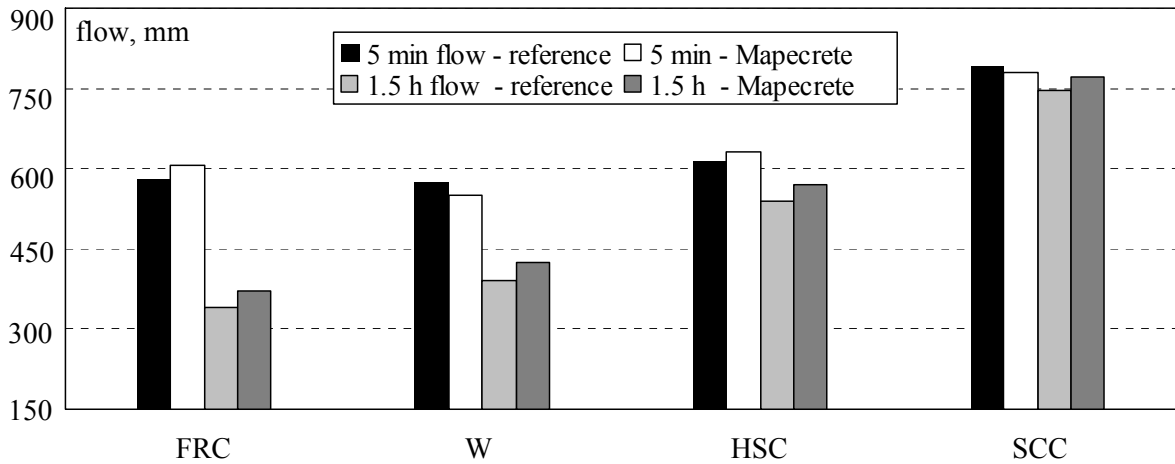


Fig. 2 Flow test results of concrete mixes without and with Mapecrete

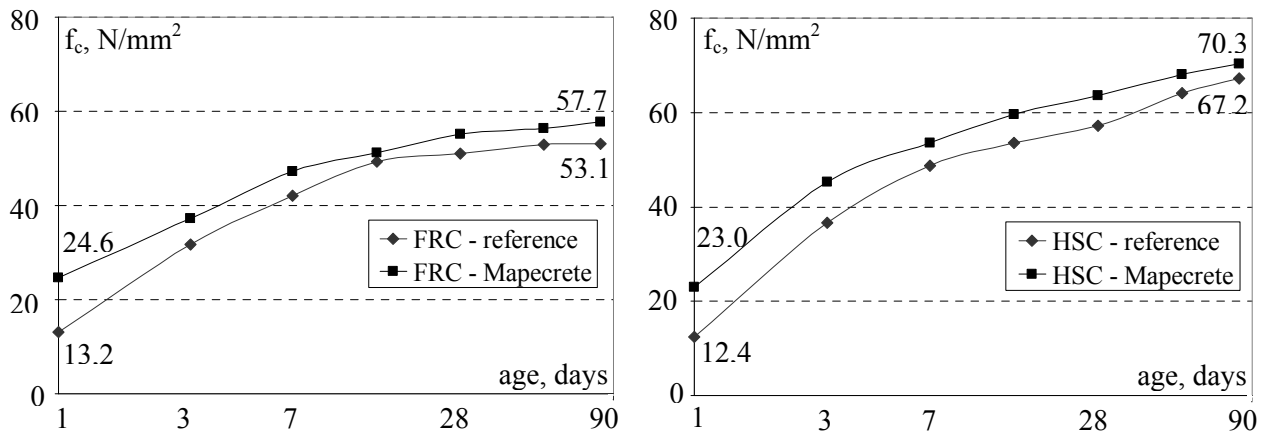


Fig. 3 Compressive strength of concrete specimens without and with Mapecrete (specimens are not moist cured and stored under laboratory conditions)

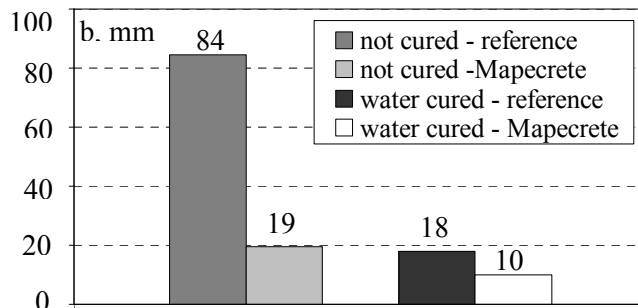


Fig. 4 Water penetration (b, mm) of concrete specimens (W) without and with Mapecrete

Water tightness was tested according to EN 12390-8:2000 at the age of 28 days and also with

the same procedure on concrete specimens that were stored at laboratory conditions up to 28 days without any moist curing. Considerable differences in behaviour are demonstrated in *Fig. 4*. *Mapecrete* provides considerably improved water tightness for concrete. The influence is remarkable especially in the case where the specimens were not water cured. Results demonstrate the efficiency of *Mapecrete* on the evolution of capillary pores of low permeability due to the combined effect of shrinkage compensation and self curing. Results indicate that use of *Mapecrete* can help the construction of watertight concrete structures where curing is of great importance and sometimes it is difficult to carry out.

## 5. CONCLUSIONS

In present experimental studies the *Mapecrete* shrinkage compensating and self curing system by *Mapei* was studied. Results indicated considerable decrease of shrinkage. The shrinkage compensation action is more effective if the concrete is more sensitive to shrinkage in its origin. Results demonstrated that compressive strength of concretes tested was improved, however, the strength level of standard moist cured concretes could not be reached by the simple use of the *Mapecrete* system as a substitute for curing. Due to the addition of fine particles to the matrix by expansive admixture the consistency and consistency endurance of concrete tested were considerably improved. Tendency against segregation of mixes was also improved; however, a higher water demand was realized for all of the tested mixes. Results demonstrated considerably water tightness. The influence was especially remarkable if the specimens were not water cured during hardening. Results also indicate the need of further experimental studies.

## 7. REFERENCES

- Maltese, C., Pistolesi, C., Lolli, A., Bravo, A., Cerulli, T., Salvioni, D. (2005) „Combined effect of expansive and shrinkage reducing admixtures to obtain stable and durable mortars”, *Cement and Concrete Research* 35 (2005) pp. 2244 – 2251
- Mapei (2006) „Mapecrete system”, *personal communication* by Csaba Szautner, 2006
- Mapei (2007) „New challenges in chemistry of superplasticizers”, *personal communication* by Dr. Francesco Surico, 2007
- Neville, A. M. (1995) „Properties of Concrete”, *Pitman*, 1995
- Valentine, L (2006) „Improving concrete durability – Shrinkage compensation components offer many benefits”, *GoStructural.com* (<http://www.gostructural.com/article.asp?id=340>)

## ENVIRONMENTAL FRIENDLY TAILOR-DESIGNED SHOTCRETE

*Olga Río, Luis Fernández-Luco, Ángel Castillo*  
*Institute of Construction Sciences Eduardo Torroja-CSIC, Spain*  
*28033 Madrid [rio@ietcc.csic.es](mailto:rio@ietcc.csic.es), [lfluco@ietcc.csic.es](mailto:lfluco@ietcc.csic.es), [acastillo@ietcc.csic.es](mailto:acastillo@ietcc.csic.es)*

### SUMMARY

Structural shotcrete can be designed and produced with an improved environmental profile when a performance-based approach (PBA) is addressed. The selection of suitable concrete constituents from a broad variety of alternatives can be ruled by the global environmental performance. Not only less energy intensive cement contribute to this objective but the use of locally available aggregates, a better efficiency and increased durability contribute as well.

This paper is aimed at highlighting a case study where the use of a PBA to structural shotcrete design and characterisation has lead to better homogeneity, increased efficiency while using less energy-intensive cements and almost any type of aggregate. The assessment of the tailored shotcrete is performed through the use of suitable performance indicators, some of them rather innovative. As a result, it can be stated that it is possible to design and produce a tailored designed structural shotcrete with an improved environmental profile. The application of PBA to the design and characterisation of shotcrete might lead also to a better harmonisation between specification and control stages.

### 1. INTRODUCTION

Since last years there has been an increasing concern on the environmental impact of construction industry. Its impact can be assessed from different approaches; energy consumption or CO<sub>2</sub> emissions associated being among them. Shortage of suitable aggregates and service life of built structures can also be regarded as environmental considerations.

The adoption of a PBA (CIB, 2001) to material selection or mix design might contribute to overcome the limitations imposed by present Standards and Codes (PrEN, 2004; EFNARC, 2002; ACI-506R, 2000), mainly prescriptive or deemed-to-satisfy-rules. But also to contribute to the development of most environmental friendly tailor-made solutions which fulfil functional needs at a time. PB criterion is characterised by the importance given to the actual behaviour of a given material or structure. The performance required is closely related to the industrial and technological needs but also other technical and not technical general considerations (*identification of goal or objective*), but these needs have to be expressed as quantitative value (*definition of requirements and corresponding indicators*) associated to specific testing methods on defined samples (Fig. 1).

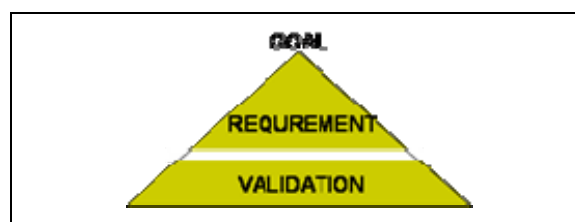


Fig. 1 Triangle of PB approach concept

These protocols for sampling and testing have to be used for validation (verification of compliance to conformity criteria) and then, according to the values obtained, to determine the acceptance or rejection of the material, structure or structural element (Andrade et al, 2005, Rio, 2005).

## 2. PB APPLIED TO SHOTCRETE

PB approach perfectly suits the needs of shotcrete or sprayed concrete (Rio et al., 2007) both fresh and hardened material related requirements but also process functionalities. As a consequence PBA can be applied to the different shotcrete stages: to the selection of concrete mix constituents, mix proportioning, shotcrete execution or, in a more integral manner, to the shotcrete or sprayed concrete material as final product.

The adoption of PBA might strongly contribute also to harmonize the specification and quality control stages, as both are ruled by the same concept (Fernandez-Luco et al, 2005). There is no need for the parameters to be assessed in terms of variables, as this criterion is flexible enough to allow for attributes as well. At present, Standards determine basic requirements for shotcrete, as well as for the parameters of the process which determine the quality of execution (Tab. 1. where both types of requirements according to EFNARC, are summarised as example) but for mix definition in general they still follows in principle a deemed-to-define-rules such maximum aggregate size, type of aggregate or type of cement, water/cement or binder relation, etc.

Tab. 1 Shotcrete Requirements

Shotcrete lining properties	Process parameters
Compressive strength and density	Pumping capacity
Flexural strength and residual strength	Rebound
Energy absorption class (plate test)	Applied shotcrete (as difference between pumping capacity and rebound)
Modulus of elasticity	Thickness of the shotcrete layer
Bond strength	Conveyor pressure
Permeability	Air consumption
Frost resistance	Air pressure
Determination of fiber content	Accelerator consumption
	Dust emission

The selection of constituent materials properties as well as its assessment and validation as part of the mix, by example, can be also based on PB approach. The advantages of using a performance criterion and its defined requirements (i.e. functional, environmental factors...), corresponding indicators (Structural stability- Safety, execution, etc. or health and sustainability..) and corresponding subindicators like (mechanical strength at different ages, or pumpability, projectability, mix efficiency or environmental effects, resources consume, etc.) are the freedom it gives to the designer and its triggering effect on technological innovations as we can see on the example described on this paper.

This attractive possibility pushed to extend the evaluation of the functions to the traditional standards but at the same time it has created confusion on the principles by mixing prescriptive and performance based methodologies and has contributed to the mistaking of definitions. PB subindicators and related tests as well are still under development for some of the cases.

### 3. SHOTCRETE MIXES SELECTED

The selection of most sustainable constituent materials for shotcrete can be based on a PBA, as mentioned in previous paragraph. For each of the constituents, main requirements have to be first identified and then, suitable performance indicators (PI) can be defined. Each of the performance indicators may lead to the use of convenient sub-indicators, which must be associated to specific sampling and testing procedures. The requirements considered in a PB approach must be seen as complementary of the ones set by Standards and Codes, which are mandatory and must be fulfilled. Under PBA, the assessment of concrete constituents and mix formulation may merge, as the performance is associated to both, constituent characteristic and mix proportions. Thus, four different formulations were prepared and tested following this criteria, as seen in Fig. 1.

One formulation, as it is used commonly, was tested as reference SRe. One formulation (SGr) was aimed at increasing the amount of aggregate, mainly the coarse, while maintaining suitable pumpability and projectability. Last two mixes are characterised for the inclusion of mineral additions, Silica fume for SSf mix and Coloidal Silica Fume for SSc mix. All mixes were projected using the same equipment onto real walls and standard shotcrete panel (PrEN, 2004). Panel cores were sampled at the age of 7d and standard cured until testing (28d).

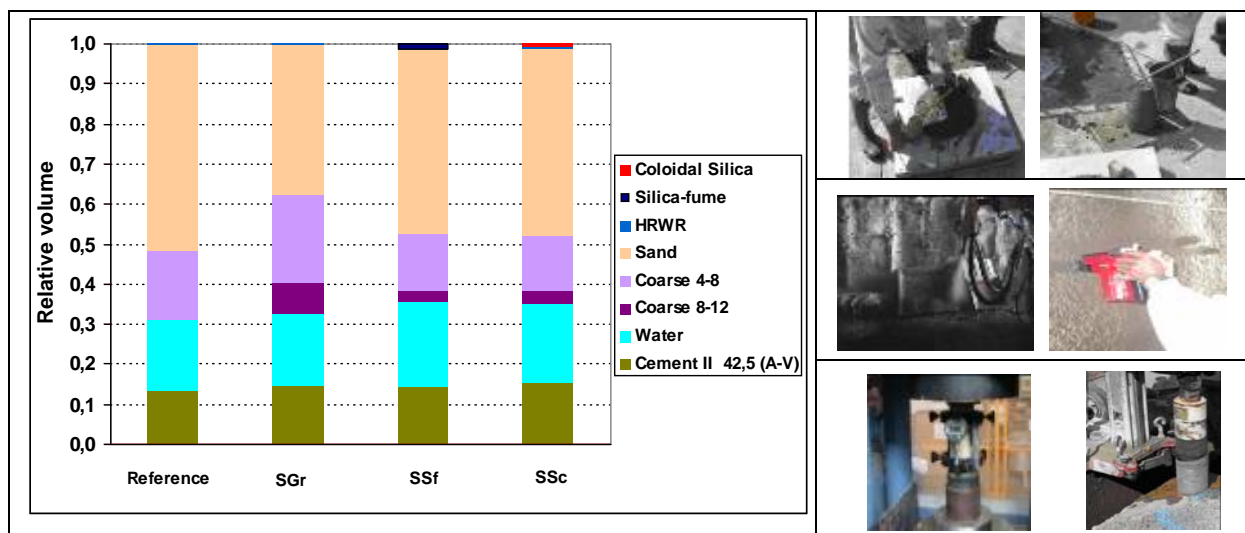


Fig. 1 Relative proportioning for all shotcrete mixes projected or sprayed and tested

#### 3.1 Aggregates

Aggregates used for shotcrete must comply with the general requirements for aggregates for conventional concrete plus extra added features to assure *pumpability* and *projectability* (see table 1). Thus, grading, shape and texture are key issues as they have a significant influence on the properties of concrete at the fresh state. Present recommendations and standards prevent crushed fine aggregates and flaky or elongated particles to be used as aggregates for shotcrete, as they might interfere with pumping and projection.

Nevertheless, adequate proportioning (Fig. 2) and the use of suitable chemical admixture may reduce the effect flaky shapes and rough textures of aggregates have on the pumpability of a concrete mix. Distance of projection, pump capacity and hose diameter are a key issue in pumping capacity and thus, the requirement may vary according to any particular situation.



All mixes showed suitable pumpability, with low pressures at the pump. The amount of rebound was low, although it was not quantitatively measured but visually assessed. The homogeneity among samples was excellent and thus, grading and mix proportioning is good at achieving low dispersion, with a mean value of  $2.23 \text{ kg/m}^3$  and a standard deviation of  $0.02 \text{ kg/m}^3$ , as well as high compacity. The reduction in density, taking the standard compacted basic concrete as a reference, was below 3 %. As a result, it can be said that the aggregate and the grading used fulfilled the performance requirements, as performance indicators show. Should additional requirements arise, such as very long pumping distances or limitations imposed by pumping equipment, conformity criteria should be adapted accordingly.

### 3.2 Cement

The cement (actually the fines content) is the main binder in any concrete formulation but it is also the main lubricant for delivery of the sprayed concrete. Very early age strength is an additional requirement, and thus, cement for sprayed concrete must always start to set extremely quickly to reach suitable very-early strength. Setting behaviour depends on the compatibility with nozzle accelerator and, as a general rule, these special admixtures work better with cement type I than with blended formulations; thus, shotcrete formulations are usually made of CEM I 52.5 R (also it is recommended by standards).

Based on the better sustainability profile of CEM II type cements and their increasing share in the European market (over 65 % in 2002 according to CEMBUREAU), a CEM II 42.5 R (A-V) was selected and tested for above shotcrete formulations after laboratory trials showed a good compatibility with chemical admixtures used. Regarding real scale testings on panels and on site fast setting was achieved at standard dosage of nozzle accelerator and early-age strength (tested according PrEN 14487 proposed methods) was only 15 % lower than the corresponding strength for a CEM I 52.5 R at the same age. Low temperatures, between 8-12 °C may have prevented the mix to achieve higher strength. Compressive strength ( $f_c$ ) of shotcrete formulations at 28-days (Fig. 3), was measured from cores taken from standard panels at 7d. The  $f_c$  achieved lies in the upper range of strength classes and in any case, all formulations tested have higher 28d strength than the reference mix (SRe). Moreover, they can all be classed as the highest group according to (EFNARC, 2002).

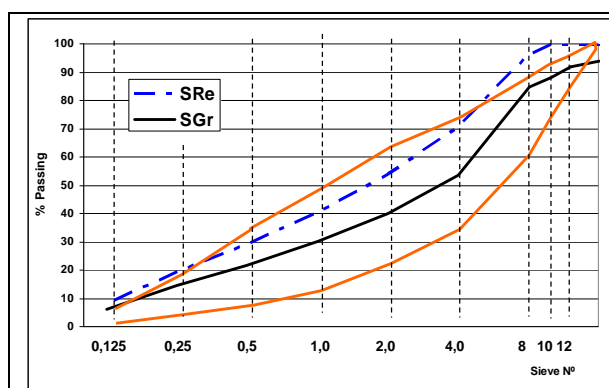


Fig. 2 SRe and SGr aggregate grading compared with SCA limits (orange)

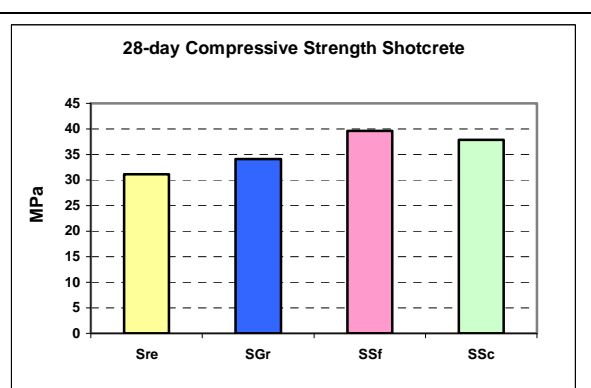


Fig. 3 28d compressive strength of different shotcrete formulations tested

### 3.3 Mineral admixtures

The use of mineral additions contributes to the sustainability profile of any concrete. They can be used to improve fresh-state properties and/or hardened state properties. These additions

may be active (like silica fume, slag and fly ash) or almost inert (mineral filler), depending on the performance requirements. Their contribution to long-term properties is well documented yet they might reduce the strength evolution at early age. Their compatibility with other shotcrete constituents should be verified in lab tests and confirmed with real scale trials, as the presence of mineral additions might interfere with the nozzle accelerator.

Real-scale trials showed that water demand for both mineral additions mixes (SSf and SSc) evaluated (Fig. 1) was increased as compared to no-addition mixes, although the difference was kept relatively low and the compressive strength at all ages was better than the corresponding for no-addition mixes, as can be seen from Fig. 3. From the results obtained, it can be stated that the mineral additions tested improved the properties of shotcrete mix.

### 3.4 Chemical admixtures

Concrete admixtures and mineral additions make concrete a complex multi-material system and the crossed compatibility becomes a key issue in achieving good results. It cannot be overemphasised that chemical admixtures should be verified jointly with other concrete constituents. A new superplasticizer (prototype under development by SIKA which feasibility has been proven on lab) was used on real scale trials. This new prototype presents a high potential for controlling water demand of the mix. Although relatively high cement content and mineral additions were used, water was kept reasonably low thus allowing for low water/binder ratios (0.38) to be achieved. Slump-loss was negligible during 1.5 hours and thus, cement used and the superplasticizer are compatible.

The fast-setting behaviour and the low reduction of shotcrete  $f_c$  as compared to basic concrete  $f_c$  confirm the very good performance of this product not available on market yet as well as the possibilities of the PBA as a way of ensuring quality while encouraging *innovation*.

### 3.5 Mix efficiency

Among the innovative proposals presented in this paper, it is worth to mention the definition of “overall efficiency” (OE) of shotcrete, which can be defined as the ratio between the compressive strength of the shotcrete samples (panel cores of projected concrete) and their basic 30x15 cm concrete samples (no projected concrete). This efficiency index is very important because it can be used to compare different mixes. Overall efficiency value represents the joint effect of constituents, mix design and execution. It cannot be overemphasised that the overall efficiency for the shotcrete mix tested averaged more than 0.85 (Fig. 3) and, for mixes SSf and SSc, it reached 0.92.

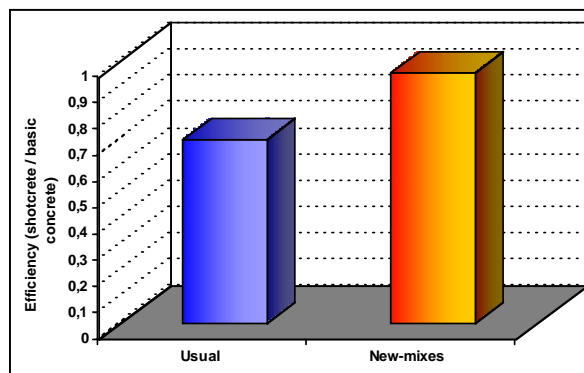


Fig. 4 Overall efficiency of new shotcrete mixes

#### 4. CONCLUSIONS

From the results shown above, the following conclusions can be stated:

1. Performance-based approach can be successfully applied to the assessment of shotcrete constituents as well of shotcrete mixes. Sustainability issues can be easily integrated in this PBA for they can be considered as primary requirements.
2. The use of blended cements, local aggregates and mineral additions contribute to the improvement of the sustainability profile of concrete and shotcrete and its inclusion as part of the mix is only possible if a PBA is applied.
3. Efforts must be forwarded to improve the overall efficiency parameter as better efficiency means less consumption of cement (less CO<sub>2</sub> emissions) per effective MPa in the shotcrete.

#### 5. NOTATIONS

$f_{c28}$	Compressive Strength at 28 days
PBA	Performance Based Approach
PI	Performance Indicator
SRe	Shotcrete <b>R</b> eference mix.
SGr	Shotcrete mix with increasing amount of aggregates
SSf	Shotcrete mix with <b>S</b> ilica <b>f</b> ume
SSc	Shotcrete mix with <b>S</b> ilica <b>c</b> oloidal.

#### 6. ACKNOWLEDGEMENTS

Authors express their acknowledgements to the Spanish Project TUNPRO:GunMat (reference BIA2004-05562-C02-01) and the European Project TUNCONSTRUCT (contract no. IP 011817-2), by its support and to SIKA España SA and AITEMIN for its collaboration on the experimental programme.

#### 7. REFERENCES

- ACI 506R-2000- Guide to Shotcrete.
- Andrade C., Martínez I. (2005), "Methodology for monitoring and assessing performance". *Proceedings of CONREPNET Special Seminar*. Madrid, November 2005
- CIB Proceedings of World Building Congress 2001: "Performance in Product and Practice".
- European Specification of Sprayed concrete Guidelines for Specifiers and Contractors EFNARC (2002).
- Fernández-Luco L., Río O., Rodríguez A. "Performance Based Concrete Design: Comparative Analysis between conventional concrete and shotcrete". Proceeding of fib Symp. Structural Concrete and Time, La Plata. September 2005.
- PrEN 14487-1:2004 Sprayed Concrete – Part 1: Definitions, specifications and conformity.
- Río O. "Partial vision on the future Underground Construction Materials", ECTP, Underground Focus Area Madrid Meeting. [www.ectp.org](http://www.ectp.org) (February 2005).
- Río O., Fernández-Luco L., Castillo A. and Rodríguez A. Is it possible to predict shotcrete actual behaviour? (¿Es posible predecir el comportamiento del hormigón proyectado?). *IngeoPres*, 52. September 2006, Pp. 82-86.

## **EFFECT OF SILICA FUME ON MECHANICAL PROPERTIES OF STRUCTURAL LIGHTWEIGHT CONCRETE CONTAINING SATURATED LECA FINE AGGREGATES**

*Masoud Hosseinpoor*  
*Iran University of Science and Technology*

*Golnaz Alsadat Mirfendereski, Ahmadreza Talebian, Ehsan Fereshte Nezhad, Majid Ebad Sichani, Behrooz Esmaeelkhanian, Morteza Madhkhan*  
*Isfahan University of Technology (IUT)*  
*Postal Address: No.25, Block 113, Taavon 1 street, Sepahanshahr, Isfahan, Iran,*  
*Zipcode:8179947768*

### **SUMMARY**

The objective of this paper is to study the influence of silica fume on development of mechanical properties and water absorption of structural lightweight concrete containing saturated Leca fine aggregates. In the experimental phase of this study, some specimens were made, cast and cured which are: 216 cylindrical specimens (150×300 mm), 48 cube specimens (100×100×100 mm) and 36 cylindrical concrete specimens (50×100 mm). Mix designs include two different 7 days saturated Leca fine aggregates, two different W/C ratios (0.3, 0.4) and three different SF/C ratios (0%, 10% and 15%). The experimental results showed significant influence of increasing SF/C ratio on development tensile and compressive strengths. Also in regression of capillary water absorption line, using logarithmic time axis instead of secondary root time axis gives better regression coefficient.

### **1. INTRODUCTION AND PRELIMINARY STUDY**

Nowadays LWAC is used in almost all over the world as a beneficial construction material. For decreasing the dead load of structures, it is recommended that LWAC is used in load carrying member instead of using concrete with normal density, but at first it is necessary to increase the mechanical properties and durability of such concrete to that of the concrete with normal density or more than it. Water absorption as an index of durability should also be noticed. It can be assessed in two fields. Volumetric water absorption indicates permeability, especially in structures which are exposed to water (i.e. piles of retaining walls). Another criterion for determining concrete permeability is the capillary water absorption, and it can be defined as the value of water absorbed by unsaturated concrete due to capillary action and has direct relationship with voids of concrete. Capillary water absorption properly indicates the durability of concrete, particularly in structures which are not exposed to the water pressure (Emerson, 1990).

The reason that causes weakness in concrete should be found in internal structure of LWAC. Low strength of LWA as a result of porosity leads to decrease in strength of the produced LWAC. In order to solve this problem, it is recommended that: using LWA with lower external porosity, using appropriate LWA grading according to the logical continuity with the size of normal density aggregates, using admixtures and pozzolan and finally propound alternative (solution) to solve the problem of water absorption of LWA from fresh concrete paste. Since Leca (light weight expanded clay aggregates) has low external porosity so in this

paper Leca is used as a part of fine aggregates in order to solve the two problems above. To realize the effect of saturating Leca aggregates on strength and water absorption of concrete, 6 mix designs with  $400 \text{ kg/m}^3$  Leca and  $W/C = 0.4$  were made. In 3 mix designs  $SF/C = 0, 10, 15 \%$  and dry Leca and in other mix designs the same  $SF/C$  ratios but 1 day saturated Leca were used. Finally it was observed that specimens containing saturated Leca have higher strength and lower water absorption. Saturated Leca act as a water reservoir and probably the evacuated water from saturated Leca participates in hydration procedure and cause a more perfect procedure and prevents considerable decrease in relative humidity of cement paste and finally, it would create a transition zone by a better performance. The surface of concrete made from saturated Leca is smoother than concrete made from dry Leca which leads to decrease water absorption.

## 2. PROPERTIES OF MIXING DESIGN COMPONENTS

### 2.1 Properties of aggregates

For making the specimens, river sand (0-5 mm), Leca and also sand (75-150  $\mu\text{m}$ ), have been used as fine aggregates. River sand grading was according to ASTM C33 with density of 2.63 and one day water absorption 0.8%. Leca grading was according to ASTM C331 with density 1.35, abrasion 34.67%, and 7 day water absorption 37.4%. River sand (75-150  $\mu\text{m}$ ) has been used as filler in mixing designs. In this study, crushed gravel (5-12 mm) has been used as coarse aggregates. Gravel grading was according to ASTM C 131-81 with compressive strength 60 MPa, abrasion 22.26%, density 2.67 and one day water absorption 0.6%.

### 2.2 Properties of other components

Portland cement type I has been used in this study. Using the plasticizers is inevitable. Plasticizers are used with the value of 1.5% of the weight of the cementitious materials. The used super plasticizer in this study, in the shape of powder, mixing with the whole water of mix designs, had melamine base.

Tab.1 Physical properties of used silica fume

Density	Specific area ( $\text{m}^2/\text{kg}$ )	Special weight ( $\text{kg}/\text{m}^3$ )	Average size ( $\mu\text{m}$ )	Maximum size ( $\mu\text{m}$ )	Minimum size ( $\mu\text{m}$ )
2.21	14000	173	0.2	0.77	0.03

## 3. MIX DESIGNS

These 12 mix designs are given in Tab.2. Also, in each mix design,  $6 \text{ kg/m}^3$  super plasticizer were used.

Tab.2 Mix designs Components (kg/m<sup>3</sup>)

Mix Design	(w/c)	$\left(\frac{SF}{C}\right)$ (%)	Dry Leca	Cement	Silica fume	Water	7day saturated Leca	Coarse aggregate (dry)	Fine aggregate (dry)	
									Sand	Filler
SN1	0.3	0	350	400	0	120	464.2	125	525	110
SN2	0.3	10	350	360	40	120	464.2	125	525	110
SN3	0.3	15	350	340	60	120	464.2	125	525	110
SN4	0.4	0	350	400	0	160	464.2	125	525	110
SN5	0.4	10	350	360	40	160	464.2	125	525	110
SN6	0.4	15	350	340	60	160	464.2	125	525	110
SN7	0.3	0	300	400	0	120	397.88	150	650	120
SN8	0.3	10	300	360	40	120	397.88	150	650	120
SN9	0.3	15	300	340	60	120	397.88	150	650	120
SN10	0.4	0	300	400	0	160	397.88	150	650	120
SN11	0.4	10	300	360	40	160	397.88	150	650	120
SN12	0.4	15	300	340	60	160	397.88	150	650	120

#### 4. LABORATORY MEASUREMENTS

In order to measure the compressive strength, cylindrical specimens 150 mm × 300 mm were used and to measure the tensile strength, cylindrical specimens 150 mm × 300mm were used according to Brazilian method. In order to measure the volumetric water absorption, cubic specimens 100×100×100 (mm<sup>3</sup>) according to ASTM C642-97 were used. After 28 days of curing the specimens were put in oven for 24 hours in temperature 110 °C and to reach the air dried condition, they were put in temperature and moisture of the laboratory. For testing, the specimens were submerged and their masses were measured each 10, 30, 60 and 120 min and also 1 day, 2 days, 7 days and 10 days after drying the surface moisture.

In capillary water absorption test, preparation conditions of specimens were the same as that in water absorption test. To measure the height of capillary water absorption, the specimens 100 mm×50 mm, according to RILEM (1994), were put in water in a way that only 10 mm of their height were in the water. After 3 and 6 hours and also 1 day, 2 days, 7 days and 10 days and after drying their surface moisture, the mass of specimens were measured to determine the height of capillary water absorption.

#### 5. EXPERIMENTAL RESULTS

##### 5.1 Mechanical Properties

The test results are shown in Tab. 3 As it's shown in the Tab. 3, specific weight of 28 days dried concrete specimens is less than 1850 (kg/m<sup>3</sup>) and more than 1440 (kg/m<sup>3</sup>), and 28 days compressive strength of specimens is more than 17.3 MPa. Therefore, all the specimens in this study have the specifications of the structural light weight aggregate concrete noticed in (ACI, 1987). According to Tab. 3 the 28 days compressive and tensile strengths increase with increment of the percentage of silica fume. The above procedure is shown for compressive and tensile strengths in Fig. 1 and Fig. 2, respectively. According to Fig. 3, there is an appropriate correlation between the tensile and compressive strength in most of the specimens. In the specimens with the amount of Leca 350 kg/m<sup>3</sup>, R<sup>2</sup> is equal to 0.936 so this correlation is more suitable. Using 15% of silica fume in specimens, results in 70% average

increase in 28 days compressive strength. Reduction in W/C ratio in the specimens containing 15% of silica fume results in 21% average increase in compressive strength. Since silica fume has a greater effect on increasing the strength, its application is more preferred in comparison with reduction of W/C ratio. Weigler found out in his studies that the tensile/compressive strength ratio changes between 5% and 15% (Weigler, Karl, 1972). In this study, this ratio was between 8% and 13%.

Tab. 3 Mechanical properties for different mixes

Mix title	Wet density (kg/m <sup>3</sup> )	Dry density (kg/m <sup>3</sup> )	Compressive strength (MPa)			Tensile strength (MPa)		
			7 day	14 day	28 day	7 day	14 day	28day
SN1	1745.33	1580.6	13.27	14.57	18.37	1.71	1.89	2.1
SN2	1747.01	1620.42	25.54	28.64	30.37	2.14	2.28	2.65
SN3	1729.72	1666.42	25.98	29.81	32.48	2.23	2.62	2.82
SN4	1781.7	1641.38	9.77	13.27	14.60	1.57	1.65	1.97
SN5	1808.42	1721.96	19.37	20.93	22.43	1.83	2.21	2.41
SN6	1831.89	1725.84	20.15	22.70	26.20	1.87	2.40	2.69
SN7	1892.46	1819.95	23.2	25.70	29.92	2.54	2.78	3.29
SN8	1943.6	1857.25	30.42	37.92	39.69	2.61	2.85	3.66
SN9	1924.42	1864.17	35.03	37.97	39.86	3.22	3.59	3.83
SN10	1902.52	1792.7	12.32	13.99	19.37	1.89	2.28	2.73
SN11	1907.45	1816.38	22.54	25.43	29.53	2.41	2.65	3.04
SN12	1933.54	1860.19	26.98	29.92	33.59	2.43	2.66	3.18

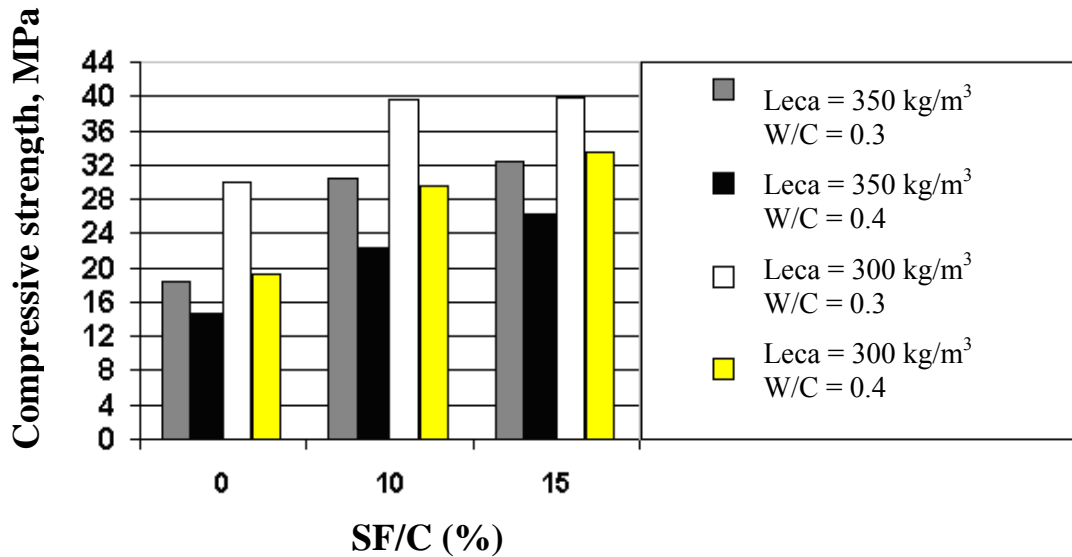


Fig. 1 28 day compressive strength to silica fume's percentage

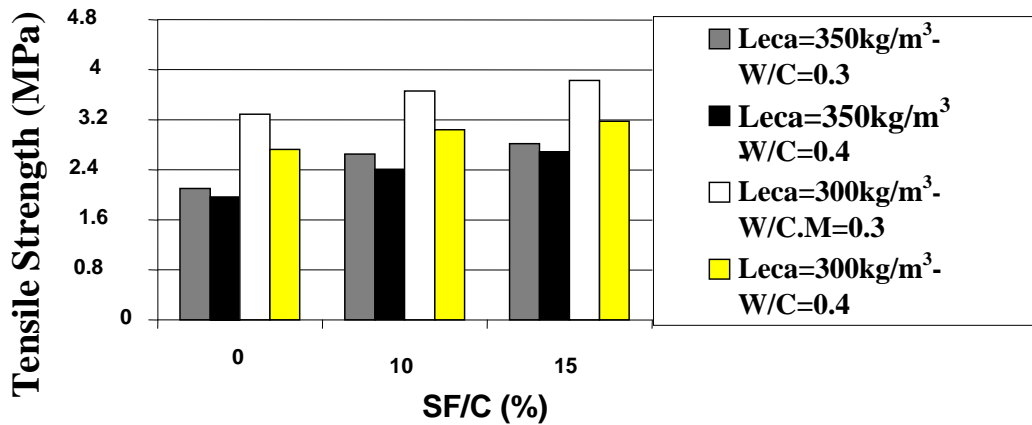


Fig. 2 28 day tensile strength to silica fume's percentage

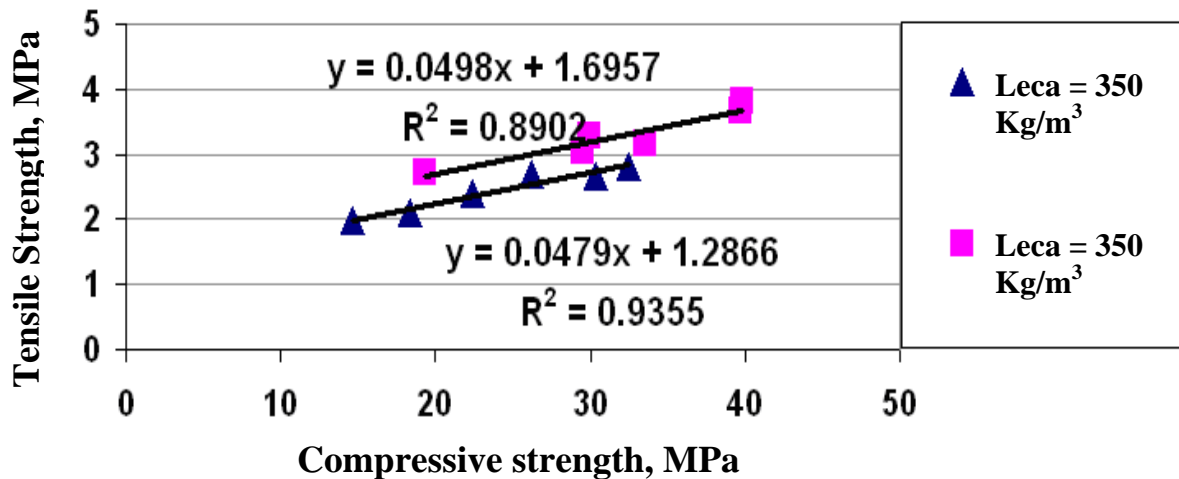


Fig. 3 Tensile strength to compressive strength (linear estimate)

## 5.2 Water absorption:

a) The results of volumetric absorption will be defined as follow:

$$A = \frac{V_w}{V} \times 100\% \quad (1)$$

where,  $V_w$  Is amount of absorbed water in ml(gr), and  $V$  is the volume of each specimen, which is equal to 1000 ml for all specimens. According to Fig. 4, the minimum volumetric water absorption belongs to SN2 and the maximum volumetric water absorption belongs to SN3. According to Fig. 5, it is concluded that the amount of 10% silica fume gives the minimum water absorption.

b) Capillary water absorption is determined by the following expression:



$$i = \frac{m}{\pi R^2} \quad (2)$$

where,  $i$  is height of capillary absorption in cm,  $m$  is the amount of absorbed water in gr, and  $R$  is the radius of specimen in cm. According to expression (3) the functions like  $i = f(t)$  is taken and two equations are expressed:

$$i = C + S\sqrt{t} \quad (3), \quad i = C' + S' \ln t \quad (4)$$

where,  $i$  is capillary water absorption in cm,  $C$  and  $C'$  are capillary water absorption constants in cm,  $S$  and  $S'$  are capillary water absorption coefficients in  $\text{cm/hr}^{0.5}$  and  $\text{cm/hr}$ , respectively.

According to correlation coefficients in Tab. 4, it is concluded that expression (4) is more accurate than the expression (3). The values of  $C$ ,  $C'$ ,  $S$  and  $S'$  are given in Tab. 4. Also according to the same table, minimum capillary absorption (with little difference) belongs to SN2 and SN5. On the other hand, SN1 with  $\text{SF/C} = 0\%$ , has maximum capillary water absorption. Also SN10 and SN12 have the minimum capillary water absorption coefficients. Tab.4 Results of capillary water absorption

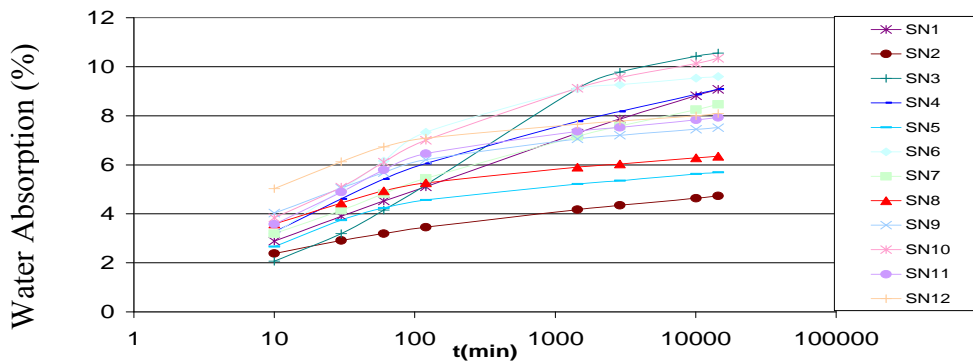


Fig.4 Volumetric water absorption versus time diagram

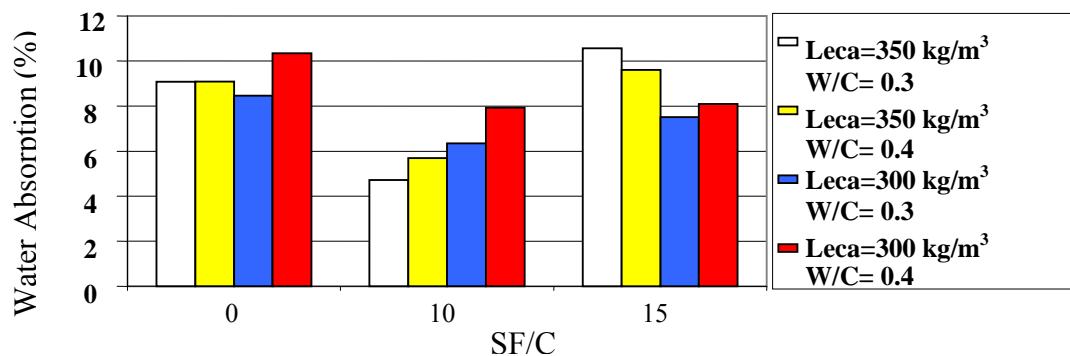


Fig. 5 Volumetric water absorption versus silica fume percentage

## 6. CONCLUSIONS

1. Compressive and tensile strengths of concrete would increase with increasing of silica fume; hence specimens with 15% silica fume have the highest tensile and compressive strengths. The concrete made by 15% silica fume has a higher density in comparison with

others, but it is about 2% or 3% and it is a very low quantity in comparison with the 70% increase in strength. So using silica fume is economically reasonable.

2. In most of the specimens, the lowest water absorption is related to the specimens with  $W/C = 0.3$ . Although this amount seems approximately low but consistency of the concrete in all the specimens is in a way that makes it possible to use this concrete as the structural one (the slump of different specimens changes between 3 cm to 10 cm).
3. The optimum value of silica fume to achieve the minimum water absorption, is suggested about 10%.
4. Expression  $i = C' + S' \ln t$  gives an acceptable approximate of capillary water absorption height, for concrete made of using Leca.

## 7. REFERENCES

ACI 213 (1987), "Guide for Structural Lightweight Aggregate Concrete", *ACI R-87*, 27 p.

Emerson, M (1990), "Mechanisms of Water Absorption by Concrete", *Transport and Road Research Laboratory*; U.K.

RILEM CP11.2-TC14\_CPC (1994), "Absorption of Water by Concrete by Capillarity ", *E and FN SPON, Chapman and Hall*.

Weigler, H., Karl, S (1972), „Stahlleichtbeton“, *Bauverlag GmbH*, Berlin.



## **INCREASE OF SAFETY OF CONCRETE PAVEMENTS BRIGHT CONCRETE PAVEMENTS WITH DARK AGGREGATES**

*Stefan KRISPEL*

*Research Institute of the Austrian Cement Association, Vienna, Austria*

*[krispel@voezfi.at](mailto:krispel@voezfi.at)*

### **SUMMARY**

The brightness of concrete pavements is, next to a multitude further, an essential advantage of this method of building vis-à-vis bituminous pavements, because brighter street surfaces affect positively the safety of the road users. Bright concrete surfaces provide above all an increase of safety in rain and in darkness (especially in tunnels).

Furthermore, the difference in brightness of both furthest common street pavements – concrete and asphalt respectively - is not only special for the road users, but rather also for the general public an essential factor, because by the efficient utilization of light surfaces energy costs can be saved and accordingly the expenses of the state, which is in the predominant majority of the cases the operator and/or upholder of infrastructure, can be minimized. This represents in times of costs consciousness and cuts in spending a significant argument.

The positive effect of bright concrete surfaces could be reached now also for the use of dark aggregates by optimization of the concrete mix and due to this a pleasing and economic solution for all participants could be found.

### **1. INTRODUCTION**

Since the beginning of the 90ies exposed aggregate concrete surfaces are used in Austria for the high-level road networks (Sommer, 1995). Main goal was not the increase of the safety of the traffic participants, because all until this time produced concrete pavements have fulfilled the requests especially the requests on skid resistance. The aim was to find a solution of the problem of generation of noise. With this development, which is based on a multitude of international studies (e.g. Descornet & Sandberg, 1980), it is possible to reduce noise emissions at the source in the interface between tyre and surface, to improve skid resistance capacities and to create concrete roads with high durability.

#### **1.1 Exposed Aggregate Concrete Technology**

For the application of washed concrete technology comprehensive adaptations and/or new developments both for the production process of the concrete surface itself and the concrete to be used were necessary.

At the beginning the concrete topping was built with a maximum aggregate size of 8 mm and a fraction as greatly as possible of polish resistant and wear resistant grit of 4/8 mm. The thickness of the concrete topping should be about 3 to 4 cm. After the longitudinal smoothing a contact retarder should be sprayed on the concrete surface and to avoid loss of humidity a plastic film or a specific curing compound should be used. On the following day the fine mortar on and between the coarse particles have to be brushed away.

Due to this treatment the surface has a median point distance of 9 to 10 mm and a texture depth of 0.8 to 0.9 mm. Due to the lack of macro texture, which would cause a deformation and as a result of this a drumming of tires, the rolling noise is reduced to a minimum. On the other hand there is enough space under the footprint of the tires so that the air could exhaust at a low noise level. Texture depths noticeable under 0.8 mm affecting the noise reduction. Noticeably larger depths are not appropriate to reduce the roll noise of passenger cars, but combined with certain concrete mix design, they provide higher wear resistance of the surface. It has been shown that a maximum aggregate size of 8 mm is an appropriate solution for mixed traffic loads (passenger cars and heavy goods vehicle). For sections of streets which are not noise sensitive but which need according to their high traffic concentrations excellent skid resistance exposed aggregate technique with a maximum aggregate size of 11 mm is been used. As a result of this the texture depth is larger but the skid resistance in wet conditions is better. A negligibly higher rolling noise level is accepted for that application.

This technology assumes the fresh to fresh concrete placing which is used in Austria in any case. The fine-grained top concrete requires adaptations for the slip-form pavers (especially for position, amplitude and frequency of the vibrator). The use of specific contact retarders is necessary to create uniform surfaces. These retarders should be independent of temperature to provide enough time to brush the concrete surface. In addition to this it is necessary to protect the concrete immediately after spraying the retarder against water loss. This protection should be very effective e.g. insulation coefficient > 90 %. In some cases the use of plastic films is unfavourable especially if the lane next to the road works is under traffic. Due to that specific curing compounds were developed which can be applied on the retarder respectively which contain the retarder. These curing compounds have enough resistance against rain and steps after a few hours (Sommer, 1995).

## 1.2 Requirements according to the Austrian standard RVS 8S.06.32

Requirements for aggregates are represented in Tab. 1.

Tab. 1 Requirements for aggregates used for washed concrete pavements

Grading 4/8 mm for top concrete (max. aggregate size 8 mm) resp. Grading 4/11 mm for top concrete (max. aggregate size 11 mm) with exposed aggregate technique	Crushed Grading (KK) LA-value (acc. ÖNORM B 3128) $\leq 19$ Coefficient of friction after polishing (acc. RVS 11.062) PSV $\geq 50$ Content of poor formed particles (L:D > 3:1) $\leq 10\%$ Mellowed particles $\leq 5\%$ Oversize $\leq 5\%$
Concrete topping max. aggregate size 8 mm resp. max. aggregate size 11 mm with exposed aggregate technique	Grading 0/1 resp. 0/2 mm and crushed grading (KK) 4/8 mm or 4/11 mm $\geq 68$ M-% resp. 68 M-% for road concrete with superplasticising agent
Subconcrete	Grading range AC32

Requirements for surfaces of concrete pavements are represented in table 2.

Tab. 2 Requirements for surfaces of concrete pavements

	Conventional concrete	Washed concrete	
		max. aggregate size 8 mm	max. aggregate size 11 mm
Depth of roughness	$\geq 0,4$ mm	0.8 – 1.0 mm	1.0 – 1.3 mm
Number of profile points	-	Recommended limit: 60/25 cm <sup>2</sup>	Recommended limit: 45/25 cm <sup>2</sup>
Rolling noise in dB(A)	-	$\leq 101$ at a speed of 100 km/h resp. $\leq 90$ at 50 km/h	$\leq 102$ at a speed of 100 km/h

## 2. ADVANTAGES OF BRIGHTER CONCRETE PAVEMENTS

### 2.1 Increase of safety

The increase of safety is an essential advantage of concrete pavements both in tunnels and in rural or urban areas. Above all two scopes can be positively influenced by using concrete. This is, beside the increase of fire safety – what matters basically for tunnel constructions, the improvement of sight by bright concrete surfaces respectively the enhancement of the subjective safety of the road users.

### 2.2 Brightness

The brightness of concrete roadways also affects the safety of the road user positively. The main factor of influence to achieve a pleasing brightness is beside the used aggregates the different matrix of both products. If dark binders e.g. bitumen are used, the brightness of the construction material cannot be influenced. However by the use of a bright binder e.g. cement the brightness can be positively influenced. The difference is shown exemplarily in Fig. 1. Fig. 2 shows the difference of the matrix of both construction materials very clearly.



Fig. 1 Difference between bright concrete pavement respectively bright guide wall and dark bituminous surface



Fig. 2 Difference of the matrix by using homogenous aggregates

### Bright concrete pavements with dark aggregates

Bright aggregates guarantee a high level in terms of brightness for more than 40 years. Recently more and more dark aggregates have been used for washed concrete pavements. The Research Institute of the Austrian Cement Industry (VÖZFI) has carried out some research to achieve also with dark aggregates comparable results. Fig. 3 shows washed concrete surfaces with bright aggregate and dark aggregate. The difference in brightness is clearly noticeable. The concrete matrix with the dark aggregate is in fact not as light as the matrix with the bright aggregate but compared with asphalt it is significant lighter.

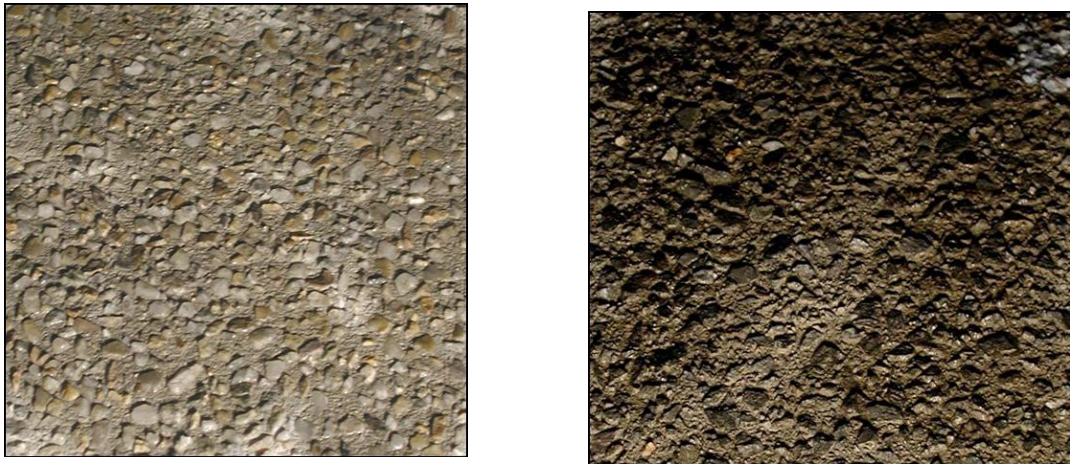


Fig. 3 Exposed aggregate concrete surface with bright aggregate (left) and exposed aggregate concrete surface with dark aggregate (right)

If a concrete pavement is produced with dark aggregates, cement and a certain pigment it is possible to reach the approved level in terms of brightness of bright aggregates. Tests with small amounts of titanium (II)oxide which was added to the concrete mix showed excellent results. The difference which is a result of the use of titanium(II)oxide is shown in Fig. 4.

If a concrete pavement produced with a bright aggregate is compared with a concrete pavement which has been produced with dark aggregates and titanium (II) oxide than it is clearly visible that it is possible to meet the approved qualities of bright concrete pavements with this alternative production method (Fig. 5).

Comparable with other areas of construction industry e. g. plaster it is possible to create different degrees of brightness of the concrete pavements. This would be useful for tender offers.

Advantages of this type of application:

- improvement of the safety aspects. In addition to an increase (enlargement) of the sight distance e.g. in tunnels the subjective safety will be enhanced (e.g. pedestrian crossings or footpaths in the night).





Fig. 4 Exposed aggregate concrete surfaces with dark aggregate (left) and exposed aggregate concrete surface with dark aggregate and titanium (II) oxide (right)



Fig. 5 Exposed aggregate concrete surface with bright aggregate (left) and exposed aggregate concrete surface with dark aggregate and titanium(II)oxide (right)

- skid resistance quality remains undisturbed which is not the case if coatings will be applied later. Another disadvantage of such coatings is the fact that they have to be renewed in certain intervals.
- the procedure of production respectively the processing is thinkable easy. Titanium(II)oxide will be simply added into the concrete mix.
- an important advantage is the factor of cost. Saving potentials arise due to the fact that if traffic areas have been examined which have to be lightened (e.g. tunnels or urban areas). The costs of lighting can be reduced drastically.



Types of application of this product innovation:

- concrete pavements
- tunnels (both for the concrete pavement and for the tunnel lining)
- urban areas:
  - pedestrian crossings
  - pedestrian zones
  - crossings
  - footpaths.

Generally this product modification can be used in each place in which brightness enforces the safety or the feeling of safety both of the motorised and non-motorised road user.

Important applications are in tunnels. The requirements on brightness in a tunnel are consequently significant higher. Fig. 6 shows a cross section of a tunnel. The given numbers refer to the brightness contribution of each construction element. Brighter pavements are helpful to cut the accident risk especially in cases in which the visual acuity of the driver is notably required (e.g. tunnels).

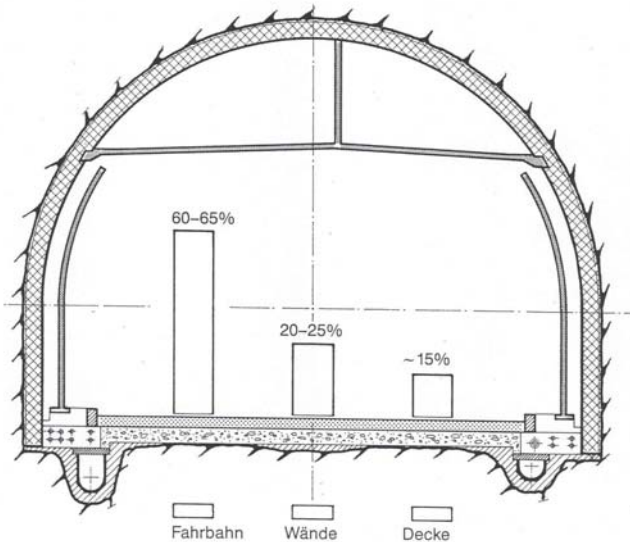


Fig. 6 Schematic cross section of a tunnel – contributions on brightness (Betonstrassen AG, Schweiz)

According to Fig. 6 accounts the contribution of the pavement for 60 – 65 %, the contribution of the walls accounts for 20 – 25 % and the contribution of the ceiling accounts for 15 % to the total brightness. Due to the fact that tunnels have to be lighted for 24 hours it is obvious that with the use of brighter concrete pavements (concrete construction elements) a significant savings potential regarding energy costs can be availed.

An important advantage of bright concrete pavements is the cost saving effect due to the reduction of the lighting costs. Lighting costs amount approximately 50 % of the environmental costs according to a Swedish survey if the costs of traffic are disregarded (Löfsjögård, 2004). Examinations on the two longest road tunnels in Switzerland were undertaken to determine the effective consumption of electricity for the operating hours and the level of lighting. One tunnel has a concrete pavement (Seelisbergtunnel) and one has a bituminous pavement (Gotthardtunnel). The result of the survey showed that in one year the tunnel to the bituminous pavement consumed 1,000,000 KWh more electricity compared with the tunnel with the concrete pavement (Betonstrassen AG, 1984). This means an energy saving of about 60 %. With this study it has been demonstrated that due to the different light

technological qualities of the coverings, significant effects of energy respectively operation costs of tunnels can be obtained. This reduction of operation costs is now also with dark aggregates by using titanium(II)oxide possible.

According to Swedish studies the saving potential of lighting costs can be demonstrated as follows (Löfsjögard, 2000):

- lighting costs for bituminous pavements have to be evaluated with the factor 1
- lighting costs for bright concrete pavements have to be evaluated with the factor 0.75
- the saving potential is accordingly 25 %.

In addition to the reduction of costs concrete can generate an air purifying effect. An admixture of TiO<sub>2</sub> to concrete elements or concrete coverings generates a purification of the air. The best effect can be achieved if the TiO<sub>2</sub> is close to the surface. For the purification process it is necessary that the concrete is exposed to ultraviolet rays which are included in the daylight.

### 2.3 Costs

To reach the effect of brighter concrete surfaces with the use of dark aggregates an amount of titanium(II)oxide of 2 M-% of the cement has to be added to the concrete mix design. The costs are approximately Euro 6 -7 per m<sup>3</sup> concrete. If we assume that the concrete topping has an thickness of about 4 cm than the costs will amount Euro 0.24 per m<sup>2</sup> concrete surface.

## 3. CONCLUSIONS

The possibility to produce bright concrete pavements respectively bright concrete construction elements even by the use of dark aggregates provides an improvement of the product concrete in several items. An increase of safety, both of traffic areas in tunnels and outside tunnels, can be reached with this modification of the concrete mix. In addition to the increase of safety the reduction of life-cycle-costs is the main advantage of this modification. Another advantage is that the application is thinkable simple.

## 4. REFERENCES

- Betonstrassen AG (1984) "Vergleichende Untersuchung der Betriebskosten für die Beleuchtung in den Straßentunnels St. Gotthard und Seelisberg", *Bericht* Nr. 5247/B Oktober 1984. Betonstrassen AG, Wildegg
- Descornet, G.; Sandberg, U. (1980) "Road Surface Influence on Tire/Road Noise", International Conference on Noise Control, Miami, *Proceedings*
- HUVSTIG, A. (2005), "Swedish experiences from LCC-calculations for pavements". In: International Conference 2005", Concrete pavements from a macroeconomic standpoint", Vienna, *Proceedings*
- Löfsjögard, M. (2004), "Optimisation Model for functional properties of concrete roads". *Proceedings*, 9<sup>th</sup> International Symposium on Concrete Roads, Istanbul, April 3-7, 2004, 10 pp.
- Löfsjögard, M. (2000), "Functional Properties of Concrete Roads – General Interrelationships and Studies on Pavement Brightness and Sawcutting". *Royal Institute of Technology*, Department of Structural Engineering. Stockholm

Sommer, H. (1995), "Optimierung der lärmindernden Waschbetonoberfläche".  
Bundesministerium für wirtschaftliche Angelegenheiten, *Schriftenreihe  
Straßenforschung*, Heft Nr. 447. Wien

## MICROSTRUCTURE OF CONCRETE WITH MICRO-FILLERS

*Aleš Frýbort, Aleš Kratochvíl*

*Transport Research Centre, Division of Infrastructure and Environment*

*Líšeňská 33a, 636 00 Brno, Czech Republic*

### SUMMARY

This paper describes research of time-dependent changes in the microstructure of self-compacting concrete. The microstructures and differences in void and pore systems of matured self-compacting concrete with commonly used micro-fillers are shown herein. The paper deals with concrete microstructure study using scanning electron microscope (SEM) method. We investigated 40 samples of SCC with varied amount of micro-fillers (fly-ash, slag, silica-fume, fine grinding limestone), two types of fine aggregates and two types of coarse aggregates with polymer-carboxylate superplasticizer. Samples are stored in water for all the time. At the present time we can compare microstructure of sample sets with age within the range from three months to four years.

### 1. INTRODUCTION

Recent concrete developments indicate applications of many types and volumes of admixtures and additions. They are added to concrete to obtain special properties of fresh concrete (e.g. SCC - Self-compacting Concrete) or properties of hardened concrete (HPC - Hi-performance Concrete, LWAC - Light-Weight Aggregate Concrete). Usage of 3 or more different types of additions (fly-ash, slag, silica-fume, fine grounded limestone or additives (plasticizers, accelerators, stabilizers, air-entered agents, etc.) is common.

This paper describes part of a work realized as a part of a project called „Long-time changes of concrete microstructure and their properties“.

Structure of hydration products (subsequent recrystallization) rising in concrete microstructure in short time after concrete mixing is well known. Generation of neoformations in cement mortar is never-ending process. The question is how the stuff (concrete or mortar additives and admixtures) influences the concrete and mortar properties in long time period. Mainly if there is some probability that the usage of additives and admixtures or their combinations, in connection to environment activity, can cause changes in concrete structure (e.g. recrystallization) that deteriorate the properties of the concrete and the realized structure.

Additions with their pozzolanic or latent-hydraulic properties enter actively into the concrete hydration process and influence chemical composition of cement mortar and mutual ratio among formed hydration products.

## 2. EXPERIMENT

For an experiment 40 different types of SCC mixtures of various types with different amount of used admixtures or for different construction purpose were designed. For this paper we bring four mixtures marked F1, F3, F4, F13 with maximum amount of each type of micro-filler (stone-dust, fly-ash, limestone and slag) we used. Complete composition of selected concrete mixtures is presented in Tab. 1.

Tab. 1 Composition of select self-compacting concrete mixtures

Concrete mixture prescriptions		F1 (stone-dust)	F3 (fly-ash)	F4 (limestone)	F13 (slag)
Cement 42,5 R	kg	400,0	400,0	400,0	400,0
Fine aggregates 0-4 m	kg	830,0	870,0	700,0	760,0
Coarse aggregates 4-8 mm	kg	165,0	230,0	230,0	230,0
Coarse aggregates 8-16mm	kg	582,0	550,0	550,0	550,0
Filler	kg	160,0	160,0	280,0	220,0
Superplasticizer	kg	4,0	4,0	4,0	4,0
Water	kg	190,0	185,0	175,0	???

Specimens (150 mm testing cubes) of this mixture were prepared in February 2003. Specimens were demoulded after 24 hours and deposited to water with room temperature. Specimens of concrete for microscope study were prepared in April 2007. The presented pictures of concrete microstructure are about 4 years old. For SEM specimen preparation we use diamond-charged saw and cut off a small piece on the edge of each cube (Fig. 1).

All concrete specimens with fracture area approximately 5x5 mm and micro-fillers were attached by self-adhesive carbon tape to specimen holder and then coated by golden film. By coating a better image resolution was obtained due to taking of the surface electric charge away (Fig. 2). Used fillers were studied too (Fig. 3).



Fig. 1 Cubes stored in water



Fig. 2 SEM specimen - raw (left) and gold-coated (right)

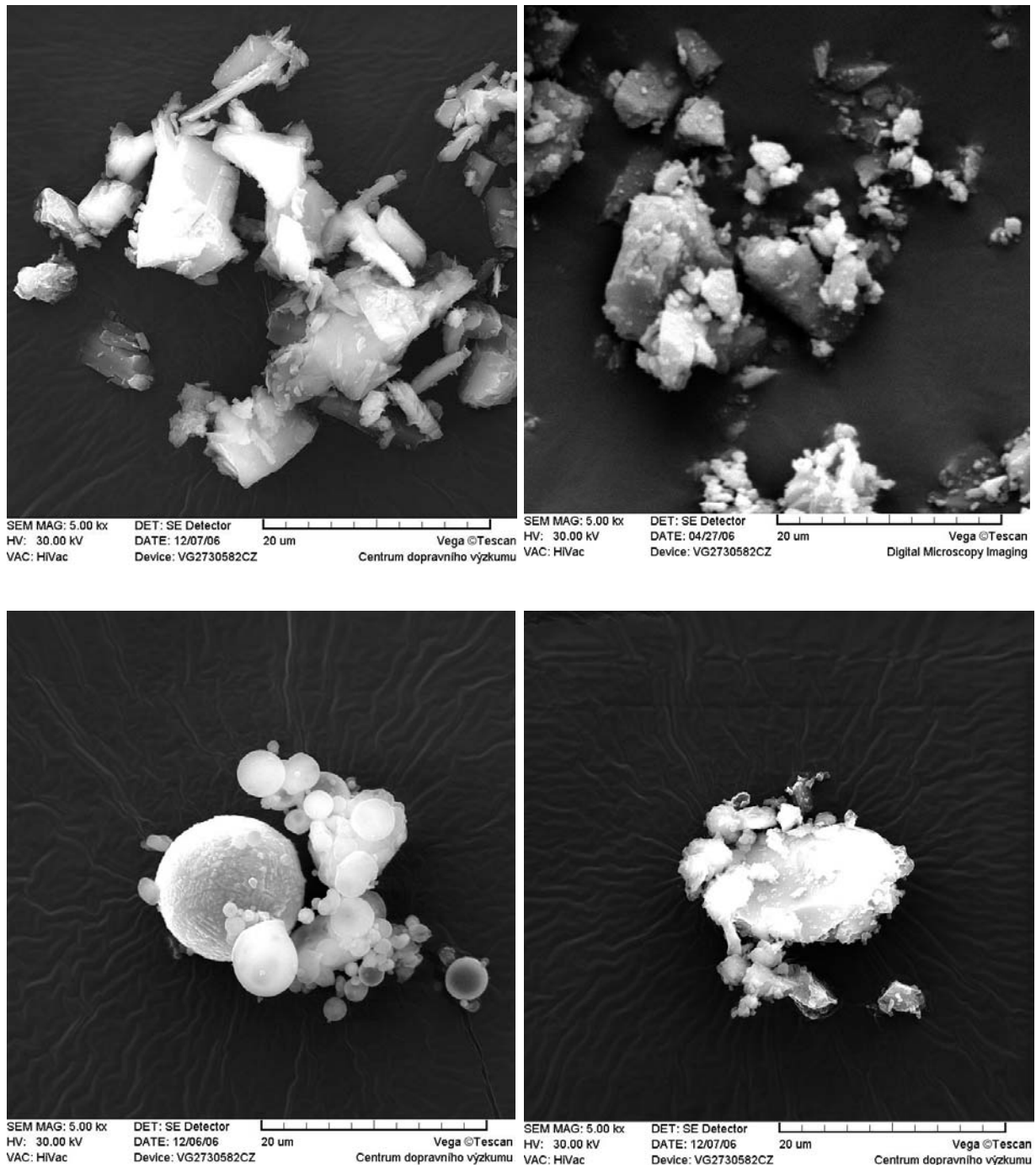


Fig.3 Used micro-fillers: A - Stone-dust, B - Fine ground limestone, C - Fly-ash, D - Slag (Magnification 5 000x)

For all microstructure study we used the Scanning electron microscope (SEM) Tescan Vega II LSU which allows work in high, middle or low vacuum mode.

### 3. CONCRETE MICROSTRUCTURE

There are some voids in concrete microstructure with crystals of ettringite  $\text{Ca}_6\text{Al}_2(\text{OH})_{12}\cdot 24\text{H}_2\text{O}$  and portlandite  $\text{Ca}(\text{OH})_2$ . Crystals of ettringite can form shapes of needles, fibres or fan-shaped agglomerations and crystals of portlandite form shapes of tables or chips in free space of voids (Fig. 4 and Fig. 5).

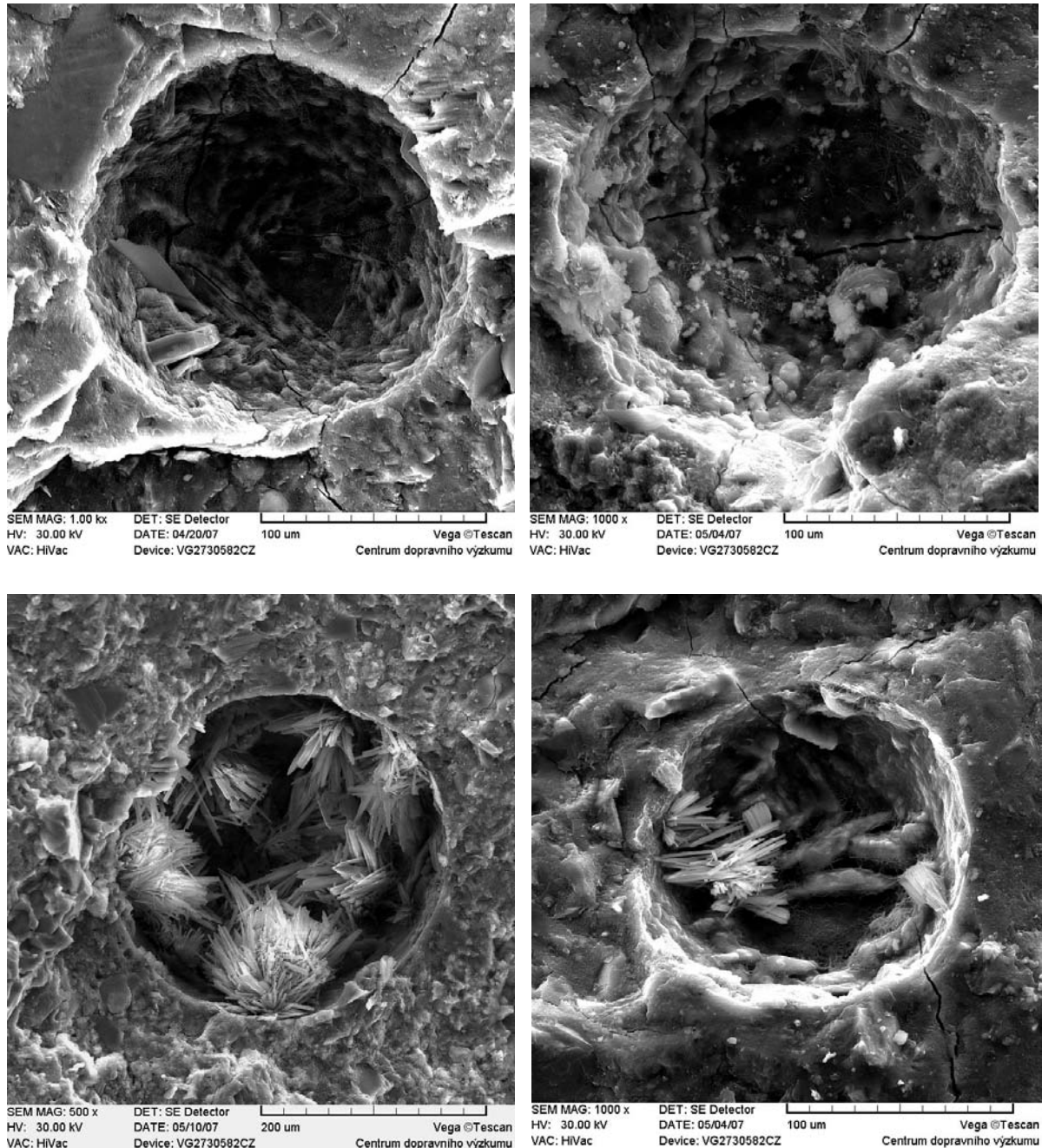


Fig. 4 Voids in concrete matrix – various amount of ettringite and portlandite crystals:

A - F1 (stone-dust), B - F3 (fly-ash), C - F4 (limestone), D – F13 (slag)

If those products of hydration reaction fill all the space of pores it can produce stress leading to crack or damage of the concrete. In this case are voids relatively unfilled, therefore, crystals of ettringite are still harmless for concrete strength.

Low amount of portlandite in concrete matrix provides better sulphate resistance. On the other way portlandite keeps high alkalic pH in concrete, which is principle of steel reinforcement passivation.

Only spherical fly-ash particles can be clearly viewable in concrete matrix (Fig. 6). Others used fillers with variform particles are indefinable in hardened concrete.

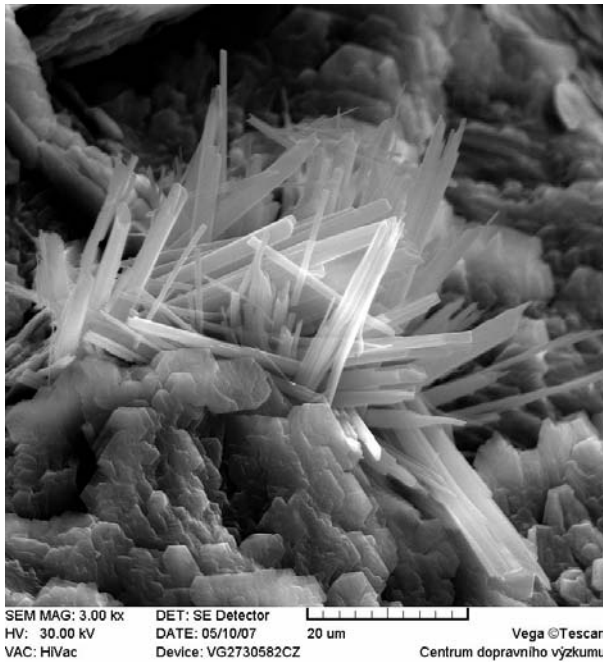


Fig. 5 Detail view of ettringite needles and portlandite tables in void space (mixture F4)

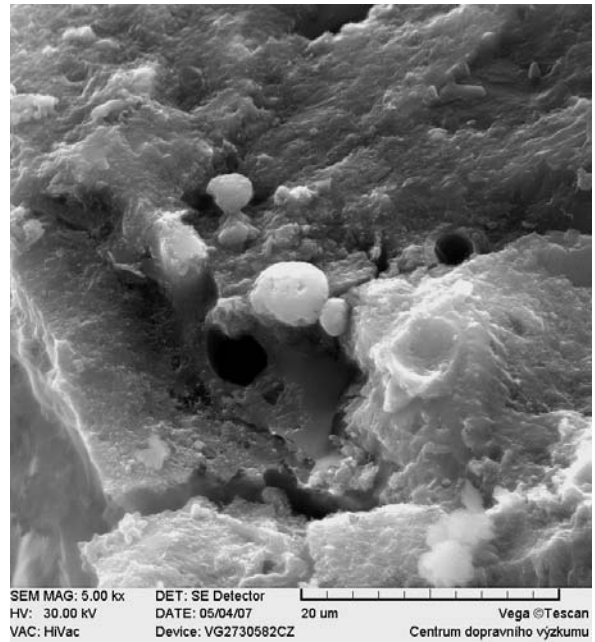


Fig. 6 Fly-ash particles clearly viewable in concrete matrix

#### 4. CONCLUSION

We suppose that microstructure investigation will lead to understanding and obtaining knowledge of relationship between concrete or mortar microstructure and their properties. As the concrete will be maturing the investigation of all specimens will be repeated periodically during solving of the project. It is supposed that different types of matured concrete specimens from existing structures with known concrete mixture composition and environment impact will be taken up and measured.

#### ACKNOWLEDGEMENT

The preparation of the article has been supported by the Ministry of Transport of the Czech Republic under contract No. MD0 4499457501.





## **PETROPHYSICAL CLASSIFICATION OF AGGREGATES FOR CONCRETES**

*Miklós Gálos, László Kárpáti*

*mgalos@freemail.hu, karpati.laci@gmail.com*

*Budapest University of Technology and Economics, Department of Construction Materials and Engineering Geology, H -1521 Budapest*

### **SUMMARY**

In this study we introduce petrophysical test results, which were performed at the Department of Construction Materials and Engineering Geology. Relationships between the different parameters were studied to decide if all of the tests are necessary.

### **1. INTRODUCTION**

Gravel, sand and gravel and sand products have been taken exclusively into consideration as aggregates for concrete for a long time, in the Hungarian practice. These products are available in high quantity and good quality to supply it to the Hungarian construction industry. The occurrences of sand, of sand and gravel and of gravel are originated from eroded territories, where first of all quartz, quartzite, plagioclase, etc., minerals can be found. It means that the minerals, mineral associations with high hardness and resistance are providing the required, expected strength of the aggregates for concrete. The acceptance of that fact has been shown very well in the former Hungarian Standard of Stone Materials, by the product standard MSZ18293 in relationship with sand, gravel with sand, and gravel.

The products were characterized according to the Hungarian Standard MSZ 18293 by the particle size distribution and the qualitative requirements depending on the mud and clay content. Cleanness requirements are depending on the sulfate- and chloride content. Fragmentation is to be characterized by the Los Angeles petrophysical test. The sulfate crystallization tests are required for the qualification of crushed products from gravel only. (Gálos et al, 2006)

European standards in accordance with the requirements of our days are differing from the Hungarian practice. The general product description is reflected in the former Hungarian standardization system by the standards “Sand, sand and gravel, and gravel”, and “Crushed aggregates”, which have been prepared with a philosophy that the suitable product should be selected from different crushed stone types.

The sand, sand and gravel, and gravel products’ characteristics are depending on the rock’s properties and on the production technology. The products’ characteristics in a concrete structure have interaction with the other materials and with the technology of construction. Consequently, the effect of the rock properties can be visible in the completed structure during its use.

## 2. PETROPHYSICAL PROPERTIES IN QUALIFICATION

The determination of the aggregate strength properties among the petrophysical properties has an accentuated role in the qualification practice. It is similar to the testing method of the uniaxial compressive strength, which has been used to the compressive strength's determination both in the Hungarian and the international qualification practice. We have the experience in the case of aggregates, that the first question is: how much is its "Los-value", which means, how high its resistance to fragmentation, measured by Los Angeles testing method.

The stones due to their natural genesis, have several different properties. The stone's properties are depending on the procedure of the rock genesis, the composition of the minerals, the binding strength between the components and the subsequent effects on the rock. In summary, it is depending on the petrological properties. The petrological properties can be studied with a descriptive way only, but we need those characteristics, which can be evaluated based on laboratory test results.

Unfortunately the material properties can't be described by a single value. Therefore, concrete technology uses several types of test methods for aggregates, in order to supplement the name and places of occurrences of the stone, which show petrological properties only. According to the test results, the aggregate types can be compared with each another and the determined limit values in the requirements. Besides the petrophysical properties, further tests might be necessary to determine the geometrical size properties of the aggregate products, as well as its contamination and ability to chemical reactions.

The knowledge of petrological, petrophysical, rock mechanical, surface properties, etc. is necessary to the application of the aggregate products. These products should be provided with a quality certification, which is containing its properties, and which guarantees its quality.

Among the quality requirements, the most important ones are the petrophysical requirements, by which the strength and durability properties of the aggregates can be qualified:

- Strength properties by the tests of resistance to fragmentation (Los Angeles testing method) and resistance to wear (Micro-Deval testing method).
- Durability properties by the tests of the sulfate crystallization and freezing.
- Surface properties by the test of resistance to polishing.

## 3. PETROPHYSICAL PROPERTIES OF AGGREGATES

In practice there are two types of testing methods of the aggregate strength properties. One is the testing with a revolving drum and second is the testing with mortar (i.e. concrete). Their common idea is that we are measuring the occurred structural change during the tests due to the applied mechanical work on the material. In the Hungarian qualification practice the procedures with the revolving drum are well known. The tests with mortars such as Hummel-crushing, Stübel-test (with falling weight), etc. Are not in the every day qualification practice.

The Los Angeles test (according to the harmonised European Standard MSZ EN 1097-2: 2000) should be performed in a revolving drum with a diameter of 711 mm, (*Fig. 1*), where the stress is ensured by steel balls with a diameter of 45-49 mm falling in the revolving drum from the partition plate to the stone material, and the friction on the inside surface of the

drum. The test is an impact abrasion test. The rotation speed of the drum is of 31-33 revolutions pro minute.

The European Standard gives the test procedure parameters to the examination of an aggregate with the limit of the particle size of 10-14 mm. 11 pieces of steel balls should be added to the aggregate specimen with the size of 10/14 mm, and with the weight of  $5000 \pm 5$  grams. The total weight of the series of the balls of 11 pieces should be of 4690 – 4860 grams. The particle size distribution of the test specimen should be in accordance with the following requirements:

- a) 60-70% should pass the examination sieve of 12.5 mm, or
- b) It should pass the test sieve of 11.2 mm.

The balls should be put first into the clean test drum, and then the test specimens. The drum should be closed and turned 500-times in the test unit. Finishing the test, the materials located in the drum should be taken out without any rest. The aggregate should be sieved with the test sieve of 1.6 mm and washed by a clean water-jet. The rest material should be completely dried, and then after having cooled off, the weight should be determined. The value of the Los Angeles fragmentation can be calculated with the following formula:

$$LA = \frac{5000 - m}{50} \quad (1)$$

where  $LA$  is the Los Angeles-coefficient (m%) and  $m$  the weight (g) of the rest material on the sieve of 1.6 mm (Gálos et. al, 2002).

The testing method micro-Deval (according to the harmonised European Standard MSZ EN 1097-1:1998) determines the wear resistance of aggregates. The micro-Deval test should be performed in revolving drums with a horizontal axis, with the diameter of  $154 \pm 1$  mm, with the length of  $200 \pm 1$  mm (*Fig. 1*), by abrasive filling of steel balls with the diameter of  $10 \pm 0.5$  mm. The friction between aggregate specimen, the abrasive filling and the inside surface of the drums are wearing the specimen. The revolution speed of the drums is  $100 \pm 5$  rpm. The micro-Deval test can be performed either by dry or wet procedures. At the procedure with water a given quantity of water ( $2.5 \pm 0.05$  litres) should be used. The rock texture will be better stressed by the effect of the water. The examination procedure regulations give the quantity of the specimen, the weight of the abrasive filling and the total rpm to the particle size of the examined specimen. The European Standard gives the test procedure parameters to the examination of aggregates with the particle sizes of 10/14 mm. The wearing of micro-Deval test should be calculated for each individual specimen, rounded to one tenth with the following formula:

$$M_{DE} = \frac{500 - m}{5} \quad (2)$$

where  $M_{DE}$  is the micro-Deval coefficient (m%) in wet condition, and  $m$  is the weight (g) of the material remained on the sieve of 1.6 mm (Emszt, 2006).

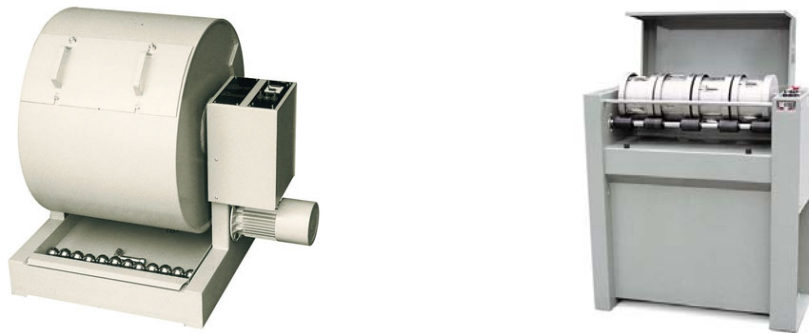


Fig. 1 Los Angeles (left) and micro-Deval (right) test equipment

#### 4. RESULTS

We can discuss the petrophysical properties of the crushed aggregates and their strengths in the visual order of the general three-phase rock model, and analyze the behavior of the rock materials. The model elements of the three-phase rock model are the followings: solid rock components, rock formatting minerals and further solid components; pores, like rock formatting components, with pore filling liquids and with gaseous materials; bindings between the solid rock formatting components (Gálos et. al 2002).

The Standard MSZ EN 206-1:2002 NAD (National Standardization Documentation) is regulating exclusively the aggregates' petrophysical classification to concretes, which have abrasion loads. There is to be checked that the concrete's aggregates should be in the petrophysical group of "Kf-B" at least in the environmental class of XK2(H), and in the petrophysical group of "Kf-A" in the XK3(H) environmental class. Furthermore, the concrete should be made of crushed aggregates of basalt or andesite (MSZ 18291:1978, ÚT 2-3.601:1998). As it can be seen in Fig. 2, there can be found in Hungary carbonated rocks (limestones, dolomites), which belong to the petrophysical class of „Kf-A”, and which are in accordance with the prescription of the environment class of XK3.

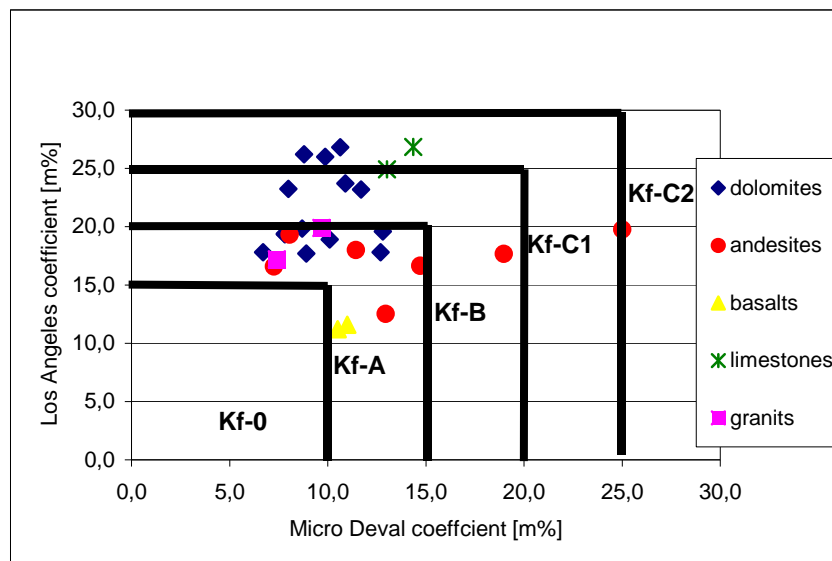


Fig. 2 Weight loss of Los Angeles and micro-Deval tests (with petrophysical categories)

No regression relationship between the Los Angeles factor and the micro-Deval factor is indicated, which is used to the determination of the resistance against fragmentation. Fig. 2

demonstrates that the two examinations ensure the qualification of both different rock properties. The water-type micro-Deval test evaluates the changes in the structure of the rock material as well, and the Los Angeles value qualifies the effect of the mechanical fragmentation.

To the evaluation of the freezing resistance of aggregates, the crystallizing with magnesium sulfate according to MSZ EN 1367-2 is considered as the most sufficient regulation, where the structure and the aggregates are exposed to seawater or de-icing salts. It can be seen in *Fig. 3* that at the majority of our Hungarian stones the magnesium sulfate crystallizing loss doesn't exceed 10% of the weight. In the Standard MSZ EN 12620 the strictest regulation is the MS<sub>18</sub>, accordingly the majority of our rocks is sufficient.

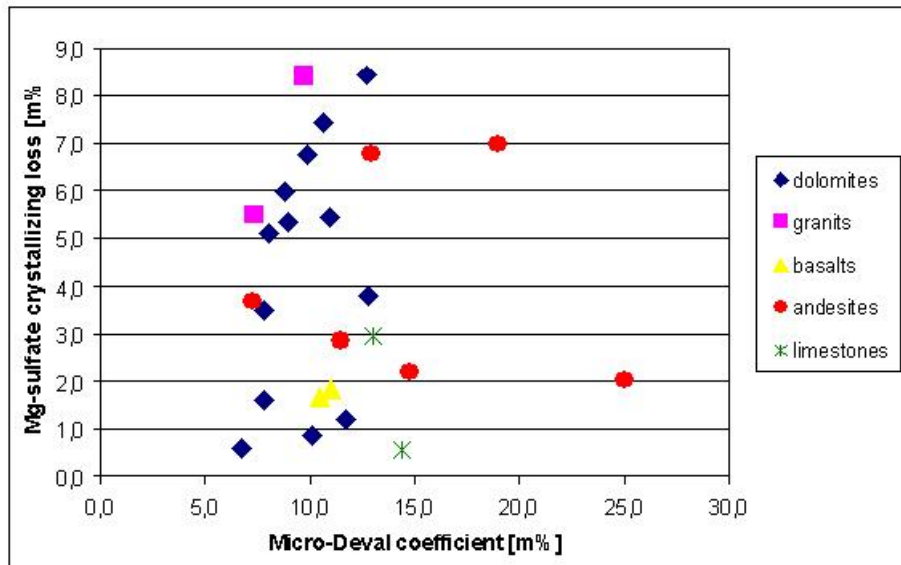


Fig. 3 Relationship between micro-Deval coefficient and Mg-sulfate crystallizing loss

It was shown in the test results of fraction 10/14, that the micro-Deval-Los Angeles coefficient connection and Mg-sulfate-micro-Deval relation was not found, therefore all of the three methods are required to characterize aggregates (*Fig. 2, Fig. 3*).

In the followings we are discussing the relationships between the values of compressive strength and tensile strength resulted of the same rock, and between Los Angeles and Magnesium sulfate crystallizing values.

Between compressive strength and Los Angeles value (on fraction 5/8 tested) a relationship could be developed. The relation describing equations show parallel lines in *Fig. 4* expect the line of andesite tuff, which runs much steeper. This phenomenon was expected, because andesite tuff has worse petrophysical parameters, than the others. Intact basalts and andesites, carbonated rocks and weathered andesites have the same tendencies, which is shown in the parallelism of the lines. This three rock types differ in their Los Angeles fragmentation values, which is probably caused by the different conditions of the bindings between the rock formatting minerals.

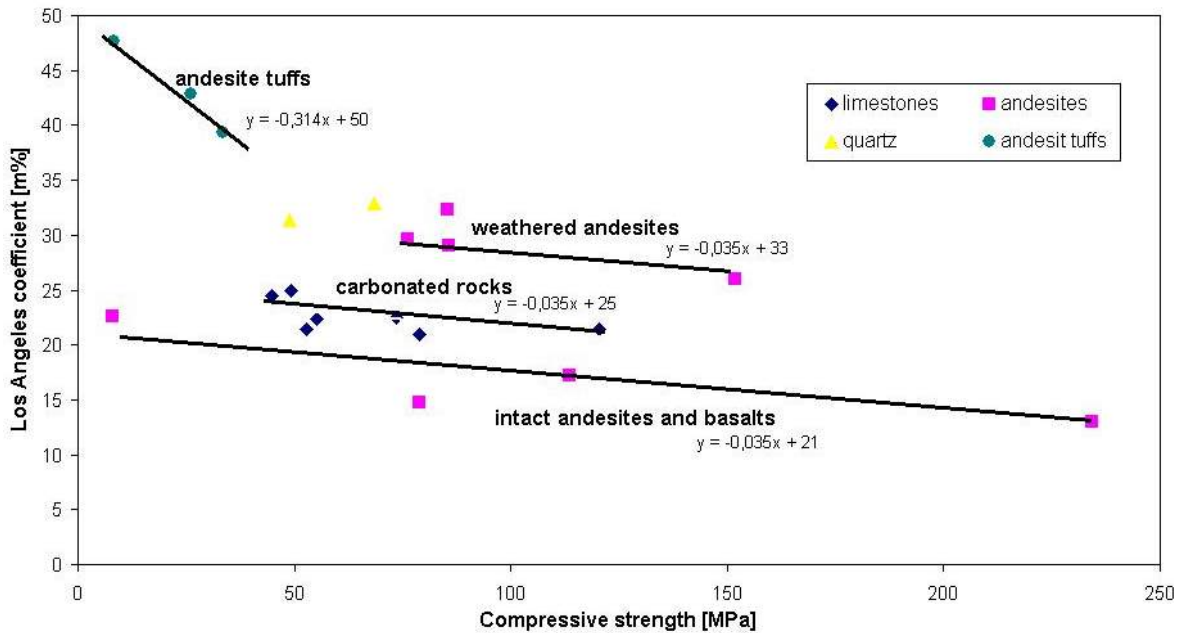


Fig. 4 Relationship between Los Angeles coefficient and compressive strength

## 5. CONCLUSIONS

In accordance with the phrasing of the Standard MSZ EN 206-1:2002 NAD: “The gravels, gravels with sand in Hungary are generally sufficient petrological, petrophysical, and chemical point of view to the production of concrete, and generally it is not necessary to examine those properties of them. The particle form of the graves is given, that's why there is no need to examine them.” That's why aggregates are received rarely into our laboratory for carry out petrophysical tests on them, but in accordance with our previous experiences there are gravels in Hungary, which show weak petrophysical properties; so we consider necessary their examination.

Relationship could be found between Los Angeles coefficient and compressive strength. There is no evident relationship between Los Angeles, micro-Deval and Mg-sulfate crystallizing test results, therefore all of the three methods are required to characterize aggregates.

## 6. ACKNOWLEDGEMENTS

The help and works of Gy. Emszt and E. Árpás in Laboratory are appreciated.

## 7. REFERENCES

- Emszt Gy. (2006) „Testing and standardization of Hungarian aggregates for railway ballast”, Bsc thesis, BME (in Hungarian)
- Gálos M., Kárpáti L., Emszt Gy., Árpás E. (2002) „Los Angeles test according to the European Standards”, *Építőanyag*, vol. 54, No. 4, pp. 106-111. (in Hungarian)
- Gálos M., Kárpáti L., Emszt Gy., Árpás E. (2006) „Determination of strength parameters of aggregates for railway ballast according to EN 13450:2002”, Research report, BME, No. 30713-003-MG-025/2005 (in Hungarian)

## **FIBER REINFORCED CONCRETE CHARACTERIZATION: ROUND PANEL VS. BEAM TESTS TOWARD A HARMONIZATION**

*Fausto Minelli and Giovanni A. Plizzari*

*University of Brescia, Dept. of Civil Engin., Architecture, Land and Environment - DICATA  
Via Branze, 43 - 25123 BRESCIA, Italy*

### **SUMMARY**

Standard test methods for determining the mechanical properties of Fibre Reinforced Concrete (FRC) are better defined if they provide parameters useful for structural design. A comparison between different test typologies for characterizing FRC is reported and discussed in the present paper, with special emphasis on the different scatter that each tests produces. Tests are performed on beams as well as on panels. All specimens have the same concrete mechanical properties and fiber content.

Aim of the investigation is to critically discuss advantages and disadvantages of each testing procedure, focusing on the applicability of the method and on the reliability of results toward a consistent characterization of the structural behaviour. A new geometry for the panel test is herein proposed and discussed in order to make the panel easier to place and handle, avoiding one of the major drawback which limits an extensive utilization of the panel tests. Suitable correlations among the different fracture and energy parameters defined in the assumed standards are finally reported, resulting very useful for a harmonization of the available standards.

### **1. INTRODUCTION**

Fiber Reinforced Concrete (FRC) is gaining an increasing interest among the concrete community for the reduced construction time and labor costs. For this reason, many structural elements are now reinforced with steel fibers as partial or total substitution of conventional reinforcement (rebars or welded mesh; di Prisco et al. (2), 2004). Besides cost issues, quality matters are of paramount importance for a construction and FRC also fulfill these requirements since fibers allow for more distributed cracks with a smaller opening that enhances durability. New construction materials requires Standards for measuring their mechanical properties and building codes or guidelines for structural design (Vandewalle, 2004; CEN, 2003). As far as FRC is concerned, design guidelines are already available in some Countries (CNR, 2006; Rilem, 2003; di Prisco et al. (1), 2004) and work is in progress for including them in the coming fib Model Code. In these guidelines, structural design is usually based on design values of the material parameters that are normally determined by dividing the characteristic values by a partial safety factor ( $\gamma_M$ ).

Mechanical properties of FRC are traditionally determined from beam tests that are usually based on a three (CEN, 2003) or four point bending schemes (UNI, 2003). Early experiences with the low volume fractions of fibers that are nowadays used in practice ( $V_f < 0.8-1.0\%$ ) evidence that the characteristic values determined from beam tests (CEN, 2003; UNI, 2003) are quite low because of the high scatter present in the beam-test results; it should be observed that the latter scatter is not related to the material itself but is mainly due to the small fracture areas (ranging from 160 to 180 cm<sup>2</sup>) that becomes particularly high when low contents



(25-50 kg/m<sup>3</sup>) of macro steel fibers (length ranging between 30 and 60 mm) are used (Sorelli et al., 2005).

It is commonly accepted that FRCs with a low volume fraction of fibers are particularly suitable for structures with a high degree of redundancy where a stress redistribution may occur. Because of this redistribution, large fracture areas are involved (with a high number of fibers crossing them) and, therefore, structural behaviour is mainly governed by the mean value of the material properties; furthermore, because of the large fracture areas, the scatter of experimental results from structural tests is remarkably lower than that obtained from the beam tests. A typical example is shown in Fig. 1, which exhibits a set of curves obtained from a standard (bending) test on notched specimens (Fig. 1a) and from structural tests on full scale slabs on grade made of the same material (Fig. 1b); the different scatter between material and structural tests is clearly evident. In order to obtain a more realistic value of the scatter from FRC material tests, specimens with larger fracture areas are needed; this suggests the use of larger beams or different specimens like slabs where a stress redistribution may also occur.

A square panel was proposed to simulate a portion of sprayed concrete in tunnel lining applications (EN 1488-5, 2004). However, since it is simply supported along the whole border, any geometrical irregularity involves that the real support may vary in different specimens; in fact, although the support can lay in a perfect (and controlled) plane, specimens are normally deformed because of shrinkage effect. The crack pattern is therefore hardly predictable and the determination of the constitutive laws for cracked concrete becomes very difficult. A Round Determinate Panel (RDP) test was proposed by ASTM (2005); it is a statically determinate test (a round slab - $\phi=800$  mm-thick=75 mm- with three supports at 120 degrees) where the crack pattern is predictable and the post-cracking material properties can be better determined. However, handling and placing such a specimen is quite complicated due to the large size and, consequently, high weight. In addition, standard servo-controlled loading machines may not fit with the geometry of the panel, which is too big for most of them. The need to have a specimen easier both to handle and to test brought the Authors to come up with a proposal of a smaller round panel having a diameter of 600 mm and a depth of 60 mm.

The present paper focuses on the comparison of different tests for FRC materials tested in the last few years at the University of Brescia. A comparison between beam and panel tests, a discussion on the smaller round panel herein proposed as well as the correlations between the different fracture properties obtained from different Standards are here presented.

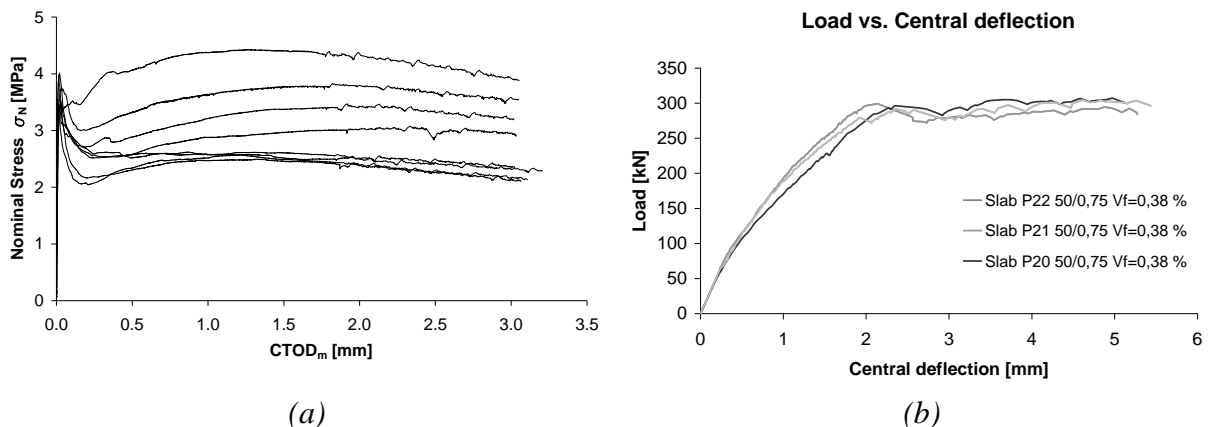


Fig. 1 Experimental results from a bending tests on a notched beam (a) and from a full-scale slab on grade (b) made of the same FRC (di Prisco et al., 2004)

## 2. MATERIALS, SET UP, EXPERIMENTAL RESULTS AND DISCUSSION

Among more than 100 comparative experiments carried out on beams and panels, the following discussion will deal with a number of tests conducted on members containing either 20 nor 30 kg/m<sup>3</sup> of hooked-end steel fibers having a length of 50 mm and a diameter of 1 mm (the aspect ratio  $L/\phi$  is 50); fibers have a circular cross section and a tensile strength of 1100 MPa. Besides the FRC specimens, plain concrete beams and panels were also made. Tab. 1 reports the main geometrical characteristics of the five testing typologies studied herein; the weight of each specimen, assuming a density of 24 kN/m<sup>3</sup>, is also outlined.

In order to study the behavior of all specimens up to failure, including any possible unstable branch after cracking, a displacement controlled testing method was adopted. The equipment shown in Fig. 2 (a) was utilized for all test beams, whereas the dimensions of the panel specimens, as already mentioned, required to utilize a different equipment, illustrated in Fig. 2 (b). In the first case, an INSTRON 1274 machine was used (having a closed loop and a maximum load of 300 kN). In the second case, the displacement was imposed by adopting an electro-mechanical screw jack (having a maximum load of 500 kN and a stroke of 300 mm) placed into a steel frame (Fig. 2 (b); no closed loop was provided in this case).

Specimen	Length [mm]	Height [mm]	Notch [mm]	Weight [kg]	Loading Scheme
Beam UNI	600	150	25	32.4	3 points
Beam CEN	550	150	45	29.7	4 points
	Dimensions [mm]	Thickness [mm]	Weight [kg]	Loading Scheme	
Round Panel Large* (RPL)	800 (radius)	75	90.5	Central point load	
Round Panel Small (RPS)	600 (radius)	60	40.7	Central point load	
Square Panel (SP)	600 (side)	100	86.4	Central point load	

Tab. 1 Main geometric characteristics of specimens. \*Large Round Panel refers to the standard test of ASTM (2005)

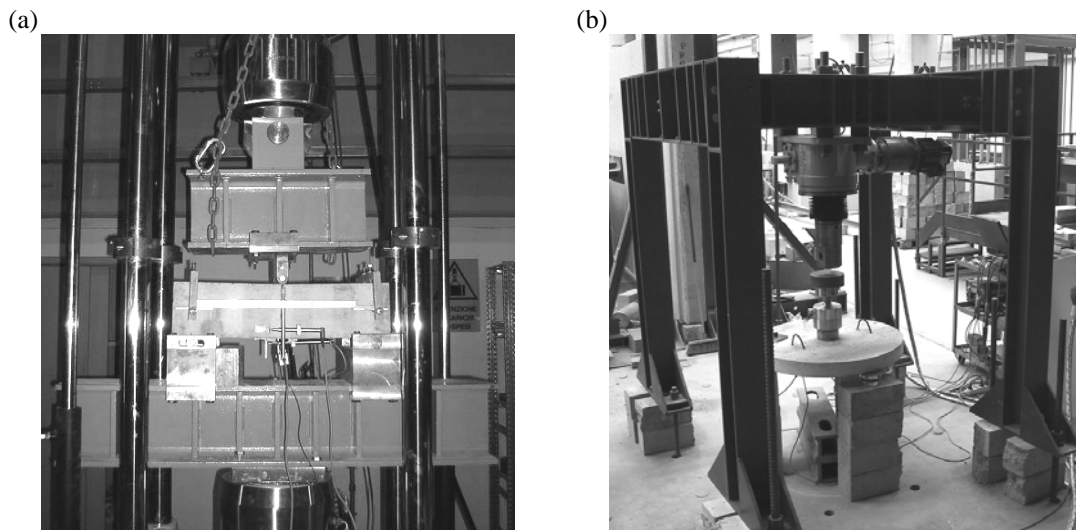


Fig. 2 Set up for performing beam tests (a), and panel tests (b)

A CMOD (Crack Mouth Opening Displacement)-controlled procedure was adopted for the notched beams (UNI and CEN prescribe a notch with a different length) whereas a

displacement-controlled test (screw control with the electro-mechanical jack) was performed with the panel tests, resulting in an instability of the test immediately after the peak of the concrete matrix. For more details concerning the geometry, tests set-up and instrumentation, one can refer to Marinoni et al. (2007). Several LVDTs (Linear Variable Displacement Transducers) were used in each test to measure the vertical displacements (under the load points and in other locations) and the crack openings (including the Crack Tip Opening Displacements in the notched beams).

Fig. 3 shows the Nominal Stress (according to a linear stress distribution in the cracked section) versus the CTOD for both CEN and UNI beam tests as well as the load versus the central vertical displacement of both large and small round panels made of the identical material. As expected, the post-peak behavior is similar for the two types of beam tests, which are characterized by a large scatter of experimental responses. Referring to Fig. 3c and Fig. 3d, the dispersion of results is definitely much smaller than in the corresponding beam tests, both for large and small round panels. It is worth underlining that, in order to characterize the post-peak behavior of panels, three LVDTs were placed to monitor the development of the crack widths, at a distance of 120 mm from the center of the panel. Crack widths greater than 20 mm were measured with a post-cracking load higher than one third of the peak load. Such an instrumentation is not required by the ASTM Standard, which states that one should only calculate the energy absorption that is defined by the vertical load and the vertical displacement. By monitoring the crack widths, whose location is predictable because of the statically determinate support system, it was also possible to come up with nominal stress (from elastic analysis) vs. crack width plots, as a suitable tool for the mechanical characterization of FRC materials (since the expected scatter from panel tests is lower). For more details concerning the experimental part, please refer to Marinoni et al. (2007).

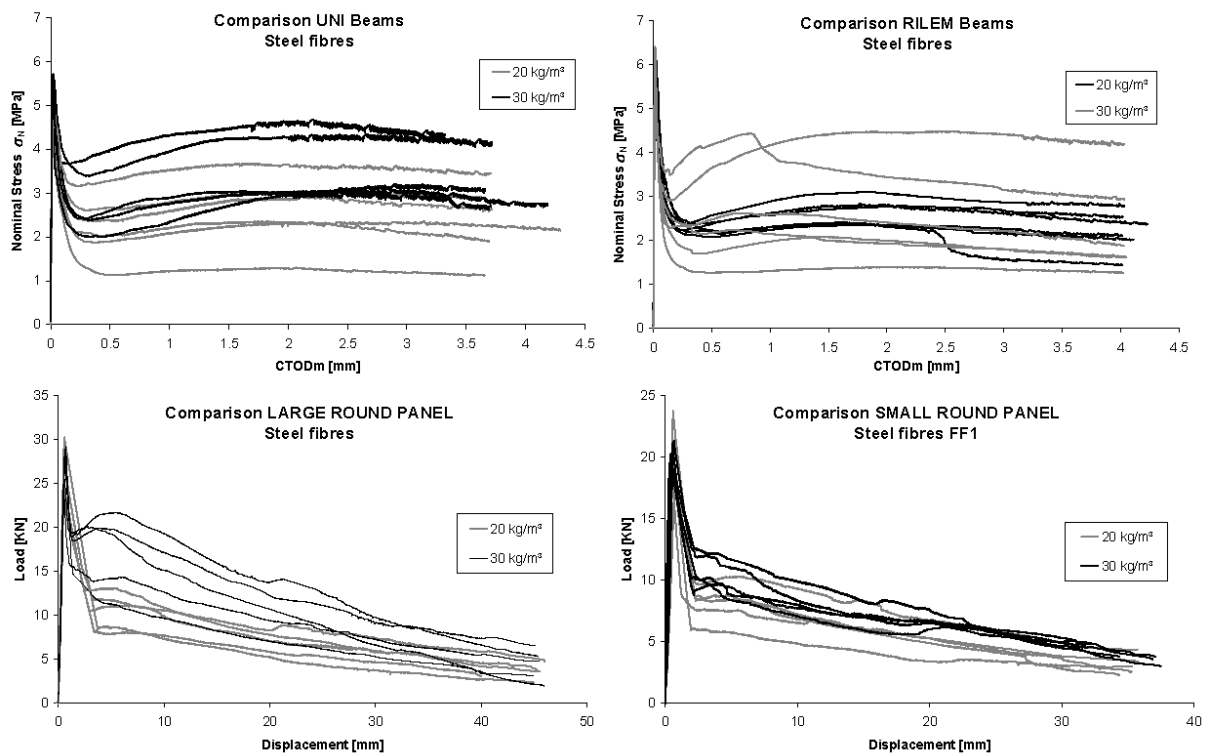


Fig. 3 Comparison of UNI, CEN and round panels tests, both for FRC with 20 and 30 kg/m<sup>3</sup>

The coefficient of variation, as an indicator of the test results scatter, was calculated for all properties and indexes defined in the different standards (Fig. 4), both for quantities which refer to the serviceability limit states (SLS) and at ultimate limit state (ULS). Once again, a

significant lower coefficient of variation can be outlined for panel tests in comparison with beam tests, according to the experimental plots aforementioned. An idea was to use the low scatter of panel tests for the determination of suitable fracture properties in accordance with the well-known procedures indicated by beam test standards. To this aim, the following procedure was undertaken:

1. Find correlation between the different parameters required by different standards;
2. Calculate average value of the equivalent post-cracking strength (according to the beam test) from the values of energy absorptions from panels;
3. Calculate the characteristic values of the equivalent post-cracking strength from panels accounting for a lower experimental scatter;
4. Compare the values of equivalent post-cracking strength determined from beam test (direct method) with those from large and small panel tests.

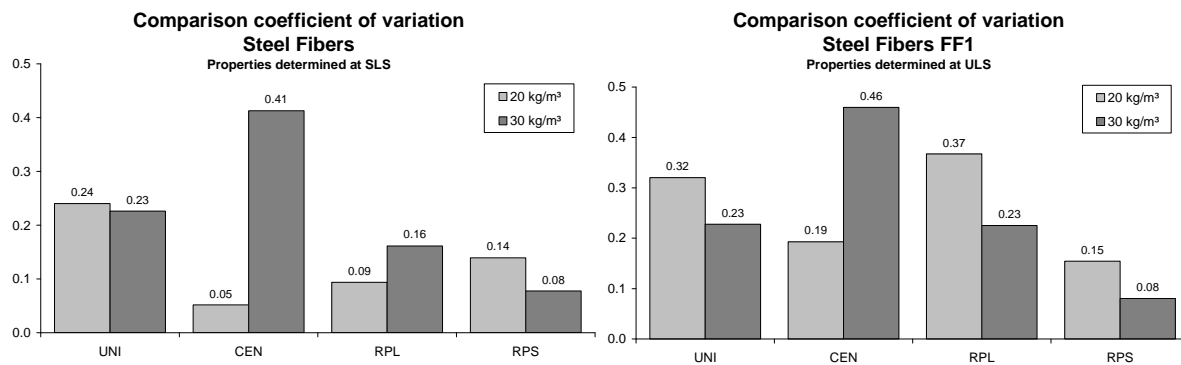


Fig. 4 Coefficient of variation calculated for all parameters required by the standards considered in the present experimental campaign

Fig. 5a, as an example, describes the correlation between the equivalent post-cracking strength of the UNI standard and the energy absorption of the ASTM panels at SLS. Among the 13 comparative studies reported (13 different points in the plots), the two bigger points refer to the two FRC materials discussed in this paper. Fig. 5b shows the identical correlation calculated with the parameters at ULS. Other correlations were also determined between panels and the CEN beam. From these two plots, one can notice that the coefficient  $R^2$  is quite small, and that a linear regression between the two quantities represents well the trend.

The two correlation found, based on 13 different experimental campaign on different FRC materials (synthetic, plastic, micro and macro fibers) brought to the following relationships:

$$E_{L,5} = 26.84 f_{eq(0-0.6)} \quad (1)$$

$$E_{L,40} = 127.23 f_{eq(0.6-3)}$$

where:

$E_{L,5}$  is the energy absorption for the large round panel up to a vertical displacement of 5 mm;

$E_{L,40}$  is the energy absorption for the large round panel up to a vertical displacement of 40mm;

$f_{eq(0-0.6)}$  is the equivalent post-cracking strength calculated for a CTOD range varying from 0 to 0.6 mm (SLS);

$f_{eq(0.6-3.6)}$  is the equivalent post-cracking strength calculated for a CTOD range varying from 0.6 to 3 mm (ULS).

From the average values of energy absorption of panel tests, using the relationships aforementioned, the average equivalent post-cracking strength according to the UNI Standard

were calculated, both using large and small (whose correlations are not herein shown) round panels. Afterwards, the characteristics values of the equivalent post-cracking strength, suitable for design purposes, were calculated in the three cases by using the corresponding experimental scatter (UNI beam, large and small round panels).

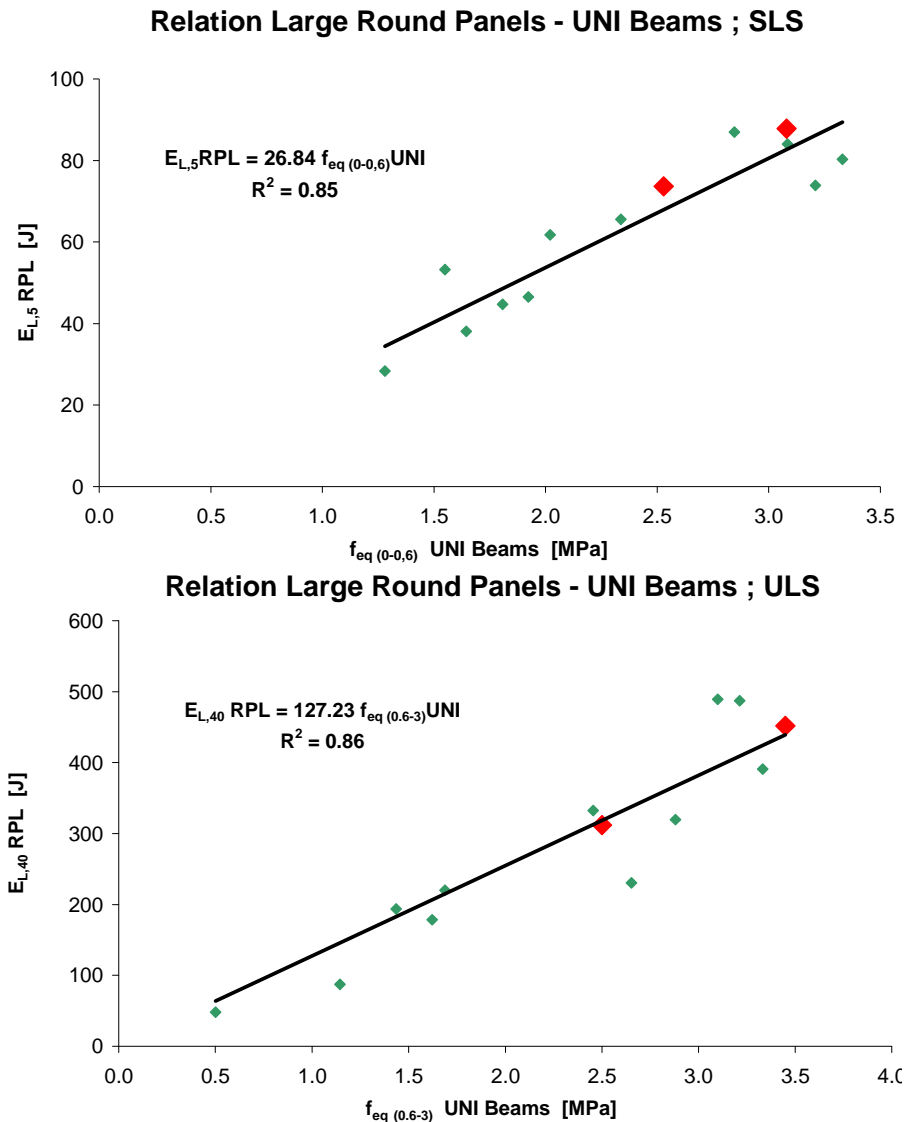


Fig. 5 Correlations among different parameters defined in different standards: Round Panel tests vs. Beam Tests UNI

Fig. 6 exhibits a comparison between the average and the characteristic values of the fracture parameter  $f_{eq(0-0.6)}$ , for FRC with 20 (a) and 30 kg/m<sup>3</sup> of steel fibers (b). Due to a very high scatter, using the beam test the characteristic values turns out to be at least 40% lower than the average one whereas, in the case of panel test, the reduction varies from 15 to 30%, with therefore a beneficial effect on the values adopted in the design process and, consequently, on the structural dimensions. One should notice that the three average values are almost identical, as a further proof of the strength and consistency of the aforementioned correlations.

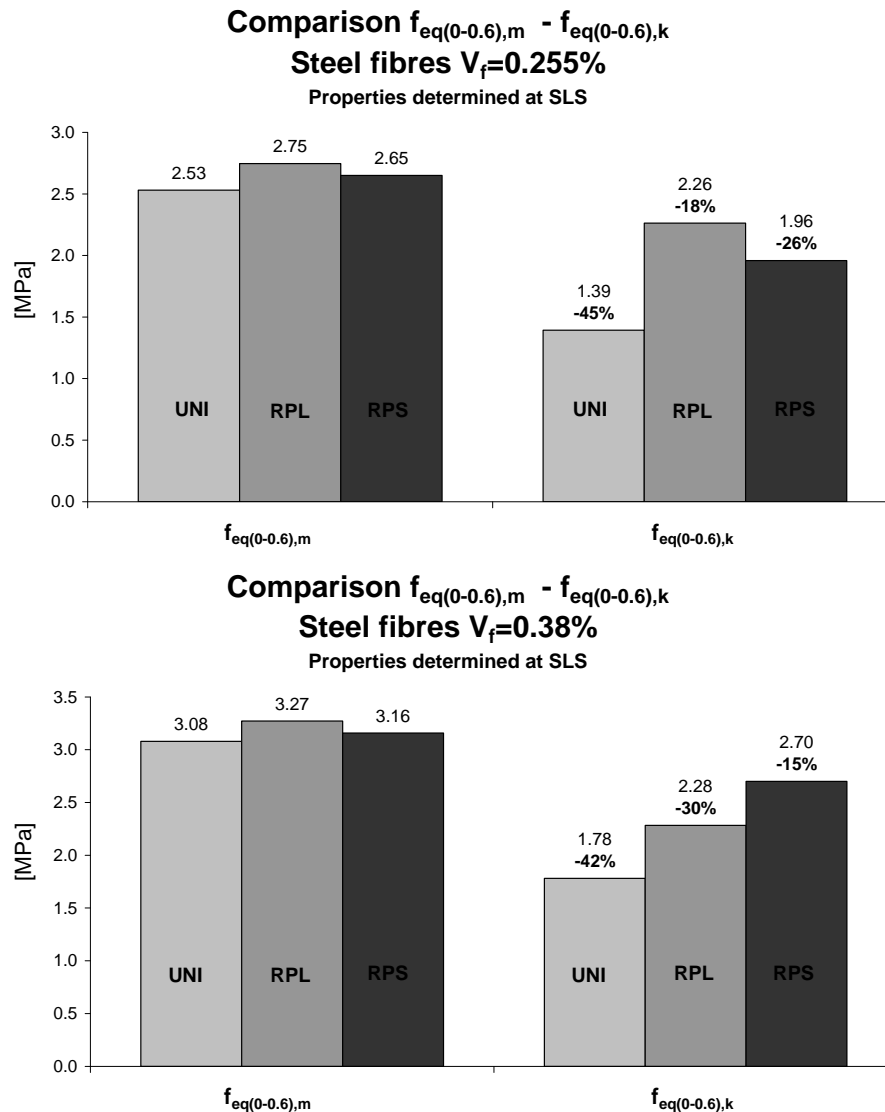


Fig. 6 Correlations among different parameters defined in different standards: Round Panel tests vs. Beam Tests UNI

### 3. CONCLUDING REMARKS

A comparative study between beam and panel tests was discussed in the present paper. The experimental high scatter generally present in beam tests is definitely caused by the small geometry and fracture area involved in the tests. It does not represent the real structures where much larger fracture areas are involved and, consequently, a lower dispersion occurs. Panel tests are therefore more suitable for representing the actual behavior of FRC materials. With a number of improvements in the test procedures (close-loop control, crack width measurements) the round panel test can be adopted for the characterization of FRC as it implies much lower dispersion of experimental results.

The proposal of carrying out panel tests on smaller specimens brought to a positive results, as such geometry does not affect the low scatter of the standard ASTM panel and, moreover, it allows for an easier placing and handling (lower weight and smaller geometry tht fits with many servo-controlled testing machines). The correlation among fracture parameters found are in general very promising and allow engineers not to repeat different tests in different Countries but to analytical calculate the fracture parameters of different tests from performing

only one or few test typologies. These correlations, that were somehow expected since we are always referring to fracture properties of the same material, are important under a practical point of view as they can give immediate indications of the fracture properties without performing expensive tests.

Finally, the round panel test could be considered as a complete test for the characterization of FRC once suitable range of crack widths will be defined. From these ranges, the corresponding equivalent (or residual) post-cracking strengths can be defined (from  $\sigma$ -w plots) following the same procedure as done for beam tests. Further studies on this topic are currently ongoing at the University of Brescia in Italy.

#### 4. ACKNOWLEDGEMENTS

The research was partially found by Officine Maccaferri (Bologna, Italy) whose support is gratefully acknowledged.

The Authors would like to thank also Engineers Yuri Marinoni, Raoul Martin Milla and Nicola Vezzoli for their assistance in performing the experiments and in data processing.

#### 5. REFERENCES

- ASTM C1550-04, "Standard test method for flexural toughness of fiber reinforced concrete (using centrally loaded round panel), pp. 9, 2004.
- CEN/TC 229 - PrEN 14651-5, "Precast Concrete Products – Test method for metallic fibre concrete – Measuring the flexural tensile strength", Europ. Standard, 2003, pp.15.
- CNR DT 204/2006. 2006. "Guidelines for the Design, Construction and Production Control of Fibre Reinforced Concrete Structures", National Research Council of Italy.
- di Prisco, M., Failla, C., Plizzari, G.A. and Toniolo, G. (2004), "Italian guidelines on SFRC", in Fiber Reinforced Concrete: from theory to practice, di Prisco, M. and Plizzari, G.A. Eds., Proceedings of the International Workshop on advances in Fibre Reinforced Concretes, Bergamo (Italy), September 24-25, pp. 39-72.
- di Prisco, M., Felicetti, R. and Plizzari, G.A. Eds. (2004), Proceedings of the 6th RILEM Symposium on Fibre Reinforced Concretes, BEFIB 2004, RILEM PRO 39, 1514 pp.
- Lambrechts, A.N., "The variation of steel fibre concrete characteristics. Study on toughness results 2002-2003", Proceeding of the International Workshop "Fiber Reinforced Concrete. From theory to practice", Bergamo, September 24-25, 2004, pp. 135-148.
- Marinoni, Y., Minelli, F., Plizzari, G.A., and Vezzoli, N.: "Prove di frattura su calcestruzzi fibrorinforzati in accordo con le principali normative internazionali", Technical Report, University of Brescia, Department DICATA, 2007.
- PrEN 14488-5-CEN/TC 104, "Testing sprayed concrete – Part 5: Determination of energy absorption capacity of fibre reinforced slab specimens", Europ. Standard, 2004, pp.1-7.
- RILEM TC162-TDF: "Test and Design Methods for Steel Fibre Reinforced Concrete: Recommendations. Bending test", Materials and Structures, 33, (225), (2000) 3-5.
- RILEM Final Recommendation TC-162-TDF, "Test and Design Methods for Steel Fibre Reinforced Concrete;  $\sigma$ - $\varepsilon$  Design Method", Materials and Structures, Vol 36, October 2003, pp. 560-567.
- Sorelli, L., Meda, A. and Plizzari, G.A., "Bending and uni-axial tensile tests on concrete reinforced with hybrid steel fibers", ASCE Materials Journal, Vol.15(5), 2005, pp. 519-527.
- UNI 11039, "Steel Fiber Reinforced Concrete - Part I: Definitions, Classification Specification and Conformity - Part II: Test Method for Measuring First Crack Strength and Ductility Indexes", Italian Board for Standardization, 2003.
- Vandewalle, L., "Test and design methods for steel fibre reinforced concrete proposed by RILEM TC 162-TDF", Proceeding of the International Workshop "Fiber Reinforced Concrete. From theory to practice", Bergamo, September 24-25, 2004, pp. 3-12.

## DURABILITY STUDIES ON STEEL FIBRE REINFORCED CONCRETE

*Attila Erdélyi, Adorján Borosnyói  
Budapest University of Technology and Economics, Hungary  
H-1111 Budapest, Műegyetem rkp. 3.*

### SUMMARY

The first aim of this research work was to study how steel fibres (diameter 0.5 mm – aspect ratio 60) influence the durability of concrete: in terms of frost and de-icing agent resistance as well as water tightness. Further aim was to study whether fibres (even after severe exposure to NaCl solution) remain still sound and effective in their reinforcing role. Also the question of changes in specific electric resistance ( $\Omega\text{m}$ ) was studied with variables of steel fibre content and saturation with NaCl solution of 3 percent. Experiments covered unexposed and NaCl solution exposed conditions, latter both in dry and wet conditions. Beside the most severe standardized (freeze-thaw) method (prEN 12390-9:2002) we developed other methods too. The developed methods enable both capillary suction and changing exposure to air ( $\text{CO}_2$ ,  $\text{O}_2$ ) while the specimens were immersed to their half thickness into NaCl solution. The changes in initial Young's modulus ( $E_0$ ), the drop of ultrasound pulse velocity (UPV), the loss of mass and the stress-strain diagrams have been studied before and after freeze-thaw cycles.

### 1. INTRODUCTION

Improved durability of steel fibre reinforced concrete (SFRC) compared to plain concrete was studied by several authors recently, in the presence or absence of chloride ions. The irreversible effect of only repeated sprayed NaCl solution without any frost attack was also studied (Cao, J., Chung, D. L., 2002; Dauberschmidt, C., Bruns, M., 2004; Fagerlund, G., 1997; Harnisch, J., 2004; Lubelli, B., Hees, R. P. J., Huinik, H. P., 2006; Maage, M., Smeplass, S., 2001; Polder, R., Rooij, M. R., 2005; Rooij, de M. R., Groot, C. J., 2006;). For example, the ASTM classification procedure accepts only the comparison of reference concretes and SFRCs after freezing-thawing cycles in NaCl solution. Therefore, present studies were focused on direct comparing methods. Laboratory tests were carried out in the last 7 years continuously and are still ongoing at the Budapest University of Technology and Economics, Department of Construction Materials and Engineering Geology to study the durability of steel fibre reinforced concretes. Experimental studies were supported by the Hungarian Research Fund (Grant No.: OTKA T032883).

### 2. EXPERIMENTAL METHODS

Two types of (intentionally chosen) non-air-entrained concrete ( $w/c=0.42$  and  $w/c=0.54$ , respectively) reinforced with 0, 25, 50 and 75  $\text{kg/m}^3$  cold drawn steel fibres of  $\varnothing 0.5$  mm and length of 30 mm (hooked-end, Bekaert, Dramix and undulated, D&D, Hungary) were tested. Beside the scaling-off test (prEN 12390-9:2002) two own-developed methods were applied: the 75×75×150 mm prisms (sawn from bigger, mature specimens) have been laid in NaCl solution of 3 percent up to their half thickness thus enabling the continuous capillary saturation of the upper half. According to one of our methods (A), the prisms were rotated after 8 cycles – and during 4×8=32 cycles all the four sides were exposed to air (i.e.  $\text{CO}_2$  and



O<sub>2</sub> is allowed to be diffused). According to our other method (B), the prisms were tested without cyclic rotation and always their same halves have been exposed to air. The decrease of Young's modulus  $E_0$  and that of the compressive and splitting tensile strength, and the loss of mass (g/g and g/m<sup>2</sup>) was measured. In extreme conditions (dry and not salt saturated, wet and dried salt saturated) the specific electric resistance was measured and plotted against fibre content and w/c ratios. Water tightness in not frozen condition and after 32 freeze-thaw cycles was found to be satisfactory. The repeatedly changed NaCl solution (maybe also due to rotation) dilutes the Ca(OH)<sub>2</sub> content of hardened cement paste sometimes in a depth of 20 mm. Steel fibres are rusted only if the matrix is totally degraded and the steel fibres come into direct contact with air at the presence of NaCl (Balázs, Csányi, 2001). Ultrasound pulse velocity (UPV) measurements confirmed the importance of contact materials used and the rate of deterioration due to freeze-thaw cycles.

### 3. EXPERIMENTAL RESULTS

#### 3.1 General findings

Non-air entrained concretes of  $f_{cm} = 45$  to  $65$  N/mm<sup>2</sup> compressive strength are not frost and de-icing agent resistant and steel fibre dosage does not significantly improve this behaviour. The scaling-off method (prEN 12390-9:2002) and even our "half thickness immersed" method with capillary suction possibility and exposure to air are more severe than all other methods applying completely immersed specimens. On the other hand 28 cycles are not enough to check freeze-thaw resistance with de-icing agent.

#### 3.2 Scaling off

In spite of heavy scaling off losses (more than 1000 g/m<sup>2</sup> after 28 standardized cycles) we continued the test till 56 cycles (i.e. 56 days). It should be mentioned that a relatively small loss of 400 g/m<sup>2</sup> means already 15 percent loss of mass. Our best slab fulfilling the limiting scaling off value of 1000 g/m<sup>2</sup> (Swedish Standard SS137244) suffered twice the loss of mass at 28 cycles as compared to our prisms. Therefore, the mentioned prEN 12390-9:2002 should be considered as a more severe test method than conventional ones.

The sum of scaling off losses (g/m<sup>2</sup>) have been calculated in three different ways: 1) for steel fibres only (separating them with a magnetic rod), 2) for concrete and 3) for an idealized total loss combining the concrete loss together with fibre losses (where fibre losses were multiplied with the ratio of densities steel/concrete, see *Fig. 1*). The results in increasing order of idealized losses can be studied in *Fig. 2*, representing a better overlook of the results.

Losses of mass did not show significant differences up to 28 cycles, independently of the applied fibre dosage of zero, 25, 50 or 75 kg/m<sup>3</sup>, respectively. Afterwards, we measured higher, randomly increasing losses. In *Fig. 2* it can be realized that the four worst results belong to a lower average fibre dosage of 37.5 kg/m<sup>3</sup> while the four best ones belong to a higher average fibre dosage of 62.5 kg/m<sup>3</sup>. It means that:

- higher dosage hinders the scaling off, independently of higher or lower compressive strength (indicated with NA or KA, respectively, in present studies),
- steel fibres cannot improve considerably the limited frost resistance of non-air-entrained concrete in the range of strength that was covered in present studies ( $f_{cm} = 45$  to  $65$  N/mm<sup>2</sup>), therefore, concretes of similar strength need air entraining,

- our non-air-entrained concretes did not correspond to the more severe test methods, though the concrete of lower water-to-cement ratio (0.42) with higher dosages (50-75 kg/m<sup>3</sup>) of fibres after only 32 cycles (with capillary suction) suffered less than 5 percent loss of mass,
- 28 cycles (e.g. according to EN 1338:2002) are not sufficient to deem the frost resistance.

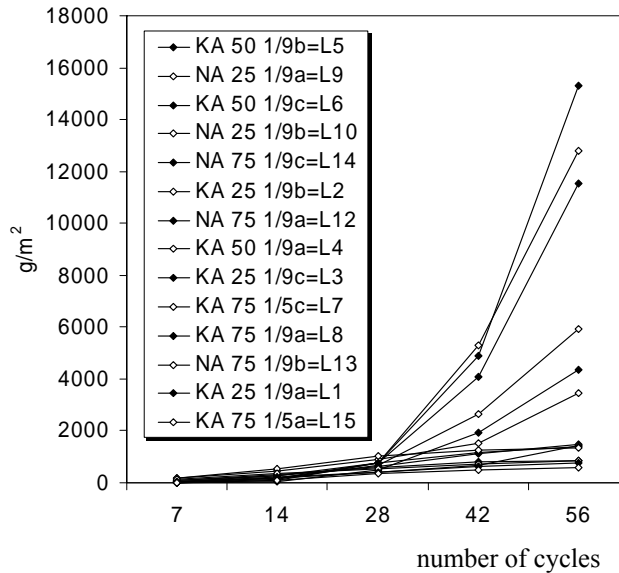


Fig. 1 Idealized total loss combining the concrete loss together with fibre losses  
 Notation: KA - lower strength concrete, NA - higher strength concrete  
 25, 50, 75 - dosages of steel fibre in kg/m<sup>3</sup>  
 L1 to L15 individual designation of specimens

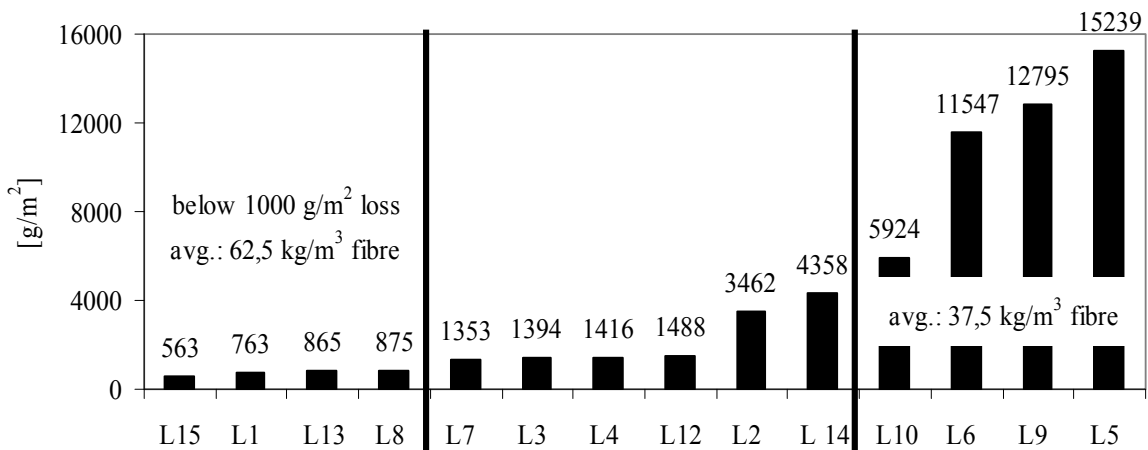


Fig. 2 Idealized total loss combining the concrete loss together with fibre losses  
 (results after 56 cycles in increasing order)

### 3.3 Mechanical properties

Initial Young's modulus ( $E_0$ ) will lose 30 to 40 percent of its original value (before freeze-thaw cycles), but compressive strength of freeze-thaw tested prisms will be decreased less. Tensile splitting strength is decreasing too, but there is evidence of the beneficial effect of steel fibres and the scaled-off slabs in spite of the worn, unsatisfactory surfaces maintain their original load bearing capacity in splitting.

Embedded steel fibres do not corrode and scaling off do not increase due to a supposed pressure of corrosion products of higher volume. The amount of steel fibres separated from the scaled off matrix is smaller than calculated from the nominal steel/concrete ratio. Exposed fibres therefore rather hinder scaling off than enhance it.

Water tightness is a useful indicator of durability of concrete. Our concrete specimens tested at 5 and 6 bars pressure showed a sufficient behaviour even after freeze-thaw cycles. Fibres render a crack arrest also against micro cracking (though  $E_0$  is decreasing due to matrix degradation) and concrete still remains water tight in its volume.

The ultrasound pulse velocity (UPV) is highly depending on the type of contact material applied, let it be grease, bentonite, suspension, vaseline, soap emulsion etc. Physical conditions (dry, saturated, etc.) also influence the phenomenon. Of course, UPV is dropping due to freeze-thaw cycles causing micro and macro cracks.

### 3.4 Electric resistance

Specific electric resistance ( $\rho$ ,  $\Omega\text{m}$ ) of reinforced or prestressed concrete is considered worldwide to be an important factor that is influencing durability – both for plain concrete and steel fibre reinforced concrete. A usual concrete of C30/37 has a resistance  $\rho \sim 10^5 \Omega\text{m}$  at a moisture content of 1 m%, but only  $\sim 10^2 \Omega\text{m}$  if it is almost water saturated (5 m%). Some of our results are indicated in *Fig. 3* and *Fig. 4*. The apparent porosity ( $p$ , V%) does not significantly influence the electric resistance though plotted points may be separated into two groups: the higher strength NA concrete with lower water-to-cement ratio 0.42 and the lower strength KA concrete with higher water-to-cement ratio 0.54. When lower strength plain concrete if dry (without any NaCl contact) is the best one from the point of view of high electric resistance, i.e. low risk of corrosion ( $\sim 14 \times 10^3 \Omega\text{m}$ ) as a consequence of its higher volume of empty pores (*Fig. 3*). The higher strength concrete of lower porosity saturated with salt solution has somewhat higher electric resistance (*Fig. 4*,  $\sim 6 \times 10^2 \Omega\text{m}$ ). Thus low water-to-cement ratio is a governing factor for all concretes in any condition, even if the electric resistance of fibre reinforced concrete specimens is similarly low as compared to non-reinforced concrete specimens. The most important factors affecting electric resistance are:

- whether concrete is dry and never exposed to NaCl solution (*Fig. 3*) or saturated with salt solution and wet (*Fig. 4*),
- whether steel fibres were applied, irrespectively of their dosage 25 to 75 kg/m<sup>3</sup>.

*It can be concluded that steel fibre dosage moderately increases the all-over corrosion sensitivity of concrete structures due to the drop or specific electric resistance.* The smallest values were measured if concrete was wet, while saturated with NaCl solution. It is advisable to keep the concrete core of structures dry (water tightness, impregnation, water repellent surface treatment, hydrophobic cover, geometrically suitable slopes of structural surfaces to keep rainwater away and before all: low water-to-cement ratio).

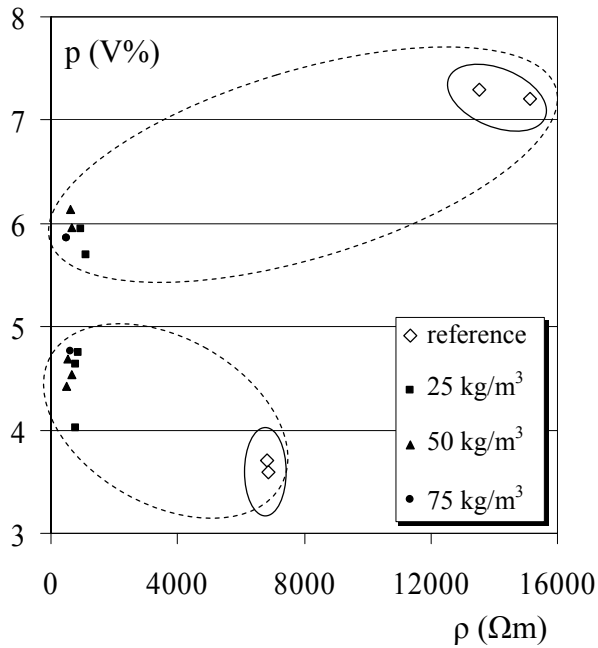


Fig. 3

Apparent porosity vs. electric resistance of dry specimens without any NaCl solution immersion

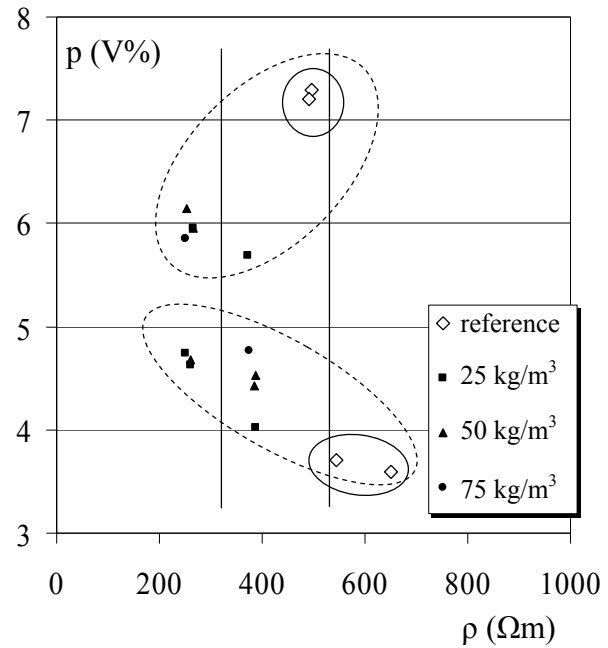


Fig. 4

Apparent porosity vs. electric resistance of wet specimens saturated with NaCl solution

### 3.5 Mineralogical and chemical properties

The chloride-ion content in samples that were never exposed to any NaCl solution is, of course, negligible. In samples immersed up to their half thickness into 3% NaCl solution a chloride-ion content (mass/mass of cement) was found to be 1.5 to 2.0m%. This is less, than the value reported by authors from the Netherlands for concrete in splash zone of marine RC structures (Polder, Rooij, 2005). Systematic chemical analyses demonstrated that the chloride-to-silicon ratio increases with higher air void volume because higher steel fibre dosages result sometimes in poorer workability, more air pocket and thus higher chloride-ion content too. During freeze-thaw cycles (in NaCl solution) the outer layer of samples has lost its  $\text{Ca}(\text{OH})_2$  – portlandite – content, became also phenolphthalein negative ( $\text{pH} < 9$ ) and both its chemical and mechanical stability was completely deteriorated. Possibly a part of  $\text{Na}^+$  ion released from the de-icing salt solution has been built into the hardened cement paste partly replacing  $\text{Ca}^{++}$  ions. It appears that reinforced concrete is endangered not only by chloride cations but also by  $\text{Na}^+$  anions too (Erdélyi et al, 2007).

### 4. CONCLUSIONS

Tests were carried out on two grades of concrete C35/45 and C45/55 made with zero, 25, 50 and 75  $\text{kg/m}^3$  of cold drawn steel fibres to study freeze-thaw resistance after saturation with 3% NaCl solution. The several years old prismatic 75×75×150 mm (1:2) specimens and 150×150×50 mm slab specimens have been tested for Young's modulus, stress-strain diagram, scaling off, specific resistance and ultrasound pulse velocity. *Non-air entrained concretes of the tested strength range are not frost and de-icing agent resistant and steel fibre dosage does not improve basically this behaviour.*

## 5. ACKNOWLEDGEMENTS

Authors gratefully acknowledge the financial support of the Hungarian Research Fund (OTKA; reg. num. T032883) and that of the Hungarian Academy of Sciences (Bolyai Scientific Scholarship). Special thanks to Nehme, S. G. for his kind contribution in UPV measurements. Our thanks are expressed to cooperating engineer colleagues: Csányi, E., Kopeckó, K., Fenyvesi, O., Gyömbér, Cs. and to all cooperating technicians.

## 6. REFERENCES

- Balázs, G., Csányi, E. (2001) „Corrosion of reinforced concrete in aggressive solutions”, *Építőanyag*, 2001/4, pp. 119-129. (in Hungarian)
- Cao, J., Chung, D. L. (2002) „Damage evolution during freeze-thaw cycling of cement mortar by electric resistivity measurement” *Cement and Concrete Research*, 32, 2002, pp. 1657-1661.
- Dauberschmidt, C., Bruns, M. (2004) „Korrosionsmechanismen von Stahlfasern in chloridhaltigem Beton“ *IBAC Mitteilungen*, RWTH Aachen, Inst. für Bauforschung, 2004, pp. 62-64.
- Erdélyi A., Borosnyói A. (2005a) „Toughness and durability of SFRC” *Conference dedicated to Professor László Palotás*, 26-27 January 2005 (in Hungarian)
- Erdélyi A., Borosnyói A. (2005b) „Durability studies on SFRC”, *Proceedings of 1<sup>st</sup> CECCC Fibre Reinforced Concrete in Practice*, 8-9 September 2005, Graz, Austrian Society for Concrete and Construction Technology, 2005, pp. 67-70.
- Erdélyi, A., Csányi, E., Kopeckó, K., Borosnyói, A., Fenyvesi, O. „The degradation of fibre reinforced concrete due to freezing and thawing with sodium chloride”, *Vasbetonépítés*, Journal of Hungarian Group of *fib*, Vol. IX., No. 2., 2007/2, pp. 45-55. (in Hungarian)
- Fagerlund, G. (1997) „Internal frost attack – State of the Art”, *Frost resistance of concrete*, Eds.: Setzer, M. J., Auberg, R., *E&FN Spon*, London, 1997, pp. 321-338.
- Harnisch, J. (2004) „Untersuchungen zum Elektrolytwiderstand von KKS (Kath. Korrosionsschutz)“ *IBAC Mitteilungen*, RWTH Aachen, Inst. für Bauforschung, 2004, pp. 126-174.
- Lubelli, B., Hees, R. P. J., Huinik, H. P. (2006) „Effect of NaCl on the hygric and hydric dilation behaviour of lime-cement mortar” *HERON*, Vol. 51., No. 1., 2006, pp. 33-47.
- Maage, M., Smeplass, S. (2001) „Carbonation – A probabilistic approach” *DuraNet*, 3<sup>rd</sup> Workshop, Tromsø, Norway, 10-12 June 2001.
- ÖVBB (2002) „Faserbeton Richtlinie” *Österreichischer Vereinigung für Beton und Bautechnik*, März 2002, pp. 1-64.
- Polder, R., Rooij, M. R. (2005) „Durability of marine concrete structures – field investigation and modelling” *HERON*, Vol. 50., No. 3., 2005, pp. 133-151.
- Rooij, de M. R., Groot, C. J. (2006) „A closer look on salt loaded microstructure” *HERON*, Vol. 51., No. 1., 2006, pp. 49-62.

## **USE OF THE ALKALI-RESISTANT GLASS FIBRES IN REINFORCED CONCRETE MEMBERS**

*María J. Álvarez-Casariego Álvarez, Juan C. Romero Ruiz, Pablo I. Comino Almenara  
Saint-Gobain Vetrotex España S.A., Spain  
Ctra. Nacional A-2 Km 34,500. Apdo 60. 28800-Alcalá de Henares*

### **SUMMARY**

Use of glass fibres for mortar and concrete reinforcement started to be taken into consideration after the good results obtained using glass fibres on synthetic resins as reinforcement. Special fibres, alkali resistant, had to be developed for this new application. It meant a big change in the world of composite materials for construction as it offered the possibility of lighter structures, with high performance, easy construction and durability. Furthermore, it opened the door for expanding and modifying the building sector.

Its first applications were small pieces like drainage channels, ornamentation and street furniture and fixtures. Nowadays, stairs, façade panels, noise barriers, tunnel linings, and other big cementitious elements are common glass fibre applications.

### **1. INTRODUCTION**

#### **1.1 A little bit of history**

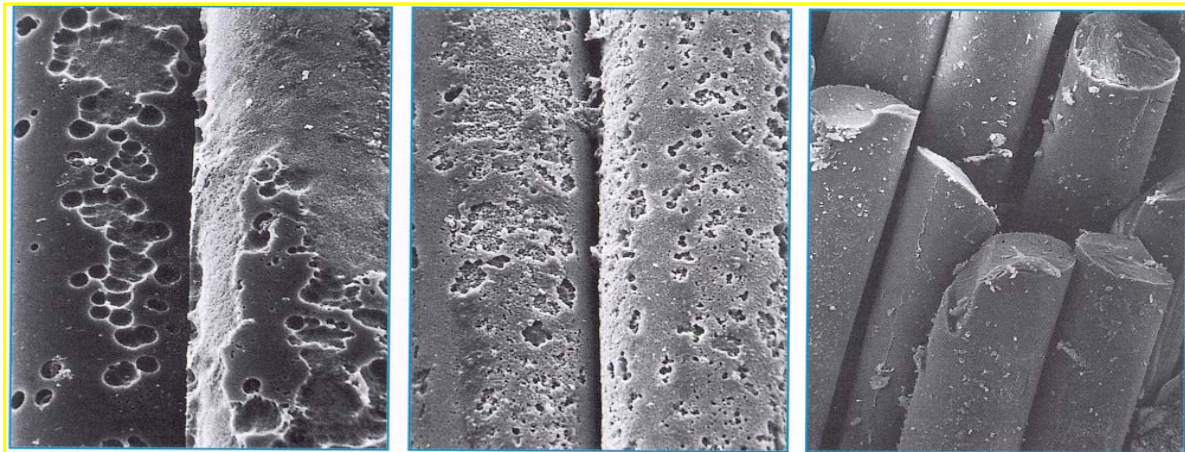
A composite material is produced with the aim of improving the properties of the base material. Mortars and concretes have a weak resistance to impact and flexure, but a very high compressive strength. The idea of reinforcing them to create a high performance composite is not new.

Steel was the first reinforcement used, but its price is increasing and possible corrosion of it motivated a lot of studies to replace it. Other reason was that steel reinforced concrete produced are always rather large and heavy pieces, well adapted for structural applications, but not for façade cladding.

First steps were done with asbestos fibres, which gave workability and cost advantages, but because of its carcinogen danger their use was stopped. Afterwards lots of different fibres, organic (aramides, nylon, rayon, polypropylene, ...) and inorganic (glass, boron, carbon, aluminium, ...) were tested. Glass fibres turned out to be the best compromise between cost and mechanical properties:

- tensile strength of glass fibres is 3 times higher than that of steel
- elastic modulus of glass is 3/4 times higher than that of cement
- glass is resistant against electrolitic corrosion and it is not combustible
- glass has no environmental impact and presents no risks for healthy
- glass has the same density of cement and high workability. Therefore, it permits entering easily into the cement matrix and can offer a three-dimensional reinforcement.

First trials were carried out with electrical glass (E-glass), commonly used in resin composites reinforcement, without complete success. It has been demonstrated, that E-glass does not resist high pH value of pore solution produced during cement hydration. In 1967, the Building Research Establishment (Dr. A. J. Majumdar) decided to develop a new type of glass suitable for the reinforcement of cement matrixes. As a result, 4 years later, a patent for an alkali resistant glass, containing zircon, was placed by the National Research Development Corporation. This glass was named AR-glass.



*E-Glass in OPC  
 after 8 days at 50°C  
 ≈ 2.2 years equivalent UK*

*E-Glass + Acrylic  
 polymer in OPC after  
 8 days at 50°C*

*AR-Glass in OPC  
 after 3 months at 50°C  
 ≈ 25 years equivalent UK*

Fig. 1 E-glass and AR-glass behaviour in alkali media

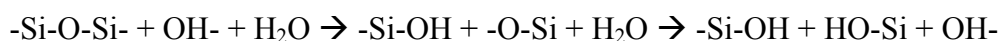
## 1. 2 Why Alkali-resistant?

Glass is an amorphous material composed in its majority by silicon dioxide and smaller amounts of other metallic and semi-metallic oxides. Main components of AR-glass are:

- Silicon dioxide: SiO<sub>2</sub> (60-70%)
- Aluminium oxide: Al<sub>2</sub>O<sub>3</sub> (0-5%)
- **Zirconium dioxide: ZrO<sub>2</sub> (16-20%)**
- Sodium oxide: Na<sub>2</sub>O (10-20%)
- Titanium dioxide: TiO<sub>2</sub> (0-5%)
- Calcium oxide: CaO (0-10%)

Glass surface is mainly a chain of Si-O bonds with variable geometry and length and inserts of other elements (Al, Ca, Na, etc.). Water molecules bonded to the glass surface grace to Van der Waals forces are very important.

When Si-O bonds are in presence of alkalis in a water media, hydrolysis happens catalyzed by hydroxyl ions:



The difference in AR-glass is that zircon on surface forms part of the chain with Zr-O bonds. The Zr atom is bigger and more electropositive than Si one. Thus, Zr-O bond has higher polarity than Si-O bond. Zr external electronic orbitals have higher level than Si ones and can allocate hydroxyl free electrons, trapping hydroxyl ions and avoiding hydrolysis reaction of

adjacent bonds. Furthermore, the excess of negative charge generated, when a hydroxyl ion is trapped in a Zr atom, is transmitted to the adjacent Zr-O-Si- bonds creating electrostatic forces that hinder Si-O hydrolysis. Steric effect is also important hindering this reaction.

## 2. FIBRE PRODUCTION AND TYPES OF PRODUCTS

Raw materials are thin milled, homogeneously mixed and melted at more than 1500 °C in a high temperature furnace. Viscous vitreous mass makes its way via canals and falls down by gravity through platinum bushings forming glass filaments. Afterwards, filaments are cooled, size covered, assembled into strands and pulled out to form the different glass products nowadays available:

- *Chopped strands*: directly from bushing of previously wound glass cakes
- *Assembled rovings*: direct from bushing wound glass cakes have thin strands that can be assembled into bigger tufts and wound again to form rovings
- *Direct rovings*: they are obtained directly from bushings, assembling all filaments into one strand
- *Mats*: assembled rovings or cakes are unwound and resulting strands are bonded with polymers to form a flat carpet, called mat.
- *Meshes*: strands from direct rovings can be used to weave meshes.
- *Rebars*: glass fibre tufts can be resin impregnated and pultruded to obtain reinforcing bars.

Size covering has a very important role in glass fibre production, as it gives to the brittle glass strand the flexural strength, abrasion resistance and cohesion among filaments needed for each specific application. Thus, size technology is one of the most important fibre glass production know-how.

## 3. GRC

There are different types of cementitious matrices. We use to call mortar to the mix of Portland cement with only fine sand particles. When other larger aggregates are added, we call it concrete.

The Glass Reinforced Cement (GRC) is a composite material with a cement based mortar or concrete and AR fibre glass as reinforcement. Other additives as plasticizers, fluxes, pigments, water-repellents, polymers, etc. can also be added depending on final properties required.

Weight ratios normally used are:

Sand/cement	→	1:1
Water/cement	→	from 0.30:1 to 0.35:1
Plasticizer or flux	→	0.01:1

GRC is normally used for producing pre-cast pieces. There are two main production methods: simultaneous spray-up and premix.

### 3.1 Spray-up

Cement, sand, additives and water are mixed up to homogeneity and sprayed with a gun simultaneously with chopped fibres. Normally for producing a piece many layers will be



sprayed up to final thickness (10 to 15 mm). After each layer spraying, compaction and air de-bubbling will be carried out with a roller.

Quantity of glass fibres used is 5% and length ranges from 30 to 50 mm. With this ratio, reinforcement gives exceptional performance to sprayed-up composites.

Pieces obtained with this method are bi-directional reinforced and simple shaped. Big flat shapes, as façade panels are made with spray-up.

### **3.2 Premix**

Cement, sand, additives and water are mixed up to homogeneity. Afterwards fibres are added and complete mortar is mixed for 30 sec. to 1 min. to achieve a homogeneous paste. Quantity of fibres may vary from 2 to 3.5 % in weight depending on shape of pieces, but also the strengths that the composite is going to suffer in its final application. About the length, strands are normally short chopped, from 6 to 12 mm, for making possible a good mixing and, thus, a three-dimensional reinforcement.

There are different kinds of premixes, depending on the using of a mould or its direct application in a building site for preparing a floor or a render (top-screed).

#### **3.2.1 Vibration-cast premix**

A mould is fixed on a vibration table and covered with a first thin layer of a liquid plank mould remover. Mortar is poured into it and vibrated to favour air de-bubbling. When pieces are hard enough they are removed from mould to finish curing.

Premix pieces have normally high volumes and complicated shapes, like ornamentation or sunscreens.

#### **3.2.2 Top screed**

Premix mixture is prepared in the building site, with the addition of a self-leveling compound in the case of flooring. Surface is covered with a flat continuous reinforcement like a mat or a mesh, which will give the structural protection. Then, premix with reinforcing chopped fibres is applied. The aim of these fibres is to prevent surface from cracking due to plastic settlement and/or shrinkage.

#### **3.2.3 Premix spray-up**

This method is the halfway between premix and spray-up, and it is an emerging application, as process is very simple and reinforcement ratio is in the middle of theirs.

### **3.3 Curing**

Curing process is one of the critical points in the GRC production, because it influences directly its final properties. The best way to control it is to keep adequate ambient conditions, at least during first 7 days:

- humidity:  $\geq 95\%$
- temperature:  $> 15^{\circ}\text{C}$

Other methods to control curing are adding special polymers that avoid too fast water evaporation.

### 3.4 GFRC Mechanical Properties

Mechanical properties after 28 days for a 10 mm GRC plate are:

Tab. 1 GRC Mechanical Properties

	<b>Units</b>	<b>SPRAY-UP</b> (manual, automatic)	<b>PREMIX</b> (vibration-cast, spray-up)
AR-Glass fibres (% w.)	%	5	3
Weigth per surface	Kg/m <sup>2</sup>	20	20
Sandwich panel(*)	Kg/m <sup>2</sup>	44	44
Coef. of thermic dilation	mm °C	10-20·10 <sup>-6</sup>	10-20·10 <sup>-6</sup>
Freeze-thaw (BS4264-DIN274)		No change on mechanical properties	No change on mechanical properties
UV Light		No degradation	No degradation
Thermic isolation	W/m°C	5.3	5.3
Sandwich panel(*)	W/m°C	0.4	0.4
Acoustic reduction	dB	30	30
Sandwich panel(*)	dB	47	47
Flexural Strength			
Modulus	MPa	20-30	10-14
Elastic limit	MPa	7-11	5-8
Tensile Strength			
Modulus	MPa	8-11	4-7
Elastic limit	MPa	5-7	4-6
Impact Resistance	Kj/m <sup>2</sup>	10-25	10-15
Modulus of Elasticity	GPa	10-20	10-20
Tensile Strain to Failure	%	0.6-1.2	0.1-0.2

(\*): Sandwich panel built with an expanded polystyrene layer of 110 mm and two GRC panels of 10 mm on each side

## 4. CONCRETE

Despite GFRC is the main application area of glass fibres reinforcement, with more than 35 years of experience; they are also used for reinforcing concrete (GRC), alone or with steel meshes or rebars. The aim is, as always, producing lighter and better performing pieces.

Most common applications are: ready-mix, dry-mix and precast concrete.

### 4.1 Ready-mix concrete

Glass fibres are added to the wet concrete just before its application to avoid plastic settlement cracking, plastic shrinkage and long-term shrinkage. Typical dosage is 600 g of fibres per 1 m<sup>3</sup> of concrete.

## 4.2 Dry-mix concrete

Fibres are added to the dry concrete to have a “ready to use” mixture. Main application is render. Fibres give better resistance to impact and less water permeability.

Ready-mix is addressed to the building sector, while dry-mix is more used in small works at home (“do it yourself”).

## 4.3 Precast concrete

Main benefits of fibres are avoiding cracking when demoulding concrete elements, in addition to it there are new applications under development:

- encapsulation: concrete pieces can be produced with a mortar permanent formwork. If this permanent formwork is produced in GRC, total composite performances improve.
- Fibre Reinforced Plastic rebars: structural steel rebars are being substituted nowadays by new materials. FRP rebar are rust and corrosion resistant and have already shown mechanical properties as high performing as steel ones.

## 5. CONCLUSIONS

AR-Glass fibres are very attractive reinforcements for mortars and concretes with high advantages compared to other types of fibres, in terms of cost and properties. Final composite is long-lasting, with high flexural, compression and tensile resistance, less water permeability, better resistance to atmospheric agents and non combustible.

Glass fibres permit also to create complicated shapes and thin elements without cracking. Load in structures is reduced as well as maintenance needed, without losing mechanical performance. Thus, glass fibre reinforcement applications in the building sector are enlarging and diversifying every day.

## 6. REFERENCES

- Majundar, A. J. and Laws, V.: “Glass Fibre Reinforced Cement”  
MANUAL FORTON: “Ciment Renforce de Fibres de verre”  
CEM-FIL INTERNATIONAL: “Guías de Proyección y Premezcla”  
CEM-FIL INTERNATIONAL: “Cem-FIL GRC Technical Data”  
Jiménez Montoya, P.; García Meseguer, A. and Morán F.: “Hormigón Armado”  
Bijen, J.: “Improved Mechanical Properties of Glass Fibre Reinforced Cement by polymer modification”  
Gliniki M. A.: “Impact performance of Glassfibre Reinforced Cement. Plates subjected to accelerated Ageing”  
Barros, A.: “El Cemento Reforzado con Fibras de Vidrio en España. Asociación Española de Fabricantes de GRC”  
Martinola, G.; Meda, A.; Plizzari, G. A. and Rinaldi, Z.: “An Application of High Performance Fiber Reinforced Cementitious Composites for RC Beam Strengthening”, Eds. By: Carpinteri, A.; Gambarova P.; Ferro, G. and Plizzari, G., 6th International Conference on Fracture Mechanics of Concrete and Concrete Structures, 17-22 June 2007, Catania, Italy, vol. 3, pp 1541-1548  
Regás, F. J. and Bolaños, J. C.: “Piedra Moldeada”, *GRC y Hormigón Arquitectónico*

## **SHEAR CAPACITY OF STEEL FIBER REINFORCED CONCRETE BEAMS**

*Minh Long Nguyen, Msc, Marián Rovňák, Assoc. Prof. PhD.  
Department of Concrete and Masonry Structures  
Faculty of Civil Engineering, Technical University of Košice  
04200 Košice, Slovakia*

### **SUMMARY**

The paper presents test results of steel fibre reinforced concrete beams (SFRCB) subjected to shear force. The effect of types and amounts of fibres on shear capacity of SFRCB was investigated. Two types of steel fibres Dramix: short straight fibres OL 6.0/0.16 and long hooked end fibres ZP305 30/0.5 were used. Experimental results were compared with theoretical results obtained by means of semi-empirical formulas, proposed new formula for estimation of shear capacity and FEM simulation. Test results indicate that fibres significantly improve shear capacity of SFRCB. The comparison of test results with theoretical predictions of shear capacity shows a very good agreement.

### **1. INTRODUCTION**

In general, adding of steel fibers to concrete matrix is to improve tensile strength as well as ductility of concrete. In case of conventional steel reinforced beams, steel fibers can significantly increase their loading capacity and improve their behaviour in shear. Using combination of short and long steel fibers can partly limit process of initiation and propagation of cracks and prevent concrete structures before sudden collapse. It is assumed that the short fibers, which are uniformly dispersed in the whole of concrete volume, bridge microcracks, and long steel fibers are effective in first stages of macrocracks initiation.

In the paper, an investigation carried out on 28 SFRC beams was reported. The main purposes of the investigation are: to study the influence of fiber volume on shear capacity of SFRC beams subjected to shear force for individual types of fibers as well as combinations; to introduce a new formula for estimating shear capacity of steel reinforced concrete beams; to present a FEM simulation of SFRC beams; to evaluate the accuracy of some existing formulas, the new formula and the FEM simulation based on experimental results.

### **2. EXPERIMENTAL PROGRAM**

The present experimental program consists of 7 series designated A to G of SFRC beams having identical rectangular cross section of  $150 \times 250 \text{ mm}$  with  $220 \text{ mm}$  effective depth. The span length of the beams is  $1050 \text{ mm}$  with a shear span length of  $265 \text{ mm}$ . A total of 28 beams were tested under non-symmetrically placed concentrated load to failure. Details of test beams can be seen in Fig. 1. The test beams were made from self-compacting concrete which contained Portland cement, natural sand, coarse aggregate, crushed limestone and plasticizer (Tab. 1). Two types of Dramix steel fibers: short straight fibers OL 6.0/0.16 and hooked-end fibers ZP305 30/0.5 (glued together into bundles) were used in the test program (Tab. 2).

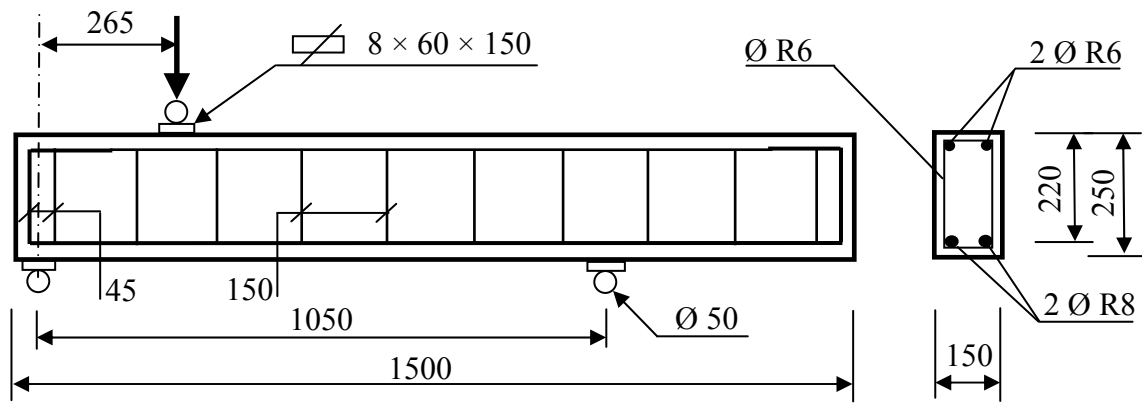
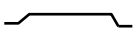


Fig. 1 Details of tested beams

Tab. 1 Concrete mix proportions

Material	Weight (/m <sup>3</sup> )
Cement 42.5 R, kg	460
Crushed limestone, kg	120
Sand 0-4, kg	1000
Coarse aggregate 4-8, kg	600
Plasticizer Stachement, l	4.5
Water, l	200.5 (w/c = 0.436)

Tab. 2 Fiber types

Fiber	Fiber shape	Length (mm)	Cross section	Cross-section area (mm <sup>2</sup> )	Tensile strength (MPa)	Elastic modulus (GPa)
OL6/0.16	—	6	circle	0.02	2000	200
ZP305		30	circle	0.2	1100	200

The beams were loaded by a 500 kN hydraulic testing machine with loading control in increments of 5 kN up to failure (Fig. 2). Loading rate was approximately 15 kN per min. At each load level midspan deflections were recorded.



Fig. 2 Test arrangement

### 3. NEW FORMULA FOR ESTIMATION OF SHEAR CAPACITY OF SFRC BEAMS

Based on fracture mechanics approach and recommendation of Rilem (Vandewalle et al., 2000) for analysis of SFRC beams subjected to shear, a new formula for estimating shear capacity of SFRC beams was proposed:

$$V_u = \frac{\sqrt{20(0.385a_T^2 + 0.707a_Tz_c)}}{a_C} \sqrt{G_f A_s E_s b} + 0.41 \sum_{i=1}^n F_i \tau b a_T + V_{sti},$$

where  $k=1$  for four-point loading tests,  $k=L/(L-a)$  for three-point loading tests, in which  $L$  is the theoretical span;  $a$  is the shear span of beam;  $a_T$  is the horizontal projection length of the diagonal crack;  $z_c$  is the arm of the internal forces;  $a_C$  is inclined-shear cracking position of beam;  $G_f$  is fracture energy of concrete;  $A_s$  is cross section area of the longitudinal tensile bars;  $E_s$  is elasticity modulus of longitudinal tensile bars;  $b$  is beam width;  $F_i$  is fiber factor  $i^{th}$ -fiber type;  $\tau$  is average fiber-matrix interface bond stress and  $V_{sti}$  is shear capacity of stirrups.

### 4. NUMERICAL SIMULATION

Two specific structural analysis programs, Lusas and Atena, based on finite elements method (FEM) were used for simulation SFRC beams subjected to shear force. The beams were modeled in plane. 2-D elements, which are used, had quadrilateral shapes with quadratic interpolation because these elements give theoretically the most accurate results. In the program Lusas, the material model “Multi Crack Concrete” was used for modeling material concrete, while, in the program Atena, concrete material was modeled by using material model SBETA embedded fixed crack model. Concrete strengths and yield stress of steel bars were given by experimental results. Elastic modulus of concrete was calculated according to Pan (Pan, 1996). Other parameters in both programs are generated automatically, except for concrete fracture energy  $G_f$  in the program Atena which was given by results from fracture tests. Bond between concrete and bars was perfectly. Loading as well as loading increments were given similarly as in experiment.

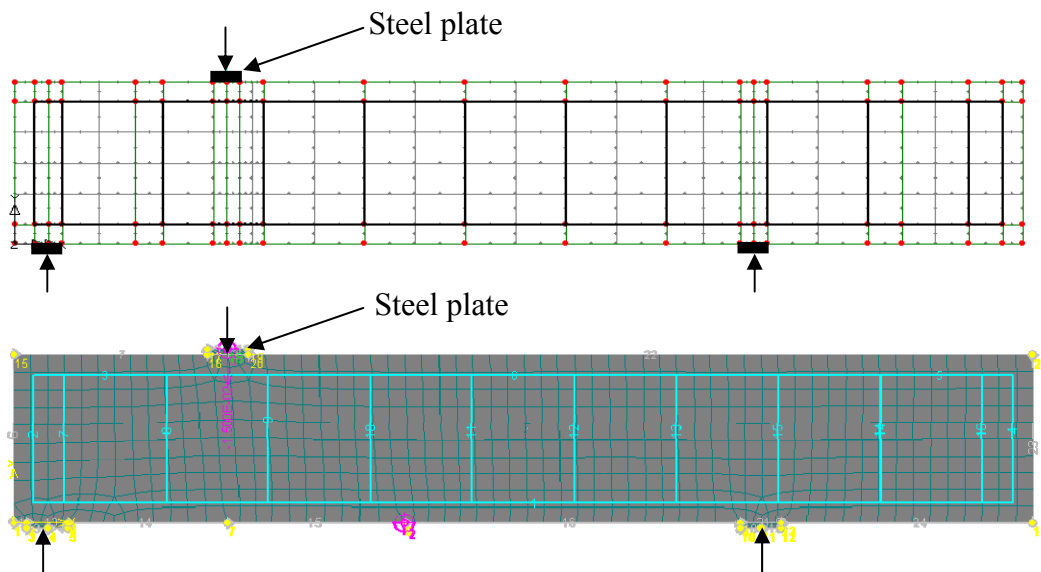


Fig. 3 FEM model of beam: (a) – Lusas, (b) – Atena

## 5. RESULTS

### 3.1 Failure of specimens

The beams without fibers failed predominantly in shear (Fig. 4). In beam series that contained fibers, the beams failed in shear, however mostly, the fibers changed the failure mode of the beams from shear to flexure or a combination of shear and flexure and in some cases, fibers changed the failure mode of the beams from shear to shear compression. The change of failure modes of beams from shear to flexure is maybe due to significant increase of shear strength of beams that is caused by presence of fibers.



Fig. 4 (a) – Shear crack initiation, (b) – Beam failure

### 3.2 Load -deflection responses

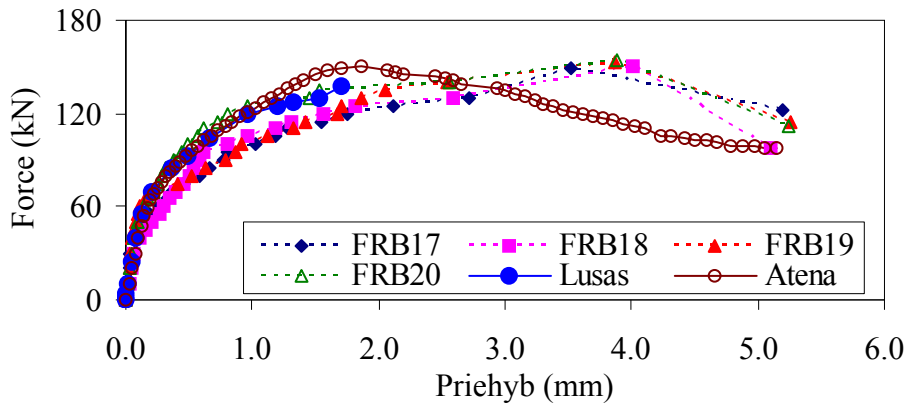


Fig. 5 Load-deflection diagrams for beams in series E

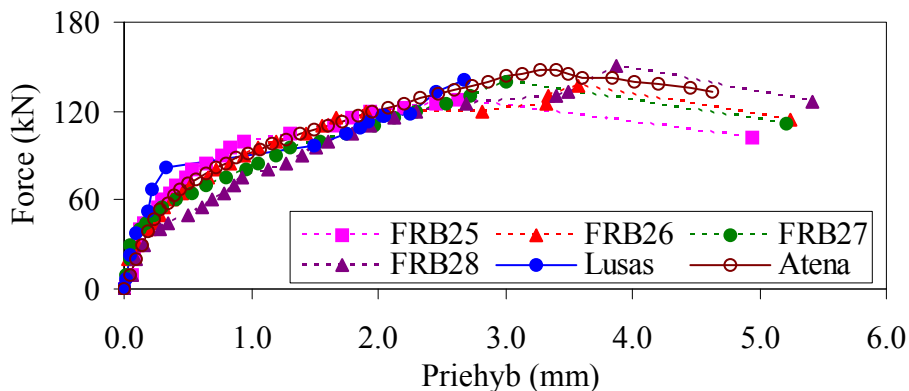


Fig. 6 Load-deflection diagrams for beams in series G

Figs. 5 and 6 show behaviour of some SFRC beams obtained from experiment and FEM simulation. The behaviour of beams from FEM simulation is nearly identical to behaviour of experimental beams.

### 3.3 Shear loading capacity

Values of shear loading capacity of beams obtained from the experiment, calculation according to existing formulas and new formula and from FEM simulation are summarized in Tab. 3. An evaluation of theoretical results obtained from formulas and FEM simulation is shown in Fig. 7. Results show that fibers improved loading capacity of the beams. Maximum increase in the shear capacity is obtained in the beams reinforced by fiber combinations of 0.6% OL6.0/0.16 and 0.6% ZP305 (series E). The increase of shear capacity of the beams contained only fibers OL6.0/0.16 is almost negligible (2.7% and 5%).

Tab. 3 Results obtained from experiment, theoretical calculation and FEM simulation

Beam series	Fiber volume		$f_c$	$f_{sp}$	$V_u$ (kN)									
	OL6/0.16	ZP305			Experiment	Sharma	Narayanan et al	Ashour et al.-ACI	Ashour- et al Zsutty	Imam et al.- fc	Imam et al.- fsp	Lusas	Atena	New formula
	$V_f$ (%)		(MPa)	(MPa)										
A	0	0	52.2	3.10	<b>121.0</b>	115	123	140	124	179	186	113.2	107.6	<b>122</b>
B	1.2	0	53.2	3.60	<b>127.0</b>	126	135	182	154	172	199	129.6	125.9	<b>130</b>
C	1.6	0	54.1	3.81	<b>123.3</b>	131	144	197	164	182	201	107.9	105.7	<b>132</b>
D	0	0.8	55.8	3.91	<b>145.3</b>	133	154	232	189	183	204	135.5	146.8	<b>139</b>
E	0.6	0.6	54.6	3.53	<b>151.8</b>	125	146	230	188	181	203	137.7	150.4	<b>138</b>
F	0.8	0.4	53.4	3.54	<b>136.3</b>	125	142	213	170	171	202	116.9	136.8	<b>135</b>
G	0.4	0.8	54.9	3.40	<b>138.8</b>	122	145	245	176	175	204	141.5	147.8	<b>140</b>

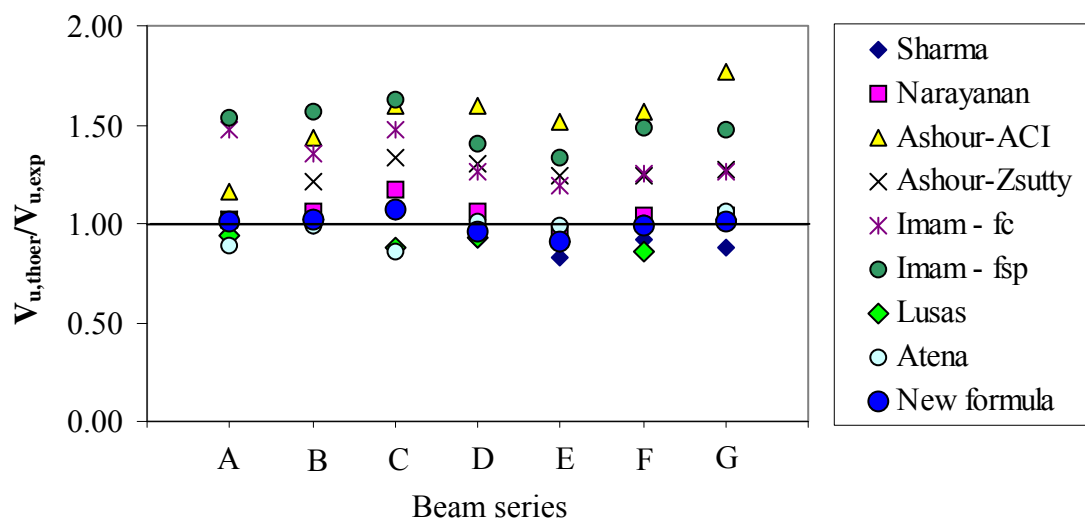


Fig. 7 Evaluation of theoretical results obtained from formulas and FEM simulation



## 6. CONCLUSIONS

Experimental results show that using fiber combinations significantly improved shear capacity of beams up to 25.5% compared to that of conventional beams. The most effective fiber combination is that contains an equal or higher volume proportion of ZP305 fibers in combination. The less ineffectiveness of OL6.0/0.16 fibers (in comparison with ZP305 fibers) in the increase of concrete shear strength could be related to unsuitable shape (straight and short) and small aspect ratio ( $l/d_f = 37.5$ ) that causes an inadequate bond with concrete matrices and this fact effects evidently in a negative way to improvement of shear capacity of beams.

The results show high accuracy of new formula for estimation of shear capacity of SFRC beams. The mean ratio of the theoretical shear capacity calculated by new formula to observed experimental shear capacity  $V_{u,theor}/V_{u,exp}$  is 1.01.

Results obtained from FEM simulation give good agreement with test results. The mean ratio of the shear capacity obtained from program Lusas and Atena to observed experimental shear capacity  $V_{u,theor}/V_{u,exp}$  is 0.94 and 0.97, so the above presented computational models could be used for a proper simulation of the behaviour of concrete beams subject to shear force and predicting their shear resistance as well as shear cracking force.

## 7. ACKNOWLEDGEMENTS

The paper was supported by the Slovak Grant Agency of Ministry of Education of the Slovak Republic and the Slovak Academy of Science (Project No. 1/2646/05 and No. 1/4201/07).

## 8. REFERENCES

- Ashour, S. A., Hassanain, G. S., and Wafa, F. F. (1992), "Shear Behaviour of High Strength Fiber Reinforced Concrete Beams", *ACI Structural Journal*, V.89, No.2, Mar.-Apr., 1992, pp. 176-184.
- Imam, M., Vandewalle, L., and Mortelmans, F. (1994), "Shear Capacity of Steel Fiber Strength Concrete Beams", *ACI International Conference on High Performance Concrete*, Singapore, SP-149, V. M. Malhotra, ed., American Concrete Institute, Detroit, USA, 1994, pp. 227-243.
- Narayanan, R., and Darwish, I. Y. S. (1987), "Use of Steel Fibers as Shear Reinforcement", *ACI Structural Journal*, V.84, No.3, May-June 1987, pp. 216-227.
- Pan, N. (1996), "The Elastic Constants of Randomly Oriented Fiber Composite: A New Approach to Prediction", *Science and Engineering of Composite Materials*, Vol. 5, No. 2, 1996, 63-72.
- Sharma, A. K. (1986), "Shear Strength of Steel Fiber Reinforced Concrete Beams", *ACI Journal, Proceedings* V. 83, No. 4, July-Aug. 1986, pp. 624-628.
- Vandewalle, L., et al. (2000), "Recommendations of Rilem TC162-TDF: Test and Design Methods for Steel Fibre Reinforced Concrete:  $\sigma$ - $\epsilon$  Design Method", *Materials and Structures*, V. 33, Mar. 2000, pp. 75-81.

## **SIMULATION AS A TOOL FOR DECISION-MAKING PROCESS FOR APPLICATIONS OF FRC IN PRECAST ELEMENTS**

*Alena Kohoutková, Iva Broukalová*  
*CTU in Prague, Faculty of Civil Engineering, Czech republic*  
*Thákurova 7, 166 29 Praha 6,*  
*[akohout@fsv.cvut.cz](mailto:akohout@fsv.cvut.cz), [iva.broukalova@fsv.cvut.cz](mailto:iva.broukalova@fsv.cvut.cz)*

### **SUMMARY**

An interesting project is developed at our department. In cooperation with industrial sphere a research project inquiring feasibility of fibre concrete precast elements is being developed. Possibilities of use of fibre concrete in precast elements, manufacturability of fibre concrete elements and suitable type of fibres for particular FRC member are inquired into. Exploitation of fibre concrete shall bring benefits and savings which lies in decrease of conventional reinforcement or reducing of thickness of elements. In the paper three members – structural element, concrete precast pipe and a non-bearing member are discussed, usefulness of the fibre concrete exploitation and possibilities of modelling and simulations in the analysis, decision-making process and considerations of fibre concrete benefits and choose of a convenient fibre concrete in a particular member.

### **1. INTRODUCTION**

Fibre-reinforced concrete is a contribution to the range of structural materials. Benefit of fibres in fibre reinforced concrete is in improvement of the performance of FRC element in comparison with the plain concrete one but also in application in reinforced concrete and prestressed concrete members. The efficiency of fibre concrete utilisation is managed only if appropriate fibre concrete with element suited to use of FRC are utilized. Several industrial manufacturers have accepted an offer of cooperation with the department of concrete and masonry structures in application of fibre concrete in structural elements. The aim of the joint work is finding out of members, where use of fibres will be a contribution, determination of a convenient type of fibre concrete and verification of manufacturability of the fibre concrete element. In the initial stage of project elements suitable for exploitation of fibre concrete were searched and a pilot plant of the elements was prepared. An analysis of a certain element was performed for service load and for ultimate load to determine critical sections of the element and shortcomings that could be modified by use of fibre concrete. A fibre concrete mixture that would improve the element behaviour was designed with proper fibres for particular element. In this stage of the project preferably smaller precast elements were chosen that are not subjected to high strain and thus they are designed to satisfy the minimal reinforcement ratio just to prevent brittle failure of the element. In these cases use of fibre concrete is especially efficient thanks to enhancement of ductility by adding of fibres.

### **2. BRIDGE CORNICE**

Cornice is not a load-bearing part of the bridge; nevertheless it can be subjected to substantial strain, salts treatment and atmospheric effects. Because of aesthetic requirements on cornice, to provide bond of anchors and prevent corrosion and pull-out of anchoring elements it is necessary to avoid excessive cracking. The main reason of cracking of cornice are principally

volumetric changes. A SSFRC (Synthetic Structural Fibre Reinforced Concrete) is usually a effective solution to this kind of cracks. Prior to detail determination of fibre content a preliminary analysis was performed where the elastic stresses were calculated.

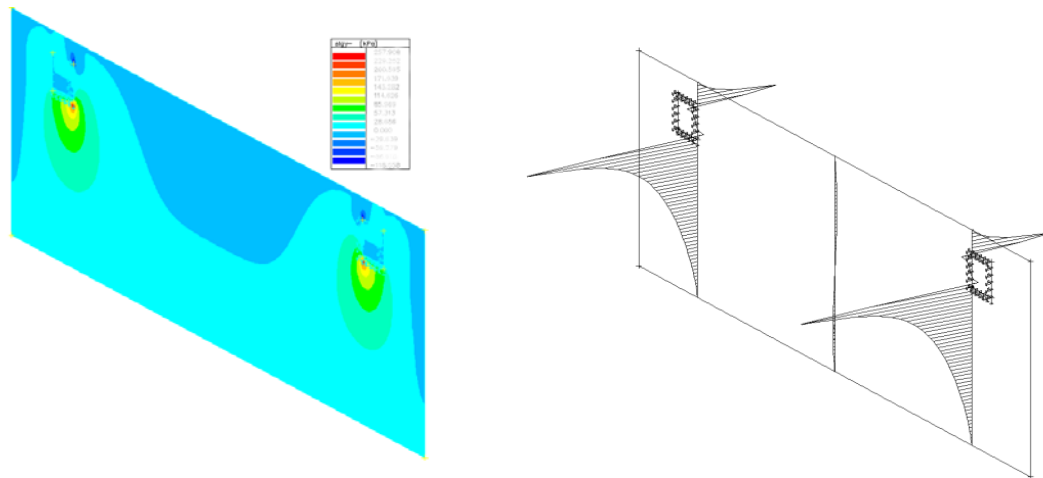


Fig. 1 Stress state from the preliminary analysis of the cornice

Knowing the stress state and considering demands on durability of the cornice a SSFRC with 1% of polypropylene fibres was chosen for the testing of workability of the fibre concrete mixture in the precast-plant devices and manufacturability of the element. Fibre concrete shall be a contribution to better service, behaviour and durability of the element. Other problem that may be solved by use of fibre concrete is cracking and failure during transport and resulting fall of the element and injure of pedestrians and damage of passing vehicles. The ductile behaviour of fibre concrete member shall enable reduction of conventional rebar reinforcement or decrease of thickness of the element. The manufacturability of the cornice has been verified in a pilot plant and the made cornice was used in a bridge build-up. Nowadays in a model simulation possibilities of reduction of conventional reinforcement are investigated.

### 3. FIBRE CONCRETE BEAM WITH CONVENTIONAL BAR REINFORCEMENT

The main goals of the fibre concrete beams research were to prove the benefits of fibre concrete in the structural element behaviour and to verify possibilities of material modelling in FEM analysis.

Since an unlimited number of fibre concretes with different properties may be designed and produced a simple procedure for determination of fibre concrete material parameters for FEM structural analysis had to be proposed. A routine exploiting results of simple laboratory test and inverse analysis has been experienced at our department. Basic laboratory specimens are tested; cubes in compression and splitting tensile test and prisms in a four-point flexural test. The flexural test is modelled in a FEM program, where compressive strength and tensile strength from cube testing are the inputs for the first run of finite element analysis. FE analysis is performed for several times and input material parameters are varied until a satisfactory coincidence of load-deflection (L-d) curve measured and L-d curve calculated by means of FE analysis is reached. This way of material parameters fitting is called inverse analysis. Material properties obtained in inverse analysis are used in further analysis of a member made of investigated fibre concrete.

To confirm correctness of proposed procedure the validity of material model from inverse analysis was checked in a research described below.

### 3. 1 Possibilities of numerical simulation of the structural element

Two sets of beams were prepared and tested in a flexural laboratory test. Setup of the test is depicted in the Fig. 1. Dimensions and load scheme of the beam for the case study were selected for the reason of separation of various parameters on structural behaviour in bending. One set of polypropylene fibre concrete beams with longitudinal steel bar reinforcement and a comparative set of beams from common concrete reinforced with identical steel bar reinforcements were prepared.

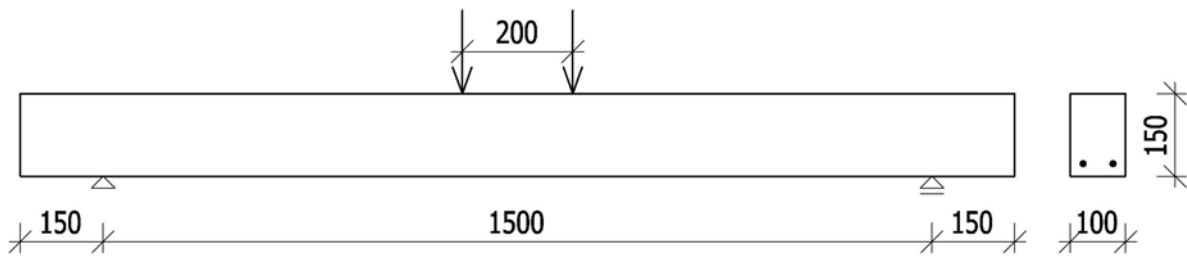


Fig. 2 Sketch of the laboratory loading setup

Comparing of results of bending test of reinforced concrete and reinforced fibre concrete beams from experiment proved benefits of fibre concrete; fibre concrete beams have higher load-bearing capacity (Fig. 3), non-brittle mode of failure and more favourable layout of cracking.

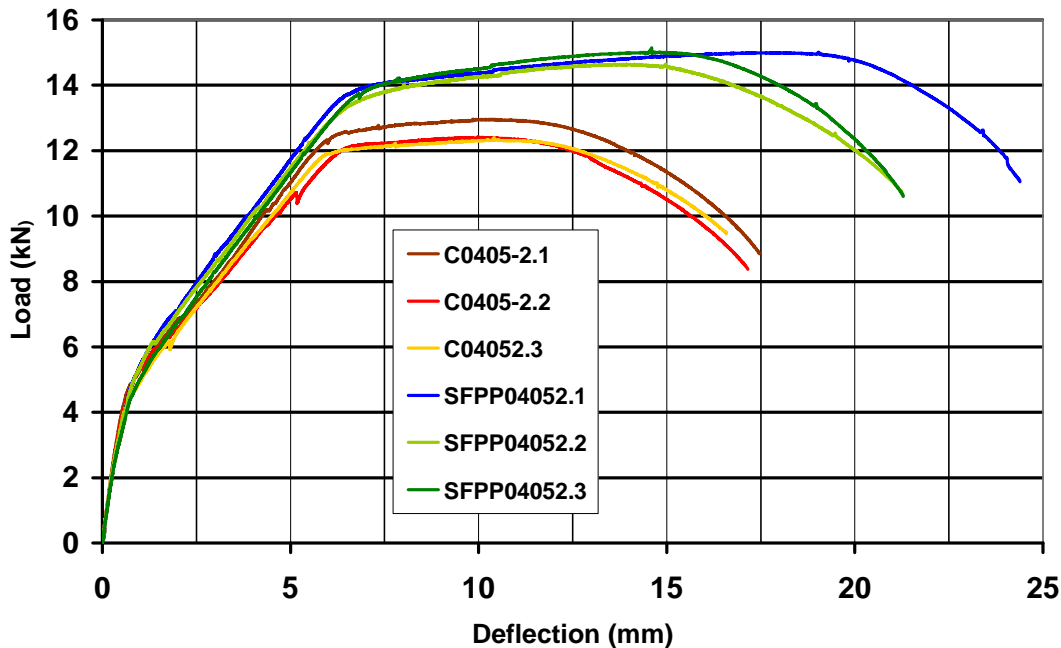


Fig. 3 Load –deflection curves for concrete beams (C) and fibre concrete beams (SFPP)

In the process of verification the main task was a simulation of a prescribed test using acquired material relation. The result of numerical modelling is load–deflection relation,

which is compared with measurements. Fig. 4 shows an output from the program for the tested beam. Material properties confirmed by the inverse analysis were used for FE analysis of a fibre concrete beam with conventional reinforcement.

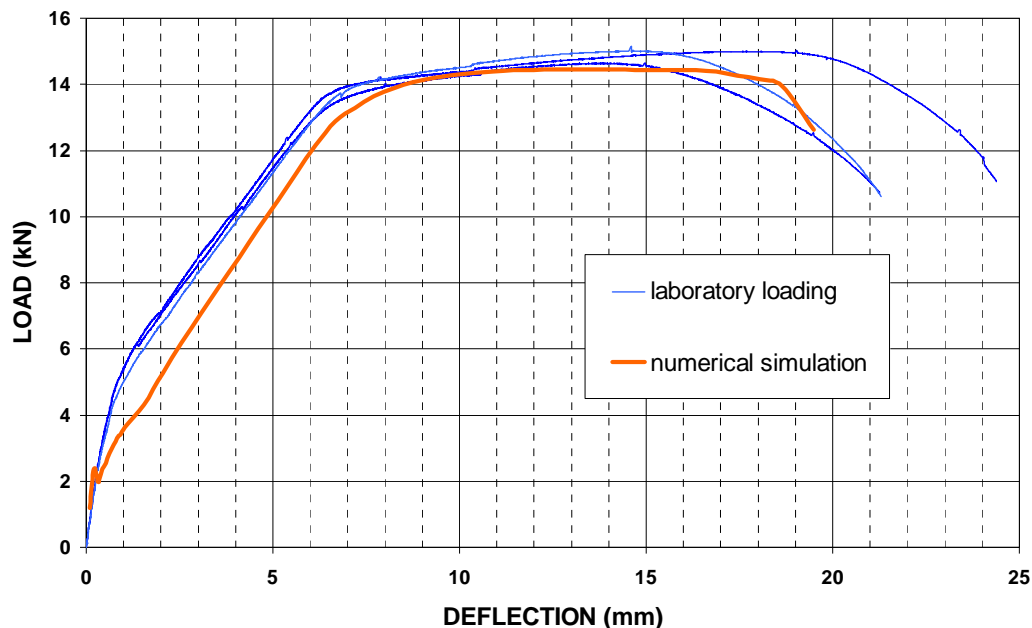


Fig. 4 Comparison of load –deflection curves of fibre concrete beams (laboratory loading) and ATENA simulation

The experiments and analysis confirmed that numerical simulation relates to real behaviour of fibre concrete member and may replace some real experiments.




#### 4. SEWER PIPES

Sewer pipes are made in two forms: one from plain concrete, second from reinforced concrete. Pipes made from plain concrete have satisfactory load-bearing capacity, but after the first crack is formed, a brittle failure of the pipe follows. To avoid brittle failure reinforcement which consists of main spiral reinforcement and secondary longitudinal reinforcement is provided. Nevertheless after forming of the first crack the use of the pipe is restricted on account of wide cracks and lost of watertight of the sewer pipe. Fibre concrete may solve both problems mentioned; fibre concrete members fail in a non-brittle mode and cracks have more favourable lay-out and may satisfy demands on water-tightness.

To prove the suppositions, an experiment with three types of fibres was performed. There were made pipes with diameter 600 mm from two different types of steel fibres and polypropylene fibres and comparative pipes from plain concrete and reinforced concrete. In the experiment the load was applied on the top of the pipe and load at first crack and ultimate load were measured.

The experiments showed that pipes from fibre concrete withstand higher load until first crack occurs than pipes from plain concrete. Pipes with polypropylene fibres have roughly the same load at first crack as pipes from reinforced concrete (with conventional bar reinforcement). Pipes with fibres have even higher cracking-load than reinforced concrete pipes (tab. 1).

Tab. 1 Table of tested materials and results of testing

Material of the sewer pipe		Load at the first crack	Ultimate load
Fibre concrete with long steel fibres ( $l = 50$ mm, strength $f_t = 1000$ MPa)		148 kN	123 kN
Fibre concrete with short steel fibres ( $l = 25$ mm, strength $f_t \sim 400$ MPa)		136 kN	collapse after first crack
Fibre concrete with polypropylene fibres		116 kN	not measured
Plain concrete		105 kN	collaps after first crack
Reinforced concrete		120 kN	145 kN

The increase of the cracking-load and ultimate load (achieved for SFRC) is not necessary from the point of view of the service of sewer pipes. Hence in subsequent steps of the development, an analysis is performed to determine either thinner wall of the pipe or fibre concrete with lower strength.

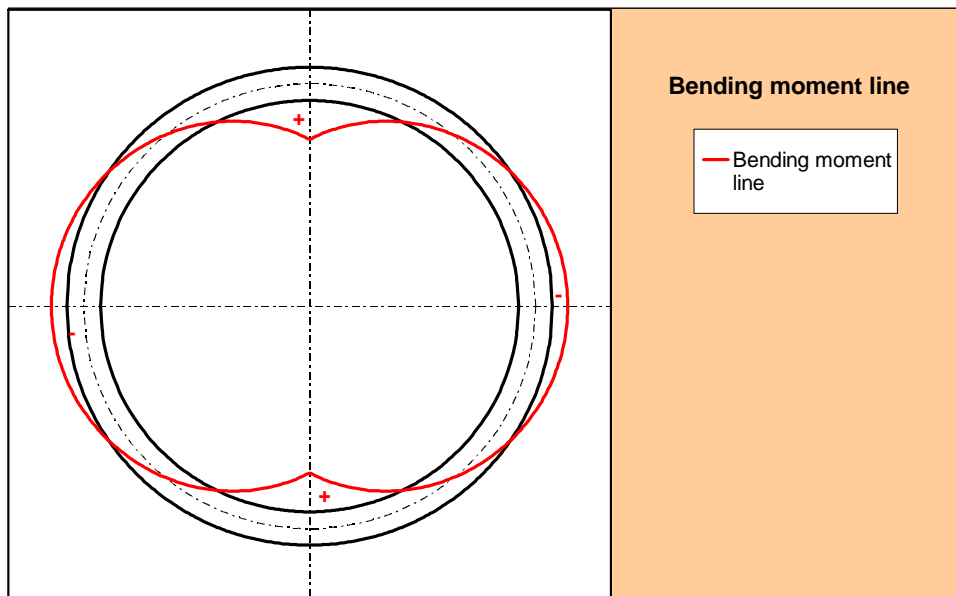


Fig. 5 Layout of the bending moment of the annular section due to the peak load

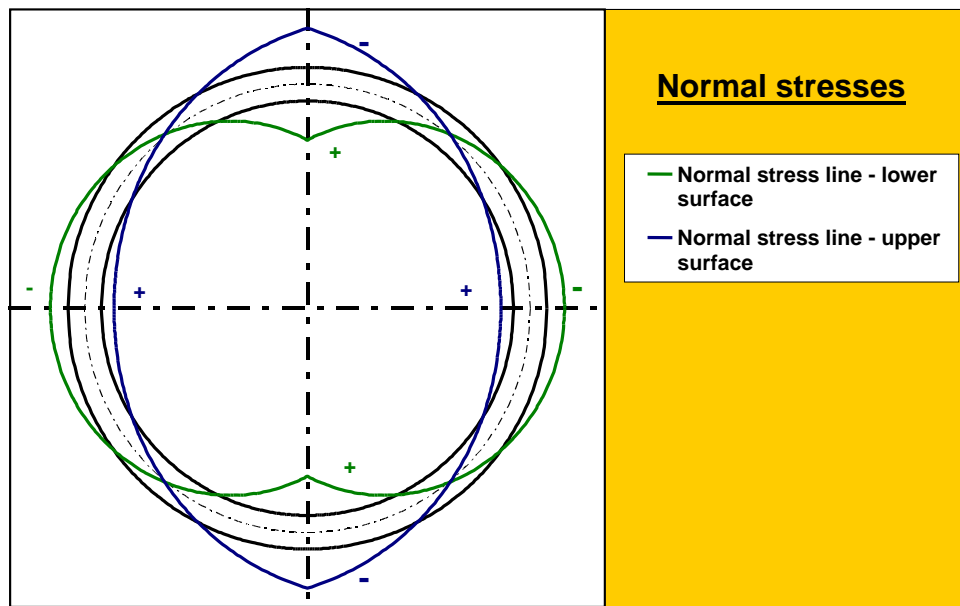


Fig. 6 Layout of the of the stresses of the annular section due to the peak load

Possibilities of decreasing of the pipe wall thickness are calculated in a simple routine (Fig. 5, Fig. 6) assuming that the material will remain same as in performed experiments, as the suitability of the material was proved. On the other hand there is an opposite way where dimensions of the pipe will remain same and a fibre concrete with new properties is sought. In this case collaboration with technologist and further verification of designed fibre concrete mixture is necessary. Which of these ways would be chosen is a matter of multi-criterion analysis considering economical aspects and possibilities of the manufacturer.

## 5. CONCLUSIONS

Use of fibre concrete brings cost saving concerning manufacturing of the element. Members from fibre concrete could be thinner which shall save transport costs and spending on expensive and energy demanding materials as rebar reinforcement and cement.

Proper choice of material plays an important role in good design of fibre concrete member. The numerical simulation may become a strong tool in the analysis; it may reduce the need of laboratory experiments and shall help in the decision-making process which fibre concrete (if any) is suitable for use in a particular structure.

## 6. ACKNOWLEDGEMENTS

This outcome has been achieved with the financial support of the Ministry of Education, Youth and Sports, project No. MSM6840770001, within activities of the research project 1H-PK2/17. The support of the Grant Agency of the Czech Republic Grant Projects No. 103/06/1559 and 103/05/2226 is also gratefully acknowledged.

## 7. REFERENCES

Kohoutková, A., Broukalová, I., Vodička, J. (2006): "Aplikace vláknobetonu v prefabrikaci", *Sborník 13. betonářské dny 2006. Praha: ČBS - Česká betonářská společnost ČSSI*, p. 189-195. ISBN 80-903807-2-7

## **APPLICATION OF GLASS METAL FIBRES TO IMPROVE THE RESISTANCE OF CONCRETE**

*Béla Magyari<sup>1</sup> and Géza Tassi<sup>2</sup>*

<sup>1</sup> *PhD, Manager, INNOIR Ltd. Kecskemét, Hungary*

<sup>2</sup> *D.Sc., Professor, Budapest University of Technology and Economics*

### **ABSTRACT**

Nowadays a wide range of fibres are used for fibre reinforced concretes. This paper deals with laboratory tests and practical application of glass metal fibre reinforcement.

Two concrete mixes were applied for test specimens. The first variable of the test series was the volume percentage of glass metal fibres. A further variable was the age of the specimens. Prism parts were tested for compressive strength and prism form beams to investigate the flexural tensile strength.

The tests results show the benefit of application of glass metal fibres by comparison to plain concrete. Macro- and microscopic analyses were carried out, too. A series of tests were completed to compare the resistance of glass metal fibre reinforced and plain concrete under frequently repeated load, to predict the applicability of glass metal fibre reinforcement. Relatively small plates and cylindrical shells were produced and tested. All the results proved that members of such materials can be advantageously used for façade elements and for various accessories of buildings and bridges.

### **1. INTRODUCTION**

Fibre reinforced concretes were widely spread all over the world in the last decades in various fields of building industry (Balázs, Polgár, 1999). Besides steel fibres non-metallic materials are also widely used for fibre reinforcement (Magyari, Tassi, 2007). Glass metal fibres are important features for practical application. Fibres represent a special area because of the composition of the material and shape of the fibres (Ackermann, Fournier, 1981).

The concrete mix, the compaction, the curing and the time of hardening and mainly the fibre dosage are important features to be studied. The knowledge on mechanical behaviour of test specimens gives good advices for practical application. Therefore some important parameters were experimentally studied and the material was applied at a few small size structural elements.

### **2. THE MATERIALS AND THE MIX**

#### **2.1 The concrete**

The optimum concrete composition for the laboratory research work was determined experimentally. The applied concrete contained in weight percentage: 64% graded sand and gravel with maximum grain size  $D_{\max}=8$  mm and 16 mm respectively for two different concretes; 28.5% Portland cement C 52.5; 7.2% water; 0.3% plasticizer Mighty 100.



## 2.2 Glass metal fibre

The fibres were manufactured at the Csepel Iron and Metal Works in Hungary with a composition of  $Fe_{74}Cr_6B_{14}Si_6$ . The length of the fibres amounted to 40 mm, the average thickness to 0.036 mm, and the width to 1.65 mm. One side was smooth, the other was rough. According to carried out tests Young's modulus was 153 GPa and the tensile strength 1.3 GPa. The glass metal due to its special composition is free of corrosion (see Chanvillard et al., 2000).

## 2.3 Casting, compaction, curing

The fibres were added by dry mixing, after adding water and mixed the FRC was poured into moulds and compacted by a table vibrator. From the mix  $D_{max}=8$  mm  $40 \times 40 \times 160$  mm prisms were made, from the mix  $D_{max}=16$  mm  $70.7 \times 70.7 \times 250$  mm ones were produced. The under water curing was continued for 28 days (or seven days if they were tested at that age).

## 3 THE LABORATORY EXPERIMENTS

### 3.1 Compressive and flexural tensile tests

Specimens described in Chapter 2.3 were tested of age of 7, 28 and 90 days respectively.

The results of the compression tests (the smaller prisms loaded at a surface  $40 \times 62.5$  mm) and those of the flexural tests are given in Tables 1 and 2. The flexural test specimens of larger size were loaded as beams with 240 mm span by two concentrated loads at the third of the span.

Tab. 1 Experimental data of glass metal FRC with  $D_{max}=8$  mm aggregate

Fibre content Vol. %	Strength [MPa]					
	7 days		28 days		90 days	
	Flex.	Compr.	Flex.	Compr.	Flex.	Compr.
0	10.5	70.9	12.4	87.0	12.7	89.5
0.25	11.3	79.3	13.4	86.5	13.3	85.9
0.50	12.5	76.1	14.2	73.5	14.6	87.3
1.00	17.4	72.8	18.8	72.4	19.6	81.0

Flex. - Flexural tensile strength

Compr. - Compressive strength

Fibre content Vol. %	Strength [MPa]					
	7 days		28 days		90 days	
	Flex.	Compr.	Flex.	Compr.	Flex.	Compr.
0	8.5	51.4	8.7	59.0	9.2	81.2
0.12	8.6	57.3	9.8	55.6	9.9	85.1
0.25	9.4	54.3	10.0	64.2	10.3	75.0
0.50	10.7	55.5	10.8	60.0	11.4	72.2

It is to be mentioned that the toughness can be gained from the stress-deflection diagrams seen in Fig. 2.

### 3.2 Behaviour of glass metal FRC under frequently repeated load

The specimens for pulsating load were of the smaller prism mentioned in Chapter 2.3, the compression was transmitted at the 40×40 mm surface.  $D_{\max}$  was 8 mm. The fibre dosage was taken for 0.5. The results were compared to the case of plain concrete. The lower stress level was 5 MPa, the frequency 250 Hz.

The results are the following: The upper stress limit belonging to  $2 \times 10^6$  repetitions amounted to 35.2 MPa, while in case of 0.5 Vol.% glass fibre FRC this value was 50.4 MPa. For both data six tests were carried out, the mentioned fatigue strength values are mean data.

The fatigue tests were begun at age of 90 days in case of each specimen.

### 3.3 Testing the structure of concrete

Parallel to strength tests slides were cut from all specimens for macro- and microscopic analysis of structure of concrete. The experiences gained by these analyses were fed back to the design of the composition. It was succeeded that the entire surface of glass fibres should be well embedded into the cement paste. According to these tests, the convenient upper limit of grain size seems to be  $D_{\max} = 8$  mm (Fig. 1).

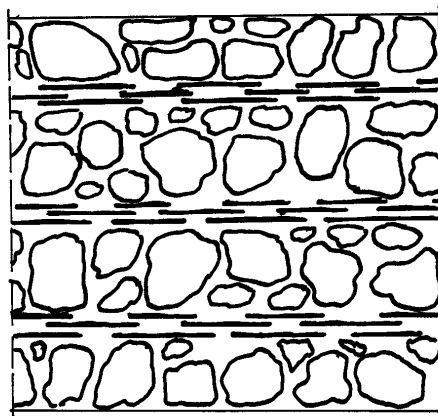


Fig. 1 Sections of glass metal FRC plate

### 3.4 Statements based on test results

As in case of FRC generally, the compressive strength is not affected by the dosage of fibres, rather more a slight reduction of strength can be observed. This can be stated in glass metal FRC, too. On the other hand, the flexural tensile strength increases by 54,3% if  $D_{\max} = 8$  mm at age of 90 days in case of 1.0 Vol.% glass metal fibre dosage. Speaking about comparison to non-metallic fibre reinforcement Based on the stress-deflection diagrams the toughness can be characterized as follows: If the toughness of glass metal FRC is taken as 100%, that in case of steel fibres is 87.6%, glass fibres 56.2%, polypropylene 44.6%, plain concrete 8.26%.

The analysis of the structure of the glass metal FRC concludes to the advice that the maximum grain size should not exceed 8 mm.

## 4 APPLICATION IN EXPERIMENTAL AND INDUSTRIAL STRUCTURAL ELEMENTS

### 4.1 Laboratory tests on plates

To study the phenomena playing role in the fibre reinforced fine mortar part of the concrete, 70×250×10 mm plates were produced with in plane arranged fibres (Fig. 1). These members were tested as simply supported elements spanning 240 mm, loaded by one concentrated line load at midspan. The fibres were arranged irregularly (Fig. 1).

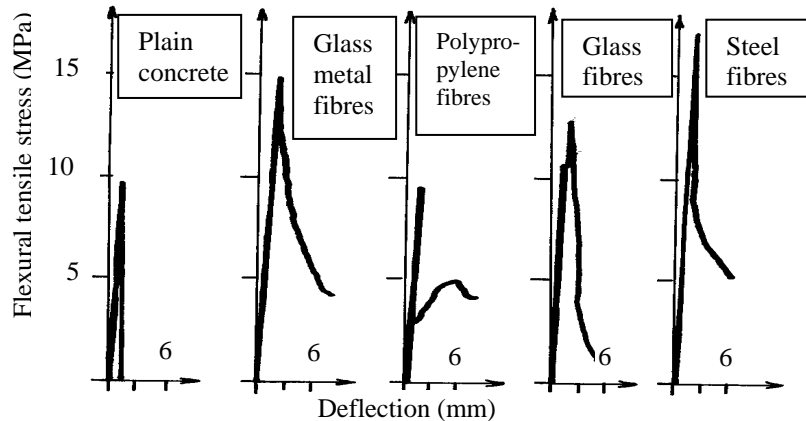


Fig. 2 Flexural tensile stress - deflection diagrams of tests on plain and different FRC plates, results of a comparative study, age: 28 days

Fig. 2 shows the flexural tensile stress – deflection curves of glass metal FRC slabs compared to plain concrete and other type FRC slabs made otherwise under the same conditions. The fibre length was 40 mm, the fibre content was 1.0 Vol. %.

### 4.2 Cylindrical shell elements and folded plates for facade

Among others, 30 mm thick glass metal FRC cylindrical members were made with 6000 mm length and 800 mm raise. The concrete mix was for 1 m<sup>3</sup>: 1493 kg aggregate with  $D_{max}=8$  mm; 600 kg Portland cement C 42.5, 22 kg glass metal fibre, 3 kg polypropylene fibre. The water-cement ratio was 0.35. The elements are used preliminarily as secondary parts of buildings.

An example for realization of glass metal FRC is the façade of an office building designed by architect I. Makovecz. The tympana are 20 mm thick folded plates produced of glass metal FRC (Fig. 3). This structural elements and many others show the practical applicability of the discussed material.



Fig. 5 Glass metal FRC folded plate elements with 20 mm thickness

## 5 CONCLUSIONS

Glass metal fibres perform an advantageous effect on mechanical properties of concrete. The influence on flexural tensile strength and on toughness is evident as shown by the laboratory tests. The behaviour of glass metal FRC is similar to concretes reinforced by metallic fibres but shows several advantages. Glass metal is stainless, this is important in case of exposed members. The higher toughness is advantageous considering the composite working of other structural parts and in case of many other effects. The high fatigue strength compared to other FRCs – to say nothing of plain concrete where the difference is 43% - enables glass metal FRC to serve structural parts under frequently repeated load.

The production of small plates and cylindrical shells as well as the use of the material in folded plates prove the practical applicability of the material. Such elements are fit to fulfil the requirements of different parts of façades and also accessories of bridges and other engineering structures.

## REFERENCES

- Ackermann, L., Fournier, G. (1981): "Reinforcement of concrete with metallic glass ribbons. *Fourth Internat. Conf. on Rapidly Quenched Metals*, Sendai, pp. 36-44.
- Balázs, L. G., Polgár, L. (1999): "Past, present and future of fibre reinforced concretes", *Proc. Fibre Reinf. Concr.*, Budapest, pp. 36-44.
- Chanvillard, G. Giraudon, G., Rogue, O. (2000): "Elements in stainless amorphous metallic fibre concrete", *Proc. 5<sup>th</sup> RILEM Symp.* Lyon, pp. 181-192.
- Magyari, B., Tassi, G. (2007): "Effect of non-metallic fibres on the concrete properties." *Proc. fib Symp.* Dubrovnik, pp. 367-374.



## **INNOVATIVE STEEL FIBRE REINFORCED COMPOSITE SLABS**

*Florian P. Ackermann, Jürgen Schnell*

*Kaiserslautern University of Technology, Institute for Concrete Structures and Structural Design*

*D-67663 Kaiserslautern, Paul-Ehrlich-Straße 14, GERMANY*

### **SUMMARY**

The paper deals with composite slabs using steel fibre reinforced concrete as topping. The conventional reinforcement will be substituted by the steel fibres. Thus, for continuous composite floors an efficient and economic slab system can be achieved. A first test series in order to verify the possible rotation capacity of continuous slabs was accomplished.

### **1. INTRODUCTION**

Conventional steel composite floors have established oneself as an extremely cost-effective floor system for domestic, commercial or industrial buildings. Significant advantages arise from the low construction costs and especially from the issue of saving time during the building process. In composite building construction the application of steel sheets keeping as long as possible and therewith the use of continuous composite floors has been proved to be an eminent productive construction method (Bode, 1998 and Sauerborn, 1995).

Researches in innovative composite slabs with steel fibre reinforced concrete topping are in progress at the Kaiserslautern University of Technology. Different types of slabs with varied geometries are looked on for the tests. Special attention should be paid to the redistribution of bending moments from the support to the field.

No conventional steel reinforcement have been applied: the hogging bending moment should only be carried by the steel fibre reinforced concrete. This innovative slab system comprises an enormous savings potential. By the use of steel fibre reinforced concrete all operations concerning the conventional steel reinforcement can be omitted. So, no labour-intensive steel fixing and reinforcement drawings are needed. The construction method allows an efficient progress of construction work. Depending on the floor area, an enormous time saving is possible.

### **2. COMPOSITE SLAB SYSTEM**

A composite slab consists of a cold-formed steel sheet covered with a concrete slab that normally contains a reinforcement mesh. A good mechanical interlock between concrete and steel sheet should be guaranteed in order to get the advantages of a composite section. This system is structurally very efficient, because it exploits the tensile resistance of the steel and the compressive resistance of the concrete. In the sagging bending moment area the steel sheeting acts as flexural tensile reinforcement of the construction. Over the intermediate supports, hogging reinforcement has to be built in, if a continuous bending action is going to be achieved. In case of the investigated innovative slab system, the hogging reinforcement will be completely substituted by steel fibre reinforcement. The attenuated hogging bending

moment is carried by the steel fibre reinforced concrete section. Its flexural resistance will not decrease considerably after cracking. Furthermore, it grants a good crack-distribution ability. Lots of small cracks will arise assuring an adequate rotation at the middle support.

The outstanding beneficial characteristics of the slab system in question are:

- Profile sheeting:
  - acts as stay-in-place formwork
  - constitutes bottom reinforcement for the slab
  - offers an immediate working platform and protects workers below
  - supports loads during construction
- Labour intensive steel fixing and reinforcement drawings can be omitted
- Enormous time saving in building process
- Due to its low weight the sheets can be placed by hand without using any crane
- Lower stock requirements needed
- Less deflection due to the continuous bending effect will occur
- Steel fibre reinforced concrete works advantageously with regard to fire protection

In Germany, the design of steel decking and composite slabs is regulated by DIN 18800-5:2007. Following this guideline their analysis may be made according to one of the following methods:

- Linear elastic
- Linear elastic with moment redistribution (up to 30 %)
- Rigid plastic global analysis provided that it can be shown that sections where plastic rotations are required have sufficient rotation capacity
- Rigid plastic global analysis without a check of the sufficient rotation capacity, only in case of usage of re-entrant steel sheeting and of reinforcement with a high ductility and in case of a maximum span of 6 meters
- Analysis of continuous slabs by approximation as a series of simply supported beams

Looking on continuous slab systems, special attention should be paid to the possible moment redistribution as well as to the plastic analysis. Thus, the use of full load bearing capacity of a continuous slab system can be made. In ultimate limit state or in case of bad workmanship (e.g. undersized fibre content - or worst case - no fibre content over the intermediate support) the system offers an adequate redundancy. A series of simply supported beams emerges and the steel sheeting keeps the slab in position.

### **3. TEST PROGRAM**

#### **3.1 First test series**

In a first test series, the possible rotation at the middle support of a two-span composite slab should be investigated. Therefore, only the area of the hogging moment was simulated and tested. The test setup is shown in Fig. 1. The span of the slab was 2.00 meters, the width 70 centimetres and the slab height 16 centimetres. In the middle of the span, the load was linearly set up by a hydraulic jack. It was increased in small load steps up to the failure load. The tests were carried out with displacement control so that as much information as possible could be recorded on the support behaviour. The loads at the crossheads were measured with load cells. The displacements and the end-slip were recorded with displacement transducers. In the middle and in the quarters of the span, strain gauges were applied to the top and the bottom of the

steel sheeting. The strain at the surface of the concrete slab was recorded with strain-measuring points.

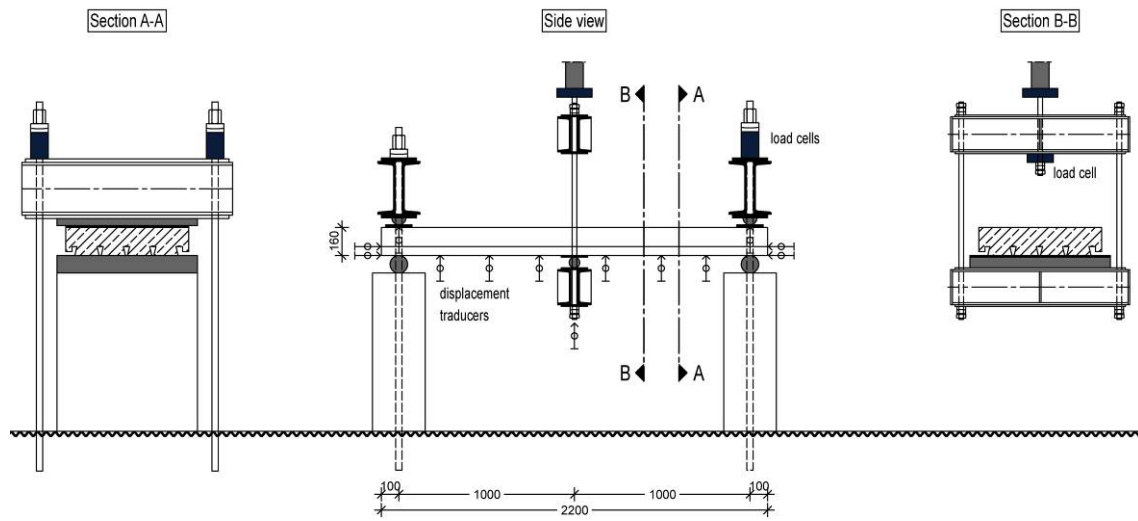


Fig. 1 Test setup

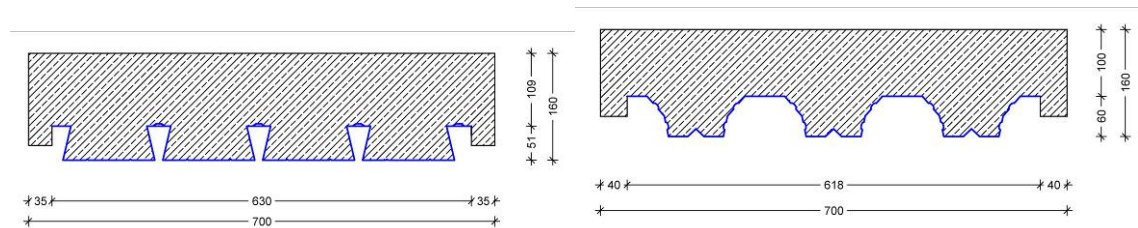


Fig. 2 Sections of the test specimens

### 3.2 Materials

#### 3.2.1 Steel sheeting

There are several types of steel sheets used for construction purposes, but they can be differentiated into two main categories: the re-entrant (dovetail) profiles with or without indentations and the trapezoidal profiles with web indentations or embossments.

In the first test series both geometries of steel sheeting were utilised. As a typical representative for the re-entrant geometry the Super HOLORIB SHR 51 sheet was used (Fig. 2 left), as typical representative for the trapezoidal geometry the HODY sheet was built in (Fig. 2 right). First of all the material characteristics of the sheeting were determined (Tab.1).

Tab. 1 Strength properties of steel sheeting

sheet type	yield strength $f_{yp}$ [N/mm <sup>2</sup> ]	tensile strength $f_{up}$ [N/mm <sup>2</sup> ]
HODY	364,71	430,64
Super Holorib SHR51	341,58	425,95



### 3.2.2 Steel fibre reinforced concrete (SFRC)

In the first test series, steel fibre reinforced concrete with a fibre content of 100 kg per cubic meter (or 1,27 Vol. %) was mixed. The corrugated TREFILARBED-TABIX fibre with a length of 50 mm and a diameter of 1.3 mm was applied. Its tensile strength averages 900 MPa. In order to get the material properties of the concrete different material tests were accomplished before starting the slab tests. The compressive strength, the modulus of elasticity, the flexural strength and - outcoming from this - the equivalent tensile strength were determined (Tab. 2). The evaluation of the SFRC-properties was carried out according to DBV-Merkblatt (DBV, 2001).

Tab. 2 material properties of SFRC

Specimen	$f_{cm}$ [N/mm <sup>2</sup> ]	$E_{cm}$ [N/mm <sup>2</sup> ]	$f_{eqm,I}$ [N/mm <sup>2</sup> ]	$f_{eqm,II}$ [N/mm <sup>2</sup> ]	$f_{eq,ctm,I}$ [N/mm <sup>2</sup> ]	$f_{eq,ctm,II}$ [N/mm <sup>2</sup> ]
SHR_51_V1	77,15	34790	5,54	4,41	2,94	1,63
SHR_51_V2	79,64	33950	5,19	3,87	2,34	1,43
HODY_V1	77,15	34790	5,54	4,41	2,94	1,63
HODY_V2	71,95	36190	5,47	4,35	2,46	1,61

with:

$f_{eqm,I}$ : mean value of equivalent flexural strength, deformation range I

$f_{eqm,II}$ : mean value of equivalent flexural strength, deformation range II

$f_{eq,ctm,I}$ : mean value of equivalent tensile strength, deformation range I

$f_{eq,ctm,II}$ : mean value of equivalent tensile strength, deformation range II

### 3.3 Test results

In the test series #1 sufficient rotation capacity was accomplished (Fig. 3). The hogging moment could be kept approximately constant over a large range of rotation. In comparison to tests on continuous composite slabs with conventional hogging reinforcement, nearly the same rotation could be attained (see Stark and Brekelmans, 1996). So a moment-redistribution is possible. This feasibility will be researched in a subsequent test series with continuous slabs.

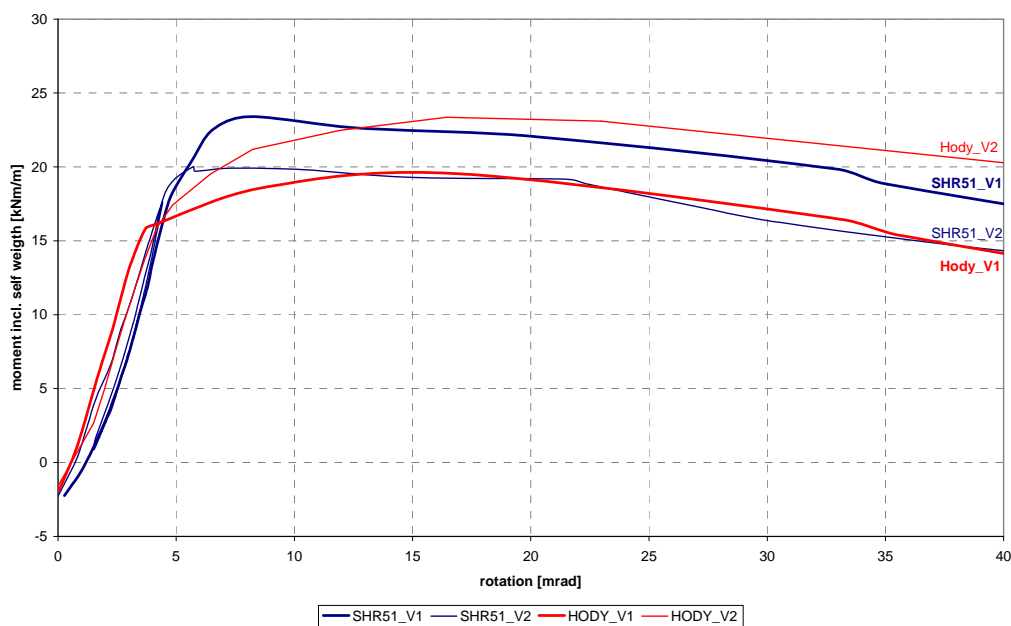


Fig. 3 Moment-rotation diagram of test series #1

No end-slip was measured during the test runs; full shear connection between steel sheeting and concrete could be realised. Fig. 4 displays the test setup and the failure crack of one specimen.

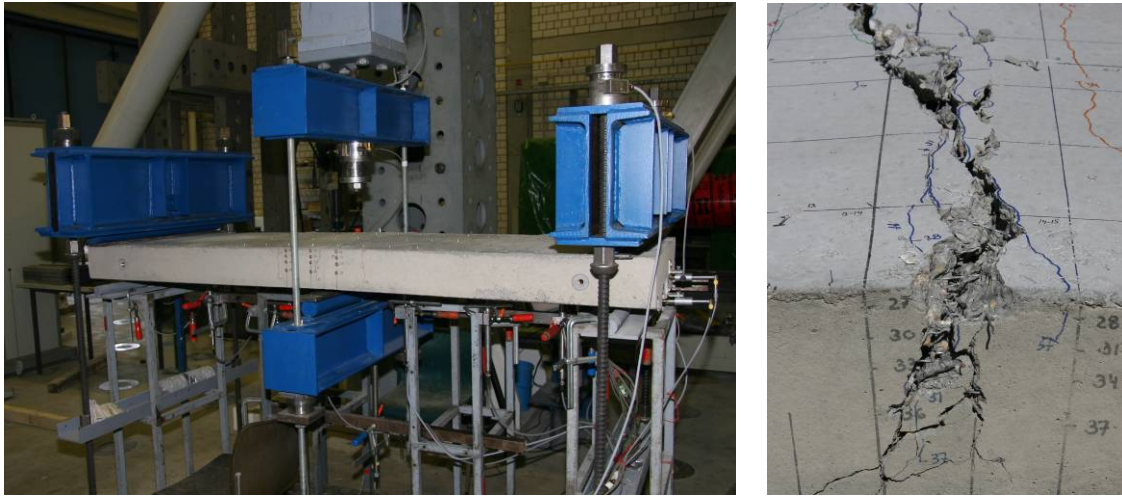


Fig. 4 Test setup (left) and crack at ultimate limit state (right)

Tab. 3 presents both, the measured maximum moment values and the previously calculated plastic moments. The calculated figures correspond very well with the reached test values. The bearing capacity of the steel sheet was taking into account. The tensile bearing capacity of the steel fibre reinforced concrete was calculated with a simplified constant stress distribution over the entire tension zone.

Tab. 3 Test results and previously calculated values

Specimen	max $M_{Test}$ [kNm/m]	$M_{pl,calc.}$ [kNm/m]
SHR51_V1	23,40	23,13
SHR51_V2	20,01	21,26
HODY_V1	19,52	20,19
HODY_V2	23,36	19,89

### 3.4 Prospective test program

In a continuative test series, the use of high strength fibres with lower fibre content will be researched. Test specimens with 60 kg per cubic meter are already fabricated. Thereafter, the main series with continuous slabs will be tested. Simultaneously, finite element parametric studies are in progress.

## 4. CONCLUSIONS

In first test series, the efficiency of the steel fibre reinforced slab system becomes apparent. The tests demonstrate that – due to the possible crack-distribution ability of the steel fibre reinforced concrete – the slabs achieve a good rotation capacity in the hogging area. In further test series the entirety of advantages of the slab system will be analysed. In statically indeterminate systems, like continuous composite slabs, the statically load bearing capacity of steel fibre reinforced concrete can be exploited. In applying nonlinear calculation stiffness

related redistribution effects and – traced of which - a more realistic bearing capacity can be considered.

## 5. ACKNOWLEDGEMENTS

This research was supported by BBR (Bundesamt für Bauwesen und Raumordnung), Trefilarbed, Dyckerhoff AG, Holorib GmbH, SAFA GmbH, Spillner Spezialbaustoffe GmbH and Woermann Degussa.

## 6. REFERENCES

- Bode, H. (1998), "Euro-Verbundbau", *Werner Verlag*, 2. Auflage, 1998.
- DBV (Deutscher Beton- und Bautechnikverein E.V.) (2001), "DBV-Merkblatt Stahlfaserbeton", October 2001.
- DIN 18800-5 (2007) German Standard: Part 5, composite structures of steel and concrete – design and construction, March 2007.
- Sauerborn, I. (1995), "Zur Grenztragfähigkeit von durchlaufenden Verbunddecken", *Dissertation*, July 1995.
- Stark, J.W.B. and Brekelmans, J. W. P. M. (1996), "Plastic design of continuous composite slabs", *Structural Engineering International*, Vol. 6, No. 1, February 1996, pp. 47-53.

## **FIBER REINFORCED CONCRETE WITH RECYCABLES USED IN EARTH STRUCTURES**

*Vytlačilová Vladimíra, Věroslav Hrubý, Hana Hanzlová, Jan Vodička, Jaroslav Výborný*  
*Faculty of Civil Engineering, CTU in Prague*  
*Department of Concrete and Masonry Structures*  
*Prague 6, Thákurova 7, Czech Republic, [vladimira.vytlacilova@fsv.cvut.cz](mailto:vladimira.vytlacilova@fsv.cvut.cz)*

### **SUMMARY**

Results of experiments of standard fine-grained concrete and concrete with recycled aggregates (crushed brick, masonry, concrete) specimens with and without polypropylene fibers are presented in this paper. Concrete with aggregate from recycled materials, which enables saving of natural aggregate in 100% content, is considered to be an advanced structural concrete. Dispersed synthetic fibers added to concrete matrix strengthen texture of concrete and brittle behaviour of material changes to tough one. The new material has enhanced tensile strength and ductility. The recycled aggregate concretes with fibres are suitable for increasing the stability of earth works. In this paper is shown modelling case, that has as one's task to verify of recycled fibre-concrete in earth-work. The experimental analyses results show that recycling of rubble brings interesting possibilities for sustainable building.

### **1. INTRODUCTION**

Construction and Demolition (C&D) waste constitutes a major portion of total solid waste production in the world, and for the present most of it is used in land fills. Preservation of the environment and conservation of the rapidly diminishing natural resources should be the essence of sustainable development. Whereas on the one hand, there is shortage of natural aggregates (NA) for production of new concrete, on the other the enormous amounts of demolished waste produced from deteriorated and obsolete structures creates severe ecological and environmental problem. Use of recycled aggregates in newly concrete provides a promising solution to the problem of C&D waste management. Among promising structural concretes one also can include that ones which are created from recycling materials together with the structural synthetic fibers (SSF). This composite with fibers and crushed brick rubble or recycled concrete aggregates (RCA) are suitable in highway construction, namely layers of pavement, slope stabilization, in hydraulic and engineering strengthening of dam crests and in structural engineering for layers of floors in commercial halls.

### **2. EXPERIMENTAL PART**

Basic mechanical-physical characteristics of recycled concretes were measured and compared with characteristics of normal concretes. A series of laboratory trials were carried out to establish the practical viability of using (C&DW) material as replacement for virgin aggregates. In a mixture proportion the water content was changed and the amount of cement was reduced from the calculated content to minimum value set in a Code ČSN EN 206-1. Specimens were made as the lean concrete (with less cement sign H – 260 kg/m<sup>3</sup>) or fat mixture (with more cement sign T – 424 kg/m<sup>3</sup>) from portland fly-ash cement CEM II/B – V

32,5R. Recycled aggregates consisted in 100% content of natural aggregates. Unclean (composed) brick rubble was shattered in laboratory breaker into fraction 0/8. As a agreement between grain brick rubble gradation and exploit aggregate fraction 0/4 with addition of shattered fraction of aggregate 4/8 in the amount of the rest of brick rubble on the sieve 4, it was decided that material properties of standard fine grain concrete with natural aggregate will be observed, and also properties of brick concrete will be under consideration in case of internal component only brick rubble will remain. The bricks arising from demolition may be contaminated with mortar and plaster, as well are often mixed with other materials such as timber, concrete or glass. In order to minimise cost an optimal dosage of polypropylene fibres (FORTA FERRO) was determined as 1% of volume content eg. 9.1 kg/m<sup>3</sup>.

### 3. RESULTS FROM EXPERIMENTS

In terms of this research were used standard test methods for determination of mechanical-physical properties as initial bulk densities, compressive strengths, flexural strengths and tensile-splitting strengths, pseudo-working diagram force – deflection. The results of experiments (Tab. 1) show that the use of crushed brick recycling for production of concrete with fibres has positive influence.

Tab. 1 Values of basic mechanical-physical properties of tested concretes from standard beams 100×100×400 mm after 28 days of curing (average from three measurements)

Specimen	Grading	Characteristics				
		Bulk density [kg/m <sup>3</sup> ]	Flexural strength [MPa]		Compressive strength of fragments [MPa]	Tensile-splitting strength [MPa]
			1 load	2 loads		
B 0T concrete no fibers	0/8	2279	4.64	-	40.2	4.60
B 1T concrete with fibers	0/8	2299	4.83	6.36	46.0	4.62
B 2H concrete with fibers	0/8	2269	-	3.70	17.83	2.55
C 0T brick concrete no fibers	0/8	1940	3.59	-	27.6	3.20
C 1T brick concrete with fibers	0/8	2035	4.13	4.77	29.3	4.06
C 2H brick concrete with fibers	0/8	1979	-	3.38	16.96	2.62
C 3T brick concrete with fibers	0/8 from 8/32	2062	-	4.53	26.27	3.51
C 4H brick concrete with fibers	0/8 from 8/32	2028	-	3.11	14.20	2.11
C 5H brick concrete with fibers	8/32	1890	-	2.01	19.11	1.82
C 6H brick concrete with fibers	0/32	1804	-	2.44	17.74	2.04
BB 1H concrete with fibers	0/32	2092	-	2.56	22.15	2.35

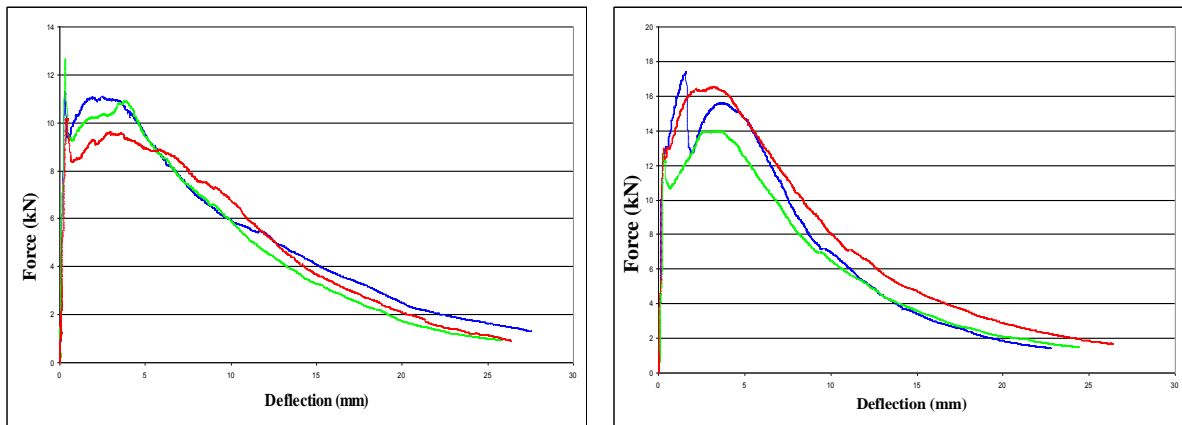


Fig. 1 Pseudo-working diagrams of three specimens C 6H (left) and BB 1H (right)

Dispersed synthetic fibers added to concrete matrix strengthen texture of concrete and brittle behaviour of material changes to tough one. The new composite material has enhanced tensile strength and ductility. For tests on watertight concrete following the standard “Determination of watertightness of concrete” samples from brick concrete with fibers aged 3 months were selected. Leakage through the parallelepipeds attained nearly the upper surface of the cubes and the area of each shattered by lateral tension was wet from more than 90%. With respect to results of the tests the watertightness of the brick concrete with fibers is negligible, but this assignment is very positive for use in earth structures.



Fig. 2 Samples with fibers and recycled aggregates

## 4. EARTH SLOPE EXAMPLE MODEL

### 4.1 Use in practice

Fibre concrete with recycled aggregate is looking for potential usage in present. As optimal use, which is offer presently, are backup strips inside of earth solid (e.g. road or railway's embankments or gradients). Next is able to find exercise e.g. improvement characters on foundation place at complicated foundations or as concrete filler.

### 4.2 Model in Plaxis

Computation of model example realize in program Plaxis. This program make use of final elements method (FEM). Present itself a lot of other simpler possibilities, than usage of FEM, but it would be “reduce” about more global and more detail behaviour of earth body. FEM also make possible to accurate setting to material behaviour. Indeed we regard on fibre-



concrete like a composite material, it` s shows, that linear material model is wanting. At over range of specific strain, it happens to material collapse that this model is unable to note. In these phase of calculation this model was used with consideration on strain.

Geological cross/section is formed only bottom and soil inside of earth-work. It is the simplest state. To it leads request to the easiest calculation free from useless complication that would occur by plotting results. It acts about modelling case, that have as one`s task to verify of recycled fibre-concrete in earth-work. In under-mentioned tables Tab.2 follows individual material characteristics.

Tab 2 Material characteristic of foot-wall, earth-work a recycle

		Foot-wall	Earth-work	Recycle	
Weight by volume	$\gamma$	21	19	18	$\text{kNm}^{-3}$
Static Young`s modulus	E	40000	10000	1500	kPa
Poisson ratio	$\nu$	0.25	0.3	0.3	
Cohesion	c	40	10	0	kPa
Angle of internal friction	$\phi$	32	22	0	°

### 4.3 Outputs

Slope was designed 15 m high. In all cases was endeavour achieve degree of safety about little bigger than 1.3 in result. Thickness every one measures was given on 0.4 m. 4 situation were under consideration:

- slope without reinforcing
- slope reinforced by one measure
- slope reinforced by two measures
- slope reinforced by three measures

By reason of article range is just small amount of outputs present. Individual variants are ranked according to before-mentioned view, i.e. fist slope without reinforcing and in the end slope reinforced by three measures of recycled fibre-concrete.

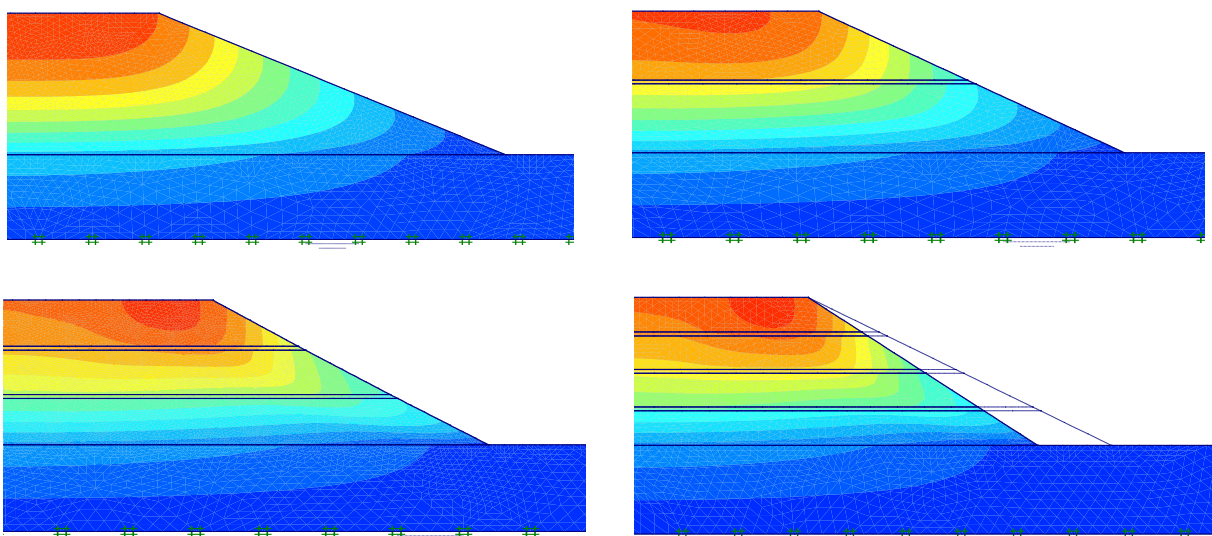


Fig. 3 – 6 Slope total deformations

It is perceptible, that with gaining measures of „recycle “ and decreasing width of slope increases, not fundamentally, slope total deformations. Spreading surface decrease and strain and deformations shoot up. Foot-wall is more loaded and building like this reinforced construction take increased requirements.

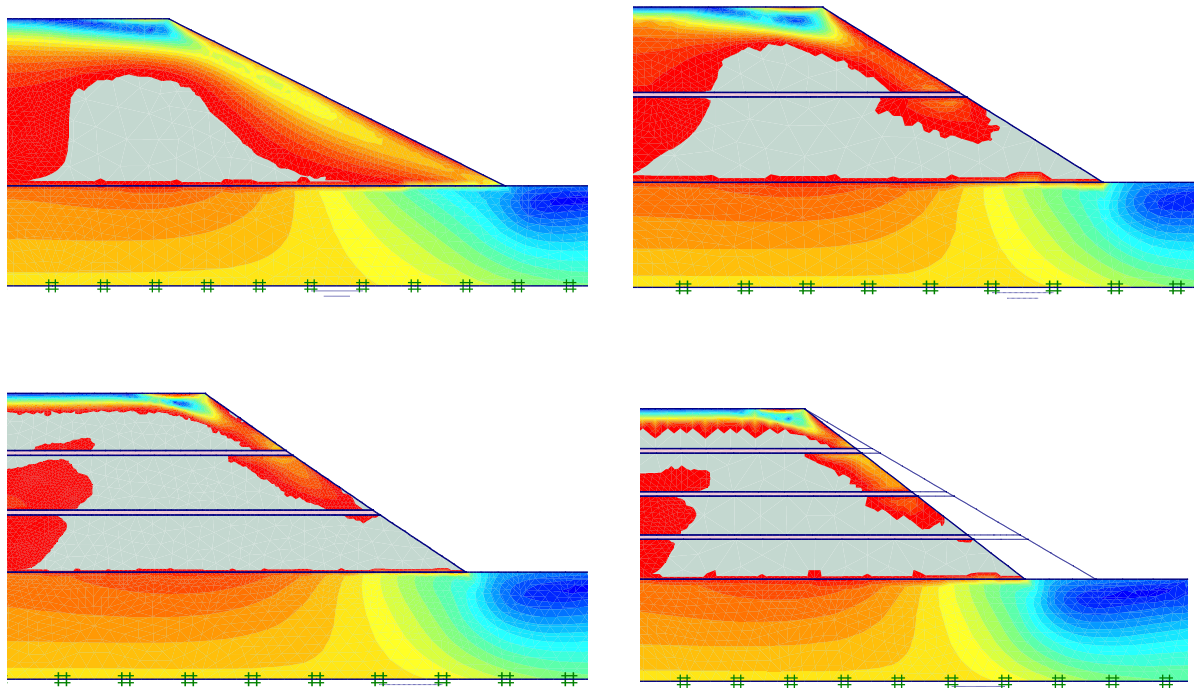


Fig. 7 - 10 Relative shear stresses

Height mentioned pictures give image about relative shear stresses. To greater visualisation are surface with over most 95 % relative shear stresses displaced. In case slope without reinforcing is used only undersized area. Usage of soil increased with accrescent measures. Taking a little flaming look on it, if would be say, that the usage of slope is more effective with acquiescent measures.

On the base analysis designed model, it is posible to suppose that composite with recycled concrete or brick rubblel in relation to fibres is exercisable in new earth construction. Real aplications can spent big capacities these recycles. It should be one of many solutions of present and future problems in enviromental. Particular variants are compared in Tab.3.

Tab. 3 Particular variants solutions compare

Variation	Stability index	Slope ( ° )	Width slope ( m )
without reinforcing	1.3288	26.57	30
1 measure	1.3469	35.54	21
2 measures	1.3616	38.29	19
3 measures	1.4175	38.29	19



## 5. CONCLUSIONS

Results are presented from the laboratory test results showing how C&DW material can be recycled and experiment testify that utilization of recycled concrete with fibres in every-day life is possible and more it is useful without plasticizer and other admixtures. Strength characteristic of recycled concrete with synthetic fibers are sufficient for structural concretes in an earth structures. Also will be attractiveness of this composite material achieved as cement is the most energy demanding component in concrete mixture manufacturing and changes of the brickconcrete material properties will not be dependent on cement dosage increase. However, the use of recycled aggregate is possible only for that with acceptable grading in the range of 0-32 mm on account of a technology simplification. Suitable technology of construction material recycling could be considered an easy alternative for future applications.

Greater efforts are needed in the direction of creating awareness, and relevant specifications to clearly demarcate areas where RAC can be safely used. The recycling of this waste will reduce environmental damages caused by incorrect disposal, extend the useful life of landfills and preserve finite natural resources. Studies are continuing with the aim of obtaining more information about concretes made with C&DW materials and reinforced with fibres and modelling situation construction with this composite. It is possible say that recycled crushed bricks and concrete as aggregate in new concrete along with polypropylene fibers are a new phenomenon in geotechnics.

## 6. ACKNOWLEDGEMENTS

The contribution was elaborated with support of research project VZ 04 Sustainable building MSM 684 0770005.

## 7. REFERENCES

- Výborný, J., Vodička, J., Hanzlová, H., Vytlačilová, V. (2006), "Structural fiber reinforced concrete with recycled aggregate". Proceedings of the workshop VZ 04 Sustainable building MSM 684 077 0005, CTU in Prague
- Vytlačilová, V., Hrubý, H., Vodička, J., Výborný, J., Hanzlová, H. (2007), "Příklad možného využiti vláknobetonu s recykláty v silničných a vodních zemnách konstrukcích", Zborník prednášok VIII. Vedecké konferencie Stavebnej fakulty TU v Košiciach, Košice.

## **STUDY ON THE PROPERTIES OF HIGH PERFORMANCE FIBRE REINFORCED CONCRETE**

*Marijan Skazlic, Dubravka Bjegovic, Mladen Jambresic  
Faculty of Civil Engineering University of Zagreb, Croatia  
Kaciceva 26, 10000 Zagreb, Croatia  
[skazle@grad.hr](mailto:skazle@grad.hr), [dubravka@grad.hr](mailto:dubravka@grad.hr), [jmladen@grad.hr](mailto:jmladen@grad.hr)*

### **SUMMARY**

High performance fibre reinforced concrete (HPFRC) is a material which contains very fine particles. Main principles for producing HPFRC were issued at the end of the last century. They recommend use of smaller aggregate grains. In most of cases maximum grain size of used aggregate is not larger than 1 mm. Currently, scientists and experts did not shared opinions about required maximum aggregate grain size for HPFRC.

In this paper influence of increasing of maximum aggregate size and selection of curing method (water curing, heat treatment) on mechanical and durability properties of HPFRC is analyzed. Experimental part of research, in which several HPFRC mixes were made, is described. HPFRC mix components, used in experimental part of research, are all available on Croatian market. Furthermore, modern laboratory test methods, adjusted to HPFRC, were used. Test results indicate that it is possible to achieve ultra high compressive and tensile characteristics and exceptional durability of HPFRC by using of larger maximum aggregate sizes.

### **1. INTRODUCTION**

High performance fibre reinforced concrete (HPFRC) is a material with characteristic compressive strength often exceeding 150 MPa (AFGC/SETRA, 2002). In its composition it has steel fibres in order to improve ductility of cement matrix. Compared to normal strength concrete (NSC), HPFRC is much more homogenous and less porous. Strength and other properties of HPFRC grow with the higher number of contacts among particles, reduced porosity and defects within the structure. Main principles for HPFRC producing were issued at the end of the last century. According to those principles and considering that HPFRC contains high quantities of binders, it is recommended that the size of maximum aggregate grain size should be reduced. In most cases maximum grain size of used aggregate is not higher than 1 mm (Richard and Cheyrezy, 1995). Currently, scientists and experts do not have shared opinions about required maximum aggregate grain size for HPFRC (Ma et al., 2004).

In this paper influence of increasing of maximum aggregate grain size and selecting of curing method (water curing, heat treatment) on mechanical and durability properties of HPFRC is experimentally analyzed.

## 2. EXPERIMENTAL RESEARCH

### 2.1 Compositions of concrete mixtures

Experimental research was conducted on two HPFRC mixtures. Compositions of mixtures were selected in order to achieve properties of concrete typical for high performance fibre reinforced concrete (Skazlic, 2003). HPFRC mixtures differ one from another only in maximum aggregate (quartz sand) sizes. Mixture M1 had maximum aggregate grain size of 0.5 mm, while mixture M2 had maximum aggregate grain size of 4 mm. Every mixture was made three times. Mixture compositions are shown in Tab. 1. The design of the compositions of mentioned mixtures, selection of their components and production were governed by the principles of design HPFRC (Aitcin, 1998, and Skazlic et al. 2004). All mix components are available on Croatian market.

Both HPFRC mixtures, M1 and M2, were made in 70 litre laboratory mixer. Period of mixing was 12 minutes. Vibration of samples was done on 150 Hz vibrating table for 120 seconds. Curing of samples was done by two different methods. First method was water curing on temperature of  $20 \pm 2$  °C for 28 days (Fig. 1). Second method was heat-treatment (water curing of samples for one day, then heat-treatment on temperature of 90 °C in duration of 48 hours, and afterwards water curing until samples were 28 days old).

Tab. 1 Compositions of concrete mixtures

Mix components (kg/m <sup>3</sup> )	M 1	M 2
Cement I 52.5	1115	1115
Silica fume	169	169
Quartz sand 0/1 mm	1073	1073
Water	204	204
Super plasticizer	32.1	34
Steel fibres 13/0.15 mm	234	234
Maximum aggregate grain size (mm)	0.5	4
Water/binder ratio	0.16	0.16
Aggregate/binder ratio	0.8	0.8



Fig. 1 Heat-treatment (left) and water curing (right)

### 2.2 Properties of mix components

Mineralogical composition of cement (CEM I 52.5) used in experimental work, calculated by Bogue formula according to the results of chemical analysis, is shown in Tab. 2. Used cement had following physical properties:

- grinding fineness 3.93 % of mass
- density 3.12 g/cm<sup>3</sup>,
- specific surface 5030 cm<sup>2</sup>/g,
- water required for achieving standard consistency 30 % of mass,
- setting period (start) 180 min
- setting period (finish) 250 min.

Tab. 2 Mineralogical composition of cement used

Cement	Mineral content (%)			
	C <sub>3</sub> S	C <sub>2</sub> S	C <sub>3</sub> A	C <sub>4</sub> AF
CEM I 52.5	70.7	3.5	8.2	9.1

Silica fume used, was in dry state and packed in bags. It had following characteristics:

- Density 2.22 g/cm<sup>3</sup>,
- Specific surface 18 595 cm<sup>2</sup>/g, and
- Content of total SiO<sub>2</sub> 93.02 %.

Preliminary investigations confirmed that used cement, silica fume and super plasticizer are compatible (Skazlic, 2005).

Two different fractions of quartz sand were used in experimental research (0-0.5 mm and 0-4 mm). Properties of above mentioned fractions of quartz sand are shown in Tab. 3.

Tab. 3 Tested properties of quartz sand

Property	0 - 0.5 mm	0 - 4 mm
Volume mass (kg/m <sup>3</sup> )	2680	2660
Water absorption (% of mass)	0.76	1.26
Small particles content (% of mass)	2.1	1.1

Straight steel fibres (*l/d* = 13/0.15 mm) with characteristic tensile strength of 2059 MPa were used.

Tab. 4 Laboratory tests conducted on HPFRC

Test method	Standard	Number of tested samples
<b>Fresh state properties</b>		
Slump test	HRN EN 12350-2	3
Temperature	HRN.U.M1.032	3
Density		3
Air content	HRN EN 12350-7	3
<b>Mechanical properties</b>		
Compressive strength	HRN EN 196-1	18
Flexural strength	HRN EN 196-1	9
Static modulus of elasticity	HRN.U.M1.025	9
Dynamic modulus of elasticity	HRN.U.M1.026	3
Toughness	ASTM C 1018 and JCI-SF 4	6
<b>Durability properties*</b>		
Air permeability	EN 993-4	3
Capillary water absorption	Modified HRN.U.M8.300	3
Diffusion of chloride ions	ASTM C 1202	3

\* Only mixture M2 was tested on durability properties.

### 2.3 Test methods

Two HPFRC mixtures were tested in fresh and hardened state. Mechanical properties of both mixtures (M1 and M2) were tested in hardened state. In addition, durability properties of mixture M2 were tested. This was done in order to research if HPFRC mixture with maximum aggregate grain size of 4 mm has satisfying durability properties. All test methods that were used are shown in Tab. 4.

## 3. EXPERIMENTAL RESULTS ANALYSIS

### 3.1 HPFRC fresh state properties

In Tab. 5 results of tested fresh state properties of HPFRC are shown. The mixtures have similar properties in fresh state.

Tab. 5 Results of tested HPFRC fresh state properties

Property	M 1 (max. grain size – 0.5 mm)	M 2 (max. grain size – 4 mm)
Slump test (mm)	200	240
Temperature (°C)	30	28
Density (kg/m <sup>3</sup> )	2510	2470
Air content (%)	4.4	3.8

### 3.2 Mechanical properties of HPFRC

HPFRC mechanical properties test results are shown in Tab. 6. From the results it can be seen that there is significant difference between mixtures M1 ( $D_{\max} = 0.5$  mm) and M2 ( $D_{\max} = 4$  mm), in a way that mixture M2 has lower values (cca 10 %) of following properties tested:

- Compressive strength in both curing methods, and
- Static modulus of elasticity when HPFRC is water cured.

There is no significant difference between two mixtures in flexural strength and static modulus of elasticity when HPFRC is heat-treated. Furthermore, mixture M1 has dynamic modulus elasticity cca 10 % higher than mixture M2. Although mixture M2 has lower values of tested mechanical properties compared to mixture M1, it still has ultra high mechanical properties. Therefore, mixture M2 mechanical properties test results are contrary to papers of scientists who invented reactive powder concrete (RPC) in which they claim that exceptional properties of HPFRC can be achieved only if quartz sand has  $D_{\max} \leq 0.6$  mm (Richard and Cheyrezy, 1995).

Heat-treatment process results in higher HPFRC compressive strength and modulus of elasticity (cca 3 %) and flexural strength (cca 15 %) compared to ordinary water curing. Toughness tests results (Fig. 2) show that increase of maximum aggregate grain size to 4 mm does not have negative affect to HPFRC toughness properties. Compared to mixture M1, up to deflection of 2 mm mixture M2 behaves even better concerning toughness.

Tab. 6 Test results of HPFRC mechanical properties

Property	Curing method	M1	M2
Compressive strength (MPa)	water cured	213.6	197.1
	heat treated	220.7	199.5
Flexural strength (MPa)	water cured	38.7	35.6
	heat treated	44.2	43.0
Static modulus of elasticity (GPa)	water cured	49.1	45.2
	heat-treated	50.4	48.2
Dynamic modulus of elasticity (GPa)	water cured	53.0	48.9

### 3.3. Durability properties of HPFRC

Durability test results in Table 7 show that mixture M2 has high quality properties. Compared to previous durability tests of HPFRC with  $d_{max} = 0.5$  mm (Skazlic, 2005), mixture M2 has similar durability properties (capillary water absorption, diffusion of chloride ions and air permeability).

Tab. 7 HPFRC durability properties test results

Durability property	M 2
Air permeability coefficient ( $m^2$ )	$3.8 \cdot 10^{-19}$
Capillary water absorption ( $kg/m^2h^{0.5}$ )	0.018
Diffusion of chloride ions (Coulomb)	148

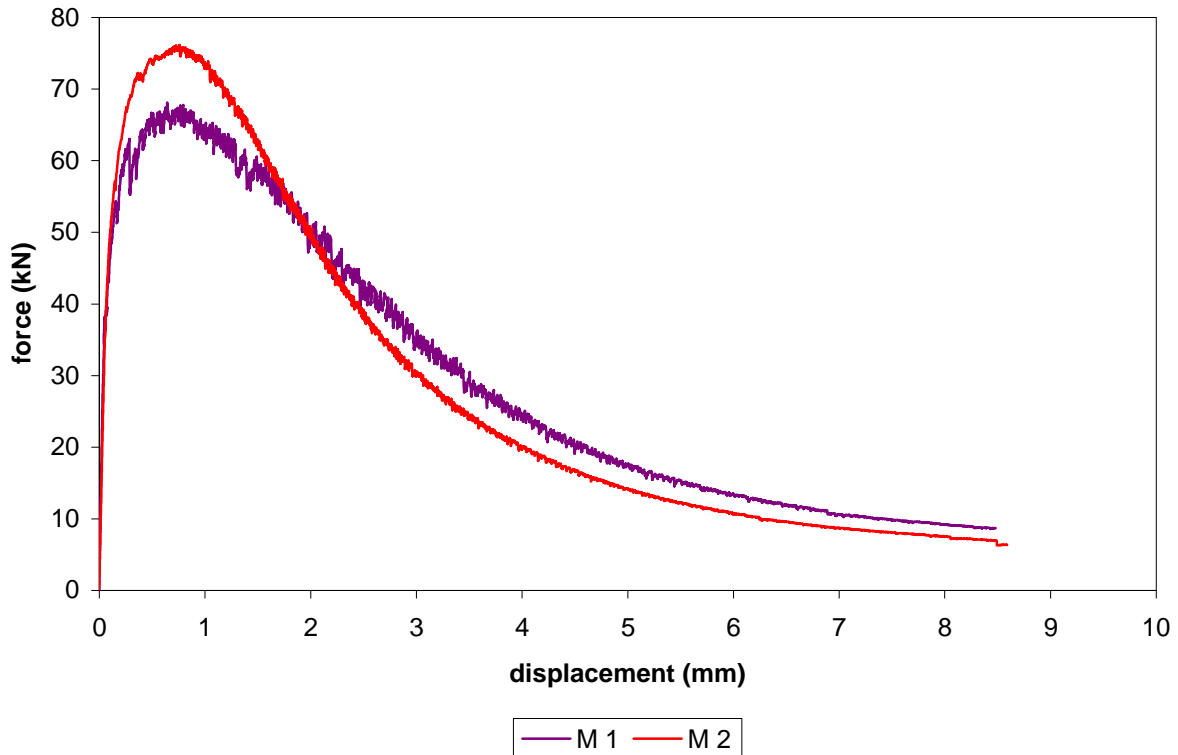


Fig. 2 Toughness test results

#### 4. CONCLUSIONS

In this paper experimental research of influence of increasing maximum aggregate size of HPFRC to 4 mm is described. The following conclusions can be drawn based on described research:

1. HPFRC with  $d_{\max} = 4$  mm has similar properties in fresh state compared to HPFRC with  $d_{\max} = 0.5$  mm.
2. Analysis of mechanical properties test results show that HPFRC with  $d_{\max} = 4$  mm has compressive strength, static modulus elasticity and dynamic modulus of elasticity cca 10 % lower than HPFRC with  $d_{\max} = 0.5$  mm. With an increase of  $d_{\max}$  flexural strength and toughness do not change significantly. Regardless the compressive strength and modulus of elasticity of HPFRC with  $d_{\max} = 4$  mm are 10 % lower, this properties are still ultra high mechanical properties.
3. Heat-treatment process improves mechanical properties (compressive and flexural strength, modulus of elasticity) of HPFRC compared to usual water curing.
4. Durability test results show that HPFRC with  $d_{\max} = 4$  mm has high quality properties. Therefore, it can be concluded that increase of  $d_{\max}$  does not have significant impact on HPFRC durability.

#### 5. ACKNOWLEDGEMENTS

Authors express their acknowledgements to Ministry of science, education and sports of the Republic of Croatia. Described experimental research has been carried out within two science projects (Modern methods of engineering materials testing, 082-0822161-2996, project manager doc. dr. sci. Marijan Skazlic, and Development of new materials and systems of concrete structures protection, 082-0822161-2159, project manager prof. dr. sci. Dubravka Bjegovic) supported by above listed ministry.

#### 6. REFERENCES

- AFGC/SETRA working group (2002), „Ultra-High Performance Fibre-Reinforced Concrete“, *Interim Recommendations*
- Aitcin, P.C. (1998), „High-Performance concrete“, *E&FN SPON, London*
- Ma, J., Orgass, M., Dehn, F., Schmidt, D., Tue, N.V. (2004) „Comparative Investigations on Ultra-High Performance Concrete with and without Coarse Aggregates“, *Proceedings of International Symposium on Ultra High Performance Concrete (UHPC)*, September 13-15, 2004, Kassel, Germany, pp. 205-212
- Richard, P., Cheyrezy, M., (1995), „Composition of Reactive Powder Concretes“, *Cement and Concrete Research*, Vol. 25, No.7, pp. 1501-1511
- Skazlic, M. (2003), „Hybrid High-Performance Fibre Reinforced Concrete“, *Master's Thesis*, Faculty of Civil Engineering, University of Zagreb (in Croatian)
- Skazlic, M. (2005), „Precast Fibre Reinforced Elements for Secondary Tunnel Lining“, *PhD Thesis*, Faculty of Civil Engineering, University of Zagreb, (in Croatian)
- Skazlic, M., Bjegovic, D., Mrakovcic, S. (2004), „High-Performance Fibre Reinforced Concretes“, *Gradjevinar*, Vol. 56, No. 2, pp. 69-78 (in Croatian)

## EXPERIMENTAL STUDIES ON CARBON FIBRE REINFORCED WHITE CEMENT LIGHTWEIGHT MORTAR AND CONCRETE ELEMENTS

*Kinga Pankhardt\*, Salem G. Nehme\*\**

*\*Debrecen University, Hungary*

*H-4028 Debrecen, Ótemető u. 2-4., [kpankhardt@yahoo.com](mailto:kpankhardt@yahoo.com)*

*\*\*Budapest University of Technology and Economics, Hungary*

*H-1111 Budapest Műegyetem rkp. 3, [sgnehme@yahoo.com](mailto:sgnehme@yahoo.com)*

### SUMMARY

The global warming up, the increasing temperatures on the earth in the future will affect also the architectural design of the continental regions. The design and the use of building materials in the mediterranean area have significant differences from continental areas such as use of white masonry or facades. The main objective was to design a high strength composite with improved ductility and use of lightweight aggregate.

The using of lightweight aggregates influences not only the body density of the construction material but also the thermal mass of the concrete. Tests were carried out at the BME Dept. of Structural Materials and Engineering Geology. We designed different mixes and tested the fresh mix and hardened mortar and concrete properties. Small construction thicknesses can be reached by high strength and reinforced materials and the dead load like self weight can be reduced by using of lightweight aggregates.

### 1. INTRODUCTION

The colour and composition of the materials greatly affect the surface temperature and the amount of absorbed solar radiation. Surfaces with lower albedos absorb more solar radiation. Traditional portland cement concrete generally has an albedo or solar reflectance of approximately 0.4, though values can vary; measured values are already reported in the range of 0.4 to 0.5. For "white" portland cement, values are reported in the range of 0.7 to 0.8. The solar reflectance of new concrete is greater, when the surface reflectance of the materials in concrete is greater (Levinson, Akbari, 2001). Important factor for thermal aspects is the thermal mass of concrete which delays the time it takes for a surface to heat up but also delays the time to cool off.



Fig. 1 Architectural example: Museum in Cagliari (Zaha Hadid, 2006)



Fig. 2 Tested specimens with recycled glass



## 2. EXPERIMENTAL STUDIES

Specimens were prepared to test the compressive and flexural tensile strength. We have chosen white cement as binder because of optical and thermal aspects, and designed different mixes and tested the fresh mix properties, like consistency, segregation, workability etc. An additional element that the concrete must also present is adequate shoot ability properties or to be self compacting to use in thin structural elements like shells.

Efflorescence, so called lime efflorescence is a natural phenomenon in cement-bound materials, which can be reduced by using of white cement. By aesthetic solutions such as exposed concrete, by preparing of elements unique surface (evenly distributed color and smooth surface) is required, which is influenced also by minimal changing in w/c-ratio of the concrete mixes. By large scale using of lightweight HPC concrete, like in prefabrication, the changing of color at same type of cement can be also a little dependent on manufacturer. To reduce colour influencing factors is preferred to use white cement in spite of the higher costs. Our experimental studies included constant and variable factors. These factors were:

- Constant factors:
- type of cement CEM I 52.5 N (white cement)
  - volume of fine aggregate (recycled glass and “00” limestone powder)
  - colour of aggregate (white)
- Variables:
- type of aggregate:
    - lightweight aggregate (recycled glass)
    - limestone aggregate
  - water/cement ratio
  - fiber reinforcement (Zoltek Panex 33 carbon fibers 0.25”).

Tab. 1 Characteristics of the applied recycled glass aggregate\*

Recycled glass aggregate	
Material	soda lime borosilicate glass
Effective particle size (microns)	65
Alkalinity	0.5 milliequivalents per gramm or less
Density (g/cm <sup>3</sup> )	0.60
Bulk density (g/cm <sup>3</sup> )	0.31-0.43
Specific surface area (m <sup>2</sup> /g)	1.9-2.7
(m <sup>2</sup> /cm <sup>3</sup> )	0.4-1.1
Thermal conductivity at 0°C (W/mK)	0.06-0.2

\*given by the manufacturer

We studied before mixing of concrete different mortar mixtures too.

- G.I. Mortar mixture with aggregate: recycled glass 10 m% of cement
- G.II. Mortar mixture with aggregate: lime stone powder “00”: 0/0.1 mm fraction
- G.III. G.I. + carbon fiber reinforcement, 2 kg/m<sup>3</sup>
- G.IV. G.II.+ carbon fiber reinforcement, 2 kg/m<sup>3</sup>

The water/cement ratio for all mortar mixture was 0.3. G.I. and G.II. mixtures contained only white cement, water, aggregate and superplasticizer. The volume of aggregate was constant and the volume proportions reference to concrete were c:a:w = 2:1:2.

G.V. Mortar Mixture was designed with very high w/c ratio:0.97 to produce lightweight mortar, with body density smaller than 1000 kg/m<sup>3</sup> only for observation purposes. We investigated 4 different concrete mixtures, which were at the first phase of our experiments not especially lightweight concrete mixtures. In the first phase our experiment we intended to study the influence of using of recycled glass aggregate and combined with

carbon fiber reinforcement. We prepared 40×40×160 mm and 30×30×30 mm specimens for testing of mortar properties and for concrete 150 mm, 100mm and 70×70×250 mm specimens and plates 300×300 mm with thickness from 10 up to 20 mm. The point of interest was to create HPC “easycrrete” which is more able to use in small construction thicknesses.

The studied concrete mixtures were:

- GB.I. Concrete mixture, where aggregate: only lime stone fractions
- GB.II. Concrete mixture, where aggregate: with recycled glass (7 m% of cement)
- GB.III. Concrete mixture, where aggregate: with recycled glass (20 m% of cement)
- GB.IV. GB.III. + carbon-fiber

The w/c ratio for all concrete mixture were 0.53.

Tab. 2 Concrete Mixtures

Materials		GB I.		GB II.		GB III.		GB IV.		
		kg/m <sup>3</sup>	l/m <sup>3</sup>	kg/m <sup>3</sup>	l/m <sup>3</sup>	kg/m <sup>3</sup>	l/m <sup>3</sup>	kg/m <sup>3</sup>	l/m <sup>3</sup>	
	CEM I 52.5 N, white	320	103.2	320	103.2	330	106.5	330	106.5	
	Water	170	170	170	170	175	175	175	175	
„00”	0-0.1 mm	Limestone	100	36.9	-	-	100	36.9	100	36,9
„0”	0-1.5 mm		675	254.7	675	254.7	575	212	575	212
I	1.5-3.5 mm		635	239.6	635	239.6	545	201	545	201
II	1.5-5 mm		205	77.4	205	77.4	151	56	151	56
III	5-7 mm		200	75.5	200	75.5	151	56	151	56
IV	7-12 mm		100	37.7	100	37.7	94	34	94	34
	65 micrum		Rec. glass	-	-	22.64	37.7	66	110	66
	0.25”	carbon fibers	-	-	-	-	-	-	2	1,15
	Superplast. Glenium 51 1%		3	3	3.3	3.3	3.3	3.3	3.3	3.3
	Air content		-	5.8	-	2.0	-	9.6	-	8.5
	Sum		2408	1000	2330	1000	2188	1000	2190	1000

### 3. EXPERIMENTAL RESULTS

#### 3.1 Influence of type of aggregate

##### 3.1.1 Influence of type of aggregate on fresh concrete or mortar properties

The quality and fineness of cement and aggregate plays important roles in the behaviour of fresh concrete. As the fine particles (cement, fine aggregate) or fineness increases, the mixture becomes more cohesive. The behaviour of fresh concrete can be significantly affected by the physical properties of aggregates. The maximum size and grading of the fine aggregate, as well as the shape and texture of both the fine and coarse aggregates, affect the water content required to produce workable concrete. Rough, angular aggregates require more cement and water for workability, than smooth, rounded aggregates. In our experiment we used recycled glass also to increase the fine aggregate content. Specific surface area of white cement was between 0.3-0.44 m<sup>2</sup>/g, of recycled glass between 1.9-2.7 m<sup>2</sup>/g (Tab 1.), which is about 6,3 time higher, then of white cement. This proportion has to be taken into account by using in concrete. This fine recycled glass aggregate is round shaped, so we expected to improve the workability. Figs. 3 and 4 show the effect of recycled glass on consistency of fresh concrete. Measured consistencies by flow table test were for mixture GBI: 370 mm and for GBII: 570 mm. By using of recycled glass aggregate in fresh mortal and concrete mixes, the flow increased of the mixture, and the workability improved.



Fig. 3 Tested fresh concrete GB I., no recycled glass added



Fig. 4 Tested fresh concrete GB II., with recycled glass

### 3.1.2 Influence of type of aggregate on hardened concrete or mortar properties

#### 3.1.2.1 Aesthetic aspects

In our experiment we have studied the smoothness of the surface of the specimens. Higher reflectance can also be reached by smoother surface. By using of recycled lightweight aggregate we have got whiter and smoother surface (Fig. 5).



Fig. 5 Tested mortar mixtures: in the middle with limestone "00", at the sides with recycled glass



Fig. 6 Low body density, mixture GV.

#### 3.1.2.2 Mechanical aspects

With white cement higher strength can be reached and therefore the element thicknesses can be reduced.

Tab. 3 Test results

Mix*	Specimen	Density kg/m <sup>3</sup>	Compressive strength N/mm <sup>2</sup>	Flexural tensile strength N/mm <sup>2</sup>
G I	40×40×160mm*	1821	89.7	19.33
G II	40×40×160mm*	2169	94.4	15.03
GB I	40×40×160mm*	2388	63.6	10.72
	□ 150 mm **		63.6	-
GB II	40×40×160mm*	2346	65	10
	□ 150 mm **		61.6	-
GV	□ 30 mm*	813	23.8	-

\* average of 3 specimens, age 28 day; \*\* average of 5 specimens, age 28 day

Body density can be reduced with recycled glass aggregate, but the strength will not decrease, and high compression strength can be reached. The flexural tensile strength increased and was more influenced by using of recycled glass in mortar, then in concrete, but the compression strength wasn't influenced by concrete.

### 3.2 Influence of carbon fiber reinforcement

#### 3.2.1 Influence of carbon fiber reinforcement on fresh concrete or mortar properties



Fig. 7 Flow test of GBIII, with limestone and recycled glass, no carbon fiber added



Fig. 8 Flow test of GBIV, with limestone and recycled glass, carbon fiber added

For better observation of fractured zone of area of specimens tested to bending we wanted to apply dark colored fibers. For higher flexural tensile strength we used carbon fibers. Fig. 7 and Fig. 8 show the consistency of fresh concrete. Measured flow were for mixture GB III.: 76 cm and for GB IV: 72 cm. The mixtures GB III. and GB IV. were so called “easycrrete” and segregation wasn’t observed.

#### 3.2.2 Influence of carbon fiber reinforcement on hardened concrete or mortar properties

Tab. 4 Test results of carbon fiber reinforced specimens

Mix*	Specimen	Density kg/m <sup>3</sup>	Compressive strength N/mm <sup>2</sup>	Bending strength N/mm <sup>2</sup>
G III	40×40×160 mm	1594	59,2	9,35
	□ 30 mm		58,1	-
G IV	40×40×160 mm	2069	77	12
	□ 30 mm		65,7	-
GB III	40×40×160 mm	2196	51,6	8,35
	□ 100 mm		51,9	-
GB IV	40×40×160 mm	2226	48	8
	□ 100 mm		51,8	-

\* average of 3 specimen, age 3 day; (by printing of paper the experiments continue)

To decrease the rigidity and to increase the ductility of the elements fiber reinforcement should be applied. High load bearing capacity can be achieved despite minimal panel thickness and large formats. This sets new standards for the design of facades, in the interior of buildings as well as for the external skin. In our future work further investigations have to be done on lightweight HPC elements by using in different application like for sandwich elements like rainscreen cladding: (A rainscreen system consists of an outer panel, a ventilated cavity and an inner leaf.) For outer panel of aesthetic and durability aspects

lighthweight HPC or HPSCC can be used. The advantages of using lighthweighth HPC or HPSCC are for example:

1. dead load of cladding can be reduced, minimal additional load applied to the existing structure;
2. energy saving - lower running costs due to greatly improved thermal insulation;
3. aesthetic colour, flexibility and shape of external facade with minimal thickness can be reached;
4. at lower dead load it is easier to remove panels for monitoring of structure etc.

#### 4. CONCLUSIONS

The following conclusions can be drawn from our experimental study:

By using of recycled glass aggregate:

- whiter and smoother surface we have got;
- increased flow of the mixture, improved workability, “easycrrete”;
- body density can be reduce with recycled glass aggregate, but the strength will not decrease, also high compressive strength can be reached.

By using recycled glass aggregate and carbon fiber reinforcement:

- to decrease the rigidity and to increase to ductility of the elements fiber reinforcement should be applied.
- to increase of bending strength fiber reinforcement (carbon, glass, PP etc.) can be applied.
- by increasing of bending strength the thickness/element size ratio can reduced.
- high quality elements with a filigree appearance can be made out of fibre reinforced concrete, which can be ideal for example as cladding solution for all modern buildings.

The experiments are now in 2<sup>nd</sup> Phase, further investigations have to be done on durability.

#### 5. NOTATIONS

SCC self compacting concrete  
HPC high performance concrete  
HPSCC high performance self compacting concrete

#### 6. ACKNOWLEDGEMENTS

Authors express their acknowledgements to Mr. András Eipl and Mr. Patrik Tóth for their laboratory work to the experiments.

#### 7. REFERENCES

Levinson R., Akbari H., (2001): “Effects of composition and exposure on the solar reflectance of portland cement concrete”, Heat Island Group Environmental Energy Technologies Division Lawrence Berkeley, National Laboratory, *University of California Berkeley*, pp.15-16.

## UNIAXIAL BEHAVIOUR OF STEEL FIBRE REINFORCED CONCRETE

*Imre Kovács, Assoc. Prof.*  
*University of Debrecen Department of Civil Engineering*  
*4028-H Debrecen, Ótemető u. 2-4.*

*György L. Balázs, Prof.*  
*Salem George Nehme, Senior lecturer*  
*Budapest University of Technology and Economics*  
*Department of Construction Materials and Engineering Geology*  
*1111-H Budapest, Műegyetem rkp.*

### SUMMARY

Mechanical modelling of the uniaxial behaviour of steel fibre reinforced concrete is discussed in this paper. A one-dimensional elastic-plastic material model has been developed for fibre reinforced concrete taking into consideration plastic matrix-fibre coupling for the irreversible deformations of the concrete and of the steel fibres. Due to the simplicity and clear physical significance of the basic mechanical model which takes into consideration elastic-brittle concrete and elastic-perfectly plastic steel fibre reinforcement behaviour, the model is extended with residual strength of the constituents and hardening or softening phenomena as well. Finally an experimental study on the uniaxial behaviour of steel fibre reinforced concrete is studied together with the characterization of model parameters .

### 1. MECHANICAL MODELL

Mechanical model is composed of two parallel sub-devices which represent the behaviour of the constituents (matrix and fibre reinforcement). Elastic-brittle concrete behaviour is composed of an elastic spring (stiffness  $C_m$ ) and a fragile crack element (strength  $f_t$ ) (Fig. 1 and Fig. 2). The behaviour of steel fibre reinforcement assumed to be governed by an elastic-perfectly plastic material law, described by an elastic spring (stiffness  $C_f$ ) together with a friction element (strength  $f_y$ ) (Fig. 1 and Fig. 2). In addition to, the two parallel sub-devices are coupled by an elastic spring element of stiffness  $M$ , which links the irreversible matrix behaviour (i.e., strain  $\varepsilon_m^p$ ) with the irreversible fibre reinforcement behaviour (i.e., strain  $\varepsilon_f^p$ ). According to Fig. 1 and Fig. 2 the overall stress ( $\Sigma$ ) is provided by the sum of  $\sigma_m$  and  $\sigma_f$  hence the overall forces ( $F$ ) of the constituents  $F_m$  and  $F_f$ :

$$\begin{aligned} F &= (1-\eta)AE_m(\varepsilon - \varepsilon_m^p) + \eta AE_f(\varepsilon - \varepsilon_f^p) \\ F_m &= (1-\eta)AE_m(\varepsilon - \varepsilon_m^p) - \eta AM(\varepsilon_m^p - \varepsilon_f^p) \\ F_f &= \eta AE_f(\varepsilon - \varepsilon_f^p) + \eta AM(\varepsilon_m^p - \varepsilon_f^p) \end{aligned}$$

Where  $A_m$  and  $A_f$  respectively represents the cross section area of the concrete and steel fibre reinforcement in a given section,  $\eta$  is the content of fibre reinforcement in volume percent,

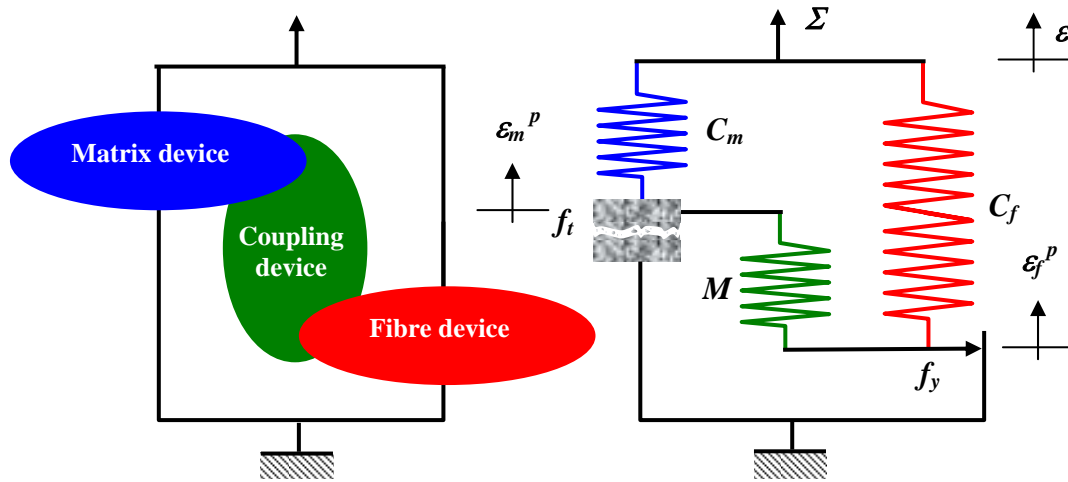


Fig.1 Mechanical model for fibre reinforced concrete in uniaxial tension

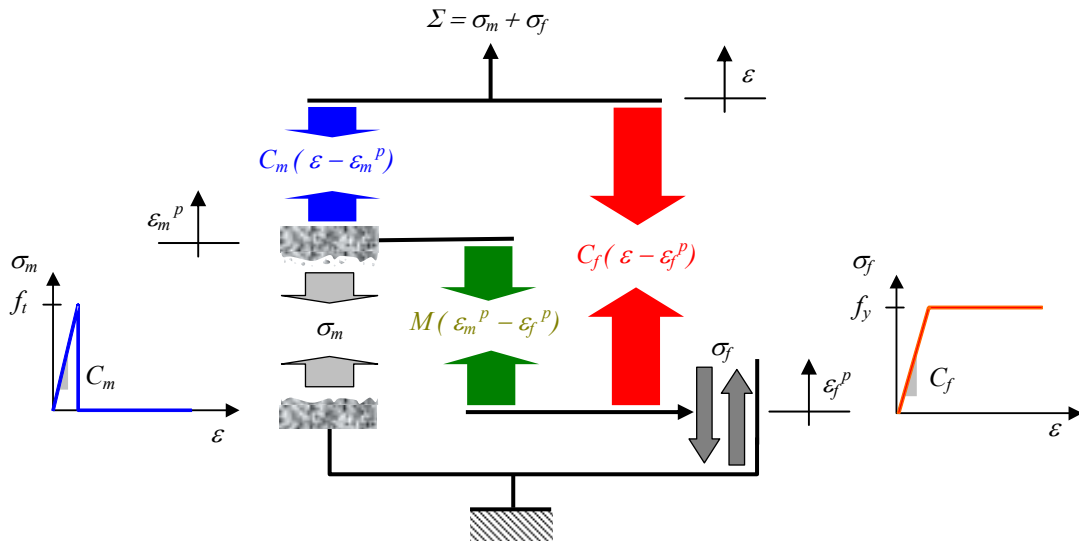


Fig. 2 Force-flow of the model and the considered material laws for the constituents

$E_m$  and  $E_f$  are the elastic modulus of constituents. All quantities are introduced at the macroscopic level of the fibre reinforced material (i.e., typical scale of laboratory test specimen). For instance, the irreversible fibre reinforcement deformation  $\varepsilon_f^p$  is a macroscopic quantity, which accounts for different mechanisms at the microscopic level of the composite, such as debonding, fibre pull-out, localized fibre yielding, etc.

Elastic-brittle concrete and elastic-perfectly plastic steel fibre reinforcement behaviour were considered, i.e., the residual stress in the matrix was zero after cracking ( $\sigma_m = 0$ ) while the fibre reinforcement stress was equal to the yield strength ( $\sigma_f = f_y$ ). For the sake of clarity, hardening and/or softening behaviour of the constituents has not been considered here before. However, due to the simplicity of the one-dimensional device element it can easily be expanded for instance by fibre reinforcement softening or hardening and matrix or fibre reinforcement residual strength as well. In this case, yield functions describe the initial elasticity domain of the fibre reinforced concrete. Further loading passes the elastic domains. Assume now brittle matrix and brittle fibre behaviour. The admissible stresses are now described by:

$$F(f_m, f_f) = \max\{f_m(\sigma_m, \varsigma_m), f_f(\sigma_f, \varsigma_f)\} = f_m = \sigma_m + \varsigma_m - \bar{f}_t \leq 0$$

$$F(f_m, f_f) = \max\{f_m(\sigma_m, \varsigma_m), f_f(\sigma_f, \varsigma_f)\} = f_f = |\sigma_f + \varsigma_f| - \bar{f}_y \leq 0$$

where  $\bar{f}_t$  and  $\bar{f}_y$  denote the residual strength of the concrete and of the steel fibre reinforcement after concrete cracking and steel fibre yielding, respectively. Note that  $0 \leq \bar{f}_t \leq f_t$  and  $0 \leq \bar{f}_y \leq f_y$ . Furthermore,  $-\varsigma_m$  and  $-\varsigma_f$  are the forces (positive in tension) in the hardening spring devices of the matrix and of the fibre reinforcement represented by a spring of rigidity  $H_m$  and  $H_f$ , respectively (Fig. 3).

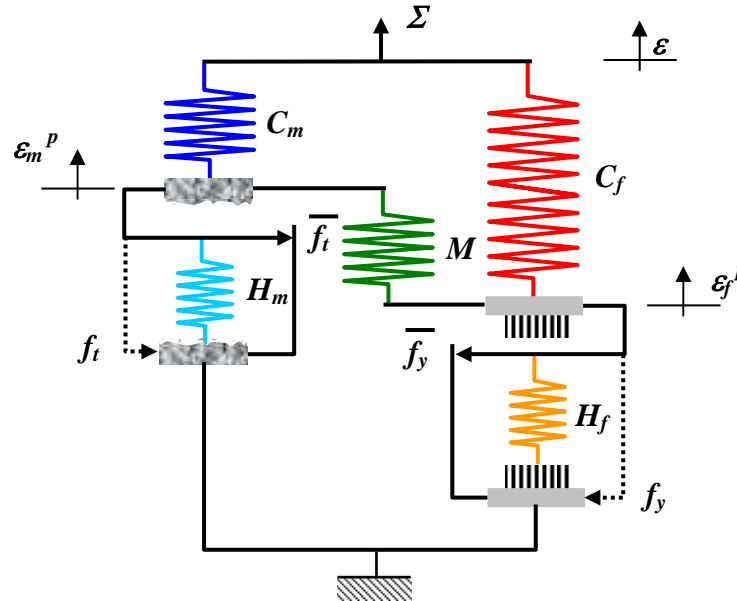


Fig. 3 Mechanical device for fibre reinforced concrete considering elastic-brittle matrix and steel fibre reinforcement with hardening or softening behaviour

## 2. EXPERIMENTAL PROGRAM

### 2.1 Material compositions and test specimens

Material properties of hardened concrete are influenced by many material parameters. Structural design requires all the material properties that have considerable influence. Appropriate values of these experimental variables are important to the mixing process and to the workability as well. Actual values of uniaxial tensile and compressive test variables were taken to obtain workable concrete mixes which represent realistic behaviour.

Concrete mix proportions are summarised in Tab. 1. Superscript and subscript indices denote the fibre content in mass ( $75 \text{ kg/m}^3$ ,  $150 \text{ kg/m}^3$ ) and the type of fibre (Dramix<sup>®</sup> ZP 305) respectively. Type of fibre Dramix<sup>®</sup> ZP 305 was used with length of  $\ell_f = 30 \text{ mm}$  and diameter  $\varnothing_f = 0.5 \text{ mm}$  (Tab. 2.). Two washed and classified aggregate fractions were used, 0-4 mm sandy-gravel and 4-8 mm gravel fractions. Maximum aggregate diameter therefore was 8 mm. CEM I. 52.5 (550 pc) type of Hungarian Portland Cements was used.

Proper workability was obtained by the addition of Sikament-10 HBR superplasticizer in order to reduce the water to cement ratio. Mixes were produced in a mixer with a maximum capacity of 50 l.




In addition to the concrete mix proportions and the fibre content, characteristic fibre orientation was the major experimental variable. Series devoted to study the effect of characteristic fibre orientation on the mechanical properties of steel fibre reinforced concretes are noted by roman numbers I and II. Numbers denote the considered two characteristic fibre orientations introduced into the slabs during casting. Fibre orientations were considered to be in the plane of slabs and hence, effect of fibres oriented in the third direction was not taken into consideration. Fibre orientation may play an important role in the anisotropy of material, particularly in the range of post cracking behaviour and hence, it is essential in structural analysis. Characteristic fibre orientations were systematically introduced in the material by a P14 type handy vibrator of 28 mm diameter. In specimens noted by I and II, the characteristic fibre orientations were perpendicular to each other. Fibre orientations were formed by moving the vibrator only in one direction in the slabs. After a week of casting specimens different specimens were sawn out of them. The sawing plan is summarised in Tab. 3. 6+6 prisms with the size of 240×100×100 mm and a small deep beam with a size of 500×170×100 mm were sawn out of specimen noted by T1...T6, C1...C6 and DB-a. T indicates that the prism will be tested in uniaxial direct tension while C denotes the prisms tested in compression. Notation DB-a denotes the type of deep beam element. Test of deep beam specimens are not discussed in this paper.

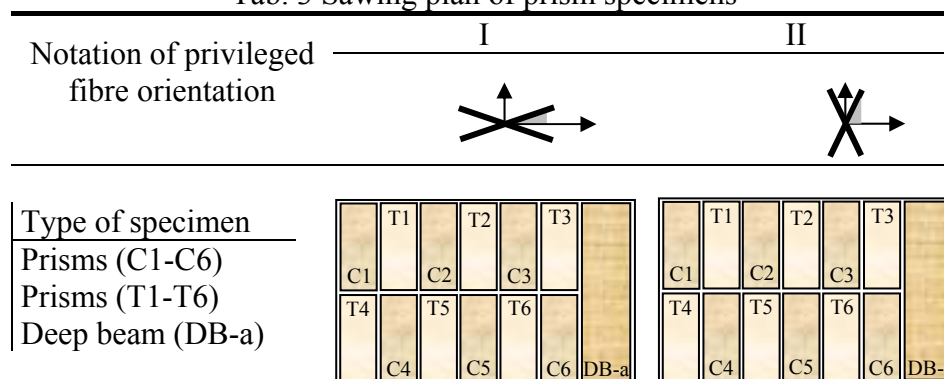
Tab. 1 Concrete composition in dry material [kg/m<sup>3</sup>] (present tests)

Nr.	Notation of mix	Fine aggregates		cement	Super plasticizer	w/c	Fibre content	
		0-4 mm	4-8 mm				V%	kg/m <sup>3</sup>
1	FRC-1 <sup>75</sup> <sub>ZP 305</sub>	1056	829	330	5,952	0.512	~ 1.0	75
2	FRC-1 <sup>150</sup> <sub>ZP 305</sub>	1056	829	330	8.571	0.512	~ 2.0	150
3	FRC-2 <sup>75</sup> <sub>ZP 305</sub>	958	752	500	9.048	0.372	~ 1.0	75
4	FRC-2 <sup>150</sup> <sub>ZP 305</sub>	958	752	500	10.476	0.372	~ 2.0	150

Tab 2 Types of fibres and their mechanical properties

Notation	Material type	Configuration	Aspect ratio $l_f/\varnothing_f$	Density [kg/m <sup>3</sup> ]	Yield strength [MPa]	Elastic modulus [GPa]
Dramix <sup>®</sup> ZP 305	Steel		60	7800	1100	200

Tab. 3 Sawing plan of prism specimens



## 2.2 Uniaxial tensile test

For testing the sawn specimens in uniaxial tension a special experimental set-up was developed. Prisms specimens (240×100×100 mm) were notched at the mid-section with a 5 mm notches. Load – displacement relationship were registered by two LVDT placed at the notches. Theoretical and experimentally determined uniaxial tensile stress – strain relationships for specimens containing 75 kg/m<sup>3</sup> and 150 kg/m<sup>3</sup> steel fibre are summarised in Fig. 5 (Kovács 1998, Kovács 1999).



Fig. 4 Test specimens for uniaxial tensile test

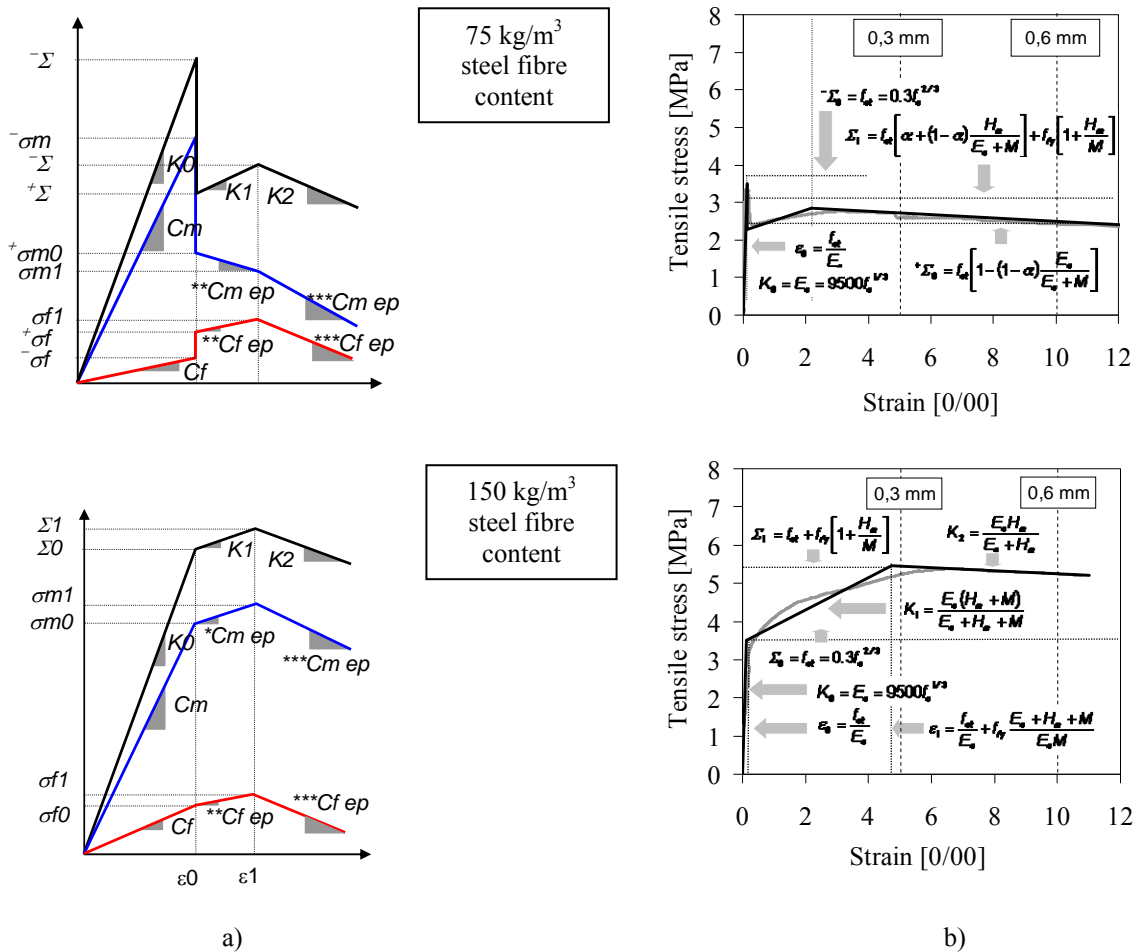


Fig. 5 Uniaxial tensile test results

- a) Tensile stress – strain relationships according to the uniaxial mechanical devices
- b) Experimental curves and characterization of model parameters

As a result indicate the developed material model can be used for determine the uniaxial stress – strain relationship of steel fibre reinforced concrete. Results of only one uniaxial compressive ( $f_c$ ) and uniaxial tensile ( $f_{ct}$ ) test, and prediction for the coupling modulus  $M$  and for the softening variable  $H_m$  are needed to characterize the model. Further, the coupling modulus  $M$  can be given as a function of the following parameters (Kovács 1998, Kovács 1999):

$$M = M\left(\frac{\ell_f}{\varnothing_f}, \alpha, \nu, C\right)$$

where  $\ell_f/\varnothing_f$  is the aspect ratio of the fibre,  $\alpha$  represents the direction parameter of fibre reinforcement,  $\nu$  takes into consideration the shape of steel fibre (crimped, hooked, etc.), while the bond characteristic of concrete – steel fibre is represented by  $C$ .

## 5. CONCLUSIONS

A 1-D material model for steel fibre reinforced concrete was developed. The model is composed of two devices representing an elastic-brittle material law for the concrete and an elastic-perfectly plastic material law for the steel fibre reinforcement behaviour, respectively. The two devices are coupled by an introduced new device element which links the irreversible concrete and irreversible steel fibre reinforcement behaviour. Due to the simplicity and clear physical significance of the developed 1-D mechanical model it was extended by different matrix and fibre reinforcement behaviour such as residual strength after matrix cracking or fibre fracture, matrix and fibre hardening or softening behaviour. Parameters of the developed model considering concrete and steel fibre reinforcement softening behaviour was characterised by uniaxial tensile test for 75kg/m<sup>3</sup> and 150 kg/m<sup>3</sup> steel fibre content. Parameters of the developed uniaxial model (stress-strain relationship) were derived from experimentally measurable (macroscopic) parameters. Determination of coupling modulus  $M$  needs further experimental investigation taking into account different fibre and concrete characteristics.

## 6. ACKNOWLEDGEMENTS

The experimental and theoretical research work has been financially supported by the Hungarian Research Establishment (OTKA Office) with the grants F021625 (Design of Steel Fibre Reinforced Structures).

## 8. REFERENCES

- Kovács, I. (1998), "Modeling of Plastic Matrix-Fiber Interaction in Fiber Reinforced Concrete", *Proceedings of the 2<sup>nd</sup> International Ph.D. Symposium in Civil Engineering*, Budapest, Hungary, 29-28 August 1998., pp.15-22.
- Kovács I., (1999), "Design Method for Steel Fiber Reinforced Concrete Based on an Engineering Model", *Proceedings of the 2nd International Conference of Ph.D. Students*, Miskolc, Hungary, August 20-22. 1999.

## PREPARATION AND HANDLING OF UHPFRC FOR THE MANUFACTURE OF THIN-WALLED BUILDING ELEMENTS

*Joachim Juhart*  
Dipl.-Ing.  
Carinthia University of  
Applied Sciences,  
school of civil  
engineering  
Spittal/Drau, Austria

*Bernhard Freytag*  
Dr. techn. Dipl.-Ing.  
Graz University of  
Technology  
Laboratory for Structural  
Engineering  
Graz, Austria

*Josef Linder*  
Dipl.-Ing.  
Graz University of  
Technology  
Laboratory for Structural  
Engineering  
Graz, Austria

*Lutz Sparowitz*  
Dr.techn. Univ.-Prof.  
Graz University of  
Technology  
Structural Concrete  
Institute  
Graz, Austria

### SUMMARY

An arch-bridge made of precast thin-walled building members shall be built in Austria using the strong and durable new building material UHPFRC. This paper deals with practice-oriented test series focusing on the preparation and handling of fresh UHPFRC with the aim to produce real size specimens. The attention was directed to the following parameters: aspects of the composition, mixing process, placing methods and formwork pre treatment. The properties under investigation were workability, de-airing behaviour, homogeneity and fibre distribution, strength and appearance of the UHPFRC-surface. A process is worked out, that leads to the production of pore free fair faced building members fulfilling the required high quality properties.

### 1. INTRODUCTION

UHPFRC (ultra high performance fibre reinforced concrete) is a strong and durable new building material. Because of its outstanding compression strength, one predestined field of application are compression elements like arch structures. Actually a bridge shall be built with an arch made of precast UHPFRC elements in Austria. The polygonal arch with a span of 71 m will be erected by the swivel in method. Single precast UHPFRC elements with a length of 5-17 m are thin walled (6 cm!) box type elements (1.20x1.20 m) assembled together before swivelling-in in a vertical position using prestressing tendons (Fig. 1 and Fig. 2).

The planning process is accompanied by several experiments regarding preparation and handling of fresh UHPFRC as well as fracture tests by means of real size specimens. This paper deals with practice-oriented test series focusing on process-parameters during the manufacture of thin-walled members. The attention is turned to the following parameters: aspects of the composition, mixing process, placing methods and formwork pre treatment. The test series lead to the production of real size specimens for following fracture test.

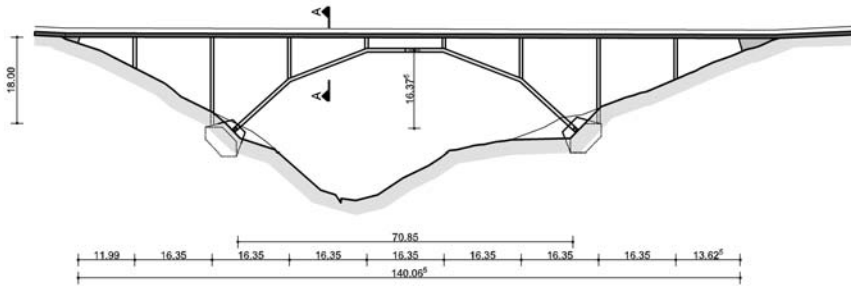


Fig. 1 Arch bridge view

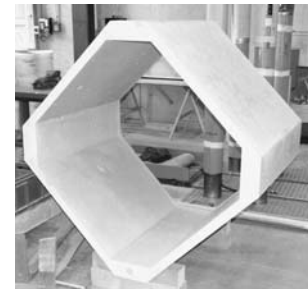


Fig. 2 Cross section

## 2. AIMS

The main task is to work out a process that leads to both, an easily workable, stable fresh concrete and a high strength, pore free fair faced building member. Therefore, the UHPFRC shall be self compacting and self de-airing. It shall be placed in a narrow formwork and the concrete shall become homogeneous with no segregation of aggregates or fibres. A high compressive strength according to a “C 165/185” concrete is aimed at and the tensile strength shall be high enough to bear secondary stresses, even if no ordinary reinforcement is used.

## 3. PROCESS PARAMETERS AND THEIR IMPACT ON MATERIAL PROPERTIES

### 3.1 Process parameters

The various process parameters and their impact on different material properties end in a complex system (Fig. 3). Any variation of a single parameter can influence other parameters (Dehn, 2003; Orgass, 2006; Seiler, 2004).



Fig. 3 Slump, “concrete cone”

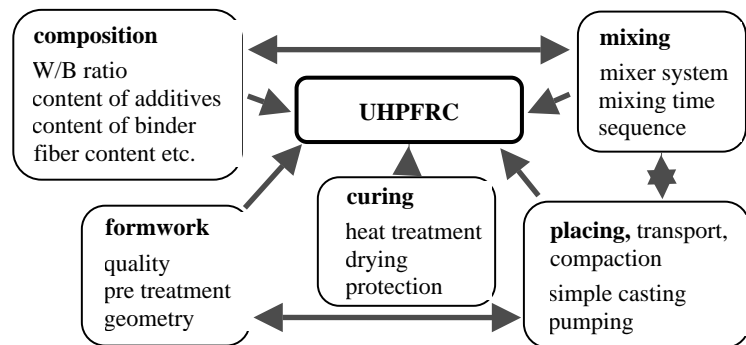


Fig. 3 Overview of process parameters

### 3.2 Properties under investigation

The *workability* is characterised by the slump flow tested following EN 12350-5 without shocks, the measurement is made two minutes after removing the cone (Fig. 3). In the laboratory the slump flow is measured in the same way but with smaller “mortar cones” (EN 1015-2, ASTM C 230).

The *air content* is measured by a pot (8 litres) with the pressure compensation method according to ÖNORM B 3303 for the test in the precast plant. Again for laboratory tests a smaller pot (1 litre) with the same function is used. The maximum *density* of the fresh concrete is determined with these pots too. The *homogeneity of the fresh* concrete is assessed

visually observing the slump and by comparing slumps and maximum densities of different samples taken from different batches or stadiums of the process. Also the *surface quality* is assessed visually. The *homogeneity of the hardened concrete* is determined by comparing the compressive strength, the maximum density and pore content of samples taken from different regions of one specimen. The fibre distribution is characterised by the measurement of the magnetic force along the specimens' height. The *compression strength* is determined on 100 mm cubes, tested according to ÖNORM B 3303, on the rule after 28 days.

#### 4. TEST SERIES AND TEST RESULTS

##### 4.1 Influence of the composition and mixing process

The used UHPRFC is a premixed product of SIKA called “ceracem”. Its standard composition “BFM Millau” is shown in Tab. 1 according to the technical product data sheet (Sika, 2003). In Ref. (Maeder, 2004) its W/B ratio is given as 0.19.

Tab. 1 Mix componets of the used UHPFRC

mix components	BFM Millau	TU Graz, range 36 tests
	[kg/m <sup>3</sup> ]	[kg/m <sup>3</sup> ]
premix ceracem, dry	2355,0	2331 – 2368
water	195,0	193 – 198
superplasticizer	44,6	40 – 49
retarder	0,0	0 – 15
steel fibres (20/0.3 mm)	195,0	150 -160

Even the composition of a preconfigured product has to be adapted to the properties of a specific task. To ensure flowability and de-airing, the amount of the superplasticizer (SIKA ViscoCrete 1030) has to be varied, depending on the different mixing procedures. A good workability is reached with a fresh concrete characterized by a slump flow of 24 cm, measured with the mortar cone that refers to a slump of 65 cm measured with the concrete cone. In the context of the project the question occurs, in how far test results of smaller laboratory mixers can be transferred to the industrial production mixers. One of the real size specimen requires a volume of about 1500 l fresh UHPFRC. It can only be realized by mixing two single batches of 750 l, one after the other in a precast plant mixer. Within the prior test series smaller specimen, smaller batch sizes and smaller mixers (30l, 150 l) with different mixer systems have to be used.

It turns out, that the slump flow of the concrete can be improved in two ways: by raising the dosage of the superplasticizer (within a small range) or by protracting the mixing time, depending on the mixer system. A too long mixing time in combination with a step by step addition of the superplasticizer leads to an over-mixing, high temperatures of the fresh concrete and a sticky, not workable concrete. The necessary mixing time until the wanted flowability of the fresh concrete is reached differs significantly from mixer to mixer. Especially the point at which the visually still dry mixture of particles and water becomes fluid after infilling the superplasticizer varies depending on the mixing process. A span of the mixing time for this period of 2 minutes to 8 minutes is observed. Differences of 10 to 17 minutes in the total mixing time are made to reach the slump flow aimed at.

Compositions or mixing processes that lead to an increase of the slump flow are always connected with a decrease of the air content. A handling and transfer of the concrete into a storage where batches are put together can increase the air content.

#### 4.2 Influence of vibration on slump flow and air content depending on time

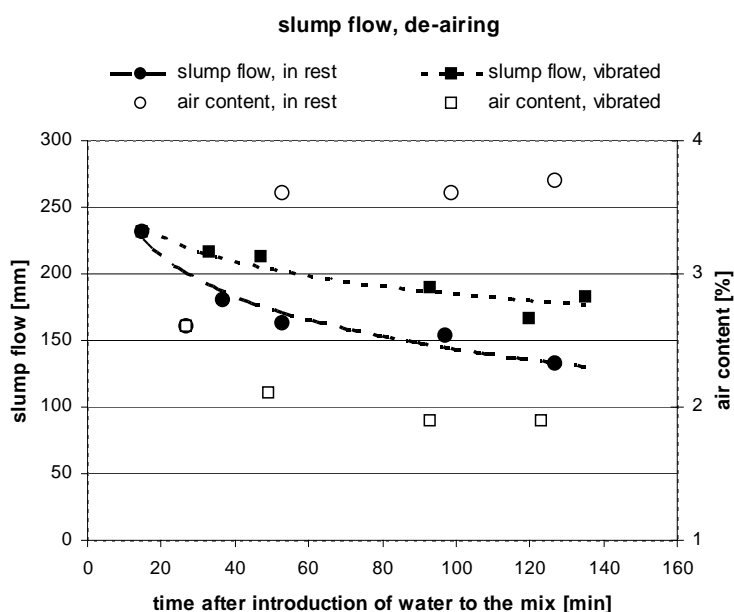


Fig. 4 Slump flow and air content with time

The slump flow turns out to decrease drastically with increasing time after the mixing and storing the fresh concrete. On the other hand the highly viscous and sticky mixture becomes more and more flowable during the process of casting it into the formwork.

To investigate this effect, the slump flow and the air content is measured depending on the storing time and depending on a re-moving of the fresh concrete. Therefore samples are taken out of two mason's hods with a content of 50 litres. The content of one hod is vibrated with an immersion vibrator for a minimum of 2 minutes before doing the tests. The other hod is let without treatment. The results are shown in Fig. 4: The slump flow, measured with the mortar cone, keeps being larger and the de-airing can be supported by vibrating the concrete.

#### 4.3 Influence of formwork pretreatment

Aiming on a pore-free surface of the test specimens, the following pretreatments of the wooden mould are studied:

Tab. 2 Pretreatment methods

	pretreatment	short description	specimen denotation
release agents	Separol®	based on mineral oil with few solvent	C OB-1
	Separol®-6W	without solvent	C OB-2
	Separol VP 233	based on emulsion	C OB-3
	floor polish	based on wax	C OB-4
draining sheets	Zemdrain® MD	draining formwork sheet using a special pastic grid	C OB-5
	Zemdrain® Classic	draining formwork sheet using a rough PP-fibre textile	C OB-6

The test series is accomplished by means of 2 m high, thin-walled members that are cast in a vertical position. The results of the surface quality are shown in Fig. 5 and 7. All release agents show the same effect: There are no pores at the concrete surface of the upper part of the specimen (about 1 m high). The lower part shows lots of pores with a maximum diameter of 10 mm. The use of the draining layers results in absolutely pore free surfaces all over the specimens. The texture of the draining layer is transferred onto the surface of the concrete.

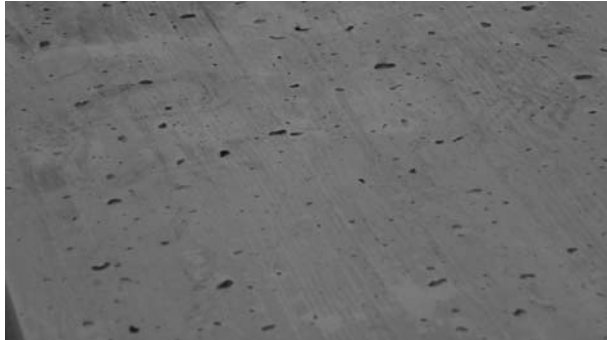


Fig. 5 Surface using release agents

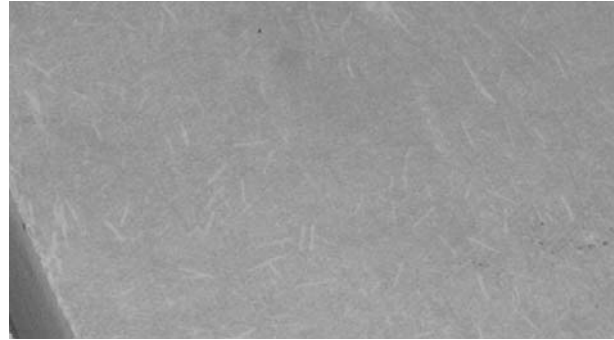


Fig. 6 Draining sheets

#### 4.4 Influence of the placing method

In order to get some information about the influence of the placing method on the homogeneity of the concrete, three specimens (3 m high) are cast using the following methods given in Tab. 3.

Tab. 3 Placing methods

specimen notation	C BE-1	C BE-2	C BE-3
placing method	continuous pulling of the filling-hose; the end of the hose is always lower than the concrete level	Simple casting by the use of a filling-hose ending at the top of the formwork	Casting from the bottom of the formwork by the use of a stand pipe



Fig. 7 shows the compressive strength of the specimens determined on drilling cores (100/100) taken from both, the upper part and the lower part of the specimen. Each value is an average of two samples. All placing methods under investigation show different strength between the top and the bottom in a range of 5 to 7%. After cutting the specimens along the height, the pores are counted also at the top and the bottom. The number of pores corresponds well with the measured density of the cores, which also show very good correlation with the strength values

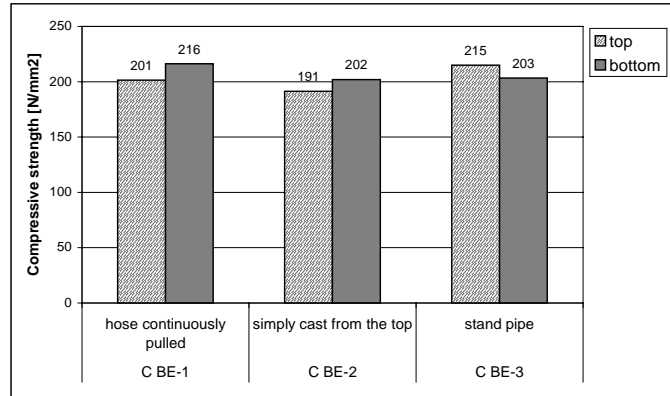


Fig. 7 Compressive strength of cores

In addition to the visual evaluation of the cut surface, the homogeneity of the fibre distribution is studied by magnetic pull-off tests along the longitudinal cut surface. The magnetic force is measured on both sides of the cut and averaged afterwards. The difference between top and bottom as well as the deviation to a linear regression are significant measures for the homogeneity of the fibre distribution (see also Fig. 8). However, one must keep in mind that the magnetic force does not only depend on the local fibre content but also on the local fibre orientation. The lower magnetic forces all over the cut of specimen C BE-3 is probably explainable by a more vertical fibre orientation caused by the upward flow during the placing and the final pulling of the stand pipe respectively. The visual evaluation confirms this explanation.

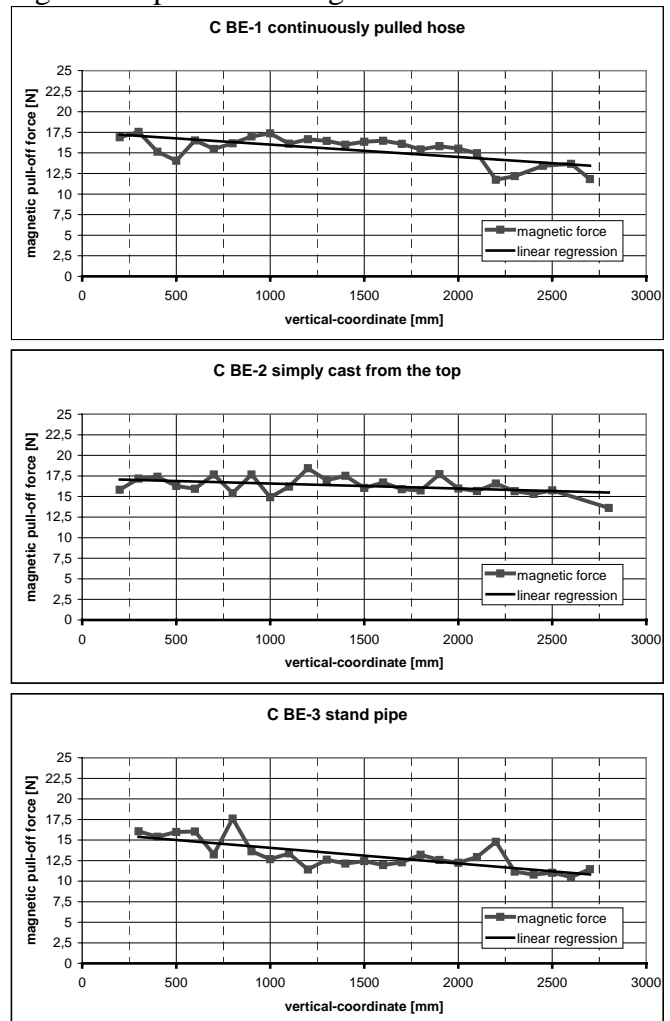


Fig. 8 Homogeneity of fibre distribution

## 5. CONCLUSIONS AND OUTLOOK

A de-airing due to vibration, moving of the concrete respectively, was observed, but also an increase of air content caused by handling and storing of a viscous mixture. The mixing process has a significant influence on the workability. A certain amount of mixing energy is required. Less power of a mixer can be compensated by extended mixing time. After reaching the transformation from granular conglomerate to viscous mixture there is a danger of “over-mixing” resulting in a loss of workability. In that case the concrete becomes too stiff and

sticky. A pore free surface of high, vertically cast elements is only reachable by the use of draining sheets.

Based on these results and the experience gained during the tests, two real size specimens for a large scale fracture test are produced. Those are a 5 m high thin-walled octagonal tube (part of the arch) and a rather compact element (coupler between two arch elements), see Fig. 9 and Fig. 10. The methods used and the properties achieved are summarised in Tab. 4.

Tab. 4 Methods, properties and results for real size specimens

	method used	results	
mixer: 1500 l batches: 800 l, 250 l	axial agitator with 2 blades running close to the rim and 2 excentric agitators running counter-currently	mixing time, mean of 3 mixes	15 min
		demand of superplasticizer	44,0 kg/m <sup>3</sup>
		slump, mean value of 3 mixes	69,5 cm
		air content, mean of 3 mixes	2,2 %
form work pre treatment	Zemdrain <sup>®</sup> MD applied	surface condition	pore free
placing method	Simply cast from the top	homogeneity of the hardened concrete	no results yet
storing of fresh concrete	Crane skip; immersion vibrator	slump, mean value, 2 batches	56,6 cm
		air content, mean of 2 batches	2,8 %
compression strength	100 mm cubes, stored and tested acc. ÖNORM B 3303	mean value of 6 specimen	203 N/mm <sup>2</sup>



Fig. 9 Octagonal tube - specimen

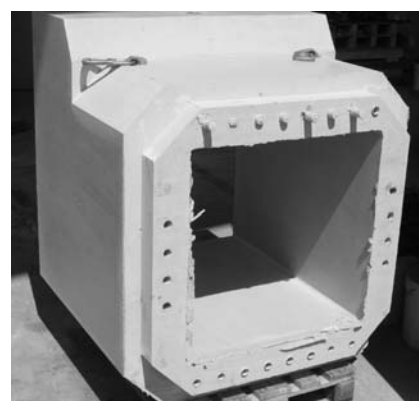


Fig. 10 Coupler - specimen

Due to the great number of influencing factors and their interdependence, very extensive test series would be necessary in order to allow general conclusions. Therefore, further research, following the systematic of Fig. 3 shall be done within the scope of a K-project “Sustainable Concrete Constructions by Saving Resources and Increasing of Quality” applied for by the FFG Austria.

## 6. ACKNOWLEDGEMENTS

We thank the companies: SIKA Austria (namely Dr. Günter Grass), “Katzenberger Baustoffindustrie Graz” (precast plant), Bekaert and IFT Fasertechnik (steel fibres) and the Carinthian local government, department for roads and bridges.

## 7. REFERENCES

- Dehn, F., "Herstellung, Verarbeitung und Qualitätssicherung von UHPC", *structural materials and engineering series, No.2*, 2003, kassel university press, p.37-47
- Maeder, U. et al., "Ceracem, a new High Performance Concrete: Characterisations and Applications", *structural materials and engineering series, No. 3*, 2004, kassel uni press
- Orgass, M.; Dehn, F., "Effect on Mixing Technology on High-Performance Concretes", *Concrete Plant + Precast Technology*, No. 1, 2006, Bauverlag Gütersloh
- Seiler, A.; Kasten, K. Seidel, M., "Conditioning and intra-company transportation of UHPC", *Concrete Plant + Precast Technology*, Jg. 70 (2004), Nr.4, p.14-20
- SIKA France S.A., "ceracem BFM-Millau", *technical data sheet*, Edition 04, 2003

## **PRODUCT-ORIENTED RESEARCH ON HIGH PERFORMANCE STRUCTURES**

*Prof. Dr.-Ing. habil. Nguyen Viet Tue, Dipl.-Ing. Gunter Schenck, Dipl.-Ing. Stefan Henze  
Leipzig University  
Institute for Structural Concrete and Building Materials  
04109 Leipzig, Marschnerstraße 31  
Germany*

### **SUMMARY**

High performance structures made of ultra high performance concrete (UHPC) are a challenge and chance for the future development of new kinds of concrete constructions. In this contribution suggestions for an application orientated material development of UHPC are presented. Furthermore promising applications for UHPC in frameworks and composite constructions are presented.

### **1. INTRODUCTION**

New perspectives in the development of concrete constructions arise by using ultra high performance concrete. The large spectrum of possible material properties allows the realisation of filigree and elegant constructions with high bearing capacity and long lasting durability. To develop a marketable product the process of development requires the investigation of structural, material technology and manufacturing technology aspects too. At present, several applications for UHPC are developed at the Leipzig University. This paper deals with some results of the research.

### **2. MATERIAL DEVELOPMENT OF UHPC**

Ultra high performance concrete represents an important source for forward-looking concrete constructions. Because of this UHPC-mixtures for different requirements were developed at the Leipzig University (Tue, Kuchler, Ma, Henze, 2006). The aim of the investigations was to determine the systematic influence of the use of steel fibres to the tensile and flexural tensile strength as well as the ductility. At the same time the workability and material costs were optimized to create a suitable and economic UHPC. Tab. 1 shows the mix proportions of the developed UHPC. All developed UHPC-mixtures reached cylinder compressive strengths in the range of 160 to 180 N/mm<sup>2</sup> after 28 days water curing without heat treatment. There are only marginal differences between the compressive strength of UHPC with and without coarse aggregates. Also the fibre content has no significant affect on the achievable compressive strength. In UHPC containing coarse aggregates the lower cementitious paste and the stiffer basalt split result in a noticeable decrease in autogenous shrinkage (Ma et al, 2004). Due to the reduced silica fume and fibre content the material costs of UHPC with coarse aggregates are lower than UHPC without coarse aggregates.

Fibre reinforced UHPC should be self-compacting to minimise the scatter of material properties in constructions. Therefore, the slump flow for UHPC without coarse aggregates

should be larger than 650 mm. The slump flow for UHPC with coarse aggregates should amount between 630 and 700 mm.

Tab. 1 Mixing proportions

material		UHPC without coarse aggregates	UHPC with coarse aggregates
cement CEM I 42.5 R	kg/m <sup>3</sup>	665-760	530-630
silica fume	kg/m <sup>3</sup>	95-230	95-115
quartz powder	kg/m <sup>3</sup>	285-425	285-340
quartz sand (0.3-0.8 mm)	kg/m <sup>3</sup>	580-1020	390-490
basalt split (2-5 mm)	kg/m <sup>3</sup>	-	750-925
steel fibres	kg/m <sup>3</sup>	95-375	60-155
w/b-ratio	-	0.20-0.25	0.20-0.25
<b>material costs</b>	<b>€/m<sup>3</sup></b>	<b>600-1500</b>	<b>500-800</b>

To assure the necessary flowability limits are set for the maximum fibre content. The maximum fibre content is addicted from the fibre geometry, the grain size and cementitious paste volume. Thereby long fibres affect the flowability more negative than short fibres. At an identical paste volume in UHPC without coarse aggregates higher fibre contents and longer fibres as in UHPC with coarse grain can be realised. Therefore, UHPC without coarse grain can reach higher tensile and flexural tensile strengths than UHPC with coarse grain.

Fig. 1 shows the range of the achievable flexural tensile strengths in the 3-point-bending-test according to RILEM TC 162-TDF (Barr, 2003). Fibre contents between 0.75 vol.-% and 4.9 vol.-% were investigated. The used steel fibres are straight or waved with a diameter of 0.16 mm and had fibre lengths between 6 and 18 mm. Fibre cocktails of short and long fibres are a good alternative to ensure the flowability on the one hand and to increase the flexural strengths on the other hand. In this context long fibres increase also the flexural strength as well as the ductility after cracking and short fibres increase primary the flexural strength.

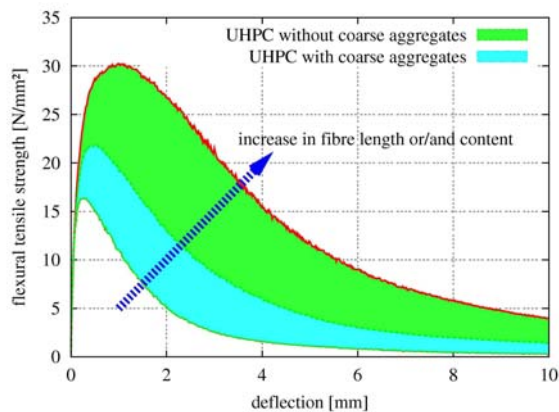


Fig. 1 Result of 3-point bending test according to RILEM TC 162-TDF

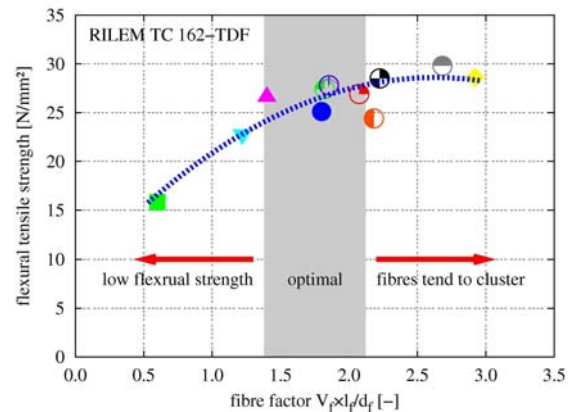


Fig. 2 Correlation between fibre factor and flexural tensile strength for UHPC without coarse aggregates

The effectiveness of the fibre addition can be described using the fibre factor (Fig. 2). The optimal fibre factor for UHPC without coarse aggregates should be in a range between 1.5 and 2.25. Lower values allow less improvement of the flexural tensile strength. Greater values

increase the flexural bending strength underproportionally and the fibre tends to cluster. Because of the wide range of possible material properties of UHPC, an application-oriented material development is necessary. In this process the different parameters of UHPC with and without coarse aggregates are considered to afford an efficient application of UHPC.

### 3. MODULAR TRUSS SYSTEM MADE OF UHPC

Truss systems afford a maximum utilisation of the material strength due to the loading with normal forces only and permit crossing large spans with low dead loads. Therefore, truss systems are appropriate applications for UHPC because of the very good density-strength-ratio  $\rho/f_c$  of the material. The expensive formwork and complex construction of the monolithic joints from conventional concrete truss systems make an economic application difficult. Furthermore, the transport and erection leads to problems due to the great length and weight of monolithic trussed beams.

At the Leipzig University a modular truss system made of UHPC was developed, which avoids the disadvantages of monolithic concrete truss systems. The modular truss system consists of separate chords, braces, posts as well as connecting and tension elements (Fig. 3). The truss members are made of steel fibre reinforced UHPC with coarse aggregates. In addition, the chords are prestressed with tension wires. Because of the high compressive strength, high prestressing forces could apply on a small cross-sectional surface. The connecting elements consists of steel fibre reinforced UHPC without coarse aggregates. Thread rods are used as tension elements. Fig. 4 shows the assembly of the truss members using the connecting and tension elements. A high flexibility for the transport and erection of the UHPC truss system is guaranteed, because the assembly can be carried out in the precast concrete manufacturing yard or on the building site. The connecting elements can realise brace inclinations between  $30^\circ$  and  $60^\circ$ . Because of this, the geometry of the truss system can be easily adapted to the current requirements. The truss members can be prefabricated in large quantities and lengths. The truss members are cut to the required length by a saw. This production method reduces the building costs substantially.

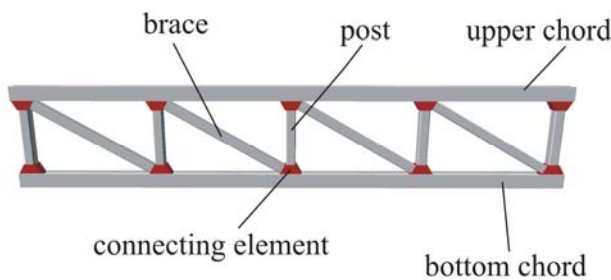


Fig. 3 Side view of the truss system

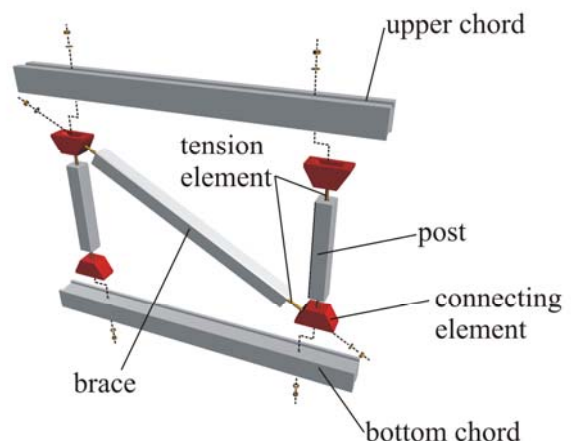


Fig. 4 Assembly of the truss system

The connecting elements transmit compressive, tension and shear forces between the connected frame members. The contact joint is designed as a dry joint to simplify the erection. The transmission of compressive strengths is carried out via contact. To transfer

tension forces the joint is prestressed with tension elements. Shear forces can be transferred via friction forces activated in the joint by prestressing.

Fig. 5 shows the test set-up to determinate the bearing capacity of the connecting element under a tension load. This case is relevant for truss systems with tension braces. In the performed tests the tension forces as well as the slip between the chord and the connecting elements, the opening of the joint and the displacement in the tension force direction are measured. During the test the prestressing force is constant at 500 kN. Depending on the construction of the connecting element, two different failures can be identified (Fig. 6). If the connecting element is designed without reinforcement the connecting element fails. The ultimate load is influenced by the orientation and number of fibres at the crack area. These parameters are significantly affected by the casting method. If the connecting element is reinforced with two stirrups in the tension zone, the element does not fail, but a ductile friction failure between the cord and the connection element occurs. In this case a tension force above 500 kN could be applied. Furthermore, the tests revealed that it is better to improve the bearing capacity with reinforcement rather than by increasing the fibre content.

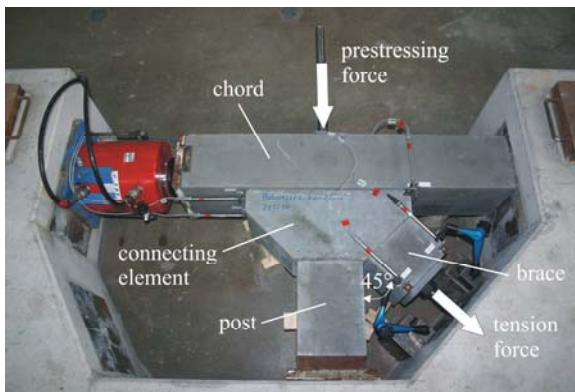


Fig. 5 Test set-up for the connecting element

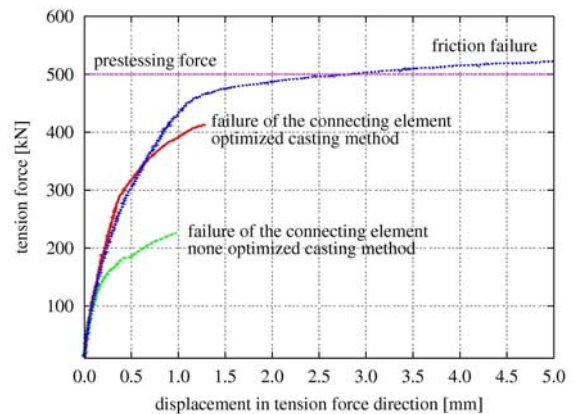


Fig. 6 Test results for the connecting element (brace inclination 45°)

For the intended practical application of the truss system the reinforced connecting element should be used. Thus on the one hand a very ductile failure can be achieved and on the other hand it is possible to increase the bearing capacity by profiling the joint area between the cord and the connecting element. Furthermore, with the reinforcement the required bearing capacity can be achieved without greater scatters. With the truss system not only the high material strength of UHPC could be utilised, but also the developed construction offers economic advantages compared to established structures. In comparison to a truss system made of steel with an identical load bearing capacity the production costs of the UHPC truss system are about 40-50 % lower at this time. Furthermore, the excellent durability of UHPC reduces the maintenance costs and increase the life time of the structure. Because the truss system can be disassembled non-destructively, most elements can be reused to build up a new construction. Thereby the developed UHPC truss system satisfies the demands on the sustainability, which must be applied to structures in future.

#### 4. UHPC-FILLED STEEL TUBES

UHPC-filled steel tubes offer good opportunities to use the high compressive strength in a composite construction. Thus the advantages of the two materials could be maximized. The developed hybrid compression element consists of an UHPC core, which is confined by a steel tube. The composite action between the UHPC and the steel tube is induced by normal

and tangential stresses without shear connectors. The required ductility of the hybrid element is guaranteed by the steel tube. Therefore no fibre additions are necessary for the UHPC. The generated confinement effect increases the ultimate load about 60 % and the fracture strain about 40 % in comparison to a non-confined UHPC (Tue, Schneider, 2003).

Fig. 6 shows the test set-up for the UHPC filled steel tube with a slenderness of  $L / D = 3.8$ . In the test two levels of measurements (center and  $D/2$  of the edge of the cross section) with three  $90^\circ$ -strain gauge rosettes were arranged for monitoring the steel strains. Additionally, the total deformations of the specimens were recorded. The geometry of the specimens was almost identical. Only the wall thickness of the steel tube was varied. For the load application it is important whether the entire cross-section (series NG) or only the concrete (series NB) is loaded. If the load is applied on the entire cross-section the stiffness of the specimen is higher as if only the concrete is loaded. The increasing of the stiffness is proportional to the ratio of the steel and concrete cross-sectional area  $A_{\text{steel}} / A_{\text{concrete}}$ , because the young's modulus of the steel and the UHPC are almost constant in all specimens. The series NB reaches slightly greater ultimate loads and significantly higher fracture strains compared to the series NG. Fig. 7 illustrate this behaviour for an UHPC ( $f_{c,\text{cyl}, 28\text{d}} = 174 \text{ N/mm}^2$ ) filled steel tube with a diameter of 168.6 mm and a wall thickness of 3.95 mm. The strength of the pipe material can be indicated for the relevant strain ranges at approximately  $350 \text{ N/mm}^2$ .

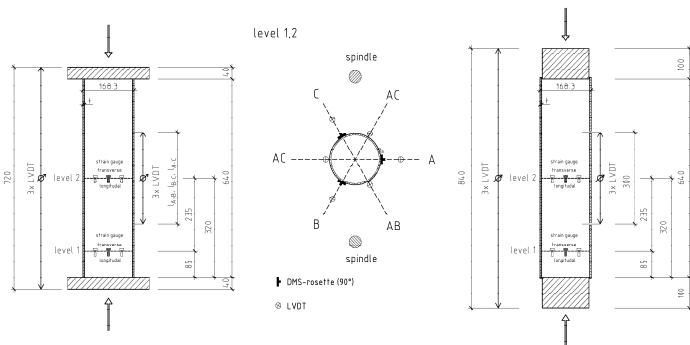


Fig. 6 Test setup for the series NG (left) and NB (right)

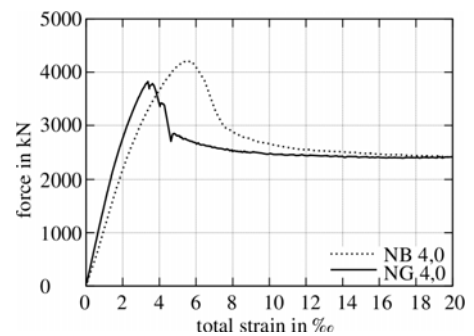


Fig. 7 Test results for the series NG 4,0 and NB 4,0

Due to the high bearing capacity and easy manufacturing UHPC filled steel tubes are a good alternative to steel composite columns in multi-storey-buildings. The high compressive strength allows designing transparent buildings with concrete. Furthermore, the costs per load unit for a UHPC filled steel tube are about 50 % lower in comparison to conventional composite columns with steel core (Tue, Schenck, Küchler, Reinhardt, 2004).

For bridges also new construction methods arise with the application of the UHPC filled steel tubes. Fig. 8 shows the concept for a hybrid arch bridge. It is possible to prefabricate the steel-arch including a thin-walled formwork of UHPC for the bridge deck in two parts. The light bridge superstructure can be transported to the building site separately and joined together. Now the required bearing capacity of the bridge is realised by filling the arch with UHPC. After casting the bridge deck and the capping concrete the bridge is completed. Furthermore by the high density and durability it becomes possible to replace the carriageway surfacing through high performance or ultra high performance concrete.



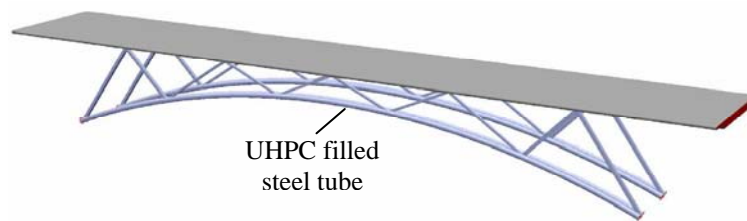


Fig. 8 Arch bridge with UHPC-filled steel tubes

## 6. CONCLUSION

Ultra high performance concrete is different from conventional concrete because of its very high compressive strength and durability. By use of steel fibres in addition the tensile strength and flexural tensile strength can be optimised for different specifications. Thus with UHPC a high performance material is available. Conventional constructions of reinforced concrete do not afford to use the full potential of UHPC from constructional and economic point of view. Because of this, new kinds of structures must be developed to permit a successful application of UHPC. Especially truss systems or hybrid constructions are suitable structures to utilize the high compressive strength of UHPC. With innovative production methods and connection techniques the construction period and building costs can be reduced. Structures made of UHPC become also attractive also under economic point of view. Finally, the excellent durability of the material contributes to increase life time and sustainability of the construction.

## 7. ACKNOWLEDGEMENT

The presented results were developed in the context of research projects financed with support of Bilfinger - Berger AG and Max Bögl GmbH & Co KG. The support of these projects is gratefully acknowledged.

## 8. REFERENCES

- Barr, B. I. G., et al (2003), "Round-robin analysis of the RILEM TC 162-TDF beam-bending test: Part 1 – test method evaluation", *Materials and Structures*, Vol. 33, No. 11, November, pp. 609-620.
- Ma, Jianxin et al (2004), "Comparative Investigations on Ultra-High Performance Concrete with and without Coarse Aggregates", *Proceedings of International Symposium on Ultra-High Performance Concrete*, Kassel, Germany, pp. 205-212
- Tue, N. V., Küchler, M., Ma, J., Henze, S. (2006), "Überlegungen zur anwendungsorientierten Stoffzusammensetzung von UHFB", *Beton- und Stahlbetonbau*, Vol. 101, No. 11, November 2006, pp. 834-841.
- Tue, N. V., Schneider, H. (2003), „Hybride Konstruktionen aus UHFB“, in: König, G., Holschemacher, K., Dehn, F. (Hrsg.): in: *Ultrahochfester Beton*, Bauwerk Verlag, Berlin
- Tue, N. V., Schenck, G., Küchler, M., Reinhardt, J. (2004), „Application of UHPC filled Tubes in Buildings and Bridges“, *Proceeding of International Symposium on Ultra-High Performance Concrete*, Kassel, Germany, pp. 807-817

## **CRACKING AND DEFORMATION BEHAVIOUR OF REINFORCED UHPC ELEMENTS**

*Dipl.-Ing. Marion Rauch, M.Sc., Prof. Dr. Viktor Sigrist  
Hamburg University of Technology  
Hamburg, Germany*

### **SUMMARY**

Ultra-high performance concrete (UHPC) is characterised by a compressive strength of more than 150 MPa as well as by improved durability properties compared to normal strength concrete. With the addition of steel fibres and in combination with reinforcing steel this material offers new possibilities for the further development of structural concrete. However, regarding the mechanical behaviour of reinforced UHPC elements only limited knowledge and experience is available. The present study is focused on the investigation of different types of reinforcing steel and their influence on the cracking and deformation behaviour of structural elements. The overall aim of this research is to develop reliable procedures for the conception and design of structures made of ultra-high performance concrete.

### **1. INTRODUCTION**

Starting with the development of reactive powder concrete in the eighties of the last century new types of concrete were invented which are now summarised with the term ultra-high performance concrete (UHPC) [here, the general abbreviation UHPC is used even if ultra-high performance fibre reinforced concrete (UHPFRC) is dealt with]. However, substantial modifications of the concrete composition have been necessary to realise this development. Compared to normal strength concrete, made of a so-called three-composite-system of water, cement and aggregates, ultra-high performance concrete consists of a five-composite-system. By adding admixtures and additions the concrete properties such as compressive strength, workability and durability can be substantially improved. The modified properties of UHPC depend on the following factors (Schmidt and Fehling, 2003):

- a low water/cement ratio of 0.20 to 0.30
- a high amount of hardened cement paste by adding suitable mineral additions
- a high density of the hardened cement paste as well as of the aggregates
- a low water demand of the fresh concrete and a low porosity of the hardened concrete
- additions, such as steel fibres, to achieve adequate ductility.

Ultra-high performance concrete has a very dense structure and is used either as fine-aggregate concrete with a maximum particle size of 0.5 mm or as coarse-aggregate concrete with a maximum particle size of 8 mm or 16 mm. As the matrix of ultra-high performance concrete exhibits a quite brittle behaviour short steel fibres are added to improve ductility in compression as well as in tension. Furthermore, the concrete strength is slightly increased with the addition of fibres. These improvements strongly depend on the type of fibres and on the fibre content and orientation.

Due to the improved properties, ultra-high performance concrete initiates a new era for the concrete industry and opens new applications (Walraven, 2004) in the field of structural concrete. UHPC is promising with regard to the design of slender and aesthetically appealing structures. Furthermore, UHPC ensures high corrosion resistance which reduces the costs for maintenance and can be seen as a first step towards no-maintenance structures. With regard to sustainability UHPC also economises with raw material and energy (Racky, 2004). For these reasons UHPC is associated with keywords like innovative or high-tech material.

The behaviour of reinforced concrete structures is significantly affected by the bond between concrete and reinforcing steel; important aspects are the control of crack widths, the anchorage of reinforcing bars, the stiffness of reinforced concrete elements and the deformation capacity of plastic hinge regions (Marti et al., 1998, Sigrist, 1999). Therefore, the cracking and deformation behaviour of ultra-high performance concrete with steel fibres and different types of reinforcing steel is investigated. The overall aim is to develop reliable procedures for the conception and the design of structural elements.

## 2. EXPERIMENTAL INVESTIGATION

To establish a basis for the ongoing research an experimental study was carried out at the structures-laboratory of TUHH (Hamburg University of Technology). The experimental programme comprised a total of 12 tension tests with longitudinally reinforced UHPC prisms (Fig. 1) and 12 pull-out tests with UHPC cubes (Fig. 2). All UHPC specimens had a content of short steel fibres ( $l_f = 9$  mm,  $d_f = 0.15$  mm) of 2.5 % in volume. In the tension and the pull-out tests conventional as well as high-strength reinforcing steel was used (Tables 1 and 2). To determine the material properties these experiments were accompanied by compression and direct-tension tests.

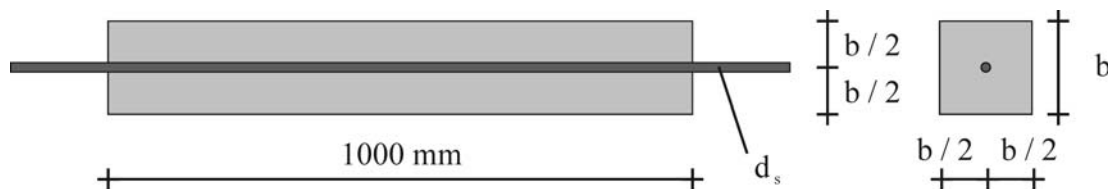


Fig. 1 Reinforced UHPC specimens for tension tests (series Z)

	Z1	Z2	Z3	Z4
type of reinforcing steel	S 500	high strength steel		strands
yield strength $f_y$ [MPa]	500	950		1570
tensile strength $f_u$ [MPa]	550	1050		1770
width of specimen $b$ [mm]	170	110	160	80
diameter of bar / strand $d_s$ [mm]	28	18	26.5	15.2
geometrical reinforcement ratio $\rho$ [-]	0.0213	0.0210	0.0215	0.0219
mechanical reinforcement ratio $\omega$ [-]	0.0533	0.0999	0.1023	0.1717

Tab. 1 Tension tests (series Z)

After taking the specimens out of the formwork (2 days after moulding) they were heat treated at 90 °C for 2 days. The concrete reached the expected strength at an age of 4 days.

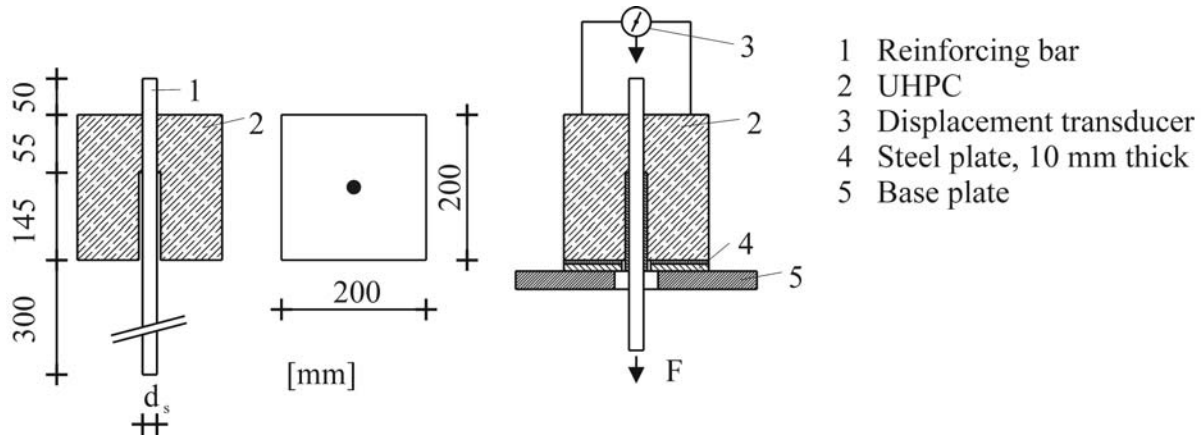


Fig. 2 UHPC specimens for pull-out tests (series A)

	A1	A2	A3	A4
type of steel	S 500	high strength steel		strands
yield strength $f_y$ [MPa]	500	950		1570
tensile strength $f_u$ [MPa]	550	1050		1770
diameter of bar / strand $d_s$ [mm]	28	18	26.5	15.2

Tab. 2 Pull-out tests (series A)

The tension tests (series Z) were carried out in two steps: First, the specimens were loaded force-controlled up to steel stresses of 750 MPa and 500 MPa, respectively, and unloaded; second, the specimens were reloaded deformation-controlled up to failure. Deformations and forces were recorded continuously, crack width have been measured at the load stages and after failure. Recordings included forces and displacements of the testing machine, deformation measurements at the free top end of the steel bars, measurements over the entire specimen length of 1 m and three measurements of local deformations over a length of 200 mm.

### 3. MATERIAL PROPERTIES

To determine the compressive strength  $f_c$  and the modulus of elasticity  $E_c$  UHPC cylinders with a diameter of 150 mm and a height of 300 mm were tested (Fig. 3).

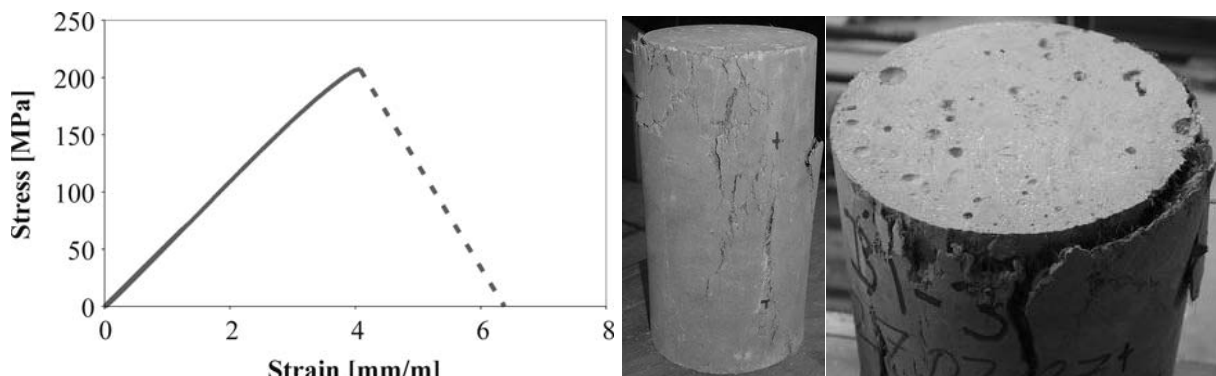


Fig. 3 Typical stress-strain-diagram of UHPC with fibres in compression

In compression ultra-high performance concrete exhibits an almost linear elastic behaviour

until ultimate load (corresponding to the strain  $\epsilon_c$ ) (Fehling et al., 2004). At failure a significant amount of fracture energy is set free. As indicated in Fig. 3, this effect made it difficult to control the descending branch of the stress-strain curve even if a stiff testing machine was used.

Tab. 3 Material properties of UHPC with fibres in compression

specimen no.	$f_c$ [MPa]	$E_c$ [MPa]	$\epsilon_c$ [mm/m]
B1-1	213.3	-	4.81
B1-3	194.5	50'769	4.05
B1-4	202.7	51'909	4.25
B1-5	203.5	51'758	4.26
mean value	203.5	51'479	4.34
B2-1	197.4	53'299	3.93
B2-2	207.3	54'572	4.07
B2-3	219.7	54'259	4.44
B2-5	204.6	-	4.19
mean value	207.3	54'043	4.16

Fig. 4 shows a typical result of a direct-tension test on UHPC with fibres. Again, a linear elastic behaviour can be observed until, in the range of 7.5 to 9 MPa, first macro cracks appear. After that no or only a slight increase of stresses is measured and at a deformation of approximately 0.2 mm (over a length of 100 mm) a drop of stresses occurs. In this softening branch of the curve, tension forces are transferred by the steel fibres that are continuously pulled out of the concrete matrix.

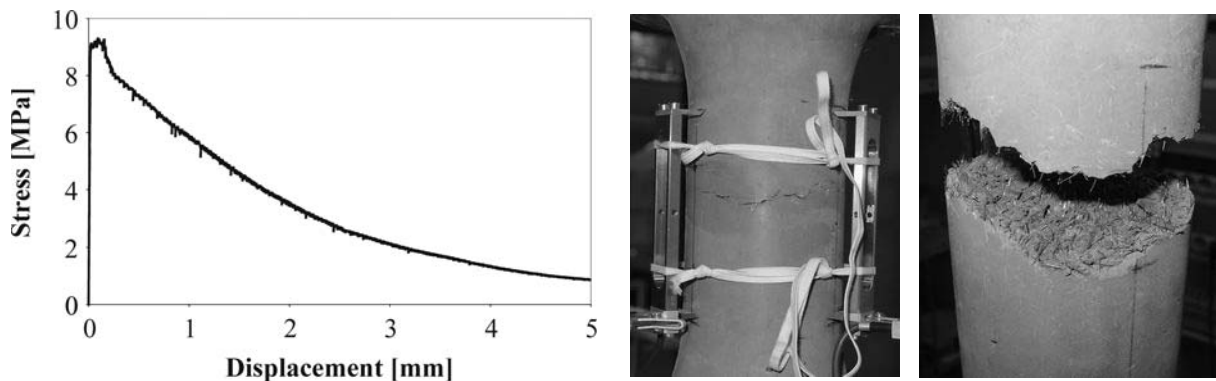


Fig. 4 Typical stress-displacement-diagram of UHPC with fibres in direct-tension

#### 4. TENSION TESTS

The test set-up of the tension tests is shown in Fig. 5. The deformation behaviour of the specimens can be subdivided in three typical phases (Figs. 6 to 9): The phase prior to cracking, the cracking phase and the phase after the onset of yielding.

Prior to cracking, the specimens exhibit an almost linear elastic behaviour; only micro cracks occur. The overall stiffness is controlled by the geometry of the components and the material properties; internal cracks due to restrained shrinkage might influence the results. After reaching the tensile strength of the concrete matrix several macro cracks appear. The force-strain-curves are linear and run more or less in parallel to those of the steel bars and strands,

respectively. Forces are transferred across the cracks by the reinforcement and the steel fibres that are pulled out. However, the overall stiffness of the specimens seems to be mainly controlled by the stiffness of the reinforcing steel in that phase.

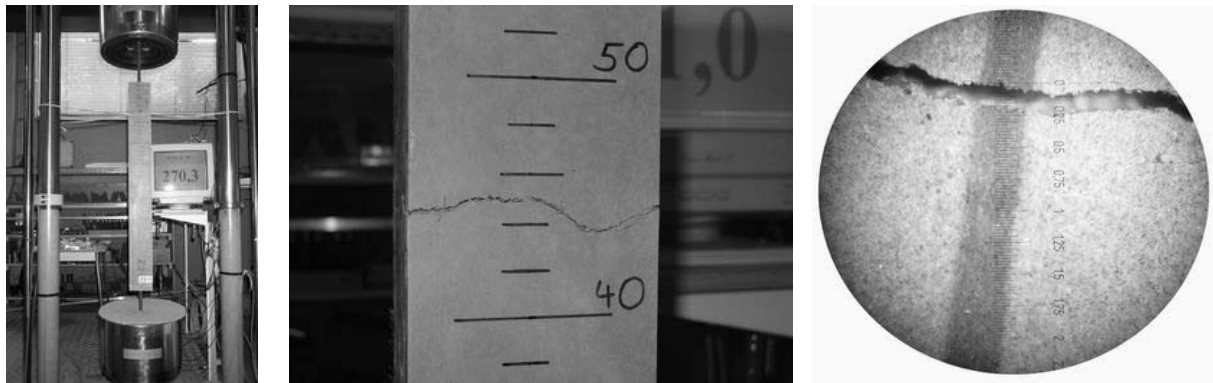


Fig. 5 Tension tests: test set-up and crack details

The third phase starts at yielding of the reinforcing steel. In that phase, stresses and deformations strongly depend on the yielding stiffness of the steel and on the softening behaviour of the cracks (Redaelli and Muttoni, 2007). Corresponding to the forces that are transferred by the steel fibres also in the yielding phase, ultimate load is increased compared to that of the bare steel. Due to this fact (and the simplicity of the test set-up) the specimens failed by rupture of the reinforcing steel at the free ends of the bars.

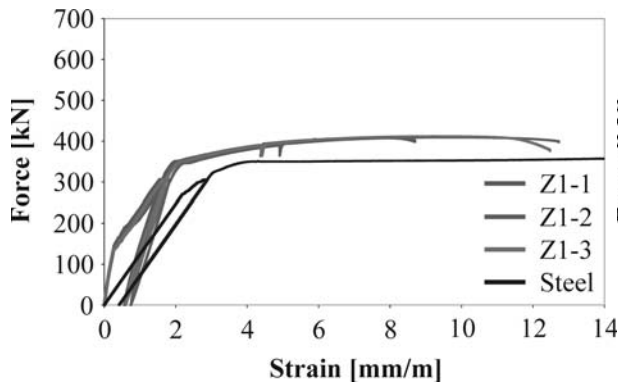


Fig. 6 Force-strain-curves of Z1 specimens

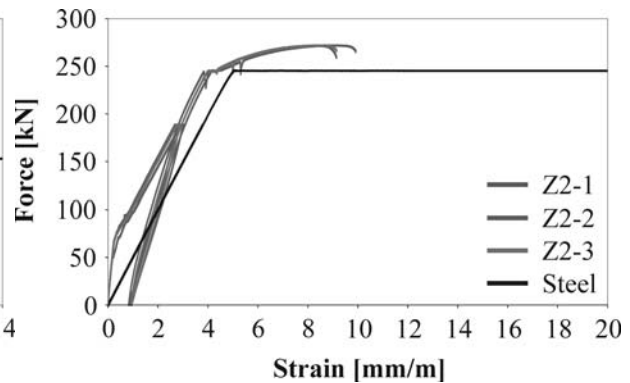


Fig. 7 - Force-strain-curves of Z2 specimens

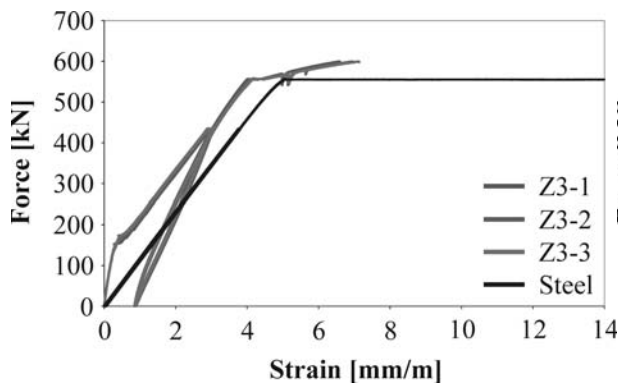


Fig. 8 Force-strain-curves of Z3 specimens

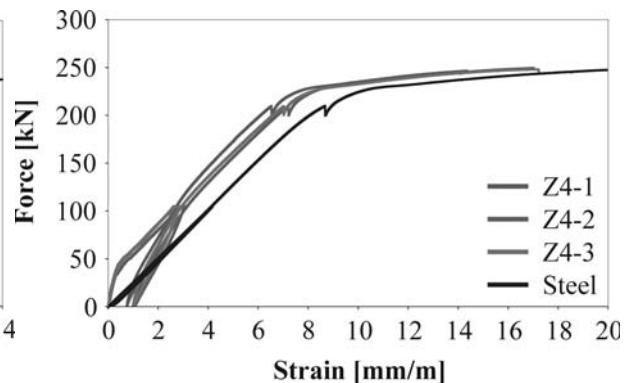


Fig. 9 - Force-strain-curves of Z4 specimens

From the tests as well as from the diagrams of Figs. 6 to 9 it can be concluded that there is a relative rigid bond between concrete and reinforcing steel; bond forces are reduced in the

yielding phase but are still relevant (Jungwirth and Muttoni, 2005). Different to the circumstances with normal strength concrete the risk of the development of longitudinal cracks at high strains is reduced or even eliminated.

Concrete structures require a minimum reinforcement to avoid brittle failure. For structural elements made of reinforced UHPC with fibres the definition of minimum reinforcement should be reconsidered, as the cracks exhibit a considerable and stable softening behaviour. Regarding ductility and failure behaviour of such structures the use of high-strength reinforcing steel seems to be reasonable.

## 5. CONCLUDING REMARKS

In this contribution an intermediate stage of an ongoing research project carried out at Hamburg University of Technology is presented. The cracking and deformation behaviour of reinforced ultra-high performance concrete elements in tensions is investigated. In parallel to tension tests, pull-out and material tests have been realized. Up to now, only first results can be shown. In the interpretation of the results not only the type and yielding behaviour of the steel but also different reinforcement ratios have to be taken into account. The theoretical study will be based on analytical (Marti et al., 1998) as well as on numerical models. The overall aim of this research is to develop reliable procedures for the conception and design of structures made of ultra-high performance concrete.

## 6. REFERENCES

- Fehling, E., Bunje, K., Leutbecher, T. (2004), "Design Relevant Properties of Hardened Ultra High Performance Concrete", *International Symposium on Ultra High Performance Concrete, Sept. 13-15, 2004, Proceedings*, University of Kassel, Heft 3, 2004, pp. 327-338.
- Jungwirth J., Muttoni A. (2005), "Versuche zum Tragverhalten von ultra hochfestem Beton - Kurzfassung", *ETH Lausanne, IS-BETON, Bericht 00.02.R8*, Lausanne, 2005, pp.27.
- Marti, P., Alvarez, M., Kaufmann, W., Sigrist, V. (1998), "Tension Chord Model for Structural Concrete", *Structural Engineering International*, Vol. 8, No. 4, November 1998, pp. 287-298.
- Racky, P. (2004), "Ultra High Performance Concrete", *International Symposium on Ultra High Performance Concrete, Sept. 13-15, 2004, Proceedings*, University of Kassel, Heft 3, 2004, pp. 797-806.
- Redaelli, D., Muttoni, A. (2007), "Tensile Behaviour of Reinforced Ultra-High Performance Fiber Reinforced Concrete Elements", *fib Symposium 2007, Dubrovnik, May 20-23, 2007, Proceedings*, 2007, pp. 267-274.
- Schmidt, M., Fehling, E. (2003), "Ultra-Hochfester Beton: Perspektive für die Betonfertigteilindustrie", *Betonwerk + Fertigteil-Technik*, Heft 3, 2003, pp. 16-29.
- Sigrist, V. (1999), "Ductility of Concrete Structures", *fib - Symposium, Prague, October 12-15, 1999, Proceedings*, 1999, pp. 289-294.
- Walraven, J.C. (2004), "Designing with Ultra High Performance Concrete: Basics, Potential and Perspectives", *International Symposium on Ultra High Performance Concrete, Sept. 13-15, 2004, Proceedings*, University of Kassel, Heft 3, 2004, pp. 853-864.

## ROTATION CAPACITY OF REINFORCED CONCRETE ELEMENTS

*Bogdan Hegheș, Cornelia Măgureanu*

*Technical University of Cluj-Napoca, Romania*

*Str. Gh. Baritiu, Nr. 25, Cluj-Napoca, 400020, [bogdan.heghes@bmt.utcluj.ro](mailto:bogdan.heghes@bmt.utcluj.ro),*

*[magureanu.cornelia@bmt.utcluj.ro](mailto:magureanu.cornelia@bmt.utcluj.ro)*

### SUMMARY

Ductility is an important property for redistribution of forces and prevention of progressive collapse. The ductility of structural members can be improved by confinement. For high strength concrete this is especially important due increased brittleness. This paper summarizes results from nine reinforced beams of high strength concrete. Ductility was explained by plastic rotation of the element, when plastic hinges appears in critical sections of the beams.

### 1. INTRODUCTION

The paper presents a comparison between the calculated values obtained through several standards and experimental values obtained by the authors.

### 2. EXPERIMENTAL STUDIES

The experimental program contained a number of eleven simple reinforced concrete beams, tested in bending. The beams were realized with concrete class of C80/90, with constant length of  $L=3200$  mm and the section of  $125 \times 250$  mm. The longitudinal percentage of reinforcement was between 2.033-3.933%, and the transversal reinforcement was the same for all the beams, with stirrups  $\text{Ø}6/300$  mm. All the beams were tested with a hydraulic press and loaded with two concentrated loads (Fig. 1).

Both ends of the beams were free to rotate under loading. At each increment of the forces, the strain on multiple heights of the section and the flexure of the beam were recorded. In Tab. 1 the compressive strength of the concrete at the date of the testing is presented.

Tab. 1 Compressive strength of the concrete

Beams	Compressive strength $f_{c,cube}$ (MPa)
FT4-1	107
FT5.1-1	78
FT5.2-1	91
I1-1, I1-2	92.4
I2-1, I2-2	85.1
I3-1, I3-2	84.9
I4-1, I4-2	89.9



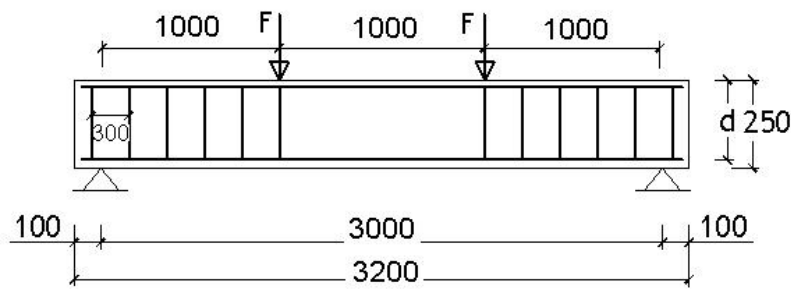


Fig. 1 Beam test sample

The longitudinal reinforcement percentage is presented in Tab. 2. Also, the mechanical percentage of reinforcement is shown. The longitudinal reinforcement was with steel type PC52, and the transversal reinforcement (stirrups) with steel type OB37.

Tab. 2 Longitudinal reinforcement and mechanical reinforcement percentage

Beams	p (%)	$\rho_m = p \cdot \frac{f_y}{f_c} \cdot 100$ (%)
FT4-1	2.061	5.779
FT5.1-1	2.033	7.819
FT5.2-1	2.033	6.702
I1-1	2.621	8.510
I1-2	2.654	8.617
I2-1	3.072	10.830
I2-2	2.990	10.541
I3-1, I3-2	3.357	11.862
I4-1	3.933	13.898
I4-2	3.682	12.287

The differences between the beams of the same series (i.e. I1-..., I2-... ) came through the transversal dimensions deviations.

### 2.1 Plastic rotation capability

The plastic rotation capability  $\theta_{pl}$  is defined by the difference between the total rotation  $\theta_{tot}$  and elastic rotation  $\theta_{el}$ :  $\theta_{pl} = \theta_{tot} - \theta_{el}$  (Fig. 2).

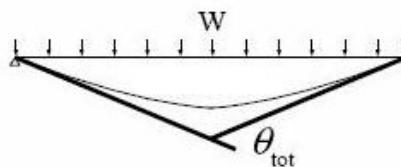


Fig. 2 Total rotation

The following definitions are adopted which apply universally to reinforced and prestressed concrete members:

- The total rotation  $\theta_{tot}$  is taken as the "sum of angles made by the difference in tensile steel elongation and shortening of outermost compressive concrete fiber, where a section reaches nominal strength".

- The elastic rotation  $\theta_{el}$  is taken as the "sum of angles made by the difference in tensile steel elongation and the shortening of the outermost compressive fibre for which neither the reinforcement nor prestress has reached its elastic limit."
- The plastic rotation  $\theta_{pl}$  is taken as the "sum of additional deformations along the beam after yielding of either the ordinary or prestressed reinforcement and until a section reaches nominal strength" or, as previously shown, as the difference of the total rotation and the elastic rotation.

The plastic theory uses the reserves of plastic hinges of static undetermined structures which are capable of forming plastic hinges in the most stressed areas, and to redistribute the efforts at less stressed areas. This hypothesis presumes that the elements have sufficient plastic deformation capabilities. To check the deformation capacity the required rotation  $\Theta_{req}$  has to be compared with the plastic rotation  $\Theta_{pl}$  as follows:

$$\Theta_{nec} \leq \Theta_{pl} \tag{1}$$

## 2.2 CEB-FIB Model Code 1990

The plastic rotation according to MC90:

$$\Theta_{pl} = \int_0^{l_{pl}} \frac{\delta}{d-x} \cdot \left(1 - \frac{\sigma_{sr1}}{f_{yk}}\right) \cdot (\varepsilon_{s2} - \varepsilon_{sy}) da \tag{2}$$

where:

- $l_{pl}$  length of plastic hinge
- $\delta$  the coefficient which taking into account the form of the stress-strain curve of the reinforcement in the inelastic range ( $\delta \approx 0,8$ )
- $x$  the depth of the compression zone
- $d$  the efficient height of the cross-section
- $\sigma_{sr1}$  the steel stress in the crack the steel stress in the crack when the first crack forms as the characteristic concrete tensile strength is reached
- $f_{yk}$  the characteristic steel yield stress
- $\varepsilon_{s2}$  the steel strain of the cracked section
- $\varepsilon_{sy}$  the steel yield strain
- $a$  the abscissa

In order to facilitate practical applications, the abscissas  $\Theta_{pl}$  and  $x/d$  represents the design values of the normalized neutral axis depth (Fig. 3)

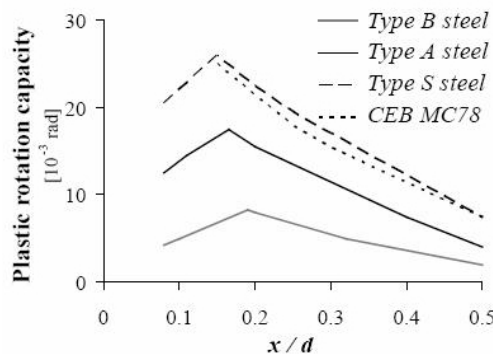


Fig. 3 Plastic rotation according CEB-fib MC90

### 2.3 Eurocode 2

Depending on the ductility class of steel, normal (N) or high (H), the plastic rotation can be taken from Fig 4. It can be seen that the plastic rotation  $\Theta_{pl}$  for  $x/d \leq 0.16$  is limited for H-steel to  $\Theta_{pl} = 20$  mrad and for N-steel to  $\Theta_{pl} = 10$  mrad.

$$\Theta_{pl} = 20 \text{ mrad for } x/d < 0.16 \quad (3)$$

$$\Theta_{pl} = \left[ 5.8 + \left( 6.22 - 11.5 \frac{x}{d} \right)^{1.8} \right] \text{ mrad for } 0.16 \leq x/d \leq 0.5 \quad (4)$$

The curvature may be used for all variations of material and geometrical parameters. Eqs. 3 and (4) describe the admissible plastic rotation (Fig. 4) using only the compressive depth ( $x/d$ ) as input parameter. Material and other geometrical parameters are not taken into account.

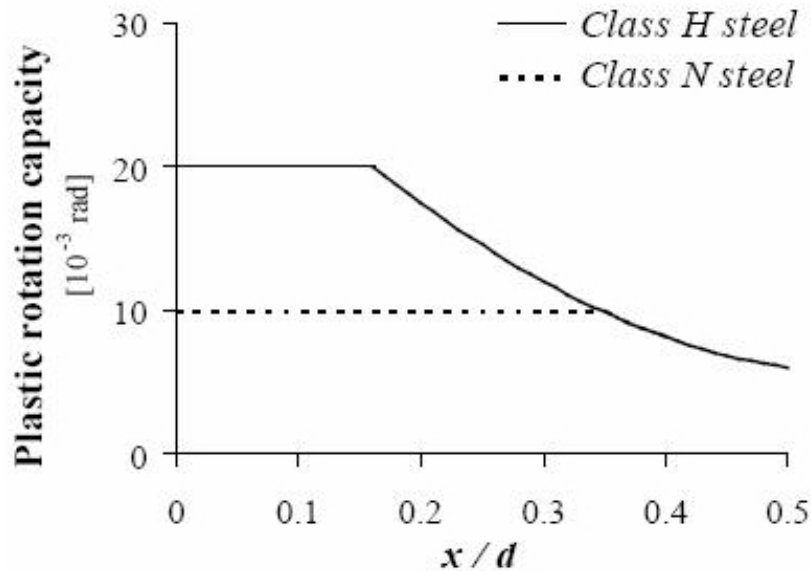


Fig. 4 Plastic rotation according Eurocode2

Simplified relationships for the  $\Theta_{pl, cap}$  are drawn up in Fig. 3 and Fig. 4 for different reinforcement types and are valid for a slenderness ratio of  $l^*/d = 6$  ( $l^*$  is the distance between two consecutive zero moment points on either side of the support). The rotation capacity can be multiplied by  $\sqrt{l^*/(6d)}$  for other values of  $l^*/d$ .

#### DIN 1045-1

DIN 1045-part 1 (2001) gives both detailed and simplified expressions for the available rotation capacity. Simplified relationships for the plastic rotation capacity are divided into concrete grades C12/16 to C50/60 and the high strength class C100/115. The relationships are reproduced in Fig. 5. The difference between Eurocode2 and DIN 1045 procedures to calculate the plastic rotation is that Eq. (5) and (6) considers the slenderness of the system  $\lambda = l/d$ . The plastic length is estimated by  $l_{pl} = 1.2 \cdot h$ . The simplified expression reads:

$$\Theta_{pl} = 20 \cdot \sqrt{\frac{\lambda_l}{20}} \text{ mrad, for } x/d < 0.16 \quad (5)$$

$$\Theta_{pl} = \left[ 5.8 + \left( 6.22 - 11.5 \frac{x}{d} \right)^{1.8} \right] \cdot \sqrt{\frac{\lambda_l}{20}} \text{ mrad, for } 0.16 \leq x/d \leq 0.5 \quad (6)$$

The plastic rotation capacity can be obtained from Fig. 5.

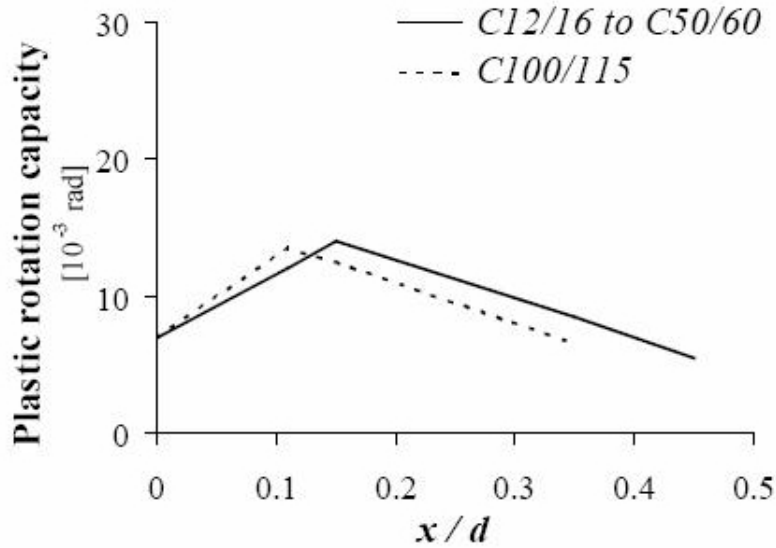


Fig. 5 Plastic rotation according DIN 1045-1

The simplified expression reads:

$$\Theta_{pl, cap} = \beta_n \beta_s \frac{\varepsilon_{su}^* - \varepsilon_{sy}}{1 - x/d} \sqrt{\lambda/3} \quad (7)$$

where:

$$\beta_n = 22.5$$

$$\beta_s = 0.074$$

$\lambda$  – shear slenderness; the distance between  $M=0$  and  $M_{max}$  after redistribution

$\varepsilon_{su}^*$  – steel strain at ultimate:

- steel failure:

-

$$(0.4 \cdot x/d + 0.13) \varepsilon_{uk} / \beta_c$$

- concrete failure:

$$1.8(x/d)^{0.7} (1/(x/d - 1)) |\varepsilon|$$

$\varepsilon_{sy}$  – characteristic steel yield strain (=0.0025)

$\varepsilon_{uk}$  – characteristic steel strain at ultimate load (= 0.05 – for high ductility steel)

$\varepsilon_{cu}$  – characteristic concrete strain at ultimate load (=0.035 – for <C50)

Fig. 5 is obtained for  $\lambda=3$ . For different values of  $\lambda$ , the rotation capacity  $\Theta$  is multiplied by  $\sqrt{\lambda/d}$ .

## 2.4 Plastic rotation due to bending

The plastic hinge can be simulated with a single beam and a single load. The length of the beam is determined by the length of the area with negative moment over the support. The plastic rotation due to bending may be calculated as follows:

$$\Theta_{pl} = 2 \int_0^{a_q} k_{(x)} dx \quad (8)$$

where  $a_q = 0.2 \cdot \lambda \cdot d$  and  $k$  - the curvature at cracking, yielding and ultimate.

The integration of the plastic area (grey area in Fig. 6) is expressible in the form:

$$\Theta_{pl} = 0.2 \cdot \lambda \cdot d \cdot \left[ k_{cr} \left( \frac{M_y}{M_u} - 1 \right) + k_y \left( \frac{M_{cr}}{M_y} - \frac{M_{cr}}{M_u} \right) + k_u \left( 1 - \frac{M_y}{M_u} \right) \right] \quad (9)$$

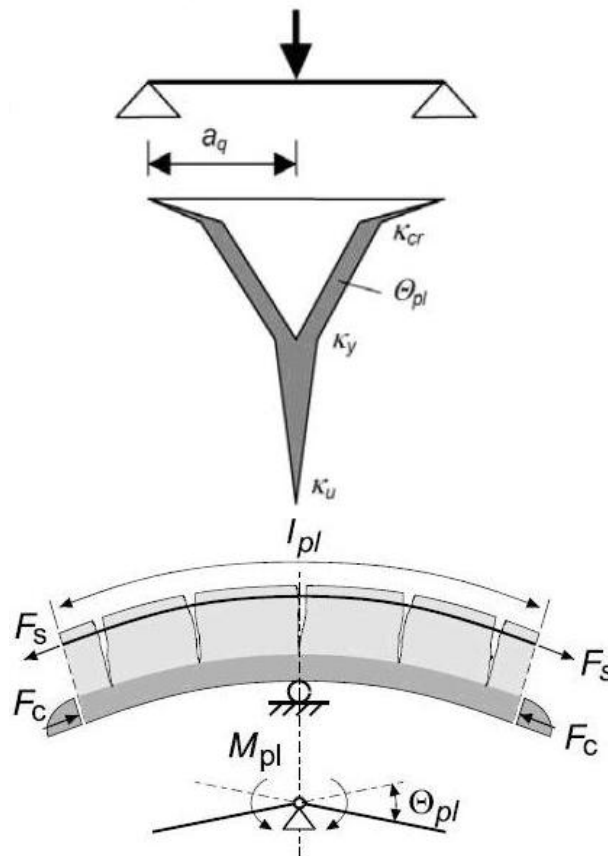


Fig. 6 Model for calculating the plastic rotation due to bending and model for a plastic hinge

### 3. EXPERIMENTAL RESULTS

The experimental program consisted in testing at bending of eleven reinforced concrete beams. In Tab. 3 the experimental data on the beams is shown.

Tab. 3 Experimental results

Beam	p%	$k_{cr}$	$k_y^*$	$k_y^{**}$ $\varepsilon_y=2\text{‰}$	$k_u$	$\mu_\Theta$
FT 4-1	2.061	0.00112	0.00642	0.00485	0.028576	5.88
FT 5.1-1	2.033	0.00394	0.00718	0.00394	0.033135	8.41
FT 5.2-1	2.033	0.00120	0.00583	0.00438	0.028669	6.55
I 1-1	2.621	0.00124	0.00698	0.00528	0.031368	5.94
I 1-2	2.654	0.00046	0.00683	0.00455	0.030362	6.67
I 2-1	3.072	0.00078	0.00970	0.00590	0.041772	7.08
I 2-2	2.990	0.00073	0.00912	0.00555	0.038536	6.95
I 3-1	3.357	0.00088	0.01007	0.00496	0.043791	8.82
I 3-2	3.357	0.00088	0.00905	0.00496	0.039704	8.00
I 4-1	3.933	0.00076	0.01062	0.00577	0.045835	8.26
I 4-2	3.682	0.00060	0.09617	0.00522	0.041436	7.63

$\mu_\Theta$  – rotational ductility ( $\mu_\Theta=k_u/k_y^{**}$ )

Beam	x/d	$\Theta_{pl\_nec}^*$ (mrad)	$\Theta_{pl\_nec}^{**}$ (mrad)	$\Theta_{pl}$ EC2 (mrad)	$\Theta_{pl}$ DIN (mrad)	$\Theta_{pl}$ MC90 (mrad)
FT 4-1	0.1000	2.6996	5.9276	20.0000	16.2063	15.3957
FT 5.1-1	0.1355	3.4381	10.7352	20.0000	16.6273	15.8178
FT 5.2-1	0.1162	2.2095	7.2124	20.0000	16.6273	14.5266
I 1-1	0.1475	1.9532	6.6228	20.0000	17.3643	16.4929
I 1-2	0.1493	1.9029	7.8116	20.0000	16.9057	16.5665
I 2-1	0.1877	1.3178	11.7126	18.2633	17.0306	16.6596
I 2-2	0.1827	2.2652	10.5410	18.5805	17.0956	16.4065
I 3-1	0.2057	2.2653	15.4767	17.1449	15.8563	15.2868
I 3-2	0.2057	3.3275	12.8320	17.1449	15.8563	15.2868
I 4-1	0.2190	0.8902	15.2446	15.8541	14.7346	14.4795
I 4-2	0.2130	1.8534	12.2871	16.7064	15.3214	15.0063

$k_y^*$  - the yield curvature is considered at yielding of the beam, from the bending moment-deflection graphic

$k_y^{**}$  - the yield curvature is considered at yielding of the reinforcement ( $\varepsilon_y = 2 \text{‰}$ ).

### 4. CONCLUSIONS

The comparison between experimental and theoretical values is shown in Tab. 3. The data obtained from this experiment and the results from the other authors leads us to the conclusion that considering yielding from the graphic of moment-deflection, actual codes are much too permissive regarding the plastic rotation. On the other hand, considering that the yielding occurs at the reinforcement yielding, the plastic rotation of the beams is much higher, in some cases at the limit that defines a non-ductile behaviour.

The rotational ductility of the beams was between 5.88 and 8.82.

The lack of an integrated and consistent concept for the development of non-linear calculation prevents a simplified calculation model for all kinds of concrete.

The number of experimental results is rather insufficient to compare the described models with the real structure behaviour.

The future studies in our Reinforced and Prestressed Concrete Department will be axed on a comparison of the same beams realized with steel type S500, others reinforcement percentage and beams with multiple openings.

## 5. REFERENCES

- Carsten, A., Jochen, K. (1998): "Development of a New Concept for the Rotation Capacity in DIN 1045, Part 1", *Lacer 1998*, pp. 213-236
- DIN 1045-1, "Tragwerke aus Beton, Stahlbeton und Spannbeton", Teil 1
- Eurocode 2, "Design of reinforced and prestressed concrete structures"
- Magureanu, C., Hegheş, B. (2006): "Experimental Study on Ductility Reinforced Concrete Beams Using High Strength Concrete", *fib Congress*, Naples
- Mark, R., (2003): "Deformation Capacity and Moment Redistribution of Partially Prestressed Concrete Beams", PH.D. Thesis

## EUROPEAN KNOWLEDGE ON REPAIR OF RIGID PAVEMENTS BY USING OF ULTRA FAST CONCRETE

*Josef Stryk, Jiri Vyslouzil, Karel Pospisil  
Centrum dopravního výzkumu, v.v.i. (Transport Research Centre)  
Lisenska 33a, 636 00 Brno, Czech Republic*

### SUMMARY

In a lot of countries there is a demand for quick solutions in case of road closures in connection to maintenance and repair works. This demand is much urgent in case of rigid pavements. The concrete normally need more time to gain sufficient strength to be exposed to a traffic. The paper is dealing with usage of ultra fast concrete for repair of rigid pavements with focus on replacement of whole concrete slabs. Current experience in this field is presented from the following countries: Austria, Belgium, Czech Republic, Germany and Switzerland.

### 1. INTRODUCTION

The trend to shorten closure time when restoring operation performance of concrete roads in Europe is basically manifested in *two ways*. The *first one* is particularly obvious in German road construction engineering. Fast best practice methods for repairs of small faults (chipped out corners or edges of slabs) are to be applied for the change of whole slabs, or even several fields. They are to be carried out in equally short deadlines which are applied for repairs of small local faults. *The latter*, e.g. obvious in Belgium, is based on reduction of strength increase time of road concretes used when constructing or reconstructing consistent traffic lane sections. The required time for fresh concrete processing has to be kept all the same.

Both ways have a number of different as well as common features. Especially the composition of mending mixtures and concretes for reconstruction, and criteria for reopening of reconstructed areas for traffic are *different*. Increased requirements for technological performance and qualification of technical as well as operating staff, higher sensitivity to changes in weather conditions, and reliability of machinery are the *common features*. The significantly higher costs for realized reconstructions is a common feature as well but may be compensated by a shorter closure time and thus also by social effects based on time and fuel savings, emission elimination, etc.

Different as well as common features of various fast ways of concrete road pavement reconstructions may best be demonstrated on characteristic applications in selected European countries. The countries are deliberately not in alphabet order, but rather refer to the two above mentioned basic ways, or in certain extent, follow fluent transition form one way to another.

### 2. GERMANY

The idea to develop material and technology for very fast restoration of operation performance of damaged concrete pavement slabs arose in the middle of 1990s with the



reconstruction of Leipzig airport (Alte-Teigeler, 2001). That time damaged slab edges were repaired during short closures within several hours and the runway was put back in operation. The repairs proved useful and consequently effort arose to implement the *system* (material and technology) in large scale reconstructions. At the same time, the term of *fast concrete* (*Schnellbeton*) for the mentioned system came to existence.

The technological pioneer of the method in Germany was a company Otto Alte-Teigeler GmbH (OAT), Bietigheim, and Institute of Construction Materials, University of Kassel (Schmidt, and Teichmann, 2005). In addition, an analysis was carried of the crucial issue of minimum compressive strength once reached that the hardened rapid concrete may be put into traffic. The results of the analysis were the values of 15 N/mm<sup>2</sup> (subgrade made from bonded layer), or 20 N/mm<sup>2</sup> (unbonded subgrade), determined with the use of Schmidt impact hammer. The relatively low values result from e.g. lower amount of traffic in first hours after the opening of the concrete road for traffic, and very fast strength increase in the first 24 hours.

According to the above mentioned analyses, determined compressive strength may be reached in approx. 8 hours under normal conditions; in exceptionally favourable conditions OAT mentions approx. 2 to 3 hours, as shown in Tab. 1.

Tab. 1 Course of works

Separating cuts	approx 1 h				
Removal, dowels, tie bars		approx 1 h			
Concrete laying			approx 1 h		
Setting time				approx 2-3 h	
Finishing works (joints)					approx 1 h

The German system of fast reconstructions is based on the following characteristics:

*Material composition* consists of a manufactured dry mixture of Portland cement, a curing agent, and sand. Manufactured mixture then prevents making mistakes in construction sites. To save costs coarse crushed aggregates and water are added into a concrete mixer in construction sites. The water-cement ratio of approx 0.40 is used and the fresh concrete is to be easily workable for about 30 minutes after mixing the dry mixture with water.

*Mixing* is principally made in construction sites in mobile concrete mixers with their drums volume corresponding with the area of road pavement for reconstruction.

*Organization work level* in construction sites must correspond with the requirements for exceptionally short time of closures. It regards the higher qualification of personnel as well as planning of required *machines, equipment, and vehicles* (reserve equipment for compensation of possible break downs are to be taken into account).

### 3. CZECH REPUBLIC

Development of so-called rapid concretes in the Czech Republic was started by SKANSKA DS a.s. about three years ago and has found its use in Czech D1 motorway when the same company reconstructed approx 100 slabs (Srutka, 2006). The development in the company took place in the close co-operation with suppliers of construction chemical materials, particularly with Sika CZ.

The development, despite having taken place gradually, was from the beginning focused on application and reconstruction of the whole road concrete pavement slabs. The initial assignment was based on that time desirable limit of three days, which included all necessary preparatory works, actual realization works (removal of damaged slabs or their parts - Fig. 1, thorough cleaning of the subbase, usual reinforcement of new slabs and their anchoring into neighbouring ones (Fig. 2), concrete laying, joints cutting and sealing) and all finishing works. For the actual realization works and especially setting and hardening of concrete only about 24 – 36 hours remained.



Fig. 1 Removal of damaged slabs or their parts



Fig. 2 Reinforcement of new slabs

Further assignment was focused on preparation of concrete with compacting and hardening time between 6 and 18 hours, which meant reducing the time to reach desirable concrete parameters *from days to hours* (according to latest experience, the time was reduced to as low as 6 – 12 hours). The following concrete parameters were reached at tests:

Compressive strength after 6 - 12 hours:  $\geq 30 \text{ N/mm}^2$ ,

Compressive strength after 28 days:	$> 60 \text{ N/mm}^2$ ,
Tensile strength after 14 hours:	$\geq 4.0 \text{ N/mm}^2$ ,
Tensile strength after 7 days:	$\geq 4.5 \text{ N/mm}^2$ .

While in Germany the reconstructed section is preferred to be reopened for traffic as soon as possible and the strength criteria are set accordingly, in the Czech Republic the technology of rapid concrete is to reach common standard concrete parameters including resistance against water and chemical deicing agents before reopening for traffic. This requirement particularly prevents the efforts for further shortening of concrete hardening time.

In contrary to Germany, the mixture is produced in a central concrete mixing plant and is brought in concrete agitators to the construction sites, where the special additives are added. However, due to very thin boundaries of all technological steps the emphasis on technological quality and qualification of technical and operating personnel is stressed.

#### 4. SWITZERLAND

Although Swiss information (Contratto, 2004) do not use the term rapid concrete directly, the character of used material and especially the attribute of application “*in working conditions*” (*unter Betrieb*) ranks the Swiss technology in this group.

The share of concrete roads in Swiss road network is still small, thus the most relevant experience with fast reconstruction come from airports, where the requirements for short closures are analogous. Similarly to Germany, experiences from small repairs (chipped slab edges) were used to change individual pavement slabs. A construction company Walo Bertschinger AG together with a producer of mending materials Sika Schweiz AG created a solution to reach minimum compressive strength of  $16 \text{ N/mm}^2$  in 3 hours. According to Swiss experience it was sufficient for runways to be opened for traffic. This *criterion is nearly identical to the German one*, even theoretically analysed (Schmidt, and Teichmann, 2005).

Special concrete based on SikaCem-501, mixed in a concrete mixing plant near to the construction site and transported by dump trucks, was used for slab changing. Similarly to Germany and the Czech Republic, damaged concrete slabs were removed in order not to have damaged the subbase. New slab joints were reinforced with tie bars and dowels in contact with the old slabs. As well as in the Czech Republic, new slabs were provided with double reinforcement. Works were generally carried out during night closures. Highly qualified team of 20 people reached average *performance of approx 30 m<sup>3</sup> concrete per night*. Regarding the planning stage, conservative philosophy proved to be more appropriate, since the situation proved the necessity to have all crucial machines and equipment in reserve.

#### 5. AUSTRIA

In Austria, the term of *12-hour-concrete (12-Stunden-Beton)* is being used instead of *rapid concrete* (Steigenberger, 2003), or in some cases even 6 or 4-hour-concrete regarding the time in which the laid concrete pavement reaches sufficient hardness for its opening for traffic. The aim of these concretes application is similar as in other countries: reduced closure times for maintenance and repairs on busiest roads and areas provided with concrete pavement to necessary minimum time not expressed *in days, but in hours*. That would reduce undesirable drawbacks of closures such as traffic congestions, dissatisfaction of road users, higher fuel consumption, and greater impact on the environment in terms of noise and emissions.

Austrian directives and specifications for road constructions (RVS 8S.06.32) have to be complied with. They state that earlier opening for traffic is possible if *70 % of required value of 28-day compressive strength*, i.e. required value of  $5.5 \text{ N/mm}^2$  at least  $3.85 \text{ N/mm}^2$ , is reached. The strength is tested on beams dimensioned of  $20 \text{ cm} \times 20 \text{ cm} \times 60 \text{ cm}$  made at the same time as the reconstructed road section and laid and treated in appropriate conditions.

*The standard practice so far* has been the usage of the so-called *24-hour-concrete*, which is made with *superplasticizers*. The lower water-cement ratio with acceptable consistence allowed to reach the strength necessary to reopen a section for traffic in one day after having prepared the mixture. This practice had complied with the requirements for closure time for several years. However, due to enormous increase in traffic the public requirements for further improvement, so that e.g. on Saturday night concrete was laid and a road section in question could be opened for traffic on Sunday afternoon. That was the case of exceptionally busy A23 motorway (Vienna Southeast Tangent).

Therefore, the Research Institute of the Association of the Austrian Cement Industry (VÖZFI) was appointed by the City of Vienna to make a *new development solution* of so-called *12-hour-concrete*. Such concrete had to meet usual requirements for road concrete in terms of strength, surface properties, water and chemical deicing agents resistance, etc. Another prerequisite was its potential production in every better equipped concrete mixing plant for production of high quality concretes from usual materials. Corresponding research works took place in a shortest possible time and in July 2002 12-hour-concrete was first used in large volume on A23 motorway. In just two weekends  $1250 \text{ m}^2$  of concrete pavement was reconstructed in this way. With the use of the concrete the closure time (started on Friday at 8 pm) was reduced by 17 hours and the road was opened for traffic as early as at noon on Sunday instead at 5 am on Monday.

## 6. BELGIUM

For fast reconstructions of concrete pavement in Belgium the technology of so-called *UFT* (*ultra fast-track concrete paving*) was developed (Lonneux, et al., 2006). The recipe was designed in a way to allow opening of the reconstructed road section for traffic up to 36 hours after concrete pavement has been laid. This concrete is to reach *the compressive strength of  $40 \text{ N/mm}^2$*  after 30 – 36 hours. The mentioned criterion used for reopening of the reconstructed pavement is significantly different (more conservative) from criteria used in Germany, i.e.  $15$  or  $20 \text{ N/mm}^2$ , determined with the use of Schmidt impact hammer.

However, the technology appeared to be suitable especially for motorway sections with heavy traffic, and its development was a common effort by administration (Roads and Traffic Administration), university (Katholieke Universiteit Leuven), research institutions (Belgian Road Research Centre – BRRC), as well as the Federation of the Belgian Cement Industry.

In contrast to the German way, in which the so-called rapid concretes used for reconstructions of local slab damage of concrete pavement roads extended to changes of whole slabs (individual as well as several or more pieces) through further development of materials and technologies, the Belgian approach is different. The effort to shorten concrete maturation and thus reduce total closure time when reconstructing cement road pavements by changing the whole road sections is being supported. Optimally, the reconstruction of road lengths between  $50$  and  $200 \text{ m}$ , i.e. area of max  $1200 \text{ m}^2$ , is stated. Faster concrete maturation while keeping

required workability is reached with the use of special *superplasticizers and reduction of water-cement ratio*, with CEM I 42.5 R LA, or CEM I 52.5 cement respectively. Thus the Belgian approach may be compared to the Austrian one. In Belgium an emphasis is put on a stress transfer from high traffic load even onto the upper subgrade layer and subbase layers; therefore, when reconstructing pavement, the *subbase* is often made with increased *load bearing capacity*, usually with the use of roller-compacted concrete – RCC. Obviously, these processes prolong total closure times, but on the other hand they contribute to longer life span of reconstruction. The longest part of closure times before reopening for traffic has been so far reserved for new concrete pavement maturation – minimum of 5 days. During approx 3-year research and testing applications in roads in the region of Flemish Brabant the 5-day period was reduced to 36 hours, i.e. the time required for reaching compressive strength of 40 N/mm<sup>2</sup>.

## 7. CONCLUSION

Fast methods of concrete pavement reconstruction overcome one of the previous drawbacks of these pavements in comparison with the bituminous ones. Different ways to reach the goal as well as different criteria for reopening roads for traffic show that satisfactory solution has not yet been found in Western and Central European countries. That concerns the approach to subgrade layers condition after damaged slabs are removed, the way to ensure water and chemical deicing agents resistance, and the life span of reconstructions in general. Only through long-term monitoring of finished reconstructions and systematic analyses comes the real, complex effect of fast technologies to life and experiences and ideas for further development are gained.

## 8. ACKNOWLEDGEMENTS

Developed with the support of Ministry of Transport R&D project no. 1F55B/090/120: Concrete Pavements - New Construction, Reconstruction, and Repair Trends and R&D project no. MD04499457501: Sustainable transport - a chance for a future.

## 9. REFERENCES

- Alte-Teigeler, R. (2001), „Erneuerung von Einzelplatten mit Schnellbeton“, In: *Betonstraßentagung 2001 Chemnitz*, FGSV Köln 2002, pp. 71-74.
- Contratto, S. (2004), „Instandsetzung von Betonverkehrsflächen unter Betrieb“, In: *Fachtagung Betonstrassen 2004 Zürich*, Cemsuisse Bern 2004, pp. 22-31.
- Lonneux, T. et al. (2006), „(Ultra)fast-Track Concrete Paving: Belgian Experience“, In: *10th International Symposium on Concrete Roads*, Cembureau Brussels, 2006, 10 pp.
- Schmidt, M. and Teichmann, T. (2005), „Instandsetzungen von Betonfahrbahnen mit Schnellbeton unter Verkehr“, *Straße+Verkehr*, Vol. 55, No. 4, April 2005, pp. 182-190.
- Srutka, J. (2006), „Oprava a vystavba cementobetonovych krytu pomoci rychlych betonu“, In: *2. mezinarodni konference Betonove vozovky 2006*, Chlumec nad Cidlinou 2006, pp. 103-107.
- Steigenberger, J. (2003), „Noch kürzere Reparaturzeiten mit dem 12-Stunden-Beton“, *Update (Aktuelles zum Thema Beto*

## **FIRE RESISTANCE OF CONCRETE TUNNEL LINING – EXPERIMENTAL RESEARCH**

*Prof. Jan L. Vitek, Ph.D., C.Eng.*

*Metrostav, a.s.*

*Koželužská 2246, 180 00 Prague 8, Czech Republic*

### **SUMMARY**

The large scale specimens made of plain concrete, fibre reinforced concrete and plain concrete with protection of Fireshield were tested against the effect of fire. The temperature of concrete during testing was measured, the damage of the specimens was evaluated and the drop of the strength was measured. The discussion of the results may contribute to better understanding of the fire resistance. Optimal design of the tunnel lining depends on many factors and the presented results can contribute to the successful choice of the best alternative.

### **1. INTRODUCTION**

During last decades a number of tunnels on roads and highways rapidly increased. Also a lot of accidents happened in tunnels, which are very dangerous due a limited space, limited possibility of ventilation and difficult access of rescue vehicles. The safety of tunnels therefore became a serious issue which must be very carefully treated in the stage of the tunnel design. The tunnel must be a stable safe structure in terms of the structural safety and also the tunnel equipment (accesses, ventilation, rescue systems, etc.) must correspond to the number of vehicles running through the tunnel. The objective of this paper is to show the problem of the performance of the concrete lining during the fire and to discuss possible consequences of the fire for the tunnel lining design.

### **2. CONCRETE TUNNEL LINING DESIGN**

The design of the concrete tunnel lining is dependent on the construction technology. In our country, most of the tunnels are driven by the NATM (New Austrian Tunnelling Method), when first the primary lining is made of the sprayed concrete and then after installation of the waterproofing the secondary lining is cast into the movable formwork. The secondary lining is designed, so that it can carry the loading induced by the earth pressure, water pressure and other factors like temperature effects, shrinkage of concrete, etc. The mechanical loading is mainly induced by interaction of the tunnel lining and rock/soil massive. If there is a fire inside the tunnel, new loading situation is developed, which has to be controlled. This is one of the issues which are not fully covered by design codes and rules, and therefore a research is highly demanded. In this case mainly the tunnels with arch cross-section are considered.

The tunnels with rectangular cross-section could be often considered as engineering structures. The slabs are reinforced and sometimes prestressed the load carrying capacity is influenced practically only by the concrete structure and almost no interaction with the rock/soil massive can be considered. The codes which define the fire resistance of engineering structures can be applied (e.g. EN 1992-1-2 Design of concrete structures – Part 1-2 General rules Structural fire design).

The secondary lining of tunnels with arch cross-section are usually reinforced, however, the number of tunnels with the lining made of the plain concrete is increasing. The tunnel segment forms an arch which is elastically supported by the rock/soil massive. If there is a fire inside the tunnel, the arch is subjected to damage. If the complete length of the tunnel segment was seriously damaged, the tunnel would collapse. However, the probability, that the complete lining will be interrupted due to the fire is rather low. It can happen that in a very serious case the lining will be deteriorated in a certain area, which could be modelled as an opening in the lining. It can be expected that such damage need not cause directly the failure of the tunnel. Therefore it seems to be rather complex issue to define, in terms of the safety of the structure, what is the fire resistance of the arch tunnel lining. (The fire resistance is usually defined as the time period, when the structure is exposed to the fire until it collapses). The definition what situation should be considered as a fire resistance is a question of further discussions. It depends not only on the concrete lining itself, but on the entire system consisting of the secondary lining, primary lining and rock/soil massive.

If the lining is reinforced, the criterion for the fire resistance could be e.g. dependent on the temperature of the reinforcing steel. However, if the lining is made of plain concrete, the criterion defining when the lining collapses is even more complex.

For the quality of lining and for the safety of the rescue works in the tunnel, there is also important if there is any spalling of concrete. It may be dangerous for anybody working in the tunnel, it reduces the thickness of the lining and it reduces the cover of steel. Therefore it is highly recommended to reduce the spalling of concrete at any type of concrete lining.

### **3. EXPERIMENTAL RESEARCH**

The experiments on the fire resistance of concrete lining started about 2 years ago, when the first lining of the road tunnel made of plain concrete was designed. It was decided to verify the performance of the plain concrete which is exposed to the fire. The main object of the experiment was to observe if there is a serious spalling or not. The first model – concrete slab 2.0 x 2.0 x 0.4 m was exposed to fire according to the Czech national code – the cellulose curve (Fig. 1) for a period of 180 minutes. The temperature gauges were located in 5 positions on the slab in 50 mm distances in the direction of the slab thickness.

The damage of this slab was very small, almost negligible. The reason may be found mainly in the fact that the temperature growth according to the cellulose curve is rather moderate. The water which is in concrete may slowly evaporate and then the surface layer of dry concrete can well withstand the high temperature and temporarily insulates the core of concrete against rapid growth of temperature. In fact it has been shown that the cellulose temperature curve did not make any serious damage of concrete lining.

Therefore, the next series of experiments was carried out, where the RWS loading curve was applied (Fig.1). The RWS loading curve exhibits very rapid growth of temperature at the beginning of the fire and then reaches temperature up to 1350 deg C which slowly drops to 1200 deg C at the time 120 minutes after beginning of the fire. The last 60 minutes of the test the temperature is kept constant 1200 deg C. This loading is rather serious since the rapid growth of temperature does not allow the water to evaporate quickly unless special precautions are accepted.



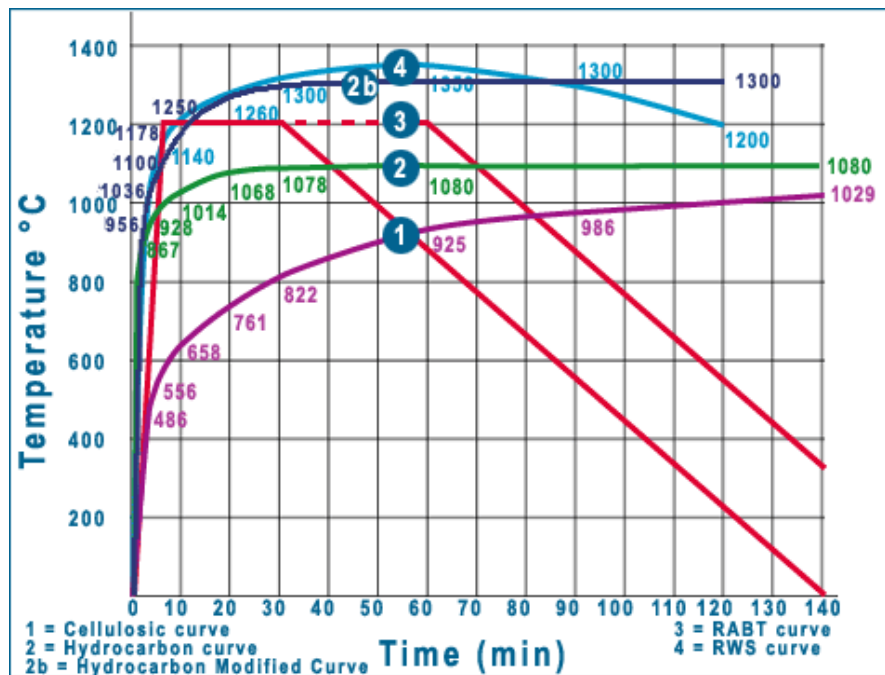


Fig. 1 Temperature loading curves

The three specimens were observed under the temperature loading. The first specimen was made of plain concrete without any special fire resisting admixtures. The second specimen was made of the same concrete; however, the polypropylene fibres were added. The third specimen was identical with the first one, but the surface was sprayed with a special protecting layer produced by BASF, which is called Fireshield. The thickness of this layer is about 50 mm. The dimensions of the specimens were  $2.4 \times 3.0 \times 0.3$  m, the third specimen was 50 mm thicker due to the Fireshield. The concrete quality was C30/37 – same at all the three specimens. The reinforcement was rather weak only in the central plane of the slabs in order to keep the slab together and in order to make possible anchorage of the hooks for manipulation with specimens.

The damage of concrete during the fire test is strongly dependent on its moisture content. Many tests are therefore carried out on the specimens, which are stored in water. This seems to be rather strong assumption, since normally the tunnel lining is not exposed to such high water content. Since there was an intention to model a realistic situation in the tunnels, the measurement of humidity in the three tunnels was carried out. The average humidity in the tunnels, which were at that time almost finished before their opening to traffic, showed that the humidity of concrete did not differ too much; it varied between 4 and 6 percent of water in concrete. Similar measurement was also made on the first two specimens prepared for fire tests. A similar humidity was measured also at the specimens, and it was concluded, that they have a similar conditions like a tunnel lining of the real tunnel.

The specimens were 3 months old at the time of the fire test. Each slab was equipped with temperature gauges, which were embedded in concrete in 3 locations. Each location involved 6 measuring points in the direction of the thickness of the slab. The distances of measuring points from the surface which was exposed to the fire were 30, 90, 150, 210, 255 and 300 mm, i.e. the last temperature gauge was situated on the surface opposite to that exposed to the fire.



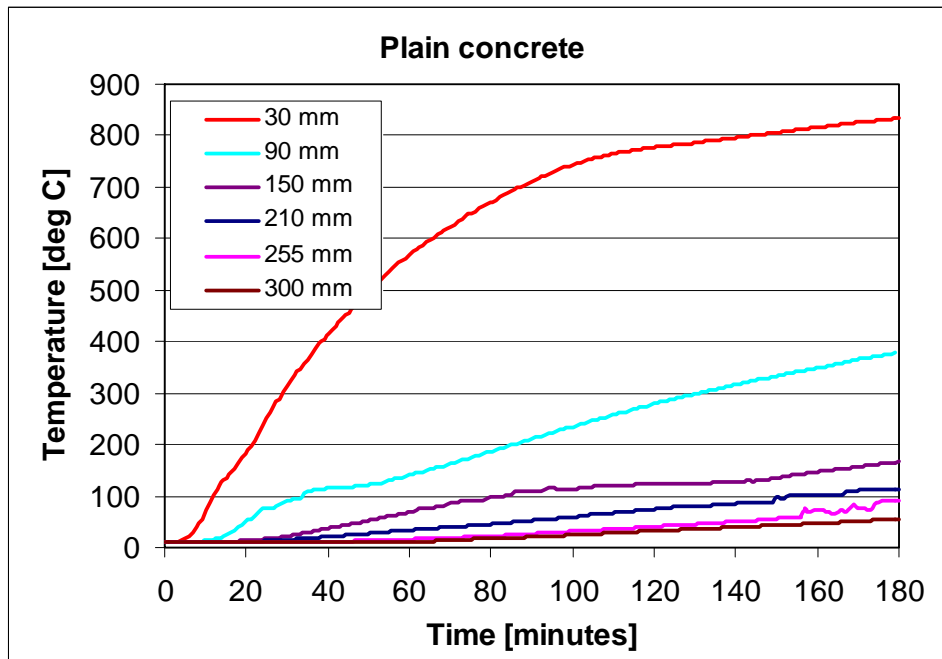


Fig. 2 Temperature variation in different distances from the surface exposed to the fire

The measured temperatures are illustrated in Fig. 2. The individual curves show the temperature development in dependence on time in different distances from the surface of the specimen which is exposed to the fire. The temperature of this surface at the time 180 minutes is 1200 deg C, and it drops rather quickly when the distance from the surface grows. E.g. 90 mm under the surface, the temperature is less than 400 deg C in the time 180 minutes. It shows that concrete exhibits a good insulation. The temperature of concrete at the opposite surface was only 56 deg C.

A similar temperature distribution was observed at the second specimen, which was reinforced by polypropylene fibres. The temperatures were slightly lower – at the distance 30 mm about 770 deg C.

The last specimen showed a completely different behaviour. The Fireshield layer 50 mm thick protected the concrete surface well from the effect of high temperature. The highest temperature in the depth of 30 mm of concrete after 180 minutes was only 125 deg C.

After the tests were completed the cores were drilled from the specimens in order to check the concrete quality after the fire. The cores had the diameter 124 mm and were about 170 mm long, taken from the surface opposite to that exposed to the fire. The concrete close to the surface exposed to the fire split up when the cores were drilled. The results are summarized in the diagram in Fig. 3. All three slabs were cast at the same day from the identical concrete of the class C30/37. The average strength at 28 days was about 41 MPa. After the tests all strengths were lower, but it could happen partly due to the testing on the cores which are smaller than the cubes for ordinary testing. The plain concrete suffered from the most severe drop of the strength. Its damage was the most severe and it was also exposed the highest temperature. The fibre reinforced concrete specimen had rather small damage on the surface. There was almost no spalling due to the presence of fibres, however, the temperatures were rather high and the strength was significantly reduced. The surface layer which did not spall

worked partly as insulation, but if the temperatures were compared no significant difference in comparison with the plain concrete specimen was observed. However, the fibres exhibited a positive effect on the strength after the fire. *The smallest reduction of the strength was observed at the third specimen, which was protected by Fireshield layer. The temperatures in concrete itself were rather low in comparison with the two previous specimens. From the technical point of view the Fireshield is the best protection of the final lining.*

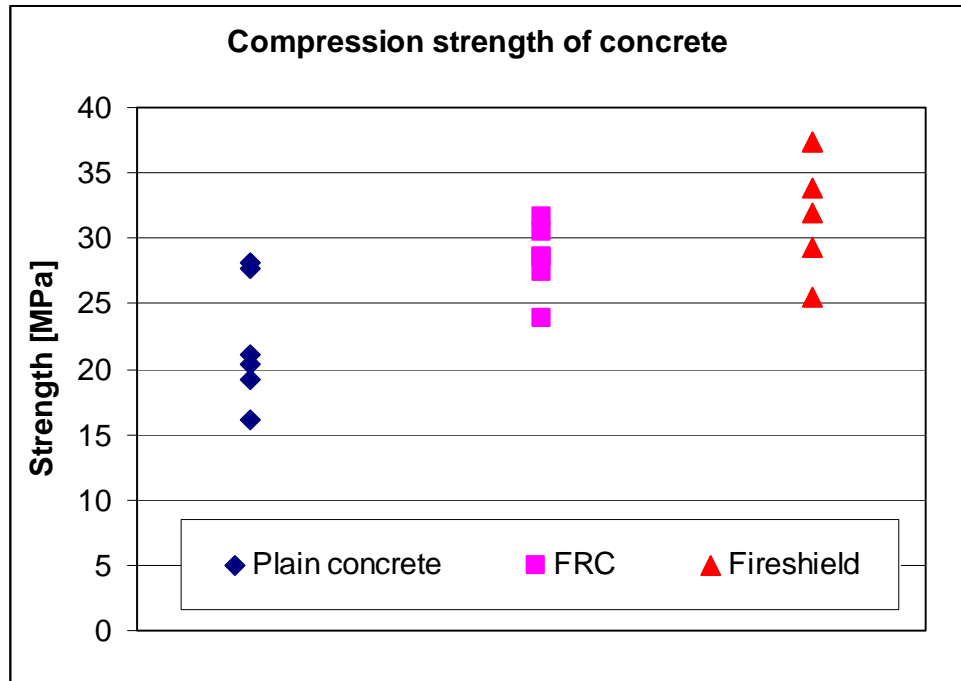


Fig. 3 Compression strength of concrete after the fire tests

#### 4. CONCLUSIONS

The four tests on the large scale specimens showed interesting results. It is necessary to evaluate them from the technical point of view, economically and also to take into account their influence on the flow of works in the tunnel. The Fireshield represents the best protection of the tunnel lining. It would be appreciated mainly as a protection of the reinforced linings, since the temperature at the level of the reinforcement is lower than 120 deg. C, which means that no damage of the steel would happen. On the other hand, the Fireshield is rather expensive; the surface of concrete requires being rough enough so that the bond between Fireshield and concrete could be guaranteed. The thickness of Fireshield - 50 mm requires that the tunnel must be larger, which means additional costs of excavations. Installation of the Fireshield represents additional operation in the tunnel which may influence the speed of construction. After a possible fire the repair is rather easy, the concrete surface would be cleaned and the new Fireshield layer would be installed.

The fibre reinforced concrete showed apparently small damage - the surface was not seriously spoilt by the fire. The strength of concrete dropped about 25 – 30 %, which is not negligible. In order to guarantee that the steel would not be damaged, the concrete cover should reach at least 70 – 80 mm. The advantage is that the spalling would not threaten the rescue teams in

the tunnel. The repair after fire requires to take away the layer of concrete exposed to the fire and to make a new layer, most probably of sprayed concrete. It assumes that the cover would be thick enough to protect the steel. The costs of fibres are reasonable and no special works are necessary on the site during construction.

Plain concrete lining suffered from the most serious damage. The drop of the strength was the most serious and the spalling appeared which made the thickness of the lining in average about 30 mm smaller. If there was reinforcement, it would be difficult to recommend the cover; the damage is strongly dependent on the aggregate used in concrete. This solution should not be recommended for reinforced linings. If the plain concrete lining is used, the repair depends on the strength reduction. If the drop of the strength was accepted than the new concrete should be sprayed on the cleaned rest of the original lining. No special costs are necessary for this type of lining.

Based on the experiments, it is not possible to formulate exact conclusions. It is necessary to evaluate the complex performance of the tunnel, the type of the lining, the density of traffic and importance of the tunnel, possibility of the alternative routes, etc. Then it would be possible to decide on the optimal fire protection.

#### **ACKNOWLEDGEMENT**

*This research was carried out in the Research Centre CIDEAS (Centre for integrated design of advanced structures) supported by the Ministry of education, project No. 1M6840770001.*

## **FIRE RESISTANCE OF STRUCTURAL CONCRETE**

*Ivanka Netinger<sup>1</sup>, Dubravka Bjegović<sup>2</sup>, Marija Jelčić<sup>2</sup>*

*<sup>1</sup>Faculty of Civil Engineering, University of Osijek, Crkvena 21, Osijek, Croatia*

*<sup>2</sup>Faculty of Civil Engineering, University of Zagreb, Kačićeva 26, Zagreb, Croatia*

### **SUMMARY**

Many studies have been directed to structural behaviour under fire conditions over the last decade. The results of these studies indicate that fire has different effects on construction materials and that concrete is the one that performs well at elevated temperatures. This good fire performance is mainly due to concrete's constituent materials (i. e. binder and aggregate) which make a material that is essentially inert up to certain temperatures and which has poor thermal conductivity. Since a lot of articles have already elaborated the special type of cement as a material that gives increased fire resistance to concrete, this paper will focus on the types of aggregates (vermiculite, perlite, expanded clay, slag) that improves its fire resistance. This paper presents properties of fire resistant aggregates mentioned above, as well as the results of preliminary testings (compressive strength, behaviour under fire conditions) of concrete made of them.

### **1. INTRODUCTION**

Some big fires in some European tunnels in the last decade induced more extensive researches with the objective of improving the system of fire protection and to diminish material and human losses (Peker, Pekmezci, 2003). The results of the studies have indicated that fire effect on a structure depends on the type of a material it is made of and concrete is proved to have good fire resistance (Stipanović, Bjegović, Planinc, 2002). Therefore, this paper aims to present some of the ways of getting increased fire resistance of concrete as a construction material. Since it is necessary, when pursuing a fire resistant material, to know the processes within a material when it is exposed to elevated temperatures, this paper describes the mechanism of concrete destruction during fire.

As the types of cement which make concrete fire resistant are already known, this paper mostly focuses on the types of aggregates with the same effect. In that sense, a short review of some fire resistant aggregates is given, as well as some of the advantages and disadvantages of their use in concrete. Some preliminary testings of mortar/concrete made of fire resistant aggregates were done and their results are also presented in this paper.

### **2. CONCRETE UNDER FIRE**

Among many types of construction materials, concrete has satisfactory fire resistance; it is inorganic, incombustible material, it does not release toxic gasses, it does not make soot and, when exposed to fire up to high temperatures, its pieces do not fall off and thus present no threat to people (Stipanović, Bjegović, 2002). Concrete is classified into the highest class of reaction to fire performance (A1) according to the standard HRN EN 13501-1. These excellent properties of concrete under fire conditions originate from its constituent materials (cement and aggregates) which, when chemically combined, form a material that is basically

inert and has low thermal conductivity. That low degree of heat transmission makes concrete an effective fire shield, not only between neighbouring rooms, but also in the protection of concrete itself from damage caused by fire (Fellinger, 2004). The only possible danger of concrete in fire comes from spalling which is typical for concrete of high and ultra high performances. Current researches aim to reduce that kind of a risk to the smallest possible degree.

## **2.1 Destruction mechanism for concrete exposed to fire**

Water pressure, chemical changes and changes of element dimensions due to raised temperatures are interconnected mechanisms which cause the destruction of concrete structure. Namely, during the transformation of water from a liquid into a gaseous state (at 100 °C) there comes to energy absorption. Considering the total amount of energy released in fire, this one is insignificant and only causes cooling effect for a short period of time. However, beside energy absorption there also comes to a great volume increase which causes spalling, i.e. the breaking off of layers or pieces of concrete from the surface of a structural element. Under the same pressure conditions, the volume of water vapour is manifold greater than the volume of water when in a liquid state, which causes pressure within concrete structure. This pressure within concrete increases until it reaches tensile strength. When pressure of water vapour in capillaries causes higher tensile stress than the one a concrete structure can resist, there comes to the destruction of concrete in the form of spalling. In concrete exposed to high temperatures, spalling can be caused, not only by pressure of water vapour, but also by chemical changes of minerals from a hardened cement paste and aggregates (Stipanović, Bjegović, Planinc, 2002).

## **2.2 Changes in concrete after fire**

Concrete is acceptably stable up to 300 °C and even above this temperature no dramatic fracture will happen. This does not mean that fire and high temperatures do not affect concrete. Changes in colour, reduction in compressive strength, modulus of elasticity, density of concrete and after-look of its surface are consequences of exposure to high temperatures. The colour of concrete is changing after cooling which indicates the exposure temperature. Namely, after 300 °C concrete becomes rosy and the intensity of the colour will depend on the amount of iron oxides in the aggregate (Društvo građevinskih inženjera, 1992).

Compressive strength of standard structural concrete also decreases after cooling. The residual strength varies depending on the maximum temperature to which concrete has been exposed, concrete structure, and load conditions during heating. Up to 300 °C compressive strength remains relatively the same. With higher temperatures compressive strength significantly decreases, so that after 600 °C concrete has no usable strength. Above 100 °C bound water in a cement paste is released from concrete, which causes a decrease in its modulus of elasticity. At 600 °C this decrease is about 90% (Društvo građevinskih inženjera, 1992).

Concrete density after cooling is somewhat smaller than the initial one due to evaporation of free water. On average, concrete density at high temperatures declines for cca 100 kg/m<sup>3</sup>. The concrete surface is also damaged; it comes to surface spalling and cracks. There are many types of spalling including: explosive spalling, surface spalling, aggregate splitting, corner separation, sloughing off, and post cooling spalling (ArupFire). Explosive spalling is the most aggressive type and usually occurs due to a combined action of pore pressures created as

moisture evaporates and high stresses as the hot material tries to expand against its surroundings including adjacent cooler concrete. In this process small pieces of concrete split off powerfully, with an explosive effect. Spalling depends on several factors, as e.g. on the kind of an aggregate, moisture content, heating condition, applied load etc.

### 3. «FIRE RESISTANT» AGGREGATES

An aggregate plays a decisive role with its thermal properties and expansion coefficient of concrete. We have already discussed the behaviour of some widely used aggregates and in the further text we will deal only with those developed for high temperatures. The later ones have the property of increased fire resistance due to way of their production.

One of the by-products, developed in the process of steel production is slag. Developed as a secondary material, slag is a valuable material used in many different applications. This non-metallic material developed during metal production can be classified into the two groups: slag developed in a blast furnace (cooled in fresh air, expanded and granulated) and slag of an electric furnace (basic and acid). If properly used, slag of blast furnaces can be used as an excellent source for making construction materials, and it finds its use in: road building, glass production, as a cement additive, as a concrete aggregate and the like.

Immediately after the production this type of slag is considered to be completely volume stable, whereas if longer exposed to weather conditions it can sometimes contain pockets of an unstable material. Sulphur, which for the most part oxidises in sulphates, often known as a gypsum, is the most common kind of instability of this slag, caused by weather conditions and mentioned in the literature. This will, under certain circumstances, lead to chemical reactions, with the sulphate-aluminate phase of hydration. This will cause a similar effect as caused by sulphate corrosion. i.e. the volume expansion of concrete resulting in its cracking. Considering the mode of cooling and strengthening, slag of blast furnace can be classified into:

- slag cooled in air - developed by slow cooling in air. It is used as an aggregate in asphalt and concrete, as well as a raw material in glass production and agro-culture
- expanded slag - developed by fast cooling of melted mass with water or vapour. The resulting material has a small volume mass which is used in light aggregate concrete.
- and granulated slag - developed as a result of cooling of liquid mass by means of great quantity of water. Crushed or ground into fine dust of the size of cement grains, granulated slag has cement properties and so can be used as a cement additive (GGBS).

Basic slag developed in an electric furnace is a by-product of steel production in which, the so called, basic flows with a high share of CaO/MgO are used. Many old kinds of slag belong to this category. Its usage is underestimated in comparison to the one developed in a blast furnace. It is partly due to its volume instability attributed to postponed hydration of free lime (CaO) and/or free magnesium (Steel slag).

Acid slag of an electric furnace is relatively stable. It contains free CaO or MgO and is generally considered volume stable (Steel slag).

Slag is currently used as a cement additive in which case it often replaces 30-70% of a cement mass. As a cement replacement it often improves concrete workability and reduces the need for water. The time of concrete bonding is increased by increasing the slag content, which can be very convenient in the conditions of elevated temperatures in which it prevents the making of cold compounds. Water extraction is also reduced by slag share. The greater the fineness of mould, the bigger the share of entrained air compared to concrete which does not contain it. Slag has been used as a cement additive for a long time, e.g., in metallurgic cement. However, the use of slag as a concrete aggregate has not been researched yet enough. Only recently

have the Japanese started to seriously consider its use as an aggregate in concrete. It is obvious in their national standard which deals with the use of this material in concrete. In Croatia there are two slag waste depots, one in Sisak and the other nearby Split. The content of these kinds of slag is mixed – a combination of slag from a blast furnace and the one from electric furnace. Their chemical analysis has not confirmed the significant presence of sulphur, which makes them suitable for placing into concrete.

*Vermiculite* is a natural mineral which, at high temperatures, has an unusual expansion property. Namely, when warming it to the temperatures of 650°C to 1000 °C, this stone of a leaf-like structure increases its volume 8-12 times, whereas single shells can increase their volume up to 30 times. During expansion it changes the colour depending on the vermiculite structure and furnace temperature. As a result, we get a material of small volume mass (60 to 130 kg/m<sup>3</sup>). It gives concrete small weight and good fire resistance, but small strength (Ukrainczyk, 1994) (Vermiculite).

*Perlite* is an amorphous volcanic glass. It develops naturally and, as vermiculite, it expands at high temperatures. When it reaches temperature of 850-900°C, it softens. Water captured in its structure evaporates causing the increasing in volume up to 7-16 times. Unexpanded perlite weights 110 kg/m<sup>3</sup> and the expanded one is only 30-150 kg/m<sup>3</sup> heavy. Due to a small volume mass, this material belongs to light aggregates. It makes concrete fire resistant, but not very strong (Perlite) (Ukrainczyk, 1994).

*Expanded clay* is developed by burning of treated and prepared clay at temperatures of 1200°C in a rotary furnace (it is commercially known in Croatia as Leca, keramzit, glinopor). It actually consists of small balls of very fine pore structures whose weight and strength can be controlled in the process of production. The form of these balls is almost perfect, and their surface is moderately rough and closed. Small weight and advantageous strength make this material very suitable for construction. Since it is developed at high temperatures, such a material can not be used as a fire resistant aggregate in concrete (Liapor).

#### **4. TESTING OF MORTAR AND CONCRETE WITH A «FIRE RESISTANT» AGGREGATE**

For our preliminary testing, a number of mortar and concrete samples were made with the above mentioned aggregates. At age of 28 days they were tested for compressive strength and their behaviour in fire conditions – inflammability (according to the standard HRN EN 13501-1) of mortar and the residual strength of concrete after its exposure to high temperatures.

Five mixtures of mortar were prepared with the same cement quantity and the same workability but with different kinds of aggregates (sand, quartz sand, slag, expanded clay and vermiculite). This research aimed to determine the behaviour of mortar made of the specific type of an aggregate in fire conditions and to establish strength values achieved by certain aggregates. Compressive strength was tested on the samples of 40/40/40 mm, whereas the behaviour in fire conditions on samples of 40/40/50 mm. The testing results are presented in the Tab. 1.

Tab. 1 Compressive strength of different kinds of mortar and the results of inflammability testing

Aggregate	Compressive strength (N/mm <sup>2</sup> )	Observations made during inflammability testing
sand	46.55	<ul style="list-style-type: none"> <li>• smoke in the first minute</li> <li>• the sample did not burn</li> </ul>
quartz sand	38.22	<ul style="list-style-type: none"> <li>• no manifestations were noticed</li> </ul>
slag	32.16	<ul style="list-style-type: none"> <li>• smoke in the first minute</li> <li>• the sample did not burn</li> </ul>
expanded clay (Leca)	0.98	<ul style="list-style-type: none"> <li>• smoke in the first minute</li> <li>• the sample did not burn</li> </ul>
vermiculite	1.23	<ul style="list-style-type: none"> <li>• no manifestations were noticed</li> </ul>

As for the achieved compressive strength, the materials behaved according to the expectations. The only exception was slag for which greater compressive strength was observed. However, when testing mortar with 56 days old slag, compressive strength was increased for even 27% in comparison to the one presented in the table, which means there was a subsequent increase of strength of mortars made of slag. Since smaller fraction of expanded clay is obtained by crushing the previously produced balls, the smaller compressive strength of that mortar was not surprising. As for fire load, all mortars met expectations and proved their inflammability according to the standard HRN EN 13501-1.

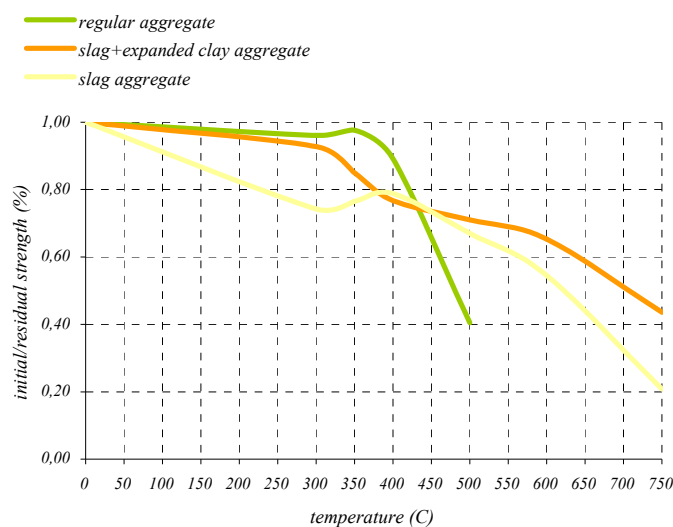


Diagram 1 - Residual strength remained after fire load

Concrete was made of the two mixes: one with slag as an aggregate and the other with the combination of slag and expanded clay (keramzite). The samples of stiffened concrete, of 40/40/50 mm in size were placed in the previously heated furnace at some of the planned temperatures (300, 400, 600 or 700 °C). We measured the time, which a thermocouple situated in the middle of the sample, needed to reach the temperature of the furnace. The residual strength was tested on the cooled samples. The interdependence of these kinds of concrete with the temperature changes they were exposed to was presented in the diagram 1. The same diagram shows the process of compressive strength decline due to fire load with concrete made of the standard aggregate, on the basis of the previously obtained testing results.



By monitoring the development of temperatures in the furnace and on the thermocouple, it has been determined that the time needed for equalizing of these temperatures was slightly shorter than with concrete made of a combination of slag and expanded clay as an aggregate, which means that concrete made of slag as an aggregate has smaller thermal conductivity. According to diagram 1, compressive strength of concrete made of a standard aggregate is stable up to the temperature of 350 °C, whereupon it abruptly declines. Compressive strength of concrete made of slag and slag and expanded clay gradually declines with the rise in temperatures, but without abrupt fractures in the curve. The diagram indicates the increased fire resistance of concrete made of slag and a combination of slag and expanded clay in comparison to concrete made of a standard aggregate, which indicates that these two kinds of aggregates can be classified into the fire resistance group.

## 5. CONCLUSION

This paper deals with aggregates which can increase concrete fire resistance and presents properties of some fire resistant aggregates (slag, vermiculite, perlite, expanded clay), as well as advantages and disadvantages of their use in concrete. The results of the conducted research confirm theoretical assumptions, according to which vermiculite and expanded clay belong to inflammable materials and concrete made of these aggregates can be classified into the group of fire resistant concrete.

## 6. ACKNOWLEDGMENT

The author would like to acknowledge the support of Croatian Ministry of education, science and sport, for the projects “The Development of New Materials and Concrete Structure Protection Systems”, 082-0822161-2159, “From Nano- to Macro-structure of Concrete”, 082-0822161-2990, “Ultimate states and sustainability of bridges”, 082-0822977-1497.

## 7. REFERENCES

- ArupFire, Fire resistance of concrete enclosures - Work Package 2: spalling categories, [www.hse.gov.uk/research/nuclear/parts1and2.pdf](http://www.hse.gov.uk/research/nuclear/parts1and2.pdf)
- Društvo građevinskih inženjera i tehničara Zagreb, Konstruktorska obnova ratom oštećenih zgrada, Zbornik radova, Zagreb, 1992. (in Croatian)
- Fellinger, J. H. H. (2004), “Shear and Anchorage Behaviour of Fire Exposed Hollow Core Slabs”, *Technische Universitaet Delft*, Delft
- GGBS, (Ground Granulated Blast-Furnace Slag)  
<http://www.fhwa.dot.gov/infrastructure/materialsgrp/ggbfs.htm>
- Liapor, <http://www.liapor.com>
- Peker, K., Pekmezci, B. (2003), “Damage Analysis for a Fire Exposed Industrial Building”, *Structural Engineering International*, Volume 13, Number 4, pp. 245-248
- Perlite, <http://en.wikipedia.org/wiki/Perlite>
- Steel slag, <http://www.tfrc.gov/hnr20/recycle/waste/ssa1.htm>
- Stipanović, I., Bjegović, D., Planinc, M. (2002), “Betoni specijalnih namjena – betoni povećane otpornosti na požar”, Materijali i tehnološki razvoj, *Akademija tehničkih znanosti Hrvatske*, Zagreb, str. 175-183 (in Croatian)
- Ukrainczyk, V. (1994), “Beton, Sveučilište u Zagrebu”, Zagreb, (in Croatian)
- Vermiculite, <http://en.wikipedia.org/wiki/Vermiculite>

## CONCRETE PROPERTIES IN FIRE DEPENDING ON TYPE OF CEMENT, AGGREGATE AND FIBRE

Éva Lublóy, György L. Balázs

Budapest University of Technology and Economics, Hungary

H-1111 Budapest Műegyetem rakpart 3 [lubeva@web.de](mailto:lubeva@web.de), [balazs@vbt.bme.hu](mailto:balazs@vbt.bme.hu)

### SUMMARY

Recent fire cases indicated again the importance of fire research. Fast development of construction technology requires new materials. Initiation and development of fire are strongly influenced by the choice of construction materials (Schneider, Lebeda, 2000). In addition to their mechanical properties, their behaviour in elevated temperature is also of high importance (Janson, Boström, 2004).

Residual compressive strength of concrete exposed to high temperatures is influenced by the following factors (Thielen, 1994): water to cement ratio, cement to aggregate ratio, type of aggregate, water content of concrete before exposing it to high temperatures and the fire process. *Results* of our experiments indicate changes of concrete properties after temperature loading as a function of the cement type, aggregate type and fibres (polypropylene).

### 1. INTRODUCTION

Constructions materials are often in interaction with each other (Fig. 1). Importance of their interaction is even more pronounced during fire.

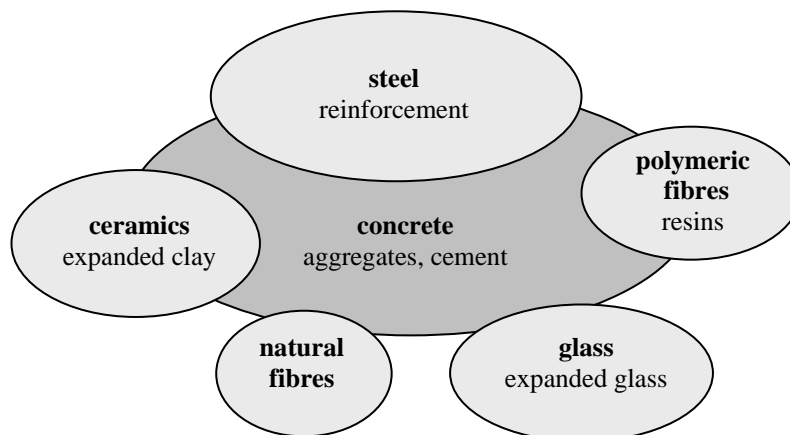


Fig. 1 Construction materials and their interaction

The residual compressive strength of concrete exposed to high temperatures is influenced by the following factors: (1) water to cement ratio, (2) cement to aggregate ratio, (3) type of aggregate, (4) type of cement, (5) water content of concrete before exposing it to high temperatures and (5) the fire process (Thielen, 1994).

## 2. EXPERIMENTAL STUDIES

Our experimental studies included various types of cements (3 types), aggregates (quartz gravel, expanded clay) and fibres (two types of polypropylene fibres (Tab. 1)).

Tab. 1 Characteristics of the applied fibre types

Fibre characteristics	macro fibre*	mono fibre**
Material	polypropylene	polypropylene
Length (mm)	40	18
Diameter (mm)	1,1	0,032
Melting point (°C)	171	160
Decomposition temperature (°C)	360	365

\* POLITON V40, Kaposplast Ltd.

\*\* FIBRIN 1832, Kaposplast Ltd.

Specimens were kept for two hours at high temperatures after heating up and then cooled down to room temperature. Maximal temperatures were: 20°C, 50°C, 150°C, 200°C, 300°C, 400°C, 500°C, 600°C or 800°C. Tests were carried out after cooling down the specimens.

## 3. EXPERIMENTAL RESULTS

### 3.1 Influence of type of cement

According to our observations type of cement have significant influence on the residual compressive strength of concrete subjected to high temperatures.

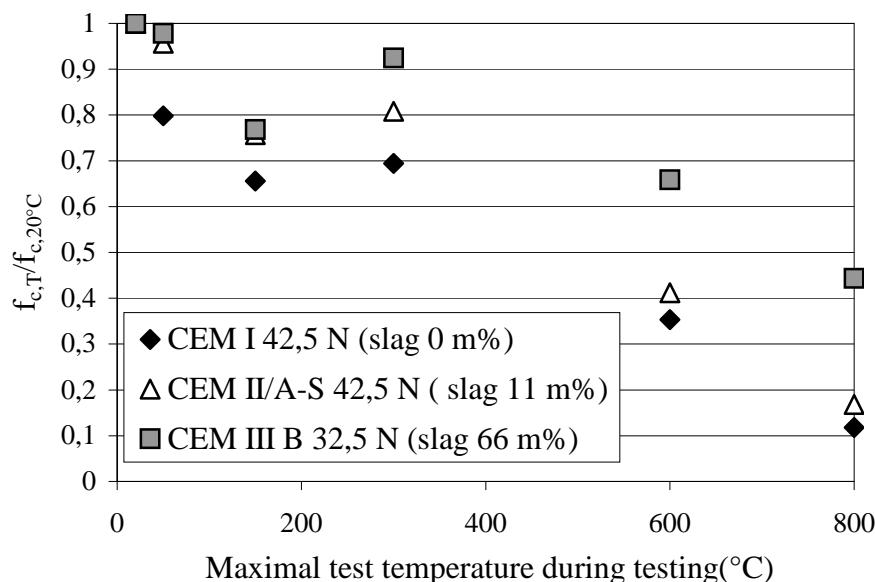


Fig. 2 Compressive strength of hardened cement paste as a function of maximal temperature and cement type. Measurements were carried out at room temperature (20°C). (Every point indicates an average of 5 measurements.)

The residual compressive strength after temperature load (300°C, 600°C and 800°C) increased with increasing the slag content (Fig. 2). The highest reduction of the compressive strength was recorded using of Portland cement (CEM I 42,5 N with slag content 0 m%) the

lowest reduction was observed using CEM III/B 32,5 N (slag content 66 m%). In case of CEM III/B 32 N cement the residual compressive strength was 40% lower than in case of the Portland cement after temperature loading of 800°C. By increasing the slag content the size and number of surface cracks were decreased (Fig. 3).

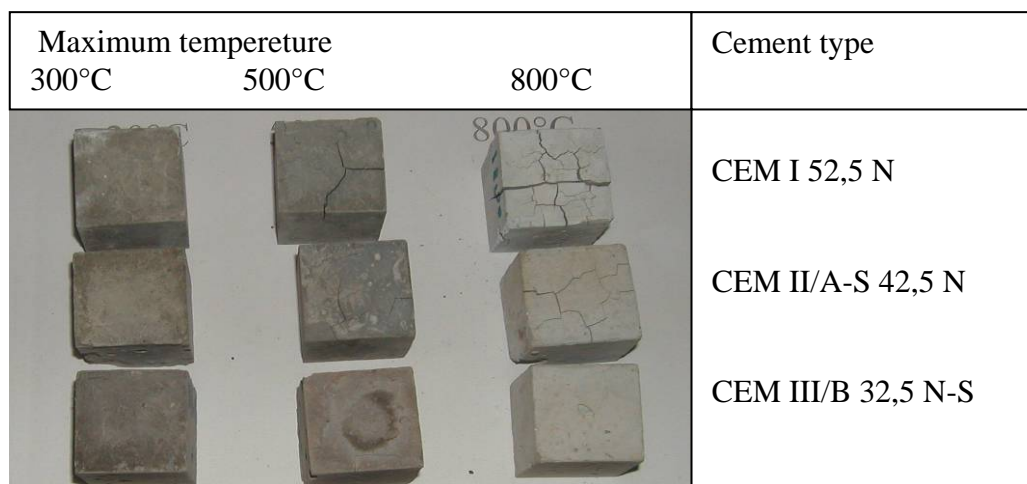


Fig. 3 Development of cracks in hardened cement stone

### 3.2 Influence of type of aggregate

In our experiments two essentially different aggregate types have been used: (1) quartz gravel or (2) expanded clay. We have used the cement type (CEM I 42.5 Portland cement) and quartz sand for every concrete mixtures. For every mixes the water to cement ratio (0.43) and water to aggregate ratio were constant. Change in the structure of the concrete was analysed by cutting sections of the test specimens. The concrete sections were fixed on glass sheets, and were ground thinner than 0.3 mm. The concrete sections prepared in this way were analysed by microscope. Coefficient of thermal expansion and coefficient of thermal conduction for lightweight aggregate concrete are lower than those of conventional concrete (Kordina, Meyer-Ottens, 1981).

Compressive strength results are presented in Fig. 4. In order to be able to show comparable results, the compressive strength of the concrete exposed to high temperature was divided by the strength value measured at room temperature. Following conclusions can be drawn from Fig. 4:

- Temperature load up to 800°C produces considerable reduction of compressive strength to all kinds of concrete mixes. This can be explained by the break down of the portlandite around 450°C and the CSH-composite around 700°C.
- The residual compressive strength of the lightweight aggregate concrete with expanded clay was higher after heating the specimens up to 400°C and then cooled down to room temperature as in the case of concrete with quartz gravel aggregate. The residual compressive strength values were by 10 to 20% lower.

The different behaviours of the various concrete mixes can be explained by the differences in the contact zones of aggregate and cement stone (Figs. 5 and 6). It can be well observed on the pictures that a layer of crystal structure can be found beside the quartz gravel (Fig. 5). The contact zone of the expanded clay is quite different (Fig. 6). The cement paste penetrates into the external pores of the aggregate of porous structure.

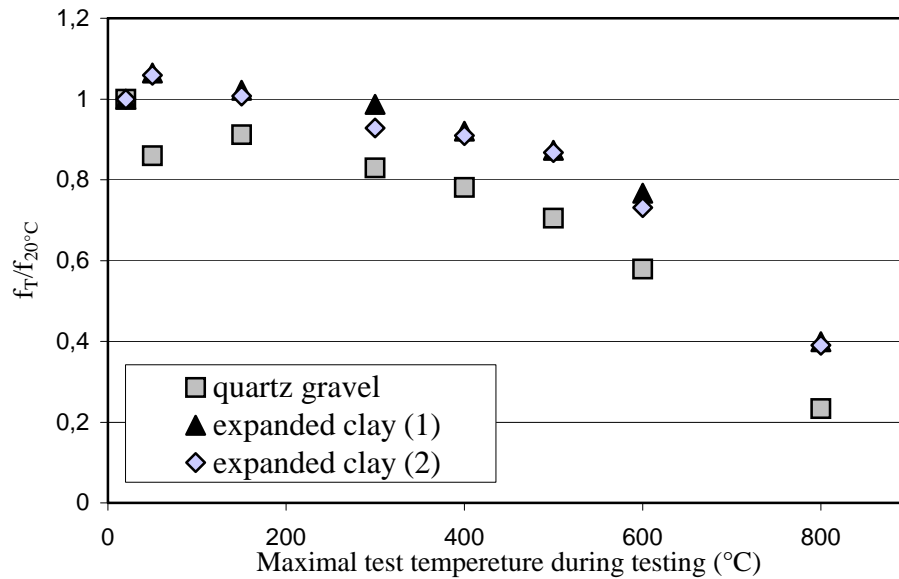


Fig. 4 Change of compressive strength after exposing the concrete to high temperature, measured at room temperature (20°C). (Every point indicates an average of 3 measurements.)

When expanded clay aggregates were used in the concrete, the specimens were deteriorated during heating up to 800°C. When the specimens deteriorated it has been observed that the aggregate particles were cracked along the surface of failure. This is may be due to the fact that the modulus of elasticity of the cement stone and the aggregate are too close to each other and, therefore, the cracks are also passing through the aggregate.

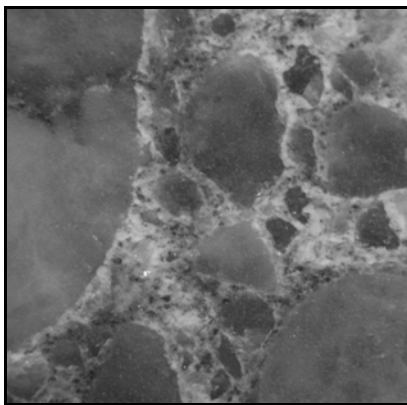


Fig. 5 Normal weight concrete at temperature of 20°C

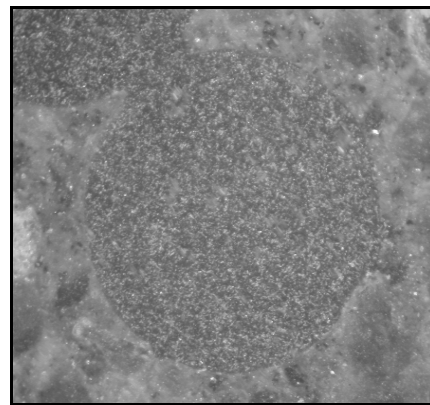


Fig. 6 Lightweight aggregate concrete with expanded clay aggregate at temperature of 20°C

### 3. 3 Influence of types of fibers

Spalling of concrete cover can be decreased by the application of synthetic fibers (Horiguchi, Sugawara, Saeki, 2004, Horiguchi, 2005). We have tested two types of polypropylen fibers (mono fibres with  $d=0,032$  mm; macro fibres with  $d=1,1$  mm).

In case of concrete with small diameter mono fibres considerable surface deformation was not observed up to 800°C (Fig. 7). In case of the reference concrete without fibres we have observed surface cracks by heating up to 800°C (Fig. 8).



Fig. 7 Mono fibre reinforced concrete (800°C temperature load)

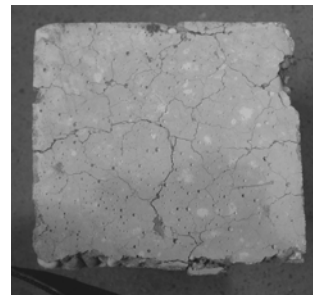


Fig. 8 Concrete without fibre reinforcement (800°C temperature load)

We observed, that macro fibres close to the surface flowed (at 200°C and at 300°C) to the surface then burnt (at 400°C) by giving colour on the surface (Fig. 9). In some places small holes could be also observed. These fibres were probably perpendicular to the concrete surface and burnt off in this position. Signs of burning could be seen on the concrete surface. These signs could be avoided by using of mono fibres instead of macro fibres (Lublóy, Balázs, 2007).

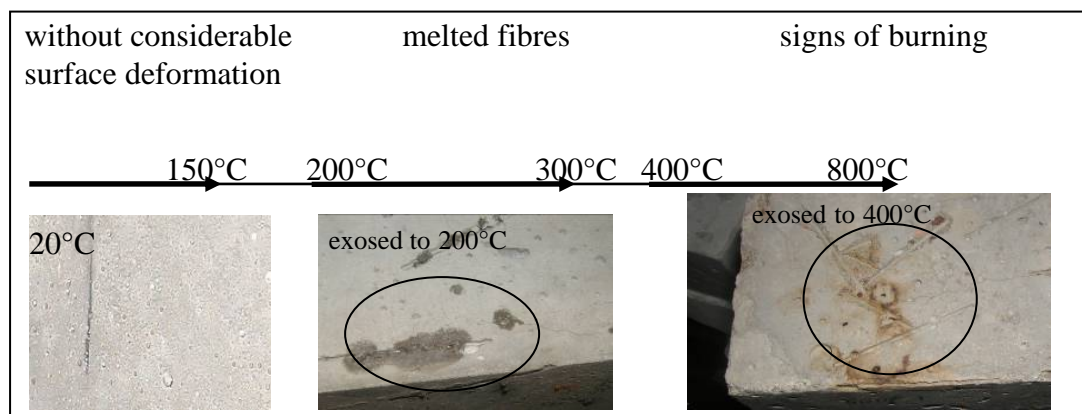


Fig. 9 Macro fiber reinforced concrete

We have analysed the behaviour of the expanded clay aggregate concrete by using also plastic fibres, with special focus on the surface of the concrete. During our experiments we observed that in the case of expanded clay aggregated concrete with synthetic fibre reinforcement, the concrete cover did not deteriorate and there were no cracks on the surface.

#### 4. CONCLUSIONS

The following conclusions can be drawn from our experimental study on cement stone (cement+water) specimens and concrete specimens (cement+water+aggregate+eventual plastic fibres). Aggregates were quartz gravel or expanded clay. Specimens were heated up to 20°C, 50°C, 200°C, 150°C, 300°C, 500°C, 600°C or 800°C. Measurements were carried out then at room temperature.

1. Temperature load up to 800°C produces considerable reduction of compressive strength to all kinds of concrete mixes.

2. *Test results with cement stone specimens* indicated that the slag content of cement has also an important influence. Strength reduction after temperature loading was smaller by increasing slag content of cement. The strength reduction with or without slag reached 40% up to 800°C.
3. *Test results with concrete specimens* indicated that the type of aggregate has also an influence on strength reduction after temperature loading. We observed 10 to 20% lower reduction of compressive strength in case of concretes with expanded clay aggregates compared to concretes with quartz gravel aggregates.
4. *Test results with concrete specimens with plastic fibres* indicated that the small diameters fibres are more favourable in case of high temperatures compared to the large diameter fibres.

## 5. NOTATIONS

- $f_{c,T}$  compressive strength of concrete measured at room temperature after heating up to max. temperature of T °C  
 $f_{c,20^{\circ}\text{C}}$  compressive strength of concrete measured at room temperature (20°C).

## 6. ACKNOWLEDGEMENTS

Authors express their acknowledgements to Duna-Dráva Cement Ltd. for providing the necessary cements for the experiments, and to the Kaposplast Ltd. for providing the plastic fibres.

## 7. REFERENCES

- Horiguchi, T., Sugawara, T., T. Saeki, T. (2004): "Fire resistance of hybrid fibre reinforced high strength concrete", Eds. by: di Prisco, M., Felicetti, R., Plizzari, G.A., *RILEM-Proceeding for 6<sup>th</sup> Symposium on Fibre-Reinforced Concretes (FRC)- BEFIB 2004*, 20-22 September 2004, Varenna, Italy pp.1125-1130.
- Horiguchi, T. (2005), „Combination of Synthetic and Steel Fibres Reinforcement for Fire Resistance of High Strength Concrete”, *Proceedings of Central European Congress on Concrete Engineering 8.-9. Sept. 2005* Graz pp. 59-64.
- Janson, R., Boström, L. (2004), "Experimental investigation on concrete spalling in fire." *Proceedings for Fire Design of Concrete Structures: What now?, What next?* (Eds.: P. G. Gambarova, R. Felicetti, A. Meda, P. Riva) Milan, Dec. 2-3, 2004, pp.115-120.
- Kordina, K., Meyer-Ottens, C. (1981): *Beton Brandschutz Handbuch*. 1. Auflage, Beton-Verlag GmbH, Düsseldorf
- Lublóy, É., Balázs, L. Gy. (2007): Residual compressive strength of fire exposed fibre reinforced concrete *Concrete Structures 2007* pp.64-69.
- Thielen, K. Ch. (1994), „Strength and Deformation of Concrete Subjected to high Temperature and Biaxial Stress-Test and Modeling“ (Festigkeit und Verformung von Beton bei hoher Temperatur und biaxialer Beanspruchung - Versuche und Modellbildung), *Deutscher Ausschuss für Stahlbeton*, Heft 437 Beuth Verlag GmbH, Berlin
- Schneider, U., Lebeda, C. (2000): *Baulicher Brandschutz*, Stuttgart; Berlin; Köln: Kohlhammer, 2000

## INSITU TEMPERATURE MEASUREMENTS TO DETERMINE PROPERTIES OF JET-GROUTED COLUMNS BY MEANS OF A THERMO-CHEMICAL ANALYSIS

*Klaus Meinhard, Martin Hopfgartner, Roman Lackner*

*[klaus.meinhard@tuwien.ac.at](mailto:klaus.meinhard@tuwien.ac.at)*

*Institute for Mechanics of Materials and Structures,  
Vienna University of Technology*

*A-1040 Karlsplatz 4, E202*

*[martin.hopfgartner@porr.at](mailto:martin.hopfgartner@porr.at)*

*PORR Technobau und Umwelt AG, Department for Geotechnical Engineering, Austria*

*[lackner@bv.tum.de](mailto:lackner@bv.tum.de)*

*FG Computational Mechanics, Technical University of Munich, Germany*

### SUMMARY

In this paper, a back-analysis scheme for the determination of the properties of jet-grouted structures using thermo-chemical couplings is presented. Hereby, the temperature increase in the center of the jet-grouted column is monitored and compared with the result of a thermo-chemical analysis of the hydration process in the column. As regards the latter, a multi-phase hydration model taking the chemical composition of the applied cement (or blended cement) into account is used.

### 1. INTRODUCTION

Improvement of weak underlying soils to support changing loading conditions during or after the construction phase of buildings and infrastructure is often required. One method standardly applied for this purpose is jet grouting, characterized by mixing the in-situ soil with cement grout discharged laterally into a borehole wall to form a column-like structure of improved soil (Fig. 1).

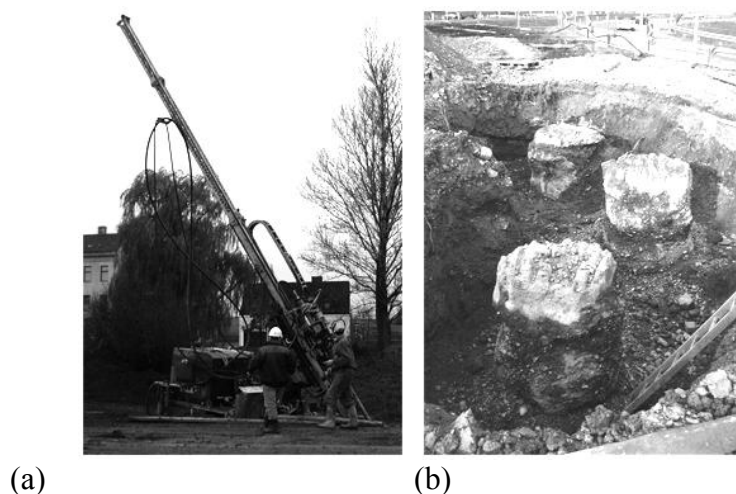


Fig. 1 (a) Drilling rig used for jet grouting and (b) test columns after excavation



Recently, the heat release during hydration of cemented soil was exploited for identification of the main properties of jet-grouted columns, i.e., the amount of cement in the improved soil determining stiffness and strength properties and the column radius (Brandstätter, Lackner, Mang, 2002); (Meinhard, Lackner, 2006). Hereby, a numerical model simulating the hydration process, i.e., the chemical reaction between cement and water taking the thermochemical couplings into account, is combined with in-situ temperature measurements. In this paper, the back-analysis scheme presented in (Brandstätter, Lackner, Mang, 2002) is improved as regards the underlying hydration model, allowing application of the back-analysis scheme in case of different types of cement and blended cements.

## 2. HYDRATION MODEL

Whereas an overall degree of hydration with one kinetic law was used in (Brandstätter, Lackner, Mang, 2002), a multi-phase hydration model, taking the main (four) clinker phases and the chemical compounds of cement into account, was proposed in (Bernard, Ulm, Lemarchand, 2003).

Fig. 2 shows the evolution of the degree of hydration  $\xi$  of the four main clinker phases  $C_3S$ ,  $C_2S$ ,  $C_3A$ , and  $C_4AF$  obtained from application of the multi-phase hydration model outlined in (Bernard, Ulm, Lemarchand, 2003) to each clinker phase and different evolution laws considering, e.g., a  $w/c$ -ratio of 0.3 and an average particle size of  $R=7\mu\text{m}$ .

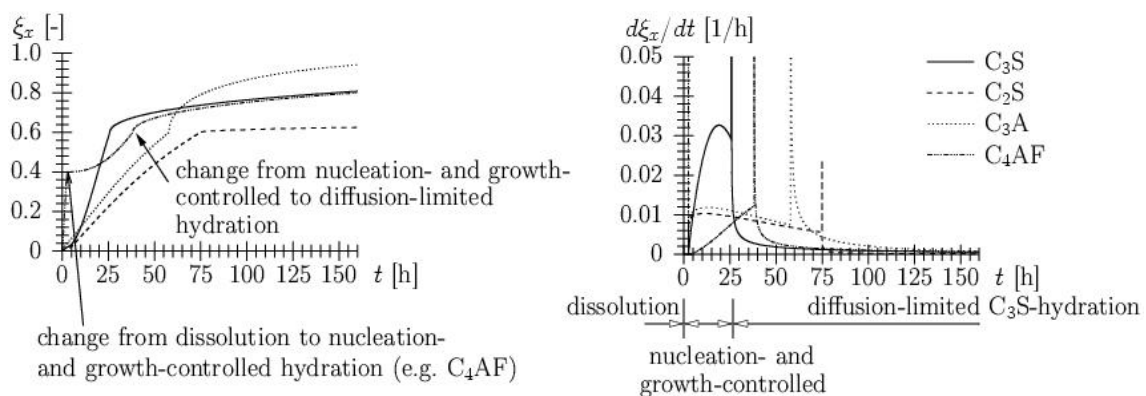


Fig. 2  $\xi_x$  and  $d\xi_x/dt$  for the four main clinker phases (water/cement-ratio=0.3; temperature=30°C; average particle size  $R=7\mu\text{m}$ )

In order to reduce costs of ground improvement, blended cements are commonly used during jet grouting (ordinary portland cement mixed with blast furnace slag, fly ash, silica fume, and lime stone). For this purpose, the hydration model presented in (Bernard, Ulm, Lemarchand, 2003) was extended towards blended cements and validated by means of differential-calorimetry (DC) experiments, see (Meinhard, Lackner, 2006). DC tests were performed for blended cements composed of ordinary portland cement, with  $4,895\text{ cm}^2/\text{g}$  blaine value ( $Q_\infty = 475\text{ J/g}$ ), and slag ( $Q_\infty = 461\text{ J/g}$  (Schindler, Folliard, 2005)), with a cement/slag-ratio ranging from 20/80 to 80/20. Fig. 3 shows the DC-results conducted at 30°C and 50°C, respectively. The dashed lines represent the heat flow and heat-flow rate of the respective cement fraction in the blended cement. It was obtained from multiplying the DC-test result for pure cement with the respective amount of cement in the blended cement. Thus, the difference between the solid and dashed line can be considered as the heat release associated with slag hydration.

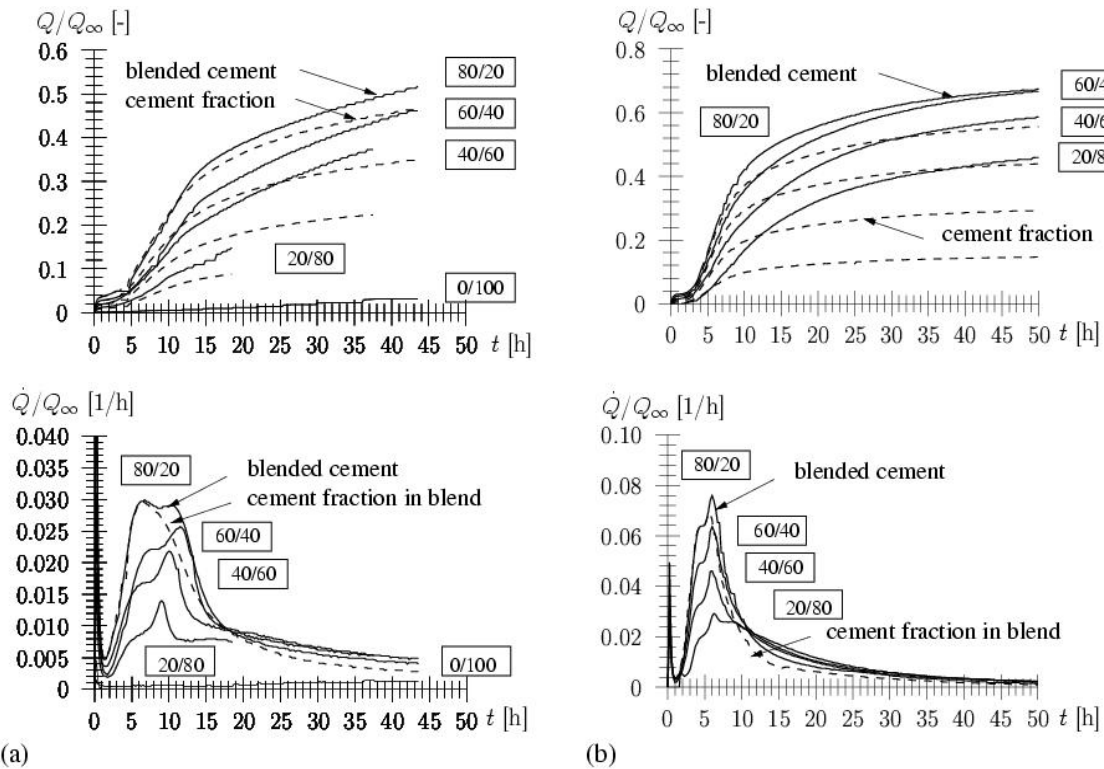


Fig. 3 DC-test results: heat flow  $Q$  and heat-flow rate  $dQ/dt$  for different cement/slag-ratios (OPC/slag,  $Q_{\infty} = 468$  J/g for all blended cements) at (a) 30°C and (b) 50°C

### 3. THERMAL PROPERTIES OF GRANULAR MATERIAL

For the solution of thermal problem, the volumetric heat capacity  $C$  [kJ/(m<sup>3</sup>K)], and the thermal conductivity  $k$  [kJ/(mhK)] of the jet-grouted soil mass and the in-situ soil are required. In order to account for the large range of these properties in granular, dry to fully-saturated material, determination of  $C$  and  $k$  from the properties of the different material phases, such as particles, water, and air is proposed. Whereas the heat capacity depends on the volume fractions of the material phases only, both material composition and arrangement (morphology) influence the thermal conductivity. In addition to models given in the literature for dry and saturated state (Lackner, Amon, Lagger, 2005), (Misra, 1995) a FEM-based model is employed to determine the thermal conductivity in the range of low and high values for the degree of saturation. Hereby, the effect of water bridging in the contact area of two particles is considered.

### 4. APPLICATION

In order to determine the diameter of a jet-grouted column and its cement content, the in-situ measured temperature history at the center of jet-grouted columns is compared with results obtained from the numerical simulation of the thermo-chemical problem. In the latter, the before mentioned hydration model and the model for the determination of the thermal properties are considered. The numerically-obtained temperature history depends on the radius of the jet-grouted column  $R$  [m], the content of cement  $s$  [(kg cement)/(m<sup>3</sup> jet-grouted soil)], and the thermal and chemical properties of the in-situ soil and the cement grout. The deviation between the measured in-situ temperature history and the respective numerical result is minimized by adapting both the column radius and the amount of cement in the

numerical model. The set of parameters yielding the lowest deviation represents the desired properties of the jet-grouted structure (Fig. 4).

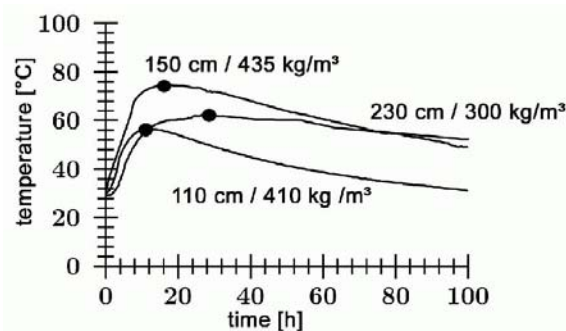


Fig. 4 Temperature histories of three different jet-grouted columns measured on site with numerically-identified properties (column radius / cement)

The so-obtained column radius was validated by excavation of the jet-grouted column giving good agreement between the predicted column diameter and the diameter measured on site.

## 5. ACKNOWLEDGMENTS

The authors thank Lafarge CTEC (Mannersdorf, Austria) for supplying the cement and blast-furnace slag used in the experimental program.

Financial support by PORR (Vienna, Austria) and the Austrian Research Promotion Agency Ltd. (FFG) is gratefully acknowledged.

## 7. REFERENCES

- Bernard, O., Ulm, F.-J., Lemarchand, E. (2003), „A multiscale micromechanics-hydration model for the early-age elastic properties of cement-based materials.”, *Cement and Concrete research*, 33, pp. 1293-1309.
- Brandstätter, Ch., Lackner, R., Mang, H.A. (2002), „Bestimmung von Materialeigenschaften zementgebundener Werkstoffe mittels Temperaturmessungen: Anwendung im Rahmen des Düsenstrahlverfahrens [Evaluation of properties of cementitious materials by means of temperature measurements: Application to jet grouting].” *Bauingenieur*, 77(2), pp. 51-57, in German.
- Lackner, R., Amon, A., Lagger, H. (2005), „Artificial ground freezing of fully-saturated soil: Thermal problem.”, *Journal of Engineering Mechanics (ASCE)*, 131, pp. 211-220.
- Meinhard, K., Lackner, R. (2006), „Validation and application of a multi-phase hydration model for the back-analysis of properties of jet-grouted structures.”, in G. Meschke, R. de Borst, H. Mang, and N. Bicanic, editors, *Computational modelling of concrete structures*, Taylor and Francis Group, London, pp. 607-615
- Misra, A., Becker, B.R., Fricke, B.A. (1995), „A theoretical model for the thermal conductivity of idealized soil.”, *Journal of Heating, Ventilation, Air-Conditioning and Refrigerating Research*, 1(1), pp. 1-21.
- Schindler, A.K., Folliard, K.J., „Heat of hydration models for cementitious materials.”, *ACI Materials Journal*, 102(1), pp. 24-33.

## PROBABILISTIC MODELING OF STEEL CORROSION IN RC STRUCTURES

*Dita Matesová, Břetislav Teplý, Jan Podroužek, Markéta Chromá*  
*Brno University of Technology*  
*Veveří 95, 602 00 Brno, Czech Republic*

### SUMMARY

The corrosion of reinforcement leads to a decrease in the effective area of the steel. The growth of rust products leads to concrete cracking, and later, the spalling of concrete cover, thus affecting the durability and reliability of a RC structure. The rate of reinforcement corrosion is governed by the availability of water, oxygen and chlorides on the steel surface. Durability limit states are explained, followed by a relevant model for degradation processes based on steel corrosion. Efficient design software is introduced which enables the probabilistic durability assessment of concrete structures. The development of the concentration of chlorides at the vicinity of the rebar surface is solved by a specific technique using cellular automata which is explained and then applied in an illustrative example showing the ingress of chlorides into a reinforced concrete cross section and the corresponding drop in the rebar's diameter due to corrosion.

### 1. INTRODUCTION

Utilization of design for durability may bring pronounced economical and sustainability impacts. Unfortunately, the prescriptive approach of current standards (e.g. Eurocodes EN 1990 and EN 1992) does not directly allow a design focused on a specific (target) service life and/or a specific level of reliability. This would require the consideration of inherent uncertainties in material and technological and environmental characteristics to be dealt with while assessing the service life of a structure. To overcome this, a full probabilistic approach should be applied.

The service life of a building or structure is determined by its design, construction, ageing and maintenance during use. While assessing service life, the combined effect of both structural performance and ageing should be considered, wherever relevant. Generally, the limit state approach is applicable, governed by the probability condition:

$$P_f = P[A t \geq B t] < P_d \quad (1)$$

In case of design for durability a new category of limit state has recently been introduced – Durability Limit States (DLS). This kind of limit state precedes the occurrence of both Serviceability Limit States (SLS) and Ultimate Limit States (ULS), and represents a simplified limit state intended to prevent the onset of deterioration. It is based on the initiation of deterioration – see the future documents (fib Bulletin 34 and ISO 13823); more can be found in (Teplý et al., in press). In Eq. (1)  $A$  = action effect,  $B$  = barrier; both  $A$  and  $B$  (and hence the probability of failure  $P_f$ ) are time dependent. This has not been considered for common cases of ULS or SLS in design practice very frequently up to now. The time  $t_s$

relevant to the limit given by (1), i.e. the service life, and the deteriorating effect  $A$  are assessed by utilization of the appropriate degradation models and the relevant LS, making use of a probabilistic approach. *Note:* Instead of the probability of failure  $P_f$ , the index of reliability  $\beta$  is alternatively (and rather frequently) utilized in practice – see e.g. (Eurocode EN 1990). The level of reliability in the context of durability should be left to the *client's decision* together with the target service life. When considering the LS caused by the degradation of reinforced concrete structures, several kinds of attack may be distinguished. The present paper focuses on *corrosion of reinforcement* and its consequences – i.e. on the propagation period of structure degradation.

The utilization of stochastic approaches (a combination of analytical models and simulation techniques) was involved in the creation of specialized software for assessing the durability of newly-designed as well as existing concrete structures - FReET-D, see (Teplý et al., 2007). This code encompasses about 30 different degradation models, for assessment of both the initiation and propagation period.

## 2. CORROSION

Once the corrosion of reinforcement starts, its detrimental effects may occur. The rate of steel corrosion is governed by (among other factors) the availability of water and oxygen. Also, the presence of chlorides in the concrete surrounding the steel bars may accelerate the corrosion. During the propagation period, i.e. after reinforcement depassivation, several states/effects may be encountered:

- (i) the volume expansion of rust products develops tensile stresses in the surrounding concrete leading to *concrete cracking* (mainly of concrete cover). The relevant limit condition should be constructed either with the tensile stress limit or the crack width limit;
- (ii) while the corrosion progress continues, which consequently is responsible for the *spalling* of concrete cover;
- (iii) a decrease in the *effective reinforcement cross-section* due to the corrosion, leading to excessive deformation and finally to the collapse of the bearing capacity of the cross section or structural member. Either general or pitting corrosion may be considered. In the following text a model suitable for handling case (iii) is shown.

### 2.1 Corrosion model

The uniform and the pitting types of corrosion are generally differentiated. The formula for the time related net rebar diameter  $d(t)$  at exposure time  $t$  [years] for the prediction of the corrosion reads according to Andrade et al. (1996):

$$d(t) = d_i - 0.0116 i_{corr} R_{corr} R_{Cl} t \quad (2)$$

where  $d_i$  is the initial bar diameter [mm] and parameter  $R_{corr}$  [-] expresses the type of corrosion. In the case of uniform corrosion, which is assumed in the example presented below,  $R_{corr}$  equals 2. Note that in the case of pitting corrosion  $R_{corr}$  equals 4-8 according to Rodriguez et al. (1996). Apart from parameter  $R_{corr}$ , other coefficients may be present in the formula, relating to the influence of chlorides, humidity, etc. Such coefficients may be applied only when appropriate data is available. The parameter  $R_{Cl}$  [-] regarding the effect of chlorides was added to Eq. (2) by the authors of this paper. The values of  $R_{Cl}$  may be determined by the results of experiments (Rovnaníková, 2002) governed by chloride

concentration, see Fig. 1. Due to the method used in these experiments and the consideration of real conditions the values of  $R_{Cl}$  are certainly somewhat on the safe side. The constant 0.0116 is a conversion factor from  $\mu A/cm^2$  to mm/years under the assumptions that steel (Fe) has  $n = 2$  (number of electrons freed by the corrosion reaction),  $M = 55.85$  g/mol (atomic mass) and  $\rho = 7.88$  g/cm<sup>3</sup> (specific gravity). The same approach may be applied to the pitting type of corrosion, see e.g. (Gonzales et al. 1995).

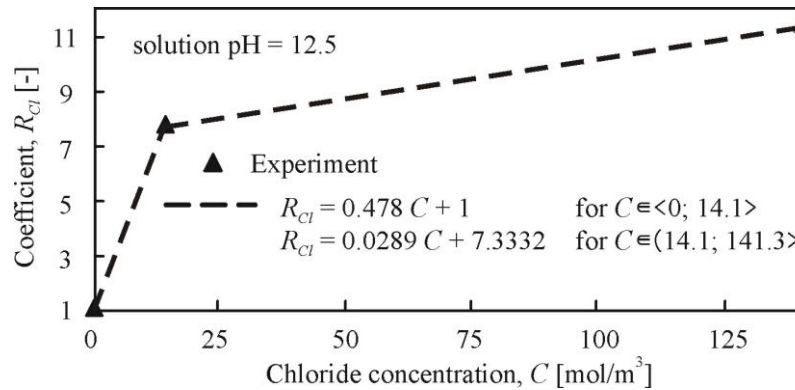


Fig. 1 The dependence of corrosion rate on chloride concentration

In order to gain appropriate information about the chloride concentration at different locations of a structural member or cross-section of complex shape a relatively sophisticated technique of cellular automata has been adopted and is introduced in the following section.

### Cellular Automata

A cellular automaton is a special class of *evolutionary algorithm*, which is a mathematical idealization of physical systems in which space and time are discrete (Wolfram, 1994). In principle, any physical system satisfying differential equations may be approximated as a cellular automaton by introducing discrete coordinates and variables, as well as discrete time steps. A cellular automaton consists of a collection of cells on a grid of specified shape that evolves through a number of discrete time steps according to a set of local rules based on the states of neighboring cells. The rules are then applied iteratively for as many time steps as desired. The overall simulation time is then the sum of all time steps.

The cellular automata solution of the diffusion equation was adopted from Biondini et al. (2004). The cross section is represented for our purposes by a 2D grid of regular uniform cells. Each cell has its state value representing the concentration of chloride ions. A visualization of the degradation evolution is shown in Fig. 2 for the time steps 0, 5, 25 and 50. The grey color represents the undamaged state of a cell while the black color represents the degraded state. The process of chloride ingress is governed by a local rule in which the evolutionary coefficients assign the level of chloride concentration redistribution within the cell's neighborhood. The relationship between the cell size, time step, evolutionary coefficient and chloride distribution constant is mandatory for the whole grid of cells within a time step. When the chloride supply changes, the distribution constant may change affecting the time step duration length. Stochastic effects may be treated as well, modifying the procedure by assuming the evolutionary coefficients to be random values with a given PDF.

In order to test the proposed methodology the standalone software SAPI is being developed by the third author (deterministic application of cellular automata). The application supports

cooperation with ATENA 2D non-linear fracture mechanics software (Červenka and Pukl, 2005). The geometry of the construction is primarily modeled in ATENA and afterwards loaded by SAPI. At this point a grid of cellular automata is created according to the initial parameters. The main parameters are: the diffusion coefficient, cell size, time step and the evolution coefficient. After defining the aggressive environment (e.g. supply of chlorides from a deicing salt solution) the transformation process may begin. After each time step a text file with the current system state is created. The whole process is displayed on the screen as a real-time graphical visualization. Proper interpretation of these results provides information about local changes to the cross section's material properties (chloride concentration) over time. For this purpose several types of boundary rule have been implemented. The best rule suitable for the comparison with conventional analytical models is the mirror neighbor rule of hemisphere action.



Fig. 2 Degradation evolution visualization

### 3. EXAMPLE

In the present example a reinforced concrete cross section is exposed to chloride ingress simulated by cellular automaton technique. Three different cases are assumed that differ by the surface areas exposed to chloride action as illustrated in Fig. 3 together with cross section geometry. The figure also documents chloride distribution in the cross sections after 30 years of exposure. The following input data for chloride diffusion simulation by cellular automata was used: surface concentration of chlorides  $60 \text{ mol/m}^3$ , cell size  $0.0032 \text{ m}$ , time step  $7.402$  days, diffusion coefficient  $2 \times 10^{-12} \text{ m}^2/\text{s}$  and evolution coefficients  $0.5$  and  $0.125$  for central and surrounding cells, respectively. The development of chloride concentration over time in the vicinity of steel reinforcements R1, R2 and R3 for three types of boundary exposed to chlorides (I, II and III) is plotted in Fig. 4. Due to certain symmetries in boundary conditions in this example some of the rebars are attacked identically - the chloride concentrations differ rather slightly.

When we apply Eq. (2) using  $R_{corr} = 2$  (uniform corrosion),  $i_{corr} = 1 \text{ } \mu\text{A/cm}^2$ ,  $d_i = 16 \text{ mm}$  and the experimental results in Fig. 1 we obtain a drop in the rebars' diameters over time due to corrosion. The results of deterministic analysis are plotted in Fig. 5 and a comparison with the case of a rebar which is not attacked by chlorides is also shown. The results of stochastic analysis performed for rebar R1\_II at time  $t = 20$  years by software FREeT-D are also depicted by means of the best fit of the probabilistic distribution function (PDF) found using the Kolmogorov Smirnov goodness-of-fit test. The input parameters for stochastic analysis were the following:  $d_i = 16 \text{ mm}$  (lognormal two parametric PDF with a coefficient of variation (COV) of  $2.5 \%$ ),  $i_{corr} = 1 \text{ } \mu\text{A/cm}^2$  (normal PDF,  $\text{COV} = 20\%$ ),  $R_{corr} = 2$  (deterministic) and  $R_{Cl} = 8.34$  (normal PDF,  $\text{COV} = 20\%$ ). The degradation of the structural capacity of the cross section would be high, so the concrete cover of  $30 \text{ mm}$  would be not

feasible in the case of such an exposition type (heavy attack of de-icing salt without consideration of seasonal application).

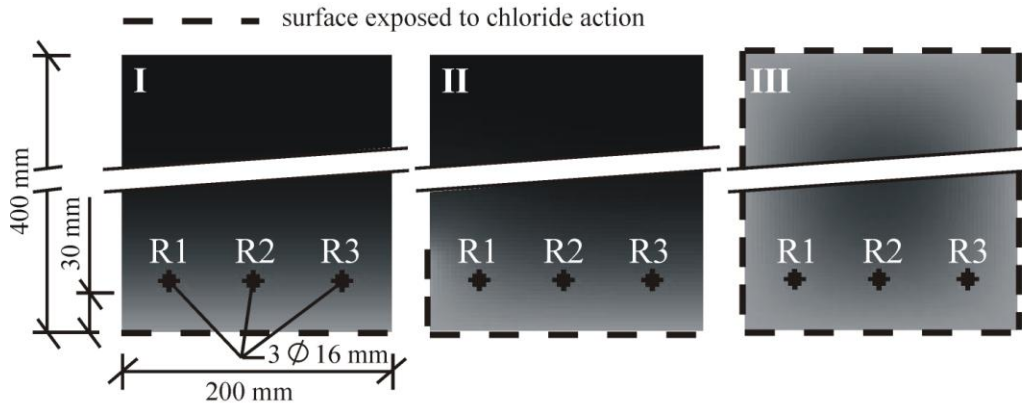


Fig. 3 Three cases of chloride ingress (I, II and III). Cross sections attacked by chloride are in grey color and sections without chloride are black

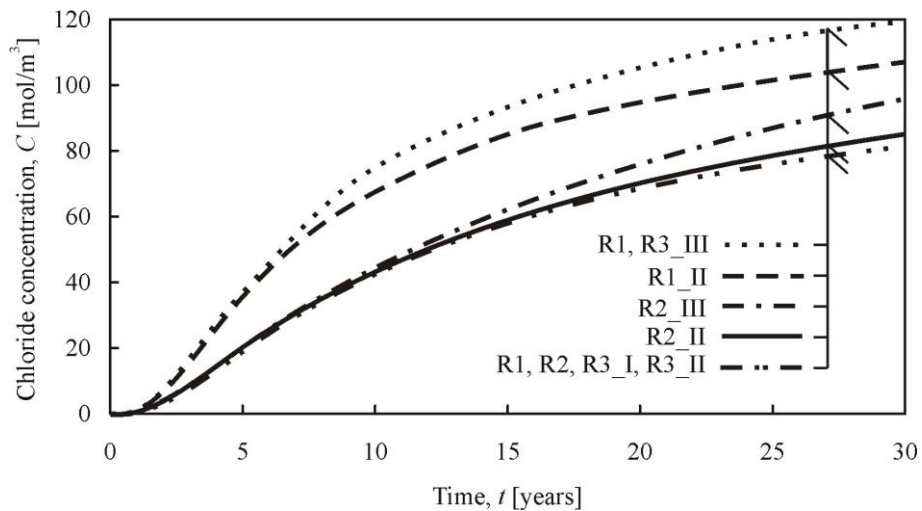


Fig. 4 Development of chloride concentration in the vicinity of steel rebars

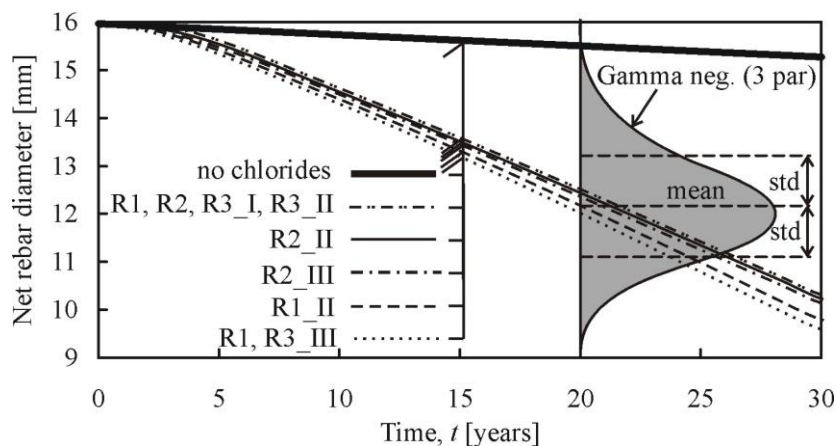


Fig. 5 A drop in rebars' diameters over time due to corrosion

#### 4. CONCLUSIONS

A probabilistic approach for the durability assessment of concrete structures, focusing on reinforcement corrosion, has been presented together with suitable numerical model and



software tools enabling the user to assess RC structure durability – the propagation period. The impact of chloride presence on corrosion rate is shown together with a special technique – cellular automata – for capturing the distribution of chloride concentration in the structural member. This creates the potential for more complex durability design, making use of statistical, sensitivity and reliability analyses of durability, serviceability and ultimate limit states. However, more complex data for the chloride concentration effect on the rate of reinforcement corrosion is lacking, as well as an assessment of the seasonal effects of de-icing salt application.

## 5. ACKNOWLEDGEMENT

This outcome has been achieved with the financial support of the Ministry of Education, Youth and Sports, project No. 1M0579, within the activities of the CIDEAS research centre.

## 6. REFERENCES

- Andrade, C., Sarria, J. and Alonso, C. (1996), "Corrosion rate field monitoring of post-tensioned tendons in contact with chlorides", in proc. of *Int. Conf. on Durability of Building Materials and Components 7* (vol. 2), Stockholm, 1996, pp. 959-967.
- Biondini, F., Bontempi, F. and Frangopol, D. M., Malerba, P. G. (2004), "Cellular Automata Approach to Durability Analysis of Concrete Structures in Aggressive Environments", *Journal of Structural Engineering ASCE*, Vol. 130, No. 11, 2004, pp. 1724-1737.
- Červenka, V. and Pukl, R. (2005), "ATENA Program Documentation", Červenka Consulting, Prague, 2005.
- EN 1990 (2002), "Basis of Structural Design", Eurocode 0, CEN, 2002.
- EN 1992-1-1 (2003), "Design of concrete structures – Part 1.1: General rules and rules for buildings", Eurocode 2, CEN, 2003.
- fib Bulletin No. 34 (2006), "Service Life Design", part of the future *fib Model Code 2008*.
- Gonzales, J.A., Andrade, C., Alonso, C., Feliu, S. (1995), "Comparison of rates of general corrosion and maximum pitting penetration on concrete embedded steel reinforcement", *Cement and Concrete Research* 25(2), 1995, pp. 257-264.
- ISO/WD 13823, "General Principles in the Design of Structures for Durability" (currently under development), ISO TC 98/SC2/WG10.
- Rodriguez, J., Ortega, L.M., Casal, J. and Diez, J.M. (1996), "Corrosion of reinforcement and service life of concrete structures", in Proc. of *Int. Conf. on Durability of Building Materials and Components 7* (vol. 1), Stockholm, 1996, pp. 117-126.
- Rovnaníková, P. (2002), "Corrosion of steel in different solutions – laboratory tests", Dept. of Chemistry, BUT Brno (unpublished).
- Teplý, B., Matesová, D., Chromá, M. and Rovnaník, P. (2007), "Stochastic degradation models for durability limit state evaluation: SARA – Part VI", in proc. of *3<sup>rd</sup> International Conference on Structural Health Monitoring of Intelligent Infrastructure (SHMII-3 2007)*, Vancouver, Canada, 2007, in press.
- Teplý, B., Chromá, M. and Rovnaník, P. (in press), "Durability assessment of concrete structures: Reinforcement depassivation due to carbonation", *Structure and Infrastructure Engineering*, in press.
- Wolfram, S. (1994), "Cellular Automata and Complexity – Collected papers", WolfrAddison-Wesley, 1994.

## **Topic 2**

Advanced reinforcing and prestressing materials and systems



## COMPARISONS IN BEHAVIOUR OF STEEL OR CFRP PRESTRESSED BEAMS

*Adorján Borosnyói, György L. Balázs*  
*Budapest University of Technology and Economics, Hungary*  
*H-1111 Budapest, Műegyetem rkp. 3.*

### SUMMARY

An experimental study has been carried out on prestressed concrete beams pretensioned either with CFRP or steel tendons at the Faculty of Civil Engineering, Budapest University of Technology and Economics. Based on present experimental data a new bilinear formula could be developed for the simplified calculation of deflections of CFRP prestressed concrete beams. Present test results demonstrated that sand coated surface of CFRP prestressing tendons gives favourable cracking behaviour of close cracks with small widths. In this way the average crack spacing can be much less than that of steel prestressed members.

### 1. INTRODUCTION

Corrosion of steel reinforcements resulted considerable deterioration of reinforced and prestressed concrete members requiring extra costs for maintenance and rehabilitation in the last decades. In order to prevent damage due to corrosion a promising alternative was developed: the application of non-metallic, entirely corrosion resistant reinforcements.

Corrosion resistant non-metallic reinforcements are Fibre Reinforced Polymers (FRP). Fibres can be made of glass, aramid or carbon. Depending on the applied fibres, FRPs have tensile strengths of 700 to 3500 N/mm<sup>2</sup>, modulus of elasticity of 38000 to 300000 N/mm<sup>2</sup>, failure strain of 0.8 to 4.0 % (Clarke, 1993; Machida, 1993, 1997; Rostásy, 1996; Uomoto, 1995). Carbon Fibre Reinforced Polymers (CFRP) show superior behaviour. Mechanical properties of CFRPs differ from those of conventional prestressing steels leading to different behaviour and design aspects (Abdelrahman-Rizkalla, 1997; ACI, 2003; Borosnyói-Balázs, 2002; Machida, 1997).

CFRP prestressing tendons are usually produced by pultrusion process (Clarke, 1993; Rostásy, 1996). Rods with almost smooth surface are not suitable for concrete structures due to the lack of adequate bond. Therefore, surface treatments (such as spiral fibre winding, indentations, periodic ribs, stranded or braided shapes, or sanded surfaces) are needed to improve bond characteristics. These treatments may increase bond strength of CFRP tendons even more than that of steel tendons (*fib*, 2000). During pull-out bond failure the outer layers of CFRP tendons can be damaged which never occurs in the case of steel tendons or steel reinforcing bars. This difference may also influence structural behaviour.

### 2. EXPERIMENTAL PROGRAMME

An experimental study has been carried out on prestressed concrete beams pretensioned either with CFRP or steel tendons at the Faculty of Civil Engineering, Budapest University of Technology and Economics. Test beams had an I-cross-section with relatively thin web and

did not contain any other longitudinal reinforcement but prestressed pretensioned tendons (Fig. 1). Beams had the same cross section, with minimum concrete cover of 12 mm. Following parameters were considered in the test programme: 1) number of prestressing wires in a beam: one, two or four, 2) prestressing material: sand coated CFRP or indented steel wire.

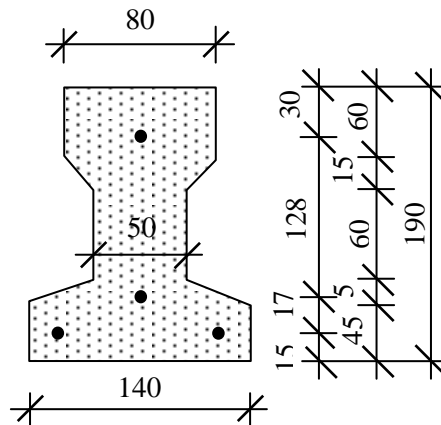


Fig. 1 Typical cross section of beam specimens with four tendons

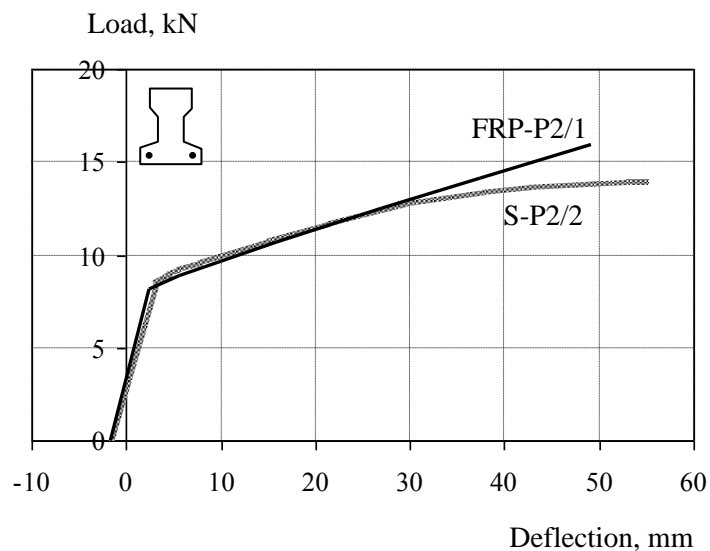


Fig. 2 Comparative load vs. deflection responses

### 3. STRUCTURAL BEHAVIOUR

#### 3.1 Deflection control

Load vs. deflection responses of concrete beams prestressed with CFRP tendons are practically bilinear in service conditions (Fig. 2 where FRP-P2/1: test beam prestressed with CFRP; S-P2/2: test beam prestressed with steel). Based on present experimental data a new bilinear formula could be developed for the simplified calculation of deflections of CFRP prestressed concrete beams (Fig. 3).

In uncracked elastic state (*State 1*) moment of inertia ( $I_g$ ) and deflections can be predicted accurately by conventional theory that is using the assumptions of CEB-FIP Model Code 1990 by simple substitution of mechanical properties of CFRP reinforcement. Evaluation of the cracking moment ( $M_{cr}$ ) is also accurate (see above). Reaching the cracking load ( $M_{cr}$ , calculated according to MC90) use of the effective moment of inertia by Eq. (1) is proposed:

$$I_{ef} = \frac{M_0}{M_{cr}} \frac{k_b \cdot \rho_{ef}}{\alpha_e} \cdot I_g \quad \text{where} \quad (1)$$

$$M_0 = -N \cdot x_{12} \frac{1/r_2}{1/r_2 - 1/r_1}, \quad \text{and} \quad x_{12} = x_1 - x_2 \quad (2)$$

$$N = A_f \cdot \sigma_{p,ef} \quad (3)$$

$$\rho_{ef} = \frac{A_f}{A_{c,ef}} \quad (4)$$

$$\alpha_e = \frac{E_f}{E_c} \quad (5)$$

In Eq. (1) parameter  $k_b$  takes bond properties of the CFRP tendon into consideration. Evaluation of present test results by the method of least square errors gave the value of the bond parameter ( $k_b$ ) for sand coated CFRP prestressing tendons to be  $k_b = 50$ . Bond parameter ( $k_b$ ) for CFRP prestressing tendons having different surface configurations needs further analysis.

The model introduced herein can provide good estimation of load vs. deflection responses of CFRP prestressed concrete beams in service conditions, tested in present experimental program. Verification of the model to further beam geometries and prestressing levels needs further analysis.

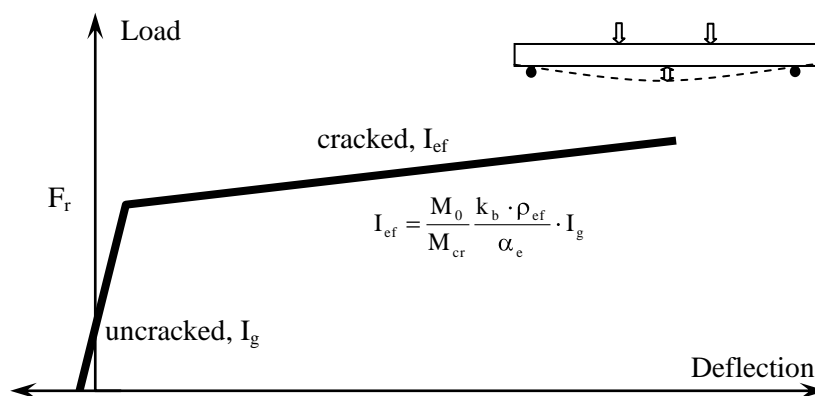


Fig. 3 Illustration for the developed bilinear formula

### 3.2 Crack control

During *crack formation phase* cracks form – independently from each other – at random positions in locally weak sections. When a crack is formed, stress in the concrete adjacent to the crack drops to zero. At the section of a crack loads are carried by the reinforcement only (*State 2*). A minimum crack spacing ( $s_{r0}$ ) can be defined based on strain compatibility. It

defines the closest point to an existing crack at which another crack can form – i.e. where stress in concrete again reach the tensile strength. If a crack spacing is equal to  $s_r \geq 2 \times s_{r0}$ , a new crack can form between the existing two cracks. If a crack spacing is equal to  $s_r < s_{r0}$ , a new crack can not form between the existing two cracks. This means that the crack spacings are expected to vary between  $s_{r,min} = s_{r0}$  and  $s_{r,max} = 2 \times s_{r0}$ . At *stabilised cracking phase* generally no more new cracks are formed, thus crack spacings can be described by ratios of minimum vs. average crack spacings and maximum vs. average crack spacings.

Present test results demonstrated that sand coated surface of CFRP prestressing tendons gives favourable cracking behaviour of close cracks with small widths. High bond strength of these tendons allows tensile stresses to be transferred along a very short distance adjacent to cracks. In this way the average crack spacing can be much less than that of steel prestressed members. Cracking force of CFRP prestressed members can be predicted accurately using formulae of CEB-FIP Model Code 1990. Further question is the load level at reaching the stabilised cracking phase. The MC90 suggests the following ratio for cracking load and load at reaching the stabilised cracking phase [MC90 Clause 3.2.3, p. 91, Eq. (3.2-7)]:

$$F_{rn} = 1.3F_r \tag{6}$$

Present experiments on the steel prestressed members result an average ratio of  $F_{rn}/F_r = 1.303$  can confirm assumptions made by Eq. (6). However, results for CFRP prestressed members with an average ratio of  $F_{rn}/F_r = 1.46$  may indicate the influence of other parameters on the load level at reaching stabilised cracking phase such as Young's modulus (was 158800 N/mm<sup>2</sup> for CFRP) or high bond capacity of sand coated surfaces.

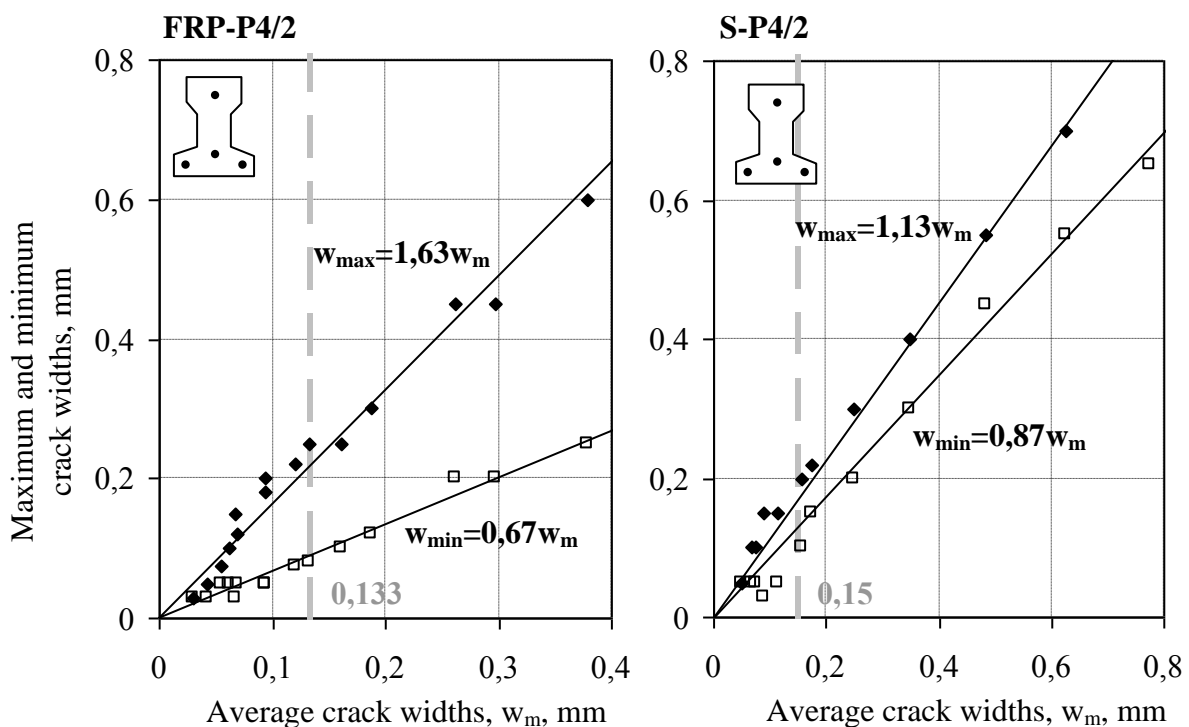


Fig. 4 Ratios of maximum vs. average and minimum vs. average crack widths

Fig. 4 represents relationships between maximum, minimum and average crack widths. Diagrams follow the whole loading procedure and linear regression lines estimate ratios between maximum, minimum and average crack widths. Here maximum crack width is introduced instead of characteristic crack width (i.e. fractile of 95 percent) that are practically equal to each other. It can be stated that the ratio of maximum and average crack widths in the case of CFRP prestressed members 50 percent greater than that of steel prestressed members. Average crack widths at reaching the stabilised cracking phase is also presented in the diagrams with dashed lines (0.15 mm and 0.133 mm for the steel prestressed and for the CFRP prestressed members, respectively). Results indicate that in stabilised cracking phase minimum crack widths also have an increasing tendency that means no more new cracks occur. During crack formation phase minimum crack width is almost constant due to the newly occurred cracks with small widths. Let us remind here to a code recommendation for the ratio of maximum vs. average crack widths: Eurocode 2 introduces value of 1.7 for members reinforced with steel. It can be seen that value of 1.7 overestimates results for steel prestressed members, however, gives reasonable estimate for CFRP prestressed members. Therefore, only one parameter seems to be not enough for the evaluation of the ratio of maximum vs. average crack widths. Fig. 5 represents relationships between maximum and average crack widths as a function of effective reinforcement ratio.

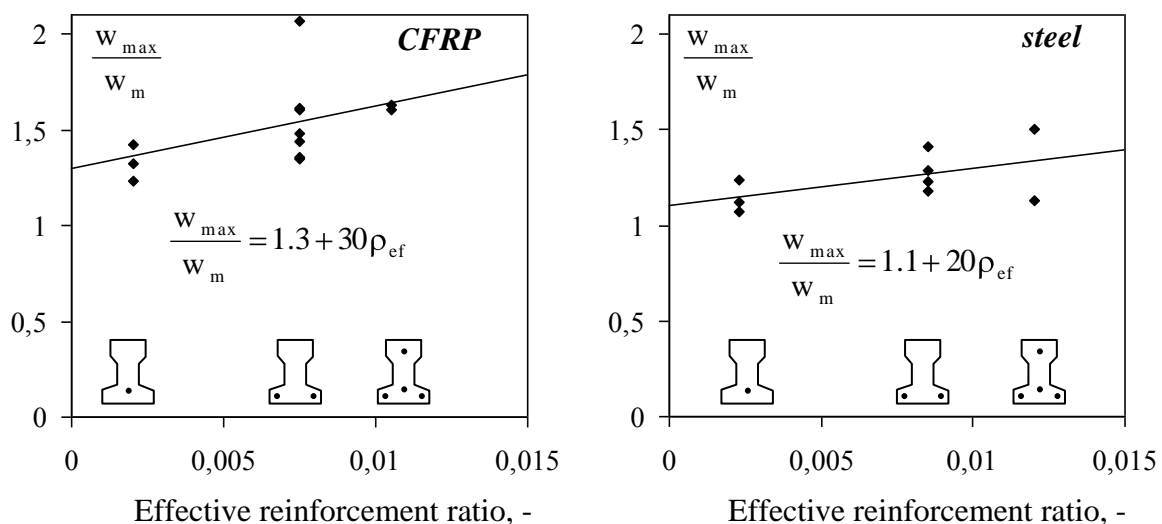


Fig. 5 Ratios of maximum vs. average crack widths

#### 4. CONCLUSIONS

Based on experimental and theoretical analyses of concrete beams prestressed with CFRP tendons the following conclusions can be drawn:

For deflection control of CFRP-prestressed beams a simplified calculation of effective moment of inertia is introduced that is not based on Branson's approach. In the formula (given by Eq. (1)) only geometrical and mechanical parameters are covered, introducing a bond parameter ( $k_b$ ) for factoring different surface configurations of CFRP prestressing tendons. The model provides good estimation of load vs. deflection responses of CFRP prestressed concrete beams in service conditions, tested in present experimental program, however, verification of the model to further beam geometries and prestressing levels needs further analysis.



Sand coated surface of CFRP prestressing tendons gives favourable cracking behaviour of close cracks with small widths. Cracking force of CFRP prestressed members can be predicted accurately using formulae of CEB-FIP Model Code 1990. Results on the ratio of cracking load and load at reaching stabilised cracking phase for steel prestressed members can confirm assumptions made by CEB-FIP Model Code 1990 with a ratio of  $F_{m}/F_r = 1.3$ . However, results for CFRP prestressed members with an average ratio of  $F_{m}/F_r = 1.46$  may indicate the influence of other parameters on the load level at reaching stabilised cracking phase such as Young's modulus (was 158800 N/mm<sup>2</sup> for CFRP) or high bond capacity of sand coated surfaces. Nature of crack formation was found to be random in the case of members with CFRP tendons, similarly to steel prestressed members. FRP reinforcements have large variety in surface configuration, therefore, the use of adopted versions of existing design code proposals for FRP reinforcements needs reconsideration of empirical parameters.

## 5. ACKNOWLEDGEMENTS

Authors gratefully acknowledge the financial support of the Hungarian Academy of Sciences (Bolyai Scientific Scholarship) and that of the Hungarian Research Fund (OTKA; contract No. F61685).

## 6. REFERENCES

- Abdelrahman, A. A. – Rizkalla, S. H. (1997) "Serviceability of Concrete Beams Prestressed by Carbon-Fiber-Reinforced-Plastic Bars", ACI Structural Journal, July-August 1997, pp. 447-457.
- ACI Committee 440 (2003) "Guide for the Design and Construction of Concrete Reinforced with FRP Bars", (ACI 440.1R-03), ACI, Detroit, USA, 2003
- Borosnyói, A. – Balázs, G. L. (2002) "Experiences and Design Considerations of Concrete Members Reinforced by FRP", Int. Congr.: Challenges of Concrete Construction, Dundee, pp. 135-146.
- CEB-FIP (1993) "CEB-FIP Model Code 1990 – Design Code", Comité Euro-International du Béton, Thomas Telford, London, 1993 (CEB Bulletin d'Information No. 213/214.)
- Clarke, J. L. (Ed.) (1993) „Alternative Materials for the Reinforcement and Prestressing of Concrete”, Chapman & Hall, London, 1993
- Eurocode 2 "Design of Concrete Structures, General Rules and Rules for Buildings", European Prestandard ENV 1992-1-1, Dec 1992
- fib* (2000) "Bond of Reinforcement in Concrete", State-of-Art Report prepared by Task Group Bond Models, August 2000.
- JSCE (1997) "Recommendation for Design and Construction of Concrete Structures Using Continuous Fiber Reinforcing Materials", Concrete Engineering Series V. 23, JSCE, Tokyo, 1997.
- Machida, A. (1993) "State-of-the-Art Report on Continuous Fiber Reinforcing Materials", JSCE, Tokyo, 1993.
- Rostásy, F. (1996) "State-of-the-Art Report on FRP Materials", FIP Report, Draft, 1996. Unpublished.
- Uomoto, T. – Nishimura, T. – Ohga, H. (1995) "Static and Fatigue Strength of FRP Rods for Concrete Reinforcement", Int. RILEM Symp. FRPRCS-2, Ghent., E & FN Spon, London. pp. 100-107.

## REINFORCING SELF-SENSING FRP RODS AS MAIN REINFORCEMENT IN CONCRETE BEAMS

*Ludovít Nad<sup>1)</sup>, Francesca Nanni<sup>2)</sup>, Gualtiero Gusmano<sup>2)</sup>, Anton Bajzecer<sup>1)</sup>, Giovanni Ruscito<sup>2)</sup>, Daniel Žarnay<sup>1)</sup>*

<sup>1)</sup> *Technical University of Košice, Faculty of Civil Engineering  
Vysokoškolská 4, 042 00 Košice, Slovak Republic [Ludovit.Nad@tuke.sk](mailto:Ludovit.Nad@tuke.sk),  
[Anton.Bajzecer@tuke.sk](mailto:Anton.Bajzecer@tuke.sk), [Daniel.Zarnay@tuke.sk](mailto:Daniel.Zarnay@tuke.sk)*

<sup>2)</sup> *INSTM research unit of Dep. Of Sciences and Chemical Technologies  
University of Rome "Tor Vergata" Via della Ricerca Scientifica, 00133 Rome, Italy  
[fnanni@ing.uniroma2.it](mailto:fnanni@ing.uniroma2.it), [giovanni.ruscito@uniroma2.it](mailto:giovanni.ruscito@uniroma2.it)*

### SUMMARY

The paper presents results of short time static test of concrete beams reinforced with self-sensing composite rod as main reinforcement. Self-sensing hybrid nanocomposite rods were made and tested in concrete beams. The self-monitoring task was performed by a dispersion of carbon particles into epoxy resin. The particles, in fact, form a conductivity pattern that allows the electrical resistance measurement. When such material is subjected to strains, it results into change of electrical resistance. Electrical resistance of rods embedded in concrete beams was measured during cure of concrete and short time static test. The deformation state of tested concrete beams – under short time loading – was simultaneously monitored also by conventional procedures. The results showed that the proposed rods present very interesting and promising self-sensing properties for monotonic load conditions.

### 1. INTRODUCTION

Corrosion of steel reinforcement is one of most frequent reasons of heavy failures of concrete structures. Use of FRP instead of steel reinforcing and prestressing units offers a reasonable solution. One of most important problems of FRP generally and especially GFRP is low modulus of elasticity and rheology of basic material. The problem leads to the strong request to pay more attention to monitoring of the concrete beams and the state of use non-metallic reinforcement and prestressing. The stress level and the deformation are the main information needed during the exploitation of the structure. As FRP generally is new material we need also to find new approach in monitoring systems and methods.

Generally, the self-sensing materials are made of polymer matrix composites (PMCs), because of their intrinsic versatility and possibility to include separate phases within the matrix. The self-monitoring task is performed by controlling the variations of an electrical property of an electrically conductive element embedded into the insulating matrix (Nanni 2003). In case when we work with PMCs, carbon is the most common electrically conductive element and therefore, usually, self-sensing PMCs are made of carbon fibres/carbon particles reinforced polymers (CFRPs - CPRPs), or hybrid composites containing aramidic/carbon or glass/carbon (CF-GFRPs). This latter choice is usually taken for those applications (for example, civil engineering) where ductility, or better pseudo-ductility, is an important parameter, which can be reached with a right selection of hybrid fibre reinforcement. In the present paper self-sensing hybrid nanocomposite rods were manufactured and tested into

concrete beams. The self-monitoring task was performed by a dispersion of carbon particles into epoxy resin. The particles, in fact, form a conductivity pattern that allows the electrical resistance measurement. Under stress the pattern, as well as the rest of the material, is subjected to positive or negative strains resulting, respectively, in an increase or decrease of electrical resistance.

The experimentation was carried out by performing simultaneously mechanical tests and electrical measurements both on composite rods and on concrete beams reinforced with the self-sensing nanocomposite rods. The deformation state of tested concrete beams – under short time as well as long time loading – was also simultaneously monitored by conventional procedures. FEM simulation was made in order to evaluate obtained experimental results.

## 2. EXPERIMENTAL STUDIES

Experimental program consists of mechanical tests of three beams reinforced with composite GFRP rods as main reinforcement. Beams had identical rectangular cross section of  $60 \times 100$  mm with 90 mm effective depth. The span of the beams is 900 mm. Scheme of beams and reinforcement is showed in Fig. 1. Two of them were reinforced with hand made self-sensing hybrid CnP-GFRP. The rest one was reinforced with factory made GFRP rods (not self-sensing) and serves as comparative specimen. In all beams as auxiliary and shear reinforcement was used steel wire with 2 mm diameter. During the concrete curing shrinkage as well as the electrical resistance on self-sensing rods embedded in concrete were simultaneously measured.

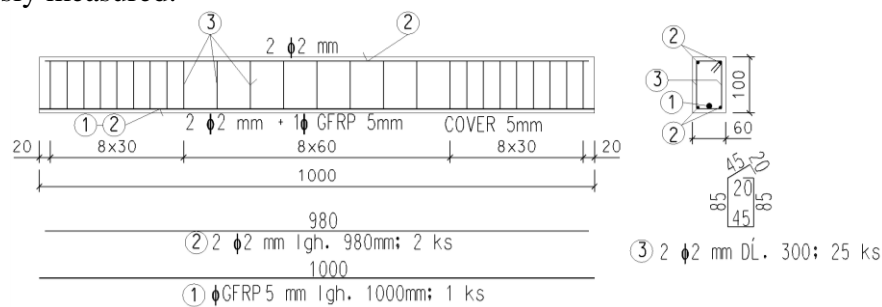


Fig. 1 Scheme of reinforcement of tested beams

All beams were tested in four point static bending tests up to failure. During mechanical test the deformation, strain and change of electrical resistance were measured. Deformation at mid span and support displacement was measured. Strain was measured on top of cross section in the mid span and along both sides of beams in level of reinforcement. Overall arrangement of mechanical tests is showed on Fig. 2.

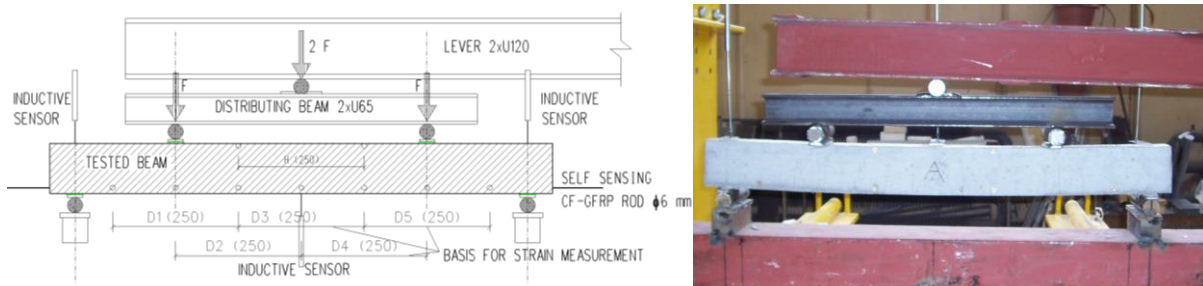


Fig. 2 Scheme of the tested beam with position of basis for strain measurement and inductive sensor for deflection measurement

## 2. 1 Materials and methods

The manufactured CnP-GFRP samples consisted of hybrid composite rods with an internal conductive core surrounded by an external insulating skin (Fig. 3). The internal core was made of glass fibres (CO.FI.TECH 475 W 2400 TEX) embedded into carbon particles-loaded (Printex, Degussa) epoxy resin (SP system). The outer coaxial skin consisted of GFRP. The final samples presented an overall diameter of 6 mm and were 1250 mm long. For better bond with concrete the finally the surface was treated by epoxy and silica sand to make rough surface.

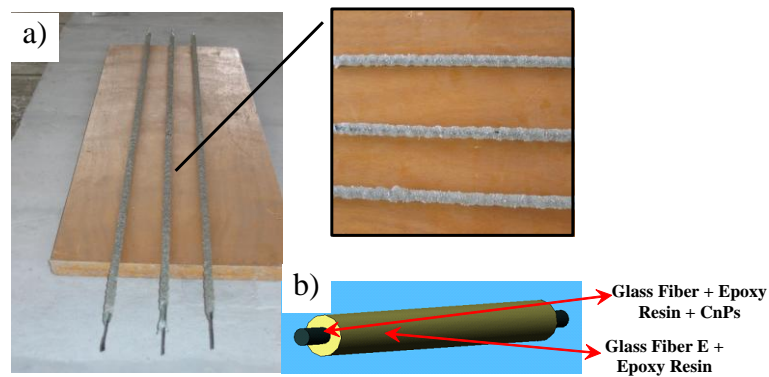


Fig. 3 a) Picture of CnP-GFRP rods with internal conductive core externally covered by GFRP

b) sketch

Mechanical properties of self-monitoring CF-GFRP rods were determined on rods which were embedded in concrete beams (sample 1 and 2) and on the sample witch was as compensative specimen not embedded in concrete (sample 3). After mechanical test of the beams the undamaged reinforcement (CF-GFRP) was selected from beams and tested in simple tension tests. There was made 2 specimens from sample no. 3 for tensile tests. Tab. 1 summarises the major properties of samples, including initial electrical resistance, strength and Young's modulus.

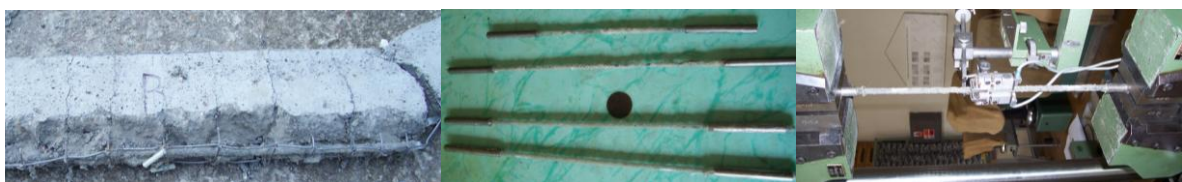


Fig. 4 Picture of selecting rod from concrete, prepared samples and test setup

Tab. 1 Major properties of CPGFRP sample

Sample #	Lenght (mm)	Total $\phi$ (mm)	Conductive Core $\phi$ (mm)	wt %	$R_0$ [MOhm]	Rupture strength [MPa]	Young's modulus [GPa]
1	1250	6	2	5%	1,25	491	26.959
2	1250	6	2	5%	1,5	445	27.637
3	1250	6	2	5%	7,9	528	25.883

Tab. 2 presents a mechanical properties of used concrete in age of 3 days and in time of mechanical tests of the beams (4 days old concrete).

Tab. 2 Compressive strength and modulus of elasticity of concrete

Age	Strength [MPa]		Young's modulus [MPa]
	Average	5 percentile	
3 days	16.70	15.21	-
4 days (test)	18.48	17.02	16 100

### 3. NUMERICAL SIMULATION

Mechanical test of beams was numerically simulated in structural analysis program “Atena” based on finite elements method (FEM). The beams were modeled as plane stress axially symmetric two dimensional task. For creating finite element mesh the quadrilateral shape elements with quadratic interpolation were used. Concrete material was modeled by using material model – concrete SBETA with fixed crack. A composite rod was modeled with linear elastic material and steel wire as bilinear material with hardening. Material properties (strength and Young’s modulus) of concrete, composite rod and steel wire were assigned according to experimentally determined value. Other parameters for concrete were generated automatically by program. Bond between concrete and reinforcement was assumed ideally bonded. Results from simulation were compared with experimental results.

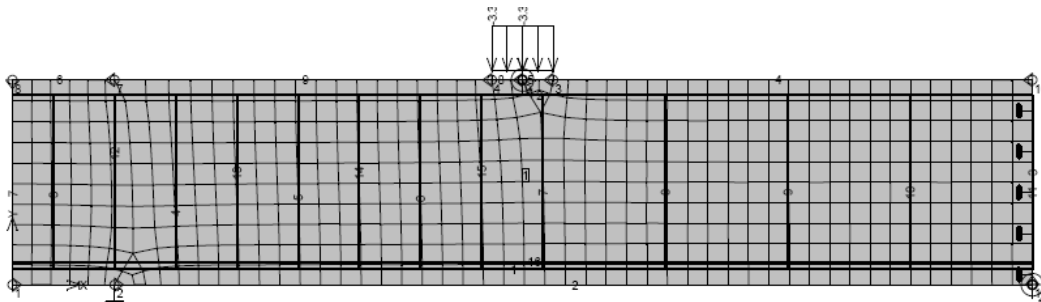


Fig. 5 FEM model of the beams in Atena

### 4. EXPERIMENTAL RESULTS

During concrete cure the shrinkage of concrete beams on top and bottom layer of beams by deformatometer and resistance variation of self-sensing rods were simultaneously measured. Fig. 6 reports recorded electrical resistance variation and measured shrinkage strains in time during concrete beams cure.

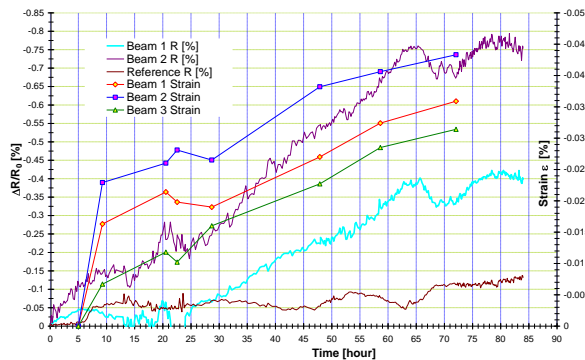


Fig. 6 Strain from shrinkage and variation of electrical resistance during concrete beam cure

The results show that, with the exception of the reference sample that was not inserted into concrete, in the other cases a noticeable negative change of electrical resistance were

recorded, referring of compression stress in reinforcement. Changes in variation trends measured around 24h can be attributed to change of environment moisture, after about 75h the resistance variation is almost constant, indicating decrease intensity of shrinkage process. The changes of electrical resistance had the same trends as strain measurements that indicate good self-sensing properties of the rods.

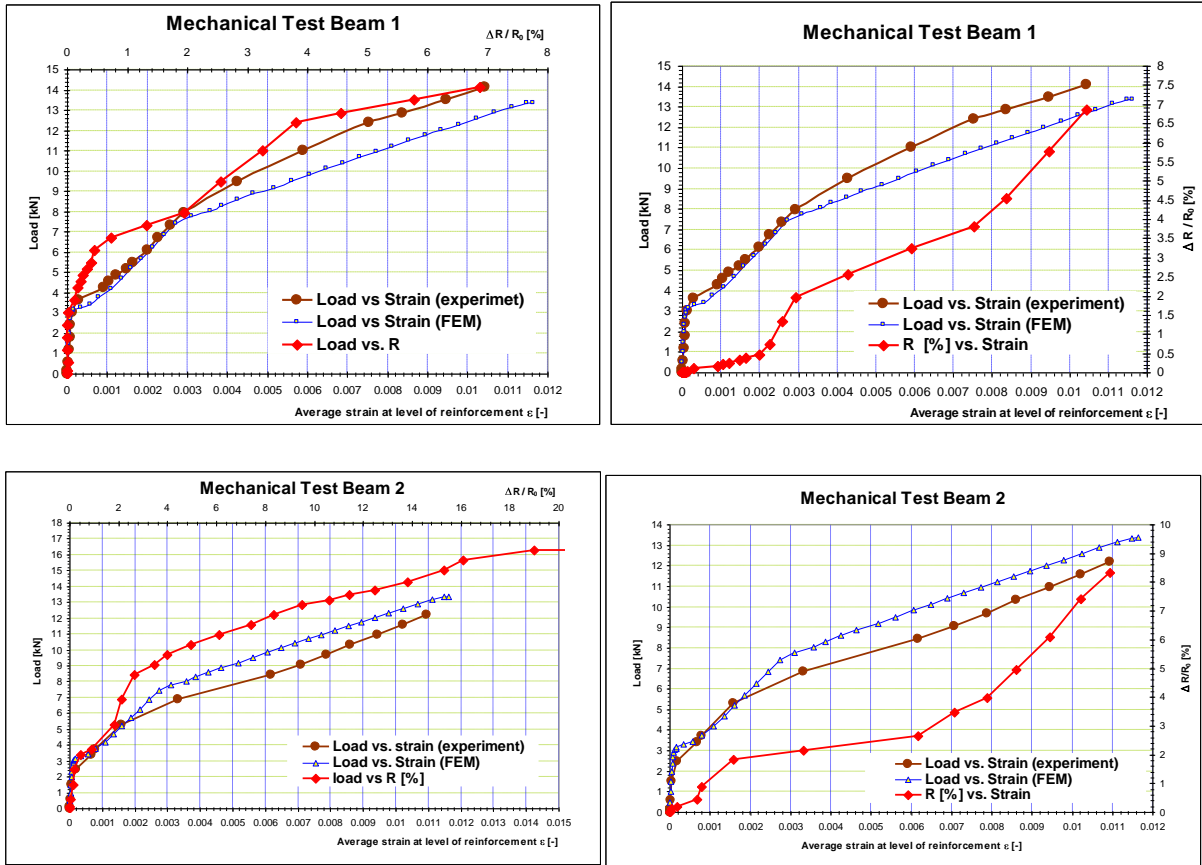


Fig. 7 Variation of resistance of rod and strain in level of reinforcement during mechanical test of beam 1 and beam 2

Fig. 7 reports the electrical resistance variation of the rods and average strain measured at level of reinforcement along entire length of beams during the mechanical test of Beam 1 and Beam 2. Fig. 8 shows the relationship between the load and deflection of tested beams.

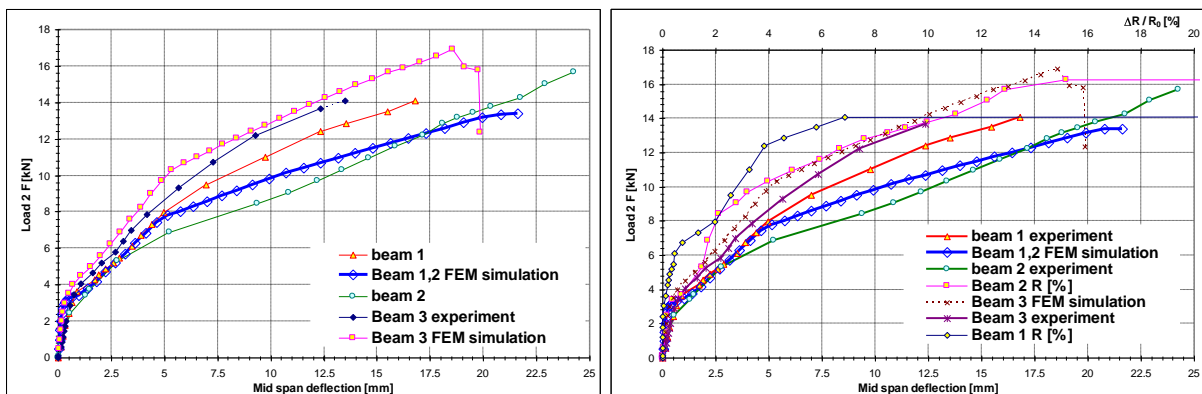


Fig. 8 Mid span deflection for four point static load test



## 5. CONCLUSIONS

The self-monitoring performance of hybrid composite bars is evident in both cases, in measure of shrinkage of concrete and in the mechanical tests. Furthermore, in the case of beam 2 a higher increase of electrical resistance was recorded due to the higher mid-span deflection and also by higher strains at level of reinforcement reached during the test. The self-monitoring function is due to the always increasing separation of carbon particles at increasing strains, which makes the current flow more difficult until, at beams collapse, the material is completely fractured with electrical resistance equal to infinity. The results showed that the proposed rods present very interesting and promising self-sensing properties.

## 6. ACKNOWLEDGEMENTS

This paper is prepared on the base of scientific cooperation supported by COST 534 “New Materials and Systems for prestressed concrete”.

The paper was supported by the Slovak Grant Agency of Ministry of Education of the Slovak Republic and the Slovak Academy of Science (Project No. 1/4201/07).

## 7. REFERENCES

- Ceysson O Risson T Salvia M (1996), “Carbon fibers sensor components for smart materials” *Third ICIM/ECSSM '96, Lyon, France* 136-141
- Muto N Arai Y Shin SG Matsubara H Yanagida H Sugita M Nakatsuji T (2001), “Hybrid Composites with Self-Diagnosing Function for Preventing Fatal Fracture” *Composites Science and Technology* **61** 875-883
- Nad' L., Špernoga B., Bajzecer A. (2006), “Behavior of Concrete Beams reinforced and prestressed with GFRP Bars”. In.: *ICCE – 14<sup>th</sup> Annual International Conference on Composites / Nano Engineering, Boulder, Colorado, USA, July 2006*, on CD
- Nanni F., Gusmano G., Forte G., Auricchio A., Sarchi F., Ramaioli F., (2003), “Italian patent Specification PV2003A000001”
- Nanni F., Ruscito G., Gusmano G. (2007), “Assessment of Self-Diagnosis properties of CPGFRP Nanocomposites for civil application”, ICCST6 22-24 January 2007, Durban, South Africa
- Prabhakaran P (1990), “Damage Assessment through Electrical Resistance Measurements in Graphite Fiber Reinforced Composites Experimental” *Techniques* **14** 16-20
- Schulte K Wittich H (1995), “The electrical response of strained and/or damaged polymer matrix-composite” *10<sup>th</sup> Int. Conf. On Composite Materials Vancouver* **5** 349-357
- Takada M Shin S Matsubara H Yanagida H (1996), “Fracture detection of fiber reinforced composite using electrical conductivity” *The 5th symposium on intelligent materials*
- Wang S Chung DDL (1999), “Interlaminar Interface in Carbon Fiber Polymer Matrix Composites Studied by Contact Electrical Resistivity Measurement” *Composite Interfaces* **6** 497-506

## **PRACTICAL EXPERIENCE OF CFRP APPLICATION FOR EXTERNAL STRENGTHENING OF REINFORCED CONCRETE STRUCTURES**

*Prof., Dr. Andrew A. Shilin, General Director  
Dr. Dmitry V. Kartuzov, Project Manager  
ZAO "Triada-Holding"  
Marshal Zhukov Ave., 6, bldg 2, Moscow, 123308 Russia*

### **SUMMARY**

The report describes a successful experience of using CFRP anchors to restore the bearing capacity of tension bars in brickwork vaults of the world famous historical building– St. Basil's Cathedral (the 16<sup>th</sup> century) in the Red Square in Moscow.

The report reviews the first application of CFRP materials in Russia - strengthening of longitudinal wharf slabs in the port of Novorossiysk (the Black Sea). The concrete cover and structural reinforcement in the bottom section of the slabs had various degrees of deterioration. The repair works were executed with the help of permanent shuttering. CFRP materials were used as structural reinforcement.

### **1. INTRODUCTION – GENERAL APPLICATION RULES**

Starting from 2000 our company – ZAO "Triada-Holding" – has executed successfully quite a number of projects on strengthening of structures with the use of composite materials. Among these there are bridges, overpasses, wharf structures, structural elements (slabs, beams, roof frames). Prior to strengthening structures have to be repaired.

First working stage envisages repair works to restore concrete cover and protect structural steel reinforcement from corrosion using polymer modified cement mortars.

At the second stage the repaired structures are being strengthened with composite materials. The surface of structures is to be cleaned in the areas where strengthening materials are to be glued afterwards. Sandblasting is recommended for the purpose because it helps to open the pore structure of the substrate.

Then the cleaned surface is grinded, the edges are rounded (min. radius of 1-3 cm). The required minimum cohesion of the substrate shall be 1 MPa when strengthening with flexible sheet materials and 1,5 MPa when stiff laminates are used. Finally the surface is vacuum-cleaned to become dust-free.

To avoid stress concentration in carbon-fibre sheets and laminates as well as to provide a uniform distribution of tensile stresses, surface evenness shall be checked with the help of a measuring bar. Minimum admissible deviation shall not exceed 1 mm over the length of 30 cm.

If the mentioned tolerance is not observed, then the surface is to be leveled by applying an epoxy-based mortar with quartz fillers. After the application is finished, there shall be a technical break of 7-12 hours to allow the applied mortar to get cured.



After the substrate is prepared, the time comes to get carbon fibre strips as well as the necessary equipment ready for application.

We worked out the following procedure. A laminate strip is unwound from the roll and placed on a special cutting table. Then it is marked to stretches of a pre-designed length, cut with a disc saw and cleaned with some organic solvent, for example acetone. This not only degrades laminates, but also removes smallest graphite particles from them.

After that the cut and degreased laminate stretches are placed in front of a special epoxy adhesive application device. One can adjust the feeding tray width as well as the passage opening height in this device depending on the laminate width thus providing a uniform application of the adhesive.

The adhesive is mixed using pre-dozed (calculated and weighed) quantities of the components.

Prior to gluing the laminates, the adhesive is applied onto the prepared substrate (layer thickness 1-1.5 mm). Then the first laminate strip is loaded into the glue application device in such a way that its edge protrudes 5-10 mm beyond the glue layer forming plate.

The adhesive is then placed into the application device and distributed evenly over the strip with a trowel. The strip is being pushed forward through the device, the adhesive being added when necessary. It is very important to keep the strip on the same level over the whole length. After the adhesive has been applied, the laminate strips are being placed in the design position either from one end of the structure to the other one or from the middle point of the structure to its ends. Immediately after placement the strips are pressed firmly to the substrate with the help of a hard rubber roller.

While the adhesive is setting (app. 12 hours) the glued strips have to be protected from any possible mechanical damage. In some cases the strips are covered with a special thermal protective coating.

## **2. STRENGTHENING OF ST. BASIL'S CATHEDRAL IN RED SQUARE IN MOSCOW**

One of the most interesting projects implemented by our company was strengthening of the metal tension bars in St. Basil's Cathedral in the Red Square in Moscow. The tension bars were made of wrought rods of rectangular cross-section. After the construction works were completed the bars started to work as part of the Cathedral's cross-tie system (anchoring and load distribution elements). Their ends were anchored into the load-bearing brickwork elements.

Over the time – the Cathedral was built in the middle of the 16<sup>th</sup> century – the tension bars deteriorated due to the metal yield, thermal deformations and corrosion.

It must be said that the tension bars worked actively during the Cathedral's construction because at that stage the walls, columns and diaphragms didn't form yet a single stable support frame for the vaults. Further on, when the Cathedral was built the tension bars worked passively, with minimum or even zero internal stress. However, periodic strains in the vertical load-bearing structures interfered with the relative horizontal displacement of the vaults' and arches' abutments. The vault loads increase as well as changing of the design model of the

building as a whole resulted in the fact that the tension bars started to work actively again, thus giving evidence that the initial equilibrium of the system was upset.

Visual inspection of the tension bars showed that the metal surface was corroded, their cross-section was partially lost; some bars broke in the areas where they had been anchored into the brickwork. To restore the load-bearing capacity of the tension bars it was decided to use CFRP sheets and laminates because metal reinforcement would impair the appearance of the Cathedral generally considered to be a masterpiece of the Russian architecture.

The works were divided into two stages. First, the cross-section of the tension bars was restored. Small laminate pieces were used for the purpose. Their size and cross-section were chosen with regard to the residual strength of the corroded or broken sections of the bars. Prior to gluing the laminate pieces, the bar surface was cleaned back to bright metal and degreased.

At the second stage the tension bars anchorage was to be restored. For this we used special carbon fibre anchors. First the holes were drilled in the brickwork. The holes were cleaned from dust. Each anchor was a combination of a sheet and a laminate, a piece of sheet being glued to a piece of laminate at one end only. Then an epoxy adhesive was injected into the pre-drilled holes. The rigid part of the anchor was placed into the hole whereas the flexible part was glued to the tension bar. Four composite anchors were used for each tension bar (Fig. 1).



Fig.1 Strengthening of metal tension bars in brickwork vaults with carbon fibre anchors, St. Basil's Cathedral, Moscow

### 3. STRENGTHENING IN PORT OF NOVOROSIJSK

Another interesting reference of ZAO "Triada-Holding" was the project in Novorossiysk, the biggest Russian trade port in the Black Sea. The project included repair works and strengthening of one of the wharfs.

Bottom sections of the wharf slabs had various degree of deterioration of their concrete cover as well as reinforcement corrosion. That's why prior to the beginning of the works our specialists conducted a thorough investigation and structural state assessment to be able to analyze the actual values of bending moments from the applied loads in all the wharf spans.

While evaluating the loads to which the structures were subject, we took into account the structural dead weight; the weight of the goods stored there, the weight of the cranes moving along the wharf. While making calculations we had to consider as well that the slabs were keyed together in the longitudinal direction to work as a single plate supported by transverse frames.

Calculations were carried out for various loading combinations (dead weight of the structure + a crane moving along the wharf, dead weight of the structure + a crane standing on the outriggers) as well as for different types of slabs.

The calculations carried out for the damaged sections requiring strengthening, showed that the most critical combination was the one with the crane, when the maximum bending moment in the span amounted to 463 ton-forces per square meter.

For the load combination with the crane, the joint work of slabs connected to form a spatial plate allowed to decrease the maximum impact on the structure (bending moment in a span) by 33% (reduction factor  $K=0.67$ ).

On the basis of the calculations it became clear that to compensate the corrosion wear of the existing reinforcement, it was necessary to strengthen each slab 1375 mm wide with the help of five carbon fibre laminate strips (Fig. 2).

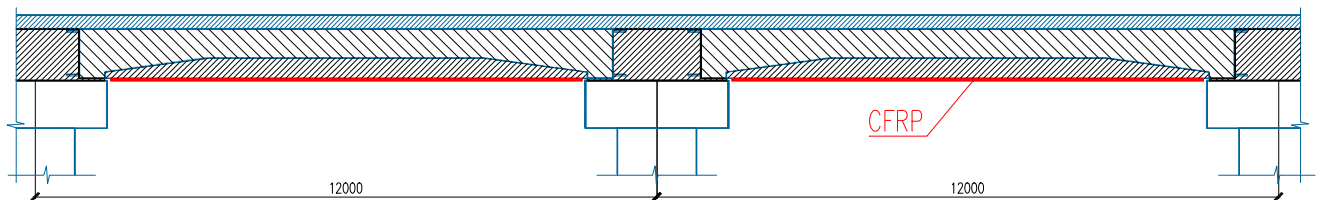


Fig. 2 Strengthening of the wharf slabs with carbon fibre laminates,  
Novorossijsk

Before we could start the strengthening works with the use of prefabricated reinforced concrete slabs, we had to do the repair of the existing wharf slabs as well as concreting of the gaps between them.

First the damaged concrete layer in the bottom section of the slabs was removed with the help of drilling hammers and high-pressure water jets (700 atm). It helped both to remove some 60-80 mm of concrete up to the sound layer and to expose the reinforcement. The reinforcement bars which had lost more than 50% of their cross-section due to corrosion were cut out from the concrete with the help of cutting machines. Then the surface was cleaned with fresh water under the pressure of 200 atm. An impregnating waterproofer was applied onto the cleaned surface. From beneath the holes were drilled in the slabs to install anchors. Then a reinforcing cage was welded to the ends of the installed anchors at the distance of 60-90 mm from the slab surface. Prior to the drilling of injection holes the joints between the slabs were cut to the width of 30-35 mm. This was done from above, from the outer surface of

the wharf slabs. The holes for the subsequent concrete injections were drilled through the joints between the slabs over the whole joint depth. 36 holed were drilled in each span.

Prior to the installation into design position, under the wharf structure, the prefabricated reinforced concrete slabs were strengthened with carbon fibre laminates.

Strengthening procedure included surface preparation (laitance removal, making dust-free, degreasing), gluing of strengthening materials as approved by design, quality control (measuring of concrete surface humidity and temperature as well as ambient temperature), application of a special coating over the glued laminates to protect them from the aggressive marine environment.

After all this being done, the prefabricated reinforced concrete slabs were installed under the wharf structure with the help of specially designed metal jig frames. Besides, special shuttering was placed at the ends of each slab to prevent the injected concrete from pouring out.

The joints between the slabs were filled in with concrete. 36 m<sup>3</sup> of concrete were injected in each span and then vibrated thoroughly.

To provide necessary adhesion between the “fresh” concrete for filling-in the joints and the “old” concrete of the wharf slabs, shrinkage cracks were injected with an epoxy-based grout through the previously placed injection tubes. Injections were carried out after the concrete in the joints gained about 70% of its design strength, i.e. 7-10 days after the placement.

#### **4. CONCLUSIONS**

The experience gained in CFRP strengthening by our company shows that each project has its own peculiarities, specific features; in other words, each project is unique.

To conclude the report, it must be said that at the moment all the strengthened structures are in good operable state, not showing any traces of either deformation or damage.

This allows us to say that the developed technological solutions for repair and strengthening were absolutely correct.



## ANALYTICAL STUDY ON TENSILE STRENGTH OF CURVED FRP REINFORCEMENT

*Thanongsak Imjai\*, Maurizio Guadagnini, Kypros Pilakoutas*  
*Department of Civil & Structural Engineering, University of Sheffield, Sheffield, S1 3JD UK*  
[\\*cip02ti@sheffield.ac.uk](mailto:*cip02ti@sheffield.ac.uk)

### SUMMARY

The use of FRP rebars as internal reinforcements for concrete is limited to specific structural elements and does not yet extend to the whole structure. The reasons for this relate to the limited availability of curved or shaped reinforcing elements on the market and their reduced structural performance. Various studies, in fact, have shown that the mechanical performance of bent portions of composite bars is reduced significantly under a multiaxial combination of stresses and that the tensile strength can be as low as 40% of the maximum tensile strength that can be developed in the straight part. In a significant number of cases, the current design recommendations for concrete structures reinforced with FRP, however, were found to overestimate the bend capacity of FRP rebars. This paper presents and discusses potential constraints relating to the use of curved FRP bars in concrete and proposes an analytical model to predict the ultimate capacity of a bent portion. The proposed model is then validated against test data obtained from specifically designed testing programme as well as tests from the literature.

### 1. INTRODUCTION

When shear demand exceeds the inherent shear capacity of concrete, transverse reinforcement needs to be provided. The presence of transverse reinforcement, most commonly in the form of vertical links, enables the transfer of tensile stresses across inclined shear cracks. Shear reinforcement is mobilised only in the tension zone of a beam and its contribution to shear resistance depends upon the maximum stress that the reinforcement can support. In the case of conventional steel reinforcement, this is equal to the yield stress while with FRP reinforcement, which is linear elastic up to failure, other governing phenomena such as slip and elongation become more relevant. Furthermore, as reported in various studies (Ishihara et al. 1997; Maruyama et al. 1995; Nagasaka et al. 1989), the tensile strength of FRP rods is largely reduced under a combination of tensile and shear stresses. Consequently, if high stresses are developed in the links, failure is expected at the corner anchorages. The reduction in strength that occurs at the corners of FRP bar depends upon radius of the bend, type of composite, bond characteristics and type of anchorage provided (Morphy et al. 1997; Ueda et al. 1995). Nakamura and Higai (1995) conducted a theoretical study on the bend capacity of FRP stirrups based on test results from Miyata et al. (1989). As a result of their study, the authors proposed an analytical model able to predict the strength of bent FRP composites as shown in Eq. (1)

$$\frac{\sigma_b}{\sigma_{1\max}} = \frac{r}{d} \ln \left( 1 + \frac{d}{r} \right) \quad (1)$$

in which  $\sigma_b$  is the ultimate strength of the bend,  $\sigma_{1\max}$  is the ultimate strength parallel to the fibres,  $r$  is the bend radius, and  $d$  is the nominal diameter of the bars. A similar study was

carried out at Hokkaido University by Ishihara et al. (1997). Building upon the finding of a previous work by Ueda et al. (1995), a 2-D finite element analysis was implemented to analyse the behaviour of a bent FRP stirrup embedded in concrete. The results of the study showed that the strength of a bar at its bent portion increases directly with the radius of the bend. Based on a finite element parametric study, Eq. 2 was proposed to predict the strength of the bent portion.

$$\frac{\sigma_b}{\sigma_{1\max}} = \frac{1}{\lambda} \ln \left( 1 + \lambda \right) \quad (2)$$

where  $\ln \lambda = 0.90 + 0.73 \ln(d/r)$

From the comparison between Eq. 1 and Eq. 2, it can be noticed that Eq. 1 is a special case of Eq. 2 in which  $\lambda$  is  $d/r$ . Furthermore, the study by Ishihara et al. showed that the reduction in bend strength was also a function of the different types of FRP composites. The authors suggested that bond characteristics and differential slippage of the FRP rod, which were not considered in this analysis, could play an important role in the strength reduction. From the analysis of the current design guidelines for reinforced concrete structures with fibre reinforced polymers, it is evident that the issue related to the use of curved FRP reinforcing elements have not been addressed in detail. All of the current existing recommendations regarding the behaviour of bent reinforcement (e.g. ACI (2006)) are based on the work done by the Japanese and included in the JSCE document. The reduction in strength that occurs at the corners of a FRP bar is hence quantified using the empirical model proposed by the Japanese Society of Civil Engineers (1997) described by Eq. 3. In this equation, the strength of the bent portion,  $\sigma_b$ , is expressed solely as a function of the uniaxial tensile strength of the composite,  $\sigma_{1\max}$ , and the bar geometry (i.e. bar diameter,  $d$ , and bend radius,  $r$ ).

$$\sigma_b = \left( \alpha \frac{r}{d} + 0.3 \right) \sigma_{1\max} \leq \sigma_{1\max} \quad (3)$$

The value of  $\alpha = 0.05$  corresponds to a 95% confidence limit, whilst  $\alpha = 0.092$  corresponds to a 50% confidence limit. Eq. 3 yields generally a conservative estimate of the maximum strength that can be developed in bent bars.

## 2. A MACROMECHANICAL FAILURE BASED MODEL

In this study, an attempt was made to develop an analytical model to predict the bend capacity of FRP composites. It is proposed that an analytical model based on macromechanical principles could adequately capture the true degradation of the strength of bent composites. When a reinforcing bent bar is embedded in a concrete element and is subjected to internal forces, the distribution of internal stresses along the element will depend upon the bond characteristics between concrete and reinforcement and the geometry of the reinforcement. If, for example, a corner portion of a shear stirrup is considered, the average stresses acting on the bent portion of the link, ignoring bond stresses, can be represented as shown in Fig. 1.

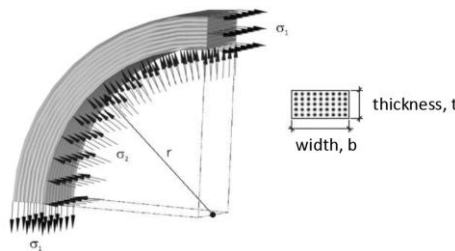


Fig. 1 Average stresses acting on a bent portion of reinforcement embedded in concrete

For the sake of simplicity, a uniform (equivalent hydrostatic) pressure is considered to be exerted by the concrete along the bent portion. The equilibrium of the rigid body may be expressed as

$$\sigma_{1.t.b} = \sigma_{2.r.b} \quad (4)$$

$$\text{or } \sigma_2 = \frac{\sigma_1 \cdot t}{r} \quad (5)$$

in which  $\sigma_1$  is the tensile stress developed in the straight bar,  $\sigma_2$  is the compressive stress applied by the confined concrete perpendicular to the fibres,  $r$  is the internal bending radius, and  $b$  and  $t$  are the width and thickness of the bar, respectively.

The proposed model adopts the Tsai-Hill failure criterion (Taranu and Isopescu 1996) for a unidirectional orthotropic lamina with fibres in the 1-direction and subjected to plane stress in the 1-2 plane (Eq. 6). As with all failure criteria for composites, this criterion regards the material as homogeneous. Accordingly, the model cannot account for failure mechanisms that occur at a microscopic level such as those due to fibre misalignment, fibre kinking or variation in the volume fraction.

$$\frac{\sigma_1^2}{\sigma_{1max}^2} - \frac{\sigma_1\sigma_2}{\sigma_{1max}^2} + \frac{\sigma_2^2}{\sigma_{2max}^2} + \frac{\tau_{12}^2}{\tau_{2max}^2} = 1 \quad (6)$$

in which  $\sigma_{1max}$  is the longitudinal tensile strength,  $\sigma_{2max}$  is the transverse tensile strength, and  $\tau_{max}$  is the in-plane shear strength. Substituting Eq. 5 into Eq. 6 for the case illustrated in Fig. 1 and rearranging, the ratio between the maximum stress that can be sustained along the bend of the composites,  $\sigma_1$ , and its unidirectional tensile strength,  $\sigma_{1max}$ , can be written in the following form (Eq. 7).

$$\frac{\sigma_1}{\sigma_{1max}} = \frac{\sqrt{1-\varphi^2}}{\sqrt{1 + \left(\frac{t}{r}\right) + \left(\frac{t}{r}\right)^2 \beta^2}} \quad (7)$$

in which  $\varphi = \tau_{12}/\tau_{max}$  and  $\beta = \sigma_{1max}/\sigma_{2max}$ . Eq (7) was derived assuming a composite bar with a rectangular cross-section. If a round bar is used, the factor  $\pi d/4$  replaces the bar thickness,  $t$ , as shown in Eq (8).

$$\frac{\sigma_1}{\sigma_{1max}} = \frac{\sqrt{1-\varphi^2}}{\sqrt{1 + \left(\frac{\pi d}{4r}\right) + \left(\frac{\pi d}{4r}\right)^2 \beta^2}} \quad (8)$$

The factor  $\varphi$  is the ratio between the shear stress,  $\tau_{12}$ , and the maximum shear strength,  $\tau_{max}$ . The maximum shear strength is equal to the interlaminar shear strength of the unidirectional composite. In general,  $\tau_{max}$  is much higher than the developed bond stress in concrete and it is not likely that interlaminar shear failure will occur. For a bent unidirectional composite subjected to tensile loading as shown in Fig. 1, the value of  $\varphi$  is very small (not more than 0.2) and can be neglected when determining the bend capacity of the material (Imjai et al. 2007a). Another important parameter included in the proposed macromechanical model is the factor  $\beta$ . This factor is the ratio of the longitudinal tensile strength,  $\sigma_{1max}$ , and transverse compressive strength,  $\sigma_{2max}$ , of the composite material. Fig. 2-right shows the effect of  $\beta$  on



the bend capacity of the composite. It can be seen that the strength of a bent unidirectional composites increases with increasing values of  $\beta$ , i.e. higher values of  $\sigma_{2max}$ .

The transverse compressive strength of the composites considered in this study, which was then used to validate the value of  $\beta$  in the proposed model was determined from direct compression tests on 10 mm cube specimens. The transverse compressive strength ( $\sigma_{2max}$ ) of the thermoplastic composite obtained from the tests was found to be 96 MPa (Imjai et al. 2007b), yielding a calculated  $\beta$  value of 7.5.

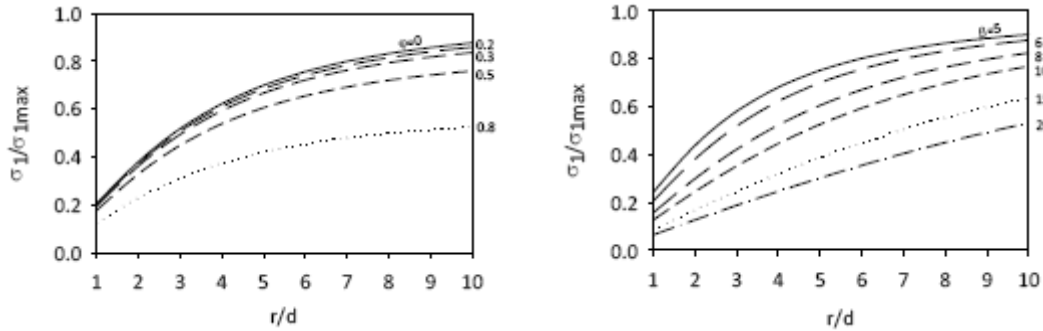


Fig. 2 Effects of factor  $\phi$  (left) and factor  $\beta$  (right) on the bend capacity

### 3. VERIFICATION OF THE PROPOSED MODEL

#### 3. 1 Bent test data by Imjai et al. (2006)

As part of the Curved NFRP Project (2003), a series of pullout tests on curved thermoplastic composite strips was carried out by the authors. In the experimental testing programme, a total of 47 specimens and 19 configurations were tested. A comparison of the test results from this study and analytical results derived according to the predictive models discussed above, as well as the newly proposed model, are shown in Fig. 3.

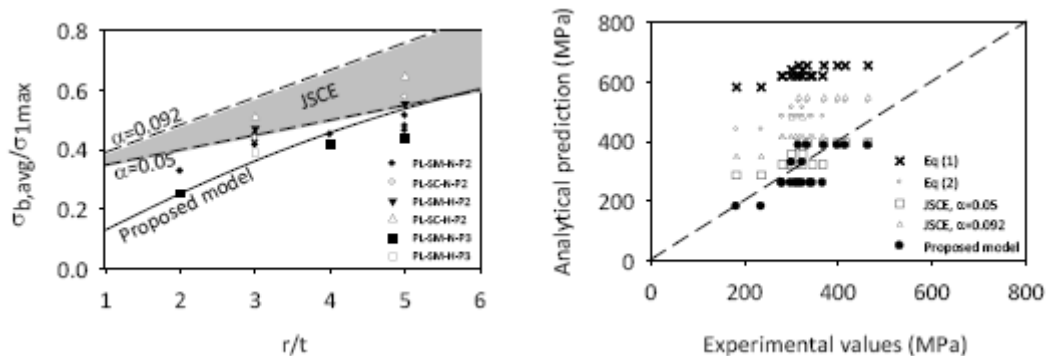


Fig. 3 Analytical predictions of bend capacity of thermoplastic strips according to the JSCE and proposed models

Fig. 3-left shows a comparison of the predicted bend capacity in terms of the average failure stress to the ultimate strength of the straight section ( $\sigma_{b,avg}/\sigma_{1max}$ ) calculated by the macromechanical based model. The value of  $\sigma_{2max}$  obtained from the tests was used here. The macromechanical based model adequately captures the variation of the bend capacity with the variation of the bending radius to bar diameter ratio. In some cases, the capacity predicted by the proposed model was found to overestimate the test results, especially when compared to specimens P3 (unbonded). This reveals that the development of bond stresses along the

bar/concrete interface plays an important role in controlling the maximum capacity that can be carried through the bent portion. Nevertheless, the predictions obtained according to the macromechanical model provide a lower bound solution, particularly when bonded specimens were used. As shown in Fig. 3-right, the bend capacity predicted by existing equations available in the literature do not agree well with the variation in the test data. It can be seen that, in a number of cases, those equations were found to overestimate the bend capacity of the composites used in the present study.

### 3. 2 Bent test data by Yang et al. (2004)

A series of tests to investigate the reduction in strength at bent corners of lamina composites was carried out by Yang et al. (2004). In their experimental programme, high strength carbon sheets were produced by the manual lay-up process using a two-part epoxy over interchangeable corner inserts. The models discussed above were tested against this set of data (Fig. 4). It can be seen that the predictions obtained according to the proposed model (Eq 6) agree well with the experimental results. A value of the ultimate tensile strength of the composite as indicated by the manufacturer was used in this analysis. An adopted  $\beta$  value of 22 was used for this set of data based on the analysis of optimum values that provided the best fit of the proposed model to the test data. The transverse compressive strength calculated according to this value of  $\beta$  was found to be 246 Mpa, which lies within the typical range for the carbon/epoxy composites, i.e 150-250 (Hollaway 1993). As seen in Fig. 4, the predictions from the various analytical models tend to overestimate the test. In addition, the predictions obtained according to the macromechanical model proposed here show a better agreement with the test data compared to other models.

Fig. 4 Performance of various models against test data from Yang et al. (2004)

## 4. CONCLUSIONS

The macromechanical failure based model that is proposed adequately captures strength degradation due to the change in geometry of the bent portion of the FRP bar. In a significant number of cases, the equations included in the literature for predicting the capacity of curved FRP composites was found to overestimate the capacity of the composites used in this study whilst the proposed model show a good agreement with the test results. Moreover, the capacity of the bent FRP specimens does not vary linearly with  $r/d$  ratio. Nor does it appear to be solely a function of the bending geometry. Rather, bond characteristics appeared to be important in controlling the development of stresses along the embedded portion of the composite as well as in dictating its ultimate behaviour.

## 5. ACKNOWLEDGMENTS

The author wishes to acknowledge the financial assistance of the European Union for the Marie Curie Research Training Network En-Core, and the CRAFT RTD project CurvedNFR.

## 6. REFERENCES

- American Concrete Institute (ACI). (2006). "Guide for the Design and Construction of Concrete Reinforced with FRP Bars, ACI 440.1R-06." *American Concrete Institution*, Farmington Hills, MI, USA. .
- CurvedNFR. (2003). "Cost effective Curved Polymer Composite Rebar." CRAFT RTD European funded project, CRAFT GIST-CT-2002-50365, <http://www.curvednfr.com/>.

- Hollaway, L. (1993). *Polymer composites for Civil and Structural Engineering*, Blackie Academic & Professional, Glasgow.
- Imjai, T., Guadagnini, M., and Pilakoutas, K. (2006). "Pull-out Tests on Bent FRP Bars. Experimental Testing Programme." *Ref. Report No ExpR5*, Centre for Cement and Concrete, The University of Sheffield, Sheffield, UK, 32 pp.
- Imjai, T., Guadagnini, M., and Pilakoutas, K. (2007a). "Pullout Tests on Plytron Thermoplastic Strips. Experimental Testing Programme." *Ref. Report No TR-FRP-07-02*, Centre for Cement and Concrete, The University of Sheffield, Sheffield, UK, 15 pp.
- Imjai, T., Guadagnini, M., and Pilakoutas, K. (2007b). "Uniaxial Compression Tests on Plytron and Aslan 100 Composites. Experimental Testing Programme." *Ref. Report No TR-FRP-07-01*, Centre for Cement and Concrete, The University of Sheffield, Sheffield, UK, 9 pp.
- Ishihara, K., Obara, T., Sato, Y., and Kakuta, Y. "Evaluation of Ultimate Strength of FRP Rods at Bent-up Portion." *In 3rd International Symposium on Non-Metallic (FRP) Reinforcement for Concrete Structures*, Sapporo, Japan, 27-34.
- Japan Society of Civil Engineers (JSCE). (1997). "Recommendation for Design and Construction of Concrete Structures using Continuous Fiber Reinforcing Materials." Tokyo, Japan.
- Maruyama, T., Honma, M., and Okamura, H. "Experimental Study on Tensile Strength of Bent Portion of FRP Rods." *Non-Metallic (FRP) Reinforcement for Concrete Structures. Proceeding of 2nd RILEM symposium (FRPRCS-2)*, 163-176.
- Miyata, S., Tottori, S., Terada, T., and Sekijima, K. (1989). "Experimental Study on Tensile Strength of FRP Bent Bar." *Transactions of The Japanese Concrete Institute*, 11, 185-191.
- Morphy, R., Sheata, E., and Rizkalla, S. "Bent Effect on Strength of CFRP Stirrups." *In 3rd International Symposium on Non-Metallic (FRP) Reinforcement for Concrete Structures*, Sapporo, Japan, 19-26.
- Nagasaka, T., Fukuyama, H., and Tanigaki, M. (1989). "Shear Performance of Concrete Beam Reinforced with FRP Stirrups." *Transactions of The Japanese Concrete Institute*, 11, 789-811.
- Nakamura, H., and Higai, I. (1995). "Evaluation of Shear Strength on Concrete Beams Reinforced with FRP." *Concrete Library, JSCE*, 26, 111-123.
- Taranu, N., and Isopescu, D. (1996). *Structures made of Composite Materials*, Editura Vesper, Romania.
- Ueda, T., Sato, Y., Kakuta, Y., Imamura, A., and Kanematsu, H. "Failure Criteria for FRP rods Subjected to a Combination of Tensile and Shear Forces." *Non-Metallic (FRP) Reinforcement for Concrete Structures. Proceeding of 2nd RILEM symposium (FRPRCS-2)*, 26-33.
- Yang, X., Wei, J., Nanni, A., and Dharani, L. R. (2004). "Shape Effect on the Performance of Carbon Fiber Reinforced Polymer Wraps." *Journal of Composites for Construction, ASCE*, 8(5), 444-451.

## BEHAVIOUR OF NEAR SURFACE MOUNTED FIBRE REINFORCED STRENGTHENINGS

Zsombor K. Szabó<sup>1</sup>, György L. Balázs<sup>1</sup>

<sup>1</sup>*Department of Construction Materials and Engineering Geology,  
Budapest University of Technology and Economics, 1521 Budapest, Hungary*

### SUMMARY

Strengthening of structures is a complex task. We can choose from various available strengthening solutions. However, in order to utilize both the strengthening and the base materials in the most efficient way an extensive knowledge of each strengthening solution is needed. Use of fibre reinforced polymer (FRP) materials for structural strengthening is an advanced novel technique, the FRP s are able to transfer considerably high stresses, therefore, special care is needed during design and application.

More detailed presentation will be given on the so called near surface mounted (NSM) fibre reinforced polymer application. Near surface mounting consist in application of FRP reinforcement in grooves pre-cut into the concrete cover. In NSM applications the strengthening reinforcement becomes more integral part of the element compared to externally bonded applications. The so developed larger bond surface induces better anchorage capacity, therefore a higher percentage of the FRP tensile strength can be mobilized, it also provides higher resistance against the unfavourable peeling-off failure. Previous experiments showed improved ductility with preferable composite action and ultimate load more independent from the near surface concrete tensile strength. Better protection against freeze/thaw cycles, elevated temperatures, fire, ultraviolet rays and local actions are also of importance.

In order to investigate the applicability and bond behaviour of FRP in NSM applications we developed an advanced pull-out test setup. Studied test variables were concrete grade, type of FRP reinforcement, FRP bond length and groove size.

### 1. INTRODUCTION

Increasing requirements for existing concrete structures need enhanced strengthening methods. In the last two decades fibre reinforced polymer (FRP) materials have emerged as promising alternative repair materials due to several advantages of FRP strengthening. However, it is important to have sufficient knowledge on behaviour and applicability of different FRP materials and techniques. FRP reinforcements are available in form of precured shapes made by pultrusion, or in the form of fabrics with fibres in one or multiple directions used in externally bonding wet lay-up technique. Carbon (C), glass (G) and aramid (A) are the largely used fibres which compose the fibrous phase of these reinforcements. The fibres are bonded together by usually epoxy matrix.

FRP materials can be bonded to the exterior of concrete structures (Fig. 1) using high strength adhesives to provide additional reinforcement to the available internal reinforcing (fib, 2001). In addition to external bonding, the FRP reinforcements can be inserted into grooves cut into

the structural members in an application called generally near surface mounting (NSM). Near surface mounting technique has many advantages vs. externally bonding technique (EBR): (i) larger bond surface induces better anchorage capacity, (ii) it provides higher resistance against peeling-off, so a higher percentage of the tensile strength can be mobilized, (iii) no preparation work is needed other than grooving, therefore reduced application time will be required (Cruz, Barros, 2002; Nanni, 2003). The surrounding concrete protects the FRP reinforcement against mechanical influences, due to the special mounting setup, therefore, this technique is attractive for strengthening also in the negative moment region. The NSM strengthening has an improved protection against freeze/thaw cycles, elevated temperatures, fire, ultraviolet rays and vandalism. Previous experiments (Cruz, Barros, 2002; Kotynia, 2005) showed also an improved ductility, preferable composite action, and an ultimate load development more independent from concrete surface tensile strength than in case of EBR reinforcements. The cross sectional properties of FRP reinforcement influence bond characteristics and ultimate load capacity of the strengthened member. Therefore, we need to distinguish from geometrical point of view three main groups of reinforcement: (1) the circular cross sectional (bars) and the rectangular cross sectional ones (2) with large (strips) and (3) small aspect ratio (rectangular bars).

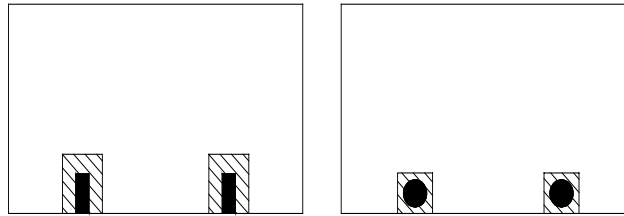


Fig. 1 Near surface mounted FRP, rectangular shapes and rods

In NSM applications the groove filler adhesive enables proper stress transfer between the FRP reinforcement and concrete. The most relevant mechanical properties (de Lorenzis, 2007) of groove filler are tensile and shear strengths. The tensile strength is especially important in case of round bars which can induce high circumferential tensile stresses in the adhesive (de Lorenzis, Rizzo, la Tegola, 2002). The shear strength is especially important when the bond is controlled by cohesive shear failure of the adhesive. The best performing groove filler adhesive is a two-component epoxy adhesive. Its material properties are strongly depending on time and temperature and influence long-term structural behaviour of prestressed near surface mounted carbon FRP strips in service (Nordin, Täljsten, 2006). Cement based adhesives can be used but with limitations.

## 2. PREVIOUS PULL-OUT TESTS

Pull-out test can be used to determine bond capacities and concrete splitting resistance along the reinforcement (Tepfers, 2004). Considering the variety of commercially available FRP rods and strips, the available experimental results are rather limited for characterization of NSM reinforcement bond capacities (Novidis, Pantazopoulou, Tentolouris, 2007).

### 2.1 Pull-out tests on C shaped specimens

The first published pull-out tests were de Lorenzis, Rizzo and la Tegola's (2002) modified pull-out tests on C-shaped concrete blocks. Their specimen offers the advantage of direct pull-out test, with minimized eccentricity, possibility to conduct the test in slip-control mode, to measure both loaded-end and free-end slips, and also enables visual access to the test zone

during loading. Test variables were: type of FRP bar, groove filling material (cement or epoxy), bond length and groove size. A typical bond stress slip curve shows a steep ascending branch and a peak followed by sudden release.

## **2.2 Eccentric pull-out test**

In experiments by Novidis, Pantazopoulou, Tentolouris (2007) 24 specimens were tested using a modified version of the conventional eccentric pullout test setup. In the experiment 12 mm CFRP bars with sandblasted surface and helical indentations were used. Investigated test variables were bond length and groove size and the passive confinement effect of an externally bonded CFRP jacket. Characteristic interfacial failure surfaces were recorded namely failure at reinforcement adhesive and at adhesive concrete interface. Influence of failure modes on ultimate load development was shown. Increasing groove size led to higher average bond strength. Average bond strength decreased while the bond length increased showing a non-uniform distribution of the bond stresses along the bond length.

## **3. ADVANCED PULL OUT-TEST FOR NSM CFRP STRIPS**

In the previous chapter pull-out tests with NSM circular rods were presented. Correspondingly, pull-out tests for FRP strips are needed to describe therein specific bond stress development. Experimental evaluation of strengthenings using FRP strips in NSM application are available in the literature (Sena-Cruz, Baross, 2002; Blaschko 2003; Hassan, Rizkalla 2003; Sena-Cruz, Baross, 2004; El-Hacha, Rizkalla 2004; Teng et al., 2006). The herein presented advanced pull-out test (Fig. 2) has some advantages compared to the beam pull-out tests presented by Sena-Cruz and Baross (2004). First, the FRP strip can be loaded with minimized eccentricity in a displacement controlled mode. In addition to it the relative displacement of FRP strip and pull-out load can be directly measured on the loaded and unloaded side with a proper visual access to the failure surface.

### **3.1 Test materials**

#### **Concrete**

The concrete specimen was designed in order to reduce eccentricities during loading. Especially in case of FRP strips the bond on lateral surfaces can be influenced considerably by the lateral confining stresses induced by frictional stresses developed at supporting planes. Therefore, the bond length will be shifted to the unloaded side of specimen. With one concrete mix 4 pull-out specimens and three control specimens were prepared. The concrete specimens were kept for 7 day under water then in laboratory conditions and tested at an age of at least 28 days. The concrete strength was verified using control specimens (Cubes of 150 mm sides) tested at the same day with the corresponding pull-out specimens. The concrete used was a middle grade concrete often used for reinforced concrete structural elements. Experiments showing the influence of concrete grade on bond stress will be available in future publications.

#### **Fibre reinforced polymer and adhesive**

For present tests, CFRP strips of medium modulus of elasticity were used. The FRP strips had a smooth surface without any surface deformations. With regards to the commonly used concrete cover thickness (25 mm), 20 mm wide strips with 1.4 mm thickness were used. According to the producer the CFRP strips have a mean modulus of elasticity 210000 N/mm<sup>2</sup>,

a mean value of tensile strength  $3200 \text{ N/mm}^2$  and a strain at failure higher than 1.35%. The adhesive used was a two-component epoxy adhesive recommended by the producer for this CFRP strips (in case of externally bonding application) with modulus of elasticity of  $12800 \text{ N/mm}^2$ .

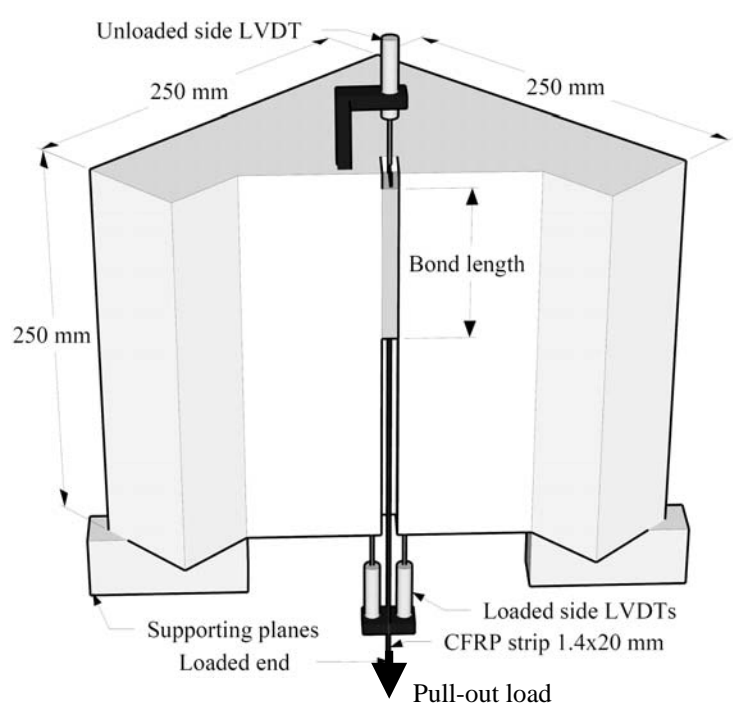


Fig. 2 Advanced pull-out tests setup used for present test for NSM reinforcement

### 3.2 FRP reinforcement application

The grooves were cut on the concrete specimens, using a two diamond blade cutting device. The strips were bonded to the concrete at the age of minimum 21 days. The adhesive was applied both on the surface of the strengthening strip and in the groove by filling it halfway. The adhesive in excess was removed and the surface levelled. The specimens were kept for at least 3 day in laboratory conditions prior to loading.

### 3.3 Test variables

The herein presented pilot test series had two variables: bond length and groove width. These variables can be expressed as multiple of the test strip thickness for general comparison. Bond length of 35 (50 mm), 70 (100 mm) and 105 (150 mm) strip thickness were used. The groove width was approximately three (5 mm), four (6mm) and six (9 mm) strip thicknesses.

## 4. EXPERIMENTAL OBSERVATIONS

In the first series of our tests, 12 pull-out specimens were tested. The purpose of the first series was to verify if the test setup is appropriate for pull-out tests. In the second test series the effect of bond length on average bond stress was investigated on 12 pull-out specimens.

### 4.1 Failure modes

Characteristic failure modes for the NSM fiber reinforced strips were recorded. Interfacial failure modes at adhesive FRP interface developed in two modes, as a pure interfacial failure

or as a cohesive shear failure in the adhesive (Fig. 3). The cohesive shear failure mode proves that the used adhesive and the preparation of the bonding surfaces are appropriate for this kind of applications.

Two different concrete cracking failures were observed. In most cases the concrete cracks near the adhesive surface a thin layer of concrete remains on the adhesive. On specimens with the bond length and free displacement on the loaded site, a conical failure surface was recorded with intense crack distribution in the concrete.



Fig. 3 Cohesive shear failure at FRP and adhesive interface

## 4.2 Bond behaviour

During the tests some specific influencing parameters of bond capacities were recorded similar to the ones presented in other publications.

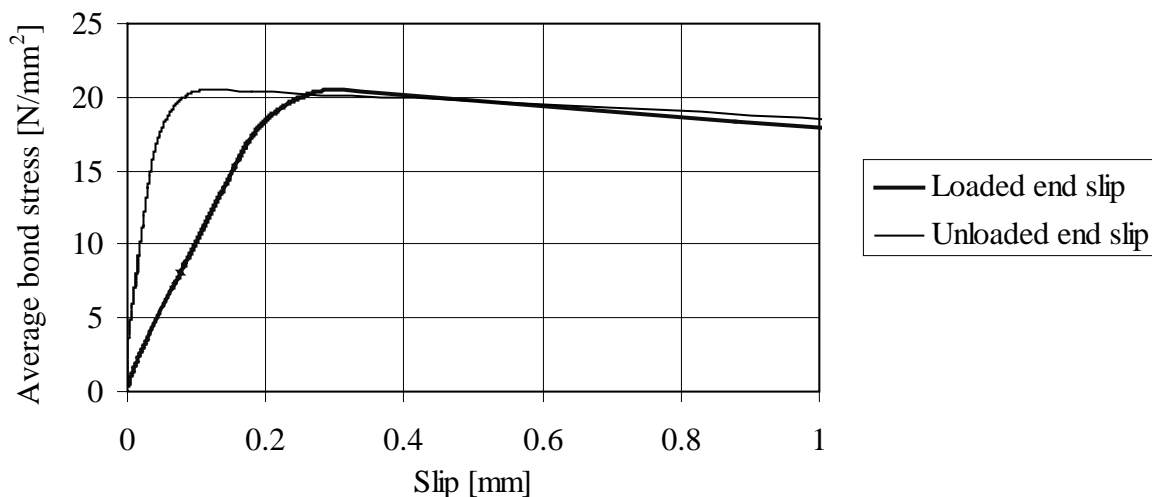


Fig. 4 Average bond stress – relative displacement diagram for bond length of 25 strip thickness (35 mm) and groove width 5 mm

The highest average bond stress (Fig. 4) was recorded on specimens with the shortest bond length (25 strip thickness) proving the non linear development of the bond stress. The groove width had also an influence on the bond stress. Higher groove widths lead to higher failure loads with higher average bond stress. At specimens with bond length of 105 strip thickness increasing the groove width from 6 mm the 9 mm resulted in an average bond strength increase from 7 N/mm<sup>2</sup> to 8 N/mm<sup>2</sup>. The most important observation is the measured difference between loaded end and unloaded end slip. By decreasing the bond length the difference between loaded and unloaded end slip increased.

## 5. CONCLUSIONS

Considering the variety of commercially available FRP rods and strips, the available experimental results are rather limited for characterization of bond capacities of NSM



reinforcement. Pull-out test results are needed in order to describe behaviour of near surface mounted reinforcements. Therefore, an advanced pull-out test setup was developed.

In the pilot test series typical bond stress development and failure modes were recorded for the used FRP strips. The highest average bond stress was recorded on specimens with the shortest bond length proving once again the non linear development of the bond stress. The average bond strength increased with the increase of the groove width, and decreased with increasing bond length. The most important conclusion is that the new developed pull-out specimens can be used economically to evaluate bond capacities of near surface mounted (NSM) with fibre reinforced polymer (FRP) strips.

## 6. ACKNOWLEDGEMENTS

Authors gratefully acknowledge the financial support of EN-CORE Research Training Network FP6 project (Grant: MRTN-CT-2004-512397).

## 7. REFERENCES

- Blaschko M. (2003), "Bond behaviour of CFRP strips glued into slits", *Proceedings of FRPRCS-6*, Singapore (ed. Kiang Hwee Tan).
- Cruz, J.M.S., Barros, J.A.O. (2002), "Bond behavior of carbon laminates strips into concrete by pullout-bending tests", *Proceeding for Bond in concrete-from research to standards*, Budapest (eds. Balázs, G.L., Bartos, P.J.M., Cairns, J., Borosnyói, A.), pp. 614-622.
- fib (2001), "Externally bonded FRP reinforcement for RC structures", *fib bulletin 14*.
- Hassan T., Rizkalla S. (2003), "Investigation of Bond in concrete structures strengthened with near surface mounted carbon fibre reinforced polymer strips", *Journal of composites for constructions*, Vol. 7, No. 3, pp. 92-105.
- Kotynia, R. (2005), "Strain efficiency of near-surface mounted CFRP-strengthened reinforced concrete beams", *Proceedings of Third international conference composites in construction*, Lyon (eds. Hamelin P. Bigaud, D., Ferrier, E., Jacquelin, E.), pp. 35-42.
- de Lorenzis, L., Rizzo, A., la Tegola, A. (2002), "Modified pull-out test for bond of near-surface mounted FRP rods in concrete", *Composites: Part B, Engineering*, Vol 33, pp. 589-603.
- Nanni, A. (2003), "North American design guidelines for concrete reinforcement and strengthening using FRP: principles, applications and unresolved issues", *Construction and Building Materials*, Vol 17, pp. 439-446.
- Nordin, H., Täljsten, B (2006), "Concrete beams strengthened with prestressed near surface mounted CFRP", *Journal of Composite for Construction*, Vol. 10, pp. 60-68.
- Novidis D., Pantazopoulou S. J., Tentolouris E. (2007), "Experimental study of bond of NSM-FRP reinforcement", *Construction and Building Materials*, Vol. 21, pp 1760-1770.
- Teng J. G., de Lorenzis L., Wang Bo, Li Rong, Wong T. N., Lam Lik (2006), "Debonding failures of RC beams strengthened with near surface mounted CFRP Strips", *Journal of Composites for Construction*, Vol. 10, No 2, pp. 92-105.
- Tepfers R. (2004), "Bond clause proposal for FRP-bars/rods in concrete based on CEB/Fip Model Code 90 with discussion of needed tests", *Chalmers University of Technology, Report 04:2*, Göteborg.

## BEAM PULL OUT TESTS OF NSM – FRP AND STEEL BARS IN CONCRETE

*D. G. Novidis and S. J. Pantazopoulou*

*Department of Civil Engineering, Demokritus University of Thrace*

*Phone: +3025410-79639, address: Vas. Sofias #12A, Xanthi 67100, Greece*

*Emails: dnovidis@civil.duth.gr, pantaz@civil.duth.gr*

### SUMMARY

This paper describes an experimental investigation regarding a relatively new strengthening method of flexural concrete members, known as NSM technology (near-surface mounting), (de Lorenzis and Nanni, 2001). The study included fourteen simply supported concrete beams, strengthened by placing either steel or carbon FRP bars in grooves cut on the tension face of the member and bonding with epoxy paste; specimens were loaded in bending till the occurrence of failure by debonding. Nine of the specimens were fabricated to have the bar fully bonded in one half-span, whereas the bonded length in the other half span of the typical member was limited. The bonded length was a parameter of study in the investigation. NSM bars were fully bonded in the case of the remaining five specimens. An objective of this experimental research was to examine the bond strength of the NSM method using realistic stress field conditions (beam pullout tests rather than standard pullout) while at the same time obtaining test results for comparison with those of the direct pull out tests. From the experimental evidence it is concluded that flexural curvature, which occurs in the beam-type tests, has a significant effect on the mode of failure of the upgraded system, the strength of the failure interface, with a magnitude that depends strongly on the mechanical properties and the surface pattern of the bar. As the height of surface deformations of the bar increase the failure mode stabilizes to the same pattern observed in standard pullout tests (failure at the epoxy-concrete interface). In this case, bond strength obtained from the beam tests is in general greater than the respective value recorded from direct pull out tests. This increase is attributed to the additional friction generated on the bar and on the epoxy filler's lateral surface owing to curvature compatibility between the bar and the surrounding concrete in the bending beam.

### 1. INTRODUCTION

The NSM strengthening method has gained renewed interest recently, with the advent of advanced composite materials which made possible solutions for strength increase without the susceptibility to corrosion, in reinforced concrete structures with diagnosed flexural strength deficiencies (e.g. slabs or beams with corroded primary reinforcement, increase of design loads etc). This option was explored as an alternative to the well known EBR (Externally Bonded Reinforcement) technique, whereby strength and failure are almost always limited by premature debonding in the ends of the attached reinforcement owing to the low tensile strength of the concrete cover (Oehlers and Moran, 1990), (Malek et al, 1998) and (Novidis and Pantazopoulou, 2007). Once placed in longitudinal surface grooves (cut in the cover of the member that requires strengthening) and surrounded by the hardened epoxy filler, the bars are subjected to compatible displacement conditions with the surrounding concrete, as occurs with the existing embedded reinforcement. Because they are generally located outside the embedded stirrups (in actual concrete members of a structure), bond and development capacity are critical parameters in determining their effectiveness as added primary reinforcement and in securing composite action with the existing member. Bond also determines the strength and the eventual failure mode of the upgraded member. In this regard, bond strength is controlled entirely by the surface characteristics and bar stiffness, the groove dimensions and the shear behaviour of the filler material (usually epoxy paste). Stress transfer and interaction occurs along the two contact surfaces: (a) at the interface between bar and epoxy and (b) at the interface between the epoxy and the surrounding concrete. In both cases, force transfer is achieved through chemical adhesion at the early

stages and through friction for higher levels of slip. Mechanical interlocking between bar and epoxy may occur if the bar used has surface deformations. Usually the failure occurs at one of the two contact interfaces; pullout tests in controlled laboratory conditions usually lead to failures at the concrete – epoxy surface (Novidis and Pantazopoulou, 2006), although failures by splitting have also been reported if a cementitious mortar is used instead of epoxy paste as a filler material. In different setups such as in beam tests bar pullout has also been reported (failure at the bar-epoxy paste interface and epoxy splitting, Novidis and Pantazopoulou, 2006). The ductility of the failure mode depends entirely on the properties of the system. If the filler material is epoxy paste, i.e. an elastic brittle material with a high tensile resistance, precipitous debonding is expected to occur in either of the two contact surfaces without stress redistribution. In the present paper, parameters of study were the material and surface pattern of the bar, the embedment length, the effect of the arrangement of the specimens (beam pull out tests – direct pull out tests) and finally the shear-span and the crack pattern of the beams. Test results are used to indicate the effect of investigated parameters on bond strength in order to facilitate and upgrade the practical design procedures for strengthening applications of reinforced concrete members with post-installed near-surface mounted reinforcement.

## 2. EXPERIMENTAL DATA OF THE STUDY

The experimental study comprised a total of 14 simply supported unreinforced concrete beams. All beams had a rectangular cross-section 150.0 mm high by 300.0 mm wide. The beams were classified in ten specimen-parameter cases (S.C.) according with the values of the parameters studied. Cases 9 and 10 concern beams 2000.0 mm long (aspect ratio of 6) whereas all other cases considered were 1000.0 mm long with an aspect ratio of 3. Surface grooves with a 20mm square cross section were preformed and the NSM bars were post-installed after curing using an epoxy paste. In all specimens, the surface of the grooves was artificially roughened using a metallic brush to improve adhesion of the epoxy paste-concrete interface through interlocking. To achieve almost uniform conditions over the anchorage so as to quantify the local bond strength, short anchorage lengths were used ( $5D_b$  and  $10D_b$ ). Commercially supplied C25/30 concrete was used, having an average 28-day compressive strength of 33.50 MPa as determined from standard (ASTM C39) concrete cylinder tests. Nominal CFRP bar properties were as follows (as specified by the manufacturer): modulus of elasticity of 124.0 GPa and 1.7% ultimate strain at tensile rupture. Bar surface patterns were either sand-coated or sand-blasted. Epoxy paste was prepared by mixing the two components (resin and hardener) and the mechanical properties, as specified by the manufacturer, were a tensile strength of 30.0 MPa and a modulus of elasticity of 3.0 GPa. When used as NSM inserts steel bars were smooth except for one case where deformed S500 bars were used, having a modulus of elasticity of 210.0 GPa. Geometrical characteristics together with test results for all beam specimens are summarized in Fig. 1 and Tab. 1 and 2 respectively.

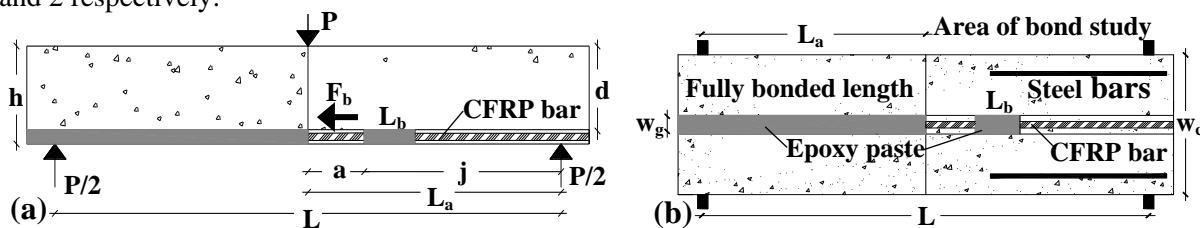


Fig. 1 Geometrical characteristics of beam specimens: (a) side view and (b) plan view.

## 3. PRESENTATION AND EVALUATION OF TEST RESULTS

Figures 2 - 6 outline the experimental results highlighting the effect of the experimental study parameters on average bond strength obtained for the group of bond specimens that had a bonded NSM-bar length of  $5D_b$  and  $10D_b$ . To avoid concrete tension failure these specimens were reinforced with two short-length deformed steel bars in the area of study, as illustrated in Fig. 1(b).

Tab. 1 Summarized test results for all beam-specimens, (beams with anchorage length of  $5D_b$  and  $10D_b$  were tested in replicas of two)

Specimen code	Length L (mm)	Actual $D_b$ (mm)	Filler material	Bonded length $L_b$ ( $D_b$ )	a (mm)	j (mm)	Bar material	Surface pattern	$P_u / 2$ (kN)	$\delta_{u,80\%}$ (mm)	$F_b$ (kN)	Slip at failure interface s (mm)	$f_b^c$ (MPa)	$f_b^b$ (MPa)	F.M.
1-BPO-5D-CF	900	9	Epoxy	5	100	350	CFRP	Sand-coated	8,64	1,70	23,98	0,14	8,88	18,85	1
2-BPO-10D-CF	900	9	Epoxy	10	100	350	CFRP	Sand-coated	11,39	2,37	31,63	0,36	5,86	12,43	1
3-BPO-10D-CF	900	9	Epoxy	10	100	350	CFRP	Sand-blasted	13,00	2,60	36,11	0,41	6,69	14,19	2
4-BPO-10D-SS	900	8	Epoxy	10	100	350	Steel	Smooth	7,25	0,60	20,14	0,15	4,20	10,02	2
*5-FB-CF	900	9	Epoxy	50	-	-	CFRP	Sand-blasted	29,50	7,31	-	-	-	-	1
*6-FB-SS	900	8	Epoxy	56	-	-	Steel	Smooth	7,50	12,60	-	-	-	-	3
**7-EM-CF	900	9	-	50	-	-	CFRP	Sand-blasted	23,25	5,17	-	-	-	-	4
*8-FB-SD	900	8	Epoxy	56	-	-	Steel	Deformed	11,25	23,45	-	-	-	-	3
9-BPO-10D-CF	1900	9	Epoxy	10	600	350	CFRP	Sand-blasted	8,13	5,39	29,02	0,33	5,38	11,40	2
*10-FB-CF	1900	9	Epoxy	106	-	-	CFRP	Sand-blasted	27,75	19,10	-	-	-	-	5

\* FB = Fully Bonded bar with epoxy paste; \*\* EM = Embodied bar in the concrete; BPO = Beam Pull Out; F.M. = Failure Modes: 1 = failure at the epoxy-concrete interface; 2 = failure by pullout at the bar-epoxy interface; 3 = steel fracture; 4 = slipping of the bar into the concrete body of the beam and 5 = splitting of concrete-epoxy cover of the bar followed by slipping bar into the epoxy. ( $f_b^c$  or  $f_b^b$  are average bond strengths).  $\delta_{u,80\%}$  is the midspan deflection in the postpeak branch corresponding to a residual strength equal to 80% of the peak value.

Tab. 2 Summarized test results of load-deflection for beams 5,6,7,8 and 10 (course of crack pattern)

Specimen code	1 <sup>st</sup> crack		2 <sup>nd</sup> crack		3 <sup>rd</sup> crack		4 <sup>th</sup> crack		Values of stable crack pattern		Failure	
	* $P'_{cr,1}$	** $\delta_{cr,1}$	$P'_{cr,2}$	$\delta_{cr,2}$	$P'_{cr,3}$	$\delta_{cr,3}$	$P'_{cr,4}$	$\delta_{cr,4}$	$P'_{cr,s}$	$\delta_{cr,s}$	$P_u / 2$	$\delta_u$
5-FB-CF	9,50	0,72	15,30	2,50	18,15	4,24	-	-	18,15	4,24	29,50	11,70
6-FB-SS	6,25	0,73	-	-	-	-	-	-	6,25	0,73	7,50	0,92
7-EM-CF	7,00	0,24	14,50	2,40	18,25	4,87	-	-	18,25	4,87	23,25	8,41
8-FB-SD	9,50	0,10	10,75	0,58	-	-	-	-	10,75	0,58	11,25	8,76
10-FB-CF	5,75	0,83	8,25	2,43	12,00	6,34	15,75	10,84	15,75	10,84	27,75	28,60

\* = Units (kN) and  $P'_{cr,i} = P_{cr,i} / 2$ ; \*\* = Units (mm)

Two alternative failure modes were observed throughout the bond tests, as depicted in Figs. 2 and 3; thus, for specimens where the surface pattern of the bar was sand-coated (S.C.: 1 and 2), failure occurred by sliding along the epoxy-concrete interface whereas for specimens having sand-blasted or smooth bars failure occurred at the other contact surface, (bar-epoxy interface, S.C.:3, 4 and 9).

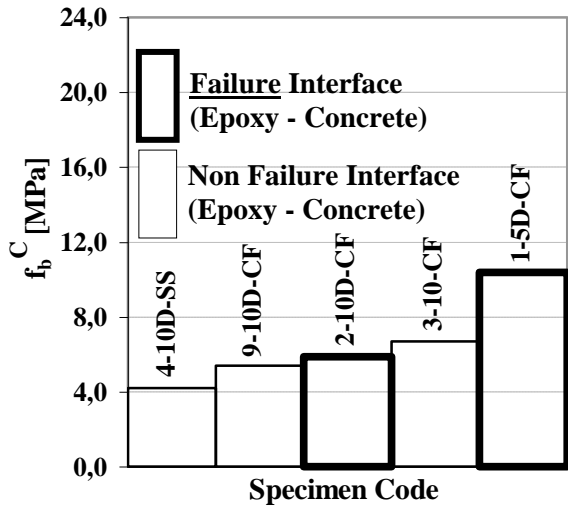


Fig. 2 Average bond strength ( $f_b^c$ ) for all bond specimens

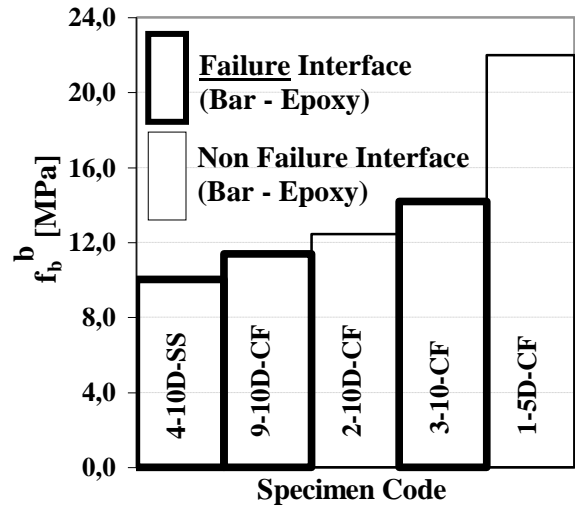


Fig. 3 Average bond strength ( $f_b^b$ ) for all bond specimens

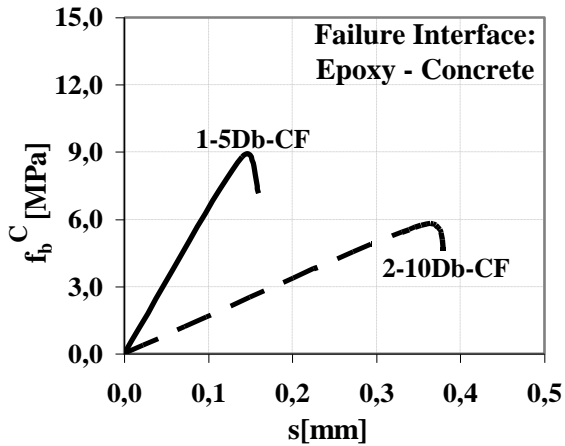


Fig. 4 Average bond strength ( $f_b^c$ ) vs. slip for different anchorage lengths

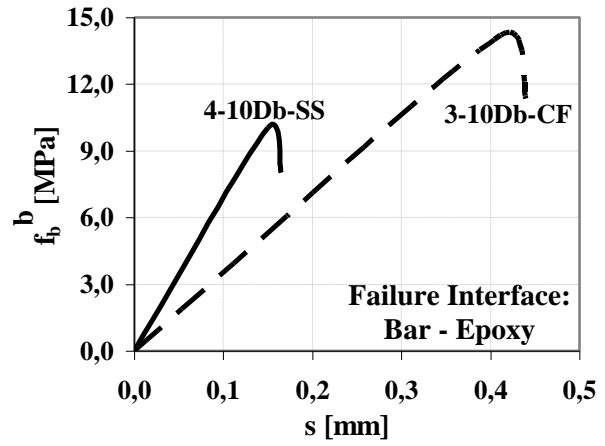


Fig. 5 Average bond strength ( $f_b^b$ ) vs. slip for different bar materials

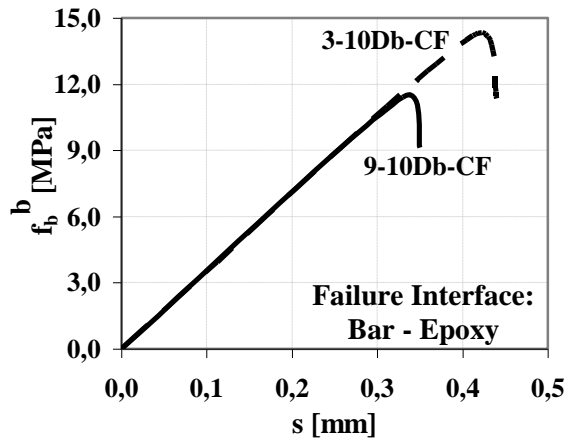


Fig. 6 Average bond strength ( $f_b^b$ ) vs. slip for different spans

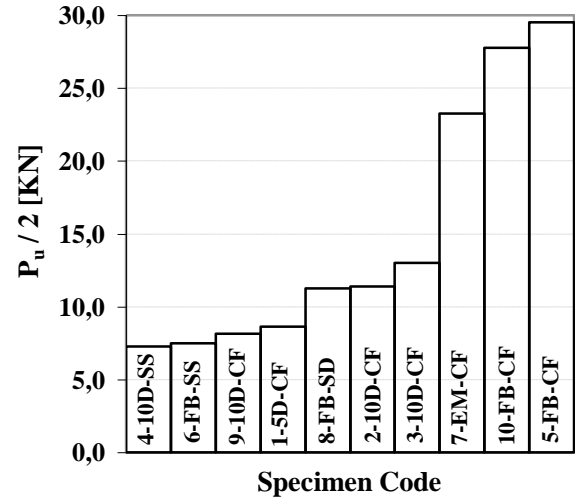


Fig. 7 Ultimate load for all specimens

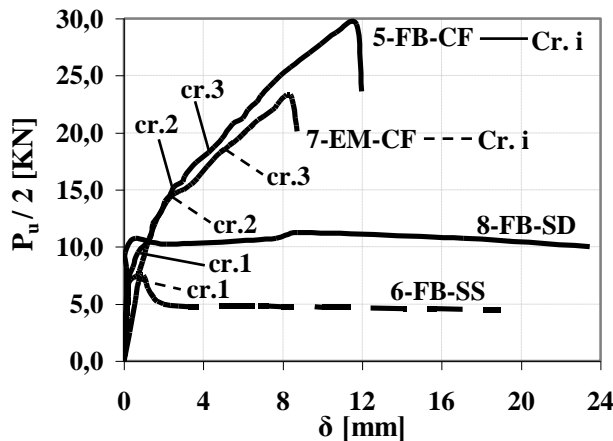


Fig. 8 Crack propagation during loading for specimens with different bar materials and bar embedment method

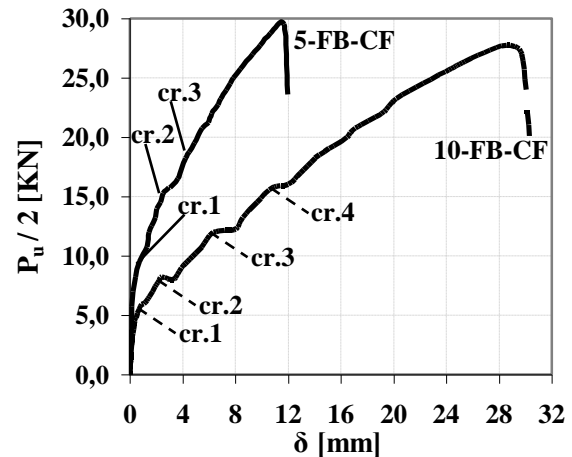


Fig. 9 Crack propagation during loading for specimens with different spans

Test results from a previous experimental study on bond of NSM bars conducted on modified direct pullout prismatic specimens with the same groove and material characteristics as those used in the present investigation showed failure at the epoxy-concrete interface even for sand-blasted bars (Novidis and Pantazopoulou, 2006). This difference in the mode of failure effected by the specimen type (beam test here, versus modified direct pullout in the former study) is confirmed also by other beam tests and is attributed to the flexural curvature occurring in the beam tests during mid-span deflection. Note that the elastic curve of the bar,  $w_b(x)$ , which is prescribed by that of the deflecting beam, is equivalent to the existence of a nontrivial normal pressure,  $q_b(x)$ , acting normal to the bar surface, through the relationship:

$$\frac{d^4 w_b(x)}{dx^4} = \frac{q_b(x)}{EI_b} \quad (1)$$

For usual cases and normal levels of deflection the estimated pressure is found to be significant. This pressure acting normal to the lateral surface of the NSM-bar encourages the development of friction and thereby mechanical interlock at both interfaces thereby enhancing the system's resistance. Considering the results of this study, it is clear that the described influence of radial pressure on the prevailing failure mode (concerning the weakest interface) has been seen in cases of specimens strengthened with the NSM procedure using either smooth bars or slightly deformed bars, such as would be the surface of a sand-blasted bar. A limit to the height of surface deformation of the bar has to be considered, as this phenomena (effect on failure mode depending on specimen type) appears to be suppressed when the surface roughness is substantial (e.g. specimens with sand-coated bars having 0.5-1.0 mm height grains of sand). Thus, beyond this limit in height deformations of the bar the cohesion between epoxy-concrete surfaces becomes the weak link regardless of specimen form or test setup.

Fig. 4 depicts the effect of different bonded lengths on average bond strength. As the bonded length increases the development capacity in terms of total load carried by the joint increases but the average bond strength decreases due to the non-uniform distribution of bond stresses. This reduction of average bond strength was observed when the available bonded length exceeds the limit value of  $5D_b$ , (Novidis et al, 2007). Average bond strength reduction was observed also when using steel smooth bar inserts (greater bar stiffness) as compared with CFRP sand-blasted bar inserts, Fig. 5. As both steel and CFRP bars used were smooth with insignificant surface roughness (sand-blasted), mechanical interlock between bars and epoxy is limited to the wedging action. Initial chemical adhesion appears to be stronger in the case of the CFRP bars at the contact surface with the epoxy, rather than in the case of smooth steel bars. Another reduction in bond strength was also observed when doubling the span length of the beam specimens, Fig. 6. This result is attributed to the higher amount of slip (quantified by crack widths) in the shear span owing to the larger amounts of deflection, leading to an earlier failure of the beam by bar pull out from the epoxy paste. Specimens with steel bars (S.C. 6 and 8, fully

bonded) failed by bar rupture after bar yield, at relative small load and high plastification in comparison with the respective specimens with CFRP bars (S.C. 5 and 10), since the shear strengths at the two contact surfaces (epoxy-concrete and steel bar-epoxy) were shown to be considerably higher than the tensile strength of the steel bars, Figs. 7 and 8. Results for the two fully bonded specimens, where in the first the FRP bar was embodied in the concrete mass of the beam (S.C. 7) and in the second the FRP bar was bonded in the groove through epoxy paste (S.C. 5), were close in all aspects (crack propagation and stiffness) except for the final strength of the beam, which was 25% higher in the latter case with the epoxy paste, Fig. 8. This result highlights the improved chemical adhesion-friction between CFRP bar and the epoxy as compared with the magnitude of adhesion in the contact between CFRP bar and concrete. Higher plastification was observed in specimens with steel bars in contrast with CFRP bars as expected owing to the different stress-strain characteristics of the two materials (brittleness of the FRP bars). Crack propagation was more intense in specimens with CFRP bars (Fig. 8), as well as in cases with longer span lengths (specimen 10-FB-CF, Fig. 9). Crack spacing was almost doubled in the latter case as compared with the corresponding specimens with CFRP bars and an aspect ratio of 3, (experimentally measured crack spacing after stabilization of the cracks was in the range of 100 to 150 mm for S.C. 5 and 7, and up to a value of 250 mm for S.C. 10).

#### 4. CONCLUSIONS

Bond behaviour of NSM-FRP bars was studied experimentally through testing of simply supported beam-specimens, after strengthening the beams with this technology. Parameters of study were the bar stiffness (steel vs. CFRP), surface roughness (sand blasted vs. bars with helical indentations, steel smooth bars, and steel deformed bars), and manner of bar placement (post-installed in surface grooves, or embedded during initial casting). An additional parameter was beam span length so as to provide data and insight regarding the influence of beam curvature on measured bond strength. The primary finding of the study is that this technology can mitigate the problems of debonding from the ends, commonly observed when strengthening beams through externally bonded FRP laminates. Beam curvature was found to increase the contact bond strengths at both interfaces moving the occurrence of failure in the weakest interface which however depends on the height of bar surface deformation; this represents a significant deviation from results obtained when the embedded bar is pulled on its axis without eccentricity. Further investigations of this problem are under development.

#### 5. ACKNOWLEDGEMENTS

This investigation was conducted in the Laboratories of the Department of Civil Engineering, Democritus University of Thrace (DUTH), Xanthi - Greece under a research program funded by the Hellenic General Secretariat for Research and Technology (PENED2001). MAC BETON HELLAS S.A. generously donated the epoxy-pastes used in the experimental program. FRP reinforcement was purchased from Hughes Brothers (USA).

#### 6. REFERENCES

- De Lorenzis L. and Nanni A. (2001), "Characterization of FRP Rods as Near-Surface Mounted Reinforcement", *ASCE J. of Composites for Construction*, Vol. 5, No. 2, pp. 114-121.
- Malek AM., Saadatmanesh H. and Ehsani MR. (1998), "Prediction of Failure Load of R/C Beams Strengthened with FRP Plate due to Stress Concentration at the Plate End", *ACI Structural J.*, Vol. 95, No. 1, pp. 142-152.
- Novidis, D. G. and Pantazopoulou, S. J. (2006), "Experimental Study of Short NSM – FRP & Steel Bar Anchorages", *Proceedings of the 2nd Int. of fib Congress, Naples, Italy*.
- Novidis D. G., Pantazopoulou S. J. and Tentolouris E. (2007), "Experimental Study of Bond of NSM – FRP Reinforcement." *Elsevier, J. of Construction and Building Materials*, Vol. 21, No. 8, pp. 1760-1770.
- Novidis, D. G. and Pantazopoulou, S. J. (2007), "Beam Tests of NSM - FRP Laminates in Concrete", *Proceedings of the 8th Int. Symposium on Fiber Reinforced Polymer Reinforcement for Concrete Structures, FRPRCS-8, Patras, Greece*.
- Oehlers DJ. and Moran JP. (1990), "Premature Failure of Externally Plated Reinforced Concrete Beams", *ASCE J. of Structural Engineering*, Vol. 116, No. 4, pp. 978-995.

## EXPERIMENTAL INVESTIGATION OF STRENGTHENED RC GIRDERS

*Peter Koteš, Patrik Kotula, Miroslav Brodňan*  
*University of Žilina, Civil Engineering Faculty, Slovakia*  
*Univerzitná 8215/1, 010 26, Žilina*  
*[kotes@fstav.uniza.sk](mailto:kotes@fstav.uniza.sk), [kotula@fstav.uniza.sk](mailto:kotula@fstav.uniza.sk), [brodnan@fstav.uniza.sk](mailto:brodnan@fstav.uniza.sk)*

### SUMMARY

The paper deals with the experimental measurements of real strengthened RC girders, which are carried out in the frame of the research work APVT-20-012204. The mentioned girders are strengthened by the S&P CFK lamella 150/2000 in bending and by S&P C-Sheet 640 in shear area. The achieved results of the experimental measurements of the non-strengthened and strengthened beams are compared.

### 1. INTRODUCTION

The rehabilitation of reinforced concrete (RC) structures using FRP (Fibre Reinforced Polymers) materials has become a growing area in the construction industry over the last decade. Many research projects in the world have been carried out to promote this efficient repair technique to increase the load-carrying capacity and to extend the service life of existing RC structures. FRP is a composite material generally consisting of carbon, aramid or glass fibres in a polymeric matrix (e.g. epoxy resin). Among many options, this reinforcement may be in the form of preformed laminates or flexible sheets. The laminates are stiff plates or shells that come pre-cured and are installed by bonding the plate to the concrete surface with epoxy. The sheets are either dry or pre-impregnated with resin (pre-preg) and cured after installation onto the concrete surface. This installation technique is known as wet lay-up (Kotula, 2006).

The lightweight and formability of FRP laminates or sheets make these systems easy to install. And since the materials used in these systems are non-corrosive, non-magnetic, and generally resistant to chemicals, they are an excellent option for external reinforcement. Just the durability and the lifetime of these systems are not still confidently verified. Externally bonded FRP laminates or sheets have shown to be applicable to the strengthening of many types of RC structures such as: columns, beams, slabs, walls, tunnels, chimneys and silos and can be used to improve flexural and shear capacities, and also provide confinement and ductility to compression structural members (Khalifa, Gold, Nanni, Abdel Aziz, 1998), (Khalifa, Nanni, 2002). Traditional methods such as for example different kinds of reinforced overlays, shotcrete or post tensioned cables are placed on the outside of the structure which normally needs much space. The FRP laminates or sheets do not require much space because they are very thin. The bending strengthening of the structures is the most common way of the structure strengthening but shear strengthening is also often needed (Täljsten, 2001). However, these structures are mostly static loaded structures.

In the last few years, some research works have started to focus on using these system on dynamic loaded structures as are bridges (Capozucca, 2006), (Casadei, Parretti, Nanni, Heinze, 2005). The bridges are considered to be an inseparable and strategically very



important part of the transportation infrastructure and they should have such parameters not to become the limiting component of the communication capacity and traffic reliability. Nowadays, the development leads to move the attention from the design of new structures towards repair and reconstruction of existing structures in order to ensure and increase the satisfactory reliability and durability of structures.

## 2. RESEARCH ACTIVITIES

In the frame of research activities (research work no. APVT-20-012204 “Remaining service life and increasing of concrete structures reliability”) of the Department of Structures and Bridges (University of Žilina), the reinforced concrete beams strengthened with CFRP lamellas in bending are investigated. The research is focused on the existing bridge structures, which do not satisfy the traffic loads. So, a bridge near village Kolárovice is observed. It is a six beams reinforced concrete bridge structure with theoretical span 10.006m, which do not satisfy the load-carrying capacity. So, it is needed to strengthen the bridge. The use of carbon fibre reinforced polymer (CFRP) materials (lamellas and sheets) is one of new ways of strengthening of concrete bridges. Firstly, the strengthening is applied on the set of specimens of the T-beam in scale 1/3. The static and dynamic load is applied on the specimens. The dynamic load is representing the real traffic load on the bridge structure.

The paper deals with the static load proof.

## 3. EXPERIMENTAL ANALYSIS

### 3.1 Non-strengthened girder

The experimental analysis was firstly focused on static load proof. The non-strengthened RC girder was made. The girder, which is three times reduced compared to the existing RC bridge girder in the village Kolárovice on the road I / 18, is shown in Fig. 1. The 1/3 scale beam was considered because of the laboratory possibilities and the beam dimensions. This beam was used as the comparison beam to the strengthened beams. The type of used concrete is C 55 ( $f_{cu} = 56.32$  MPa) and the beams are reinforced in bending by rebars of diameter 6 mm ( $f_{yk} = 358.073$  MPa) in one layer ( $3 \phi 6$ ) and in shear by rebars of diameter 4 mm ( $f_{yk} = 693.793$  MPa) ( $\dot{\lambda} 108$  mm).

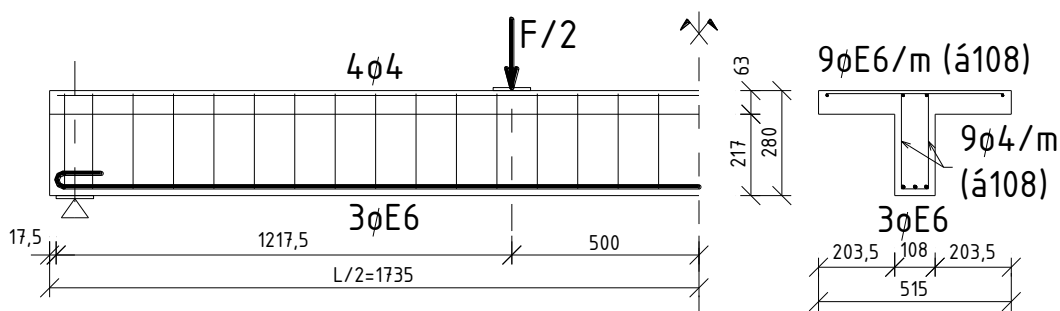


Fig. 1 The three times reduced RC girder of RC bridge girder in the village Kolárovice on the road I/18

### 3.2 Strengthened girders

The measurement of strengthened beams was the main part of the research work. The five strengthened RC girders were created (Fig. 2). The girders were strengthened with one

MBrace<sup>®</sup> S&P CFK lamella 150/2000 in bending and with three S&P C-Sheet 640 of width 100mm in shear. Three of these girders were static loaded and two of these girders were dynamic loaded. The denotation of all girders including non-strengthened is shown in Tab. 1.

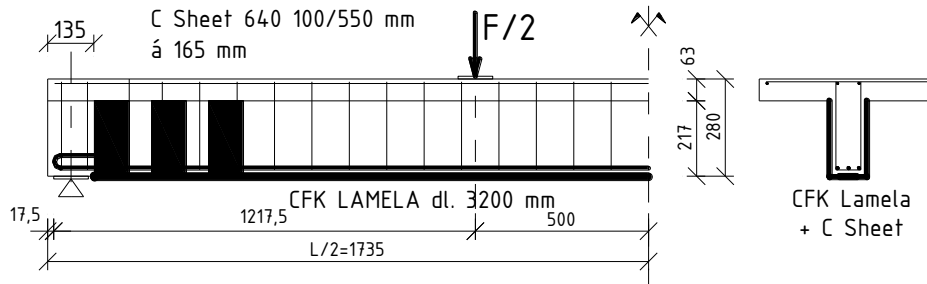


Fig. 2 The three times reduced RC girder strengthened with one MBrace<sup>®</sup> S&P CFK lamella 150/2000 and S&P C-Sheet 640

Tab. 1 The review of all made laboratory RC T-beam subjected to bending

Denotation	Description
TO_0	Non-strengthened specimen for comparison; bending static proof
TO_1	Strengthened specimen: 1 lamella S&P CFK 150/2000 50/1.2 mm in the bending area + S&P C-Sheet 640 strips in the shear area; bending static proof
TO_2	Strengthened specimen: 1 lamella S&P CFK 150/2000 50/1.2 mm in the bending area + S&P C-Sheet 640 strips in the shear area; bending static proof
TO_3	Strengthened specimen: 1 lamella S&P CFK 150/2000 50/1.2 mm in the bending area + S&P C-Sheet 640 strips in the shear area; bending static proof
TO_4	Strengthened specimen: 1 lamella S&P CFK 150/2000 50/1.2 mm in the bending area + S&P C-Sheet 640 strips in the shear area; bending dynamic proof
TO_5	Strengthened specimen: 1 lamella S&P CFK 150/2000 50/1.2 mm in the bending area + S&P C-Sheet 640 strips in the shear area; bending dynamic proof

#### 4. RESULTS OF THE EXPERIMENTAL MEASUREMENTS

The analysis was focused on the influence of the externally bonded MBrace<sup>®</sup> S&P CFK lamella 150 / 2000 on the bending capacity of the RC girder. The value of the additional bending capacity was controlled with the deflection in the middle of the RC girder span. According to the standard (STN P ENV 1992-1-1, 1999), the considered limited deflection is  $L / 250$  which means  $w_{lim} = 13.88$  mm. Firstly, the non-strengthened girder TO\_0 was statically loading till failure in order to obtain the maximum force at the failure and to compare it with the maximum force at the failure of the strengthened girders. At the same time, the cracks formation and development was observed. Also, the deflections were measured (Fig. 3). The maximum force at the failure is equal to  $F_{max,TO_0} = 30.0$  kN.

Next, the three T-beams TO\_1, TO\_2 and TO\_3 were static loaded. The deflections and the strains were measured by the resistance sensors.

The program of the static proof of the RC T-beams series „TO“ were consisting of

- 1) prior to testing, the non-strengthened girders were cracked (the partial failure) in the bending area to simulate an overload condition that were corresponded to the limited bending crack width  $w_{lim} = 0.02$  mm; RC T-beams „TO\_1“, „TO\_2“, „TO\_3“.

- 2) the strengthening of the partially failed RC T-beams „TO\_1“, „TO\_2“ and „TO\_3“ using 1 lamella S&P CFK 150/2000 50/1.2 mm in the bending area that were strengthened in the anchorage by C-Sheet 640 strips.
- 3) the loading tests of the strengthened RC T-beams as far as bending failure.

The dependence of the deflection on the loading force  $F$  in the middle of the span is shown in Figure 4 and in the place of the force  $F/2$  is shown in Fig. 5.

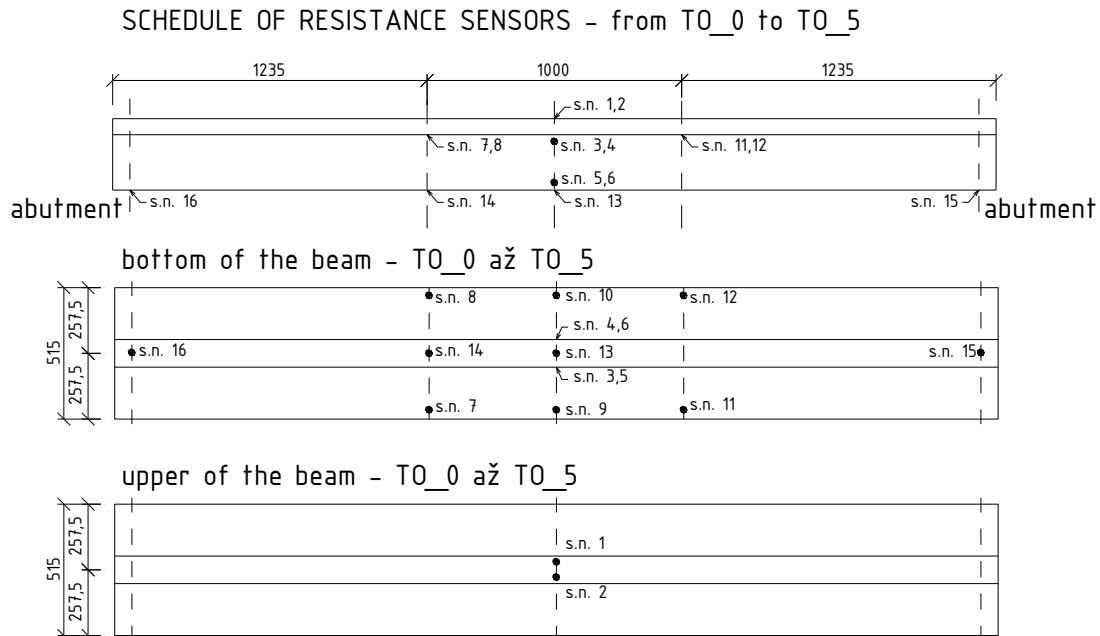


Fig. 3 The locations with the measured deflections

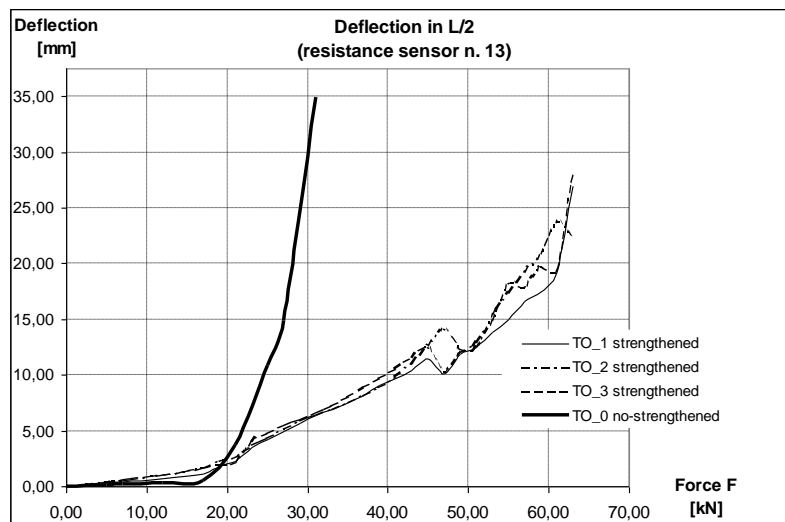


Fig. 4 The deflection in the middle of the beams depending on the load force  $F$

The value of the maximum force at the T-beams failure after strengthening (step 3) was the same for all girders TO\_1, TO\_2 and TO\_3 and the value is equal to  $F_{\max, TO_1} = 63.0$  kN. It means, that the load-carrying capacity increased about 110%. So, the degree of the strengthening  $\eta$ , which is equal to ratio between the resistance bending moment  $M_{Rd,f}$  of strengthened cross section and the resistance bending moment  $M_{Rd,0}$  of non-strengthened

cross section, is higher than 2.0. The moments can be replaced by forces, so the degree of strengthening is defined:

$$\eta = M_{Rd,f} / M_{Rd,0} = F_{max,TO_0} / F_{max,TO_1} = 2.10 \geq 2.0 \quad (1)$$

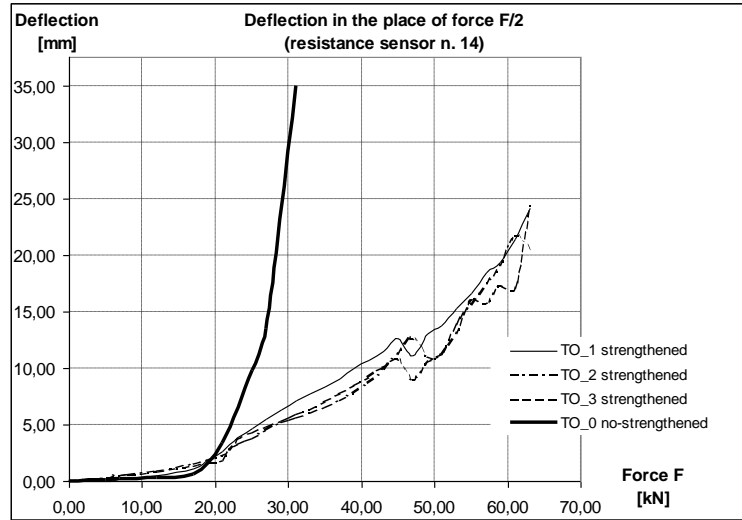


Fig. 5 The deflection in the place of force F/2

The degree of strengthening should be less than 2.0. Since it is higher than 2.0, the maximum load force, which can be used practically, is equal to  $F_{max,TO_1}=60.0$  kN.

The high value of the maximum load  $F_{max,TO_1}$  represents the high quality of the strengthening.

The maximum forces corresponded to the ultimate limit state (ULS) or to the limited deflection in the middle of the RC beam span are shown in Tab. 2. The degree of the strengthening  $\eta$  is also shown.

Tab. 2 The maximum forces at the beams failure

Denotation	The maximum forces achieved in the ultimate limit state (ULS)		The maximum forces corresponds to the limited deflection in the middle of the RC beam span		
	$F_{max}$ [kN]	$\eta$	$F_{max}$ [kN]	w [mm]	$\eta$
TO_0	30.00	1.00	26.00	13.20	1.00
TO_1	63.00	2.10	53.00	13.81	2.04
TO_2	63.00	2.10	51.00	12.47	1.96
TO_3	63.00	2.10	51.00	12.87	1.96

#### 4. CONCLUSIONS

The paper deals with the influence of the CFRP strengthening on increasing the load-carrying capacity. The girders are strengthened with one MBrace<sup>®</sup> S&P CFK lamella 150/2000 in bending and with three S&P C-Sheet 640 of width 100mm in shear. The three of the girders were only statically loaded as far as the girders failure. The comparison beam TO\_0 was not strengthened and was also statically loaded and corrupted.

Firstly, the large influence of the CFRP strengthening on the load-carrying increasing was achieved. The degree of strengthening corresponding to the ultimate limit states is higher than

2.0. If the limited deflection  $w_{lim}$  in the middle of the girder span ( $L/2$ ) and the corresponding force  $F$  are considered, the degree of strengthening is equal to 1.96.

It is needed to point that just the load-carrying capacity and the deflection in  $L/2$  were observed. Further limit states like maximum width of the cracks were not verified due to arrangement of the static proof load.

At the same time, the numerical modeling and analysis of mentioned non-strengthened and strengthened beams is carried out. The Atena software is used for numerical modeling. The achieved experimental results will be compared with the result from numerical analysis.

## 5. ACKNOWLEDGEMENTS

This work was supported by the Science and Technology Assistance Agency under the contract No. APVT-20-012204 and by the Slovak Grant Agency, Grant No. 1/3332/06.

## 6. REFERENCES

- Capozucca, R. (2006): Comparison at Short and Long Term of Static-dynamic Response of RC Beams Strengthened by CFRP. *The Second International fib Congress 2006, Proceedings of the abstracts, Proceedings of the papers on CD*, Napoli, 5-8 June 2006, ID 10-16
- Casadei, P. & Parretti, R. & Nanni, A. & Heinze, T. (2005): In situ Load Testing of Parking Garage Reinforced Concrete Slabs: Comparison between 24h and Cyclic Load Testing. *Practice periodical on structural design and construction*, February, pp. 40-48.
- Frangopol, D.M. & Estes, A.C. (1997): Lifetime Bridge Maintenance Strategies Based on System Reliability. *Structural Engineering International 3*, pp. 193-198.
- Khalifa, A. & Gold, W.J. & Nanni, A. & Abdel Aziz, M.I. (1998): Contribution of Externally Bonded FRP to Shear Capacity of Flexural Members. *ASCE-Journal of Composites for Construction 4(2)*, pp. 195- 203.
- Khalifa, A. & Nanni, A. (2002): Rehabilitation of Rectangular Simply Supported RC Beams with Shear Deficiencies Using CFRP Composites. *Construction and Building Materials 3(16)*, pp. 135-146
- Koteš, P. (2005): Contribution to determining of reliability level of existing bridge structures. *PhD Thesis*, Žilina: EDIS (in Slovak)
- Koteš, P. & Vičan, J. (2006): Experiences with Reliability-based Evaluation of Existing Concrete Bridges in Slovakia. *The Second International fib Congress 2006, Proceedings of the abstracts, Proceedings of the papers on CD*, Napoli, 5-8 June 2006, ID 16-6
- Kotula, P. (2006): Chosen theoretical and practical problems about strengthening of concrete structures using bonded reinforcement. *PhD Thesis*, Žilina, EDIS (in Slovak)
- Nowak, A.S. (1995): Calibration of LRFD Bridge Code. *Journal of Structural Engineering*, pp. 1245-1251.
- Omishore, A. & Kala, Z. (2006): Application Limits of Conventional Models of Systems. Structures reliability; *Proceedings of VII. International Conference*, Prague, 5 April 2006. Prague, CVUT
- Täljsten, B. (2001): Strengthening Concrete Beams for Shear with CFRP Sheets. In *Structural Faults and Repair 2001; Proceedings of 9th International Conference and Exhibitions*, London, 4–6 July 2001, CD-ROM Version
- Vičan, J. at all. (1999): Guideline - Evaluation Methodology of Existing Concrete Road Bridge. *Final Report for Slovak Road Administration*. Žilina, University of Žilina (in Slovak)

## **Topic 3**

Advanced production and construction technologies



## **CONCRETE GIRDER BRIDGES WITH LONG PREFABRICATED GIRDERS**

*Prof. Jure Radnić, PhD. Civ. Eng.; Prof. Alen Harapin, PhD. Civ. Eng.; Marija Smilović, BSc. Civ. Eng.,  
University of Split, Faculty of Civil Engineering and Architecture,  
Matice hrvatske 15, 21000 Split, Croatia*

### **SUMMARY**

The paper presents a short discussion on some specific features of design and construction of concrete girder bridges with long prefabricated girders. Namely, design and construction of prefabricated girder bridges with spans up to about 35 m are almost a routine engineering task. However, with the increase in prefabricated girder length, there is also an increase in problems associated with girder design and construction, which is discussed in short in this paper. The paper also gives an overview of three concrete girder bridges, with spans of 36-50 m, recently built in the framework of construction of new Croatian freeways.

### **1. INTRODUCTION**

Concrete girder bridges with prefabricated longitudinal girders are still the most common bridges in the Republic of Croatia. There are almost no other bridge types to compete with them for spans up to about 50 m. Namely, prefabricated concrete longitudinal girders are a well proven solution, easy in design and construction; they require small concrete and steel consumption, enable fast construction process and are more efficient than other girder types for the aforementioned spans. Those bridges are constructed as either continuous beams or simple beams on two supports and continuous slabs above the piers. The most efficient solution for bending at midspan are prestressed cables, while conventional reinforcement shall be used to withstand bending moments above the piers. The previously described bridges, of up to about 35 m span, are almost a routine task for design engineers and contractors. However, with the increase in prefabricated girder length, requirements concerning their design, fabrication and assembly become stricter. The paper starts with the discussion on some specific features of design and construction of girder bridges with long prefabricated girders. After that, the paper gives an overview of three bridges with spans 36-50 m, recently built in the framework of construction of new Croatia freeways.

### **2. SOME SPECIFIC FEATURES OF LONG PREFABRICATED GIRDERS**

As is well known, bending moments in a beam, due to uniformly distributed load, increase with the squared length. Thus, ratios among bending moments for beams of e.g. 30, 40, 50 and 60 m spans are 1:1.77:2.78:4. For uniform load, there is a linear dependence between transverse forces and beam span. Beam deflection increases proportionally with the fourth exponent of its span. Thus, with the increase in girder span, there is a drastic need for an increase in its height, as well as width of chords and web. Also, increase in girder span leads to significant increase of girder mass. Due to great girder mass, there is a problem of transport and assembly of long prefabricated girders.



With the increase in girder span, the need for greater prestressing force increases i.e. for a greater number and bearing capacity of prestressed cables. Because of limited compressive stresses immediately after prestressing, long girders require increased width of the bottom chord at midspan. Due to limited compressive stresses in exploitation, top chord width of the girder shall increase with the increase in span. Furthermore, cables with greater profiles require wider girder web.

For prefabricated long continuous girder bridges, there is the problem of compressive stresses of concrete in the girder bottom chord above the piers. Precise calculation of bending moments in the beams above supports, after establishing their continuity, shall be carried out, taking into account all subsequent loads and actions (other permanent load, traffic load, creep, temperature changes, etc.). For the purpose of concrete compressive stresses limiting, the bottom chord of the girder above the support shall have sufficient width. With the same aim, there is a need for as great as possible concrete strength and conventional compression reinforcement.

In order to eliminate the prestressing force impact on the increase of compressive stresses in the bottom chord of continuous girders above the piers, the centroid of the prestressing force at the end of prefabricated girders shall be at the upper edge of the cross-section core or above it. This will require classical reinforcement in the upper girder chord at the ends, and its proper construction.

Greater height and wider bottom chord of long girders makes their concreting more difficult. The formwork of such girders is also more complex. With the increase in girder span, proper construction of details as well as cable positioning becomes more and more demanding.

Long girder spans are usually directly associated with high piers of viaducts and bridges. Regarding the great girder mass and the usually very high bridge gradient in regard to the surrounding terrain, assembly of long girders, using truck crane, is often impossible. Those girders are usually assembled with mobile launching trusses. They can assemble girders of mass up to about 300 t and up to about 65 m in length, which is considered the limit in application of prefabricated prestressed concrete bridge girders.

### **3. SOME CONTEMPORARY BRIDGES WITH LONG PREFABRICATED GIRDERS IN THE REPUBLIC OF CROATIA**

A short overview of Severinske Drage Viaduct on the Zagreb-Rijeka freeway (Radnić, 2000), and Kličevica Bridge (Radnić, 2004) and Dabar Bridge on the Zagreb-Split freeway (Radnić, 2005), is presented hereinafter. They were all constructed using prefabricated reinforced concrete girders that were assembled using mobile launching truss. Main span structures are continuous girders, prestressed by cables to withstand bending moments at midspan and reinforced by conventional reinforcement above the piers. Some girders have wide top chords, while the others have narrow ones. All girder webs are 0.24 m wide. Piers have box cross-section of 5x3.4 m external dimensions and 0.30 m thick walls, of the same dimension along the entire length. At the pier top, there is a massive head beam. Pier foundations are shallow footings.

### 3.1 Severinske Drage Viaduct

Longitudinal and cross-section of the viaduct are shown in Fig. 1 (Radnić, 2000). Its appearance in construction is shown in Fig. 2. The total length of the viaduct span structure is 716 m, divided in three dilatation units. Axial distances between span structure supports are:  $38.8+16\times 39.9+38.8 = 716$  m. Above the piers, the span structure is supported by two rows of supports at the longitudinal distance of 2.2 m.

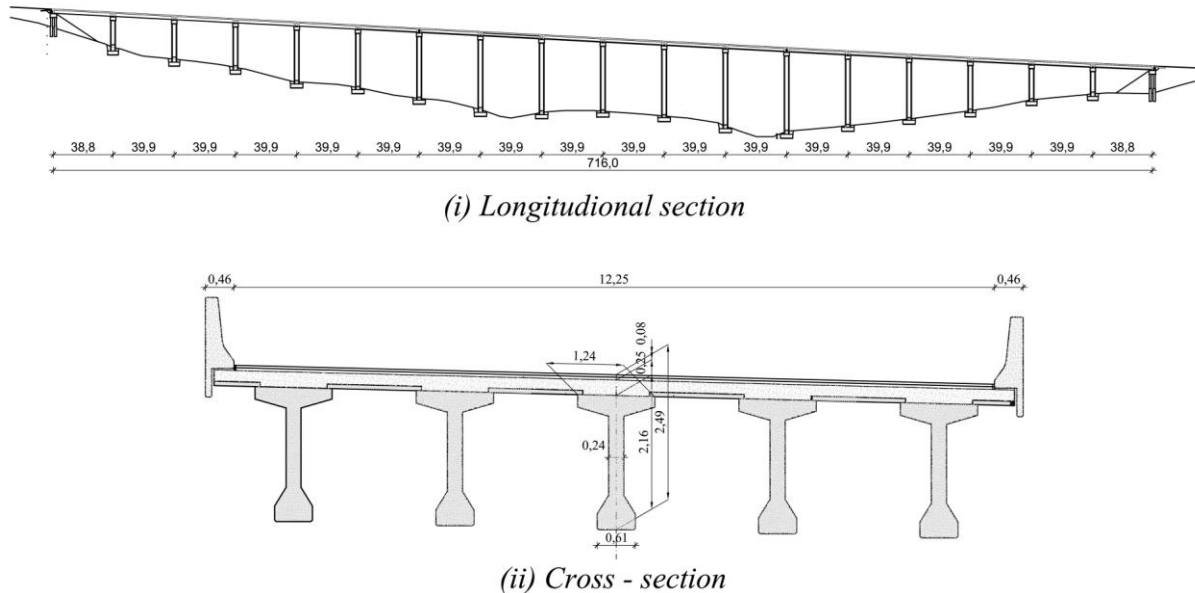


Fig. 1 Longitudinal and cross – section of the Severinske Drage Viaduct

The actual spans of main girders are:  $18\times 37.7+17\times 2.2=716$  m. Prefabricated girder height is 2.16 m. Top and bottom chords are 1.24 m and 0.61 m wide, respectively. Each girder has four prestressed cables. The initial force at the press is 2460 kN for each cable. Average girder mass is 96 t. Total bridge deck is 0.25 m thick and consists of a 0.08 m thick prefabricated part and a 0.17 m thick monolithic part. The span structure is supported by piers and abutments via conventional elastomeric bearings. Piers are 20-55 m high.



Fig. 2 Appearance of the Severinske Drage Viaduct in construction

### 3.2 The Kličevica Bridge

The longitudinal and cross-section of the bridge are shown in Fig. 3 (Radnić, 2004). In regard to the cross-section, the bridge has two separate bridge decks. The span structure consists of 4 spans as follows:  $40+2\times 50+40 = 180$  m. The span structure is supported by supports via conventional elastomeric bearings. Prefabricated girder height is 2.4 m. Average mass of girder with 50 m span is 140 t. Top and bottom chords are 2.55 m and 0.64 m wide, respectively. Girders in end spans are prestressed by three cables, each cable with the force of 2600 kN at the press. Girders in middle spans are prestressed by four cables. Monolithic part of the bridge deck is 0.2 m thick and made composite with the girder top chord. Piers are 24-45.5 m high. Appearance of the bridge in construction is shown in Fig. 4.

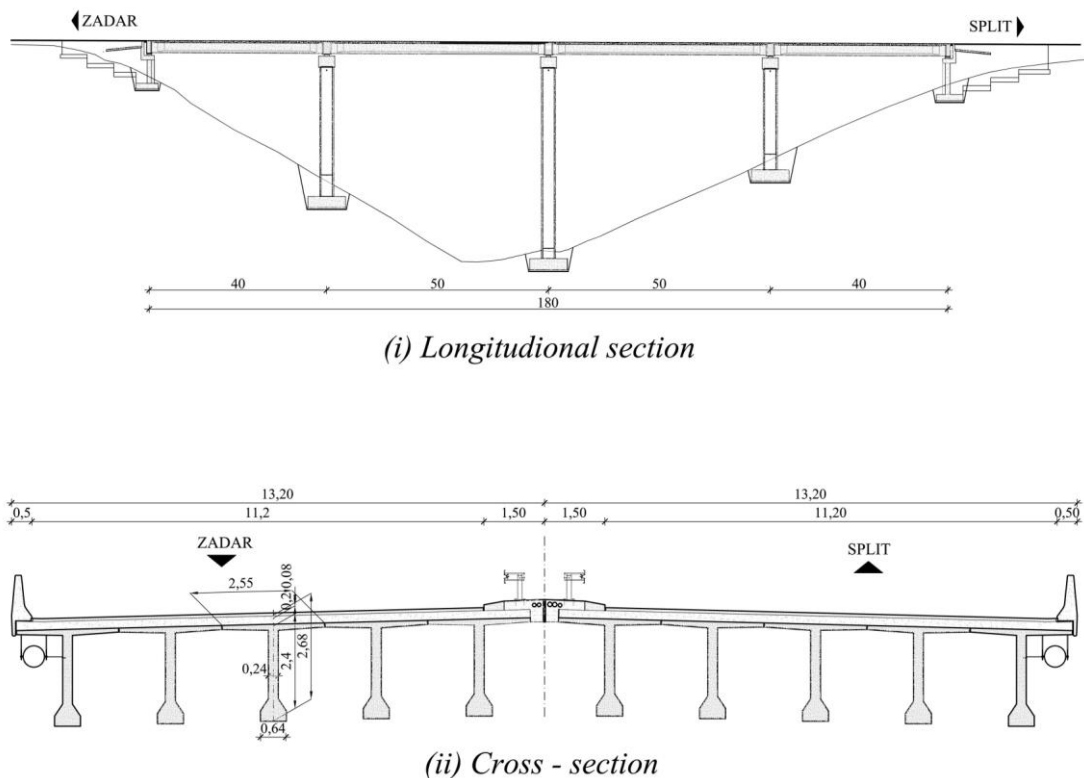


Fig. 3 Longitudinal and cross – section of the Kličevica Bridge



Fig. 4 Appearance of the Kličevica Bridge in construction

### 3.3 The Dabar Bridge

The longitudinal and cross-section of the bridge are shown in Fig. 5 (Radnić, 2005). The appearance of the bridge in construction is shown in Fig. 6. In regard to the cross-section, the bridge has two separate bridge decks. The span structure consists of 7 spans as follows:  $40+5 \times 50+40=330$  m. Above the supports  $U_1$ ,  $U_2$ ,  $S_1$  and  $S_6$ , the span structure is laid on pot bearings, mobile in longitudinal direction. Piers  $S_2$ ,  $S_3$ ,  $S_4$  and  $S_5$  have rigid connection with the span structure. Longitudinal girders, as well as other span structure solutions, are analogue to those for the Kličevica Bridge. Piers are 15.6-62.8 m high.

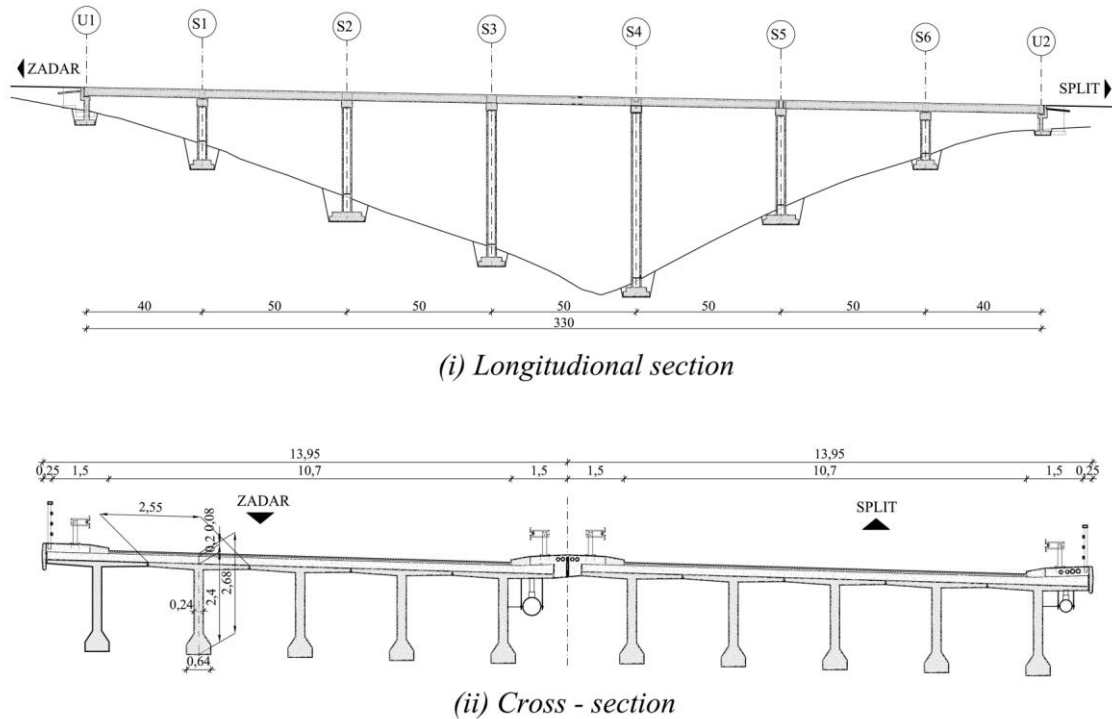


Fig. 5 Longitudinal and cross – section of the Dabar Bridge



Fig. 6 Appearance of the Dabar Bridge in construction

#### **4. CONCLUSION**

Concrete girder bridges with prefabricated longitudinal girders longer than about 35 m, require much more attention in design and construction than short prefabricated girders. The limit length of prefabricated girders is about 65 m, with the limit mass of about 300 t. The girder cross-section dimensions and mass, as well as number and bearing capacity of cables, increase with the increase in girder length. For continuous girders of long span, the limiting factors are usually compressive stresses of concrete in girder bottom chord above the piers. Cable at the ends of those prefabricated girders shall be anchored above the top edge of cross-section core, so that prestressing force does not increase compressive stresses in girder bottom chord. For long girders, particular attention shall be given to detail solutions, reinforcement and cable positioning, as well as girder fabrication and assembly.

#### **5. REFERENCES**

- Randić, J. (2000), "Final and construction design of the Severinske Drage Viaduct", IKON d.o.o. Split, (in Croatian).
- Radnić, J. (2004), "Final and construction design of the Kličevica Bridge", Civil Engineering Institute of Croatia – regional Unit in Split (IGH PC Split), (in Croatian).
- Radnić, J. (2005), "Final and construction design of the Dabar Bridge", Civil Engineering Institute of Croatia – regional Unit in Split (IGH PC Split), (in Croatian).

## CONCRETE SLAB WITH INTEGRATED INSTALLATIONS

*Andreas E. Kainz, Stefan L. Burtscher, Johann Kollegger  
Vienna University of Technology – Institute for Structural Engineering, Austria  
A-1040 Wien, Karlsplatz 13/212  
[sek212@pop.tuwien.ac.at](mailto:sek212@pop.tuwien.ac.at)*

### SUMMARY

A new slab system was developed, which allows large and easily accessible installations. This goal was achieved by integrating the building services into the slab structure instead of a suspended ceiling or false floor. The load carrying structure consists of a thin concrete slab connected to girders on the upper side. The girders are produced with large openings, to produce ducts for the installations. On top of the girders plates that can be removed establish the floor. Therefore the installations are easily accessible. Since the installation is integrated into the slab structure the load carrying structure can be higher than in conventional floor systems, while the overall height is still smaller. The increased structural height allows for larger spans.

### 1. INTRODUCTION

At the Institute for Structural Engineering an optimized slab system for department stores, industrial and office buildings is under investigation. For such buildings a lot of installations are necessary and a high degree of flexibility is desirable. The developed slab system is considering these high requirements and the improvements in contrast to conventional systems are

- reducing the overall height of the load carrying and installation parts.
- easier accessibility and higher flexibility of the installations.
- allowing for larger spans.
- lower self weight.

Installation in conventional slab systems are discussed first. The schematic representation of the systems discussed, is given in Fig. 1. Most often the installations are positioned in the floor construction embedded in a layer of sand. The disadvantage is that the floor has to be destroyed, when the installations have to be accessed. Another more flexible option is to produce a false floor system, where the floor can easily be removed. Then, the accesses and the repositioning of the installation is easy. When installations with large dimensions are required a suspended ceiling is usually chosen. A high degree of flexibility and easy accesses are possible.

The load carrying components and the space that is occupied by the installations are existing independently of each other. In order to keep the overall height small in conventional systems it is necessary to optimize both parts independently.



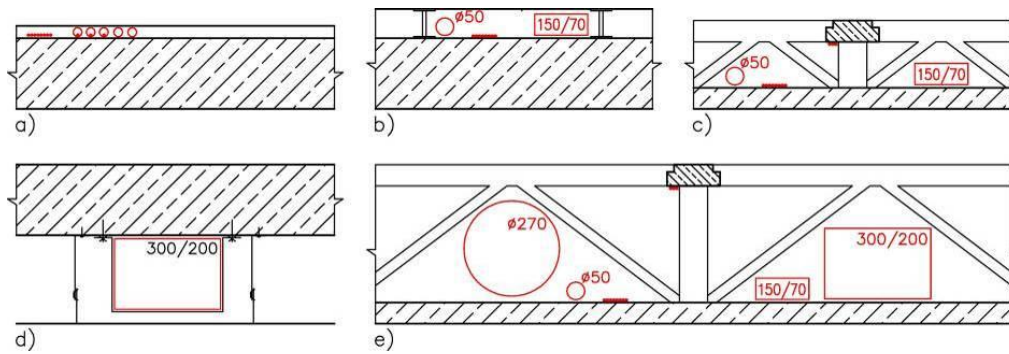


Fig. 1 Installations in different slab systems

- a) Installations in a layer of sand b) false floor system c) slab for installation  
d) Slab with a suspended ceiling e) slab for installations for large installations

This is in contrast to the new system proposed, where the space occupied by the installations is integrated into the plate. The load carrying structure can be much higher, while the overall height can still be lower than in conventional systems. The load carrying structure is not made of a massive plate, but is made up of a girder grid with a plate on the bottom. The girders can have the form of a framework with large openings. Figs. 1c and 1e show one example for small installations and another for large installations. In Fig. 2 a point supported slab with a girder grid and a thin plate at the bottom is shown. The girders show large openings to produce ducts for the installations. The girders are covered with plates, that are usually used for false floor systems and can be easily removed.

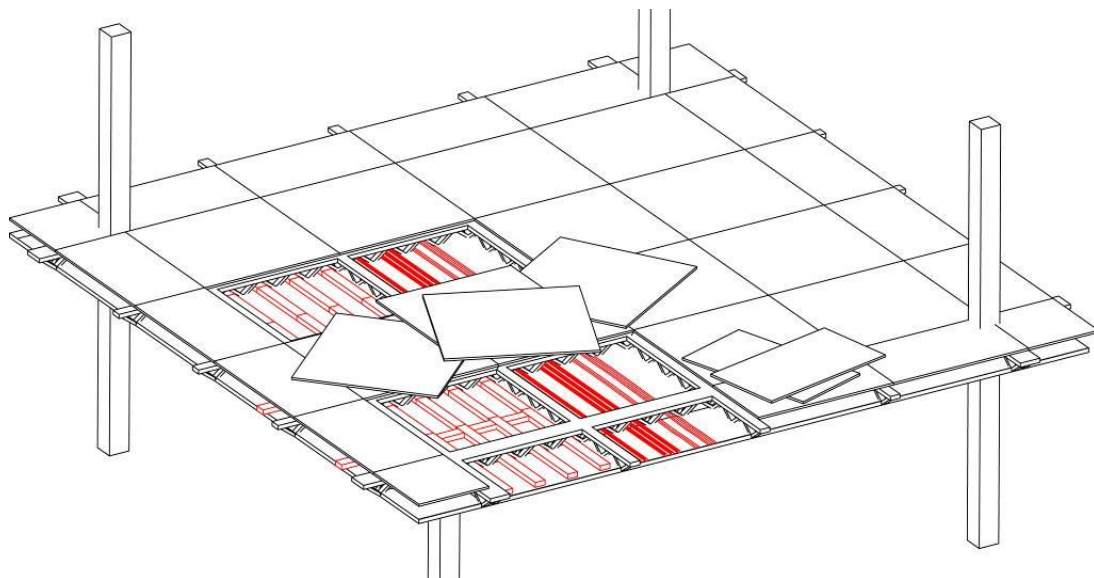


Fig. 2 Slab for installations

## 2. LAYOUT OF THE SPECIMENS

In cooperation with Katzenberger Beton- und Fertigteilewerke GmbH, Graz and Gerasdorf, the slab system was designed, produced and tested. The length of the specimens was 16.80m and the width 2.40 m. The specimen 1 and 2 represent parts of a point supported slab, where the slab is founded on three supports (Fig. 3). Specimen 1 has one main span direction (Fig. 3, left), while specimen 2 (Fig. 3, right) shows a grid girder in two span directions. The load was

applied to the specimens in 6 locations, to simulate realistically the forces from the slab system.

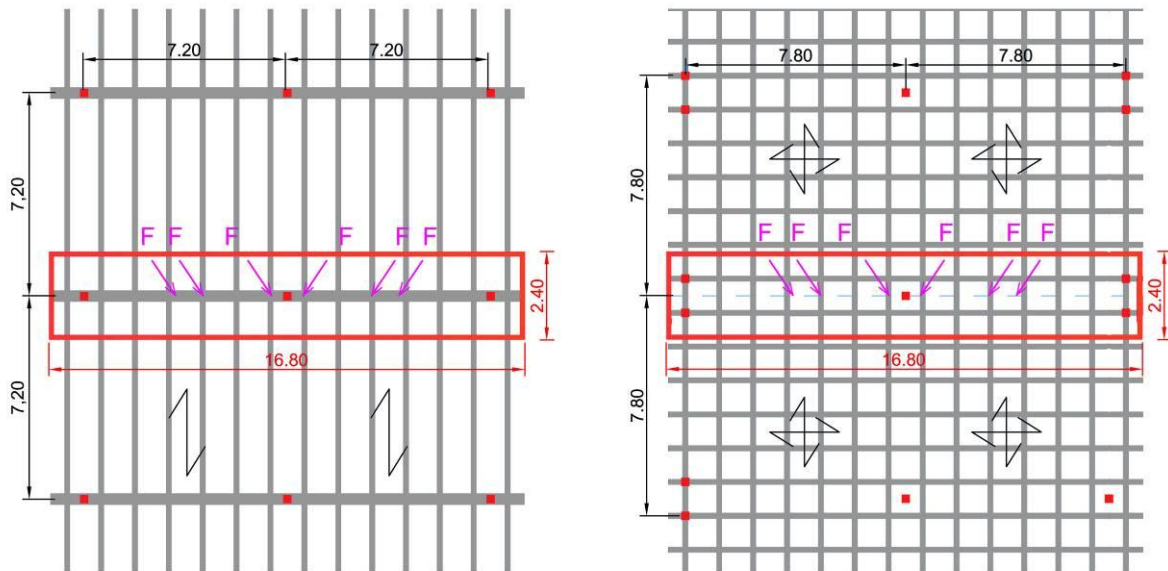


Fig. 3 Point supported slab system with specimen 1 (left) and 2 (right) colored in red and applied force positions.

Specimen 1 consists of one main girder made of reinforced concrete with a height and width of 40 cm. The cross section of the openings is 0.2 m<sup>2</sup>. The thickness of the plate was 10 cm. The grid girders of specimen 2 have the same dimensions in both span directions with a height of 40 cm and a width of 14 cm. The girders also contain steel profiles that were used as formwork during production. The thickness of the profiles was 4 mm. Fig. 4 shows a view of the girders of specimen 1 and 2 before testing.

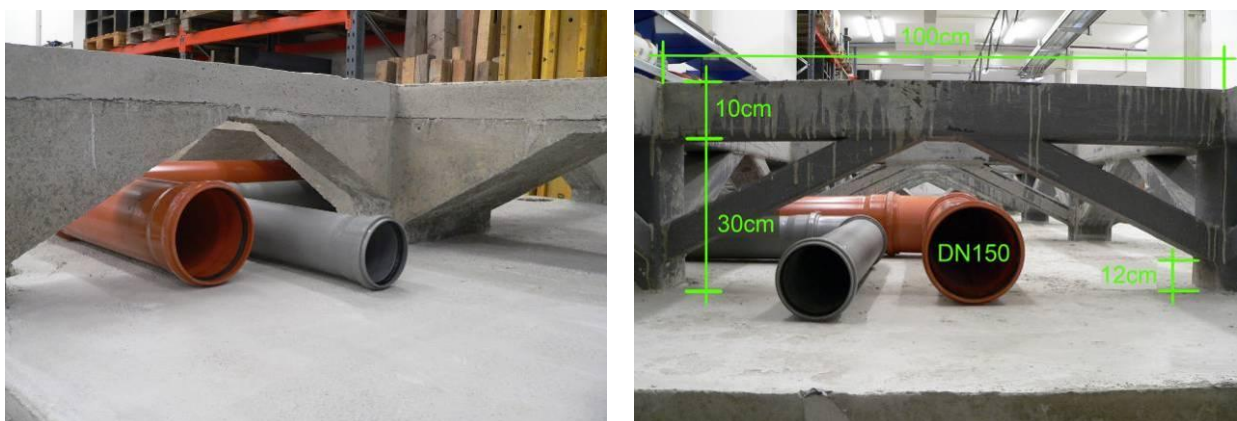


Fig. 4 Cross sections of specimen 1 (left) and specimen 2 (right).

### 3. PRODUCTION OF SPECIMENS

The specimens were produced of 7 prefabricated elements with dimensions of 2.40×2.40 m. Fig. 5 shows the prefabricated elements of specimen 1 and 2 positioned in a row and the reinforcement for the connection. The elements of both specimens were produced with a 5 cm thick reinforced concrete plate. The connection was established on site with reinforcement



bars and another 5 cm of concrete. At the final stage the thickness of the concrete plate was 10 cm. The girders of specimen 1 were produced similar to the plates by adding concrete and reinforcement bars on the top of the girder. For the connection of the girders it was necessary to produce a formwork on site. The girders of specimen 2 were made of steel profiles that are welded together. The connection between the prefabricated elements was made also on site with reinforcement bars and concrete. The steel profiles served as formwork and were filled with concrete over the whole girder height. Fig. 6 shows the specimens after connection of the prefabricated elements.

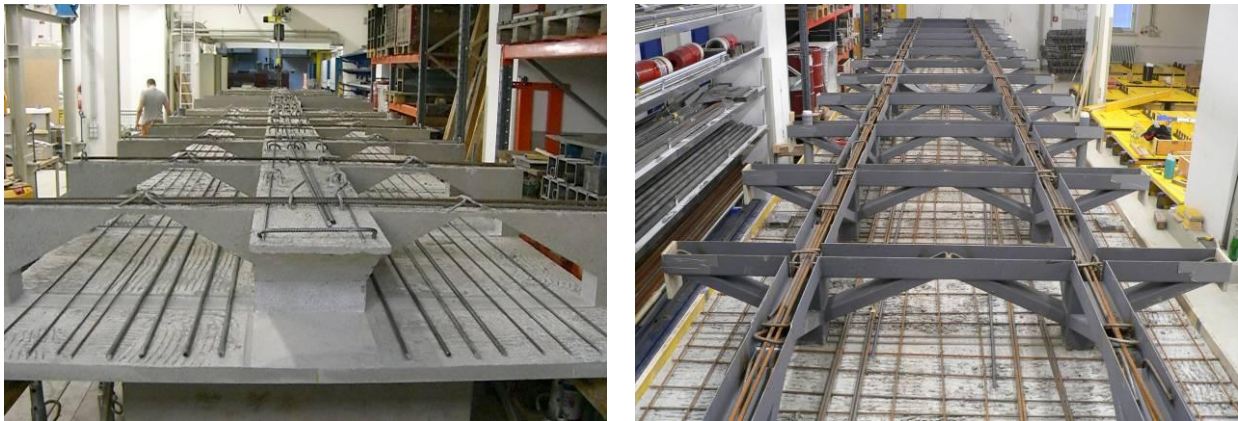


Fig. 5 Prefabricated elements of specimen 1 (left) and 2 (right) before casting with concrete



Fig. 6 Specimen 1 (left) and specimen 2 (right) after connection of the prefabricated elements

#### 4. EXPERIMENTAL RESULTS

Fig. 7 shows specimen 2 under high loads. Due to the high construction height, the large openings and the layout of the reinforcement shear was more critical than bending. The transfer of shear forces in the girder was critical due to the large openings. The failure in specimen 1 occurred close to the opening. Specimen 2 contained a higher amount of shear reinforcement and the concrete failed in compression at very high loads. The failure was at the upper side of the girder at midspan (Fig. 8).



Fig. 7 Specimen 2 during testing



Fig. 8 The failure of specimen 2 after ultimate load

## 5. CONCLUSIONS

The investigations showed that the concrete slab with integrated installations is able to satisfy high demands on flexibility of the installation and is also able to house installations that require a large space at a low overall height. Due to the low self weight and the high construction height large spans up to 10 or 12 m can be built at low cost with high quality.

## 6. ACKNOWLEDGEMENTS

The authors like to thank Fa. Katzenberger Fertigteilewerk GesmbH, for the production of the prefabricated elements and the Österreichische Forschungsförderungsgesellschaft mbH (FFG) for funding the project.

## 7. REFERENCES

Kollegger, J., Kainz, A. E., and Burtscher, S. L. (2006), „Flächige Beton - Tragkonstruktion

sowie Verfahren zur Herstellung derselben.“ *Austrian Patent application*  
Kollegger, J., Kainz, A. E., and Burtscher, S. L. (2007), „Flächige Beton - Tragkonstruktion  
sowie Verfahren zur Herstellung derselben.“ *PCT Patent application*

## **APPLICATION OF HIGH STRENGTH CONCRETE AT THE PRODUCTION OF RAILWAY UPPER LINE POLES.**

*János Beluzsár, Levente Beluzsár, Zoltán Sziklai*  
*Lábatlani Vasbetonipari Zrt.*  
*H-2541 Lábatlan*

### **SUMMARY**

Lábatlani Vasbetonipari Co. has installed technology for production of spun poles in 1994. The new technology has started with the production of pre-stressed spun poles for the electric distribution network and for the lighting system. Many kinds of round shape cross-section of spun poles are produced with this technology. The technology has offered good possibility to increase the strength of concrete. The cross-section of round-shape gives good opportunity to exploit the higher strength of concrete at relatively small production cost. The applied silica fume and additives have relatively increased the production costs of concrete, however, due to the smaller concrete demand the production is running at lower total cost. The laboratory tests and internal quality control has proved the proper concrete strength.

### **1. INTRODUCTION**

The spun concrete production technology process is well known and applied from the beginning of the precast concrete production. It is mainly used for the precast elements of circular shape. All over the world production capacities were installed, which fulfills the demand of the industry.

In Hungary this kind of production was neglected for a long period. The Lábatlani Vasbetonipari Co. after its privatisation invested for the spun production technology and started to supply this kind of elements as prestressed spun poles mainly for the electrical distribution network and as the lighting poles.

### **2. COMPACTION WITH SPINNING**

The spinning is a compaction method under pressure, where the compaction pressure occurs due to the centrifugal force. The size of the pressure depends on the speed of rotation and the distance of the spun concrete mass from the rotation axis. The average pressure on the wall of the mould can be calculated very easily from the following equation:

$$p_t = 2,89 \cdot 10^{-8} \cdot d \cdot r \cdot n^2 \left( \frac{kp}{cm^2} \right) \quad (1)$$

where:

d - wall thickness (cm)

r - the distance of the inner wall surface from the mould axis (cm)

n - speed of rotation (1/ min).

The necessary pressure depends on the consistency of the concrete. To find the right concrete parameters a lot of test is needed. It is an optimum searching among the w/c value, cement content and additives of the concrete mixture.

#### *Compaction carried out on the vibrating table*

During the compaction on the vibrating table the air bubbles will be driven out by the vibration pressure. The high strength concretes are produced from concrete mixtures, which have surplus cement paste. In that way the aggregate is “swimming” in the cement paste. In this paste the grain has its own frequency during the compaction process. The grain creates a paste skin around it, as long as there is surplus cement paste.

#### *Compaction carried out in the spinning process*

The aggregate grain has bigger specific weight as the cement paste, that's why the aggregate particles will move towards the wall of moulds creating in the wall some kind of aggregate skeleton. First the air bubble and then the surplus of the cement paste will be pressed out from the skeleton, remains inside the skeleton the only cement paste which can fill the space between the aggregate grains. In that way the well designed spun concrete consists only the cement paste for the saturation, the surplus will be gathered in the inner surface of the element, and can be removed easily. There is an advantage of the spinning, the outside surface of the elements have optimum concrete mixture, closed surface almost like glass.

### **3. THE CONCRETE**

The size of the aggregate depends on the wall thickness and the reinforcement of the elements. The maximum size of aggregate has to go through the reinforcement. The grading curve has to ensure minimum free space in the aggregate skeleton. The w/c factor depends on the concrete strength, normally it is 0.4. Consistency of the concrete mixture is 45-50 cm measuring on flow table. Of course as the consistency and the cement content can be chosen as the wall thickness and the pressure determined.

There are different demands against the concrete mixture:

- During the filling phase, high consistency is needed; the concrete has to move alongside the mould axis.
- During the compaction phase the constituents of concrete move in radial direction. The first the aggregate skeleton will occur, the air and the surplus of cement paste will be driven out of the skeleton to the inner surface of the element. At the same time the free water which remains in the cement paste will be pressed out. The w/c value in the skeleton will be higher as was planned.

There are some reports about the concrete of w/c = 0.5-0.6 after spinning the w/c value of concrete will be 0.38-0.42. The surplus of water and cement paste “the slum” can be removed from the mould.

### **4. SPECIFIC CHARACTERISTIC OF THE SPUN CONCRETE**

The spinning is one of the most effective compaction methods. The strength of the spun concrete is 10-30 % higher as the strength of the basic mixture. This increment can be taken into account during the calculation process according to national standard for example: DIN 4228-89.

This increment in our case was checked by the ÉMI at 1996. There were test specimens 300 mm high and diameter 150 mm produced on vibrating table or spinning process. The result, that the spun specimens have 18 % higher compressive strength as the vibrated.

From the beginning of 2000 years we started to produce high strength concrete.

The applied concretes are certified by the LGA München. The test results are as follows:

Tab. 1 Data of the concrete mixture C 80/95 (2004)

	Quality			Mixture
		kg/m <sup>3</sup>	Lit/m <sup>3</sup>	kg/m <sup>3</sup>
Cement	C52.5	500	161	
Water		150	150	
Aggregate	0/4	777	294	
	5/12	706	262	
	12/20	265	98	
Micro silica	Pulver 940 U	40	17.1	
Additive	FM 28	20	16.8	
Air		0	1.1	
<b>Total</b>		<b>2458</b>	<b>1000</b>	<b>2461</b>

The LGA München continuously checks the production. The test result is in the Tab. 2.

Tab. 2 Data of the concrete mixture C 80/95 (2004)

		Density	Compressive strength	Average
Year	No	kg/mm <sup>3</sup>	N/mm <sup>2</sup>	
2003	1	2430	103	<b>101,7</b>
	2	2430	102	
	3	2430	100	
2005	1	2500	123	<b>121</b>
	2	2490	121	
	3	2490	118.5	
2006	1	2460	112.5	<b>112</b>
	2	2450	113	
	3	2460	111	

## 5. SPINNING AT THE FACTORY OF LÁBATLAN

The technology for spun concrete was installed in 1994 in Lábatlan, suitable for the production max 16 m long spun poles, the lifting capacity 2×12.5 Mp bridge crane, so max 24 Mp total weight can be produced. On the spinning machine can be produce products up to 24 m length, in that case the heat curing needs special solution. There are bottom and top parts of the mould, which will be fixed together with screws. There are insulating strips between the two parts of moulds to prevent the leakage of concrete during the production process. The moulds are connected from 2 m long sections.

The production process is as follows:

- the empty moulds will be cleaned and oiled,
- the inserts will be fixed in the bottom part of moulds,
- the anchorage heads will be fixed both ends of the moulds,



- the pre stressing wires or strands and the spiral cage will be placed, and then the pre stressing wires will be slightly prestressed,
- the moulds will be filled with concrete and closed with the top of moulds,
- the prepared moulds will be spun on the spinning machine, during this process the concrete will be distributed along the wall of moulds and compacted, After the process the surplus of concrete will be removed from the moulds,
- after eight hours heat curing the elements will be remoulded.

## 6. HIGH STRENGTH CONCRETE AT THE SPUN RAILWAY UPPER LINE POLES

The railway upper line poles are standard products of the spinning technology. It has 1 to 15 conicity and 30 mm concrete cover on the pre stressing wires. Increasing the concrete strength offers lower transport cost and in that way lower total cost. In order to exploit the benefit of the spinning we increase the concrete strength using micro silica fume.

The recalculation is based on the principle: the top load remains the same for both poles type-8 kN.

We are able to decrease the weight of poles 14 %. Now there are mass production for railway upper line poles where the concrete strength is C80/95. The manufacturing cost of poles is a slightly higher at the high strength poles (Tab. 3).

There is a chance to reduce further the material cost replacing the microsilica with limestone powder. Our experience shows that there is a possibility to produce the same practical value poles at lower manufacturing cost (Tab. 4).

Tab. 3 Manufacturing cost at the poles produced from C 50/60 and C 80/95 concrete

	C50/60			C80/95 – (with Silica)		
	Kg/poles	HUF/kg	HUF	Kg/poles	HUF/kg	HUF
Cement (CEM 52,5)	364.7	22.4	8169.3	289.5	22.4	6484.8
Water	114.2	0.12	13.7	86.8	0.12	10.4
Aggregate 0/4	414	1	414	449.8	1	449.8
4/8	355	1	355	-	-	-
8/16	414	1	414	-	-	-
5/12	-	-	-	408.7	1.98	809.2
12/20	-	-	-	153.4	1.83	280.7
Additives FM 28	-	-	-	11.58	260	3010.8
Stabiment FM 95 E	4.09	217	887.5	-	-	-
Micro silica	-	-	-	23.16	184	4261.4
Concrete weight (kg)	1666			1423		
Cost of concrete			10253.5			15307.1
Feszítőhuzal - 7/16"	84	203.6	17102.4	84	203.6	17102.4
Spiral Ø3mm	12.78	144	1840.3	11.47	144	1651.7
Támgyűrű Ø8mm	4.29	130	527.7	2.16	130	280.8
Steel weight (kg)	101.1			97.63		
Cost of steel			19470.4			19034.9
Pole weight (kg)	1767			1521		
Cost of poles			29723.9			34342

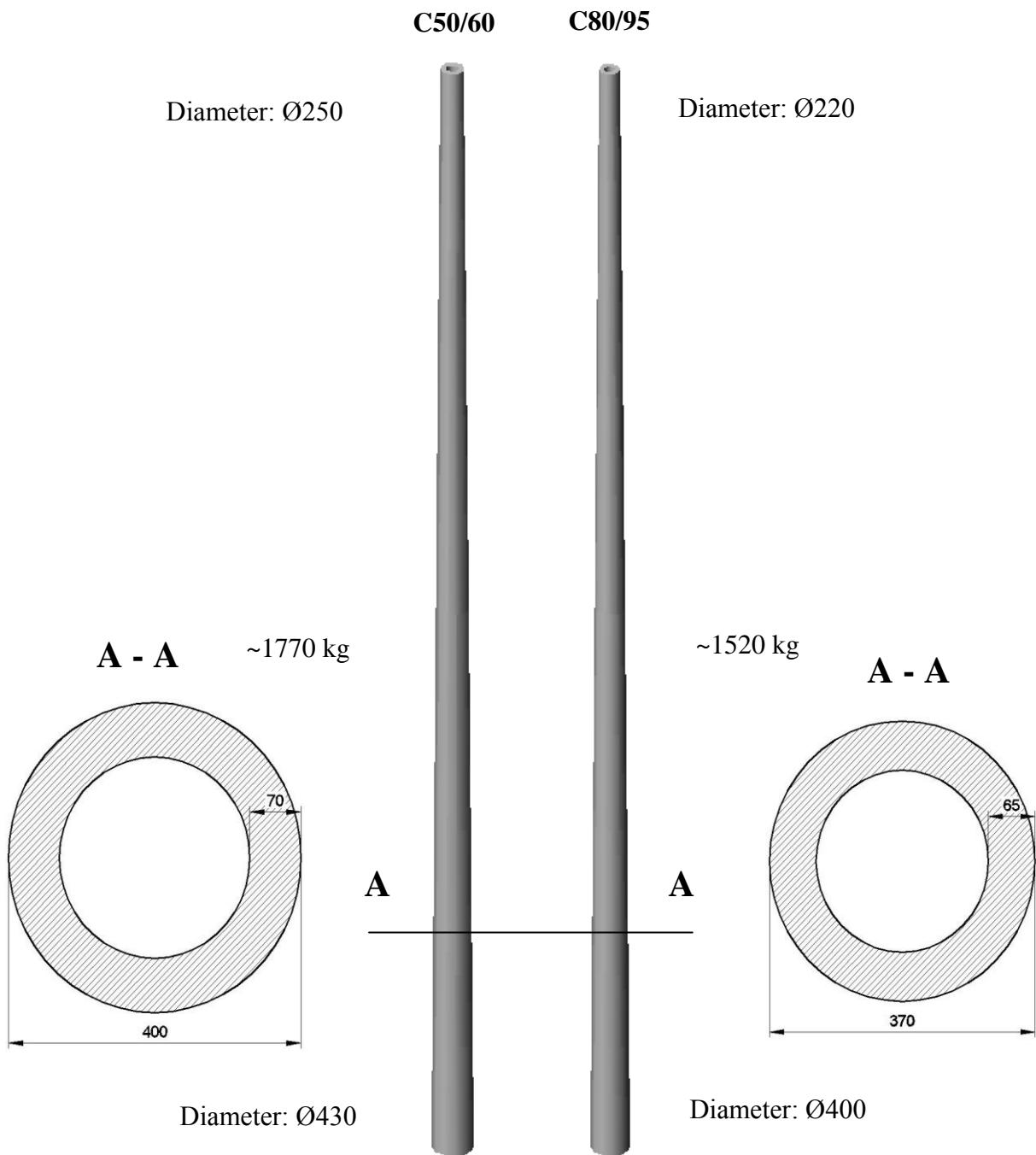
Tab. 4 Manufacturing cost of poles produced with limestone powder

	C80/95 – (without Silica)		
	Kg/poles	HUF/kg	HUF
Cement (CEM 52,5)	289.5	22.4	6484.8
Water	86.8	0.12	10.4
Aggregate 0/4	463.7	1	463.7
4/8	-	-	-
8/16	-	-	-
5/12	421.5	1.98	834.6
12/20	158.1	1.83	289.3
Muraplast FK802	2.89	481	13090.1
Stabiment FM 95 E			
Micro silica	-	-	-
Concrete weight (kg)	1423		
Cost of concrete			9472.9
Feszítőhuzal - 7/16''	84	203.6	17102.4
Spiral Ø3mm	11.47	144	1651.7
Támgyűrű Ø8mm	2.16	130	280.8
Steel weight (kg)	97.63		
Cost of steel			19034.9
Pole weight (kg)	1521		
Cost of poles			28507.8

## 7. CONCLUSION

The spinning technology has given a possibility to replace the vibrated poles with spun poles. The new technology extends the applied concrete strength to the higher range. It is more economical and through the durability the products have longer lifetime. There is a chance to reduce further the cost replacing the expensive microsilica with limestone powder.





## **DURABILITY-DESIGN OF PRECAST CONCRETE MEMBERS**

*Kálmán Koris*

*Budapest University of Technology and Economics, Hungary*

*H-1111 Budapest Bertalan L. u. 2. [koris@vbt.bme.hu](mailto:koris@vbt.bme.hu)*

### **SUMMARY**

Aspects of durability are important during the design of engineering structures. A possible method for the durability design is the probabilistic approach considering changes of material properties and structural dimensions during time. This paper is dealing with durability design of pre-cast concrete members using the stochastic finite element method. The use of the theoretical method is also presented by a numerical example.

### **1. INTRODUCTION**

The importance of issues concerning durability during the design process is continuously increasing. Reduction of maintenance costs is becoming a more and more important aspect in case of larger projects. Maintenance costs are partially generated by deterioration of structural elements due to usage, which is usually difficult to predict. Rheological changes of material properties due to environmental effects can be however modeled and this change can be considered during the design. The ability of comparing the load carrying capacity with the expected loads at any point of time can help us design structures which are statically adequate during the whole lifetime. Design codes generally include directives for durability design, however it can be sometimes necessary to perform more precise calculation on the load carrying capacity in a desired point of time.

Design of prefabricated, reinforced concrete structures is a possible field for such detailed calculations to assure durability. The demand of different prefabricated, reinforced and prestressed concrete members significantly increased during the last decade. Considering the large number of produced elements, the amount of work and materials can be optimized by the application of durability design. We intend to evaluate the stochastic distribution of load carrying capacity of pre-cast concrete members in different points of time and use them for durability design. The implemented method can help us design prefabricated elements with appropriate load carrying capacity during the desired lifetime.

### **2. CALCULATING THE PROBABILITY OF FAILURE OF A STRUCTURE**

#### **2.1 Explanation of probability of failure**

The ability of a structure to resist the acting loads can be described by a performance function. This function can be usually written as:

$$G = R - S,$$

where structural resistance ( $R$ ) and the loads ( $S$ ) are deterministic functions of certain parameters. At a positive value of  $G$  the structure is functioning according to the expectations, negative value refers to structural failure and in case of  $G = 0$  the structure is exactly in

ultimate limit state. Load carrying capacity of a structure and the acting loads are probabilistic values, thus the  $G$  performance function will be a probabilistic value too and it can be described by an  $F_G$  distribution function. Assuming that the parameters of the distribution are known, the probability of failure ( $p_G$ ) can be calculated as:

$$p_G = \int_{-\infty}^0 f(G) dG,$$

where  $f(G)$  is the probability density function of  $G$ . In case of engineering structures, the system is usually too complex thus we are not able to evaluate the probability of failure by one performance function. The system must be decomposed to smaller subsystems, the performance functions of the subsystems must be calculated separately and the failure of the structure can be evaluated from the combination of these separate functions. The way of combination depends on the type of the system. We can distinguish serial, parallel and mixed systems. However in case of buildings and other structures, these subsystems are statistically not independent, thus the application of the above method could be difficult. A possible solution for such systems is the geometrical approach, where we use the geometry of the range of integration. In this case the  $G$  performance function can be written as linear function of  $x_i$  normally distributed random variables:

$$G = c_0 + c_1 x_1 + c_2 x_2 + \dots + c_n x_n = c_0 + \underline{c}^T \underline{x}$$

Assuming that  $M_x$  and  $s_x$  are the mean value and standard deviation of the  $x_i$  variable,  $\rho_{ij}$  is the coefficient of correlation between  $x_i$  and  $x_j$  as well as  $M_G$  and  $s_G$  are the mean value and standard deviation of  $G$  performance function. Let us standardize the  $x_i$  random variables:

$$\underline{r} = \underline{L}^{-1} \cdot \underline{T}^T \cdot (\underline{x} - \underline{M}_x),$$

where  $\underline{L}$  is a diagonal matrix composed from the eigenvalues of the covariance matrix and columns of matrix  $\underline{T}$  are the eigenvectors of covariance matrix. Using the standardized variables, the performance function can be written as:

$$G = c_0 + \underline{c}^T (\underline{L} \cdot \underline{r} + \underline{M}_x)$$

With the use of standardized variables, the  $G = 0$  ultimate limit state defines a hypersurface of  $n-1$  dimensions in a space of  $n$  dimensions. The closest point of this surface to the origin of coordinates means the failure of highest probability. The minimum distance between the origin and the hypersurface is (Bolotin, 1970):

$$\frac{c_0 + \underline{c}^T \underline{M}_x}{\sqrt{\underline{c}^T \cdot \underline{T} \cdot \underline{L} \cdot \underline{L} \cdot \underline{T}^T \cdot \underline{c}}} = \frac{M_G}{s_G} = \beta,$$

where  $\beta$  is usually called the safety index. Fig. 1 represents the geometrical explanation of safety index where the  $G$  performance function is linear function of two standardized random variables ( $r_1, r_2$ ).

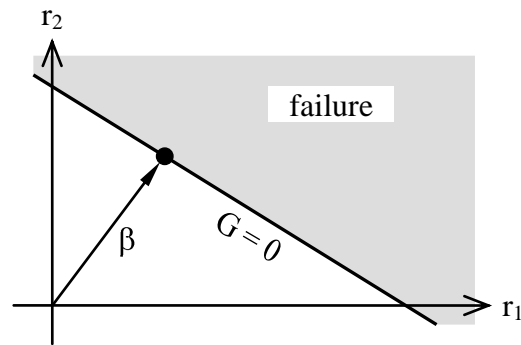


Fig. 1 Geometrical explanation of safety index ( $\beta$ )

The probability of failure of the structure can be finally expressed as (Bolotin, 1970):

$$p_G = P[G < 0] = \Phi\left(\frac{0 - M_G}{s_G}\right) = \Phi(-\beta) = 1 - \Phi(\beta)$$

The performance function is indeed non-linear function of the random variables, thus the hypersurface is not flat. However, an appropriate solution for the probability of failure can be achieved by first order estimation where the hypersurface is linearized in the point of highest failure probability (Bolotin, 1970). The reliability of the structure can be described as  $p_G \approx \Phi(-\beta)$ .

## 2. 2 Evaluating stochastic parameters for the distribution of structural resistance

To be able to calculate the probability of failure we need to know the stochastic distribution of structural resistance and the load effect. We are dealing with the stochastic analysis of the structural resistance only, assuming that the distribution of acting loads is known. Parameters for the distribution of resistance can be derived by different analytical or numerical methods. The reliability analysis (second moment analysis) is a common analytical solution for the problem while the Monte-Carlo simulation is the most prevalent numerical approach. These methods have, however, certain disadvantages. The reliability analysis compares cross-sectional resistance with locally acting forces only while the Monte Carlo method can be very time consuming in case of complex structures.

These problems can be eliminated by the use of stochastic finite element method (SFEM). The stochastic finite element method is an extension of the deterministic finite element method to accommodate random functions. This method allows the comparison of the acting loads with structural resistance at system level. Major advantage of SFEM is that the multivariate distribution function of the resistance is not needed to be known, but only the first two moments. It is computationally less expensive than the Monte Carlo simulation, but it is still accurate enough in structural engineering. The limitation of SFEM is that the uncertainties cannot be too large. The allowed maximum coefficient of variation is around 15%. Application of prefabricated concrete elements can be complied with this condition.

According to the previous, the first two parameters (mean value and standard deviation) of the distribution of resistance must be evaluated in order to be able to calculate the probability of failure (Mist eth, 2001). The sizing of prefabricated elements can be carried out by the comparison of calculated and permitted probabilities of failure. The permitted value can be

determined in different ways. We might use the desired level of probability given by design standards or we can evaluate a different value for permitted probability (e.g. optimum risk) according to the current conditions (Mistéth, 2001).

### 3. LOAD CARRYING CAPACITY OF STRUCTURAL ELEMENTS

#### 3.1 Application of finite element method for beams

The finite element method (FEM) is used to calculate the deflections of structural members subjected to compression (e.g. prestressing) and bending (Bojtár, Gáspár, 2003). To obtain the mean value of the structural resistance, the mean values of structural dimensions and material properties are used for the calculation. Structural members are modeled by bar elements with deformations of order three. Shear deformations are significantly smaller than flexural deformations therefore they are neglected in the analysis. Deformation functions are approximated with  $C^{(0)}$  continuous functions (Lagrange polynomials) since the equation for the potential energy contains the first order derivatives of these functions only.

#### 3.2 Design method not involving the modular ratio

While no forming of cracks has occurred in the concrete, the material can be considered homogenous and isotropic. The reinforcement can be neglected during the calculation of deformations. Due to the low level of stresses, linear stress-strain relationship can be used. The stiffness matrix of a finite element holds elastic cross-sectional properties, resulting in a linear connection between forces and deformations. After forming of cracks in concrete, the problem cannot be handled with assumption of plane state of stress. Stiffness of the structure significantly decreases, the material properties, such as Young modulus cannot be interpreted. Any kind of deformation will be affected by all kinds of stresses, thus the stiffness properties will depend on the acting forces as well. Under these conditions, deformations can be calculated using the method of increments. The applied load is single-parameter load as presented on Fig. 2. The value of the load-intensity is increased in steps until the structure fails. The chord of the stiffness matrix is calculated and applied for each load increment.

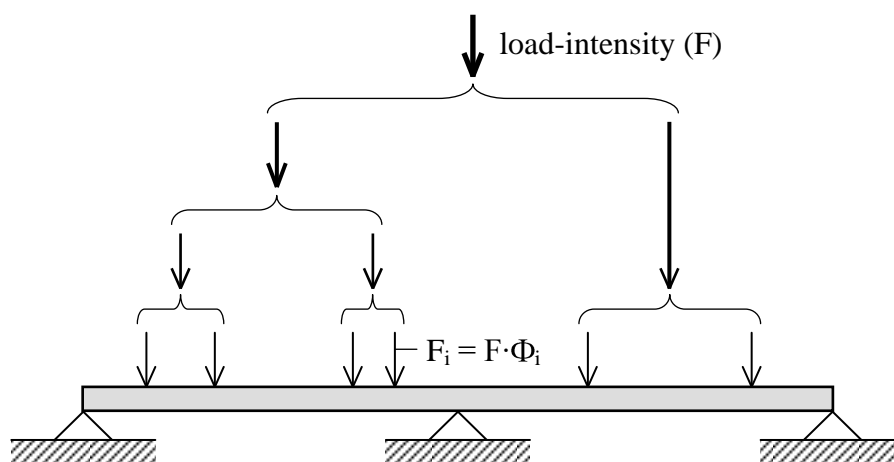


Fig. 2 Single-parameter load with  $\Phi$  load-distribution function

A parabolic-elastic stress-strain relation for the concrete can be used for the analysis. The behavior of reinforcing steel bars and prestressing tendons can be described with bilinear stress-strain relation.

#### 4. SCATTER OF LOAD CARRYING CAPACITY

Material properties and geometrical sizes are fluctuating around an expected value ( $M_x$ ) due to inhomogeneity of materials and errors in manufacturing. These fluctuations can be described by a continuous random variable  $\alpha(\zeta)$ . Scatter of any material property or geometrical size ( $x$ ) can be described as (Eibl, Schmidt-Hurtienne, 1995):

$$x = M_x \cdot [1 + \alpha(\zeta)]$$

The continuous  $\alpha(\zeta)$  function is discretized along the finite elements by the use of stochastic finite element method. The  $\alpha(\zeta)$  function can be approximated by interpolation functions ( $N_i$ ) for any given finite element:

$$\alpha(\xi) = \sum_{i=1}^n N_i(\xi) \alpha_i, \quad 0 \leq \xi \leq 1$$

It is reasonable to assume a constant shape for the approximate  $\alpha^{(k)}$  function within separate elements ( $N_i(\xi) = 1$ ) so the probabilistic degree of freedom of the system will be equal to the number of finite elements. The covariance of the structural resistance can be expressed by the covariance of input parameters. The covariance ( $\underline{C}_x$ ) of a given  $x$  input parameter can be written in the following form:

$$\underline{C}_x = \underline{s}_x \cdot \underline{C}_\rho \cdot \underline{s}_x^T$$

where  $\underline{s}_x$  includes the standard deviation of  $x$  in the diagonal and  $\underline{C}_\rho$  is the correlation matrix. The correlation between different elements can be described by an exponentially decaying function of the distance between two elements and the length of correlation. If the  $\underline{q}$  load vector is function of any  $x$  random parameter (standard deviation of  $x$  is  $s_x$ ), its standard deviation can be approximately expressed by the first term of Taylor's series:

$$\underline{s}_q \cong \frac{\partial \underline{q}}{\partial x} \cdot s_x$$

Using the above equations, the covariance of the load vector can be expressed as:

$$\underline{C}_q = \frac{\partial \underline{q}}{\partial x} \cdot \underline{C}_x \cdot \frac{\partial \underline{q}}{\partial x}^T$$

If we evaluate the covariance of the load vector for the highest load the structure is able to resist, we practically get the covariance matrix of structural resistance itself. Standard deviation of the resistance can be obtained as square root of the diagonal elements of  $\underline{C}_q$ .

This method is, however, difficult to be directly applied, so we use an extended method for the practical analysis suggested by Eibl and Schmidt-Hurtienne, 1995.

## 5. EXAMPLE OF APPLICATION

Fig. 3 represents the change of the probability of failure for a one-span prefabricated concrete beam over a certain period of time, evaluated by SFEM. According to Eurocode, the quality of concrete is C40/50 and the quality of reinforcement is S500B. Height and width of the cross-section, value of concrete cover and the strength of concrete and steel were treated as random numbers. Mean values of random variables are presented on Fig. 3. Standard deviations of parameters and their changes during time were considered according to Koris, 1998 and Mistéth, 2001.

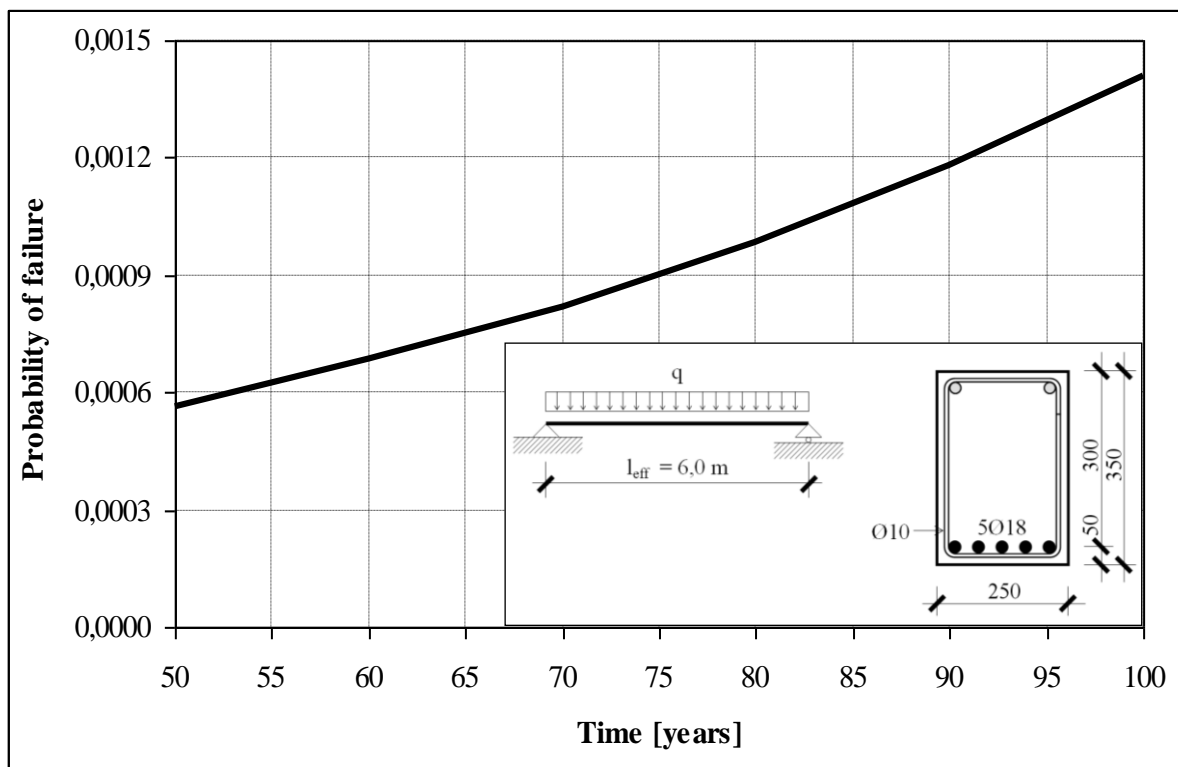


Fig. 3 Change of the probability of failure during time

## 6. SUMMARY

A method using probabilistic approach was presented for the durability design of prefabricated concrete members. The implemented method can be used for the design of precast elements with appropriate load carrying capacity during the desired lifetime. The use of the theoretical method was also presented by a numerical example.

## 7. REFERENCES

- Bolotin, V. V. (1970), "Static methods in the mechanics of structures", *Műszaki Könyvkiadó*.
- Koris, K. (1998), "Stochastic distribution of structural resistance of reinforced concrete beams", *Proceedings, 2nd International Ph.D. Symposium in Civil Engineering*, Budapest pp.127-134
- Eibl, J., Schmidt-Hurtienne, B. (1995), "Grundlagen für ein neues Sicherheitskonzept", *Bautechnik* 72(8), pp. 501-506
- Mistéth, E. (2001), "Design philosophy", *Akadémiai kiadó*, Budapest
- Bojtár, I., Gáspár, Zs. (2003): "Finale element method for engineers", TERC Kft.

## **APPLICATION POSSIBILITIES OF FIBRES IN PRECAST ELEMENTS**

*Dipl. Ing. Markus Schulz*

*KrampeHarex GmbH & Co. KG*

*Pferdekamp 6-8, D-59075 Hamm, Email: [markus.schulz@krampeharex.com](mailto:markus.schulz@krampeharex.com)*

*Internet: [www.krampeharex.com](http://www.krampeharex.com)*

### **1. INTRODUCTION**

The norming process for fibre concrete in Europe has undergone a continuous development over the past few years. The federal authorities in Germany issued a “Merkblatt Stahlfaserbeton” in October 2001 (DBV, 2001) a guideline for the general approval process of fibre concrete.

In March of 2002, the federal authorities in Austria published a general guideline (ÖVBB, 2002), which does not only deal with the application of fibre concrete but also with the utilization of polypropylene fibres in the segments for the purpose of fire protection as well as for the improvement of the shrinkage behaviour. Both guidelines are currently under review.

In Germany one can observe the development of fibre concrete from a commodity which was solely used for constructive purposes to a comprehensive construction material with a wide range of application purposes: production of load bearing elements, foundation slabs, walls and even steel fibre reinforced prestressed concrete beams.

### **2. FUNDAMENTALS**

The increasing acceptance and importance of steel fibres as reinforcement in Germany (DIB, 2005) was encouraged by higher requirements for the certification of fibres by the federal authorities. A few years before, one just had to prove that the fibres do not damage the concrete, nowadays one also has to prove the effectiveness. This can be the following:

- reduction of the shrinkage behaviour
- improvement of the mechanical features of the concrete
- reinforcement-function with static effects
- improvement of the fire resistance.

### **3. APPLICATION OF STEEL FIBRES**

Usually, steel fibres are deployed for reinforcement with static effects. In order to ensure the reinforcement-function, test must indicate a minimum post-cracking tensile strength of 1 N/mm<sup>2</sup> according to the German DBV (2001) guideline.

The effectiveness of steel fibres depends on their aspect ratio (length/diameter), the anchorage of the fibre and their tensile strength. However this is limited through the integration of the fibres and the workability of the fibre concrete. With an increasing aspect ratio special dosing equipment becomes necessary, it is possible to dose the fibres by a special integration machine or a dosing machine with automatic weighing (Fig. 1).





Fig. 1 Mixing and dosing machines for fibre reinforced concrete

Steel fibres are only one aspect of steel fibre concrete. The same dosage of identical fibres at a different concrete design leads to diverse results. Example: looking at the results of a fibre type DE 50/1.0 N (length: 50 mm, diameter: 1.0 mm) as absolute values, one can observe different results (up to 100% more/less in value) despite applying the same dosage. When the results are shown in percentage of the flexural tensile strength becomes obvious that the concretes themselves had different flexural strengths. The pure effect of the steel fibres was between 40 – 47%.

To produce an effective steel fibre concrete it is necessary to create a proper concrete design. That includes that the tensile strength of the steel fibres which has to be related to the strength of the concrete. To achieve a strongly ductile performance of the material the end hooks of the steel fibres must only be slowly embedded and pulled out of the concrete. Steel fibres with a standard tensile strength which are used in a high strength concrete will be broken instead of being pulled out slowly by applying high strength steel fibres in a standard concrete the fibres would be pulled out of the concrete (Fig. 2).



Fig. 2 Failure with fibre pull-out

Concretes for precast elements usually have higher strengths. This has to be considered when a suitable steel fibre shall be recommended. Tests with concrete for tubings have proved that steel fibres with higher diameters deliver higher equivalent flexural strength. Even if their dosage has to be increased up to 20% that solution was more economical. By increasing the tensile strength of the steel fibre it was possible to increase the equivalent flexural strength up to another 20%. The higher stiffness of thicker fibres enables to use only 15 – 20% more fibres especially for high quality concrete.

#### 4. STEEL FIBRE CONCRETE IN PRACTICE

Due to the properties of steel fibre concrete (the post-cracking level of the deflection curve is underneath the crack value) a limitation of the crack width is not possible with steel fibre concrete only. For steel fibre concrete the complete system has to be considered. In case of bending of foundation slabs for example the spring-effect of the substrate helps to obtain an equilibrium. In case of walls or tunnel shells the axial force helps to guarantee a defined compression zone. Therefore, non-brittle rupture can be obtained. For precast elements the future lies with the combination of steel fibres and conventional reinforcement. In this case the limitation the crack width can be calculated with steel fibre concrete too. The post-cracking tensile strength of the steel fibre concrete can be deducted from the tensile strength of the normal concrete. So it is possible to save up to 40% of the reinforcement which is normally necessary for limitation of the crack width. Moreover steel fibres can reduce or replace shear reinforcement at prestressed elements.

Prestressed precast trusses are produced successfully at Rekers Betonwerk GmbH & Co. KG. The shear reinforcement was further replaced by a middle strength KrampeHarex steel fibre. For the IKEA central store 780 beams each 20 m of length have been installed after an approval has been effected (Fig. 3).



Fig. 3 Steel fibre reinforced beams for the IKEA Central Store

#### 4. APPLICATION OF PP FIBRES

First of all polypropylene fibres significantly reduce the risk of shrinkage cracking. Test which have been carried out for an approval in Germany at the Ruhr University of Bochum confirming that the fibre type “PM” reduces the risk of shrinkage cracking up to 95%. Due to the requirements of the Deutsches Institut für Bautechnik concrete slabs of 160 cm × 60 cm × 8 cm were clamped, concreted and put in a wind tunnel and exposed to a wind speed of 5 m/s. The total area of the cracks of the slabs with and without PP fibres were compared. In the Austrian guideline “Faserbeton”, edition March 2002, the positive properties of polypropylene fibres results in early-cracking classes. These classes are determined by shrinkage-rings.

The most important property of PP fibres regarding the application for tunnel constructions and precast elements is the improvement of the fire resistance. In case of fire, the concrete will spall off explosively. So the load bearing reinforcement is exposed and the structural integrity will be endangered (Fig. 4). Moreover, the bearing cross-section of the concrete is reduced. The quantity of the spalling depends on the moisture content of the concrete, kind of aggregates, temperature of the fire, development of temperature, concrete quality and possible compression stress in the construction. The reason for the explosive spalling is the high vapour pressure which occurs because of vaporisation of chemical and physical bounded water. If spallings have to be reduced PP fibres shall be used among the reduction of the moisture content and the application of suitable aggregates.



**Abbildung 6**

Fig. 4 Temperature fire tests

The purpose of the PP fibres is to provide sufficient pores to allow the vapour to evaporate. Polypropylene fibres melt at 160°C and form capillary pores. Moreover, the zone between the aggregates and the binding material becomes more permeable.

Different classes of fire resistance are mentioned in the guideline of the Austrian concrete society “Faserbeton”. Fire tests have to be carried out at specimens 60 cm × 50 cm × 30 cm

using concrete with and without fibres. The effect is determined by the reduction of the spalling. Tests based upon that guideline are showing impressively the positive influence of the PP fibres whereas the influence of an axial force (which occurs in tunnel elements) is not recognised. Therefore a bigger concrete dice of 180 cm × 140 cm × 50 cm with an additional normal force has been determined in a recent guideline “Innenschalenbeton”, published 2003.

## **5. POLYPROPYLENE FIBRES IN PRACTICE**

Polypropylene fibres are applied at present for the production of tubing's at Max Bögl for the project “City Tunnel, Leipzig”. Two railway stations shall be linked by two subterranean single-tracked tunnels. For the tubing's fire tests have been carried out at the MFPA Leipzig to get the required approval. 2 kg of the PP fibre “KrampeFibrin PM 6/15” were applied. Beside that tests a general federal approval was achieved from the German Institute of Structural Engineering. Further test in cooperation with the MPA in Brunswick have confirmed that spellings can be significantly reduced if suitable PP fibres are applied.

## **6. REFERENCES**

- DBV-Merkblatt „Stahlfaserbeton“, Fassung Oktober 2001, Deutscher Beton- und Bautechnik-Verein E.V.
- Dehn, Werther, Knitl, „Großbrandversuche für den City – Tunnel Leipzig, Beton- und Stahlbetonbau, August 2006
- Grundsätze für die Erteilung von Zulassungen für Faserprodukte als Betonzusatzstoff (Zulassungsgrundsätze), Deutsches Institut für Bautechnik, Fassung Januar 2005
- Richtlinie „Innenschalenbeton“, Österreichische Vereinigung für Beton- und Bautechnik, 2003
- Prüfbericht “Prüfung von Betonplatten ohne und mit unterschiedlichen Additiven (multifilamenten Polypropylenfasern) in Anlehnung an den „Prüfplan zum Nachweis des Anwendungsbereiches „Verbesserung des Brandverhaltens“ bei Fasern“ des Deutschen Instituts für Bautechnik, Berlin bei einer Brandbeanspruchung in Anlehnung an die RABT/ZTV-ING Tunnelkurve“, Materialprüfanstalt für das Bauwesen Braunschweig, 2006
- Prüfbericht (Teilbericht 1) „Zulassungsprüfungen an Kunststofffasern des Typs PM“, Lehrstuhl für Baustofftechnik Ruhr-Universität Bochum, 2006
- Richtlinie „Faserbeton“, Österreichische Vereinigung für Beton- und Bautechnik, 2002
- Untersuchungsbericht „Vergleichende Untersuchungen von Stahlfasern“, Hochtief Consult Materials, 2006



## **CYCLIC BEHAVIOUR OF PRECAST COMPOSITE SHEAR WALLS: EXPERIMENTAL RESULTS AND ANALYSIS**

*Seng Kiong Ting and Hongsheng Han  
Nanyang Technological University, Singapore.*

### **ABSTRACT**

A total of six specimens, two monolithic composite walls acting as prototypes and four precast composite walls, were tested under cyclic load. Steel sections, channels and I-beam, were used in these walls as flexural reinforcement at these walls' boundaries. Basically, the precast walls showed similar shear capacity to their monolithic prototypes. However, the major differences between behaviors of the monolithic and precast walls include stiffness, displacement ductility, pinching effect, capacity of energy dissipation, and failure modes and locations. In this paper, stiffness, flexural, shear and sliding deformations, vertical dilation and capacity of energy dissipation are used as valuable tools to evaluate performance of these specimens. Strut-and-tie models are built before yielding and plastic stages, respectively. The built strut-and-tie models give clear explanation on behavior of these walls.

### **1. LITERATURE REVIEW**

The use of steel reinforced concrete (SRC) composite structures to resist lateral load due to earthquake or wind have been widely explored and developed, with increasing recognition of the benefits from several different types of composite structures. Makino et al (1980), Makino (1984) and Wakabayashi (1984) presented that buildings of composite construction showed good earthquake resistant capacity under the Kanto earthquake as compared with ordinary reinforced concrete structures. Tupper (1999) studied the reinforced concrete walls with steel boundary elements and concluded that the design used for ductile flexural walls can be modified to enable comparable design of reinforced concrete walls with steel boundary elements.

Up to now, the limited use of this type of wall is due to the construction sequence, i.e. the vertical steel shapes must be erected before the concrete is placed. This may cause instability of the steel sections before concrete is placed, use of substantial vertical formworks and low construction speed. In order to overcome these weaknesses of composite shear wall, the concept of "precast" is introduced into this type of wall in this paper, that is, the composite shear wall is cut into several portions horizontally at floor levels and these portions are prefabricated in plant with high quality. Finally these separate components are transported to the site and assembled. This kind of wall is named precast composite shear wall (PCSW).

### **2. RESEARCH SIGNIFICANCE**

As monolithic concrete walls are divided into several portions at floor levels and manufactured in plant, which later were assembled on site by horizontal connections, the internal load paths are different from the original monolithic wall. This causes changes in cyclic response of the walls, including strength, stiffness, failure mode and capacity of energy

dissipation. The different configurations of embedded steel shapes also affect behavior of the walls. The experimental programs presented herein aim at addressing these issues.

### 3. EXPERIMENT DESIGN

The experimental work described in the following involves the testing of six composite shear walls: two monolithic walls and four precast ones. Such walls are considered to represent the critical story element of the structural wall system with a rectangular cross section. The dimensions of walls are 1800 mm wide, 2300 mm high and 140 mm thick and the aspect ratio is  $\alpha = h_w/l_w = 1.41$  (where  $h_w$  and  $l_w$  are the height and width of specimens, respectively). In all these specimens, horizontal bars are T10 and vertical bars are R10 with same spacing 200mm. Horizontal rebars are welded to steel sections. Channels (76x38x6) are embedded in W1 to W3 and acting as flexural reinforcement as shown in Fig. 1. All properties of W4 to W6 are same to W1 to W3 accordingly except with I-beams (152x89x16). One shear connector is used in W2 and W5, while two shear connectors are used in W3 and W6. Steel sections at wall ends are spliced with bolt connection. Shear connector consists of rebars and steel plates. After bolting, the gap between upper and lower walls is filled with concrete with same strength in precast walls. Cyclic load was applied at top beam (Park, 1988) of these specimens until failed them. Material properties are listed in Tabs. 1 and 2.

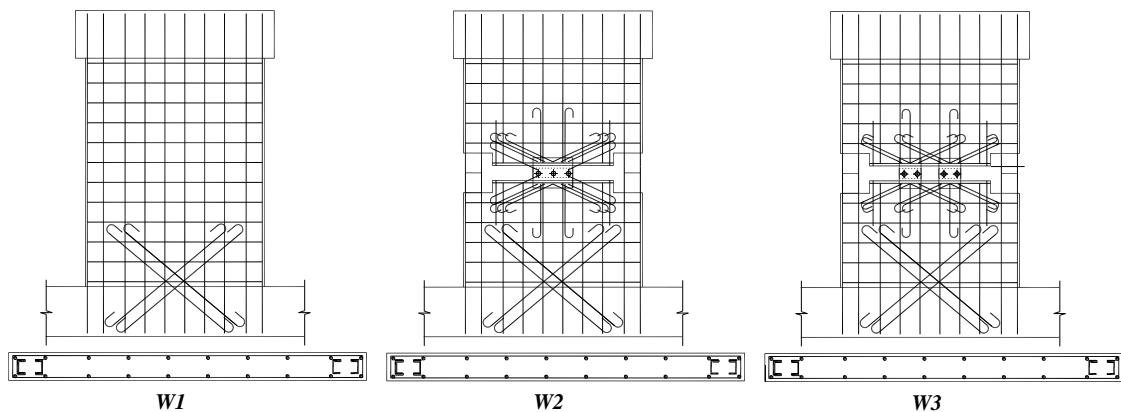


Fig. 1 Layout of specimen W1, W2 and W3

Tab. 1 Average concrete cylinder compressive strength

Specimen	W1	W2	W3	W4	W5	W6
Strength(MPa)	35.58	33.53	34.04	35.45	34.02	33.24

Tab. 2 Properties of reinforcement and steel sections

Types	R10	T10	Channel	I beam
Area of cross section $A_s$ (mm <sup>2</sup> )	78.5	78.5	856	2050
Modulus of Elasticity $E_s$ (MPa)	192721	185553	192460	177279
Yield strength $f_y$ (MPa)	384.63	485.91	307.74	322.16
Yield strain ( $\mu\epsilon$ )	2200	2700	1800	2000
Ultimate strength $f_u$ (MPa)	544.5	603.68	470.97	487.78



Tab. 3 Characteristics of experimental results

	W1	W2	W3	W4	W5	W6
Yielding strength (kN)	522.8	522.8	522.8	608.9	608.9	608.9
Yielding displacement (mm)	9.74	13.35	11.23	7.96	11.16	-
Ultimate strength (kN)	562	559	574	757	740.5	723.7
Ultimate displacement (mm)	53.67	52.02	45.99	58.65	53.67	16.8
Drift (%)	2.11	2.05	1.81	2.31	2.11	-
Stiffness (kN/mm)	58.33	39.16	46.56	77.4	55.12	-

## 4. EXPERIMENT RESULTS

The main characteristics of test results are listed in Tab. 3. The precast walls exhibited similar strength with their monolithic prototypes with lower stiffness in all testing stages. Lower ductility and energy dissipation capacity were also observed compared to their own monolithic prototypes. Precast walls experienced higher vertical dilation than monolithic ones. The monolithic walls fail in flexural while precast walls fail in sliding shear in lower wall. Ratio of strength of wall with I-beam and that with channel is bigger than rate of sectional area of I-beam to channel, which means the dowel action of I-beam is higher. Precast walls exhibited lower ductility compared to their monolithic prototypes as shown in Fig. 2.

### 4.1 Stiffness

The stiffness properties of these specimens are evaluated by their secant stiffness  $K$ , as shown in Fig. 2, which is defined at the peak value of the first cycle of each displacement level. In the whole loading phase, monolithic wall W1 and W4 showed higher stiffness than that of its precast counterparts, W2 and W3, W5 and W6, respectively. The two precast walls with embedded channels manifested similar stiffness throughout the test, same as W5 and W6. Monolithic wall showed highest stiffness in walls with same steel section.

### 4.2 Deformation

Horizontal displacement is decomposed into flexural, shear and sliding deformations to reflect roles of these components in overall behavior of these specimens. In specimen W1, flexural deformation is the main deformation. As shown in Fig. 3, in specimen W2, the ratio of the shear deformation to the total horizontal deformation is higher than that in specimen W1. It is a hint that higher energy is dissipated by flexural deformation in W1 than in W2. Flexural stiffness of W1 is higher than that in W2. In precast wall, *built-in* tolerance between bolts and bolt holes, discontinuity of vertical reinforcement and lower friction between upper and lower wall panels are the main causes. Pinching is more serious in W2 than in W1, which can be seen from Fig. 3 (b) and (d). The sources are shear deformation, bond slip and sliding of the wall relative to the base beam. In reloading phase, stiffness is very low before the load reaches one third of the ultimate load, especially in specimen W2. At the same time, the records of the gauge on the reinforcement in extremity show positive strain. It hints that one source of pinching is closing of cracks previously opened. After cracks closed, concrete took over the role of resisting compression, which is indicated by increasing stiffness in later reloading stage.



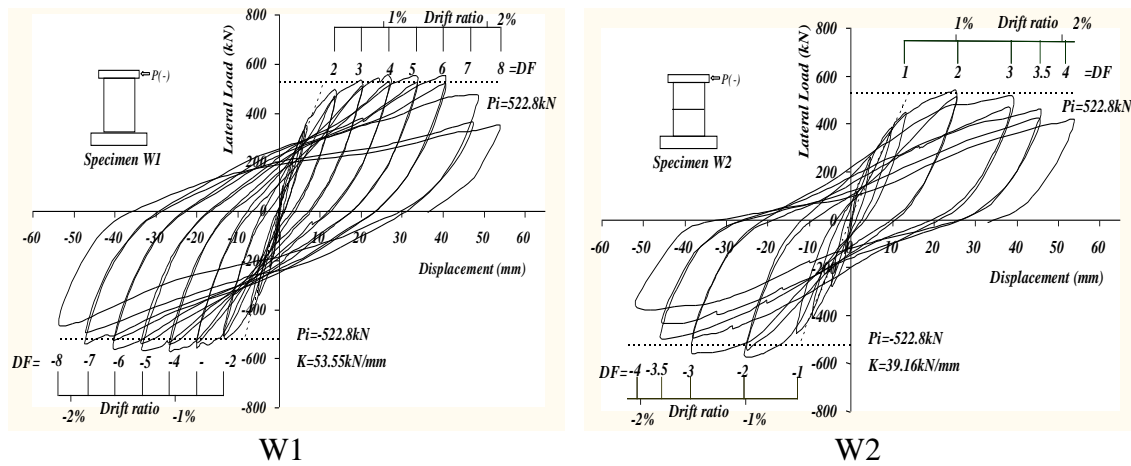


Fig. 2 Hysteresis loops of W1 and W2

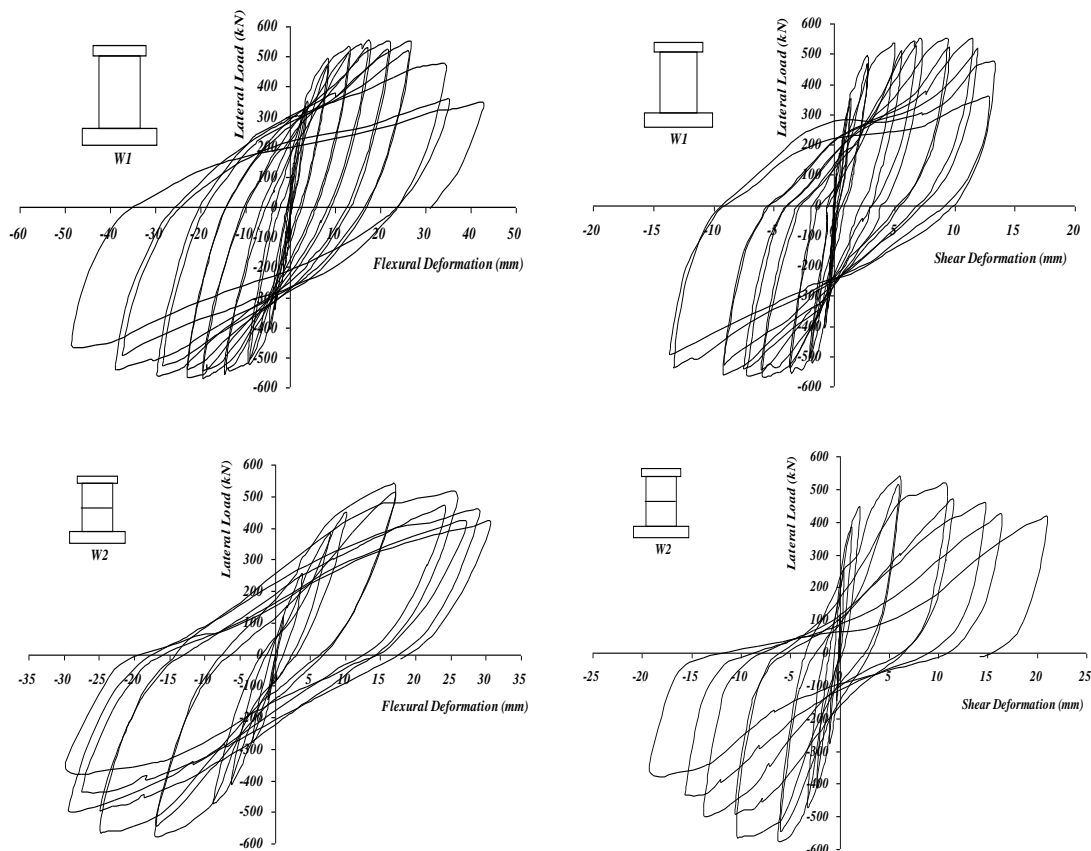


Fig. 3 Load versus Deformations of specimen W1 and W2 (a) flexural deformation of W1; (b) shear deformation of W1; (c) flexural deformation of W2; (d) shear deformation of W2.

### 4.3 Energy Dissipation Capacity

As one of the significant factors in seismic design, capacity of energy dissipation is also investigated in this paper. The most convenient approach of obtaining the energy in the dynamic situation is using the area enclosed by the hysteresis loops. The energy is normalized by dividing loops' area by displacement. As shown in Fig. 4, it is found that in the early loading stage, all specimens exhibit faster increase in energy dissipation. With increasing displacement level, the increasing rate decreases and reaches a constant, and a drop appears in final loading stage. The decrease in increasing rate is due to increasing pitching caused by

shear deformation that is known for its lower energy dissipation. When the lateral load exceeded the ultimate load, it displays decreasing trend. This is another reason for lower energy dissipation in the final stage.

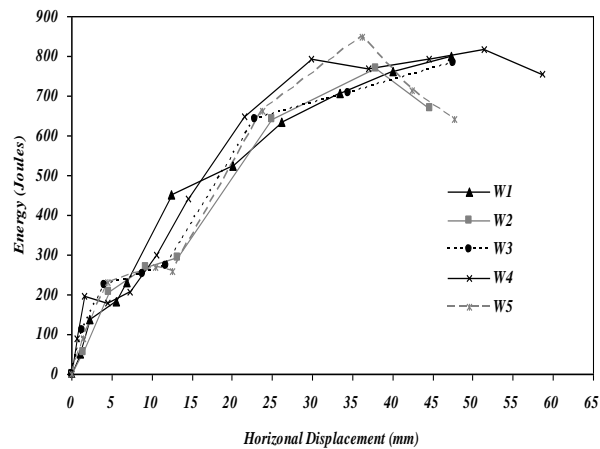


Fig. 4 Comparison of energy dissipation per displacement of all specimens

### 5. STRUT-AND-TIE MODEL

A combined strut-and-tie model is developed incorporating the first and second mechanism according to the minimum energy dissipation theorem. The minimum energy dissipation theorem is principle of minimum strain energy for linear elastic behavior of the struts and ties after cracking as shown in following:

$$\sum F_i l_i \varepsilon_{mi} = \text{minimum}$$

where  $F_i$  = force in strut of tie  $i$ ,

$l_i$  = length of member

$i, \varepsilon_{mi}$  = mean strain of member  $i$

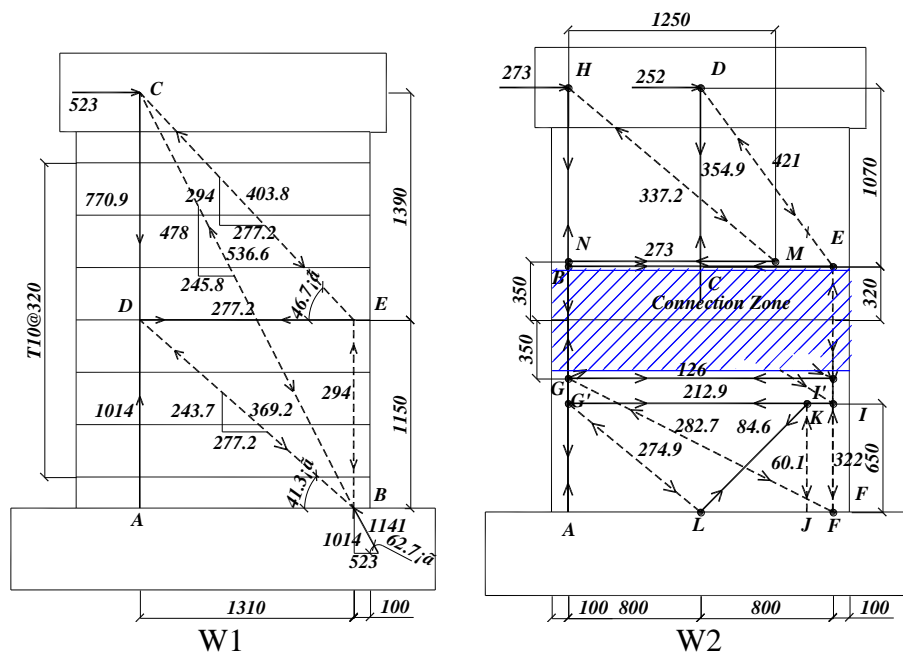


Fig. 5 Strut-and-tie model for specimen W1 and W2

Before loading reached yielding strength of the specimens, diagonal cracking from upper corner to the lower opposite corner was observed. This means, in the first stage, a diagonal strut and flexural reinforcement formed a load-resistant system. After loading passed the yielding strength, in the second stage, diagonal struts with lower inclined angle appear. This indicates change of internal load paths. For each stage of every specimen, strut-and-models were built and combined into to one with minimum energy dissipation theorem. The combined strut-and-tie model for typical specimens W1 and W2 are shown in Fig.5. It can be seen that all lateral load in W1 was resisted by diagonal struts and would crush the lower corner. However, lateral load in W2 was taken by horizontal rebars just below the horizontal connection and would fail them in tension. This was observed in experiment.

## 6. CONCLUSIONS

Analysis on six composite shear walls, namely, two monolithic walls and four precast ones, is carried out in this paper. The following conclusions can be drawn:

- Horizontal connections in the precast walls successfully transfer the lateral load acting on the top beam. Precast specimens exhibit lower stiffness compared to their monolithic prototypes.
- Decomposition of total horizontal deformation is used as worthy tool to gain insight into the seismic behavior of specimens. By comparing average energy dissipated in each loading cycle, precast walls exhibited similar capacity of energy dissipation.
- Strut-and-tie models for typical monolithic wall and precast wall gives a clear explanation for the failure mode.

## 7. REFERENCES

- Makino, M., Kawano, A., Kurobane, Y., Saisho, M. and Yoshinaga, K. (1980) "An Investigation for the Design of Framed Structures with Infill Walls", *Proceedings of the Seventh World Conference on Earthquake Engineering*, Istanbul, Turkey, September 8-13, Vol. 4, 1980, pp. 369-372.
- Makino, M. (1984) "Design of Framed Steel Structures with Infilled Reinforced Concrete Walls", *Composite and Mixed Construction*, Roeder, C.W. (ed.), ASCE, New York, 1984, pp. 279-287.
- Park, R. (1988) "Ductility Evaluation for Laboratory and Analytical Testing", *Proceedings, 9 WCEE*, Vol. III, Tokyo-Kyoto, 1988, pp. 605-616.
- Tupper, B. (1999) "Seismic Response of Reinforced Concrete Walls with Steel Boundary Elements", (Thesis), McGill University, Canada, 1999.
- Wakabayashi, M. (1986) "Earthquake-Resistant Buildings", McGraw-Hill, New York, 1986.

## **NOISE PROTECTION BARRIERS BY CONCRETE TWO-LAYER PANELS**

*Stjepan Lakusic<sup>1</sup>, Vesna Dragcevic<sup>1</sup>, Dalibor Bartos<sup>1</sup>*  
*<sup>1</sup>University of Zagreb, Faculty of Civil Engineering*  
*Croatia, 10000 Zagreb, Kaciceva 26*

### **SUMMARY**

In this paper protection of residential areas located near asphalt mixing plant in Zagreb (Croatia) from industrial noise is presented. The concrete wall as noise protection barrier formed by two layer panels was applied and built in February 2007 year. Two layer concrete panels consist of reinforced concrete slabs (with static function) and a sound-absorbing layer of lightweight porous concrete (on the noise source side). The short-term noise level measurements before and after the construction of the barrier were performed. Noise level measurements after the construction of the barrier were carried out at the same time in front of and behind the barrier using two sound-meters. In that way the effect of the applied protection was determined more precisely. The result of measurements on the site compared with the result of calculations and very good agreement was obtain.

### **1. INTRODUCTION**

Increase of urbanisation is linked with a great increase in the number of vehicles on European roads, even Croatia is not lagging behind. It can be seen in the multiple increase of motor vehicles on city roads, but also on roads out of towns. It is a well known fact that road traffic is one of the greatest environment pollutants, especially from the view of traffic noise. From all noise sources (traffic, industry, construction activities, free time activities) the biggest percentage falls off on traffic (about 81%), whilst on road traffic it measures 50% from the total of noise produced by the traffic (Lakusic, Dragcevic, Rukavina, 2003).

Republic of Croatia, although not a member of European Union, made a regulation about noise protection, which is synchronized with the European Directive 2002/49/EC. But, in spite of that, noise protection in cities of Croatia is carried out only sporadically. Certain protective measures are carried out only for the areas near the roads, where the noise level is extremely high, and the remarks of the local population to the City Council are frequently repeated over several years. If populated areas near motorways are observed, the situation is completely different in the case of excessive noise levels. Joint stock companies, which control motorways, are following the strategy of the Republic of Croatia to pay more attention to looking after the environment, as well as after noise protection. Ten years ago, Croatia started an intensive traffic infrastructure construction and so 1062 km of new motorways were constructed until today. Project documentation of planned solutions for noise protection, regular noise protection walls, is partially carried out. These are mostly wooden walls in mountain parts of Croatia and in northwestern part of Croatia the walls are made of aluminum and transparent panels. In general, noise protection constructions present significant cost estimate items, especially if they are made of aluminum and transparent panels of foreign manufacturers. So we turned in other direction. Concrete and concrete elements production technology in Croatia is on enviable level, from experts as well as scientific research point of

view. As part of two scientific projects of Faculty of Civil Engineering "Noise and vibrations on tram and railway tracks" and "Road traffic noise – monitoring and mitigation measures" financed by Ministry of Science, Education and Sports of the Republic of Croatia, the Faculty of Civil Engineering has in cooperation with the firm VIADUKT made a pilot project Noise protection of the settlement Svibje from the noise of asphalt mixing plant Trstenik. The realisation of the pilot project was conducted in three phases: making of project documentation, noise protection wall construction and applied protection efficiency analysis. Noise protection is carried out through the use of absorbent concrete panels, the efficiency of constructed barrier was analyzed with respect to the improvement of the state of environmental noise, and all with the goal of usage and development of own technology and usage of own resources in construction expert practice.

## **2. DESIGNING NOISE PROTECTION**

Planning of noise protection included acoustic calculation and mechanical resistance calculation as well as barrier stability was carried out.

### **2.1 Calculation for noise level and barrier optimization**

Increased noise levels caused by industrial plant of asphalt base are a result not only of work of machines, which are directly included in the asphalt production process, such as sand and small stone dosage equipment, a drum for drying of stone aggregate, mixer with constituent material dosage equipment, boiler for warming the connective materials and measurement devices for scattering stone flour, but also of transportation, either that driving over the components for production of asphalt to the dumpsites or that transporting to dosage devices or that of finished asphalt mixtures transport from the area of the industrial plant. Concerning it is an industrial plant, the existing state of noise in the plant and the surrounding area of the asphalt mixing plant were simulated on a computer according to the measurements on the site. Measurements on the site were conducted on two measuring points (MP) on the height of 1.2 m. The first measuring point was next to the plant, and the other one next to the objects, which need to be protected. For the needs of calculation, the source was set as spotted on the computer, on the height of 1.2 m and on the location of the plant. Immission values of the noise level of the receiver measured on the site were used to determine noise emission of the source. The calculation method of industrial noise ISO 9613-2 was implemented in accordance with European (Directive, 2002) and Croatian regulations (Noise Protection Act, 2003) for the needs of the calculation. Emission noise level of source was calculated based on the familiar data for receivers, which is the result of superposition of emission noise levels of all sources. The asphalt base of the firm VIADUKT, is located in "Zone 5: the zone of economic purpose – production, industry, warehouses, services", whereas the settlement Svibje, located next to the asphalt base is located in "Zone 3: the zone of mixed, mostly residential purpose". For zone 3, according to [4] allowed noise level at daytime is 55 dB (A). Evenings and nights noise levels are not relevant since the plant is not active at that time.

Noise maps for the existing situation without the wall and for the situation with the absorbent wall were made for the analyzed area, Fig. 1. In both cases, immission values for noise levels were calculated on facades of objects located next to the asphalt mixing plant on heights of 1.2, 2, 3.2 and 4.4 m. First analyzed solution was with only one noise protection wall located next to the western fence of the industrial plant. Optimizing the barriers, supported by the computer program, the optimal solution for dimensions of the noise protection wall was determined (length, height). By supposition it were an absorbent wall of absorption coefficient 4, the noise level on the facades of the object next to the western fence would be

reduced on values allowed by the Regulation (Official Journal, 2004). The calculation included reflection of the area within a diameter of 30 m with respect to each receiver.

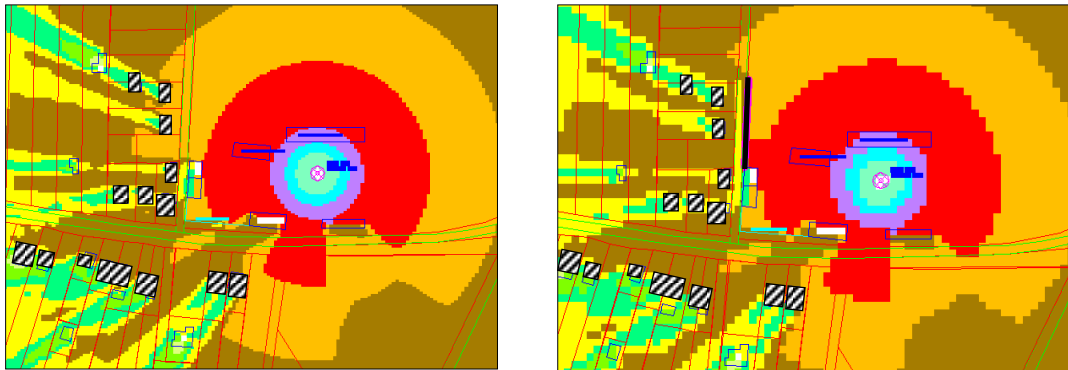


Fig. 1 Noise levels at the height of 1.2 m (without and with noise protection wall)

## 2.2. Mechanical resistance and stability

For the needs of noise protection from the industrial plant (asphalt mixing plant), a protective wall was projected of two-layered concrete elements (two-layered concrete units). Two layer concrete panels consist of reinforced concrete slabs (with static function) and a sound-absorbing layer of lightweight porous concrete (on the noise source side), (Lakusic, Dragcevic, Bartos, 2007). The construction was calculated on basic load according to HRN EN 1794-1:2003 standard. Wind load was calculated according to ENV 1991-2-4:2004 with reference speed ( $V_{ref}$ ) for the area (wind zone), where the sound wall is located. The city of Zagreb belongs to the wind zone I in which  $V_{ref} = 22$  m/s and  $q_{ref}=0.303$  kN/m<sup>2</sup>. The construction consists of adjusted prefabricated AB column and its intersection of external dimensions is 30×30 cm. The column is laid in a 'base' of concrete prefabricated foundation and is filled with cement mortar of minimum quality of C25/30. Before putting up the column it is necessary to adjust the projected height of the steel plate on the bottom of the base of the foundation. Concrete foundation can be made on spot or it can be put down on the prepared base as a prefabricated foundation. Since the dominant load is the wind load, foundation dimension depends on the bearing capacity of the foundation ground and on the wind zone the construction is located at. Filling of the sound protection wall is projected as a two-layered concrete panel of thickness  $d = 12$  cm, with reinforced wire screen Q 131 on both sides, Fig. 1.

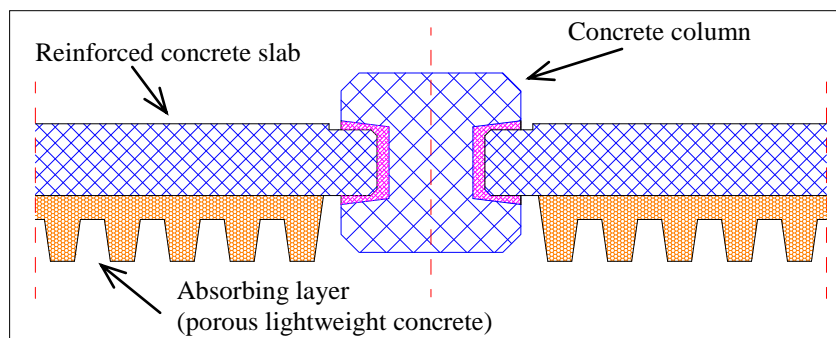


Fig. 2 Cross section of two-layer concrete panel and concrete column

The porous surface of the absorption layer with a trapezoidal structure is facing the noise source for a high absorption effect. The porous material of the structure and the porous surface of the absorption layer achieve the absorption capacity. The general rule is, the larger the active surface is, the higher the degree of the noise absorption. The optimal requirements of acoustic absorption are attainable by various combinations of rib thickness or rib spacing of the lightweight porous concrete that may be harmonized with the architectural requirements of the noise barriers to provide the best final effect. The surface of the absorption layer (the face) is made in wooden forms, which enables a large selection of shapes. The rear side of the units may be surface-finished as well, as required. With this pilot project there was only one of the absorption layer surface geometry, as can be seen on Fig. 2. The material of concrete columns and filling slabs is concrete of class C 30/37, and the foundation concrete of class C 25/30. Armature is made of checker plate RA 400/500 and wire screens MA 500/560.

### 3. THE CONSTRUCTION OF NOISE PROTECTION BARRIER

On the lower part of the noise protection wall, building in of concrete plank backplanes of thickness of 12 cm, height of 50 cm and length of 382 cm was planned, and the space between columns is 4.0 m. Concrete planks are common solution for the lower parts of noise protection walls. It is built in between concrete columns, and is leaned on column foundations. On built in concrete planks the cement absorbent panels of appropriate dimensions were erected. Panels are built in between columns, specially formed for this purpose. Mutual horizontal joining of panels is achieved on the *tongue and groove* principle using '*fugenband*'. Vertical joining was done with adequate neoprene jointing on the edges (column and panel joint). Illustration of the construction method and joining of individual elements can be seen in Fig. 3. Receipt points were planned to make loading the panels, transporting and erecting them, easier. Fig. 4 shows the erected noise protection wall, using two-layered concrete absorbent panels.



Fig. 3 Building of the noise protection wall



Fig. 4 Constructed noise protection wall

### 4. APPLIED PROTECTION EFFICIENCY ANALYSIS

The measurements were carried out during the day on the asphalt base location, when the plant is working with full capacity. With a goal of determining the usability of the calculation method, a verification of the results was carried out according to the measurement results for the state before and after the erection of the barrier, (Lakusic, Dragcevic, Bartos, 2007).



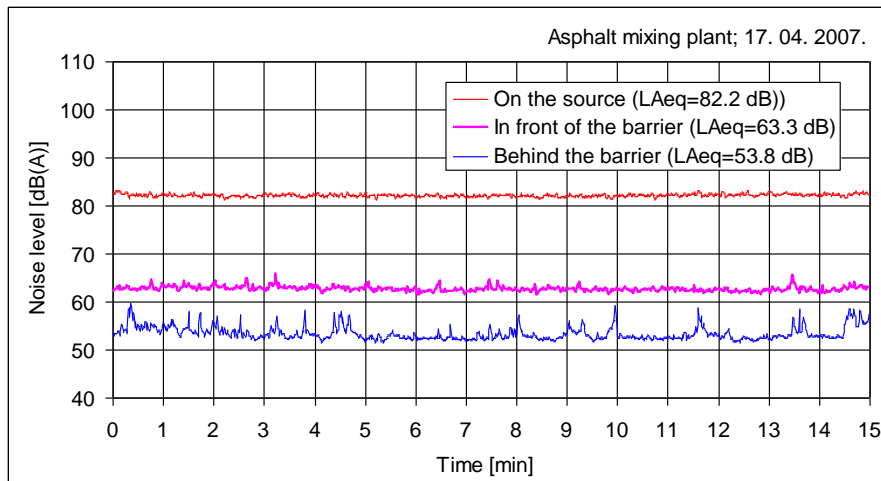


Fig. 5 Representation of noise level changes over measuring time period

Efficiency of the erected barrier determined by the calculation was tested after the erection of the barrier with measurements on the site in front of and behind the barrier, Fig. 5. From measurement data, Tab.1, it can easily be seen that this type of barrier achieved a noise decrease of 9.5 to 10.3 dB(A). Comparing noise levels on the source (asphalt base) and on the location behind the barrier, decrease of the noise measures 29.4 dB(A), and the plant is located 80 m from the erected noise protection wall.

Tab. 1 Noise level measured in front of and behind the barrier, LAeq [dB(A)]

Time period of measuring \ Measuring of noise	On source	In front	Behind	Noise reduction
11.18 – 11.33	-	63.3	53.8	9.5
11.35 – 11.50	-	62.9	52.6	10.3
11.54 – 12.09	82.2	-	52.8	29.4
12.15 – 12.30	81.6	59.7	-	21.9

The noise level acquired by the calculation on the location of the wall before it was erected was 58.5 dB(A). Measured values of the noise level after the erection of the wall right in front of the wall depending on the production process type (mixing of small or bigger fractions for asphalt production) were between 59.7 and 63.3 dB(A), Tab. 1. The calculation showed, that after erecting the wall of height of 4 m, the noise level on the height of 1.2 m behind the wall (right next to the object it protects) would measure 51.3 dB(A).

## 5. CONCLUSION

Noise protection of the settlement Svibje from making an asphalt base is carried out with the use of cement absorbable panels, which were for the first time used in Croatia. Measurements on the site, before and after constructing the noise protection, have shown, that with this kind of walls a decrease of noise level of approximately 10 dB(A) can be achieved. Acquired results are encouraging and confirm that all procedures in the production process and the construction of the wall were carried out according to the project presumptions. Nonetheless, the erected wall also achieved esthetic appraisal from the local population, but also from



experts. The achieved result of the first use of two-layered concrete wall composed of reinforced concrete slabs (on reverse side) and a sound absorbing layer of light-weight porous concrete (on the noise source side) have encouraged Croatian Roads Company on the wide range of possibilities of their usage. The erection of such a wall on state road D-502, a section from Zadar to Zagreb-Split motorway (junction Zadar 2) is in progress. Experts are becoming more informed about this new product, and further contacts for the usage of such walls on other locations, not just near roads, but also near railways, are in progress. The system of concrete noise barriers provides not only for high acoustic efficiency, but also provides for easy assembly with minimum maintenance requirements and with an extensive variability of architectural design.

## 6. REFERENCES

- Directive 2002/49/EC of European Parliament and of the Council relating to the assessment and management of environmental noise, *Official Journal of the European Communities*, L 189/12, 2002.
- ENV 1991-2-4 (2004), "Basis of design and actions on structures: actions on structures - wind actions".
- Highest permitted noise level Regulation for places where people work and reside, *Official Journal* NN 145/2004.
- HRN EN 1794-1 (2003), "Road traffic noise reducing devices. Non-acoustic performance. Mechanical performance and stability requirements".
- Lakusic S., Dragevic V., Rukavina T. (2003), "Pregled europske regulative o buci od cestovnog prometa", *Građevinar* 55 (2003) 6, str. 349-356
- Lakusic S., Dragevic V., Bartos D.(2007), "The Noise Protection of Settlement Svibje from the noise of the asphalt mixing plant Trstenik", *Working design*, Zagreb, 2007.
- Noise Protection Act (2003), *Official Journal* NN 20/2003.

## **PARAMETRIC ANALYSES OF PRECAST REINFORCED CONCRETE PIPES**

*István Bódi, László Erdődi, Kálmán Koris*

*Budapest University of Technology and Economics, Hungary*

*H-1111 Budapest Bertalan L. u. 2. [bodi@vbt.bme.hu](mailto:bodi@vbt.bme.hu), [erdodi@vbt.bme.hu](mailto:erdodi@vbt.bme.hu), [koris@vbt.bme.hu](mailto:koris@vbt.bme.hu)*

### **SUMMARY**

Precast reinforced concrete pipes are the most commonly used elements for drainage systems due to their advantageous properties. The statical calculation of pipes according to the Hungarian Standard allows the use of design charts. In order to speed up this design process, a specific software tool has been developed for the analyses of precast reinforced pipe sections. The software combines calculation methods and design charts of Hungarian standard with sophisticated programming algorithms. This makes the software an easy to use and effective tool for measuring Precast reinforced concrete pipes sections and optimizing of the reinforcement under many specific circumstances. With the use of the software, design charts and diagrams were produced. Design charts and diagrams can be used for preliminary pipe cross-section design.

### **1. INTRODUCTION**

Precast reinforced concrete pipes are widely used for construction of gravity drainage systems. Before their application, pipe segments must be measured similar to other structural elements. However, calculation of the acting loads according to the Hungarian Standard is more complicated since the value of ground pressure depends on many parameters (type of bedding, sizes of trench, material properties of soil, etc.) which can be considered by use of design charts only. To smooth the progress of reinforced pipe section design, a computer software has been developed in cooperation with an industrial partner. With the use of the software the necessary reinforcement for the pipe under given circumstances can be uniquely determined which results in more economical utilization of materials. A set of design charts and diagrams were also produced using the developed software. These charts and diagrams can be used by civil engineers for quick and exact preliminary design.

### **2. ANALYSES OF REINFORCED CONCRETE PIPE CROSS-SECTIONS**

#### **2.1 Determination of loads**

The pipe is usually affected vertically and horizontally by ground pressure. The level of ground pressure depends on the weight of the soil above the pipe, on the self-weight of the pipe (including the weight of the fluid inside the pipe), and on the loads acting on the surface.

The value of vertical ground pressure will be different than geostatic pressure according to the laying technology. In case of narrow trench, the surrounding soil mass can be considered solid thus the consolidation of backfilling will be obstructed by the sides of trench. This means a lower level of ground pressure than geostatic pressure on the pipe. If the pipe is laid in wider trench or into bank, the pipe itself obstructs the consolidation of backfilling which results in higher ground pressure than geostatic pressure. This means that we have to consider the width

of the trench during the calculation. The Hungarian Standard uses the value called limit width of trench to determine witch state to assume. The value of vertical ground pressure coming from the weight of the soil depends on the diameter of the pipe, on the width of the trench, on the distance between the stable ground and the top of the pipe cross-section, on the solidity of stable ground and on the volume weight of the backfill.

The self-weight of the pipe and the fluid flowing inside the pipe can be considered by an equivalent, evenly distributed, vertical load. Loads acting on the surface can be divided into two groups. Ground pressure caused by evenly distributed surface loads is a linear function of the surface load intensity and the vertical ground pressure coming from the self-weight of the soil. In case of soil cover less that 1 meters, a concentration coefficient must also be applied. The effect of vehicular load is considered by an equivalent, evenly distributed, vertical load. The value of equivalent load intensity depends on the vehicle type according to the Hungarian Standard, on the thickness of soil cover and on the pavement conditions.

The horizontal ground pressure reduces the stresses caused by vertical pressure inside the pipe cross-section, therefore it can be considered only if it is acting permanently. It is usually difficult to decide, if the horizontal pressure is permanent or not, but the following thumb rules can be generally applied: Horizontal ground pressure can be always considered if the pipe is laid into bank. The effect of horizontal ground pressure is insignificant in case of narrow trenches (trench width is smaller than the trench width limit) so it can be neglected. In case of trenches wider than the trench width limit it is possible to consider the horizontal ground pressure if conditions are corresponding (we have granulous soil with a solidity of at least 85% and there is at least 0,5 m space between the pipe and the trench wall). The horizontal ground pressure can be considered (if it is reasonable) by an equivalent, evenly distributed, vertical load witch will reduce the effect of vertical ground pressure. The value of equivalent load intensity depends on the diameter of the pipe, on the thickness of soil cover and on the material properties of backfilling.

## 2. 2 Determination of stresses in the pipe cross-section

Different types of vertical loads (multiplied by corresponding safety factor) must be summarized to obtain the of design load. The design stresses acting to the pipe cross-section (axial force and bending moment) are usually obtained by the method of elastic centroid.

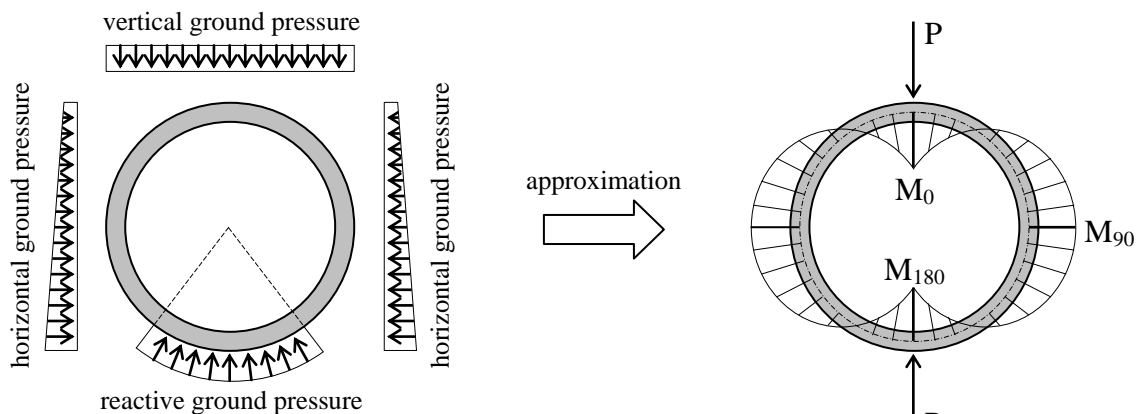


Fig. 1 Ground pressure acting to the pipe and the substituting knife-edge load

It is sufficient for the practical application to use a substitute knife-edge load instead of the actual ground pressure distribution. Fig. 1 represents the actual ground pressure distribution and the substitute knife-edge load with the corresponding bending moments. The bending moment diagram has three maximums ( $M_0$ ,  $M_{90}$ ,  $M_{180}$ ). The cross-section of the pipe must be designed to resist these forces considering the simultaneous axial force. For special types of bedding might other places of pipe cross-section must also be checked.

### 2. 3 Statical analysis of the pipe cross-section

First the fiber-stresses on the inner and outer side of the cross-section are determined. For pipes without reinforcement we perform elastic analysis, that means fiber-stresses are compared to the limit stresses. In case of reinforced concrete pipes (one or two layered) we calculate the ultimate bending moment in the cross direction considering plastic behavior of the materials. For pipes with reinforcement, the crack-width is also determined and compared to the limit value.

### 3. SOFTWARE FOR THE ANALYSIS OF REINFORCED CONCRETE PIPES

The software for the design of reinforced concrete pipes uses object oriented programming (OOP). This is the most up-to-date programming method, where the frame of the software is built up by single objects. These objects contain the necessary input data for the calculations (variable fields) and procedures for manipulating the fields (methods). Fig. 2 represents the object oriented structure for pipe analysis. The child object inherits the properties from the parent object, eg. the *Trcpipe* (reinforced concrete pipe) inherits all the variable fields and methods from *Tpipe* (concrete pipe) object.

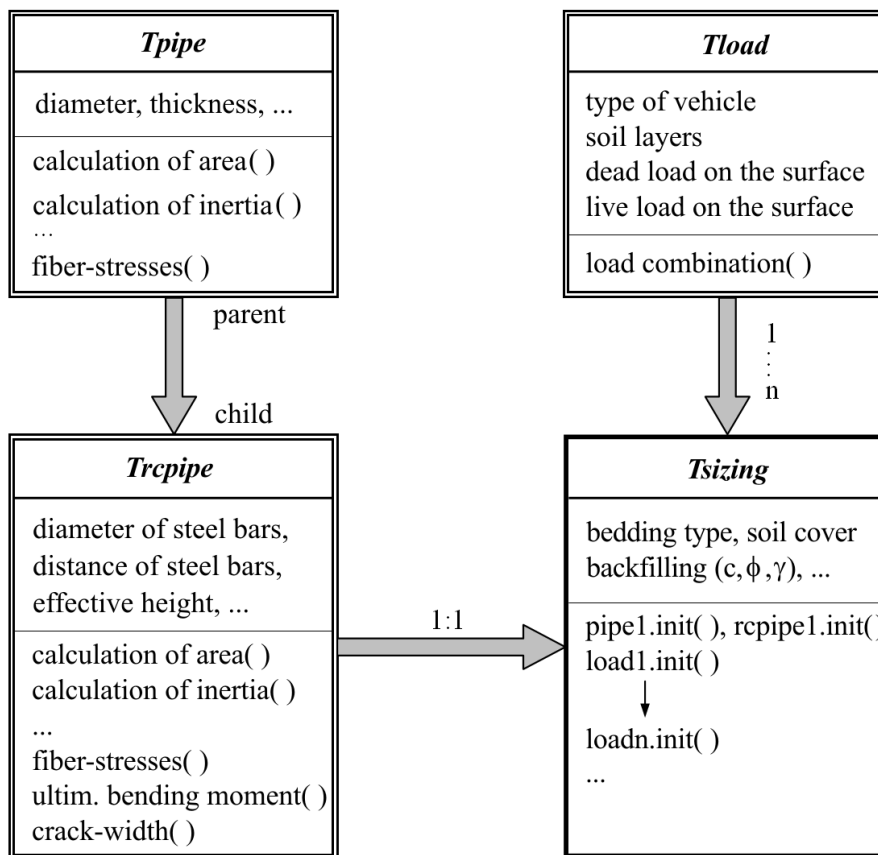


Fig. 2 Object-oriented software structure

The base object was the *Tpipe*, which contains the geometrical data and the procedures for calculating cross-sectional properties and fiber-stresses. As indicated on Fig. 2, *Trcpipe* extends the *Tpipe* object by additional properties for handling the reinforcement. A procedure for calculating the ultimate load-carrying capacity is also available, which calculates the ultimate bending moment considering the actual value of the axial force as well as the crack width. *Tload* object involves the surface loads including the vehicle loads, pavement loads and live loads. The most sophisticated object is called *Tsizing*. It contains several copies of *Tload* object (load combinations) and the pipe laying conditions (type of bedding, geometry, soil properties, horizontal ground pressure, etc.).

A run-time copy of the *Tsizing* object is created during the analysis to consider all available circumstances. Based on the parameters entered by the user, the software creates one copy of the necessary objects (depends on which type of pipe was selected). The software uses a database containing the pipe templates provided by the manufacturer. In case of a pipe with non-standard geometry, parameters can be separately modified by the user.

After obtaining the necessary input data from the user, the software executes the verification process of the pipe cross-section according to the procedure described in Chapter 2. A runtime view of the software is presented on Fig. 3.

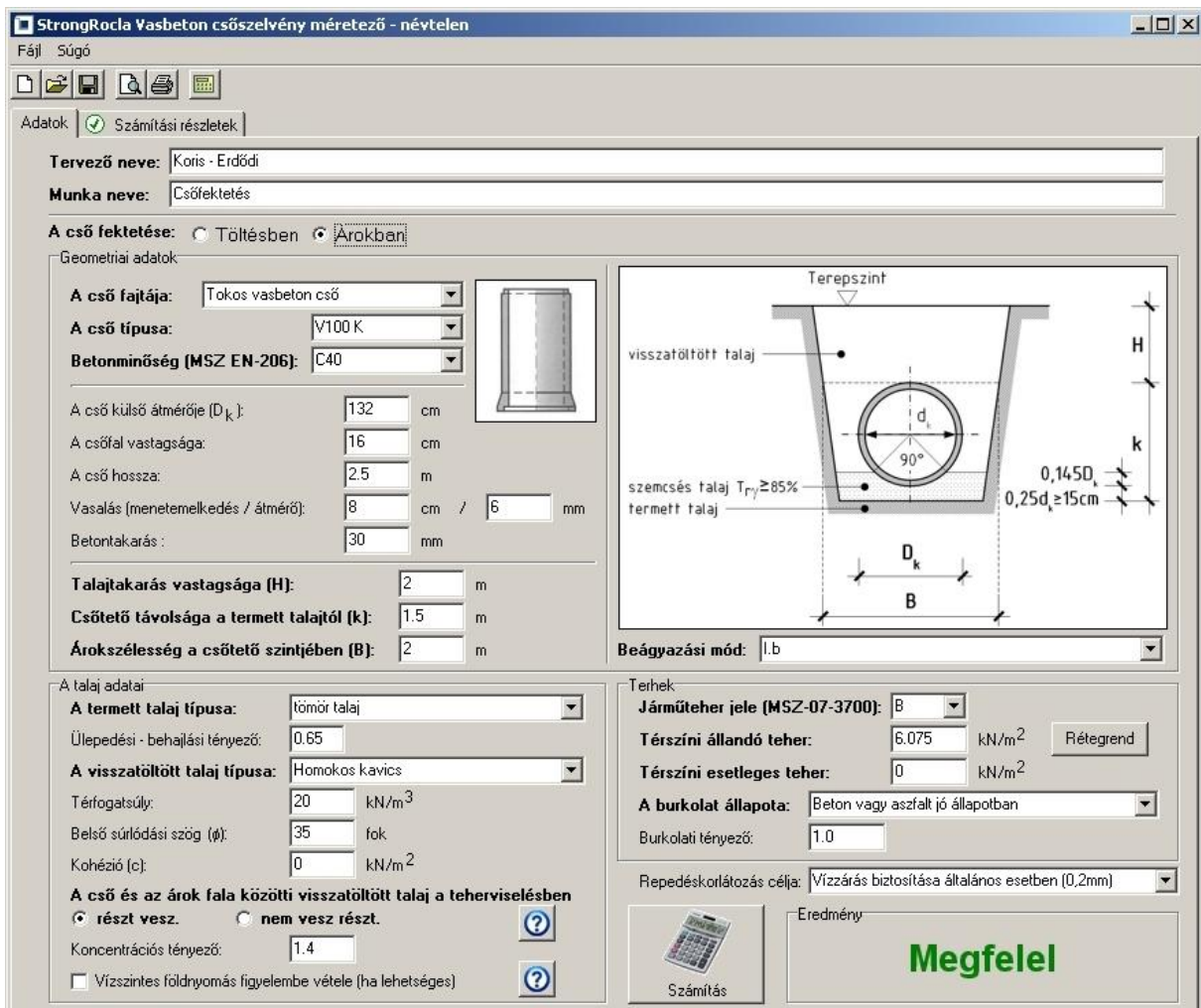


Fig. 3 Runtime view of the software

#### 4. PARAMETRIC ANALYSIS OF PIPES

The software described in Chapter 3. is an efficient tool for the calculation of concrete or reinforced concrete pipes and for the optimization of the reinforcement. However it is usually more convenient to use design charts for the preliminary design of pipes. Therefore a set of design charts have been created using the developed software.

There are different charts for different kinds of soil as well as for different pipe types. In addition, pipes laid into trench are differentiated from pipes laid into bank. The thickness of soil cover is indicated on the horizontal axis while the vertical axis represents the design value of the allowed surface load. One single chart usually contains a set of curves which stand for different types of bedding and different crack-width limit. A design chart for the reinforced concrete pipe type R100T in case of clay soil is presented on Fig. 4. It is supposed that the width of the trench (B) is the double of the pipe's diameter (D). The notations I.a., I.b., II.a. and II.b. indicate the different bedding types. Some available bedding types are illustrated on Fig. 5.

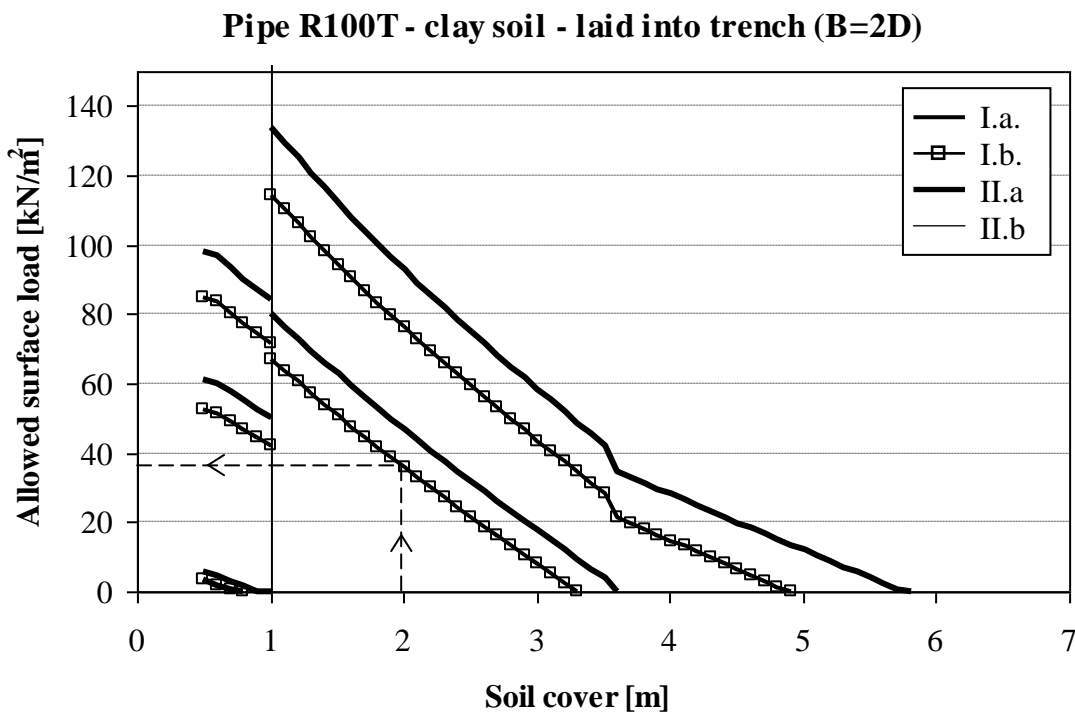


Fig. 4 Design chart for pipe type R100T

The created charts can be used for quick and exact preliminary design. Let us suppose we have to use reinforced concrete pipe type R100T which will be laid into trench. The planned value of soil cover is 2,0 meters, we have clay soil and bedding type I.b. (see Fig. 5) will be applied. The intensity of the dead load is 6 kN/m<sup>2</sup> and we also have a live load of 8 kN/m<sup>2</sup> on the surface. According to the design chart indicated on Fig. 4 we get a value of about 36 kN/m<sup>2</sup> for the allowed surface load in case of the given parameters. The design value of the surface load is 6 + 8 = 14 kN/m<sup>2</sup> which is smaller than the allowed load. This means that the load-carrying capacity of the selected pipe is sufficient and it can be safely applied under the current conditions.

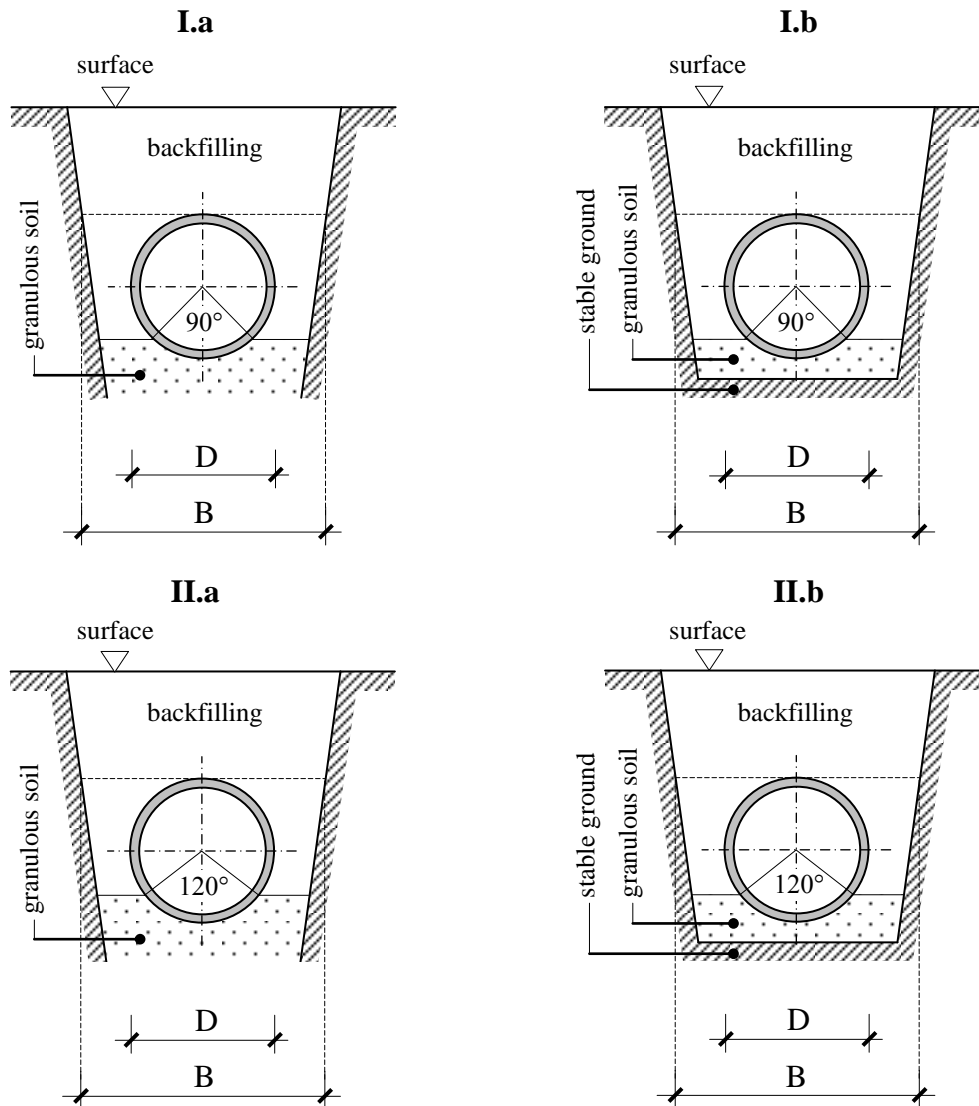


Fig. 5 Different types of bedding for the pipe

## 5. CONCLUSIONS

A software tool has been developed for the analyses of precast reinforced pipe sections. The software combines calculation methods of Hungarian standard with sophisticated programming algorithm. The software is an effective tool for the analysis of reinforced concrete pipes as well as for optimizing the reinforcement. Design charts were also created with the use of the software. These charts can be used for quick preliminary design.

## 6. REFERENCES

- György, I. (1978): *Vízügyi létesítmények kézikönyve*, Műszaki Könyvkiadó, Budapest
- George, J. F. (2004): *Object-oriented system analysis and design*, International ed, Upper Saddle River, N.J. Pearson Prentice-Hall
- LEIER (2004): *Mélyépítési elemek*, Technical Guide
- MI-10-167-4-78 (1978): *Közcsatornák tervezése. Csatornák erőtani tervezése*, Műszaki Irányelvek, Országos vízügyi hivatal
- StrongRocla Kft (2006): *Beton és vasbeton csövek*, Product Manual

## THE NEW AMALIA RODRIGUES PARK IN LISBON

*Jorge de Novais Bastos*

*Faculdade de Arquitectura – Universidade Técnica de Lisboa*

*Rua Sá Nogueira, Alto da Ajuda, PT 1349-055 LISBON, Portugal*

### SUMMARY

During this last century and after several different design proposals, the Lisbon City Council decided, some years ago, to complete right in the heart of Lisbon, the central city park top sector. A well-known senior Portuguese landscape architect was retained to develop a unique urban park design solution for this sensitive location. The constructed area included several facilities: a large concrete round slab, a lengthy “biological lake”, a glass wall pavillion and a large underground technical area. Special design needs and aesthetic requirements in a singular large environmental impact project were met. Although architects can raise objections on the extensive use of concrete in public works, in this particular project, a “constructive” approach existed towards different performance concrete types and other structural materials.

### 1. INTRODUCTION

After the dreadful 1755 Great Lisbon Earthquake, a newly designed Cartesian-grid city emerged from the rubble, following the principles of the Enlightenment, Fig. 1. The construction started under the King’s Prime Minister leadership – the Marquis of Pombal and the two brilliant royal military engineers – the Hungarian born Carlos Mardel and the Portuguese Eugénio dos Santos. During the next 250 years while the city was expanding new public spaces were deemed necessary – the Rossio, the Public Promenade (Av. da Liberdade).

The new Amalia Rodrigues top-of-the-hill garden is one of the best visible public works built by the City of Lisbon in the last ten years, Figs. 1.(b), 2. The 42.000 sq. m. of public land were subjected to several studies during the last century with imaginative solutions that were never materialized due to excessive costs, public opinion and, unrealistic urban needs. In the early 1990’s, Prof. Gonçalo Ribeiro Telles, a senior landscape architect, was able to implement an adequate design solution to enclose one the main city public garden N-S axis. Although the design concept limited the traffic solutions and encouraged the public use by pedestrians, the adjacent streets are still intense “corridors” in the “east-west” city traffic jam.

Late XIX<sup>th</sup> century design studies were done and, in 1903 during is royal visit to Lisbon, a new public garden was dedicated to H.R.H. the British Crown Prince Edward. The current hill top design solution completes this centenary Park Edward VII with a generous open air theatre, located 114.0 m above sea level. A magnificent view of Lisbon can be experienced from this spot – St. George Castle, Tagus River estuary, left bank villages and the distant Moorish castles in the Arrabida peninsula. The complete construction program included an artificial hill on the east side, a large cleanwater artificial lake with a jet outlet, a pavilion with a restaurant, a biological contour lake with an observation platform, and the open air amphitheatre. This study main purpose is to present several different design limitations that the constructed solution, the site constraints, and time cost requirements had to be met adequately.





(a) 1902-03 Plan (1)



(b) 2000-02 Plan

Fig. 1 The City of Lisbon

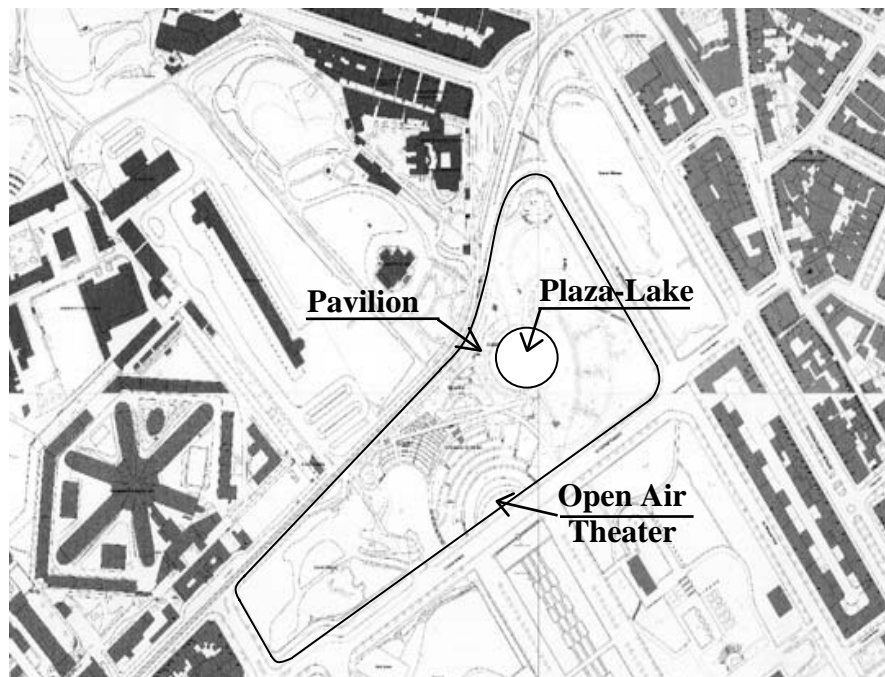


Fig. 2 The new Amália Rodrigues Park

## 2. THE AMALIA RODRIGUES TOP-OF-THE-HILL PARK

### 2.1 Design Concepts

The design concepts that underline the general guidelines followed during the design phase were: (a) aesthetics; (b) public space/leisure quality; (c) construction costs; and, (d) long-range sustainability of this intervention. The aesthetics requirement was a must which had to be closely observed in this very sensitive public area. During several decades and since the public park early beginnings, this top-of-the-hill region was subjected to several studies depending on the current day-to-day policies. A well-designed, carefully detailed solution had to be built under close public scrutiny. The general layout called for a public open air theatre in order to enjoy the panoramic local views, a pavilion with a reflecting pond and the surrounding earth-modeled artificial hills (landfills). Secondly, the leisure concept had to be discretely available to the passing-by citizen. A subtle arrangement of trees, bushes, viewing spots, lighting, was planned so that in this particularly crowded area anyone could enjoy an open space garden during leisure time. Thirdly, the budget constraints the design group had to follow were not very stringent considering the importance of this area. Consequently, readily available materials were adopted – reinforced concrete (RC) structural systems (foundation piles, retaining walls, slabs, beams, columns) and structural steel for the glazing façade and aluminium blinds to shade the pavilion. Last, the long-term sustainability of this intervention required the Park had to have some “anchor” areas. The pavilion with a restaurant is able to attract not only “lunch hour” people from the surrounding offices and businesses, as well as, evening family visitors. The open-air amphitheatre is a great attraction with public events.

### 2.2 The Water Area – the lakes

The existence of a reflecting pond is a classical concept in landscape design. The light reflected on the water surface increases the space dimension (e.g. Villa Adriana, Versailles) and provides a refreshing environment during the hot summer days. A very large circular “plaza-lake” solution was conceived. In summer when filled with water, a shallow refreshing lake ( $D_{\max}= 60$  m;  $h_{\text{water}}= 0.20$  m - 0.80 m) and a central single water jet ( $H_{\max}= 15$  m) to circulate/renovate the water is available. During the winter season, the lake can be emptied to clean the basin surface and to use the available  $2,500$  m<sup>2</sup>, as a recreational plaza. Therefore, this design concept was labeled by the landscape architect as a “plaza-lake” (Fig. 3).

A 56.0 m diameter circular RC waffle slab (“plaza-lake”) was supported on several 0.60 m diameter piles and on a longitudinal (N-S) ground-buried service gallery. The geotechnical studies showed soil strata with a variable depth landfill clay/silt type soils. These heterogeneous, disturbed soil materials were the result of several dumping deposits created in the early 1960`s when the new metro line was built. Due to the soil properties random behavior, the structural designer adopted a cast in-situ RC pile foundation solution, at a maximum 8.0 m spacing, to support the two half-circle cantilevering slabs. The design dead loads (DL) were the RC slab self weight, concrete leveling top layer and 0.12 m side granite cubes surface finishing, placed with cement mortar, topping the water-proofing membrane layers. The materials used were pozzolanic added concrete class B25 ( $f_{cd}=13.3$  MPa) and steel deformed rebars class A400NR ( $f_{syd}=346$  MPa), with 0.15 m to 0.20 m o.c. maximum spacing for crack control.

The underground gallery has a dual purpose: (1) water-jet pipe and connections need to be maintained; and, (2) the 600 m<sup>3</sup> water reservoir may require to be quickly emptied.

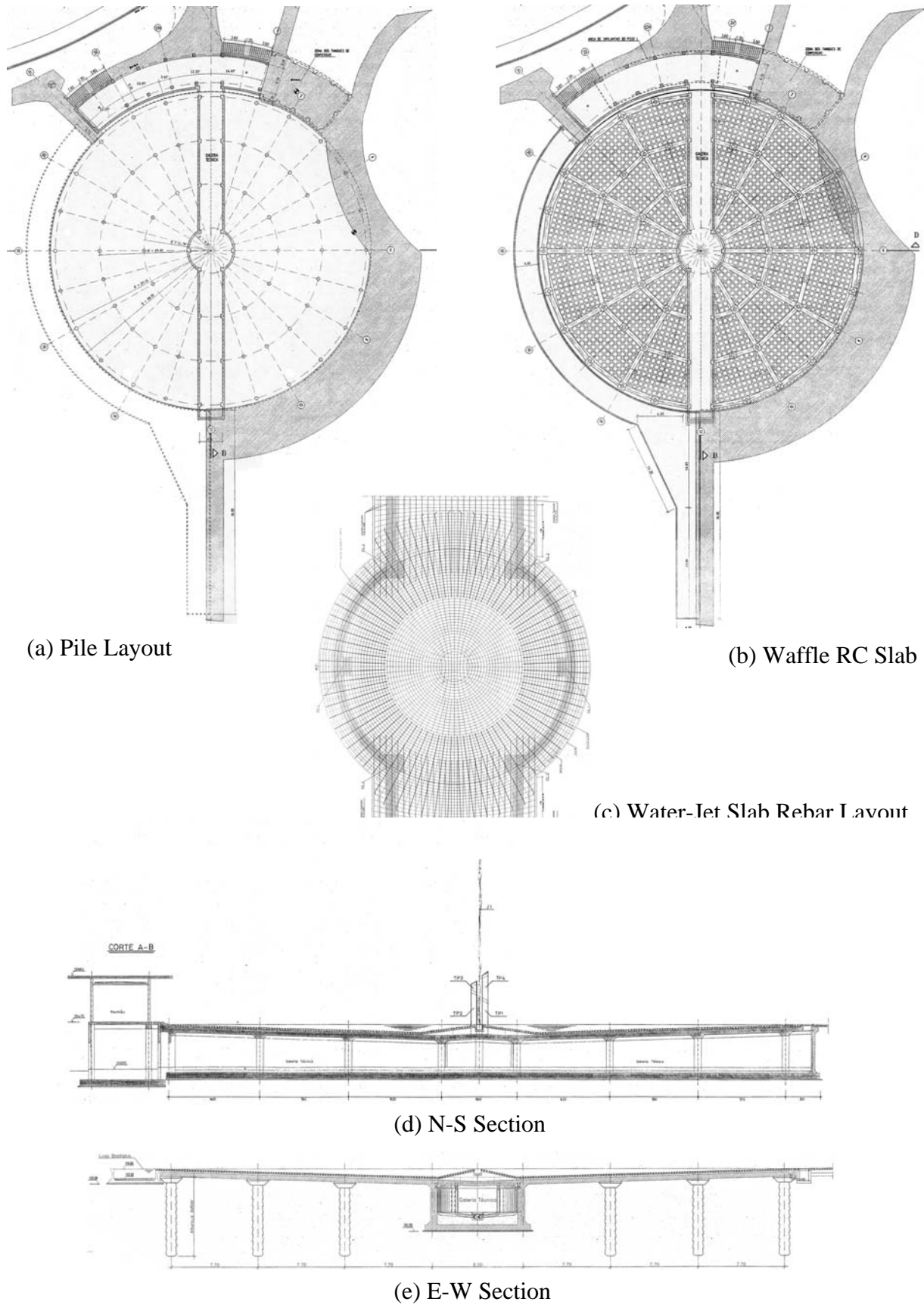


Fig. 3 “Lake-Plaza” and Pavilion structural system

Frequent pipe joint collapses need to be repaired due to the sudden water shock created by the water on-off system pumped into the network lines (e.g. “water hammering”, “coup-de-bellier”) albeit shock absorbing connections are used. The surface contour drainage may occur due to a possible sensor water-level malfunction. To avoid major flooding four water surface intakes were provided, near the central water jet. Nearby, the lower bottom drainage is also located to empty the lake and to remove the accumulated mud and sand deposits, (Fig. 4).

The adjacent sickle-shaped biological lake is very extensive  $L_{\text{approx.}} = 100.0$  m, with a maximum depth of 1.00 m, Fig. 4. The water stored in this reservoir is “static” and it is supposed that plants and fish will provide an adequate environmental balance. The structural solution consists of a U-shaped RC slab-on-ground with similar materials, i.e., class B25 concrete and A400 NR steel rebars. The floor slab and the side walls were cast monolithically without any construction joints along its length. To provide better crack control performance the steel rebars were placed at a maximum 0.15 m o.c. spacing and an epoxy-coating waterproofing layer applied.

### 2.3 The Surface Pavillion and the Technical Support Areas

The restaurant sleek design with its curved glass facades required the use of a slender roof system. A composite lightweight concrete slab connected to structural steel beams was used in order to reduce the total flat roof thickness. Above this roof system a structural steel grid with aluminum fixed blades provide extra shading on the pavilion esplanades, Fig. 5. The large twin-cell water tanks, placed over concrete short columns supports above the ground floor, are located in the technical support area, with a 52.0 m length by 8.5 m width and 4.0 m height. Possible contour surfaces water leaks can be easily accessed and the cracks repaired. The total capacity is 60 cu. m which corresponds to nearly 10% of the “plaza-lake” total water volume. The concrete admixtures also included pozzolanic cements in order to improve concrete long-time behaviour and waterproofing resistance.

## 3. CONCLUSIONS

The new Amália Rodrigues top-of-the-hill park is an enjoyable experience to any visiting pedestrian. From the initial conceptual stages to the final built solution more than three years went by due to continuous improvements. Special care was taken in conceiving the different water cycles. The biological lake with muddy water was separated from the clean water “plaza-lake”, and in both lakes the “trop-pleins” discharges were carefully detailed. The pavilion near the lake was designed with a lightweight structural steel frame system in order to enhance the curtain glass façade. The general utilities garden network system – water supply, drainage, public lighting, was also studied to integrate the different equipments. At a total cost of 2.0 m euros, this new public park is a matter of achievement for the City of Lisbon.

## 4. ACKNOWLEDGEMENTS

The Author is greatly indebted to The City of Lisbon, the Faculdade de Arquitectura, the Magnifico Rector of The Tech. Univ. of Lisbon, for their support in this work. Sincere appreciation to *fib*- CEB-FiP –Hungarian Group, The Tech. Univ. of Budapest – Dept. of Civil Engineering, for their efforts in organizing the 3<sup>rd</sup> European Congress on Concrete Engineering.

## 5. REFERENCES

City of Lisbon – “Old Plans (1904 – 1911) by Silva Pinto and

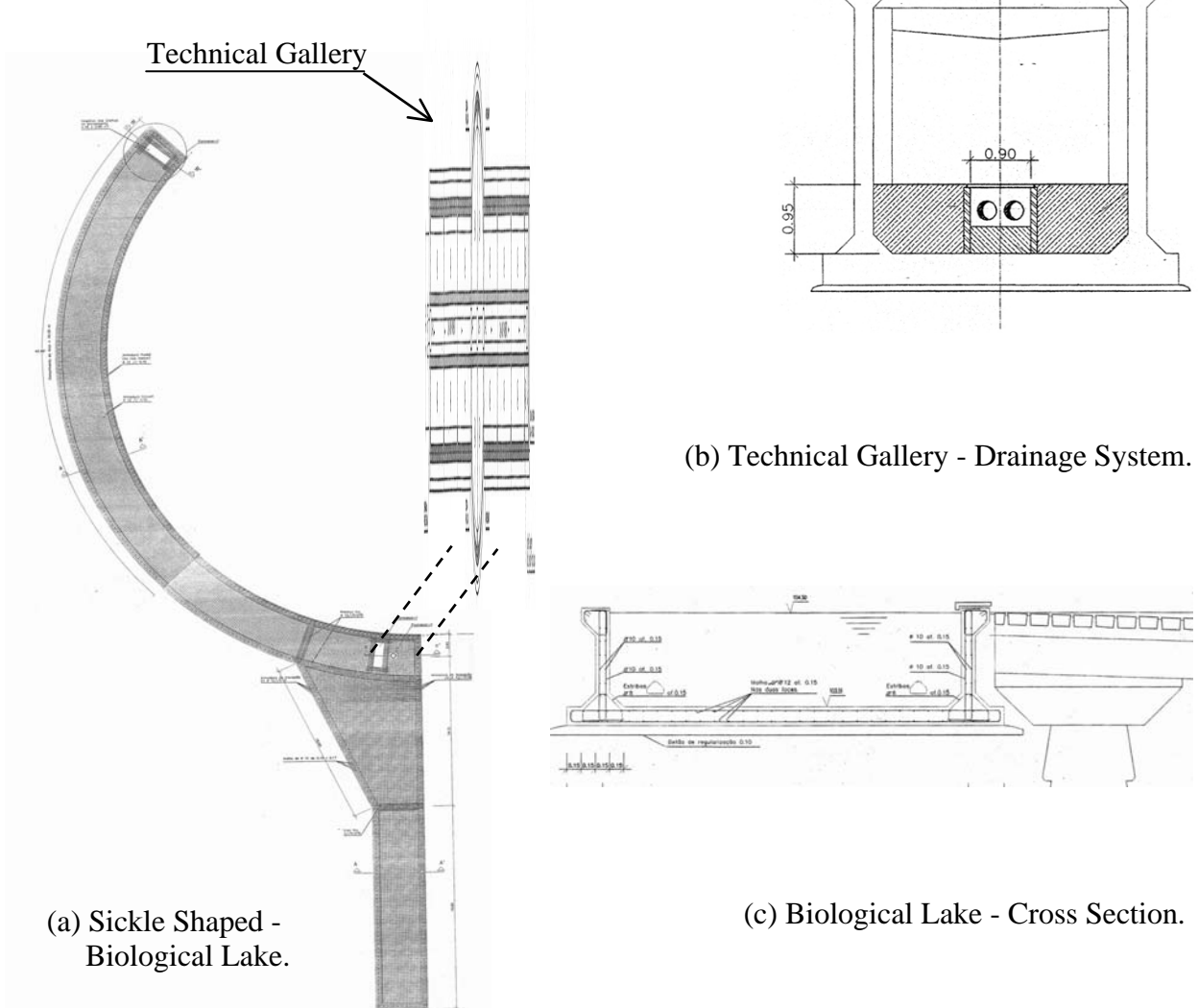


Fig. 4 Open-Channel Drainage System



Fig. 5 The Plaza-Lake and The Pavilion

## **INNOVATIVE APPLICATION OF HIGH PERFORMANCE SELF COMPACTING CONCRETE**

*Mr. S. Kanappan*  
*General Manager & Head ,*  
*Engineering Design and Research Centre – (Buildings & Factories Sector),*

*Mr. Sthaladipti Saha,*  
*Chief Engineering Manager,*  
*Engineering Design and Research Centre – (Buildings & Factories Sector),*

*M/s Larsen & Toubro Limited,*  
*Engineering Construction & Contracts Division*  
*P.O. Box 979, Manapakkam,*  
*Chennai 600 089, Tamil Nadu,*  
*India.*  
*Tel: 0091 - 44 - 22528101.*  
*Fax: 0091- 44 – 22526064.*

### **SUMMARY**

Technology Centre II, located inside M/s. Larsen & Toubro Ltd.- ECC Division ( L&T ) campus at Chennai, India is an exclusive office building with built-up area of 15000 sqm, designed with an innovative structural system implemented for the first time in India. The basic concept of the building is an expanding floor plate having a curvilinear profile, with the ends of the building anchored to the ground through shear walls. The innovative structural system implemented comprises posttensioned composite flat slabs with expanded polystyrene for main office areas, supported by central Reinforced Concrete core and peripheral Reinforced Concrete shear walls/Columns resting on pile foundation. Self Compacting Concrete (SCC) has been used on massive scale for concreting. Addition of high performance admixtures like Sulphonated Naphthalene Formaldehyde (SNF) resulted in a high strength concrete, making the mix cohesive with a free flow of slump  $625 \pm 25$  mm.

### **1. INTRODUCTION**

L&T, the principal consultant of the project has provided complete Design and consultancy services for Technology Centre II, Chennai. L&T offered turnkey design and consultancy for this prestigious project from concept to commissioning of all the services viz. structural, electrical, public health engineering, fire protection systems, building automation, air-conditioning, interior design, landscaping, kitchen equipment and acoustic design.

Technology Centre II is surrounded by roads on three sides and canal on the other side. The building has been constructed on turnkey basis including interiors and completed in a period of 17 Months.





Fig. 1 Exterior View

## 2. ARCHITECTURAL FEATURES

The basic concept of the building is an expanding floor plate to provide a lighter base in harmony with the existing development in the campus. The building has curvilinear profile to provide a softer edge in a rectangular profiled site, with the ends of the building anchored to the ground through shear walls. The building has been organized with a central core containing service facilities with an organization of plan providing for large column free office space.



Fig. 2 Curvilinear Wall



Fig. 3 Formwork for Curvilinear Wall

All the common facilities are organized in the ground floor to provide secure office space in the upper floors. The building form was articulated through a controlled use of Glazing and Punch Windows. It was further enhanced through the use of pattern in concrete and texture finish and the curvilinear profile of the silhouette of the building. The building outer faces are profiled to an inclination of  $0^{\circ}$  at ends to  $11^{\circ}$  at centre.

Technology Centre – II is a ground plus four storied building, with built-up-area of 15,000 Sq.m and floor to floor height of 4.05 m to create a clear space of 3.45m in each floor to host Electro-Mechanical services. The ground floor houses the corporate facilities. The first to fourth floor has been detailed for housing modular office facilities. The Terrace, houses the service back bone facilities like chiller plant, Lift machine room, pump rooms and water tank. Soft and hard landscaping has been provided around the building to enhance the aesthetics.

### 3. STRUCTURAL SYSTEM

An innovative and exclusive structural system implemented for the first time in India has been adopted here. It comprises *Posttensioned composite flat slabs with expanded polystyrene* for main office areas, supported by central reinforced concrete core and peripheral reinforced concrete shear walls/columns resting on pile foundation. Due to this structural system a *large column free space of span 20 x 45 m* was achieved.

The building has been designed for seismic zone-III (4 % lateral shear ) with ductile detailing as per latest Indian codes of practice and other relevant Indian standards. Reinforced Concrete walls on either sides of the building and central reinforced concrete core act as rigid lateral load resisting system to take seismic and wind forces. 3-Dimensional Finite Element Analysis of the structure has been carried out using ETABS and SAP software packages. Appropriate loads and its combinations as per Indian Standard codes, for most unfavourable effects are chosen for design. In analysis, slab has been modelled as an equivalent rectangular section and density of the material in the model adjusted to account for the equivalent I-section.

#### 3.1 Use of High Strength and High Performance Concrete

Each post tensioned flat slab floor plate of 60m x 45m size is 600mm thick and has been *cast composite with expanded polystyrene to reduce the self-weight component*. Cross section comprises 75 mm thick top and bottom slab with infill. The infill has been placed as shown in Fig. 4.

##### 3.1.1 Infill Material

Expanded polystyrene blocks of sizes 875 x 875 x 450 mm and 875 x 750 x 450 mm thick have been used to reduce the self-weight of slab by 33% and overall weight on foundation by 27%. Prestressing system with 5/13 flat ducts and 12/13 circular corrugated GI ducts have been adopted.



Fig. 4 Polystyrene Blocks with Top Mats in place





Fig. 5 View of Curvilinear Wall

### 3.1.2 Self Compacting Concrete (SCC)

Self Compacting Concrete (SCC) has been used on a massive scale for the first time in India.

SCC has been chosen due to its high performance and excellent deformability in the fresh state and high resistance to segregation. Since there is no need for external compaction and to avoid noise pollution, this unique material has been selected in place of ordinary concrete.

SCC used in a thin slab, being a better flowing material can be used effectively in reinforcement congested areas. It had helped us to use formwork for more repetition resulting in greater productivity.

### 3.2 Production of Material

The concrete was manufactured at the Ready Mix Concrete (RMC) plant located about 6 kms. from the site. The close proximity of the RMC plant aided in reducing the time taken for placing of concrete and increased the speed of construction invariably.

The concrete was poured in two stages. The first casting was done to the 75 mm thk. flat slab at a duration of 24 hours. The second casting of concreting was done to the ribs and top slab at a duration of 48 hours. This has been followed mainly to overcome floating of infill material due to buoyant force.

#### 3.2.1 Use of High performance Admixtures

*Sulphonated Naphthalene Formaldehyde (SNF)* was the admixture added to SCC . 300 ml to 400 ml of admixture was added to 50 kg of cement. Addition of SNF to SCC made the mix cohesive with a flow of slump  $625 \pm 25$  mm.

*Class F-Fly ash* - an environmentally friendly material was used as a cementitious material at 15 to 20 % of Ordinary Portland Cement (OPC). The use of fly ash gave multiple benefits as Greener concrete, enhanced cohesiveness and better slump retention. Fines which were available in plenty were used extensively more than the coarse aggregates.

### **3.3 Benefits of Using Fly ash in Concrete**

Benefits of using fly ash in concrete are listed as follows:

- a) Reduction of water demand producing equivalent workability, equivalent early stripping & handling performance, lower permeability & reduced bleeding,
- b) Improved cohesion due to higher volume of fines, reduced fines deficiency & better particle size distribution improved pumping performance.

## **4. INNOVATIONS**

*Post-tensioned composite flat slabs with expanded polystyrene* for main office areas supported by central reinforced concrete core and peripheral reinforced concrete shear walls/columns resting on pile foundation. Due to this structural system a *large column free space of span 20 x 45 m* was achieved.

Each Post tensioned flat slab floor plate of 60 x 45 m size is 600 mm thick and is *cast composite with expanded polystyrene to reduce the self-weight component* thus bringing about quantity and hence cost savings to the client.

## **5. LEARNINGS AND PRECAUTIONS TAKEN**

The use of SCC resulted in a high workable slump giving rise to buoyant force which was faced with a great challenge during the execution. Two stage concreting has been done to avoid upliftment of insulation materials.

## **6. CONCLUSIONS**

The building is an example of Innovative and Pioneering technology implemented for the first time in India. The swank building is architecturally and structurally an outstanding masterpiece. As a result of its unique structural system, the building has the *flexibility* to undergo any modifications in its functional requirements and when need arises even after 50 years.

## **7. LIST OF NOTATIONS**

SCC - Self Compacting Concrete  
SNF - Sulphonated Naphthalene Formaldehyde  
RMC - Ready Mix Concrete  
OPC - Ordinary Portland cement

## **8. ACKNOWLEDGEMENT**

We acknowledge the contribution made by Architect-M/s R.Chakrapani & Sons, India who had fully co-operated in achieving a better and efficient structural system.

We also express our heartfelt thanks to the in-house Research & Development Team-Concrete Technology Cell for their continued support in developing this innovative material and Mrs. Febin, MAVENS team head for preparing this article .

We are grateful to our management for the encouragement and freedom to carry out the experimentation.

## **9. REFERENCE**

“The European Guidelines for Self Compacting Concrete–Specification, Production and Use”- May 2005.

## PRELIMINARY RESULTS ON A FULL SCALE EXPERIMENT ON SEISMIC ROCKING OF STRUCTURAL WALLS

*Marco Preti and Ezio Giuriani*

*Department of Civil, Architectural, Environmental and Land Planning Engineering, DICATA,  
of the University of Brescia, via Branze 43 – 25123 – Brescia – Italy  
[marco.preti@unibs.it](mailto:marco.preti@unibs.it)*

### SUMMARY

In the present work a full scale structural wall referring to a five storey building was studied. A non traditional technique, based on the use of un-bonded steel tendons, instead of longitudinal reinforcing bars, combined with steel hollow dowels was adopted. In this way the compressed concrete damages due to plastic instability and low cycle fatigue, which are typical of ordinary longitudinal reinforcing bars, were avoided as the un-bonded tendons worked only in tension up to structural collapse. The shear over-strength was assured adopting vertical un-bonded hollow dowels in the critical region. These hollow dowels, in practice, substituted the sheaths for the tendons. The preliminary experimental results are here presented and discussed.

### 1. INTRODUCTION

Structural walls are widely adopted in seismic resistant building structures because they offer both sufficient stiffness to avoid damages to the non structural elements under frequent earthquakes and adequate ductility under stronger events (Paulay and Priestley, 1992, Fintel, 1995). Recent research (Riva et al., 2003, Preti et. al., 2007, Preti and Giuriani, 2007) showed that the flexural ductility is not always guaranteed. Sufficient ductility can actually develop only when appropriate detail is adopted in the critical region. As a matter of fact the risk of sliding shear failure becomes relevant when little vertical load is carried by the wall. Furthermore, anticipated crushing of compressed concrete may occur due to the local plastic buckling of reinforcement. Strong and closely spaced stirrups are not sufficient to avoid the plastic buckling of steel bars and the shear collapse. A solution of this problem was proposed by using uniformly distributed longitudinal reinforcement in the cross section. The effectiveness of the solution was confirmed by the results of one full scale test (Preti and Giuriani, 2007).

Nevertheless, at very large values of drift (about 2.5%), under few cycles of loading, significant damages were observed such as the extensive concrete cover spalling and the fracture of the most loaded longitudinal bars. In order to provide large drift capacity without significant damage, the solution adopting rocking walls was proposed by some authors (Priestley et al., 1999, Kurama et al., 2002, Holden et al., 2003, Seo and Sause, 2005).

Prestressed un-bonded tendons, instead of the usual reinforcement bars, make controlled rocking possible avoiding damages due to plastic buckling of the compressed bars. Nevertheless, some authors raised and underlined the uncertain reliability of the shear resistance at the base of the wall (Kurama et al., 2002). As a matter of fact the friction of the compressed concrete at the base of the wall providing shear capacity can be compromised by

the decrease of the concrete interlocking resistance due to repeated impact and local dynamic effects.

In the present paper a new solution is proposed for structural rocking walls to prevent shear slip and failure. In the critical region un-bonded and thick steel sheaths around each tendon were adopted to provide effective dowel resistance against the shear sliding. Such a solution was adopted and tested in a full scale structural wall, under cyclic loading up to very large drift. Due to the complexity and the efforts required by the full scale testing, only one test was possible to be carried out. Then the aim of the present research work is to show the effectiveness of the proposed solution and to provide early experimental results which can be useful for calibrating further theoretical and numerical formulations.

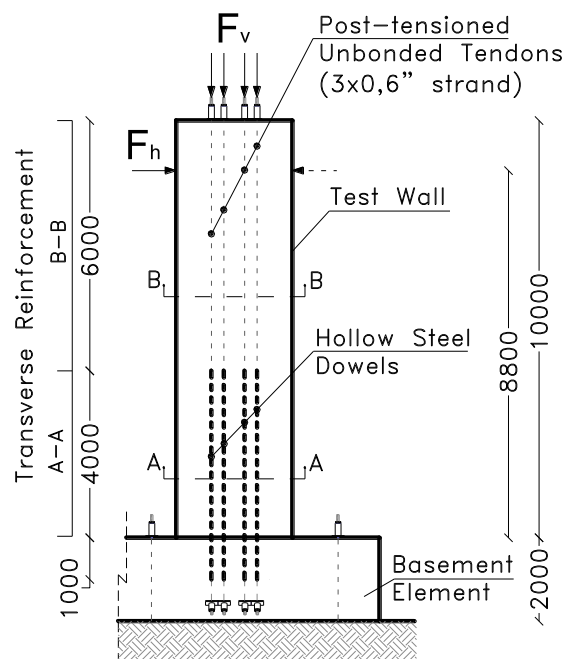
In the present paper some preliminary results are presented which show the global behaviour of the wall. The course of the experimental research will focus more in detail on the effectiveness of the dowels and the critical region behaviour.

## 2. GEOMETRY AND MECHANICAL CHARACTERISTIC OF THE STRUCTURAL WALL

The full scale experimental structural wall (Fig. 1) was preliminary designed and proportioned referring to a hypothetical ordinary five storey building, subjected to a strong earthquake. The lateral force on the wall was assumed as 30% of the weight of the building tributary area, which was assumed equal to 50 m<sup>2</sup>.



(a)



(b)

2Fig. 1 Full scale test wall (a) and position of the post-tensioned un-bonded tendons and dowels (b)

The test wall was 10 m in height, equal to two thirds of the case study height  $h_d$ . A constant section 2800×300 mm was adopted. So the wall geometric aspect ratio in the case study building was  $h_d/l_w = 5.4$ , where  $l_w$  was the overall section depth of the wall, while the shear span, defined as the ratio of the resultant lateral force height on the section depth, was

$M_b/V_b \cdot l_w = 3.9$ , being  $M_b$  and  $V_b$  the moment and shear action at the base of the wall in the case study. The position of the applied force over the base in the experimental test was equal to 8.8 m about one meter below the level of 2/3 of the case study building height.

Figs. 1 and 2 illustrate the test wall geometry and the location of the un-bonded tendons and the dowels. The wall was embedded at the base on a stiff basement element. Details concerning the experimental set up are widely illustrated in the paper (Preti and Giuriani, 2007). The global axial force provided by the tendons was 2500 KN (8 unbonded tendons made of three 0.6" strand, of 11.5 m total length). Note that referring to the case study, this adopted axial force was assumed as the addition of the structural weight of the tributary floors and of the prestressing load.

In order to avoid a shear collapse at the wall base, a shear over-strength of 50% was adopted. The task of resisting shear action was completely assigned to eight steel hollow dowels. These dowels are made of steel pipes (48 mm diameter and 8 mm thickness) which replace the sheaths of cables at the base of the wall (Fig. 1). The dowels are wrap in thin polythene sheaths to avoid bond and thus axial stress. Their resistance was evaluate according to (Eurocode 8, 2004). The wall was reinforced with strongly confining stirrups in the critical region, up to 4 m from the base (Fig. 2), in order to improve the concrete ductility. No vertical ordinary reinforcing steel bars were placed in the wall to avoid any damage produced by buckling. The stirrups were sustained by plastic pipes (diameter 12 mm). The confinement allowed to achieve large inelastic deformations of concrete and, thereby, a large curvature in the critical region. The volumetric confinement steel ratio, constant along the section, was  $\rho_c = 1.80\%$ . Besides this transverse confining reinforcement other ordinary stirrups (8 mm diameter) were placed along the total wall height.

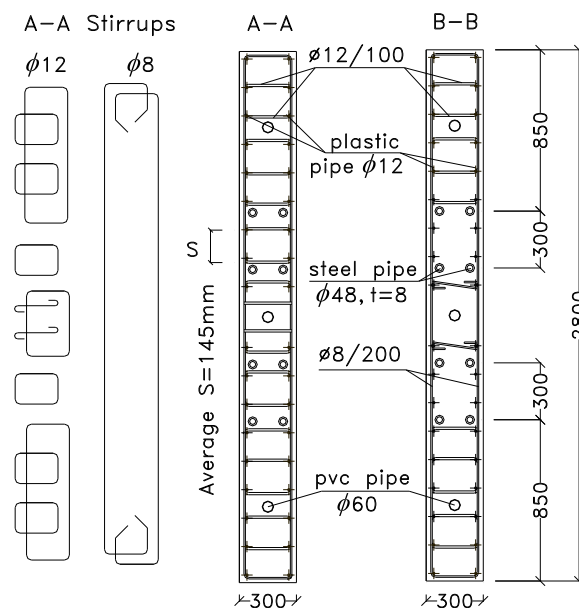


Fig. 2 Details of the wall transverse reinforcement and position of the hollow dowels and tendons

The mechanical characteristics, as determined by means of standard tests on three concrete cube specimens (150x150x150 mm), are summarized in Tab. 1. The computed confining stress was  $\sigma_2 = 2.5 \text{ MPa}$ , having adopted FeB44k steel stirrups, ( $f_{ym} = 550 \text{ MPa}$ ). The theoretical confined compressive strength  $f_{cc} = 55.3 \text{ MPa}$  e ultimate compressive strain  $\varepsilon_{cc,u} = 1.6\%$  were obtained from Collins and Mitchell (1997).

Tab. 1 Concrete mechanical characteristic based on UNI-EN 12390 standard test on cubic specimens

Concrete Specimen		1	2	3
Size, mm	Height	150	150	150
	Length	150	150	150
	Width	150	150	150
Mass, kg		8356	8256	8292
R <sub>c</sub> , MPa		49.6	50	50.8
R <sub>cm</sub> , MPa		50.1		
E <sub>c</sub> <sup>*</sup> , MPa		28300		
f <sub>ct</sub> <sup>**</sup> , MPa		4.1		
ε <sub>c,u</sub> %		0.35	0.35	0.35
Water Cement Ratio		0.54	0.54	0.54
Aggreg. max diam, mm		25	25	25

\*Indirect test value at 1<sup>st</sup> application of load. \*\*  $f_{ct} = 0.63\sqrt{f_{cm}}$  (Collins and Mitchell, 1997)

### 3. EXPERIMENTAL APPARATUS

The horizontal load was applied at the top of the wall, by means of pushing and pulling jacks, for seven cycles of increasing amplitude under displacement control. The horizontal reactions of the jacks were supported by a second reaction wall. The average loading rate, defined by adopting the displacement settling criterion at each step, was equal to about 180 mm/h (Preti and Giuriani, 2007). The instrumentation was defined to measure the top wall horizontal displacement, the applied lateral load, the curvature and the sliding at the wall base. The displacements and deformations were measured by 18 potentiometric transducers. More details on the instrumentation will be illustrated in a future report.

A plumb line system measured the wall horizontal displacement at the applied load; the plumb was immersed in water to damp its oscillation. The horizontal force was measured indirectly by the jack oil pressure using a full bridge resistive pressure transducer. The maximum jack loading capacity was 800 kN and the maximum inaccuracy was about 1%, measured by means of experimental calibration.

The crack pattern of the front face of the critical region was recorded at each load step by means of a high resolution camera. A 200x200 mm grid painted on the wall surface was adopted as reference system for the cracks.

### 4. EXPERIMENTAL RESULTS

The experimental results are illustrated in the following Force-Drift diagrams (Fig. 3). The total drift was obtained by the measured horizontal displacement at the level of load application. Fig. 3(a) shows the first two cycles. The first, in the un-cracked stage, allowed the set up of the test apparatus and instrumentation together with the evaluation of the initial stiffness of the wall and, indirectly, of the Young's modulus of concrete. The first crack opening occurred at about 0.03% drift and 160 kN lateral force (point A in Fig. 3(a)). Fig. 3(b) illustrates the seven cycles applied to the wall up to the maximum investigated drift. The behaviour was characterized by a small amount of energy dissipated. The curves of each loading and unloading cycle show a trend to a bilinear behaviour. The branches of the curves at increasing loading practically superpose each other. The loading branches B-C and



unloading D-E are nearly parallel. The branches O-B and E-O are practically superpose. A family of ideal bilinear curves could be obtained by the coordinates of point B, C, D and E provided in Fig. 3. Basically the same behaviour occurred for cycles in reverse loading. Due to the lengthening of the tendons in consequence of the wall drift increment, hardening of the wall strength occurred. The slope of the ideal linear branch B-C and of D-E are about 1/12 of the first linear branch O-B. No residual drift was obtained at the end of each cycle.

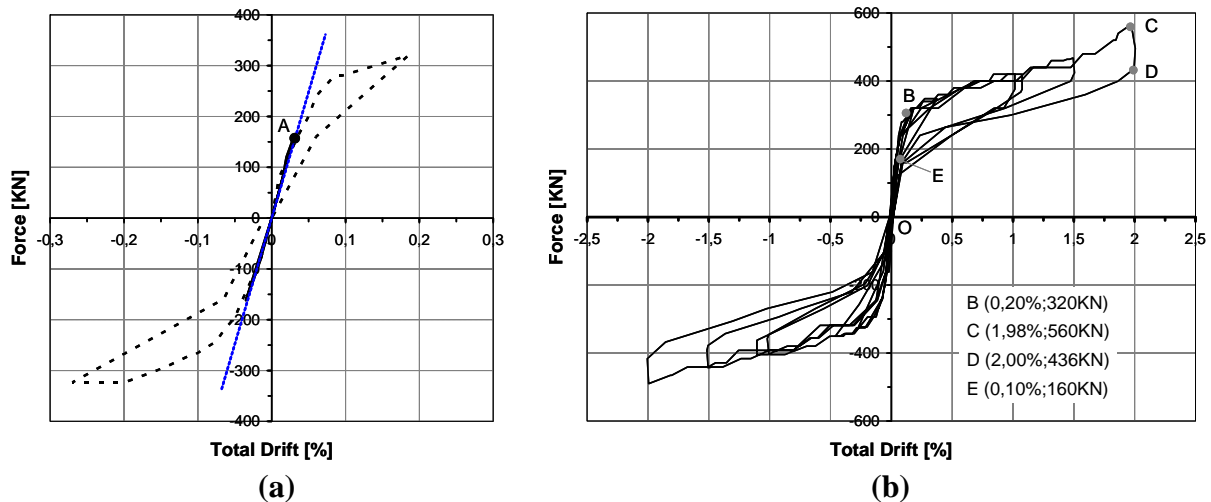


Fig. 3 Lateral Force versus Total Drift diagrams of loading cycles I and II (a) and of the all cycles (b)

The wall underwent a typical rocking deformation with only one large crack opening at the base (Fig. 4(a)), while the rest of the wall remained un-cracked. Minor damage occurred in the compressed concrete (Fig. 4(b)), where cover spalling started at 1,5% drift, without affecting the overall bearing capacity of the wall.



Fig. 4 Details of the single large crack opening at the base of the wall (a) and of the minor spalling of concrete cover in the compressed region (b) at maximum displacement

#### 4. CONCLUSIONS

Based on these preliminary results of the experimental investigation on a full scale rocking structural wall, the following concluding remarks are drawn:

1. The global behaviour of the wall showed very little damages and no signal of shear sliding up to large deformations.



2. Large values of total drift up to 2% drift were obtained under reversed cyclic loading and no stiffness or stress degradation were measured.
3. Even at very large drift the compressed concrete maintained its bearing capacity suffering only minor damage in the external concrete cover after 1.5% drift.
4. No residual drift and little hysteresis was observed after each cycle.

The course of the research program will investigate more in detail the role of the un-bonded hollow dowels in providing reliable shear over-strength against sliding. In order to evaluate the only contribution of the dowels to the shear resistance, an artificial drop of friction in the cracked section will be created.

## 6. ACKNOWLEDGEMENTS

The experimental test was partly financed by MIUR (Ministry of Education, University and Research) within the Research Program of National Interest Prin 2004. The contribution of UNIECO s.c.r.l., Calcestruzzi s.p.a., Ferriera Valsabbia s.p.a., Axim Italia s.p.a. allowed the construction of the experimental wall and apparatus. The authors gratefully acknowledge all the supporters. Finally, the authors are grateful to P. Spatti and D. Fiorillo who, together with the authors, carried out the design and testing of the wall respectively, and to the staff of P. Pisa Laboratory of the University of Brescia.

## 7. REFERENCES

- Collins M.P., Mitchell D. (1997), "Prestressed concrete structures", *Response Publications, Canada*.
- Eurocode 8, (2004), "Design of structures for earthquake resistance", EN 1998-1:2004.
- Paulay T., Priestley M.N.J. (1992), "Seismic design of reinforced concrete and masonry buildings", *Wiley-interscience*.
- Fintel M. (1995), "Performance of buildings with shear walls in earthquakes of the last thirty years" *PCI Journal*, 1995, 40(3), pp. 62-80.
- Holden T., Restrepo J.I., Mander J.B. (2003), "Seismic performance of precast reinforced and prestressed concrete walls", *Journal of structural engineering, ASCE*, march 2003, pp. 286-296.
- Kurama Y.C., Sause R., Pessiki S., Lu L.W. (2002), "Seismic Response Evaluation of Unbonded Post-Tensioned Precast Walls", *ACI Structural Journal*, V.99, No.5, Sept-Oct. 2002, pp. 641-651.
- Preti M, Riva P., Giuriani E. (2007), "Indagine Sperimentale sulla Duttibilità dei Setti di Controvento in Scala Reale Sottoposti a Carichi Ciclici", *Proceeding of the XII Convegno L'ingegneria sismica in Italia*, June 2007, Pisa, Italy, 47, pp.163. (in Italian)
- Preti M., Giuriani E. (2007), "A Full Scale Test on the Structural Wall Ductility under Cyclic Loading", *Università di Brescia, Dipartimento di Ingegneria Civile, Architettura Territorio e Ambiente, Technical Report n.9*, 2007.
- Priestley M.N.J., Sritharan S., Conley J. R., Pampanin S. (1999), "Preliminary Results and Conclusions from the PRESSS Five-Story Precast Concrete Test Building", *PCI Journal*, V.44, No.6., Nov-Dec 1999, pp. 42-67.
- Riva P., Meda A., Giuriani E. (2003), "Cyclic behaviour of a full scale RC structural wall", *Engineering Structures* 25, 2003, pp. 835-845.
- Seo C.Y., Sause R. (2005), "Ductility Demands on Self-Centering Systems under Earthquake Loading", *ACI Structural Journal*, V.102, No.2, Mar-Apr. 2005, pp. 275-285.

## INNOVATIVE TECHNIQUE FOR SEISMIC UPGRADE OF RC SQUARE COLUMNS

*A. Prota, G. Manfredi, A. Balsamo, A. Nanni, and E. Cosenza*

*University of Naples, Federico II – Italy*

*[aprota@unina.it](mailto:aprota@unina.it), [gamanfre@unina.it](mailto:gamanfre@unina.it), [albalsam@unina.it](mailto:albalsam@unina.it), [nanni@unina.it](mailto:nanni@unina.it), [cosenza@unina.it](mailto:cosenza@unina.it)*

*G. Morandini*

*Mapei S.p.A. – Italy*

*[composite@mapei.it](mailto:composite@mapei.it)*

### SUMMARY

The preliminary results of an experimental investigation on under-designed RC square columns are presented in the paper. The seismic upgrade was achieved by combining steel spikes (*MAPEWRAP S30*) and GFRP fabrics (*MAPEWRAP G UNI-AX*). Two parameters are investigated: the lap splice of the longitudinal steel reinforcement and the level of axial load. A comparison between as-built and strengthened columns is presented in terms of strength and ductility. The shear-top displacement relationships of strengthened columns are analyzed to assess the influence on the global performance of the lap splice. This preliminary analysis confirms that the proposed solution for the seismic strengthening of under-designed columns is very effective when it is necessary to relocalize the potential plastic hinges of columns by increasing their flexural strength. The obtained results will represent the basis for developing design criteria for the strengthening of similar interventions and will represent a reference for the calibration of a model of the strengthened column.

### 1. INTRODUCTION

Many existing reinforced concrete (RC) structures that are nowadays located in seismic zones have been designed about 40-50 years ago in order to withstand only gravity loads. The upgrade of their seismic performances represents an important issue that involves economic and social aspects in different areas of the world. These RC structures designed without seismic provisions are often characterized by an unsatisfactory structural behavior due to low available ductility and by a weak column-strong beam construction that, under a seismic event, yields most likely to the formation of local hinges in the columns. This failure mode represents the lower bound of the strength hierarchy because it is characterized by brittle and catastrophic structural crisis.

Different techniques can be selected to upgrade under-designed columns. Reinforced concrete jacketing, steel profile jacketing and steel encasement have been widely used in the past. All of them were characterized by disadvantages related to constructability (i.e., difficulty of ensuring perfect bond and collaboration between old and new parts, loss of space, construction time and high impact on building functions) and durability issues; in the case of reinforcing concrete jacketing, significant mass increase could also be generated. Innovative techniques based on FRP materials have become valid alternatives to those solutions; along with high structural effectiveness, composite materials are light and easy to install, their application does not imply loss of space and, in some cases, it can be performed without interrupting the use of the structure.

Laboratory experiments have confirmed that FRP laminates can significantly improve the seismic performance of RC columns. CFRP strips were used by Ye et al. to confine square columns; tests were conducted under an axial load ratio of 0.48. Iacobucci et al. (2002) investigated the behavior of columns simulating members typical of multistory structures and designed with non-seismic provisions; the columns were wrapped using Carbon FRP (CFRP) laminates and the axial load ratio ranged between 0.33 and 0.56.

The effectiveness of CFRP confinement to improve the seismic performance of rectangular under-designed columns was assessed by Shaheen et al.; the confinement provided by a continuous laminate was compared to that given by discontinuous strips. Bousias et al. (2004) investigated the seismic behavior of rectangular under designed columns with axial load ratios ranging between 0.34 and 0.40; the columns were wrapped with either CFRP or GFRP and the effect of corrosion was also studied. The opportunity of using FRP to repair damaged columns has been also verified. Ilki and Kumbasar tested the effectiveness of longitudinal and transverse CFRP laminates to restore the performance of damaged square columns with axial load ratios ranging between 0.05 and 0.20. Chang et al. (2004) tested 2/5 scale rectangular columns repaired using CFRP confinement and the pseudo-dynamic tests confirmed that the original seismic performance could be recovered after the FRP repair.

## **2. TEST SPECIMENTS**

A total of 8 column specimens were constructed and tested under monotonic lateral load. All had the same square cross-section with side equal to 300 mm and were internally reinforced using smooth steel bars. The specimens were characterized by height of 2.0 m above the footing 0.60 m deep. 8-mm diameter ties spaced at 100 mm on center were placed along the height; rules typical of old construction were followed for the first tie above the footing (placed at 50 mm from the column-footing interface) as well as for the geometry of the hooks. Two different layouts of the longitudinal reinforcement were realized. In type C columns, each of the three 12-mm diameter longitudinal bars disposed on each side of the cross-section had no lap splice from the footing; type LP columns had instead lap splices of the longitudinal reinforcement. Tests on cylinders taken during specimen construction provided an average cylindrical concrete strength of 24.9 MPa; the mechanical characterization of the used smooth bars provided a yield strength of 358 MPa and 327 MPa, a maximum strength of 449 MPa and 439 MPa, and a strain corresponding to the ultimate strength of 21.5% and 23.1%, for 8 mm-diameter and 12 mm-diameter smooth bars, respectively.

## **3. STRENGTHENING CONFIGURATION**

The design of the strengthening of the columns could not be done without considering the consequences of the column upgrade on the global performance of the structure. When operating on underdesigned structures, the local upgrade with composites should aim at improving the global deformation capacity of the structure. One way to reach this goal is to relocalize the potential plastic hinges; this means to establish a correct hierarchy of strength, that is a key criterion in the seismic design of new structures as suggested by seismic codes of Europe, USA, New Zealand and Mexico. Therefore, the strategy is the following: by increasing the strength of some elements (i.e., columns) it is achieved that the failure of others (i.e., beams) occurs before and then prevents that of the upgraded members. This allows protecting those elements whose failure could be critical from a global standpoint and then improving the seismic behavior of the structure.

Tests performed on RC columns and numerical analyses (Grasso et al., 2003) have demonstrated that the FRP wrapping can provide a significant benefit in terms of ductility of the confined cross-section, but the strength increase is negligible for axial load ratios that characterize typical columns of buildings or bridges. Since the goal of the strengthening was to modify the strength hierarchy, it was necessary to design a strengthening scheme that could allow increasing also the strength of the column. An innovative system was then proposed based on the combination of steel spikes and GFRP laminates. The steel spikes (*Mapewrap S30*) were made of 3x2 steel cords, each of them being obtained by twisting 5 individual zinc coated wires together; they were realized by cutting a roll of steel cords. The density of the 3X2 tape used in this research program consists of 87 cords per mm, which is considered high-density tape. The steel cords have an ultimate tensile strength of 3070 MPa, Young modulus of 184 GPa and ultimate strain equal to 0.017. A two-component thixotropic epoxy resin Adesilex PG1 (Mapei) was used to impregnate and bond the steel tape to the concrete substrate. GFRP uniaxial laminates having a density of 900 gr/m<sup>2</sup> (Mapewrap G uni-ax 900) were used. The supplier provides the following properties of these laminates: ultimate tensile strength equal to 1370 MPa, Youngs modulus equal to 65.6 GPa and ultimate strain equal to 0.021.

#### 4. EXPERIMENTAL PROGRAM

A total of 8 columns were tested, 4 as-built and 4 strengthened. Within each series of 4 specimens, two parameters were studied: the axial load ratio and the lap splice of the longitudinal steel reinforcement. The two selected axial loads were 270 kN and 540 kN corresponding to axial load ratios of 0.12 and 0.24, respectively. For each of those two axial load ratios, one type C and one type LP columns were tested. Each specimen is denoted in the following by a letter (C for columns without lap splice and LP for those with lap splice) followed by a number that indicates the value of the axial load (270 kN or 540 kN). The test setup is shown in Fig. 3. Two post-tensioned bars were used to connect the footing of each specimen to the strong floor. Even though the post-tensioning of the bars was computed in order to avoid the sliding of the specimen during test, lateral restraints were also provided on the short sides of the footing in order make the test system more safe. The vertical and horizontal hydraulic actuators were put in place; then, the axial load was applied. Once the column was under the fixed level of axial load, the lateral load started to act. Tests were performed in a displacement control mode.

#### 5. PRELIMINARY EXPERIMENTAL RESULTS

A detailed analysis of the experimental performance of the as-built columns is done elsewhere. The strengthened columns showed significant strength increases compared with those as-built. In terms of strength, the results show an average increase of 54% for the columns subjected to axial load of 270 kN and 33% for those whose axial load was 540 kN. The drift at 90% of the maximum shear force on the descending branch was less than that given by the as-built columns for the low axial load, whereas it almost doubled when the axial load was 540 kN. In terms of ductility index, the strengthened columns provided in all cases values lower than the corresponding as-built members. In terms of global behavior of the strengthened columns expressed in terms of shear-top displacement relationships, it appears that for axial load of

270 kN the trend was not very influenced by the lap splice of the longitudinal reinforcement Fig. 4. A different situation was observed for columns under 540 kN (Fig. 5): the specimen LP-540 showed a higher stiffness compared with C-540. This could be due to the different

failure mode: in the case of C-540 it was characterized by a reduced crack at the footing interface and by another significant crack that opened at the height where the spike was cut (Fig. 6 and 7); the crack pattern of LP-540 until failure showed only one significant crack at the footing interface Figure 16. In terms of strength, for both axial load levels type LP columns had a slightly higher strength compared with the corresponding of type C; this is consistent with the fact that for the length of the lap splice the amount of steel longitudinal reinforcement was double.

## 6. CONCLUSIONS

The paper presented the preliminary outcomes of an experimental analysis concerning monotonic and cyclic behaviour of under-designed RC square columns. An innovative technique based on the combination of steel spikes as flexural reinforcement and GFRP laminates as external confinement was validated in the laboratory. The comparison between as-built and strengthened columns provides strength increases ranging between 33% and 54% with increase also of the drift corresponding to maximum shear force. The obtained results allow also assessing the influence of the lap splice of the longitudinal reinforcement on the global behaviour of the column. The obtained results will be used as a reference for the calibration of a model of the strengthened column and they will be also the basis for the development of design criteria that engineers could use to design similar strengthening interventions.

## 7. ACKNOWLEDGMENTS

The authors would like to thank Mapei Spa, Milan, Italy, for donating the FRP system and supporting its installation. The activities here presented are included within the research project PRIN 2003 "Performance and Design Criteria for the Upgrade of RC Structures with Composites", funded by the Italian Ministry for University and Research.

## 8. REFERENCES

- Chang, S.; Li, Y.; and Loh, C., "Experimental Study of Seismic Behaviors of As-built and Carbon Fiber Reinforced Plastics Repaired Reinforced Concrete Bridge Columns," *ASCE Journal of Bridge Engineering*, V. 9, No. 4, July-August 2004, pp. 391-402.
- Chung, Y. S.; Lee, J. H.; and Kim, Y., "Experimental Seismic Performance Evaluation of Lap-spliced Bridge Piers," *Proceeding CD-ROM of the Seventh U.S. National Conference on Earthquake Engineering*, Boston, Massachusetts, July 21-25, 2002, Paper N. 150.
- Grasso, V.; Manfredi, G.; Prota, A.; and Realfonzo, R., "Effectiveness of the Confinement of UnderDesigned Columns using Composites," *Proceedings of the International Conference Composites in Construction*, Cosenza, Italy, September 16-19, 2003, pp. 343-353.
- Iacobucci, R.; Sheikh, S.A.; and Bayrak, O., "Seismic Behaviour of Square Concrete Columns Retrofitted with Carbon Fibre Reinforced Polymers," *Proceeding CD-ROM of the Seventh U.S. National Conference on Earthquake Engineering*, Boston, Massachusetts, July 21-25, 2002, Paper N. 326.
- Kono, S.; Matsuno, K.; and Kaku, T., "Bond-slip Behaviour of Longitudinal Reinforcing Bars Confined with FRP Sheets," *Proceedings CD-ROM of the 12 th World Conference on Earthquake Engineering*, 2004, Paper N. 642.

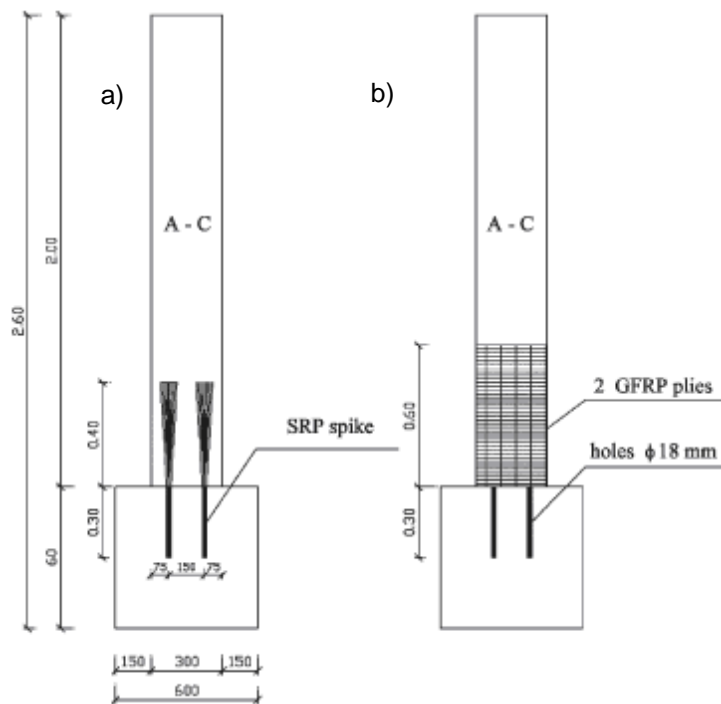


Fig. 1 Cross-section parallel to sides A and C: steel spikes (a) and final strengthening configuration (b)

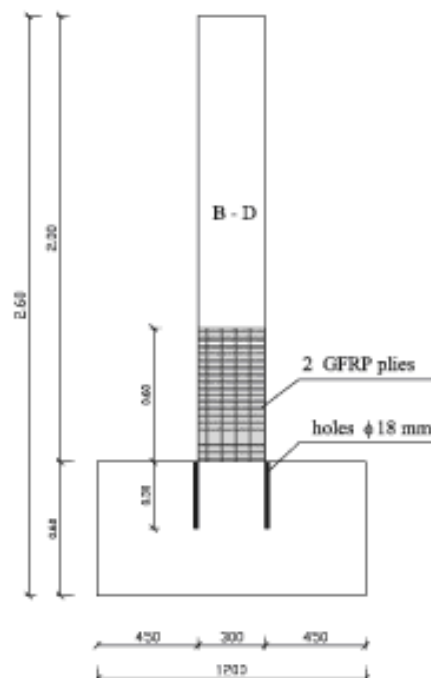


Fig. 2 Cross-section parallel to sides B and D: final strengthening configuration

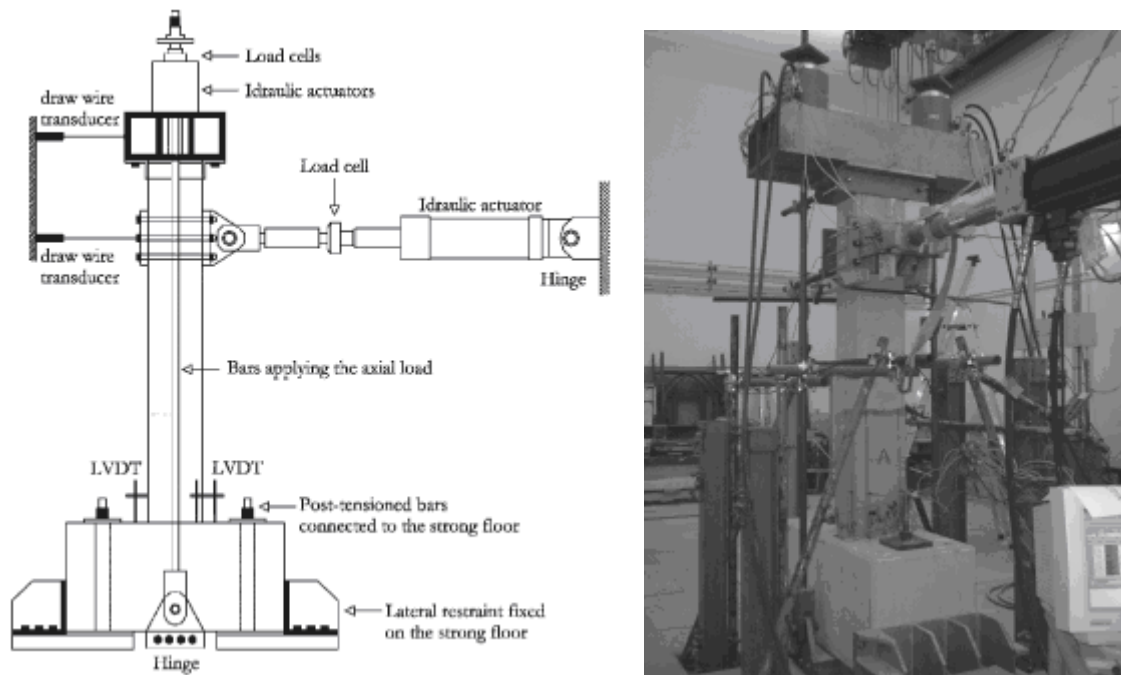


Fig. 3 Test setup and view of a column prior to testing

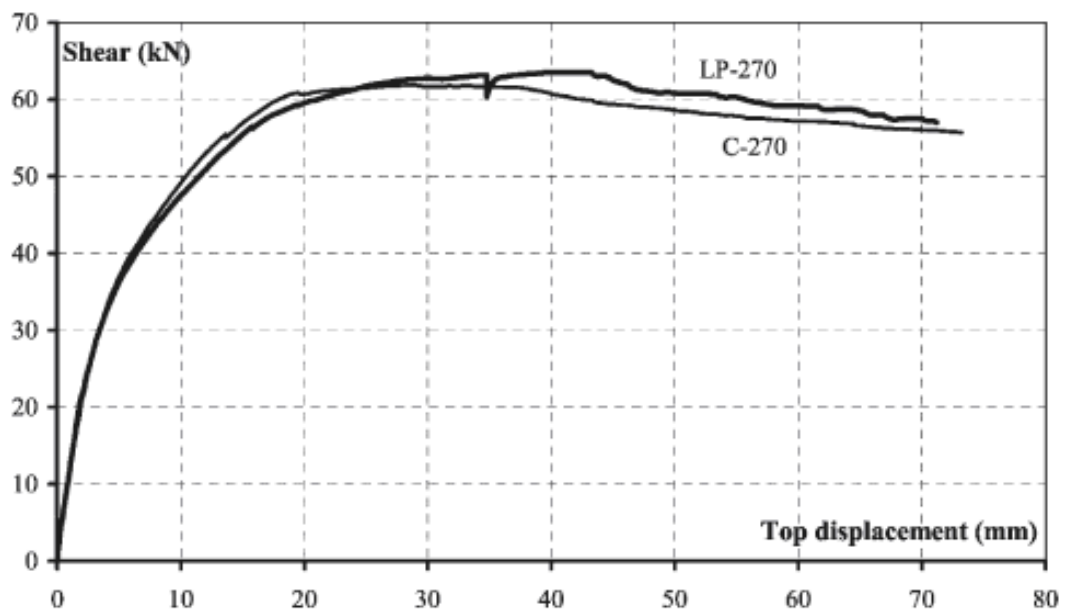


Fig. 4 Shear-top displacement curves for C-270 and LP-270 columns

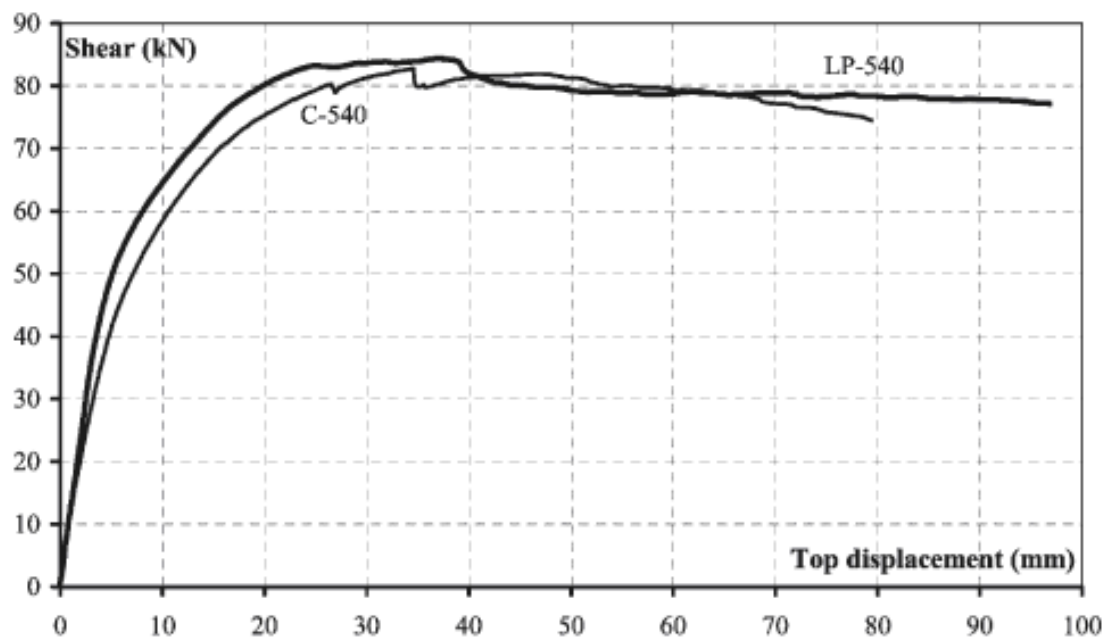


Fig. 5 Shear-top displacement curves for C-540 and LP-540 columns

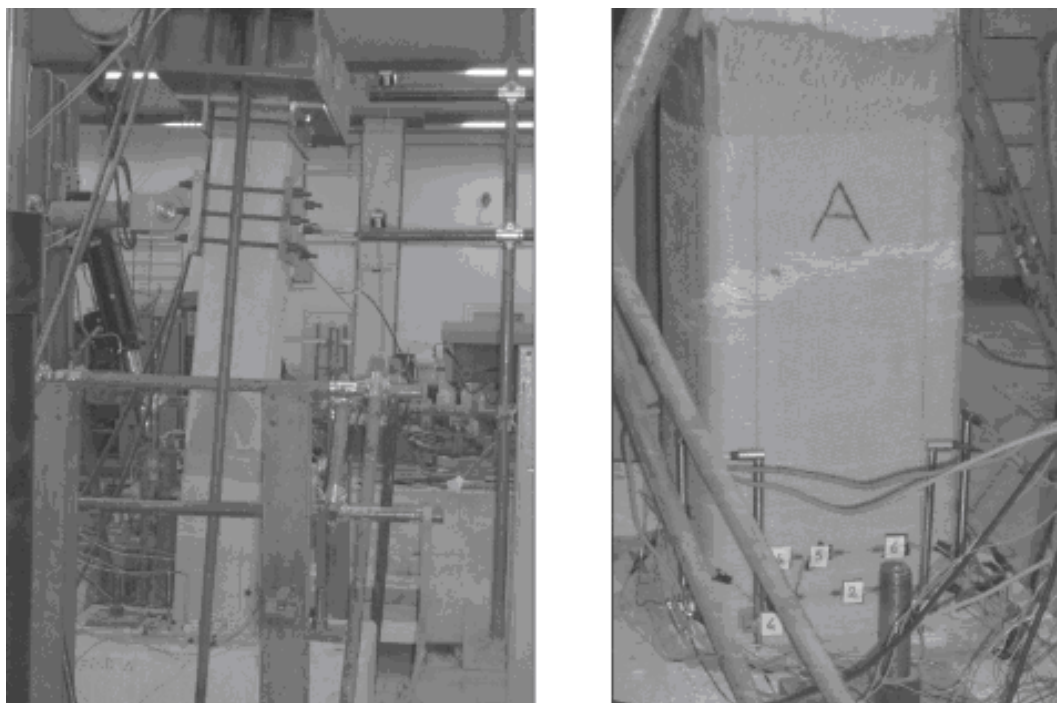


Fig. 6 Failure mode of C-540 column



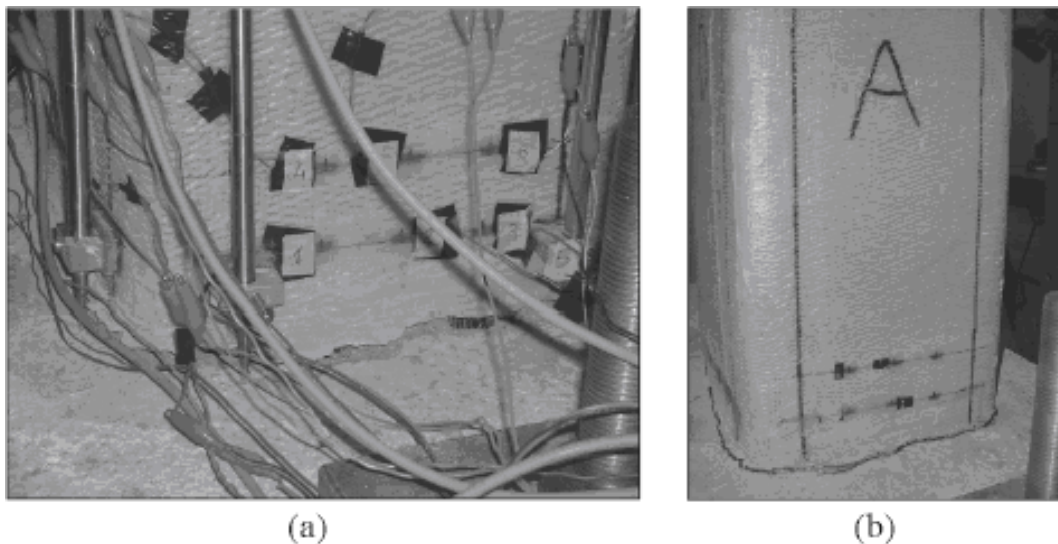


Fig. 7 Column LP-540 at end of the test: crack at column-footing interface (a) and view of side A (b)

## FOUNDATIONS FOR OFFSHORE WIND TURBINES

*Dr.-Ing. Christian Dehlinger, Ed. Züblin AG*

### SUMMARY

The design and dimensioning of the loadbearing structures for wind turbines – especially offshore systems – are a complex task. Stochastic waves, a turbulent three-dimensional wind field, complex control mechanisms, difficult geotechnical effects (the problem of pore water pressure during load cycles) affecting the dynamic interaction with the mass- and stiffness-distribution of the entire system determine the design. Any type of foundation has to pay close attention to this interaction. Although, in this case, concrete is more difficult to manage than steel, concrete foundations may not only be highly efficient, robust and maintenance-free, but also dynamically fine-tuned systems. It is a major advantage of prestressed concrete that the appropriate choice of prestress will result in the appropriate foundation for a certain situation.

### 1. INTRODUCTION

Wind turbines have been in use since the early 1980s. Recently there has been an unexpected push for this type of power generation which is mainly due to ecological reasons but also due to the desire for independence from fossil fuels. However, many people react highly critical towards the wind parks and single units existing throughout Europe. Not only do they question the efficiency of such land-based units, but there are also conflicting views regarding the use of the sites. The future offshore sites will hold a large potential for development and utilization. Since those sites are usually located far beyond the 12-mile-zone, there is a greater social acceptance than in case of the land-based sites and, in addition, the offshore units operate 30 % more total load hours annually since the wind offshore has a higher velocity and is less turbulent (Fig. 1). All this contributes to a considerably higher energy output, thus possibly compensating for the higher cost of developing offshore sites.

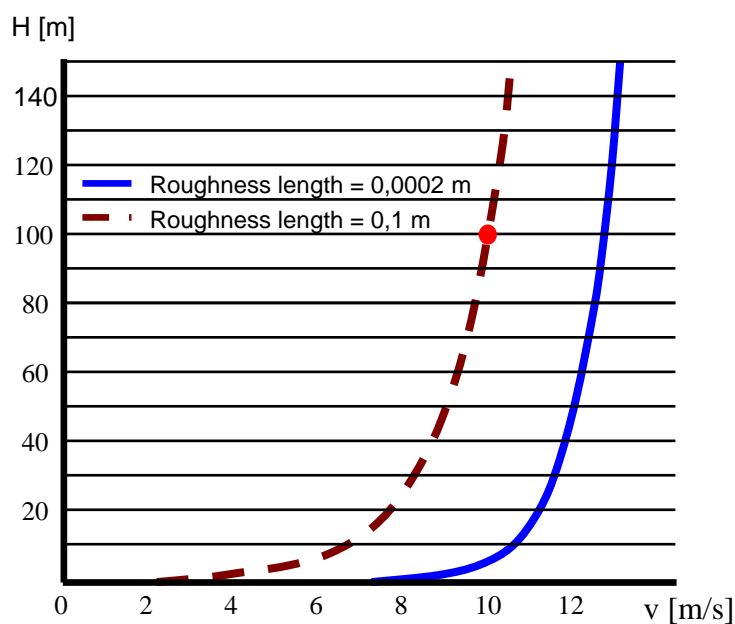


Fig. 1 Comparison between wind velocity onshore (brown) and offshore (blue)

## 2. FOUNDATION TECHNOLOGY

There are three different types of foundation commonly used for offshore wind turbines depending on the water depth and the condition of the ocean floor (Fig. 2). The type of foundation shown in the center of Fig. 2 depicts a single driven pile or monopile. Depending on the size of the wind turbine, this is an economic alternative for more shallow water and ocean floor permitting a monopile. In case of water depth exceeding 25 m the values of wave stimulation obtained during the fatigue strengths analysis might render an economic dimensioning is impossible.

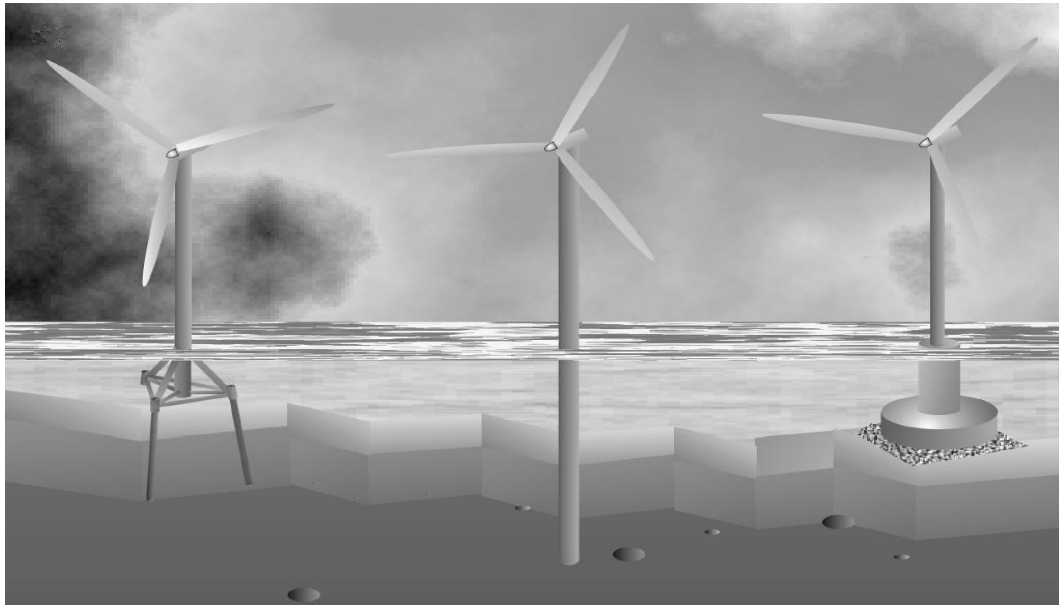


Fig. 2: Major types of foundation systems used for offshore wind turbines  
(source: Essener Unikate 23/2004)

The resonant frequency of the entire system may reach the induced frequency of the predominant waves and the monopile weakens, especially in the area exposed to wave impact, i. e. from the ocean floor to the surface. For water depth of up to 35 m and a sound ocean floor – consisting of compacted sand often found in the Northern Sea – the shallow foundation or gravity foundation on the far right in Fig. 2 is suitable. This type of foundation system also suits some sites in the Baltic Sea where large erratic boulders might occur in certain depths causing problems for both types of deep foundation described here. It is possible to design these shallow foundation systems with sufficient strength to withstand the wave impact. However, in this case the strength of the foundation joint might be insufficient, which may lead to similar effects. For greater water depths – up to approximately 50 m – very stiff tripod- or jacket- (steel truss) structures are appropriate. These, in comparison to the two previously described systems are sometimes more expensive and – as with the monopile – the conditions have to allow for the foundation piles to be driven into the ocean floor. Floating, submerged or semi-submerged foundation systems are being developed for water depths exceeding 50 m.

## 3. DESIGN OF THE FOUNDATION SYSTEM

Wind turbines with their towers and foundation systems are structures exposed to great dynamic stress. Therefore, the resonant frequencies of the entire system consisting of rotor,

generator, tower, foundation system and foundation soil play a major role in the design. During operation offshore wind turbines are subjected to a multitude of dynamic stresses with varying frequencies. This has to be taken into consideration when designing the tower and the foundation. The rotor frequencies may be subjected to major, periodically occurring impacts from the rotor caused by a possible unbalance (for example such as an uneven accumulation of ice) or to stimulations from the connection of blades to the face of the tower. Large modern turbines have a rotor frequency of  $f_{err,1p} = 0.15 \dots 0.25$  Hz; consequently the frequency of the blade connection of a three-blade-rotor increases by the factor 3 ( $f_{err,3p} = 0.45 \dots 0.75$  Hz).

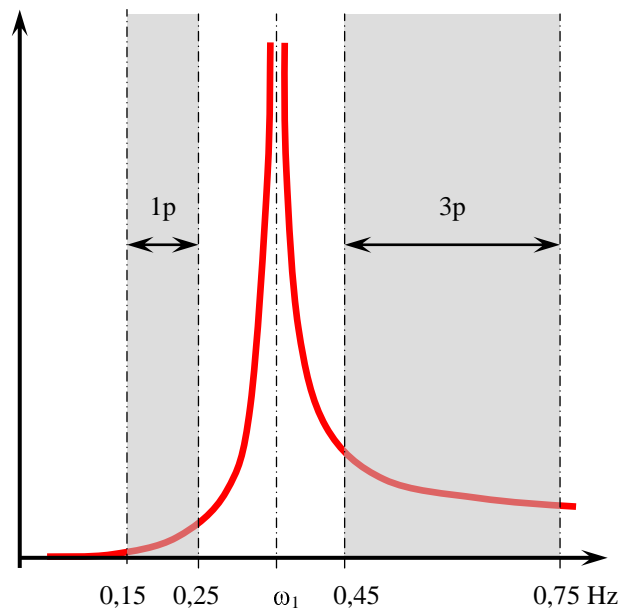


Fig. 3 Areas of the induced frequencies and the desired resonant frequency  $\omega_1$

The control mechanism of the wind turbine causes additional dynamic stress, for example due to a change in the rotation speed of the rotor or the generator, in the output or the blade angle. Further dynamic loads occur due to the swell (usually within the range of  $f_{err,w} < 0.25$  Hz) and due to wind gusts which in turn depend on the intensity of the turbulences. Since the loadbearing structures of wind turbines usually exhibit very little damping (logarithmic damping value  $\zeta < 5\%$ ), the dynamic design calls for the initial resonant frequency to be at least 10 % above the rotor frequency, but significantly below the blade frequency. This results in a rather narrow range of approximately  $\omega_1$  between 0.3 and 0.4 Hz (Fig. 3) for the initial resonant frequency. After determining the dimensions of the loadbearing structure and of the foundation, and after assessing the ultimate limit state while adhering to the target resonant frequency, additional assessments of the limit states of serviceability and, above all, fatigue assessments are conducted using time range aeroelastic simulation analysis comprising the following inducements:

- electrical and mechanical controls/control devices of the wind turbine
- dynamic behaviour of the entire system (foundation soil, foundation, tower, engine, rotor)
- aerodynamic inducements (including aerodynamic damping; this is up to 10 times greater than the structural damping)
- turbulent, stochastic 3D-wind field around the rotor and the tower
- loads due to waves and hydrodynamic effects (a resonant body of water around the system, hydrodynamic damping)

#### 4. SELECTING A SUITABLE FOUNDATION

In addition to the static and dynamic requirements described above, the choice of an efficient foundation suitable for a certain type of system and a certain offshore site is governed by several additional factors, with the erection method and the corresponding offshore logistics playing a major role. Just in this field there are several variations with construction management and the requirements being of a similar complexity as the static and dynamic aspects described earlier. Consequently, logistics may contribute up to 50 % of the construction cost of the foundation – depending on the number of systems to be constructed. Due to the multitude of possible variations and aspects, this paper will not cover the construction and erection, even though they require the same close attention during the design process.

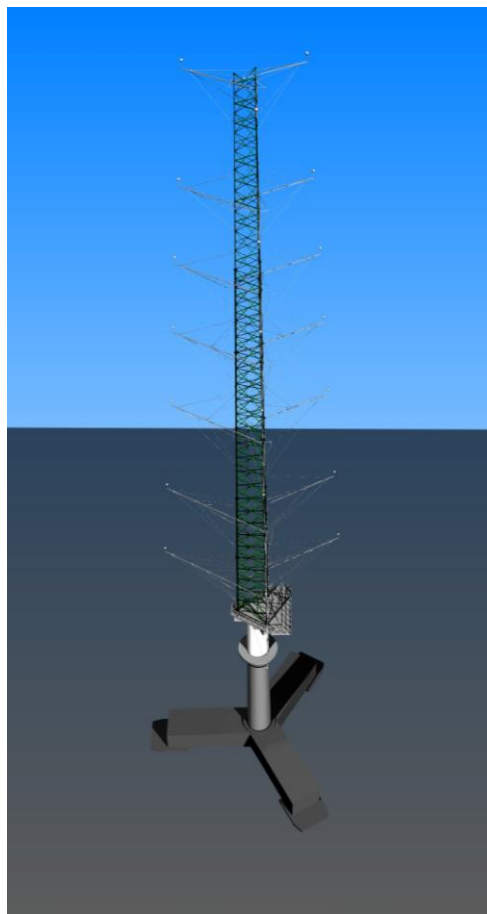


Fig. 4 Prestressed concrete gravity foundation for the tower in Arkona Basin in the Baltic Sea

Since the oil- and gas-industry largely dominate the offshore sector, steel is used predominantly for the foundations of offshore wind turbines, a solution strongly supported by the mechanical engineers who design the turbine-technology. Due to the history of (onshore) wind energy structural engineers were reduced to play a minor role. Therefore, reinforced and prestressed concrete foundations are still the exception. Closely following the recent developments in the development of offshore wind turbines, the Ed. Züblin AG has been applying the concept of prestressed concrete gravity foundations. In 2006 a gravity foundation was constructed for the tower in the Arkona Basin in the Baltic Sea (Fig. 4).

## 5. DYNAMIC BEHAVIOUR OF A PRESTRESSED CONCRETE STRUCTURE

The above described the requirements for a finely tuned dynamic system. The following explains the interrelations applying for the case of a prestressed concrete structure. First a concrete structure is subject to greater fluctuations of the structural dimensions compared to a steel structure (for example wall thickness of the structural elements). This is due to the manufacturing procedure (onsite-production as opposed to the production in a steel-mill). This may result in a deviation from the planned structural strengths. In addition, compared to steel, there are greater fluctuations in the E-modulus of concrete. Another major aspect is the fact that the stiffness of prestressed concrete elements depends on the load due to the transition of partial cross-sections of the prestressed concrete from state I to the cracked state II. These three factors influence the stiffness of certain areas of the structure and thus influencing the dynamic behaviour of the entire structure. In view of the above, the question arises whether or not concrete is suitable for the foundations of wind turbines.

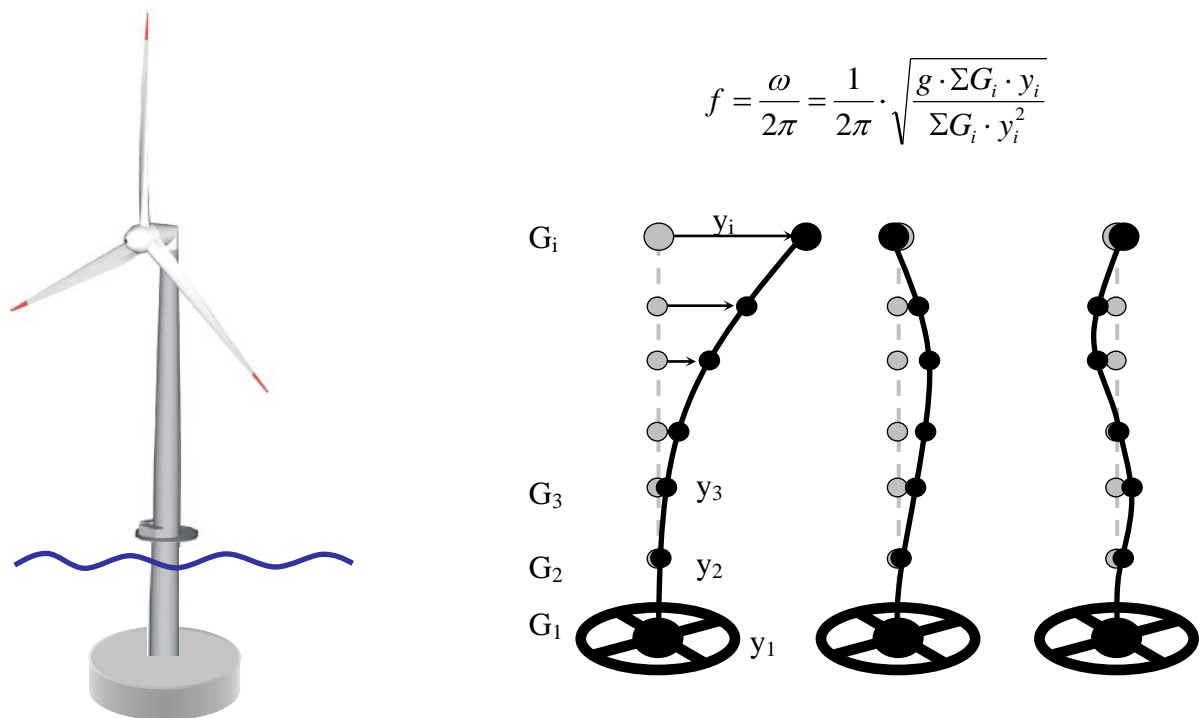


Fig. 5 Determination of the resonant frequencies and of the eigenforms of the complete system

The technical office of the Ed. Züblin AG conducted extensive tests to assess the magnitude of these impacts. The manufacturers of the generators require deviations from the target resonant frequency to be below five percent depending on the difference between the initial resonant frequency and the governing induced frequency. However, usually only the system's first natural frequency is of any relevance, since a higher resonant frequency results only in a slight acceleration of the rotor and generator. Fig. 5 shows for example the top of the systems remaining almost stationary in the 2<sup>nd</sup> resonant mode since the analysis of the affects on the initial resonant frequency proved that the impacts on the resonant frequencies caused by the deviations in the geometry of the cross-sections or in the E-modulus of the concrete were

justifiable (Tab. 1). In comparison: a change in the mass at the head (for example when using a different type of generator) will lead to a significant change in the dynamic behaviour.

The weight of engines in the same power category (for example the current 5 mega-watt-category) varies from approximately 280 tons to 450 tons, i. e. more than the examined 30 %. However, assumptions of 20 % fluctuations in the E-modulus of concrete of the same mixture were unrealistically high.

Tab. 1 Impacts on the 1. resonant frequency of the complete system

	<i>Basic values</i>	<i>Variation of the basic value</i>	<i>Change in the 1. resonant frequency</i>
<i>E-Modulus of the concrete</i>	<i>Mast C55/67 foot C 45/55</i>	+ / - 20%	<i>ca. 5%</i>
<i>Horizontal/ vertical foundation</i>	<i>Kz = 30 MN/m<sup>3</sup> Kh = 6 MN/m<sup>3</sup></i>	+ / - 50%	<i>ca. 3%</i>
<i>Wall thickness of the shaft</i>	<i>85 to 95 cm</i>	+ / - 15%	<i>ca. 3%</i>
<i>Head-mass</i>	<i>3000 kN</i>	+ / - 30%	<i>ca. 20%</i>

The loss of stiffness due to crack formation in the concrete (transition phase to state II) may be perfectly controlled by choosing the appropriate prestress for the cross-sections. A wind turbine experiences 30 different modes of operation. In some modes neither the generator, nor the rotor or the controls are operating. For example, this is the case when the system "trundles" in strong wind. These modes of operation do not necessarily require adhering to the resonant frequency since the dynamic stress also differs from the regular mode of operation. In this case it is acceptable for the stiffness of the loadbearing structure to decrease due to cracked sections; consequently the natural frequency is also reduced. Therefore, the choice of prestress has to ensure that the foundation remains in state I throughout the major modes of operation. During stress peaks the system will be out of operation, therefore changes in stiffness and resonant frequency are acceptable. A prestressed concrete gravity foundation with the appropriate type of prestressing will perfectly match all the requirements of a wind turbine, or may be designed to exactly fit a certain type of power generator.

## **MODELLING CAST-IN-SITU REINFORCED CONCRETE FRAME STIFFENED BY BRICK WALL USING FEM SOFTWARE**

*István HARIS*  
*PhD. Student*  
*BUTE*  
*Budapest, Hungary*  
[haris@vbt.bme.hu](mailto:haris@vbt.bme.hu)

*Zsolt HORTOBÁGYI, Ph.D.*  
*Ass. Professor*  
*BUTE*  
*Budapest, Hungary*  
[horto@ep-mech.me.bme.hu](mailto:horto@ep-mech.me.bme.hu)

### **SUMMARY**

The major advantages of the surface modelling procedure include the fact that the load bearing phase following the production of contour cracks can also be properly modelled, and that the model can also be used to calculate tensile stresses perpendicular to the pressed zone and can be compared to material characteristics. Owing to the surface model, it is not a problem, either, to calculate stiffening walls broken through by openings. So, this method can be used to examine the compressive stress and the tensile stress of the filler walling and its destruction by local impact (seal pressure). Furthermore, more accurate results are yielded for the bearing forces and deformations of the reinforced concrete framework as well.

### **1. INTRODUCTION**

In Hungarian engineering practice, the global spatial stiffness of buildings with cast-in-situ reinforced concrete pillar frames is ensured mostly by so-called connected or individual stiffening wall systems. Stiffening walls are mostly realized in the form of cast-in-situ reinforced concrete walls or frame structures filled by brick walls. This article presents the modelling – taking practical aspects into consideration – of the joint behaviour of a separate planar filler brick wall and cast-in-situ reinforced concrete frame. In everyday engineering design practice, cast-in-situ reinforced concrete frames are mainly dimensioned only by the supplementary slanting bar rod model known as the 'traditional method'.

### **2. SLANTING PRESSED BAR ROD MODEL**

Stiffening walls are characteristically dimensioned for horizontal action (e.g.: wind loads, earthquake loads). When producing a slanting pressed bar model, cast-in-situ reinforced concrete structures (columns, beams) are taken into consideration with their actual geometric and material characteristics in the calculation, whereas frame filler brick walls are modelled by a so-called supplementary slanting bar. This fictitious rod's cross-sectional dimensions and material characteristics taken into consideration must always be specified in accordance with the stipulations of the applicable standard; (Fig. 1).



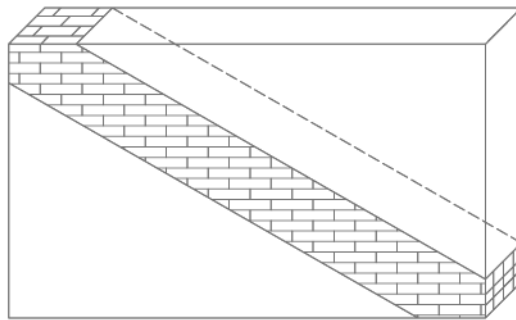


Fig. 1 Interpretation of a supplementary slanting bar

Horizontal impacts are reduced to the nodes specified along the respective floor slab levels; then the stresses are determined in the pressed slanting bar rod, supported by joints at both ends; the static scheme of the model is shown in Fig. 2.

Perhaps the major disadvantage of this model is that although the supplementary slanting pressed bar can be defined by non-linear material characteristics (working only upon pressure), still only axial forces can be generated in the bar, therefore tension perpendicular to the pressure cannot be studied in the brick wall. Furthermore, connection between the reinforced concrete frame and the brick wall cannot be modelled at all; only an ideal joint can be taken into consideration, which may considerably differ from actual behaviour.

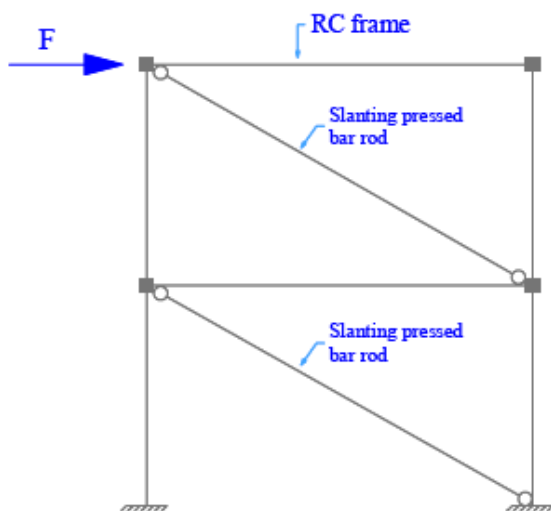


Fig. 2 Static scheme of slanting pressed bar model

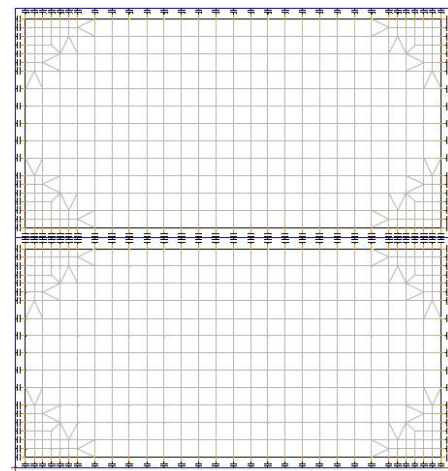


Fig. 3 Mesh design

### 3. SURFACE MODEL

The reinforced concrete frame can be modelled by several types of linear elements; however, it is expedient to apply elements capable to take shear deformations into consideration as well. The frame filler brick wall is modelled either by disc elements in the state of planar deformation, or by plane shell elements in accordance with its actual location. In order to model the connection between the reinforced concrete frame and the brick wall, we defined spirings demonstrating non-linear behaviour along the edges of connection as well as contact elements. By reason of the easier specification of stiffness characteristics, it is advisable to define an FEM mesh distribution which is even along the contact elements (Fig. 3).

In order to be able to model the connection between the reinforced steel framework and the brick wall, a spring and a contact element are aligned 'serially' as in Fig. 4. A fictitious spring

support of the lateral displacement of the node between the 'serially connected' elements is required so that the stiffness matrix of the structure should not become singular.

The contact element is designed to make the reinforced concrete structural element and the brick wall work together only to the impact of pressure. In the present case, it is a property of the FEM software applied that the non-linearity of the behaviour of the contact element only means that it cannot take up tension, but to the impact of pressure it demonstrates perfect linear flexibility (Fig. 5).

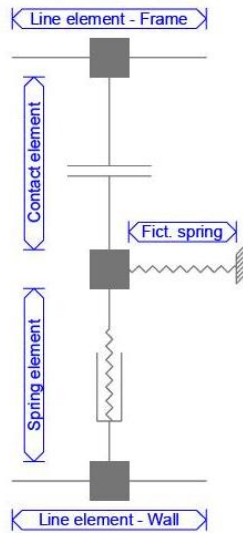


Fig. 4 Static scheme of connection model

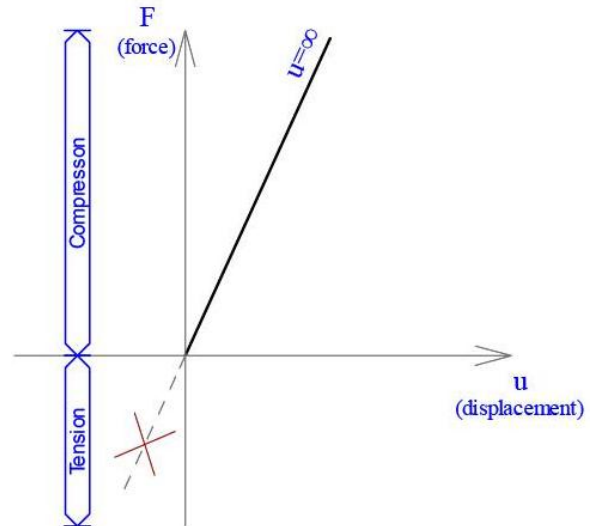


Fig. 5 Contact element behaviour

The spring element ensures the control of the upper limit value of resistance generated along the contact area in a form that the element can be uniquely associated with the design value of load bearing ( $F_{Rd}$ ), characteristic of the given brick wall, to be calculated according to the applicable standard (Fig. 6).

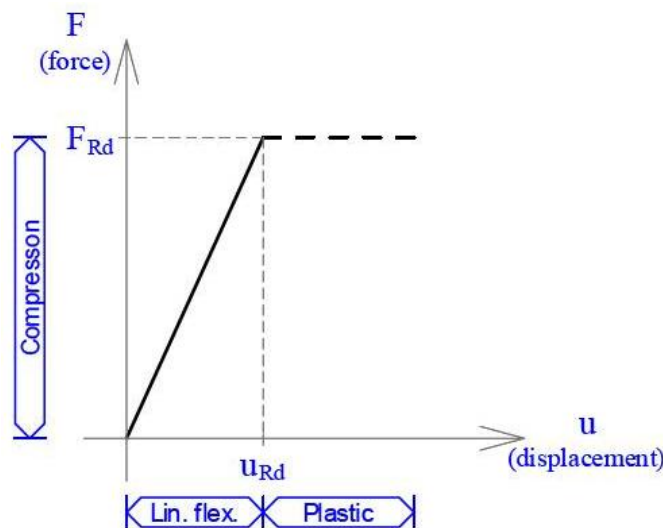


Fig. 6 Joint behaviour of the contact and spring elements

Thereby the spring element can be used for modelling the destruction of node connections, meaning that the impact of load is 'transferred' to the adjoining contact elements after the exhaustion of the load bearing capacity of an element.

#### 4. BRIEF INTRODUCTION TO THE FEM SOFTWARE APPLIED

The procedure presented can be used by practicing engineers to examine the joint behaviour and load bearing capacity of the two different structural components by an FEM software. Therefore, our aim is to complete the calculation using a commercially available software in a way to approximate reality better.

In the present case, modelling was performed using the FEM software AxisVM 8.0, the one most widely spread in Hungary. The software applies isoparametric flat quadrilateral (8/9-node) or triangular (6-node) elements to model surfaces. Their shape functions are of the second degree. 3-node rib elements are recommended for modelling linear elements as they also take the impact of shear deformations into account in the course of calculation. It is important to note, however, that any other commercially available FEM software can be used to complete the procedure presented; the software is only required to have the types of the elements used.

#### 5. RESULTS

The modelling procedure is presented on a structure of freely recorded geometry using the software mentioned in the previous section. Modelling of the static frame and of the connection nodes was defined as specified above.

In the course of calculations, fictitious material properties were utilized; accordingly, the design value of the strength of the walling were only inferred. The model of the FEM calculation and the results of the non-linear static calculation are presented below, without striving for completeness.

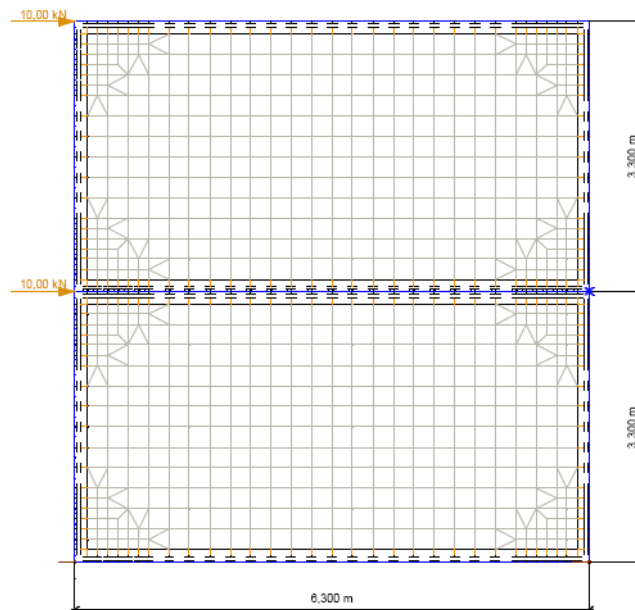


Fig. 7 Static model

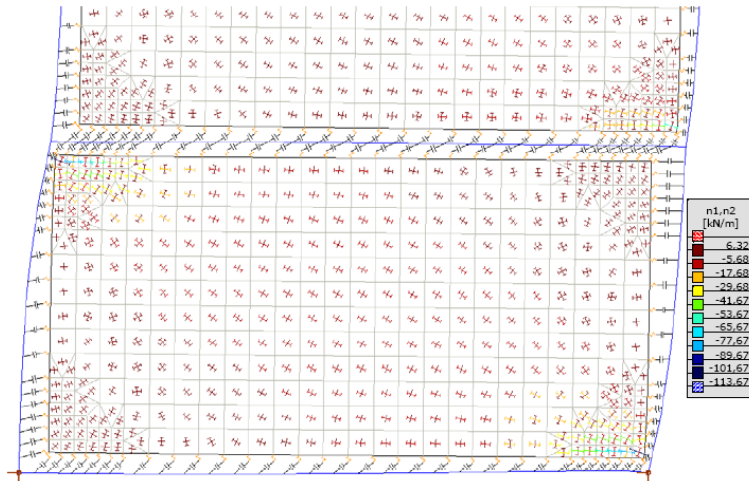


Fig. 8 Main directions of normal bearing forces

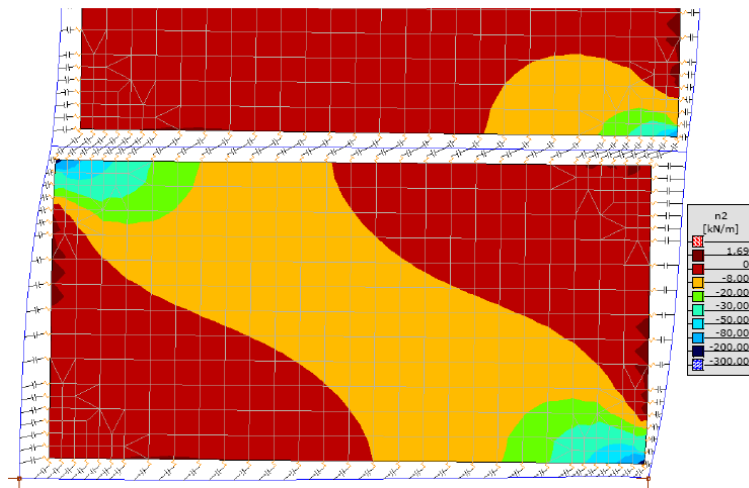


Fig. 9 Main directions of normal bearing forces

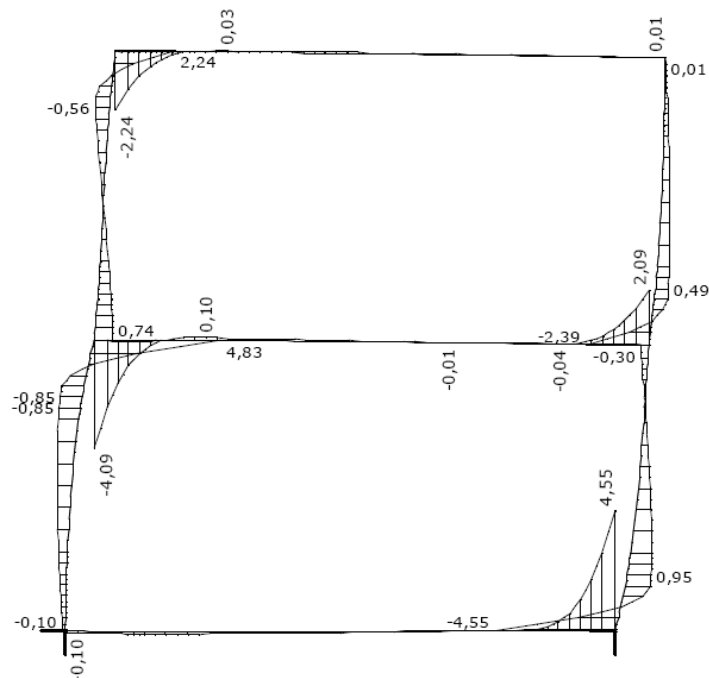


Fig. 10 Figure of bending momentum on the deformed shape [kNm]

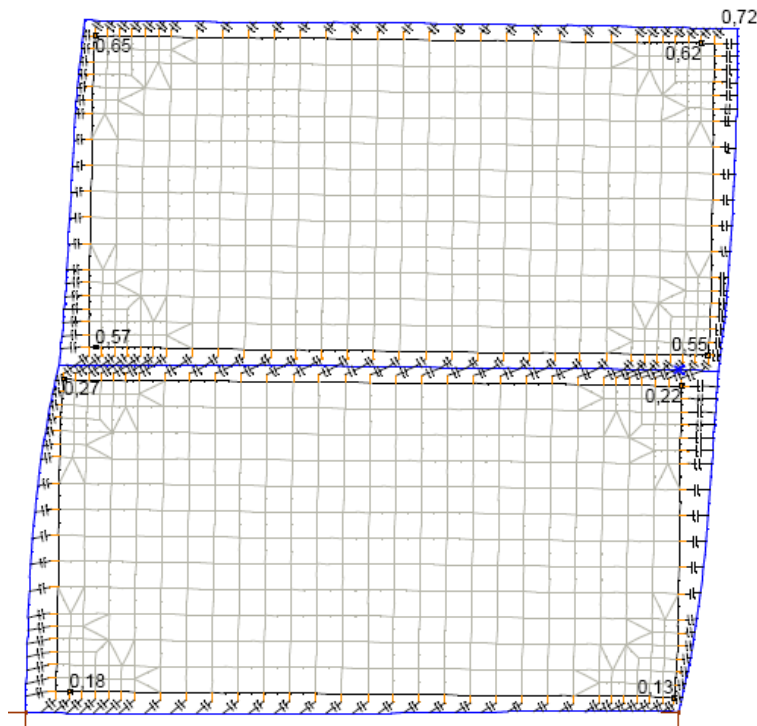


Fig. 11 Horizontal displacements [kNm]

## 6. OBJECTIVE OF FURTHER RESEARCH

Modelling according to the procedure presented was performed using a FEM software applied by practising engineers, necessarily developed only for demands directed to everyday design practice. Further studies are required; however, they must surely be performed by a FEM software developed for scientific use in order to be able to define more detailed and much more accurate models.

## JARUN CITY BRIDGE – PRELIMINARY DESIGN

*Jure Radić, Alex Kindij, Ana Mandić*  
*University of Zagreb, Faculty of Civil Engineering*  
*Croatia, 10000 Zagreb, Kačićeva 26*

### SUMMARY

A new bridge across the Sava River in the city of Zagreb is to be built to link the south entrance into the city with the west of the city. The City Council of Zagreb and the Croatian Society of Structural Engineers organized a public competition for the preliminary bridge design.

Ten alternative proposals were entered by different design teams, comprising both bridge engineers and architects. In this paper all ten bridge proposals including beam type bridges, through and half through arch bridges and cable-stayed bridges, made of concrete or steel or of composite type are shown.

Particular emphasis is given on the asymmetrical cable-stayed concrete bridge, which was awarded the first prize. The main span is 150 m with the overall bridge length of 625 m. The superstructure is a continuous box type prestressed girder with constant depth of 280 cm over eleven spans. The inclined concrete box-type pylon is 88 m high of which 75 m are above the superstructure.

### 1. INTRODUCTION

Jarun is southwestern part of the Zagreb city, where the lake of Jarun is located. The Jarun Lake is a popular recreational and sports area consisting of three connected lakes with the largest comprising a 2 km long rowing track. The Jarun Bridge will be situated in the proximity of the Lake.



Fig. 1 The Jarun Lake in Zagreb



The Jarun Bridge is a part of a major traffic network improvement. The main aim is to connect the western part of the City Zagreb with the main road towards the Adriatic Sea. This high capacity road will also connect two very attractive recreation and sports areas, northern and southern, now divided by the Sava River.

The Jarun bridge is situated outside the city limits with a nice view from the southeast corner on the city and the Medvednica mountain. The Sava River in Zagreb is about 105 m wide. During flooding the water covers the whole area between embankments and is 293 m wide..

The main assumption for the bridge design is that this large area will not be left unregulated and unused but that in not so distant future some additional facilities will be built in this area to enable the city to come near to the river and benefit from the fact that a major river flows through the city.

## 2. OPEN DESIGN COMPETITION

For this bridge the City Council of Zagreb and Croatian Society of Structural Engineering organized an open design competition. Ten different design teams, comprising both bridge engineers and architects submitted their proposals, including beam type bridges, through and half through arch bridges and cable-stayed bridges, made of concrete or steel or of composite type.

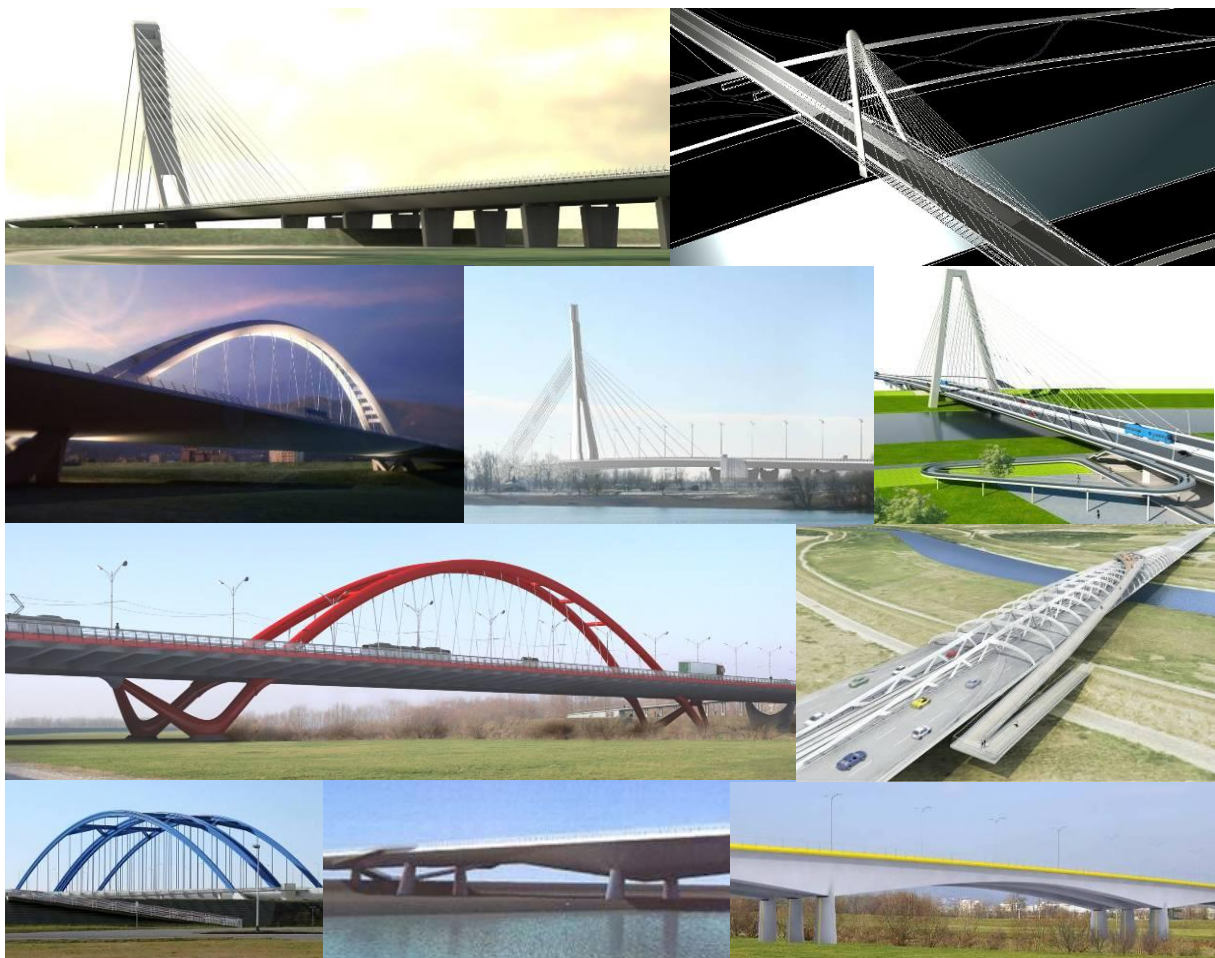


Fig. 2 Computer simulations of various solutions for the Jarun bridge

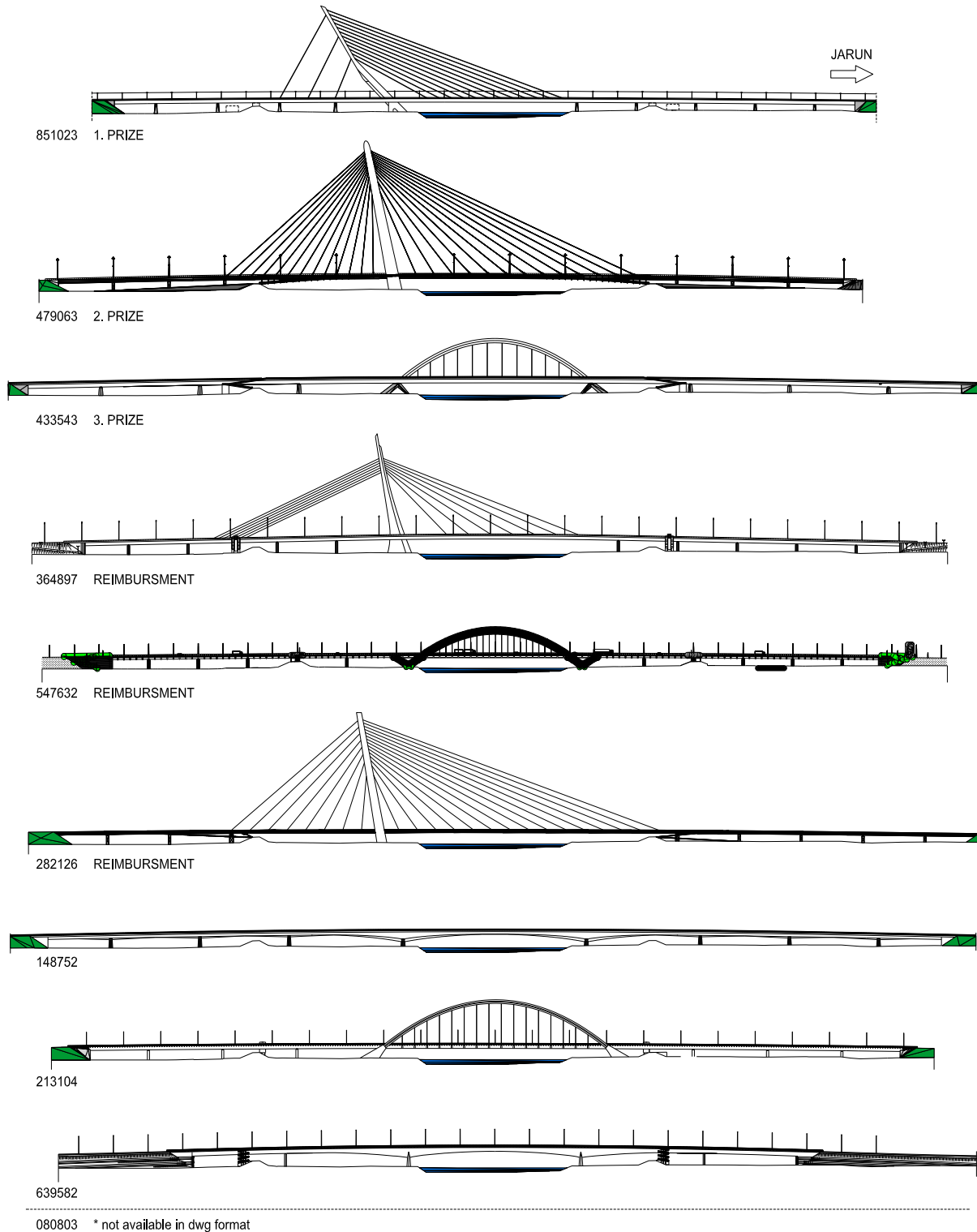


Fig. 3 Longitudinal sections of alternative Jarun Bridge structures

The appointed Competition Evaluation Committee, consisting of eminent bridge engineers and architects rated all submitted designs on the basis of aesthetics, buildability, costs and durability. The first prize was awarded to the cable-stayed bridge, described later in more detail, the second prize to another cable-stayed solution and the third prize to through steel arch bridge, while three other submitted design proposals were reimbursed. All submitted designs are shown in the Figs. 2, 3 and 4.



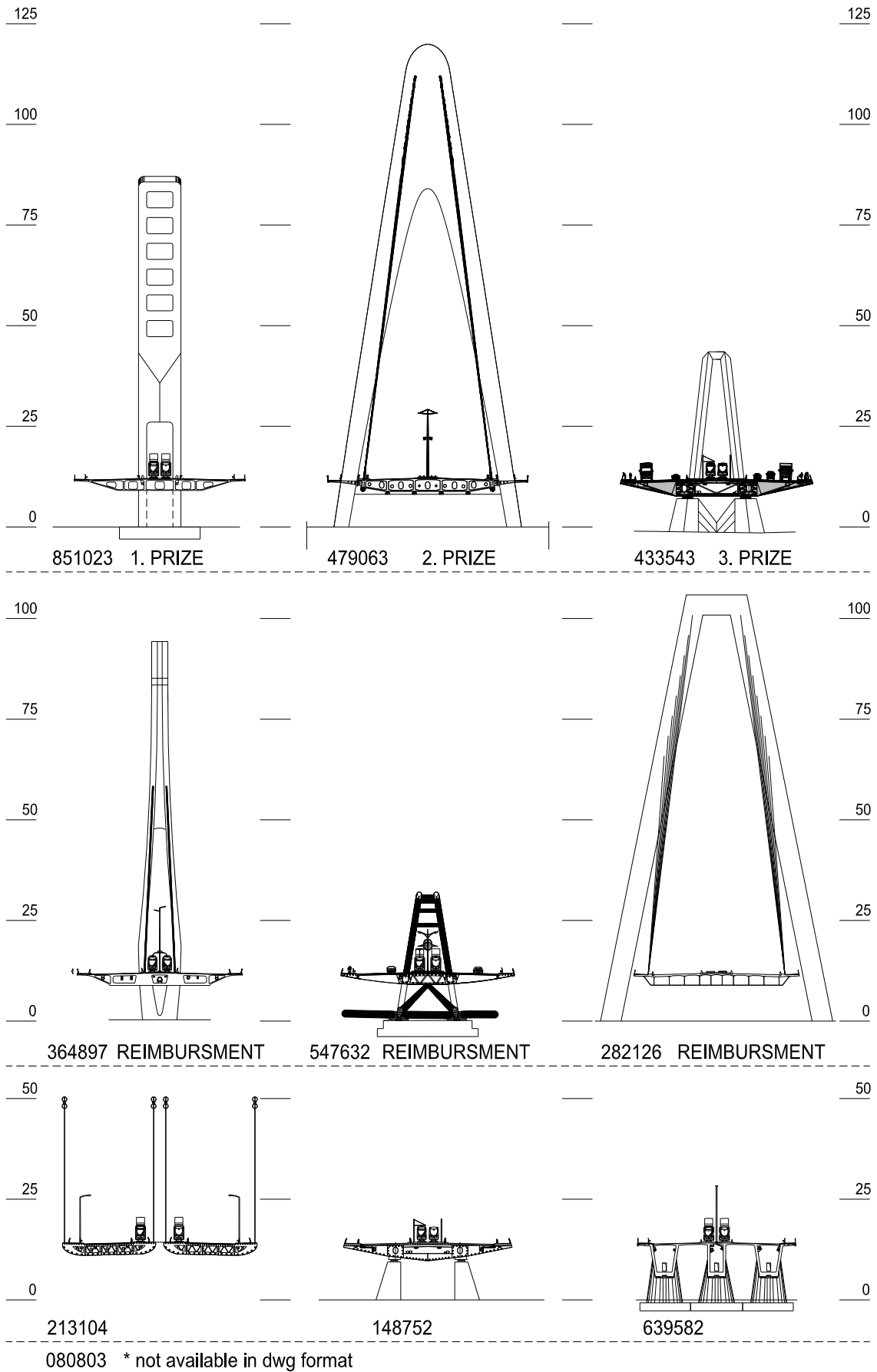


Fig. 4 Cross sections of the proposed solutions for the Jarun bridge

### 3. THE JARUN BRIDGE PROJECT

The Jarun Bridge is designed as a city bridge and is inserted in the urban structure at the outside perimeter of the city. For this city bridge asymmetrical layout with one inclined pylon was chosen.

The main span is 150 m with the overall bridge length of 625 m. The main span is an asymmetrical cable-stayed bridge with twelve (12) pairs of stays and three (3) pairs of back stays. The superstructure is a continuous box type prestressed girder with constant depth of 280 cm over eleven (11) spans 35 + 2\*50 + 2\*45 + 150 + 4\*48 + 34 meters long (Fig. 5). The grade line at the bridge lies in a straight line in ground plan and the vertical alignment is in radius of 25750 m and enables free passage on the river embankments. The longitudinal layout of the cables is of modified fan type with partial suspension. Cable-stays in two parallel planes are spaced at 10 m longitudinally and 8.5 m in transversal direction.

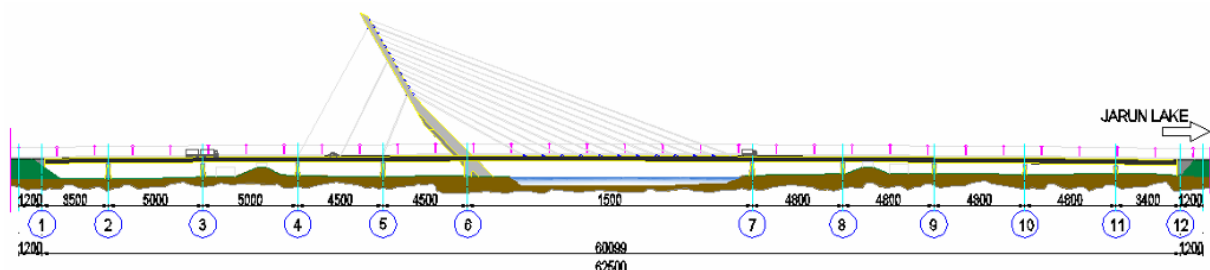


Fig. 5 Longitudinal view of the bridge

The width of the six (6) lane carriageway and city railway is  $11.5 + 12.0 + 11.5 = 35$  m and the overall width of the superstructure is 42 meters (Fig. 6).

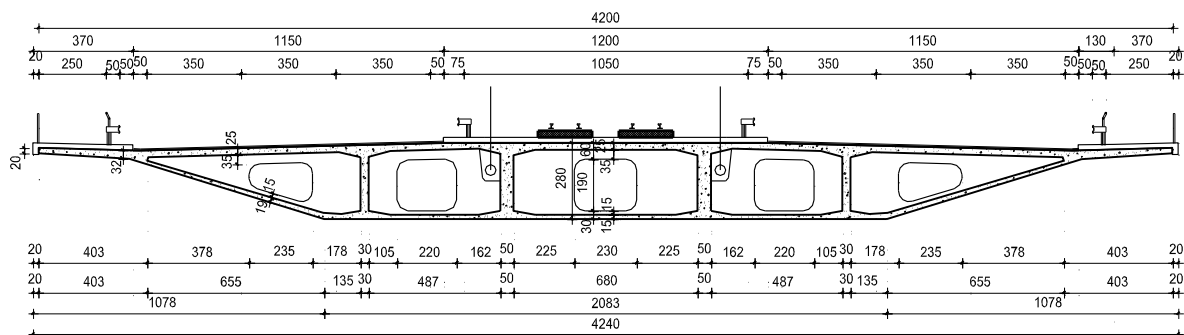


Fig. 6 Cross-section of the bridge

The inclined concrete box-type pylon is 88 m high of which 75 m are above the superstructure. The pylon cross-section is 10.5 m wide. At the superstructure level the city railway passes through the 6.5 m wide opening in the pylon. At the level of 15 m above the superstructure, immediately below the stays, the pylon is inclined for additional  $10^\circ$  towards the main span. Above this level six (6) vertically shaped openings in the pylon provide the necessary lightening of the structure and provide some interesting views (Fig. 7).

The columns comprise two concrete wall piers with variable dimensions in both directions. At the foundation level the pier is convex hexahedra with outside dimensions  $300 \times 450$  cm, and at the bearings level the cross section is a concave hexahedra with outside dimensions  $200 \times 720$  cm. The height of piers vary from 6.5 to 8.5 meters (Fig. 8).

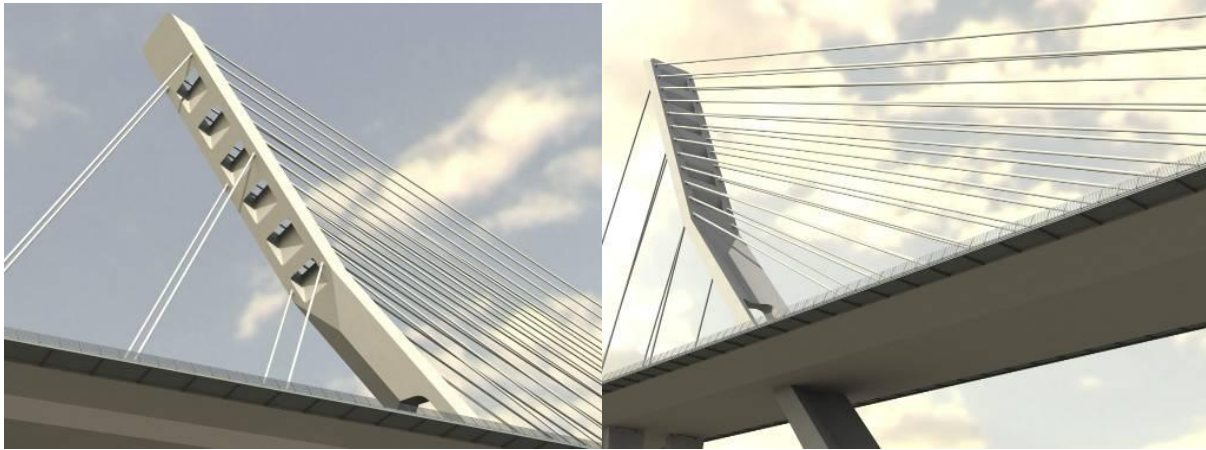


Fig. 7 Shape of the pylon and openings

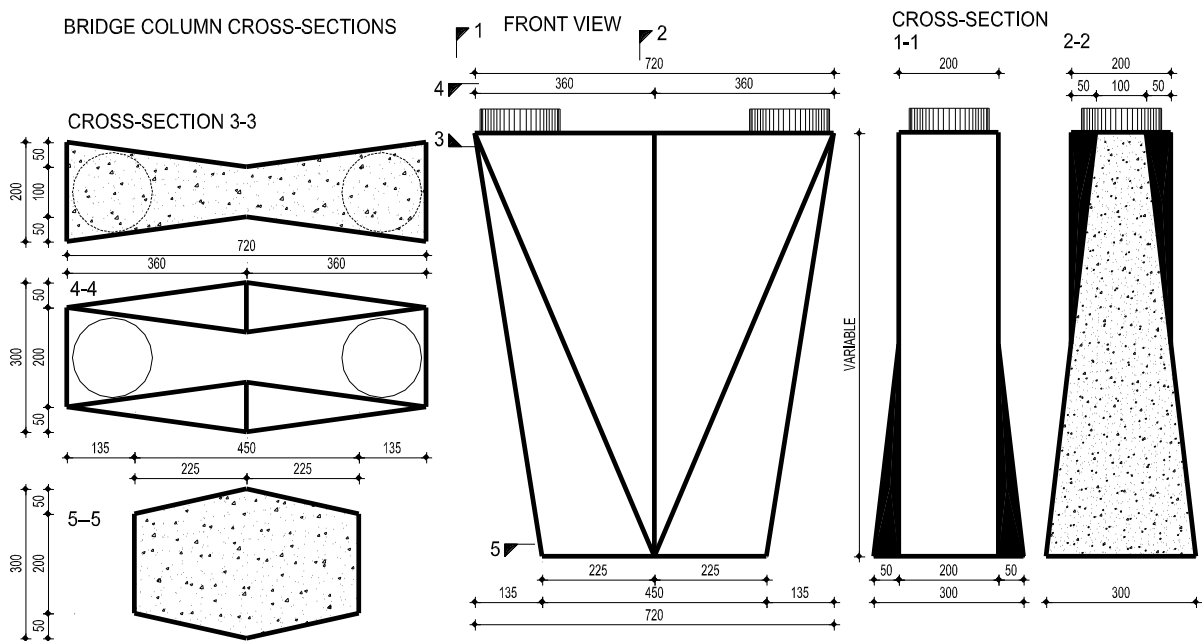


Fig. 8 Bridge column with variable dimensions

For this city bridge decorative lighting is also planned. Roadway lighting is designed at the railing level at approximately 10 – 20 m distance concentrated on the roadway. Also lighting of the railway, stays and direct lighting in the pylon openings and indirect lighting of the superstructure from the pylon is designed.

Numerical models for static and dynamical analysis of the main load bearing system will comprise the whole bridge structure, the pylon, columns, structural bearings and prestressed superstructure. All loadings are based on the Croatian standards HRN ENV 1991, Parts 2 and 3 except for the seismic loading which was assessed on the basis of EC8. Detailed analyses of all construction phases of the pylon erection and construction of the superstructure will be performed. The project is still under way. It is expected that the construction will start in February 2008.

With this bridge the City Council of Zagreb wants to solve the present problem of the inadequate capacity of bridges across the Sava River and in this way improve traffic connections of the parts of the city divided by the river.

## THE HIGHWAY BRIDGE AT RZAVÁ

*Ladislav Šásek*

*Mott MacDonald Praha spol. s.r.o.*

*Národní 15, 147 00 Prague 1, Czech Republic*

*sasek@mottmac.cz*

*Petr Štědronský*

*Metrostav, a.s.*

*Koželužská 2246, 180 00 Prague 8, Czech Republic*

*stedronsky@metrostav.cz*

### 1. THE LAUNCH OF A COMPLETE COMPOSITE SUPPORTING STRUCTURE ALONG THE BRIDGE DECK

The bridge on the D3 highway was constructed using an unusual technique which had never been used before. The highway bridge at Rzává was designed in the form of two independent bridge constructions. Each of them has 7 spans in lengths  $24.0 + 5 \times 36.0 + 24.0$  m (Figs. 1 to 3).

The bridge deck consists of two steel beams coupled with the reinforced and prestressed (longitudinally and transversally) concrete bridge plate. The complete composite bridge deck including the steel bracing and supporting reinforced-concrete cross beams was launched along the bridge deck.

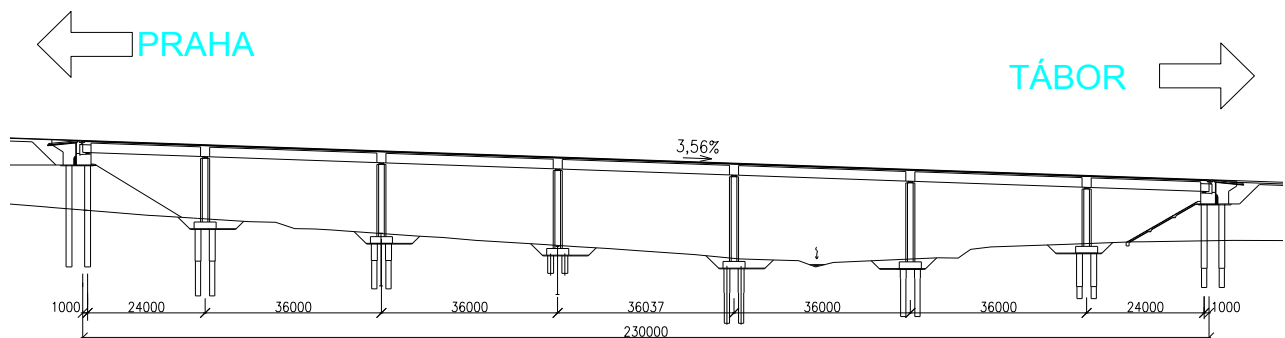


Fig. 1 Elevation



Fig. 2 Bridge at Rzava

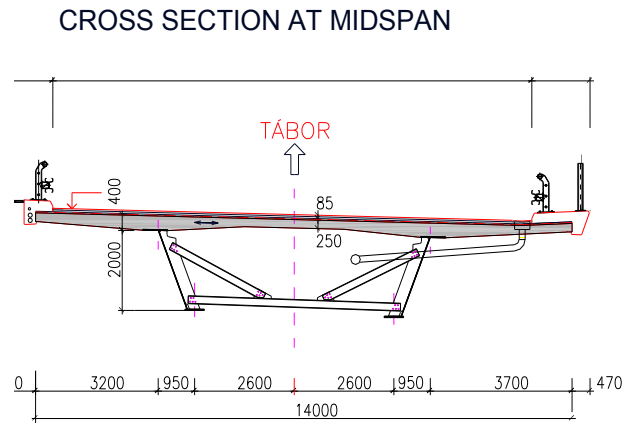


Fig. 3 Cross section

Considering the height of the bridge being 15 - 20 m above the terrain and its constant direction curve the originally proposed building technology was to launch the steel structure alone with additional in situ concrete-casting of the bridge deck on the launched construction.

When launching stand-alone steel structures of composite bridges, relatively low reaction forces originate and also the local stress of the beams in the supports is low and it is easy to design them. On the contrary – when launching the complete composite bridge one has to move approximately 4-times greater dead load of the structure, because the reinforced concrete bridge plate represents 75-85% of total dead load of the cross-section.

Large mass of launched composite structure induces substantial reaction in the slide bearings at launching. Those reactions then migrate along the whole length of the structure. If the construction had been placed on those supports via the bottom flange of the steel beams, a huge local stress of the bottom flange and the steel diaphragm would have occurred, which could be compensated only on the account of a substantial rise of the steel mass.

*For this reason the launching of the bridge on the outer side of the upper flange was proposed.* The upper steel flange was connected to the concrete slab by the means of studs. Close to this sliding support the slab was reinforced with steel beam web being rigid enough and with sufficient bearing capacity (Figs. 4 to 7). This supporting mode was not causing any increase in the usage of the structural steel of the bridge deck.

Due to this solution the idea of launching the complete composite bridge deck has emerged. The steel structure assembly and the concrete-casting of the bridge slab in the workshop allowed to achieve higher precision and accelerate the speed of construction.

Tensile stress inside the slab above the supports was lower than allowed stress of the concrete. The only unknown factors were the inaccuracy of the trajectory and steel construction geometry as well as the height slump of the intermediate temporary piers. Those inaccuracies could have caused further increase of stress. Although such a stress was not exceeding the stress caused by the service load, the slab was initially prestressed by four

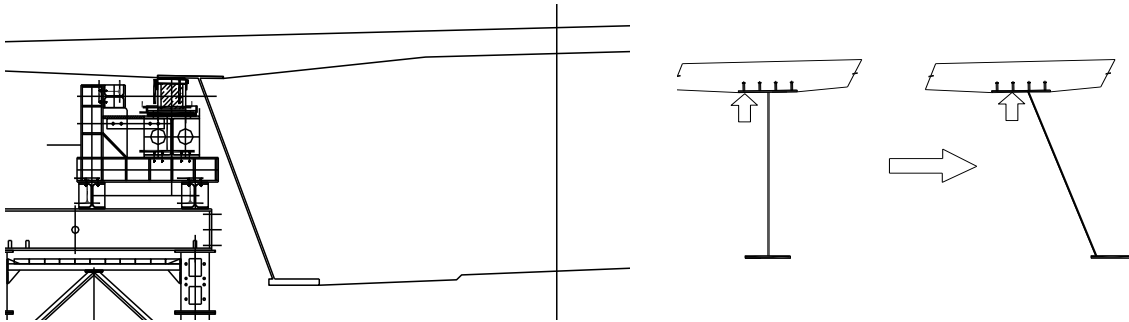


Fig. 4 Sliding bearing

cables to avoid arising of cracks at launching. On the piers, the special fixtures with sliding bearings were fitted on which the bridge deck was launched along the above mentioned surface of upper flange. To be able to place those constructions as close as possible to the girder's side, the shape of the construction in its cross-section was adapted in such a way that the steel beams were made with sloping diaphragms.

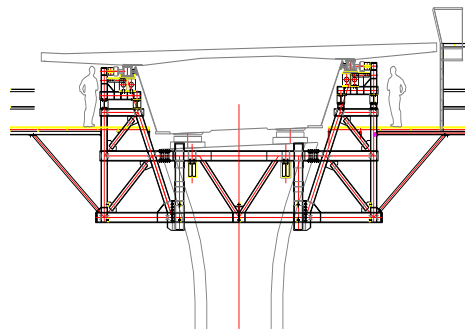


Fig. 5 Steel head on concrete piers



Fig. 6 Sliding bearing

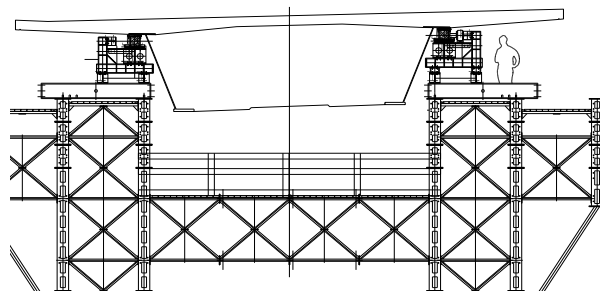


Fig. 7 Temporary pier head



## 2. THE WORKSHOP

On an embankment in the Tabor bridgehead behind the Tabor abutment the workshop (Fig. 8-9) with the launching track was established. This is where the steel construction in length up to 90 m was assembled. The space for casting the concrete slab was 18 m in length. On the track made of steel construction a support frames were embedded and on those frames the steel beams and cross-bracing were mounted from separate parts. Behind the abutment a scaffolding formwork was made with boarding outside the steel beams for casting the concrete slab.

The support frames were always located under the cross bracing of the girders walls, that is every 6 m. Supports located in this manner and in this distances transferred reliably the load of steel beams and concrete slab without any problems with the local strain of the girder's wall.



Fig. 8 Workshop



Fig. 9 Casting of the 18 m long segment

## 3. THE LAUNCHING TRACK

Another innovation of this launching technology was the construction of a launching track (Fig. 10). In order to lower the stress of the bridge deck due to its dead load during the launching, the fixed supports were complemented with one temporary support in each field. The final piers were designed for the service load, where the horizontal frictional forces acting in the longitudinal dimension of the bridge are compensated with a greater vertical reaction. On the contrary, relatively huge horizontal forces could be activated during the launching in the slide bearings, especially when the move started or in the case of casualty – wrongly inserted sliding element (teflon).

A launching unit was resting on the abutment. The abutment was fixed on the piles in the embankment. The total force induced by the launching unit would be greater than the "horizontal bearing capacity" of the abutment.



Fig. 10 Launching track

In order to decrease the horizontal load of the compliant abutment and at the same time to reduce the stress on the piers and to ensure the stability of temporary piers in the longitudinal bridge direction, a balanced static system was proposed where the heads of all supports including the abutment were interconnected with prestressed bars. All bars were prestressed from one abutment to another and all piers and intermediate supports were fixed to those bars.

Uniform temperature differences along the whole bridge length will then cause only changes of the tension in the bars.

Regarding the stiffness and the degree of prestressing of the bars this static system is preset so as not to exceed both the allowed stress or displacement of all structural elements during the launching. The hydraulic launching unit placed on the Tabor abutment launched the bridge towards the 3.56% elevation using the prestressing wires. The wires were anchored to the edge of the concrete slab using a special fixture. After launching of one phase these fixtures were dismantled and fitted at the end of the slab in the next phase. The hollow double-acting hydraulic launching units were equipped with a dual system of wires anchoring, so the bridge was braked against regression when the cylinder was shifting in.

After finishing the launching phase the whole bridge was safely braked against regression using screw bars which connect the concrete slab with the Tabor abutment using the fixtures. Then the fixtures of the towing wires could be dismantled and relocated into the next phase. The above mentioned anchoring system was very simple and reliable and totally independent on the vertical load effect.

#### 4. MONITORING

In looking for the maximal security of the construction process an automatic system for monitoring the horizontal displacements of piers and supports in the longitudinal direction of the bridge was proposed (Fig. 11). Through the center of the bridge in the pier heads level, a string was pre-tensioned independently on the supports and piers. In the pier heads sensors measuring the displacements against the string were installed. Measuring data were downloaded into the evaluating center which was adjusted to stop the launching automatically when the limits of the pier displacement were exceeded. Regarding the speed of launching the non-permissible displacement of the pier would occur within a few seconds. Therefore it was



not advisable to rely solely on the manual breaking of the launching by the operating personnel.

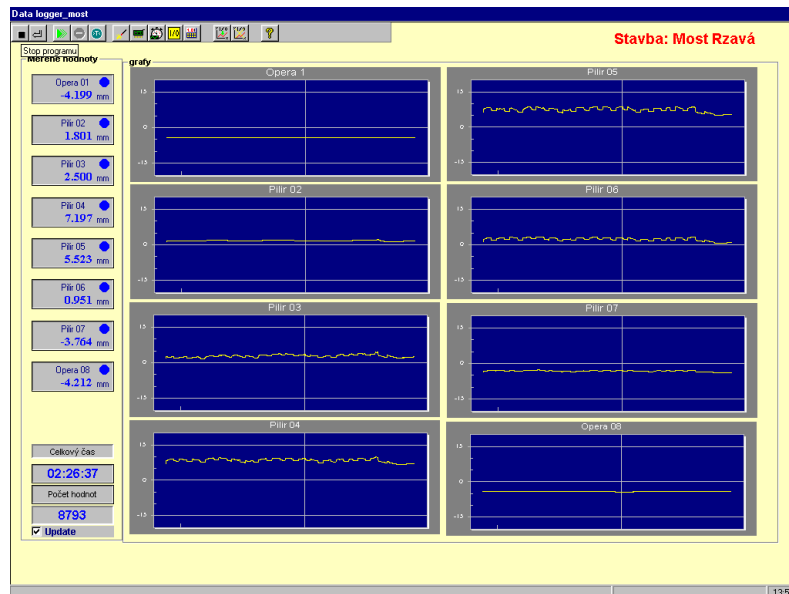


Fig. 11 Monitoring

The actual measured values of displacements were corresponding exactly to the computed values. The effectiveness of the measuring system was already verified when the bars were prestressed between the piers.

The functionality of the securing measuring system was checked out randomly as a minor accident occurred unrelated to the launching itself, when the signal cables from the deformation sensors were damaged. In an instant the system reacted properly and stopped the launching and the risk of uncontrolled launching was avoided.

## 5. CONCLUSION

The presented system of launching the complete construction with the slab in such an extent is probably unique. In the preparation of building a series of problems, technological procedures and construction details had to be solved. Today, when the whole bridge is launched, it can be said that all effort invested into the solving of many details comes back in the form of a perfect work.

The contractor of the bridge was very pleased with the quality and speed of the construction – in one week 18 m of a complete bridge deck of the bridge was made. From the designer's point of view a lot of time was saved by the static calculation of the bridge geometry and in many constructing phases, because the structure was made in the workshop in the final shape and with a great precision.

## **NEW TECHNOLOGIES ON THE PROJECT WIENERWALDTUNNEL, AUSTRIA – OPTIMIZATION OF BACKFILL MATERIAL FOR SEGMENT RINGS AND USE OF LONG FORMWORKS**

*Andreas Rath*  
*Porr Tunnelbau GmbH*  
*A-1103 Vienna, Absberggasse 47*  
*[andreas.rath@porr.at](mailto:andreas.rath@porr.at), [www.porr.at](http://www.porr.at)*

### **SUMMARY**

The Wienerwald Tunnel, approximately 13.35 km in length, will form part of the new high-capacity railway link between Vienna and St. Pölten in eastern Austria. A length of 10.75 km of the project has been designed as a twin tunnel. The tubes were driven by two single-shield tunnel boring machines of 10.6m diameter. This gave a total length of as much as 21.5 km to be driven by TBM and thus provided the opportunity to improve construction materials and methods. In fact, several of the new developments were prompted by technical needs and challenges.

New construction technologies and construction materials were developed and field-tested to answer special requirements, with an emphasis on the backfill material – mortar and grouted pea gravel – for the annular space between the outer surface of the segment ring and the excavation surface. The TBM-driven twin tunnel section of the Wienerwald Tunnel will receive a plastic liner plus a secondary lining. The straight tunnel alignment enables the use of long formwork systems for the watertight invert slab plus the inner lining shell. Thus, it is possible to pour several blocks with concealed construction joints within a single concrete-pouring step. Prior to construction, it was necessary to analyse and solve special technical details in conjunction with concrete and formwork experts.

### **1. GENERAL**

The driving operations on the Wienerwald Tunnel contract, going on since the end of 2004, are facing completion: A length of 21,450 m was excavated by two single-shield TBMs and more than 4,000m was driven by conventional means, i.e. by excavator and drill and blast methods.

The advance rates achievable in both sections – the East Section driven by conventional means and, especially, the TBM-driven West Section – were very much a matter of the logistics of haulage to and from the site. A great number of optimisations and innovations were implemented as the long and technically challenging tunnelling work proceeded, so as to reach daily advance rates of up to almost 52 m for each TBM.

This report will be confined to the outstanding measures carried out to optimise the backfilling process for the annular space as well as to develop long formwork systems for the construction of about 25km of secondary lining.

**WIENERWALDTUNNEL**  
 Project Overview

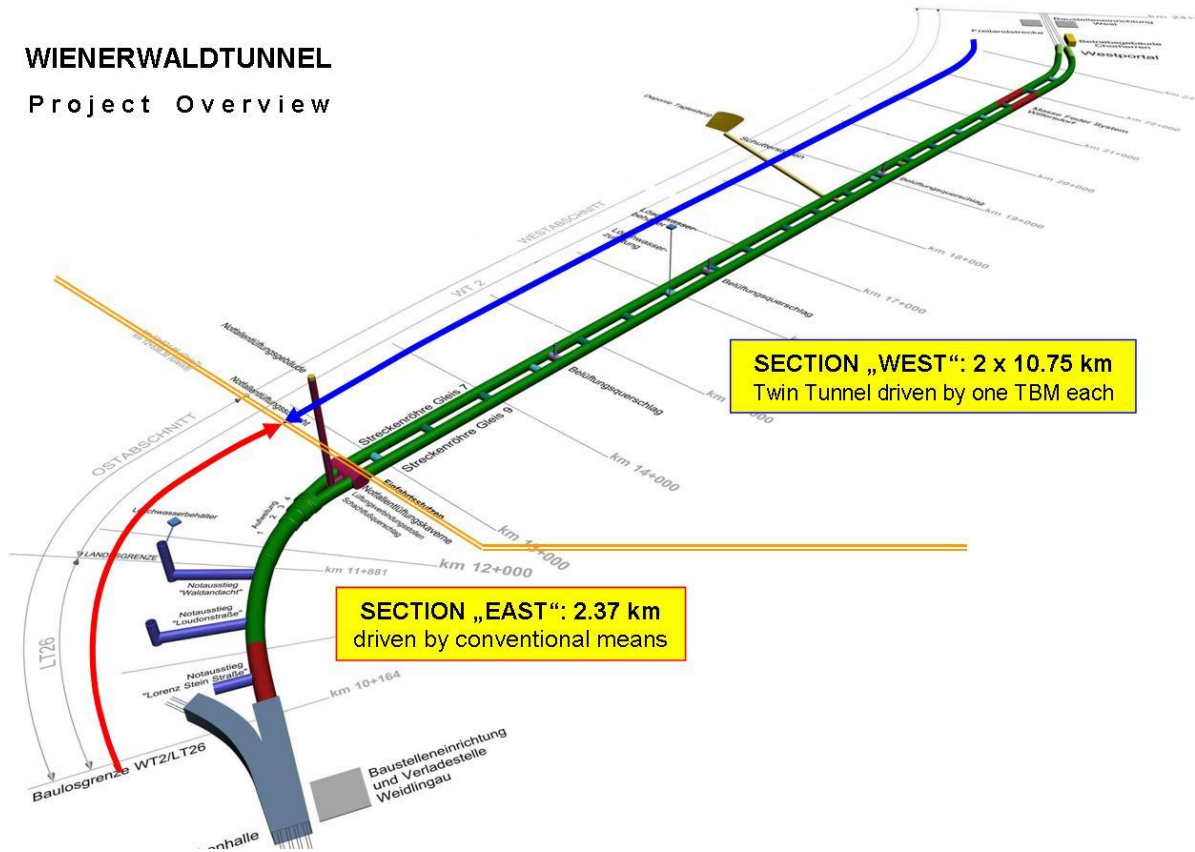


Fig. 1 Project overview

**2. OPTIMISATION OF ANNULAR-SPACE BACKFILL MATERIAL**

The excavated underground opening of the TBM-driven West Section is supported by a secondary lining consisting of segment rings 35 cm in wall thickness and 2.25 m long. The ring, composed of 5 segments weighing 12 tonnes each plus a key stone 80cm wide, is cast on site.

The annular space between the outer surface of the segment ring and the excavation surface is backfilled with mortar in the lower portion and pea gravel in the upper portion (Fig. 2). Subsequent grouting of the pea gravel was originally planned only for short sections, and all the intermediate storage facilities and installations were planned to be accommodated on the back-up gears of the TBMs.

**Pea gravel**

The pea gravel of size 4 to 8 mm used for backfilling comes from the Danube riverbed. During the blowing-in process gravel particles have been seen to get crushed on their way from the rotor pump to the feed opening in the segment ring. This reduces the rounded proportion of originally 100% and jeopardises the satisfactory distribution of the gravel within the annular space.

**Mortar for the annular space**

The mortar, mixed on site using sand and cement, is placed through special openings in the shield tail. This should ensure appropriate mortar backfilling of the invert to an angle of 120°. But practice has shown that in places the pea gravel tends to penetrate to this area.

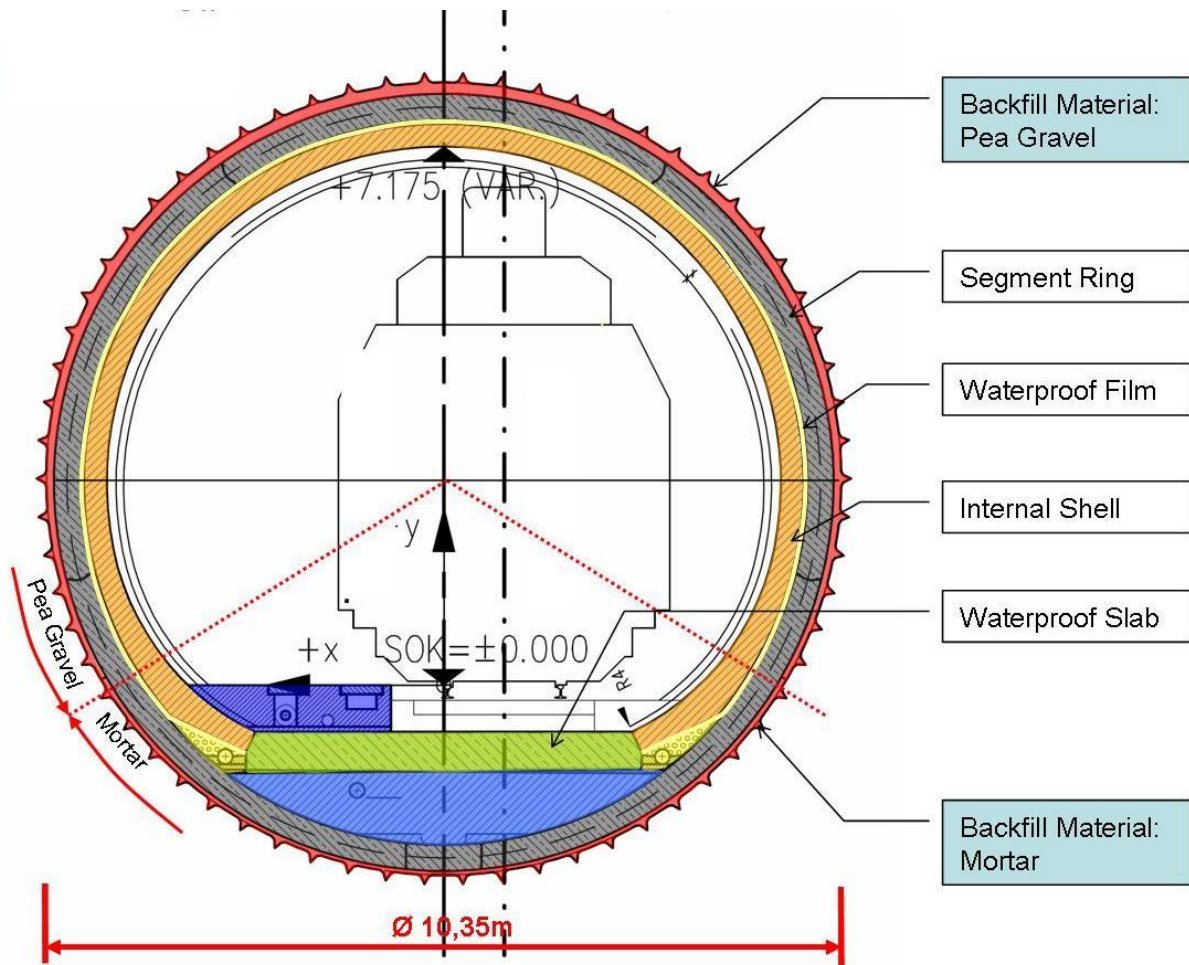


Fig. 2 Cross section through West Tube

### Backfill material

Backfilling the annular space must ensure the rapid build-up of sufficient bedding forces between the excavation wall and the segmental lining. However, loose rocks falling onto the segment ring made it impossible in places to introduce the pea gravel. This prompted the need for developing a new system for backfilling the annular space.

The requirements to be met by a new backfill material have been defined as follows: The material should

- fill remaining cavities and run off over the pea gravel without penetrating into it;
- form a stable mix showing sufficient flowability and pumpability to a distance of 250m;
- stiffen early in filled cavities so as to be able already to absorb the forces from the segment ring being erected next.

A solution to the problem has been found by injecting a tixotropic fine-grained mortar mix provided with a setting accelerator at the injection packer. For the workability an open time of about 4 hours has to be achieved. Conducted Experiments with standpipes showed a penetration into the pea gravel of 3-5 cm independent of the mortar level. The mix is monitored by density measurements. Because of its viscous and tixotropic consistency the mortar needs increased pressure to penetrate narrow spaces. Thus a feeding pressure of at least 3 bar is necessary for a 100 m pump line.

The required equipment must now be accommodated on the back-up trailer in the area originally reserved for the installations needed for subsequent pea-gravel grouting where necessary.

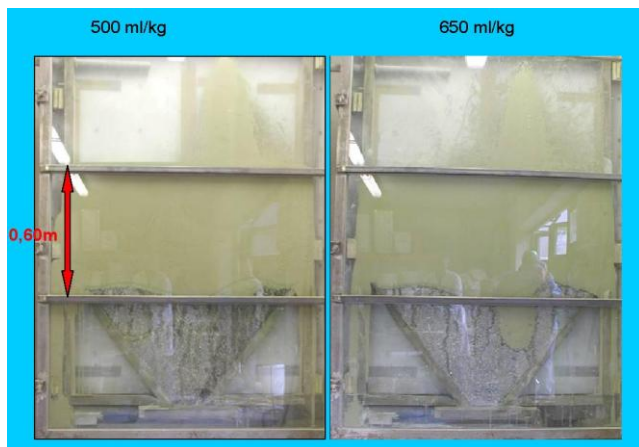


Fig. 3 Backfill Material



Fig. 4 Grouting Material

### Secondary grouting of pea gravel

A new concept had to be developed for the back-up train in view of the changed grouting process and the new quantities needed. In normal case a pore volume of about 40% had to be grouted, i.e. 1.8 m<sup>3</sup> suspension per meter.

The requirements to be met by the grout and the installations involved can be summarised as follows:

- separation from the back-up installations so as to avoid reducing the system performance of the TBM;
- use of pumping lines to transport the material to the point of placement so as to avoid the need for additional supply travels in the tunnel;
- highly viscous suspension pumpable over a distance of about 6,000 m;
- ensure that the material penetrates the pea gravel and reaches a final strength of 5 N/mm<sup>2</sup> after 28 days, as corresponds to the strength of the surrounding rock mass.

A special unit has been developed for subsequent pea-gravel grouting. This consists of a mixer and pump carriage as well as a carriage for packer erection and a grouting-carriage. Control and data collection are automation supported.

This unit works independently between 500 m and 1000 m behind the TBM; material supply is from a mixing plant at the portal, through pumping lines. Only closure of the unsealed segment joints is from the TBM back-up system.

The grouting material, like the backfill material, was developed and optimised in close cooperation with the Central Laboratory installed at the site and the supplier of the cements and aggregate.



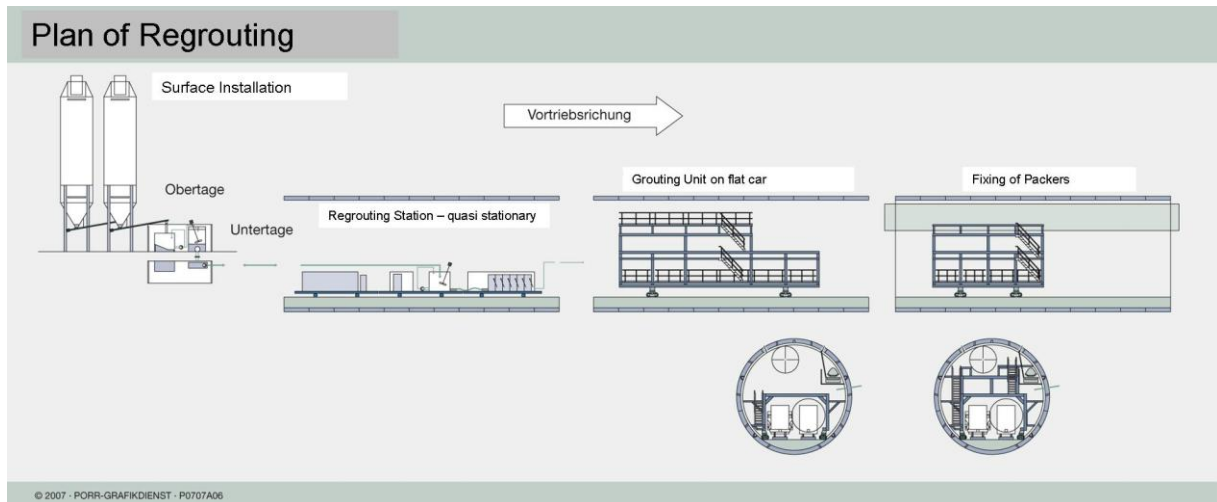


Fig. 5 Schematic drawing showing back-up train

### 3. LONG FORMWORK UNITS

The straight tunnel alignment and the time schedule permit erection of the secondary lining for the west portion of the Wienerwald Tunnel in 36 m concreting sections. Based on this length, special formwork has been developed for pouring both the watertight invert slab and the arch.

#### 3.1 Watertight invert slab

The formwork system for the invert slab consists of two lateral units of 36m length, which can be connected by braces. Free access between the two units is needed for the reinforcement and concrete-pouring works.

The individual 3 times 12 m concreting sections are separated by construction joints. The standard joints in between, spaced at 12 m intervals, are designed as concealed joints using hardboard inserts. Invert slab reinforcement is by means of reinforcement cages erected in advance for each standard block length of 12 m.

Concrete is hauled to the site in 4 agitators on rail-mounted flatbed carriages. A pump placed by the side of the train feeds the concrete into the formwork through a rotating distributor. Pouring proceeds from the head of the formwork unit in the direction of the portal, towards the completed preceding concreting section, with the concrete line being continuously shortened.

A self-propelling portal frame equipped with three independently operating cranes serves for all sealing and reinforcement processes as well as for moving formwork and the concrete pump and distributor.

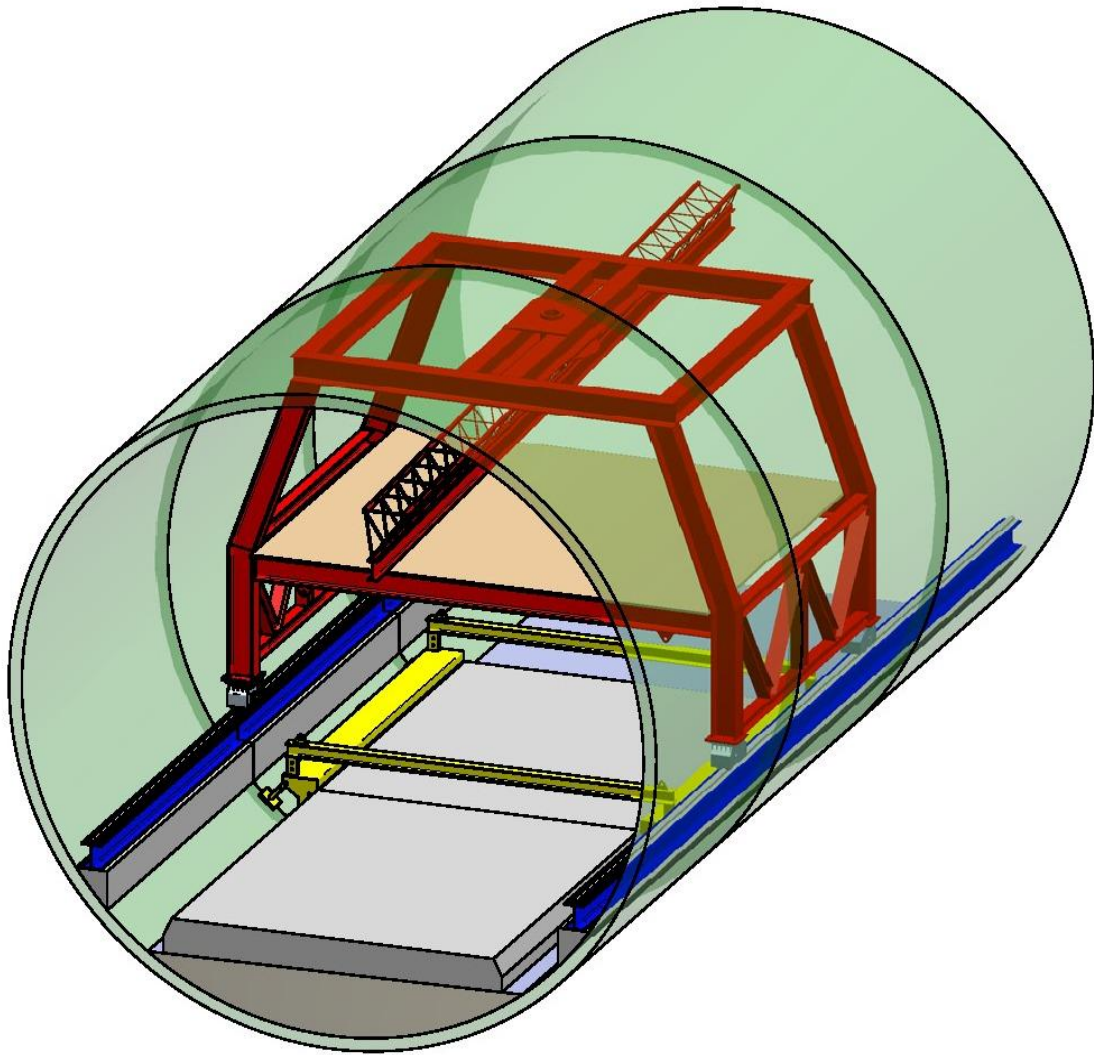


Fig. 6 Systematic drawing of the portal crane system for the invert

### 3.2 Arch concrete

The standard design of the inner shell for the single-track tube provides for a plastic liner, without reinforcement.

Reinforcement is provided at intersections with crosscuts and where necessary for geotechnical reasons. The self-supporting reinforcement units are carried on steel arches mounted on a travelling carriage of 12 m length equipped with a lazytong platform for carrying the reinforcing material.

The travelling arch formwork unit is composed of three couplable formwork carriages 12m in long each, which together pour a total length of 36 m. The formwork units are mounted on self-propelling haulers which are moved one by one to the next concreting section by a hydraulic drive. Then, in the new concreting section, they are placed in position by means of hydraulic lifting devices and connected via the tail plates, which are provided with trapezoidal forms for the concealed joints.

This system allows pouring three standard blocks totalling 36m in length on a daily basis. The formwork unit can be decoupled so that it is possible also to pour a single 12 m standard block.

The three-block pouring rhythm and the block-division plan have been harmonised so as to permit special blocks (e.g. special shapes or an isolated reinforced block) to be poured in a single process.

Trapezoidal profile forms are mounted radially around the formwork skin for the concealed joints that separate the blocks. Reinforcement where necessary needs to be designed so as to harmonise with these concealed joints.

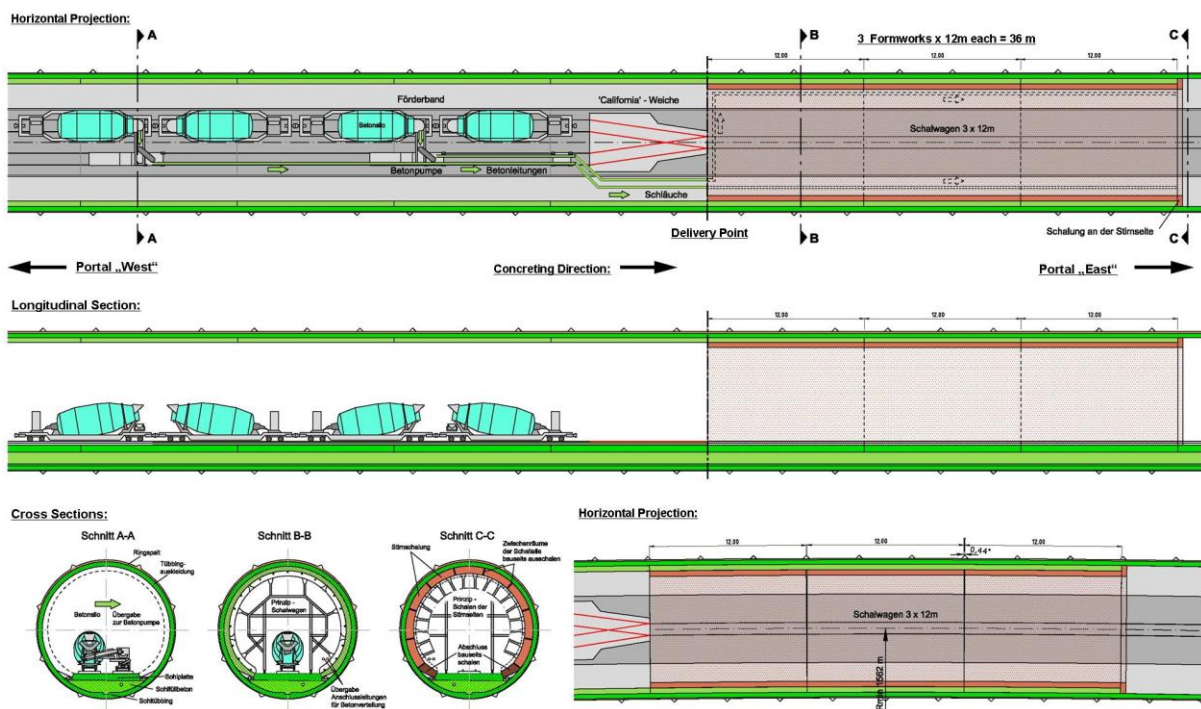


Fig. 7 Schematic drawing of 36 m travelling formwork

The concrete is hauled to the arch formwork by rail-mounted agitators on flat-bed carriages. Two parallel rail-mounted concrete pumps empty the agitators. Each pump feeds one half of the total formwork system through a fixed concrete line. The concrete distributors are capable of feeding a total of 32 hoppers with their respective pump connection pieces. Only for the last pouring operation closing the ring, a single pump is used to cover the entire length of the formwork carriage.

Detailed phase-dependent pouring regulations concerning rising speed and differential concrete surface levels have been prepared to avoid unacceptable uplift forces. During pouring, the hauler carries no weight and in fact serves as ballast for the self-supporting formwork skin. The rising velocity is limited to 1.5m/s in the lower portion and to 3.0 m/s in the upper portion. The concrete-surface differential is 1.0m in the lower portion and 1.5m in the upper portion.

Lateral braces stabilise the formwork units. They are extended after the formwork is placed in position and retracted as concrete pouring proceeds.



Secondary treatment by spraying on a continuous film of a liquid anti-evaporation agent begins as early as possible at the tail of the arch formwork system.

### 3.3 Logistics

Material for the construction of the inner lining shell is hauled to the site on vehicles running on two tracks situated at the tail end of the arch formwork carriage. The two outer rails serve at the same time as a track for the whole concreting train (sealing, reinforcement, arch formwork and scaffolding for roof-gap grouting).

An additional construction track needs to be provided between the arch and invert formwork carriages to permit the passage of the arch formwork carriage and the scaffolding. Passage from the two outer rails to the central track is via mobile Y points travelling in front of the arch formwork carriage.

## 4. CONCLUSIONS

The solutions discussed above are the answer to the need for improvement. They have helped to implement an optimisation potential identified as the work proceeded. It has become clear in every individual case that new ideas and innovative measures can be developed during construction provided:

- requirements and targets are clearly defined
- problems are treated in open technical discussions in consultation with specialists from theory and practice;
- the construction schedule leaves enough time to permit specific laboratory and in-situ testing as well as model analyses;
- the client takes a positive view of new ideas and is included in the decision-making process.

It has been possible to create such a setting on the Wienerwald Tunnel contract, which is once more evidence of the fact that the desired targets are reached only by joint efforts among all partners to a project.



Fig. 8 Section „East”, Widenig before twin tunnel

## **ERECTION OF REINFORCED CONCRETE SEGMENTS IN BUDAPEST METRO 4 LINE**

*Julius Hirscher, Richard Dietze*  
*BAMCO Management, General Construction Manager*  
*H - 1113 Budapest Etele ter*  
*julius.hirscher@bamco.hu*

### **1. INTRODUCTION**

The construction of the TBM tunnels is part of the Metro 4 Line Project stage I running tunnels and associated structures in Budapest and will be carried out with two earthpressure balance shields with a diameter of 6.1 m.

The *DBR Metro Project Directorate* awarded the contract to the consortium *Vinci-Strabag-Hidepitő* at the beginning of 2006 and the first TBM was launched on the 3. April 2007 and the second TBM 5 weeks later.

The installation of rings takes place in the north and the south running tunnels between Etele tér and Keleti station on a length of approximately 10.5 km.

13 cross-passages, 6 ventilation tunnels, 1 crossover and the mined station at Gellért are also included, as are the launching shaft at Etele and the shaft at Gellért.

### **2. GENERAL RING DESCRIPTION**

The ring is assembled by 6 reinforced concrete segments: 3 ordinary segments, 2 counterkeys and 1 keystone.

A ring is a cylinder in section with an average width of 1500 mm. The width of ring is 1525 mm at the widest point and 1475 mm at the narrowest.

The rotational position of the ring determines the direction of drive for the concrete tunnel lining.

Eleven possibilities of ring orientation are given through the positioning of the key stone as shown in the Fig. 1 below.

### **3. TYPE OF RINGS:**

The lining consists of a precast universal tapered reinforced concrete ring.

Two different types are used with the following functions.

The functions of the standard ring are:

1. to create the final tunnel lining of the permanent structure for the metro trains
2. abutment for the shield to move forward and finally
3. to avoid infiltration of groundwater and soil into the tunnel.

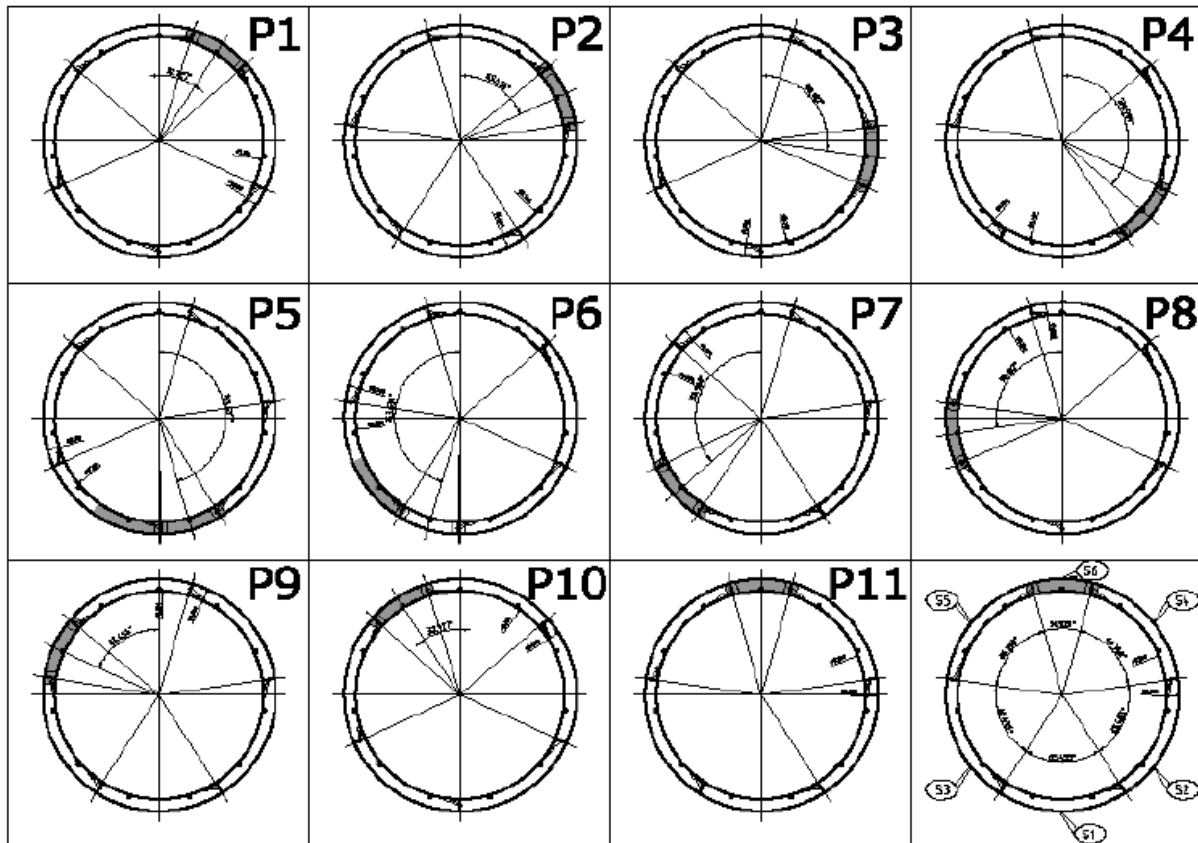


Fig.1: Ring orientation

The functions of the special ring are:

1. to support the openings for the ventilation tunnels and cross-passages
2. to create the final tunnel lining of the permanent structure for the metro trains
3. abutment for the shield to move forward and finally
4. to avoid infiltration of groundwater and soil into the tunnel.

The construction of ring follows always the same sequence of segments and the transport is via segment car and segment feeder to the erector.

Before and after transport in the tunnel, the segments are checked for damage. Damaged segments must not be erected into the tunnel.

The construction of ring starts with segment S1 and the follow others alternatively from the right to the left side of the first one. The ring will be closed with the keystone. Even if the first segment S1 starts at the crown the ring building follows the same order. A triangular mark allows a quick check on the angular position to ensure the clearance of the key stone.

The installed CAP system calculates the new necessary orientation and TBM parameters for the next ring to follow the theoretical tunnel axis.



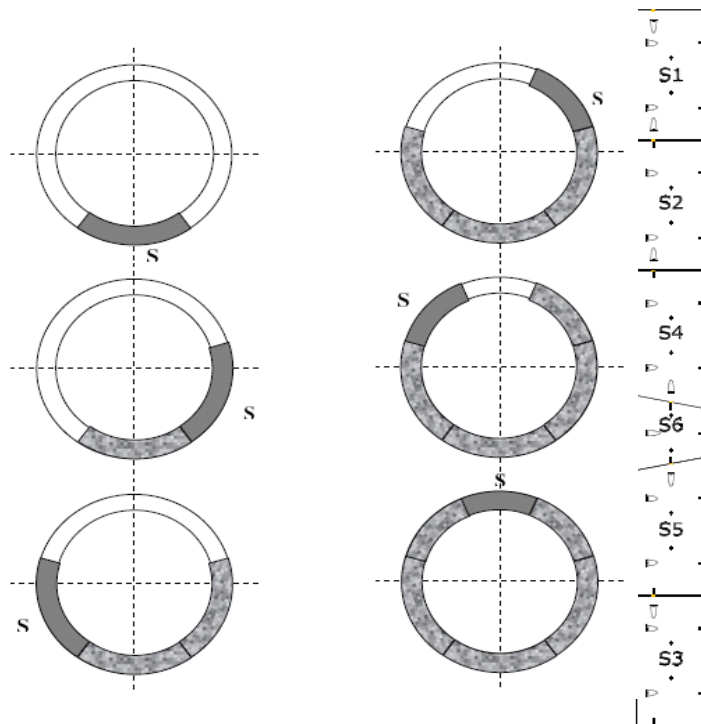
Frame with segment ring on flat car



Segment feeder



Tunnel entrance launching shaft



Sequence of segment assembly – Ring orientation P11

#### 4. OPERATING PROCEDURES

After every process of advancing, a new segment ring must be built in under the protection of the tail skin of the TBM. The segment rings acts as a counter bearing for the machine advance process and serves as an extension of the tunnels resistance to pressure and water.

The constructed ring should not touch the tail skin to avoid damaging either the ring or the wire brushes.

The TBM driver determines with the CAP System, the keystone segment position of the desired ring orientation.

The segment joints must be staggered to avoid cross joints and the risk of leaking (Fig.1 ring orientation).



Segment joints

Before ring erection a check of the tail skin is required that no mortar, no grease, no water, etc... can interfere with the erection of the segments and also the check of the vacuum plate and ring erector.

The length of one excavation stroke can be controlled on the screen in the pilot cabin and with the stroke of the thrust cylinder of the TBM to be sure that the length is sufficient to install the ring.

To be sure that the pre-calculated laying plan for the ring erection is identical with the TBM drive a control measurement between the tail-skin and the intrados of the segments is necessary to compare the measured figures with the CAP calculation and to adjust the next laying plan.

##### 4.1 First segment: S1

For the positioning of the first segment S1 the thrust cylinders in this area are retracted. Two cylinders are linked to one cylinder shoe. Eleven pairs of cylinders are installed on the TBM for the full ring.

Depending on the laying plan determined by CAP the erector operator picks up the segment with the vacuum plate from the segment feeder and transports it in the tail skin to align and install it.

Positioning rams on the vacuum plate allows it to be manoeuvred in any direction in order to build the ring with minimal steps, lips and misalignments.

For the fine alignment a triangle mark is located on the centre line of the segments. The mark shows the edge of the adjacent segment. The first segment S1 is the reference stone for the remaining segments. To guaranty an accurate positioning of the following segments the segment S1 must be installed with a high exactness and with particularly care.

When the segment S1 is in the correct position the push rams are applied, the segment checked again for lips and steps on the seat and circle joints and bolted to the adjacent segments. If the segment needs to be adjusted again, the pairs of cylinders are released and the position corrected before bolting.

Finally the vacuum can be released and the next segment can be picked up.

The alignment is checked for:

- straight alignment with aluminium ruler
- angular position with the triangular marks
- minimum lips with a 2 cm piece of straight staff.

#### **4.2 Second segment: S2**

Before erecting segment S2 it is checked that it is clean on the segment feeder to avoid problems on the vacuum plate. Then two sets of push rams retract corresponding to segment S2 on the right side of the first segment and the segment is aligned and installed.

*Example:* the first segment had been built at the invert; the second will stand to its right.

*Example:* The first segment had been built at the crown; the second will stand at its right but at your left.

The alignment reference is taken with the previous segment. The two edges of each segment have to be in line. This is checked by eye. Then the segment will be rotated against the previous one to compress the gasket. The face of the segment is not in contact on the previous ring. The segment will be kept in place by the two sets of push rams. If the segment needs to be adjusted again the pair of cylinders is released and the position corrected before bolting.

Finally the vacuum can then be released and the next segment can be picked up.

#### **4.3 Segments three - five: S3 –S5**

The erection of segments S3 to S5 follows the same steps as the second segment S2 only the positioning is alternated: Segment S3 on the left of segment S1, Segment S4 on the right of segment S2 and segment S5 on the left of segment S3.





Segment S4

#### 4.4 Keystone: S6

Before erection of the keystone a check of the clearance between the two counter-keys S4 and S5 are necessary. The clearance is measured with a tape measure along the straight line between the two counter-key corners. If necessary an adjustment of the two counterkey lips will be carried out to maintain the theoretical clearance. For a better positioning of the keystone soap or grease on the gaskets supports the erection.

The keystone is erected.

It is aligned, centred and levelled between the two counter-keys by eye.

The erector is moved and the key positioning is adjusted if necessary.

When gaskets are in contact the key is pinned with the pair of cylinders.

The key is bolted.

The ring position is checked and parameterized for the next ring.



Keystone S6

After finalisation of the ring erection the control of the annular gap with the distance at 3h, 6h, 9h and 12h between the ring and the tail skin is required to allow an adjustment on the laying plan.

Also a roll check is done on the previous ring built, prior to the next ring build, to adjust the next ring accordingly.

Any lips, steps or damage caused during the erection will be recorded on the ring repair check sheet and handed over to the QA manager for filing and finally for use by the reconstruction and commissioning of the tunnel.

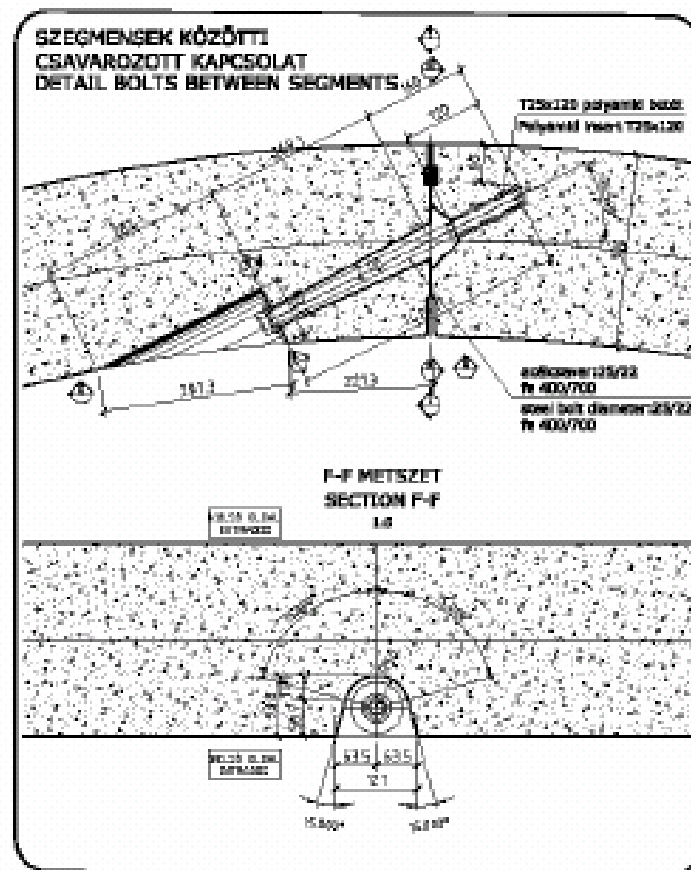
## 5. AUXILIARY TOOLS

For the ring erection and alignment of the segments special auxiliary tools are required. For the standard ring and its temporary connection will be used a normal black bolt is used, for permanent fixing a hot dip galvanized bolt is used.

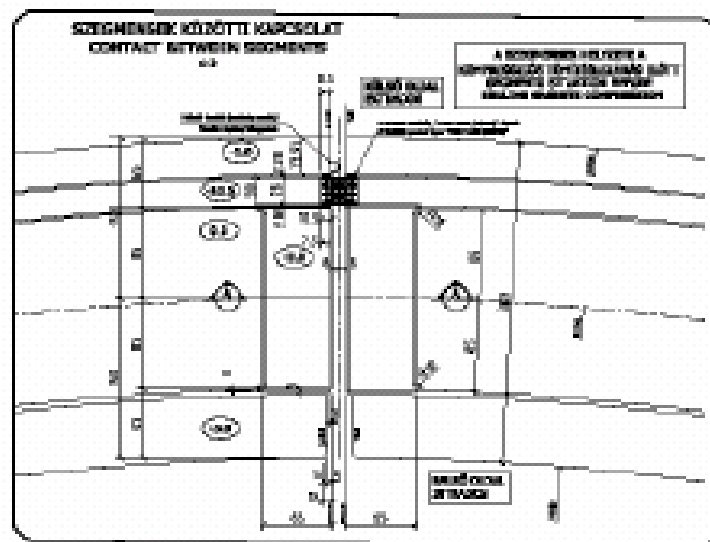
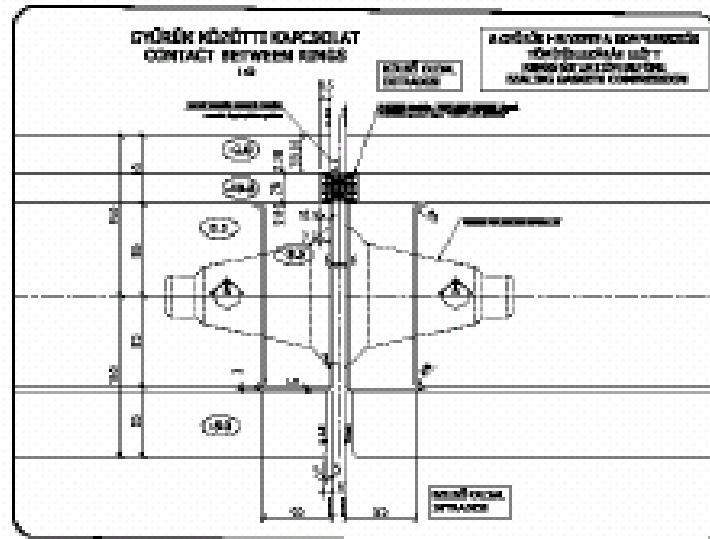
Additional to these bolts is a special shear cone inserted for the special rings for openings by cross passages or ventilation tunnels and by sections with higher loads.

In order to guaranty water-tightness of the joints of the segments an elastomeric sealing gasket complying with the clients requirements is fixed to the segments. Due to the fact that the segment has only a thickness of 30 cm is a very small profile used with a width of 29.2 mm.

This situation requires a highly precise installation of the segments.







## CONCRETE TO CONCRETE INTERACTION BY CONSTRUCTING THE 4<sup>TH</sup> METRO LINE IN BUDAPEST, HUNGARY

*Tamás K. Simon*

*Budapest University of Technology and Economics (BME), Hungary*

*H-1111 Budapest Múegyetem rakpart 3.; t.simon@eik.bme.hu*

### SUMMARY

During the construction of the 4<sup>th</sup> metro line in Budapest rose the question of the interacting capacity of a hardened and a later, next to it poured concrete layer. At some locations the ground water table is close to the surface. The stations are built in such a way that at first a slurry wall is constructed at the perimeter of the construction pit. In this “slurry wall box” is the station constructed. The mass of the slurry wall is to be involved against the up thrust of the ground water. So the accepting slurry concrete would interact (work together) with the adjacent walls of the station. Furthermore there was a need of a watertighting layer between the two walls. The study shows that a slurry watertighting layer would decrease the interacting capacity of two concrete layers, while passing through reinforcement does not effect it until a relative movement is experienced between the two.

### 1. INTRODUCTION

SWIETELSKY Construction Ltd. instructed the Department of Construction Materials and Engineering Geology of BME to experimentally study the interacting capacity for shear stresses in the construction joint formed by a hardened concrete layer with a surface roughness of a slurry wall and a later, adjacently poured concrete layer.

The actuality for the study was very practical, since the company has won the tender for the construction of several stations of the 4<sup>th</sup> metro line in Budapest in close locations to River Danube (Fig. 1). At these locations the level of the ground water is quite close to the surface. The architectural design of the metro stations were prepared so that these structures are practically hollow RC boxes as can be seen in Figs. 2 and 3.

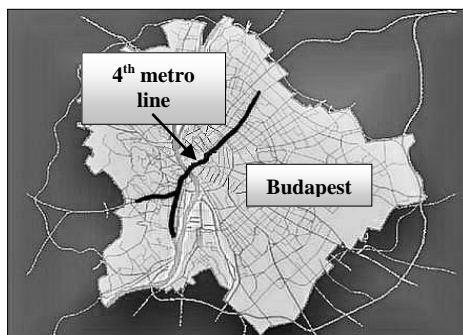


Fig. 1 The 4<sup>th</sup> metro line under construction in Budapest

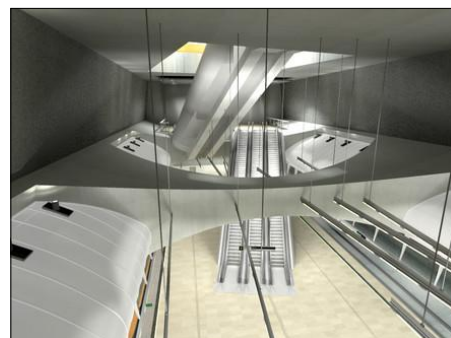


Fig. 2 The 3D drawing of Kálvin square station, as an example

The construction method of the structures, since the areas are affected by dense traffic, is to be such that the surface construction time is minimized. At first slurry walls are constructed at the outer perimeter of the stations final walls. Following this an RC slab is constructed on the

top of the slurry walls on which the traffic can be restarted. Then the earth is excavated and the floor is poured out of concrete. In the so constructed RC box the building of the structure can be completed (Fig. 3).

The tunnel boring machines are able to bore through the slurry walls, since at the place, where the tunnels are connecting to the structures the slurry wall reinforcement is prepared out of non metallic reinforcing material instead of steel.

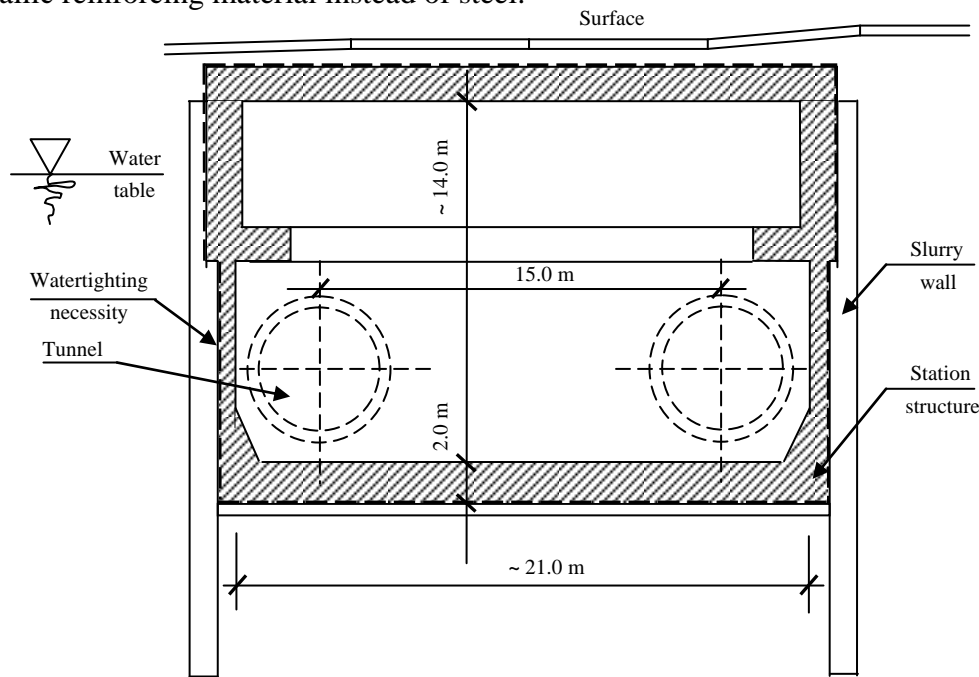


Fig. 3 Sketch of a station structure at the 4<sup>th</sup> metro line in Budapest

The station structures are submerging into the ground water in a large extent so they suffer a considerable up thrust what must be counterbalanced by self weight and/or anchoring. If the mass of the slurry walls could be involved into the counterbalance of the up thrust, it would be a cost effective technology, but for this the interacting capability of the slurry wall and the station structure must be determined.

Further difficulty is the safety requirement of the tender to have an extra waterproofing layer between the two walls. One of the ideas to eliminate this difficulty was to add to the concrete of the slurry wall an admixture which through growing crystals in the pores would increase the watertightness of the concrete. However, no concrete mixing plant in the town was willing to take the responsibility of adding a powdery admixture to the fresh concrete, due to lack of experience. The next idea was to apply a coating layer named Penetron on the internal surface of the slurry wall, which material would form the necessary crystals in the concrete pores to make it waterproof.

To be able to take into consideration the interacting capability of the two concrete layers due to adhesion, an old, but valid Hungarian Standard, (MSZ 15022/4-86) requires a connecting reinforcement which has a cross sectional area of 0.1% of the adjacent concrete surface. Due to this reason no other type of Damp Proofing Course (DPC) could have been applied.

## 2. EXPERIMENTAL STUDIES

Earlier studies showed that one of the most significant influencing factors of the interacting capacity is the surface roughness of the accepting concrete (Júlio, Branco, Silva, 2004; Santos, Julio, Silva, 2007). For modelling the situation, several sample types are used (Momayez, Ehsani, Ramezaniapour, Rajaie, 2005; Simon, 2003), we chose for our experimental studies the following test samples:

Using C20/25- $d_{max}=16$  concrete mixture of V1 consistence in steel formwork, accepting concrete samples of the size 300x300x100 mm were cast. The accepting concrete surfaces were prepared by having the imprint of a stamp, made out of gypsum to model the roughness of the surface of a slurry wall (Fig. 4 and 5). The preparation of the stamp was necessary to be able to obtain equally rough surfaces, At such considerable roughness the sand patch method to measure SCD value (Garbacz, Courard, Kostana, 2006; Simon, 2003) is already impossible. Three of such samples surfaces were left intact as reference, three received Penetron slurry coating and three was prepared with reinforcement (5 pcs BHB55.50; diameter 5 mm rebar to model 0.1% passing through reinforcement) leaning out of the surface.



Fig. 4 Gypsum stamp to imprint equal surfaces      Fig. 5 Imprinted accepting concrete surface

These nine accepting concrete samples were mix cured at first for 14 days (1 day in formwork, 6 days under water then 7 days in laboratory conditions).

Following the 14 days curing cycle, in steel formworks with heightened walls, a new layer of concrete was poured onto the 9 accepting concrete surfaces out of such kind of a concrete mixture from which we expected to reach similar strength as of the accepting concrete, but after 14 days. In such a manner, after a further 14 days of mixed curing cycle the accepting concrete was just 28 days old, and the samples were ready for testing. During the preparation of the samples we obtained three of each sample types, altogether nine samples (Tab. 1).

The slurry for the three samples which were treated for the increase of watertightness of the accepting concrete was prepared according to the technical specification (Penetron), out of the powdery material. Since the instructions of the employer were not aiming to check the

effectiveness of the watertighting capability of the slurry, we have not carried out such, watertightness tests.

Tab. 1 Types, sign and the number of test sample specimens

Type of test sample	Sign of sample	Number of samples	Total number of samples
Construction joint model, the accepting concrete surface was prepared with a stamp. No further surface treatment.	I/4/P–I/5/P–I/6/P	3	9
Construction joint model, the accepting concrete surface was prepared with a stamp, and coated by PENETRON slurry.	II/1/P–II/2/P–II/3/P	3	
Construction joint model, the accepting concrete surface was prepared with a stamp. No further surface treatment but rebars are crossing the joint having 0.1% cross sectional area of the area of the joint.	III/1/P–III/2/P–III/3/P	3	

### 3. EXPERIMENTAL RESULTS

#### 3. 1 Setup of the experiments

Following the 14 days hardening period of the second layer of concrete, we have subjected the above modelled construction joints to shear according to the setup shown on Fig. 6.

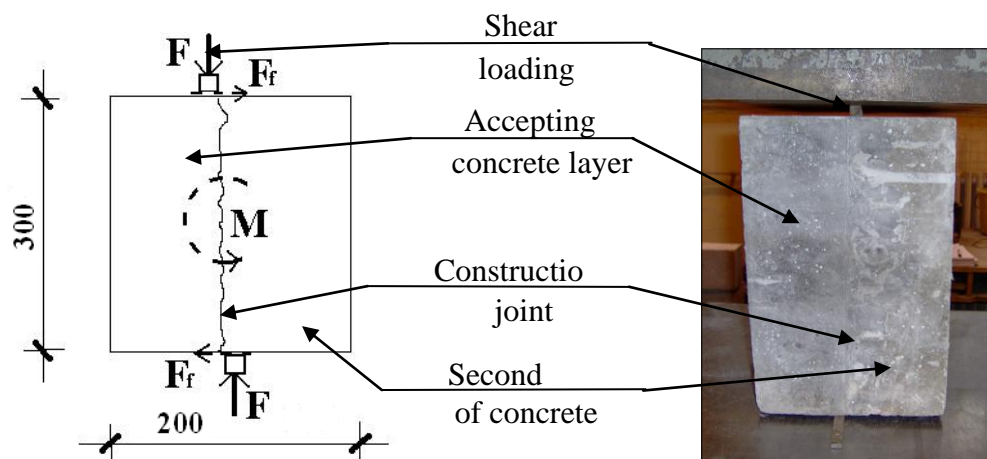


Fig. 6 The layout and real time photo of the shear loading of construction joints

On the layout the shear force is marked with  $F$ , and the possible moment  $M$ , arising from the small eccentricity of  $F$  is counterbalanced by the frictional forces  $F_f$ .

During the execution of the experiments we measured the maximum of the shear force  $F$ , and calculated the shear stress in the construction joint, using the nominal sizes of the specimens which was 300x300 mm.



### 3. 2 Influence of the PENETRON slurry coating

Visually it was possible to apprehend that the slurry – due to it's very fine particle size distribution, has produced a fine, smooth coating on the accepting concrete's surface. This occurrence may be visualized (Fig. 7).

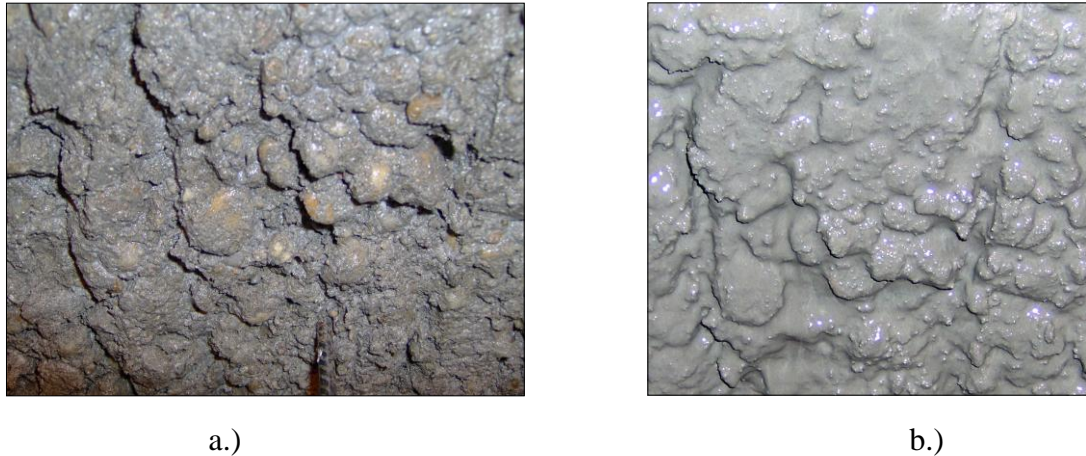


Fig. 7 The intact rough concrete surface a.) and concrete surface treated and smoothed by the slurry b.)

The untreated and slurry treated construction joints were tested for shear load bearing capacity according to point 3.1, and the results summarized (Tab. 2).

Tab. 2 The results of testing and comparing the shear strength of construction joints, where the accepting rough concrete surface is untreated, with those, which are treated with slurry

Sign of sample	Comment	Shear force [kN]	Nominal shear stress [N/mm <sup>2</sup> ]	Average shear strength [N/mm <sup>2</sup> ]	Shear strength %-age of the average of the reference	Average [%]
I/4/P	Samples without slurry treatment for reference	210.0	2.33	2.35	--	--
I/5/P		240.0	2.67			
I/6/P		185.0	2.06			
II/1/P	Samples with slurry treated surfaces	120.0	1.33	1.22	56.69	<b>51.97</b>
II/2/P		85.0	0.94		40.16	
II/3/P		125.0	1.39		59.06	

It is evident from the above results: A slurry like coating of a rough accepting concrete surface decreases the shear load bearing capacity of the construction joint nearly to 50% of that of the untreated connection by smoothing the surface.

### 3. 3 Influence of 0.1% reinforcement across the construction joint

At last we have tested the shear load bearing capacity of those samples which contained reinforcement in cross sectional area of 0.1% of that of the connecting surfaces. These surfaces were not treated with any slurry. The results of the experiments are summarized (Tab. 3). From these results it can be clearly seen that the joining reinforcement (in the extent

of 0.1% of the joining concrete surfaces) – until the two concrete layers do not suffer any relative movement – does not increase the shear load bearing capacity of a construction joint.

Tab. 3 The results of comparing the shear strength of construction joints. The accepting rough concrete surface is untreated, against where connecting reinforcement is applied

Sign of sample	Comment	Shear force [kN]	Nominal shear stress [N/mm <sup>2</sup> ]	Average shear strength [N/mm <sup>2</sup> ]	Shear strength %-age of the average of the reference	Average [%]
I/4/P	Samples without slurry treatment for reference	210.0	2.33	2.35	--	--
I/5/P		240.0	2.67			
I/6/P		185.0	2.06			
III/1/P	Samples with connecting reinforcement	210.0	2.33	2.33	99.21	<b>99.21</b>
III/2/P		195.0	2.17		92.13	
III/3/P		225.0	2.50		106.30	

#### 4. CONCLUSIONS

We tested the shear load bearing capacity of construction joints if a slurry like coating is applied on the accepting concrete surface, and when 0.1% of the area of the joint quantity of connecting reinforcement is applied. The followings are the conclusions.

1. A slurry like coating of a rough accepting concrete surface decreases the shear load bearing capacity of a construction joint nearly to 50% of that of the untreated connection due to smoothening (decreasing) the roughness.
2. The joining reinforcement (in the extent of 0.1% of the joining concrete surfaces) – until there is no relative movement between the two layers of concrete – does not change the bond in a construction joint if the accepting concrete surface is rough.

#### 5. REFERENCES

- Garbacz, A., Courard, L., Kostana, K. (2006), „Characterization of concrete surface roughness and its relation to adhesion in repair systems” *Materials Characterization* 56 2006, pp. 281-289.
- Júlio, E. N. B. S., Branco, F. A. B., Silva, V. D. (2004), „Concrete-to-concrete bond strength. Influence of roughness of the substrate surface” *Construction and Building Materials* 18 2004, pp. 675-681.
- Momayez, A., Ehsani, M. R., Ramezani-pour, A. A., Rajaie, H. (2005), „Comparison of methods for evaluating bond strength between concrete substrate and repair materials” *Cement and Concrete Research* 35 2005, pp. 748-757.
- MSZ 15022/4-86, „Design of loadbearing building structures – prefabricated concrete, – reinforced and stressed concrete structures” (Hungarian standard), *Magyar Szabványügyi Hivatal*, p 4.
- Penetron, „Technical specification” [www.penetron.com](http://www.penetron.com)
- Santos, P. M. D., Júlio, E. N. B. S., Silva, V. D. (2007), „Correlation between concrete-to-concrete bond strength and the roughness of the substrate surface” *Construction and Building Materials* 21 2007, pp. 1688-1695.
- Simon, T. (2003), „Sand patch method for evaluation of concrete-to-concrete interaction” *Concrete Structures 2003*, Journal of the Hungarian Group of fib pp. 67-71.

## **BRIDGE DECK CONCRETE OVERLAYS AS RENEWAL STRUCTURES**

*Velimir Ukrainczyk,  
"Mostprojekt"  
Zagreb, Sv. Duh 36, Croatia*

### **SUMMARY**

In the past ten years several reinforced concrete bridges have been renewed with latex modified high performance concrete. As compared to the reconstructions with waterproofing and asphalt, concrete pavements provide the possibility of simple widening and strengthening the span structure. The bituminous waterproofing and asphalt layers have been replaced by water-resistant pavement with low permeability for chloride ions and the durability of the pavement has been increased. Completion deadlines have been reduced to 1/2 of the time required for the classic reconstruction.

The concrete mix design and the construction methods have been aimed at obtaining waterproof, abrasion and skid resistant, freezing/thawing cycles and chloride ions resistant overlay. In addition, the concrete surface layers were impregnated with styrene-butadiene latex solution.

### **1. INTRODUCTION**

In the past ten years in Croatia several reinforced concrete bridges have been renewed with styrene-butadiene (SB) latex modified high performance concrete. As compared to the classic solutions of pavements reconstructions, with waterproofing and asphalt, high-performance concrete pavements in particular cases, presented in this contribution, have the following advantages:

- in some cases within the existing layout, the bridge has been strengthened, which has been significant because of increased loadings in comparison with previous normative;
- in some cases widening of the bridge by cantilever extension of the bridge cross-section has been rather straightforward;
- durability of the pavement has been increased (higher resistance to wear, freezing and de-icing salts);
- bituminous waterproofing as the least durable part is replaced by water-resistant pavement with low permeability for chloride ions;
- completion deadlines have been reduced to 1/2 of the time required for the classic reconstruction.

The mix design and the construction methods of special SB latex modified (PM PCC) concrete overlays have been aimed at obtaining waterproof, abrasion and skid resistant, freezing/thawing cycles and chloride ions resistant overlay. Special properties have been obtained by admixing 5 % of SB latex, and then the solution with 12 % SB polymer solids was subsequently applied as surface protection. Volcanic crushed aggregate sizes above 4 mm and PP fibres  $L/d=30/0,3$  mm were used to improve resistance to wear. Results of



laboratory tests on concrete impregnated with SB latex solution for improved durability are also presented in this contribution.

## 2. EXAMPLES OF RENEWAL

### 2.1 Strengthening and widening the bridge in Stupno

The bridge had been constructed about the year 1920. The total length of the bridge was 39,20 m, the total width was 7,15 m, and width between curbs is 5,60 m. The bridge has three spans, the middle one 16,0 m, and the outer ones 10,0 m each. The bearing system is Gerber beam with two joints in the middle span. The reinforced concrete slab was degraded by water leakage, reinforcement corrosion and freezing. The depth of asphalt layers was 5 - 6 cm. Under the asphalt layer cca 5 thick was the old layer of setts 9 cm high layed on the sand layer about 4 cm thick.

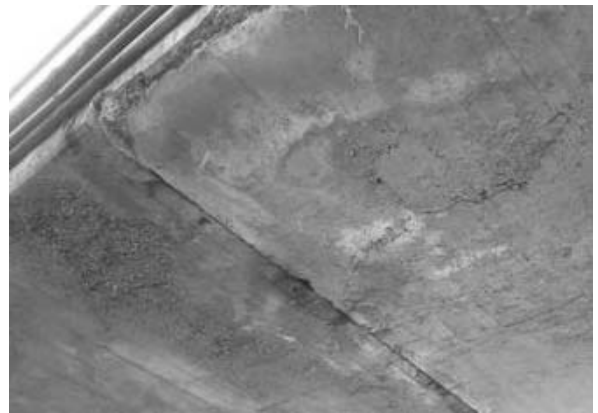


Fig. 1 The bridge lanes were too narrow for trucks      Fig. 2 Lower side at the place of Gerber joint

The renewal work (Fig. 3a-e) consists of pavement layers removal and constructing the new bridge deck, total width 10,0 m. Reinforced concrete deck is simultaneously concrete pavement on the bridge and on the abutments. They were cast with SB latex modified concrete class C25/30, water impermeable, resistant to abrasion and freezing and deicing salts. The lower side of the bridge, after removal of deteriorated concrete and cleaning the existing reinforcement, is strengthened by additional reinforcement protected by the layer of latex modified sprayed concrete. At the same time the Gerber joints are “locked”, changing the Gerber beam into the continuous bearing system.

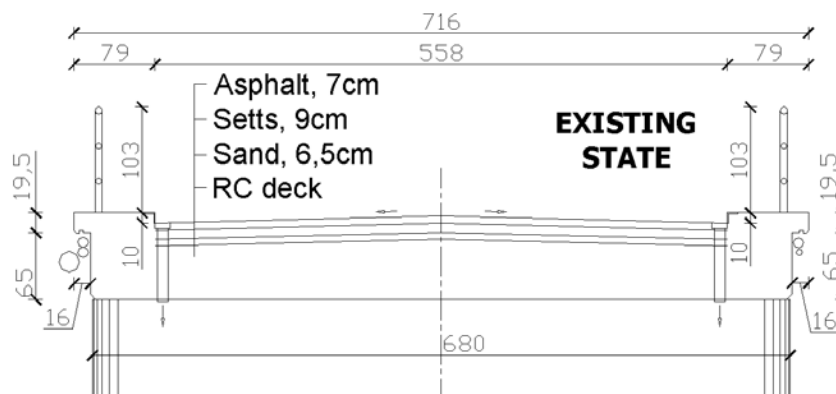


Fig. 3a Cross-section before renewal and widening

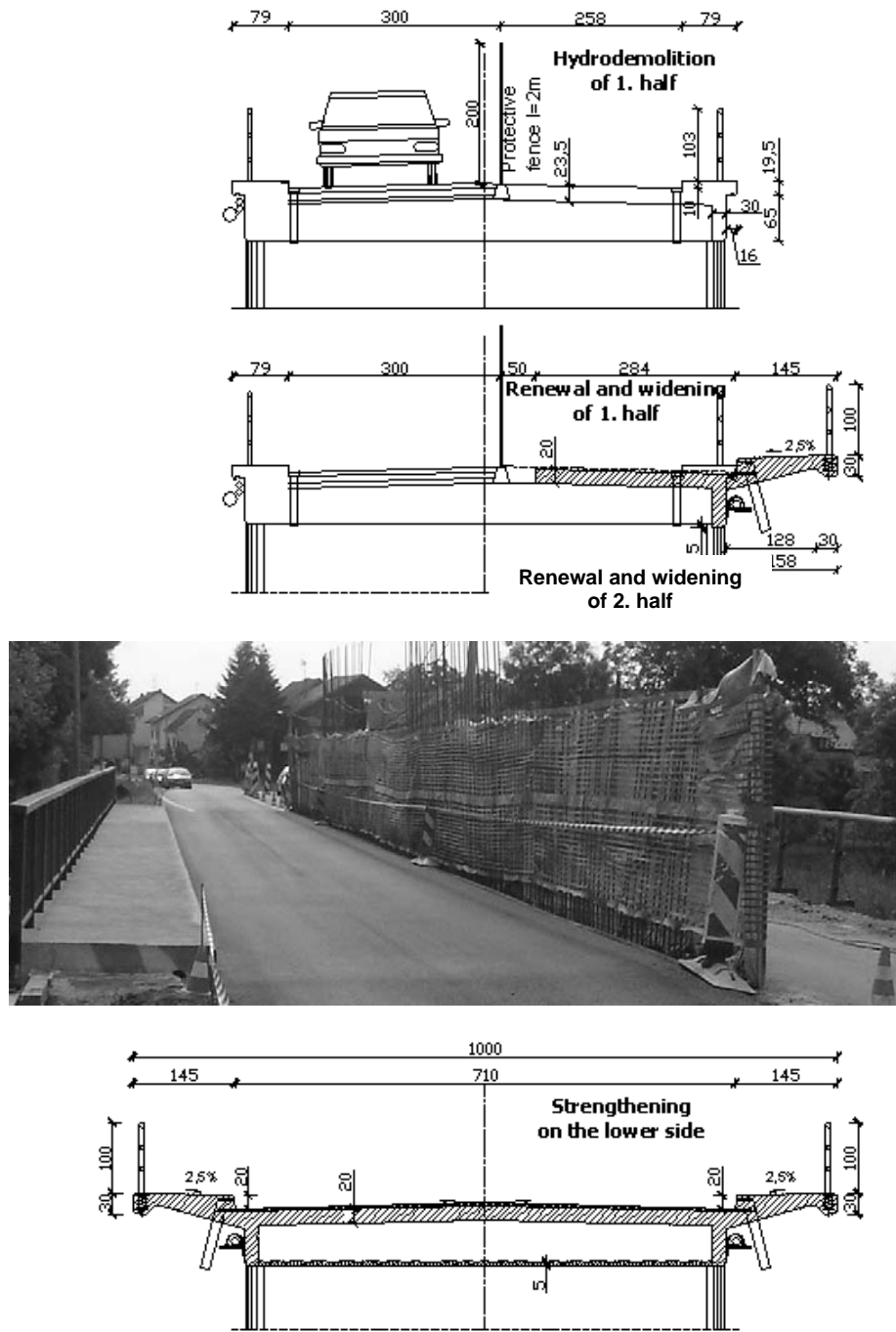


Fig. 3a-e Phases of renewal and widening bridge Stupno

## 2.2 Replacing the span structure and widening the bridge Kamenmost

The original stone arched bridge on the land road had been destroyed at the end of the World War II, and then immediately renewed by low quality concrete, reinforced with old small profile rails. In the next 50 years on the both sides of the bridge the settlement has been built. The bridge has five spans  $L = 7,17+7,27+7,27+7,27+7,21$  m (FIG. 4). The width between the curbs was 5,74 m and the side walks were too narrow.



The old stone piles and abutments were used for the new bridge. However, the old span structure was used only as «scaffolding structure» for the new deck. On each stone pile the support reinforced concrete beam has been built (Fig 5.).

Fig. 4 After the World War II the arch stone structure was replaced by continuous plate

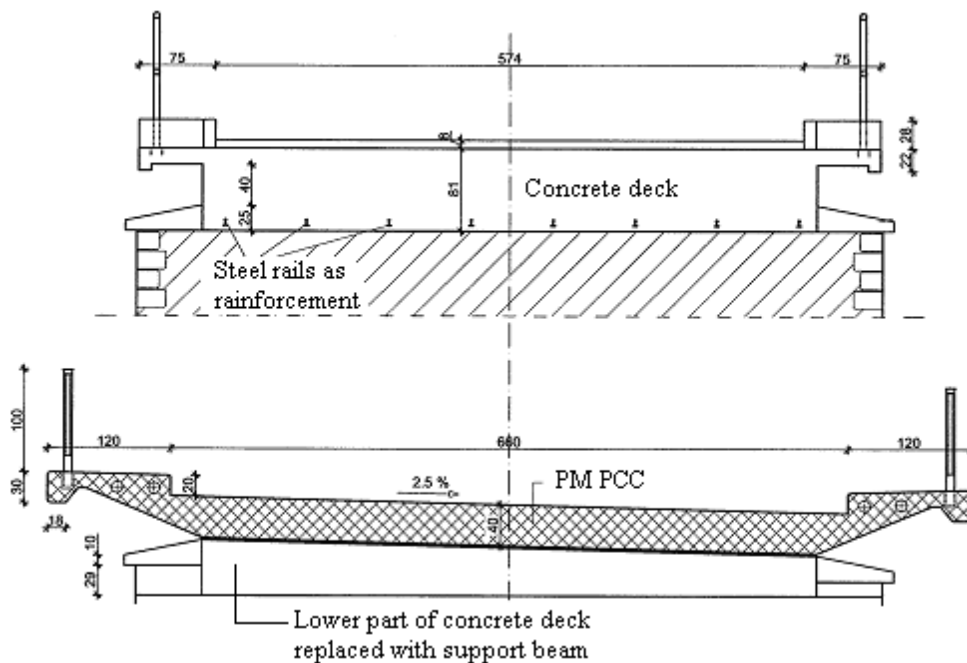


Fig. 5 Cross-sections before and after renewal

### 2.3 Strengthening the Bridge Oštarije

The bridge had been constructed in winter 1972, and the young concrete surface layer was damaged by freezing. The inspection in the year 2000 has ascertained low concrete strength ( $f_{ck} = 15$  MPa), damaged waterproof membrane and reinforcement corrosion.



Fig. 6 Deteriorated curbs



Fig. 7 Deteriorated lower side, bridge Oštarije

The latex modified concrete was designed for strengthening the bearing deck structure by replacing the old concrete layer 10 cm and increasing the deck depth for 10 cm on the account of the former asphalt and waterproofing membrane layers. It is resistant to freezing and deicing chemicals, to abrasion and adhesion wear, and serves as waterproof impermeable layer instead of membrane.

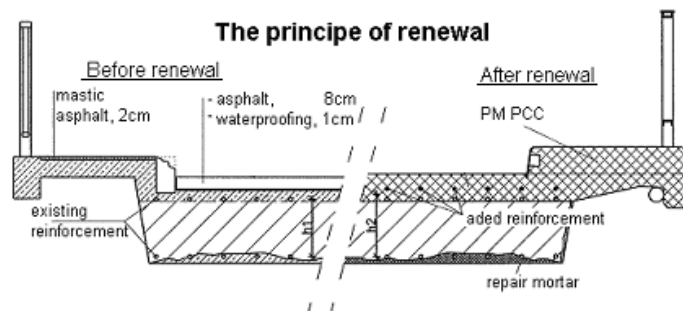


Fig. 8a-c Principle of renewal, final state and during reconstruction

### 3. Latex modified concrete as bridge deck overlay

It is well known that 10 to 15 % of SB latex solids improves durability and mechanical properties of concrete bridge deck overlays [ACI Recomm., 2003, Ohama 1995]. It significantly reduces the penetration of chloride ions into concrete, improves resistance to freezing cycles, increases bond of old to new concrete and decreases the cracking risk. However, the admixture of 10 to 15 % of styrene-butadiene polymer significantly increases the price of repair works.

The influence of SB latex impregnation was laboratory investigated by comparative test with commercial protection materials: two types of silane and one type of siloxane. Hardened ordinary concrete specimens, cylindrical-shaped, with a 10 cm diameter, 5 cm height and characteristic strength 30 MPa, were first tested unprotected and than impregnated for the following durability parameters:

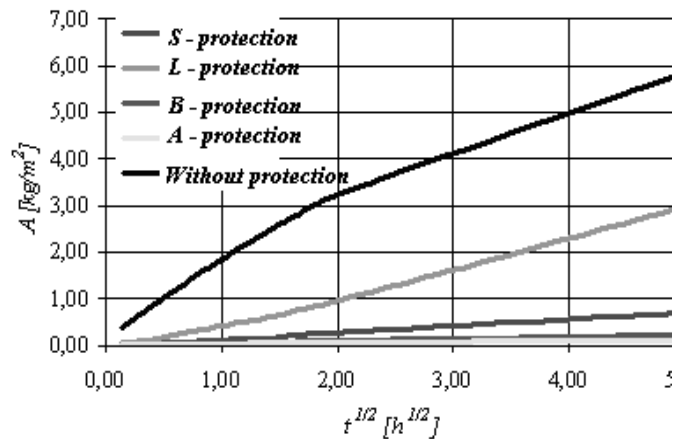


Fig. 9 Average results of three waterabsorption tests

capillary absorbtion, gas permeability, porosity, chloride ions diffusion, depth of protection material penetration, resistance to wear.

The results of laboratory testing are shown in Fig. 9 and Tab. 1. and summary effects of surface type protections on concrete properties are shown in Tab. 2.

Tab. 1 Results of laboratory testing of surface protection material.

Protection type Protection label	Depth of protection material penetration	Cl <sup>-</sup> ions after 90 days %	Wear (Böhme) cm <sup>3</sup> /50 cm <sup>2</sup>
Unprotected	-	0.109	19.5
SB LATEX (L)	5 - 6 mm	0.053	11.16
SILANE A (A)	20 - 26 mm	0.029	22.94
SILANE B (B)	9 - 32 mm	0.032	18.54
SILOXANE (S)	on the surface	0.063	19.92

Tab. 2 Evaluation of surface protection materials on concrete properties

Surface protection	Capillary absorbtion	Water penetration	Gas permeability	Cl <sup>-</sup> ions diffusion	Wear	Evaporable toxic matter
Siloxan	++	+	+	+	o	o
SB latex	+	+	++	+	++	o
Silane A	++	+	o	++	o	-
Silane B	++	++	+	++	o	-

+ - good; ++ - very good; o - no effect; - environmentally harmful effect

## REFERENCES

- ACI Recommendation 548.3R-03 „Polymer Modified Concrete“, 2003.  
 Ohama, Y.: Chapter 7. 1995, «Polymer-Modified Mortars and Concretes» Concrete Admixtures *Handbook*, V.S.Ramachandran,ed., Noyes Publications, Park Ridge, N.J.

## **M0 NORTH DANUBE BRIDGE IN BUDAPEST, HUNGARY – CONSTRUCTION TECHNOLOGY**

*Réka Szécsényi  
Hídépítő Co.  
1138 Budapest, Karikás F. u. 20.*

### **SUMMARY**

The longest river bridge in Hungary is being built at the northern border of Budapest, as the 1861 m part of the m0 motorway's 3.2 km section currently under construction. Construction works started at the spring of 2006 and the expected completion date is August 2008 Hídépítő Co. is the head of the consortium responsible for the project.

### **1. TECHNICAL SPECIFICATIONS OF THE NORTH-DANUBE BRIDGE OF THE M0 MOTORWAY**

The route of the northern sector of M0 Motorway crosses the main branch of the river Danube, the southern part of Szentendre island, the Szentendre branch of the river and the adjacent floodland (Fig. 1). The total length of the bridge, as part of the 3.2 km section of the motorway, is two kilometers, supported by 29 pylons. The width of the bridge will be 47 m, which will include 2×2 lanes plus an emergency lane. The width, which exceeds the minimum required size, will offer an opportunity for future widening to be required by possible traffic increase, because the cable-stayed bridge spanning over the river will not allow any widening in the future. Separate lanes at both sides of the bridge will provide a connection between regional pedestrian and bicycle roads located on the Pest and Buda side of the bridge.



Fig. 1 Layout of the M0 North Danube bridge

### **2. 5-IN-1 BRIDGE**

Although the North Danube Bridge is a single project, it will be made up by various types of structures, the almost 2 km long section will include 5 bridges, which follow each other.

## 2.1 Floodland bridge on the left side of the river

This section is a four-span beam bridge, made of pre-stressed reinforced concrete box blocks (Fig. 2). Two parallel bridges will be built, according to the two traffic directions. Precast sections of both bridges will be manufactured at platforms established behind the abutments, using gradually advancing technology.

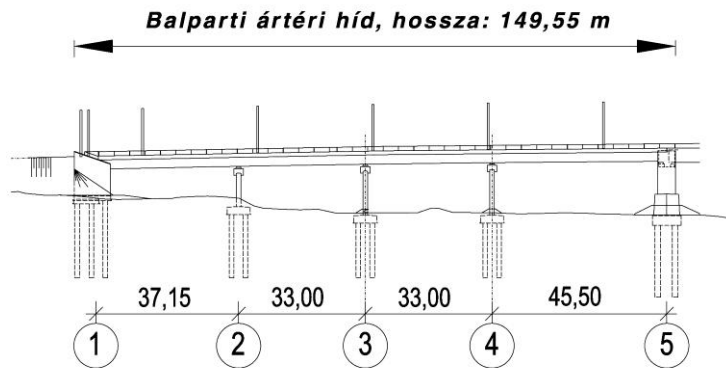


Fig.2 Construction of the left-side floodland bridge

## 2.2 Bridge over the main branch of the river Danube

This is a three-span, two pylon fan-type stayed-cable bridge (Fig. 3). Cables run into the two sides of the support pylon in the shape of two fans, anchored at distances of 12 m. The structure of the two pylons is a pre-stressed, reinforced concrete box, forming a letter "A". The pylons will be made of a hollow rectangle with gradually decreasing wall thickness. Stairs or industrial elevators will be installed inside this hollow space, which provides access to the anchoring chambers of the cables, located at various levels of the pylon. Cables will be anchored into steel anchoring beds installed into the reinforced concrete floors. The triangle between the pylons and the connecting beam will be decorated by a glass façade, which will enhance the look of the bridge.

The support structure is a fine-meshed carriageway grid, made of welded steel profiles, with an enclosed box under the two cable fans. This section will be assembled by using 12.0 m long, full-size sections, with cantilever technology.

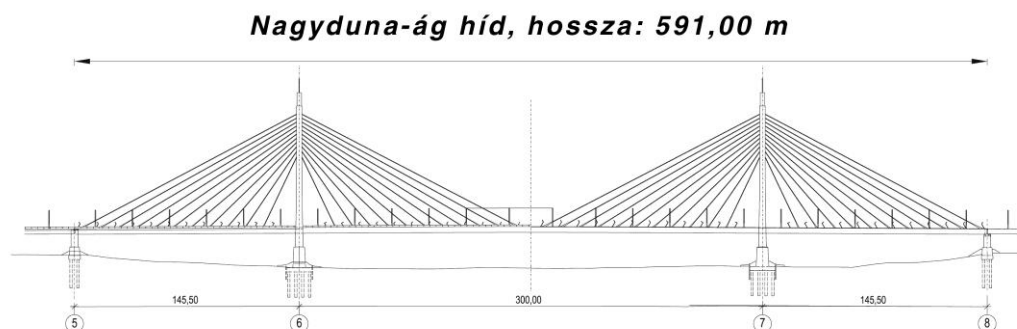


Fig. 3 Structure of the bridge over the main branch of the river Danube

### 2.3 Bridge over the floodland at Szentendre-island

This is a 12-span beam bridge made of prestressed, reinforced concrete box sections (Fig. 4). Similar to the bridge over the left floodland, two bridges will be built for the two directions, separated by a narrow gap. The superstructure will be manufactured at assembly platforms located between pylons No. 19. and 20. and moved to its final position by gradual advancing.

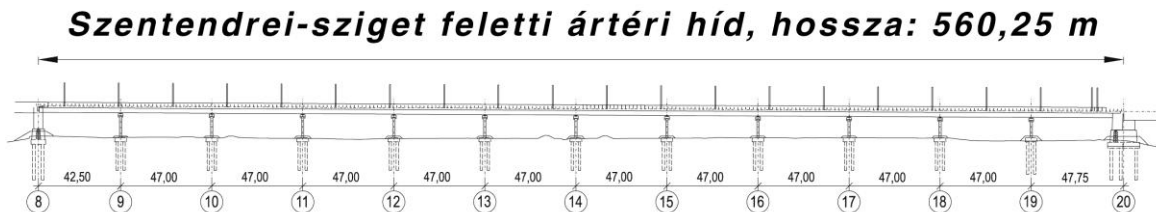


Fig. 4 Structure of the bridge over the floodland of Szentendre Island

### 2.4 Bridge over the Szentendre branch of the river Danube

This bridge will run in the angle of 80° to the main stream of the river. Pillars will be in parallel with the main stream, but the superstructure will be perpendicular.

The bridge is a three-span fine-meshed carriageway grid, with a single-cell, continuous box structure (Fig. 5). Girder webs are installed in an angle. Similar to the above, the two bridges will be built for the two directions, separated by a narrow gap. All factory and in-situ joints will be welded. Sections of the bridge will be floated to their final locations.

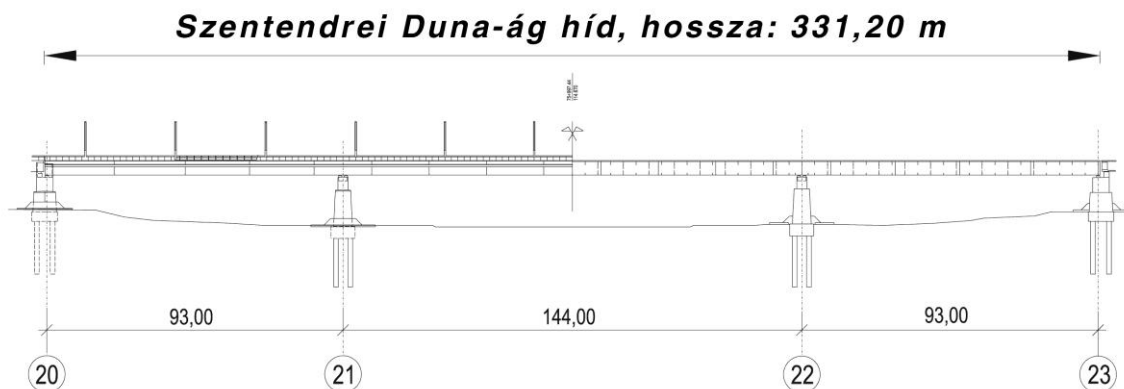


Fig. 5 Structure of the bridge over the Szentendre branch of the river Danube

### 2.5 Bridge over the right-side floodland

This section is a five-span beam bridge, made of prestressed reinforced concrete box blocks. (Fig. 6). Similar to the above two bridges built with advancing technology, two separate superstructures will be built for the two directions. Precast sections of this bridge, similar to the above two ones, will be manufactured at platforms established behind the abutments, using gradually advancing technology.



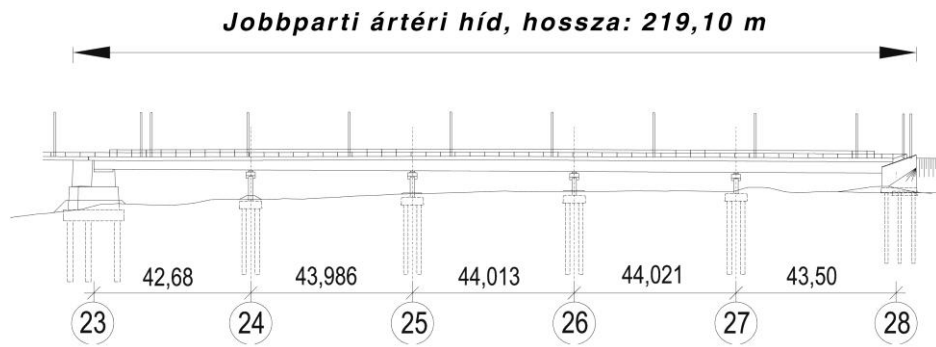


Fig. 6 Structure of the bridge above the right-side floodland

### 3. BUILDING THE BRIDGE OVER THE MAIN BRANCH OF THE RIVER DANUBE

We use bridges day after day without even noticing them. There are smaller and larger, simpler and more complicated ones. Even we, who work in bridge construction tend to forget about the days of construction, how the bridge we just crossing was built. Building a bridge is like an adventure, especially the construction of such a unique fan-type, cable-stayed bridge like the bridge of M0 Motorway across the river Danube.

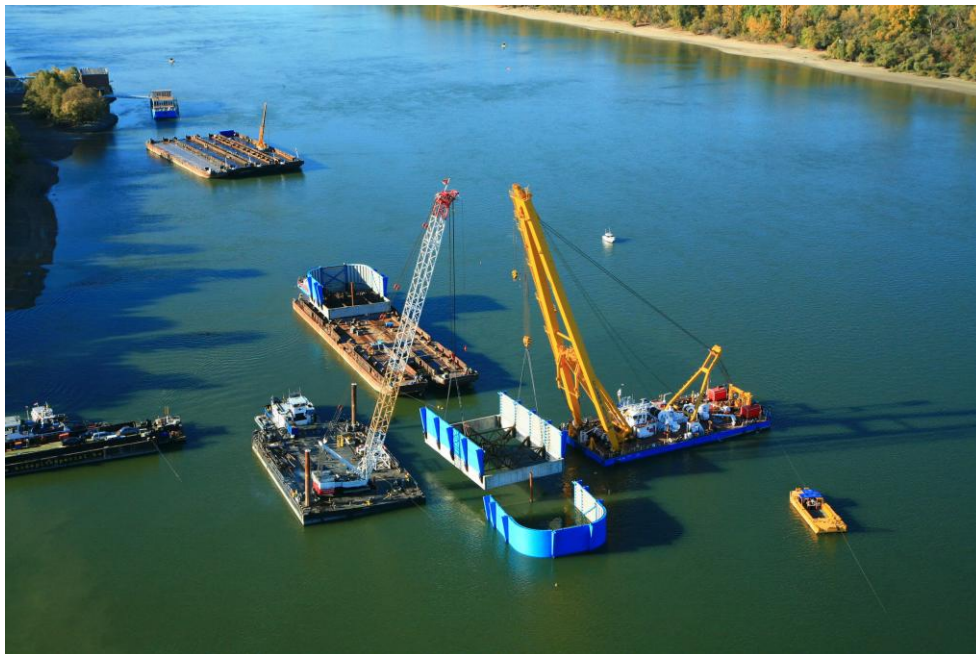


Photo 1 Installation of the casing

Pylons in the river Danube are constructed by the method called reinforced casing element technology, patented by Hídépítő Co. (Photo 1). According to this technology, reinforced concrete and steel piling walls are erected to provide waterproof working area. The casing will be used as a non-removable shuttering for the preparation of underwater concrete structures and the head beam. In contrary, the steel piling wall is recyclable, to be used for the construction of the next pylon.

Preparation of drilled piling is very similar to the traditional method, the only difference is that the piling machine is not standing on the ground but installed onto a custom-made floating platform. As soon as all boxing plates and piling walls are installed with the help of geodesic advisors and divers, they start pouring underwater concrete in order to stabilize the riverbed and to prevent floating of the whole structure. After pumping water out from the space guarded by the piling walls, construction is continued with using traditional pylon-building methods. The only worry is the water level; it must not exceed the level of safety.

Construction of the „A” frame pylons starts at the last stage of the bottom part of the pylon, when the so-called structural beam is installed. Fittings of the tower crane to be installed into the concrete are put into place also at this stage. This tower crane will be used for the construction of the upper section of the pylon. At the same time, the  $\Phi$  40 dywidag rods, to be used for tensioning the pillar arms, are also anchored into the pillars, into the depth of 2 m. The installation of these fittings indicates the actual start of the almost 100 m high pylons. Pylons will be built with using automatic climbing shuttering technology, in 4 m long stages (Fig. 3). The system includes five operating levels. The main level (0. level) is the level of the shutters. The hydraulic system, which moves the climbing shuttering, is controlled at the level -1, beneath level 0. Slippers of the climbing shuttering system are removed at level -2. Bindings of the shutters are installed at the level above the main level (level 1). Concrete is poured at the highest level (level 2).



Photo 2 Construction of pylons with using climbing shuttering technology

Construction steps of an average pylon:

1. step: Installation of the inner shutters. Since this is not part of the automatic climbing system, this section is lifted into its place by a crane. After moving the internal shutters into their place, they are adjusted to their final location with the help of geodesic experts, with a tolerance of 5 mm.

2. step: Installation of the fittings. Fittings are mostly taper sockets used for fastening the climbing shutters, with the exception of a few other components, such as temporary supports, concreted fittings of the tower crane and anchoring parts of the cables to be installed in future steps.
3. step: Installation of steel reinforcements. In order to save time on time-consuming in-situ assembly, we will install as many prefabricated components as possible at the factory.
4. step: In parallel with the installation of reinforcements,  $\Phi$  40 dywidag rods and their accessories - used for tensioning - are installed.
5. step: Installation of the external shutters, helped by geodesic experts, with an accuracy of 5 mm.
6. step: Pouring concrete with using concreting container.
7. step: As soon as the strength of the concrete reaches  $26 \text{ N/mm}^2$ , shutters can be removed.
8. step: After installing the internal working platform onto the upper level of the completed section and the strength of the concrete exceeds  $32 \text{ N/mm}^2$ , the structure will be tensioned.
9. step: To advance the automatic climbing shuttering system to the position for preparing the next section.

After completing step 9., the procedure starts from the beginning. A layman may think that from here it is only a repetition of monotonous steps, but as every construction work, new problems emerge all the time. We, the contractors, have got used to these challenges and as the result, we will never get bored. To work at the top of the pylon arms is really fantastic, like working on our private island, far away from the world and enjoying the excellent view.

#### **4. CONCLUSIONS**

Most of us have a desire to participate in creating something special, something everlasting; at least once in our lifetime. Some of us, after Kőröshegy, believed that we have achieved this aim with no similar project to come. But this current project offers to us, to dedicated bridge builders, another opportunity to participate in something special and to build a long-lasting creation. We believe that we are really the lucky ones.

Although we passed half of the project, we are sure that many challenges are still waiting for us.





## AUTHOR INDEX

Aciu, C.	155
Ackermann, F. P.	251
Adámek, J.	105
Asztalos, I.	123
Badesso, L.	135
Bajzecer, A.	351
Balázs, Gy. L.	1, 111, 275, 327, 345, 369
Balázs, Gy.	87
Balsamo, A.	455
Bartos, D.	425
Beluzsár, J.	401
Beluzsár, L.	401
Bjegovic, D.	321
Bódi, I.	431
Borosnyói, A.	221, 345
Brodnan, M.	381
Broukalová, I.	239
Burtscher, S. L.	395
Castillo, Á.	179
Černý, V.	93, 99
Chromá, M.	337
Clemente, P.	135
Consenza, E.	455
Corradi, M.	129
De Novais Bastos, J.	437
Dehlinger, C.	463
Desmyter, J.	67
Dragcevic, V.	425
Eisenhut, T.	81
Erdélyi, A.	221
Erdódi, L.	431
Esmaeelkhanian, B.	185
Fernández-Luco, L.	179
Ferrari, G.	135
Francišković, J.	143
Freytag, B.	281
Gálos, M.	207
Gamba, M.	135
Giuriani, E.	449
Gunter, S.	289
Han, H.	419
Hanzlová, H.	257
Harapin, A.	389
Heghes, B.	301
Hirscher, J.	495
Hopfgartner, M.	333
Hosseinpoor, M.	375

Hrubý, V.	257
Imjai, T.	363
Jambresic, M.	263
Józsa, Zs.	61, 155
Juhart, J.	281
Juránková, V.	105
Kainz, A.	395
Kalová, V.	93
Kárpáti, L.	207
Kartuzov, D. V.	357
Kassai, Zs.	55
Khurana, R.	129
Kindij, A.	475
Kohoutková, A.	149
Kollegger, J.	395
Kopecskó, K.	87
Koris, K.	407, 431
Kotes, P.	381
Kotula, P.	381
Koukal, P.	105
Kovács, I.	55, 275
Kratochvíl, A.	201
Kremnitzer, P.	117
Krispel, S.	193
Kucharczyková, B.	105
Lackner, R.	333
Lakusic, S.	425
Linder, J.	281
Lublóy, É.	327
Macht, J.	75
Madhkhan, M.	185
Magarotto, R.	129
Magyar, J.	21
Magyari, B.	245
Manfredi, G.	455
Matesová, D.	337
Meinhard, K.	333
Mihalik, T.	13
Mikšić, B.	143
Minelli, F.	213
Mirfenderesk, G. A.	185
Nad, L.	351
Nagy, A.	29
Nanni, A.	351, 455
Necas, R.	35
Nehme, S. G.	269, 275
Nemes, R.	61
Netinger, I.	321
Nezhad, E. F.	185
Nguyen, M. L.	233

Nischer, P.	75
Novidis, D. G.	375
Pankhardt, K.	269
Pantazopoulou, S. J.	375
Pekarek, A.	81
Pilakoutas, K.	363
Plizzari, G. A.	213
Podroužek, J.	337
Pollet, V.	67
Pospisil, K.	309
Preti, M.	449
Prota, A.	455
Rath, A.	487
Rauch, M.	295
Río, O.	179
Rogan, I.	143
Rovňák, M.	233
Ruscito, G.	351
S. Kanappan,	443
Schnell, J.	251
Shilin, A. A.	357
Sichani, M. E.	185
Sigrist, V.	295
Simon, T. K.	503
Skazlic, M.	263
Smilović, M.	389
Sparowitz, L.	281
Štědroňský, P.	481
Stefan, H.	289
Strasky, J.	35
Stryk, J.	309
Surico, F.	135
Szabó, Zs. K.	369
Szautner, Cs.	173
Szécsényi, R.	515
Sziklai, Z.	401
Szilágyi, H.	167
Szilágyi, K.	111, 173
Tassi, G.	245
Teplý, B.	337
Terzijski, I.	35
Ting, S. K.	419
Tomičić, M.	143
Tue, N. V.	289
Vítek, J. L.	315
Vladimíra, V.	149, 257
Vodička, J.	257
Výborný, J.	257
Vysloužil, J.	309
Zsigovics, I.	111, 161, 173